ProQuest LLC.
789 East Eisenhower Parkway
P.O. Box 1346
Ann Arbor, MI 48106 – 1346

Enzymatic Cleavage of Chemokines CCL2 and CXCL10: Implications for Multiple Sclerosis Pathogenesis

Helen Ann Denney

A thesis submitted in partial fulfilment of the requirements of Sheffield Hallam University for the degree of Doctor of Philosophy

April 2008

This thesis is dedicated to my wonderful parents,
who have provided enduring love and support,
fostered my love of learning,
and encouraged cerebration.

Abstract

In multiple sclerosis (MS), lymphocytes and monocytes penetrate the blood brain barrier (BBB), causing inflammation and leading to myelin damage and subsequent loss in the white matter of the central nervous system (CNS). Chemotactic cytokines (chemokines), contribute to the recruitment of immune cells into the CNS, and are expressed by astrocytes, the most abundant cell type in the CNS, and endothelial cells. CCL2 and CXCL10 are chemokines expressed in MS lesions, which are thought to be pivotal in chemoattraction of T cells and monocytes into the CNS. Astrocytes, microglia, and endothelial cells produce proteases, such as matrix metalloproteinases (MMPs), which contribute to the destruction of the BBB, facilitating cellular entry. Increased expression of MMP2 and MMP9, amongst others, has been shown previously in autopsied MS brain, and increased levels of the cell surface peptidase CD26, expressed by T cells and endothelial cells, have been linked to disease activity. Interactions between proteases and chemokines expressed in the same milieu can result in chemokine processing that dramatically increases or decreases their activity. To assess the potential effects of chemokine cleavage in MS, recombinant proteins were used in an *in vitro* study which examined processing of CCL2 and CXCL10 by MMP2, MMP9 and CD26, using mass spectrometry to identify enzymatic cleavage products. MMP9 removed four residues, and CD26 cleaved a dipeptide, from the N-termini of both CCL2 and CXCL10. MMP2 N-terminally cleaved four residues from CCL2, and five from CXCL10. C-terminal truncation of CXCL10 was observed with MMPs 2 and 9, which each removed four residues. Cleavage by CD26 was rapid, and complete with CXCL10 within 30min. MMP truncation of CCL2 was complete within 3h, but with CXCL10, remained incomplete by 48h. Astrocyte supernatant was examined by mass spectrometry for the presence of these truncated chemokines, but low levels prevented detection. Protease expression was investigated, to identify the likelihood that cleaved CCL2 and CXCL10 arise *in vivo* in MS. The MMP mRNA expression profile of cytokine-treated and untreated astrocytes examined by real time PCR showed that MMP2 mRNA was highly expressed with and without cytokine treatment, and MMP9 mRNA was increased following treatment with the pro-inflammatory cytokines tumour necrosis factor and interleukin-1β. MS brain tissue was examined using dual-labelling immunofluorescence for CD26 expression, which was found in lesions to be associated with T cells and monocytes in perivascular cuffs, and macrophages within the parenchyma, but not with astrocytes. The chemotactic activity of the cleaved forms of CCL2 and CXCL10 identified in this study was investigated using real time *in vitro* migration assays. THP-1 cells, a monocytic cell line, exhibited a two-fold reduction in migration to cleaved CCL2 isoforms, compared to the intact form. Preliminary experiments with Jurkat cells, a T cell line, indicated that migration remained unaffected, or was slightly increased, by cleaved CXCL10 compared to the intact form. Collectively, this study demonstrated that cleavage of CCL2 and CXCL10 by proteases, found at elevated levels in MS, may be an important regulator of chemokine activity. In particular, CD26 may play a key role in regulating chemokine activity, and thus cell migration into the CNS, as it demonstrated rapid and highly specific proteolytic activity and is highly likely to encounter chemokines as it was associated with T cells and macrophages that express the appropriate chemokine receptors.

Contents

List of Figures

Chapter 1

Chapter 2

Chapter 4

List of Tables

Abbreviations

APC	antigen presenting cell
BBB	blood brain barrier
BM	basement membrane
BSA	bovine serum albumin
CD	cluster of differentiation
CHO	Chinese hamster ovary
CNS	central nervous system
CSF	cerebrospinal fluid
CV	coefficient of variation
DPPIV	dipeptidyl peptidase IV
EAE	experimental autoimmune encephalomyelitis
EBV	Epstein-Barr virus
EC	endothelial cell
FCS	foetal calf serum
GA	glatiramer acetate
Gd	gadolinium
GFAP	glial fibrillary acidic protein
GM-CSF	granulocyte-macrophage colony-stimulating factor
H&E	haematoxylin and eosin
HBSS	Hank's balanced salt solution
HLA	human leucocyte antigen
HRP	horseradish peroxidase
HSCT	haematopoietic stem cell transplant
HSA	human serum albumin
ICAM	intercellular adhesion molecule
IFN-β	interferon-beta
IFN-γ	interferon-gamma
Ig	immunoglobulin
IL	interleukin
iNOS	inducible nitric oxide synthase
IP3	inositol triphosphate
LDS	lithium dodecyl sulfate
LFA-1	leukocyte function antigen-1
LPS	lipopolysacharide

MAC	membrane attack complex
MAG	myelin associated glycoprotein
MALDI-TOF	matrix assisted laser desorption/ionisation - time-of-flight
MALDI-QTOF	matrix-assisted laser desorption/ionisation - quadrupole/time-of-flight
MBP	myelin basic protein
MHC	major histocompatibility complex
MES	2-(*N*-morpholino) ethanesulfonic acid
MMP	matrix metalloproteinase
MOG	myelin oligidendrocyte glycoprotein
M_r	relative molecular mass
MRI	magnetic resonance imaging
mRNA	messenger ribonucleic acid
MS	multiple sclerosis
MSpec	mass spectrometry
NAWM	normal appearing white matter
NF-κB	nuclear factor-kappa B
NK	natural killer
NO	nitric oxide
OCB	oligoclonal bands
OLG	oligodendrocyte
ORO	oil red O
PBMC	peripheral blood mononuclear cell
PCR	polymerase chain reaction
PHA	phytohaemagglutinin
PLP	proteolipid protein
PP	primary-progressive
PR	progressive-relapsing
ROS	reactive oxygen species
RR	relapsing-remitting
RT	room temperature
SDS-PAGE	sodium dodecyl sulphate-polyacrylamide gel electrophoresis
SELDI-TOF	surface-enhanced laser desorption ionisation
SEM	standard error of the mean
SFM	serum-free media
SP	secondary-progressive
TCR	T cell receptor

TCV	T cell vaccination
TGF-β	transforming growth factor-beta 1
Th	T helper
TIMP	tissue inhibitor of metalloproteinase
TLR	toll like receptors
TNF	tumour necrosis factor
TREM2	triggering receptor expressed on myeloid cells - 2
VCAM-1	vascular cell adhesion molecule-1
VEGF	vascular endothelial growth factor
VLA-4	very late antigen-4

Acknowledgements

I wish to express my gratitude to my supervisor, Professor Nicola Woodroofe, for her guidance, expertise, and feedback throughout this project, and to Dr Rowena Bunning and Professor Malcolm Clench for their input. I am thankful to the BMRC for funding my studentship.

Thanks are extended to Dr Nacho Romero for providing primary human astrocytes, and to Dr Robert Nuttall and Professor Dylan Edwards for accommodating me in their lab at the University of East Anglia for a week of intensive PCR. I would also like to acknowledge Dr Stephen Wharton from the University of Sheffield, for pointing out some neuropathological features on brain sections.

A special mention must go to the donors of the brain tissue used in this project for their very valuable contribution. Dr Abhi Vora and Nirali Patel kindly organised the provision of tissue from the UK MS Tissue Bank, and provided a warm welcome during my visit.

For help with various techniques throughout this project, I wish to acknowledge Jessica Surr, Dr Gail Haddock, Dr Alison Cross, and Antoine Fouillet. I am grateful to those who donated blood samples, and to Dr Omer Suliman, Dr Shri Suryakant Pujari, and Dr Yong Zhou, for obtaining them.

Many colleagues in the lab have become good friends, and have offered support and vital humour when needed. They are too numerous to list, but include both past and present BMRC inhabitants, especially the "elite PhD office crew". Thanks to them, my PhD journey was littered with many happy, if somewhat bizarre, memories. Erdinger anyone?

Last but not least, a huge special thank you to my family and friends for their love, understanding, motivation, gifts of chocolate, and support. I realise this PhD has been a painful process for them too and I respect them for their patience.

~

Since completing this thesis, I have sadly learnt of the death of my undergraduate project supervisor, Professor Carl Pearson. It is to Carl that I owe my initial interest in neuroscience, and wish to commemorate him with the thought that he planted the seed that finally developed into completion of this PhD.

Chapter 1

General introduction

1.1 Immune regulation in the central nervous system (CNS)

The brain is a delicate organ with a limited regenerative capacity, which could suffer catastrophic damage if subjected to significant inflammation. Axons and dendrites, in particular, are very sensitive to inflammation due to their long, thin processes, high energy requirement, and low capacity for regeneration (Neumann and Takahashi, 2007). In the past, the brain was thought of as an 'immunologically privileged' site, not subject to infiltration of immune cells as part of routine surveillance. It was known that leukocytes existed in large numbers in the CNS during diseased states, but they were thought to be absent in healthy brain tissue (Antel and Owens, 1999). More recent discoveries have clarified that immune cells enter the CNS without it being subject to disease, but that this is highly regulated, and varies with age and brain region (Galea *et al.*, 2007).

The CNS can be thought of as a collection of compartments: the parenchyma; the ventricles, housing the choroid plexus and cerebrospinal fluid (CSF); and the meninges (Fig. 1.1). It was shown in 1923 that antigens injected into the brain parenchyma did not elicit an immune response, but did so if implanted into the ventricles. Almost 60 years ago, Medawar showed that the efferent immune response, i.e. the 'effector' phase designed to eliminate pathogens, is mostly intact in the CNS, but the afferent, or 'sensing' phase involving antigen recognition, is significantly lacking. The protective barrier formed by blood vessels and glial cells of the CNS, namely the blood brain barrier (BBB), was investigated in a quest to explain these differences observed in the CNS. The BBB was previously held wholly responsible for the CNS immune privilege, but it is now known that other features, such as details of the microenvironment, and specialised afferent communication to nearby lymphatic organs, are more important (reviewed in Galea *et al.*, 2007). As such, the CNS is best considered an immunologically *specialised* site, where immune reactions are present. There are several cell types involved in the immune response of the CNS, including T cells, B cells, phagocytes, and glial cells.

1.1.1 T cells

Maintaining an appropriate balance between reacting to pathogens and self-tolerance is essential for normal function of a healthy immune system. T cells develop in the thymus and play crucial roles in cell-mediated immunity. T cells recognise peptide antigens, displayed by major histocompatibility complex (MHC) molecules expressed on other cells. All nucleated cells express MHC class I proteins, which bind to T cell receptors (TCRs) on T cells expressing the coreceptor CD8 (Burrows *et al.*, 2008).

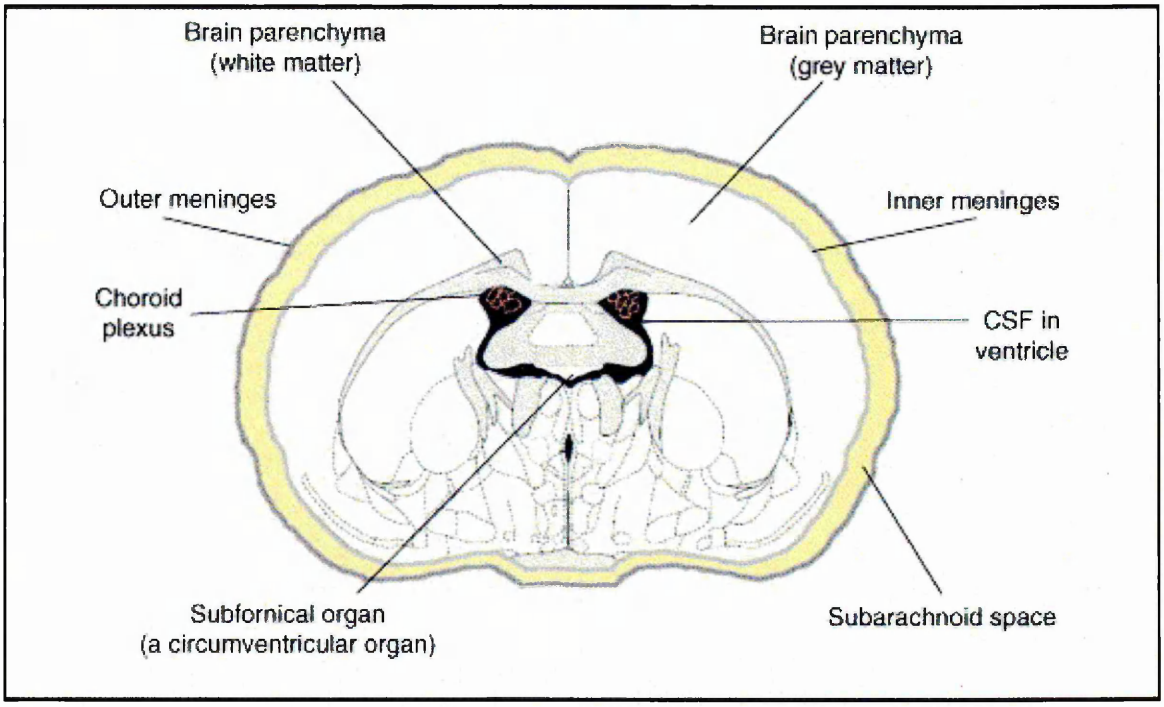

Reprinted from (Galea *et al.*, 2007) © (2007), with permission from Elsevier.

Figure 1.1 Compartments of the central nervous system

Within the ventricles, the choroid plexus produces cerebrospinal fluid (CSF), which bathes the brain parenchyma. Ventricular CSF is continuous with CSF found in the subarachnoid space, between the inner meninges covering the brain surface, and the outer meninges. Antigens injected into the ventricles elicit an immune response, demonstrating that these are not immunologically privileged sites. In the case of adaptive immunity, the immune privilege of the CNS is restricted to parenchymal compartments. The subfornical organ is circumventricular, in that it lacks a blood-brain barrier (BBB), and does not experience immune privilege (Galea et al., 2007)

T cell possession of the CD4 coreceptor, however, restricts TCR binding to cells expressing MHC class II, namely antigen presenting cells (APCs). Immune responses are geared towards detection of pathogens by breaking down the proteins involved into peptides, which are captured by MHC molecules on APC, and then presented to TCRs. The capacity of an antigen-MHC complex to activate T cells correlates with the duration and strength of TCR binding, with lengthy, high affinity binding being characteristic of TCR agonists (Mantzourani *et al.*, 2007). T cells that recognise self-peptides are largely eliminated during negative selection processes in the thymus (Yan and Mamula, 2002).

T cells can be broadly divided into effector or memory populations, with an additional subset that includes natural killer (NK) T cells and γδ T cells, which recognise antigen using molecules other than MHC class I or II (La Rosa and Orange, 2008). Memory T cells can be either $CD4^+$ or $CD8^+$, and facilitate a rapid proliferation of T cells in response to previously encountered antigens (Sprent and Suhr, 2001). Effector T cells cover diverse functions, as discussed below.

Effector T cell populations include helper, regulatory, and cytotoxic T cells. Helper T cells (Th) are of the $CD4^+$ subset, secrete cytokines involved in T cell and B cell proliferation, and attract and activate other immune cells, such as macrophages. $CD4^+$ T cells can also differentiate into regulatory, or suppressor, T cells, which are vital in maintaining immunological tolerance as they suppress auto-reactive T cells, and shut down T cell responses (La Rosa and Orange, 2008). Cytotoxic T cells (CTLs), mainly of the $CD8^+$ subset, are implicated in direct killing of resident target cells via secretion of perforin and granzymes (Trapani *et al.*, 2000).

CTLs are rarely found in the normal CNS, but during inflammation and microbial infection, their numbers can increase dramatically, and stimulation of brain cells may result in antigen presentation to T cells via expression of MHC molecules (Pedemonte *et al.*, 2006). CTLs surround, and accumulate in, CNS lesions during many neurological diseases, such as multiple sclerosis (MS) and virus-induced inflammatory brain diseases, and are known to be important in autoimmune CNS diseases.

In addition to categorising T cells according to the presence of either CD4 or CD8 surface molecules, $CD4^+$ T cells can be further subdivided according to the profiles of the cytokines they secrete. Cytokines are secreted proteins, critical in most immune responses, acting in either pro-inflammatory or anti-inflammatory ways. $CD4^+$ T cells, termed Th0 cells when in an undifferentiated state, are considered to produce the majority of cytokines, once activated (Berger, 2000). Activated Th0 cells can become

either Th1 or Th2 cells, depending on the local environment, with interleukin (IL)-12 stimulating Th1 activity, and IL-4 promoting Th2 differentiation (Berger, 2000). Recently, a third subset of CD4 T cells, namely Th17 cells, has also been identified (Korn *et al.*, 2007).

Pro-inflammatory cytokines, such as interferon (IFN)-γ, IL-2, and tumour necrosis factor (TNF), arise from Th1 cells, and are responsible for destruction of intracellular parasites and perpetuation of autoimmune responses, such as in MS (Frossi *et al.*, 2008). Th1 cells increase the production of immunoglobulin (Ig) G antibodies and encourage cell-mediated immunity (Berger, 2000). Th2 cells produce anti-inflammatory IL-10, and IL-6, and cytokines associated with allergic responses and promotion of IgE, such as IL-4, IL-5, and IL-13 (Frossi *et al.*, 2008). Th2 cells are involved in defense against extracellular pathogens. Th1 and Th2 cytokines are antagonistic in action, and the correct Th1:Th2 balance is critical in maintaining appropriate immune responses, thereby limiting tissue damage caused by pro-inflammatory Th1 responses, or allergic responses created by an excessive Th2 response (Berger, 2000). Th17 effector T cells produce the cytokine IL-17 and are implicated in defense against some pathogens, tissue inflammation, and organ-specific autoimmunity (Korn *et al.*, 2007).

T cells can engage in immune surveillance of the CNS, albeit to a lesser extent than in other organs under basal conditions, and contribute to inflammatory and immune responses (Xiao and Link, 1998). In addition to evidence that activated T cells can migrate from the blood into the CNS, using a sheep model, it has been shown that T cells do not need to be activated to enter the CSF (Seabrook *et al.*, 1998). Suggestions about the pathways taken by T cells when entering the CNS include infusion into the CSF, and exiting along major cranial nerves or arteries, meaning they would enter deep cervical lymph nodes and be able to engage in an immune response if the appropriate antigen was present, or rejoin the circulating lymphocyte pool (Seabrook *et al.*, 1998). In healthy individuals, the number of T cells entering the CNS is low (Hickey, 1999), but the efficiency with which they gain access varies according to area. T cells enter the spinal cord with greater efficiency than when accessing the brain (Phillips and Lampson, 1999), probably because recruitment mechanisms differ (Engelhardt and Ransohoff, 2005). Studies have indicated that the migratory phenotype of T cells necessary to cross the BBB is induced by several signals, including interleukin-2 (IL-2) (Pryce *et al.*, 1997). It is thought that T cells enter the CNS in a random fashion, as no receptors have yet been identified that serve to target specific leukocytes to the CNS (Hickey, 1999).

In patients with inflammatory disorders of the CNS, T cells are one of the most common cell types found in affected areas and in the CSF (Pedemonte *et al.*, 2006). It has been suggested that the CSF experiences an enrichment of Th1 T cells capable of differentiation into effector cells upon discovery of antigen, and that these cells are recruited by chemotactic cytokines called chemokines (Giunti *et al.*, 2003).

1.1.2 B cells

B cells are important in the humoral immune response, particularly in responding to microbial infections. They are produced in the bone marrow, circulate in the blood and lymph, and undergo differentiation after encountering an antigen, and signals from T helper cells. Activated B cells can become long-lived memory cells, specific to previously encountered antigens, or plasma cells, which produce antibodies (immunoglobulins: IgA, D, E, G, and M). Antibodies can bind antigens, preparing the product for phagocytosis by macrophages, for example, and they can also activate the complement system (Briere *et al.*, 2001).

When inflammation is not present in the CNS, B cells are mainly absent, but inflammatory CNS diseases are associated with significant numbers of them in the CNS and CSF (Cepok *et al.*, 2006). During CNS inflammation, immunoglobulins produced within the subarachnoid space, namely oligoclonal bands (OCB), are often detected and demonstrate that B cells have a role in the immune response (Thompson and Keir, 1990). B cells may also have antibody-independent roles in CNS immune responses, as they can function as antigen-presenting cells (APC) (Antel and Bar-Or, 2006).

The role of B cells in routine CNS surveillance is poorly understood. One study indicated that B cells can target their antigen in the CNS and produce oligoclonal IgG against it, suggesting memory B cells can be receptive to antigens as they drain from the CNS to deep cervical lymph nodes (Knopf *et al.*, 1998). Given the short life span of antibody-secreting cells, and the limited ability of antibodies to cross the BBB, it is most likely that the B cells involved in CNS immune surveillance are of the memory subset. Memory B cells have been found to accumulate in the CSF during CNS inflammation, particularly the subset with an IgD^-/IgM^- phenotype (Cepok *et al.*, 2006). Several findings indicate that, unexpectedly, B cells might undergo rapid division in the CNS akin to a germinal centre reaction, as short-lived plasma blasts (immature precursors of plasma cells) are found in the inflamed CSF (Cepok *et al.*, 2006), together with all B cell subsets (Corcione *et al.*, 2005).

1.1.3 Mononuclear phagocytes

Monocytes are produced in the bone marrow, circulate in the bloodstream, and can move into tissues, where they mature into macrophages. In the CNS, these macrophages occur as microglia. Monocytes/macrophages and microglia are likely to play a substantial role in the immune surveillance of the CNS, as aside from their phagocytic activity, they are involved in antigen presentation and control of T cell responses (Aloisi *et al.*, 2000), as discussed in Section 1.1.4.1 below. The phagocytic ability of these cells is mediated by opsonins, such as IgG, or complement, on the target antigen. Mononuclear phagocytes may also alter the ability of T cells to penetrate the CNS parenchyma via their upregulation of inducible nitric oxide synthase (iNOS), leading to increased nitric oxide (NO) expression, as well as increased production of TNF (Tran *et al.*, 1998). These mediators act on endothelial cells (ECs), causing an upregulation of adhesion molecules and contribute to the compromised state of the BBB seen in MS. Activated macrophages secrete IFN-γ and IL-3, in addition to TNF, all of which interfere with myelination by damaging oligodendrocytes (OLGs) (Merrill *et al.*, 1993).

1.1.4 Glial cells

Glial cells represent the non-neuronal, supportive cells of the CNS, including macroglia (astrocytes and OLGs), and microglia. Collectively, glial cells support neurons in a number of ways, including OLGs providing insulation of neurons with myelin, and astrocytes providing nutrition, maintenance of homeostasis, and participation in signal transmission. They produce many molecules involved in inflammatory and immune functions, such as cytokines and proteases (Von Bernhardi and Ramirez, 2001).

1.1.4.1 Microglia

During both development and adulthood, bone marrow derived myeloid cells enter the CNS and become perivascular macrophages, or more rarely in adults, microglia (Simard and Rivest, 2004) (Fig. 1.2). Microglia represent approximately 5 - 20% of resident glial cells, and are the major immunocompetent cells in the brain, capable of presenting antigen (Farber and Kettenmann, 2005). The exact precursor subtype responsible for microglia is unknown, but microglial cells are reportedly similar to uncommitted myeloid precursors, with the capacity to differentiate into dendritic-like cells (Servet-Delprat *et al.*, 2002). Following antigenic stimulation, for example, microglia become activated, adopt an amoeboid morphology, migrate to sites of injury, proliferate, and engage in phagocytosis (Imai *et al.*, 1997). Microglia possess highly motile and long, interdigitating processes which form a network that covers the entire

CNS, strongly suggesting a role for resting microglia in immune surveillance (Neumann and Takahashi, 2007).

An innate immune receptor expressed on cell membranes, namely Triggering Receptor Expressed on Myeloid cells - 2 (TREM2), is expressed on microglia (Kiialainen *et al.*, 2005). The TREM2 receptor associates with the adaptor protein and signalling molecule DnaX-Activating Protein of 12 kDa (DAP12), thereby enabling TREM2 stimulation to initiate signalling via DAP12. DAP12 triggers a protein tyrosine kinase called extracellular signal-regulated kinase (ERK), which is involved in an intracellular signal transduction pathway (Takahashi *et al.*, 2005). TREM2 signalling has been found to be essential for phagocytosis of apoptotic cellular membranes (Neumann and Takahashi, 2007). Without this TREM2-DAP12 receptor-signalling complex, CNS tissue homeostasis would be disturbed by delayed debris clearance and increased production of inflammatory cytokines by microglial cells.

In addition to phagocytosis, microglia can respond to threats to the CNS by releasing cytotoxic and inflammatory modulators (e.g. cytokines such as IL-1β, and complement proteins) and cell killing via release of NO and superoxide ions (Von Bernhardi and Ramirez, 2001). Aside from this pro-inflammatory role, evidence is accumulating that microglia might have neuroprotective properties, through stimulation of myelin repair, eradication of toxins in the CNS, and prevention of neurodegeneration in chronic brain diseases (Glezer *et al.*, 2007). There is evidence that microglia may function co-operatively with astrocytes in generating responses to brain injury, exhibiting reciprocal regulation (Martin *et al.*, 1994).

1.1.4.2 Astrocytes

Astrocytes are the most abundant glial cell, and are highly diverse, exhibiting varied reactive responses to pathogenic brain insults. In the healthy CNS, they remove excess ions (particularly potassium) from the external environment of neurons, recycle neurotransmitters, are involved in uptake of glucose and glutamate, and glycogen storage (Fatemi *et al.*, 2004), and are considered to be a major component of the BBB (Fig. 1.2) (Kramer-Hammerle *et al.*, 2005).

Astrocytes signal to each other using calcium: the messenger molecule inositol triphosphate (IP3) diffuses from one astrocyte to another via gap junctions, activating calcium channels on organelles, and resulting in calcium release into the cytoplasm, which may prompt production of more IP3 and culminate in a calcium wave propagating from cell to cell (Bellinger, 2005).

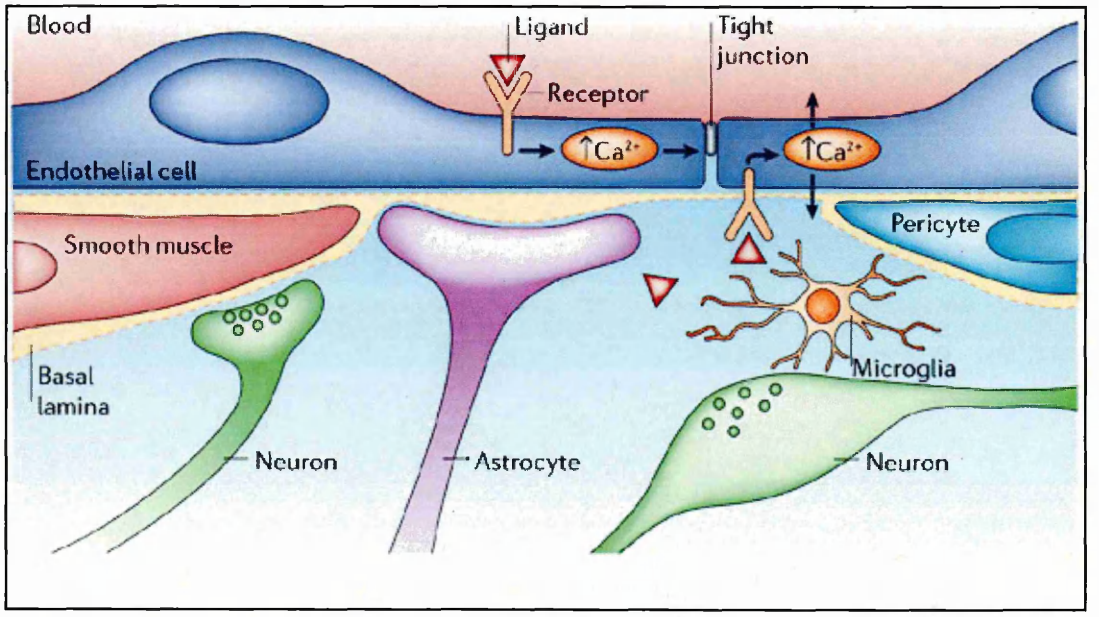

Figure 1.2 Complex cellular interactions at the blood–brain barrier

A brain capillary wall is shown, with the major cell types capable of signalling to each other. Pericytes form a close association with the endothelial cells due to their enclosure within the basal lamina. Astrocytic end feet contact the outer surface of the basal lamina. Microglia share the perivascular space with synaptic terminals, neurons, and, in arterioles, smooth muscle cells. Endothelial cells are influenced by ligand-receptor interactions arising on both their blood or brain surfaces. Some of these interactions lead to increases in intracellular calcium. Following receptor activation of endothelial cells, the arrows indicate their ability to release substances to either the blood or brain side (Abbott et al., 2006).

They respond to the firing of adjacent neurons by exhibiting rapid electrical activity, and are receptive to neurotransmitters such as norepinephrine and glutamate (Murphy *et al.*, 1993). Astrocytes can release glutamate, thereby signalling back to neurons (Carmignoto, 2000). Calcium signalling from astrocytes can contribute to neuronal plasticity and learning by influencing synaptogenesis and synaptic transmission (Ostrow and Sachs, 2005).

Activated astrocytes contribute to CNS diseases by the production of proinflammatory cytokines, proteases, adhesion molecules, such as intercellular adhesion molecule (ICAM)1 and ICAM2, chemokines, and NO (Von Bernhardi and Ramirez, 2001). Unlike microglia, astrocytes cannot generate large amounts of free radicals, but they do have some phagocytic ability. Astrocytes produce cytokines that are able to act on microglia, such as colony-stimulating factors, which can stimulate microglial migration after injury. The interaction between astrocytes and microglia is complex, but it is thought that microglial-derived products are neurotoxic, while astrocytes tend to play a neuroprotective role by producing neurotrophic factors and eliminating neurotoxins (Von Bernhardi and Ramirez, 2001). Astrocytes respond to CNS trauma by becoming hypertrophic and proliferating. This astrocytosis, however, can restrict repair in MS by hindering migration of remyelinating cells (Malik *et al.*, 1998).

1.1.4.3 Oligodendrocytes

OLGs are glial cells that produce and maintain the 'myelin sheath' that surrounds axons, providing insulation to facilitate salutatory conduction. The sheath can be of a simple cytoplasmic type, or composed of multiple myelin lamellae. In addition to this vital role of myelin production, OLGs can also contribute to the growth and maintenance of axons within white matter (Edgar *et al.*, 2004).

OLGs that produce myelin have been categorised as types I – IV according to their morphology and axonal interactions. Type I OLGs are found around blood vessels, neurons, and fibre tracts, in the forebrain, cerebellum, and spinal cord. Type II OLGs are seen in white matter, near to nerve fibres. Type III OLGs are found in the medulla oblongata, spinal cord, and cerebral and cerebellar peduncles. Type IV OLGs adhere to nerve fibres at the entrance of nerve roots (Baumann and Pham-Dinh, 2001). When OLGs approach axons to begin myelination, the OLG exhibits an undifferentiated structure, and it is not known if the microenvironment or genetic programming determines the subtype the OLG will become. The maturation of OLGs is characterised by stages of expression of myelin-related genes and cell surface markers, such as

myelin basic protein (MBP), proteolipid protein (PLP), and myelin oligidendrocyte glycoprotein (MOG) (Webber *et al.*, 2007).

Microglia can directly interact with OLGs, damaging them, and contributing directly to the demyelination of axons and other tissue injury (Irani, 2005). Different mechanisms of myelin destruction have been suggested in MS, with either the OLG, or the myelin sheath being the target (Kornek and Lassmann, 2003). Antibodies against various myelin proteins have been found in MS patients, such as anti-MOG antibodies, although their exact role is unclear (Reindl *et al.*, 1999). Remyelination is potentially a powerful neuroprotective therapy to ameliorate disability in MS. Cytokines of the IL-6 superfamily can promote OLG survival - a significant finding given that astrocytes and microglia are the predominant source of IL-6 cytokines in the inflamed CNS (Ransohoff *et al.*, 2002).

1.1.5 Endothelial cells (ECs)

Brain ECs comprise the main component of the BBB (Fig. 1.2) and contribute to the immune response of the CNS by responding to, transporting, and secreting cytokines (Verma *et al.*, 2006). ECs are unique in possessing differing compositions of their cell membranes according to the environment they face, with lipid, receptor, and transporter components differing between the face in contact with the blood, and the membrane facing the brain. This polarisation is thought to help with the functions of the BBB, namely preventing harmful substances from entering the brain, and controlling the passage of substances to and from the brain. ECs comprising the BBB differ from those elsewhere in the body due to their absence of fenestrations, reduced pinocytic vesicular transport, and more extensive tight junctions between them, which limit the flux of hydrophilic molecules between cells (Ballabh *et al.*, 2004).

Tight junctions consist of three membrane proteins (claudin, occludin, and junction adhesion molecules), and also cytoplasmic accessory proteins, including zonula occludens (ZO) -1, -2, and -3 (Ballabh *et al.*, 2004). Occludins and claudins collectively form intramembranous strands which contain channels that allow diffusion of ions and hydrophilic substances (Matter and Balda, 2003). Junctional adhesion molecules are little explored, but are thought to play roles in adhesion between cells, and monocyte transmigration through the BBB (Aurrand-Lions *et al.*, 2001). In MS, leukocyte migration into the brain can trigger signalling cascades that result in the loss of occludin and ZO proteins from tight junctions, thereby contributing to BBB breakdown (Bolton *et al.*, 1998).

Brain ECs can receive immune challenges from one side (e.g. the blood), and respond by secretion of cytokine into the other (i.e. brain) (Fig. 1.2). Brain EC secretion of cytokines IL-1α, IL-10, granulocyte macrophage colony-stimulating factor (GM-CSF), IL-6, and TNF has been demonstrated, with a preference for secretion into the blood, rather than the brain (Verma *et al.*, 2006). Lipopolysaccharide (LPS) induces release of specific cytokines from brain ECs, and is known to disrupt the barrier function of the BBB (Singh and Jiang, 2004). When brain ECs are exposed to TNF, IL-1β, IFN-γ, or LPS, the transendothelial electrical resistance is decreased due to increased permeability of the tight junctions, thus reducing the ability of the BBB to impair the passage of peripheral blood mononuclear cells (PBMCs) into the CNS (Wong *et al.*, 2004). Brain ECs are important in the immune response of the CNS, as they constitute a major component of the BBB that can secrete cytokines in an inducible, varied, and polarised fashion.

1.1.6 The blood brain barrier

Ehrlich's seminal observation that injecting dyes into peripheral blood vessels resulted in poor staining of the brain, compared to other organs, sparked further experiments that led to an increasing elucidation of the specialised structure of the BBB. The BBB was linked to the state of immune privilege by Barker and Billingham, who described how the scarcity of transport vesicles in brain ECs, and the occluding junctions between their plasma membranes, together with neuroglial end processes (Fig. 1.3), could significantly restrict immune cell infiltration. The barrier function of the BBB is well established, but routine transport across the BBB is possible, however (reviewed in Bechmann *et al.*, 2007). Lipophilic substances (e.g. oxygen and carbon dioxide) diffuse freely along concentration gradients; smaller molecules, such as glucose and amino acids, utilise transporters to cross the BBB; and receptor-mediated endocytosis is employed for larger molecules (e.g. insulin and leptin) (Ballabh *et al.*, 2004).

All brain regions possess a BBB, except for circumventricular organs (Fig. 1.1), such as the pineal gland. These areas are important sites for communicating with the CSF, and have blood vessels with fenestrations that allow diffusion of blood-borne molecules, thus helping to regulate the autonomic nervous system and endocrine glands (Ballabh *et al.*, 2004). The BBB is not simply composed of ECs, as it includes the capillary basement membrane (BM), astrocytic end-feet enrobing the vessel walls, and pericytes within the BM (Fig. 1.2), that wrap around ECs. The astrocytic end-feet enhance the barrier properties of ECs by inducing and maintaining a tight junction diffusion barrier (Ballabh *et al.*, 2004). Pericytes are thought to be involved in angiogenesis, vessel structural integrity, and the formation of tight junctions (Allt and Lawrenson, 2001).

Figure 1.3 Location of the three main barrier sites in the CNS

The CNS presents 3 main barriers to penetration by cells or substances. The first is mainly created by brain ECs, which form the BBB (1). The basement membrane (BM) of the blood vessel, pericytes within the BM, and astrocytic end feet also contribute to the composition of the BBB. Circumventricular organs contain specialised neurosecretory or chemosensitive neurons and are the only brain region to lack a BBB. Their leaky endothelium is separated from other brain regions by a glial barrier and from the CSF by an ependymal barrier (Ballabh et al., 2004). The second barrier is the arachnoid epithelium (2), which comprises the middle layer of the meninges. The outer layer of the meninges is composed of the dura mater, and the pia mater constitutes the inner layer. The epithelium of the choroid plexus (3), which is responsible for CSF secretion, forms the third physical barrier. All 3 barriers utilise tight junctions to reduce the permeability of the intercellular pathway (Abbott et al., 2006).

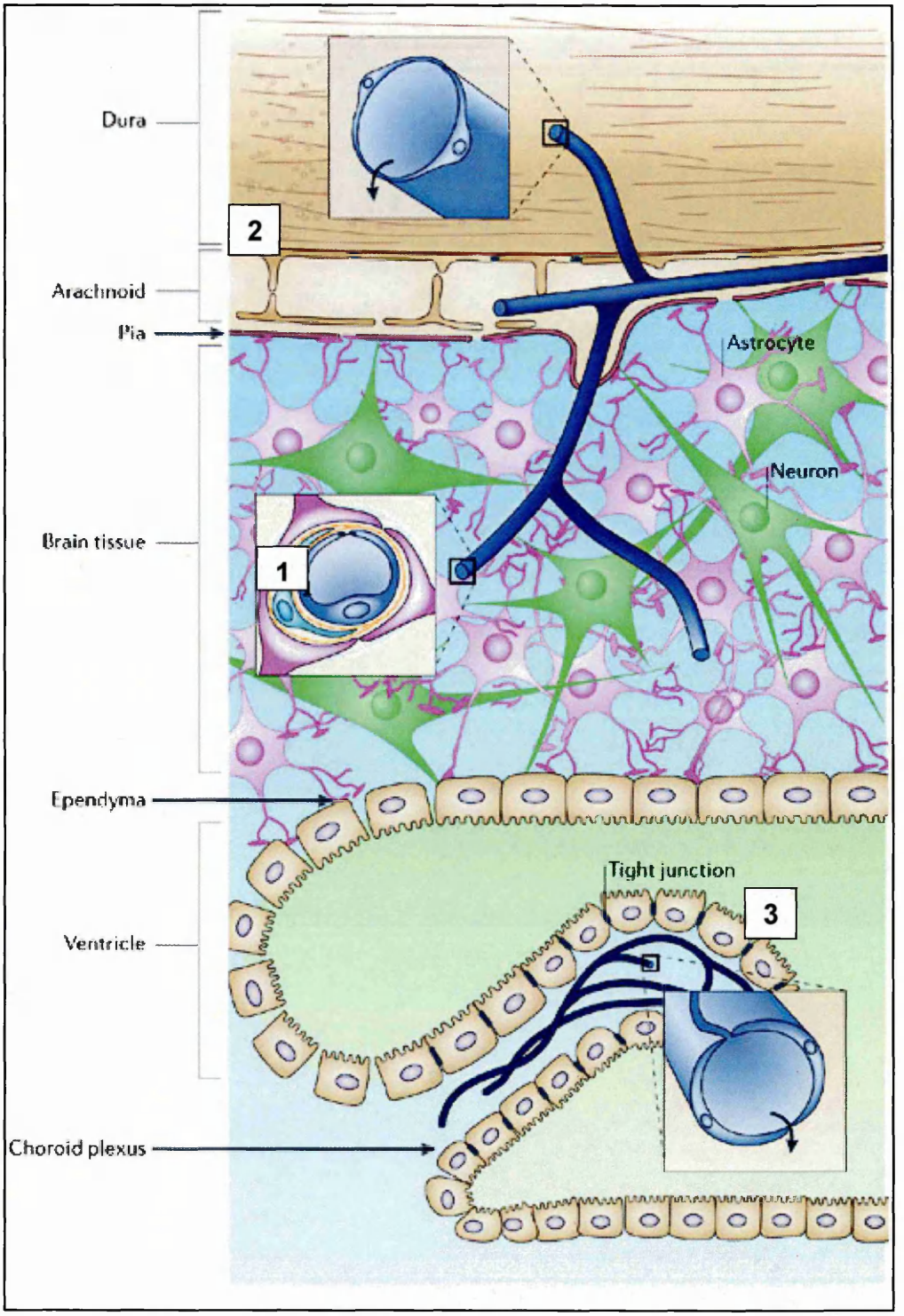

Reprinted by permission from Macmillan Publishers Ltd: Nature Reviews Neuroscience (Abbott *et al.*, 2006) © (2006)

The barrier created by tight junctions between ECs is tightest in the capillary endothelium (Ge *et al.*, 2005), so leukocytes tend to traverse the endothelium at postcapillary venules (Bechmann *et al.*, 2007). The vessel wall in pre- and post-capillary zones of the BBB is separated from the neuropil by an additional compartment, or perivascular space, created by protrusions from the pia mater of the brain surface. This compartment, termed the Virchow-Robin space, is partially filled with CSF via its connections with the subarachnoid space. Cells crossing the vessel in this region do not directly enter the neuropil, but are instead often retained in this perivascular space. Accumulation of inflammatory cells in the Virchow-Robin space is one of the hallmarks of MS, and some other neuroimmune diseases, creating characteristic 'perivascular cuffs'. The Virchow-Robin space may be responsible for initiating and sustaining an immune response to foreign antigens in the brain, as macrophages found there express MHC class II, and are well positioned to interact with lymphocytes from the blood (Vos et al., 2005). As neuroinflammation proceeds, cells may then pass the glia limitans, which underlies the pia mater, in a considerably more restricted step than the process of passing from the blood into the perivascular space. For cells to pass the glia limitans, APCs must present antigen in the perivascular space (Greter *et al.*, 2005). The glia limitans serves as both a mechanical and functional barrier. Astrocytic end feet of the glia limitans constitutively express the death ligand CD95L, which may account for perivascular apoptosis, designed to prevent activated T cells from stimulating immune responses (Bechmann *et al.*, 1999).

1.2 Multiple sclerosis

MS was first identified by Jean-Martin Charcot in 1868, and was considered a rarity by American physicians for the next 50 years. Many cases were misdiagnosed, but increased training of neurologists, and ensuing improvements in diagnosis, saw MS rated as one of the most prevalent neurological diseases (Talley, 2005). MS is commonly described as a disease of the CNS white matter, involving immune-driven inflammation and demyelination, culminating in sclerotic plaques and axonal damage (Bar-Or *et al.*, 1999). It is a complex disease, often resulting in severe disability for the individual, whilst presenting a significant economic burden to society. The estimated lifetime costs incurred by health care and social systems in the UK are £1 million per MS patient (Altmann and Boyton, 2004; Orton *et al.*, 2006). Whilst treatments for the symptoms of MS have improved substantially, as has diagnosis, utilising magnetic resonance imaging (MRI), a cure remains elusive.

1.2.1 Symptoms of MS

Symptoms of MS are many and varied within and between patients, depending on which areas of the CNS are damaged, to what extent, and on how the disease progresses. Physiological symptoms are related to the CNS, and the musculoskeletal and autonomic nervous sytems. Commonly, fatigue, spasticity, muscle weakness, pain, depression, cognitive dysfunction, deterioration of speech, visual disturbance, bladder and bowel disturbances, and sexual dysfunction, are experienced (Crayton and Rossman, 2001; Huijbregts *et al.*, 2006), The fatigue experienced by MS patients can result from either the disease, or as a side effect of treatment, is often worsened by heat, and can exacerbate the morbidity of MS by limiting the patient's reserves to deal with accompanying symptoms (Bakshi, 2003).

1.2.2 Diagnosis of MS

MS is often misdiagnosed as other conditions can mimic it, such as the demyelinating inflammatory disease, neuromyelitis optica (Charil *et al.*, 2006). MRI has emerged as playing a prominent role in the diagnosis of MS, but this is combined with information from the clinical history and physical examination of the patient by a neurologist, together with laboratory tests for the presence of OCB in the CSF and increased IgG, to establish as firm a diagnosis as is possible. MRI criteria for diagnosing MS has changed frequently over the last two decades. Currently, disease dissemination must be shown in 'space and time', whereby evidence of multiple lesions detected at least six months apart, and occurrence of at least two distinct attacks, is required (Charil *et al.*, 2006).

1.2.3 Clinical subtypes of MS

MS can be divided into different clinical subtypes based on the clinical course of the disease. Approximately 90% of patients exhibit relapsing-remitting MS (RRMS) initially, with acute attacks involving worsening of neurological function (relapses), alternating with periods of full or partial recovery (remissions) (Fig. 1.4) (Schwarz *et al.*, 2006). A minority (30%) remain with this disease course, but 60% of RRMS patients find as the disease progresses, recovery from attacks is incomplete, leaving permanent axonal damage, and eventually the disease course is often described as secondary progressive MS (SPMS). SPMS is characterised by the frequency of relapses levelling off, and steady deterioration occurring, without remission (Fig.1.4) (Compston, 2004; Guttmann *et al.*, 2006). Approximately 10% of patients present with what is described as primary progressive MS (PPMS) in onset, which typically involves a progressive decline without distinct relapses or remissions (Fig. 1.4) (Schlaeger *et al.*, 2006; Al-

Araji and Mohammed, 2005; Lublin and Reingold, 1996). The rarest disease course is progressive relapsing MS (PRMS), where progressive disability occurs from the onset, with clear relapses, with or without recovery (Fig. 1.4) (Podojil and Miller, 2006).

1.2.4 Epidemiology

MS accounts for the majority of neurological disability of young adults in the Western World, affecting approximately 1.1 – 2.5 million people worldwide, with a prevalence of 1/1000 in the UK (Compston, 1998). MS is generally considered to be increasing, as seen in Canada (Orton *et al.*, 2006), Australia (Barnett *et al.*, 2003), and the USA (Noonan *et al.*, 2002), for example. Women are approximately twice as likely to suffer from MS as men (Reipert, 2004). This sex ratio can vary regionally, however, exceeding 3.2 females to every male in Canada, for example (Orton *et al.*, 2006). The onset of this complex disease often occurs between the ages of 20-40 years, with over 90% of patients experiencing onset before 50 years of age (Noseworthy *et al.*, 1983). Childhood-onset MS is rare, with only 3-10% of patients developing MS before the age of 18 years (Banwell *et al.*, 2007).

In general, there is an increasing prevalence of MS in climates more distant from the equator, where it is almost zero (Fig. 1.5) (Sharpe, 1986). Migrant studies suggest moving from high-risk to low-risk areas generally decreases the chance of MS developing, particularly if the migrant is under 15 years of age, strengthening the theory that environmental factors are most important before or around adolescence (Marrie, 2004). Substantial evidence supports a geographical link, including the study of over 5000 World War II veterans, which also suggested racial and environmental factors are involved (Kurtzke *et al.*, 1979). This higher prevalence of MS with increasing latitude has been linked to levels of exposure to ultraviolet-B (UVB) radiation in early life and associated vitamin D production (Fig. 1.5) (Grant, 2006). A latitudinal gradient has also been proposed in the British Isles, as the Orkney and Shetland Islands have a very high prevalence of MS of 309 and 184 per 100,000, respectively, whereas the southerly Channel Islands have a much lower prevalence, of 113 and 87 per 100,000, in the Bailiwicks of Jersey and Guernsey, respectively (Sharpe *et al.*, 1995). A gradient has also been observed within Ireland, with a prevalence of 185 per 100,000 in County Donegal in the north, and 121 per 100,000 in County Wexford in the south (McGuigan *et al.*, 2004). Regional differences can also be attributed to factors other than latitude, however, as variations in genetic predisposition and diagnostic accuracy may play significant roles. Interestingly, seasonal variations of the onset of MS have been identified, with fewer outbreaks being observed in winter months, suggesting wintertime radiation is associated with greater protection (Abella-Corral *et al.*, 2005).

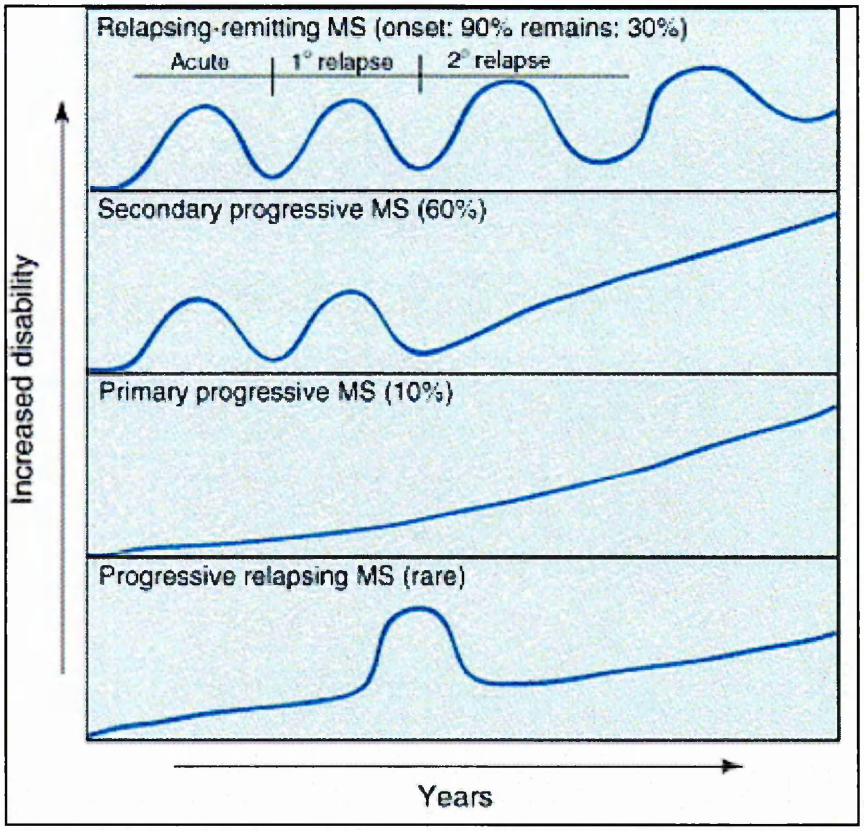

Reprinted from (Podojil and Miller, 2006) © (2006), with permission from Elsevier.

Figure 1.4 Clinical disease courses of multiple sclerosis

Four disease courses of MS have been identified, according to their characteristics and progression over time. Relapsing remitting MS (RRMS) involves periodic attacks followed by full recoveries, and is the most common disease course at onset. Many patients progress from RRMS to secondary progressive MS (SPMS), where fewer attacks are experienced, with incomplete recovery. Primary progressive MS (PPMS) involves a progressive accumulation of disability with no clear relapses or remissions. The rarest disease course is progressive relapsing MS (PRMS), characterised by progression from onset, with distinct relapses, with or without full recovery (Podojil and Miller, 2006).

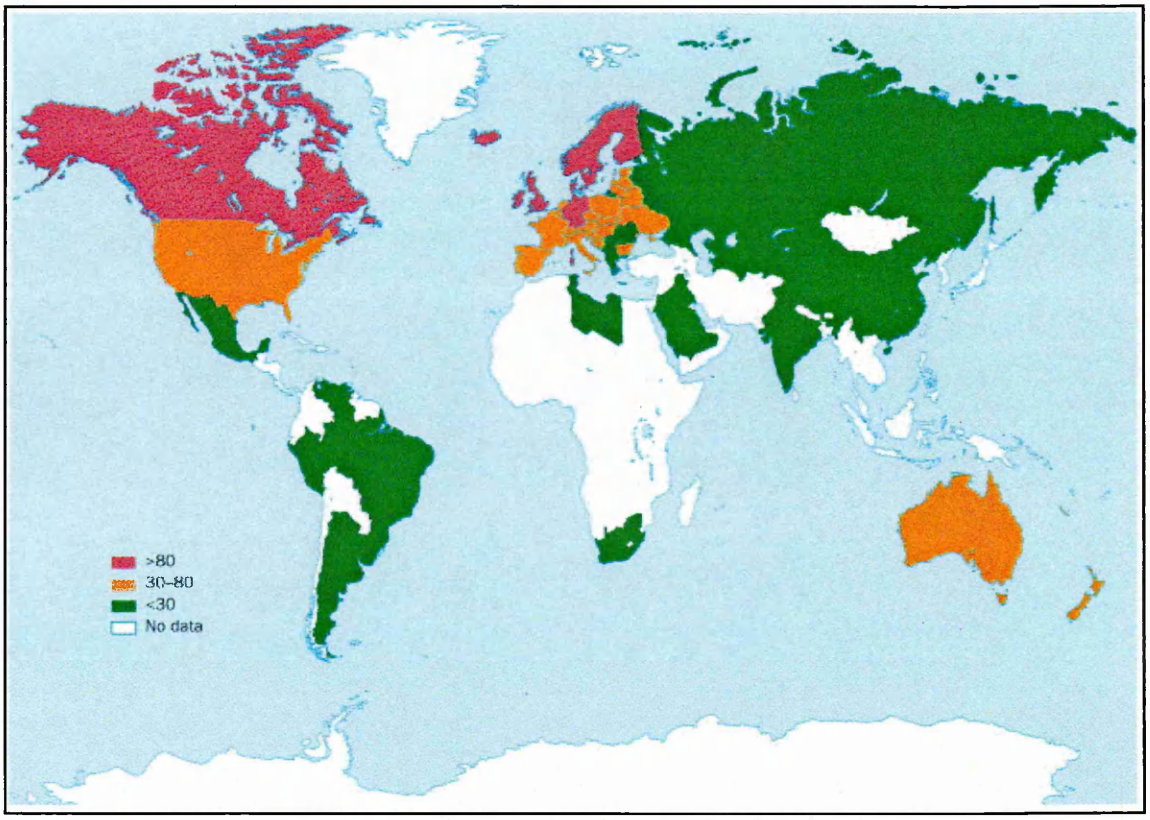

Reprinted from (Marrie, 2004) © (2004), with permission from Elsevier.

Figure 1.5 Geographical variation in prevalence of multiple sclerosis per 100,000 population

The prevalence of MS increases with increasing distance from the equator. Tropical areas, such as Asia and South America, tend to have lower levels (shown in green) of <30 per 100,000, but temperate areas, including northern Europe, northern USA, and Canada, experience a high prevalence of >80 per 100,000 (shown in red). Intermediate levels of MS of 30-80 per 100,000 (shown in orange) are found in southern Europe and the southern USA, for example (Marrie, 2004)

Evidence exists that the symptoms of MS, as well as the risk, are reduced by experiencing higher levels of UVB, and hence, vitamin D (Embry *et al.*, 2000). This protective effect of vitamin D was confirmed in a large longitudinal study of over 90,000 women in the USA which showed that taking vitamin D supplements reduced the life-time risk of MS by 40% (Chaudhuri, 2005). The exact role vitamin D plays is unknown, but it has been suggested that differentiation of oligodendrocytes (OLGs), and their adhesion to axons, is dependent on sufficient vitamin D during development (Chaudhuri, 2005). Vitamin D can reduce inflammatory cytokine production by controlling gene expression, so a deficiency could contribute to the inflammation observed in MS (Mark and Carson, 2006). Higher levels of vitamin D from dietary intake, as found in fish and dairy products, are also associated with a reduced risk of MS (Munger *et al.*, 2004). In addition, lower levels of vitamin D were found in MS patients during relapses, compared to in remission (Soilu-Hanninen *et al.*, 2005).

Clusters of the disease within countries exist, particularly on islands, such as in Sardinia (Sotgiu *et al.*, 2004). Worldwide epidemiological clusters of MS have also been found, for example those which mirror the distribution of the tick-borne bacterial pathogen *Borrelia burgdorferi*, responsible for Lyme disease. Lyme disease can also lead to CNS demyelination (Batinac *et al.*, 2007), and it has been postulated that MS might be prevented or cured by the use of antibiotics against this microorganism, but this is yet to be investigated (Fritzsche, 2005).

1.2.5 Aetiology

The aetiology of MS remains obscure, but is believed to involve exposure to unknown environmental factors in those with a genetic susceptibility (Ristic *et al.*, 2005). The genetic element is thought to result from variants of alleles in several genes, which increase susceptibility in some people, but not others, depending on post-transcriptional regulation and external influences (Baranzini and Oksenberg, 2005). Genes coding for human leukocyte antigen (HLA) class I antigens were first associated with MS in 1972, with HLA class II, T-cell receptor β, *CTLA4, ICAM1,* and *SH2D2A* genes being amongst those that are also thought to contribute (Dyment *et al.*, 2004). The major histocompatibility complex (MHC) region of chromosome 6, and chromosomes 17p11, 3q21-24, 18p11, and 17q22-24 have been identified as potential areas linked to MS. An association between MS and type-I diabetes has also been postulated, based on HLA genetic susceptibility factors (Sotgiu *et al.*, 2004). It is clear, however, that factors other than genetics are involved in the risk of developing MS, as studies of monozygotic twins have shown a concordance of approximately only 30%, and dizygotic twins display approximately 5% concordance (Sadovnick *et al.*, 1993).

Environmental factors implicated in MS aetiology are many and varied. One study has found immigrants from low risk areas coming to the UK do not adopt the high risk seen here (Dean *et al.*, 1976). Other studies have shown people migrating from high risk areas to low risk ones achieve an intermediate risk (Visscher *et al.*, 1977). In the UK, children of immigrants are born with a similar risk to those from non-immigrant parents, demonstrating that environmental factors can act rapidly (Elian *et al.*, 1990).

Other bacterial infections in addition to *Borrelia burgodorferi* have been implicated in MS aetiology. The common respiratory pathogen *Chlamydia pneumoniae* is known to infect ECs, which is thought to assist in the migration of monocytes into the CNS (Stratton and Wheldon, 2006). *C.pneumoniae* is associated with CNS infections, and is also commonly detected in white blood cells. Once cells carrying this bacteria have entered the CNS, they are capable of infecting microglia, astrocytes, and neuronal cells (Ikejima *et al.*, 2006). The incidence of *C.pneumoniae* infection in 155 MS patients, 70 patients with other neurological diseases, and 499 healthy controls, was examined in an attempt to clarify the prevalence of this pathogen in MS patients. Chlamydia infection was found to be more frequent in MS patients than healthy controls, adding further weight to the suggestion that the pathology of some MS cases may be an infectious syndrome triggered or fuelled by such a pathogen (Parratt *et al.*, 2007).

Viral infections have been linked with either the aetiology or progression of MS, including Epstein-Barr virus (EBV), human herpes virus 6 (HHV-6), and multiple sclerosis-associated retrovirus (MSRV) (Sotgiu *et al.*, 2004). Epitopes of viral pathogens exhibiting similar conformations to myelin antigens may invoke an anti-viral immune response that can also result in T and B cells mounting an anti-myelin response in MS; a process known as molecular mimicry (Batinac *et al.*, 2007). No one specific pathogen has been pinpointed as being the molecular mimic in MS, and it is possible that infection with several pathogens is responsible. Furthermore, the diversity of the disease phenotype may be explained by variability in the mechanism of molecular mimicry, i.e. whether HLA class 1 or 2 restricted T-cells, and antibodies, are involved. Induction of MS by molecular mimicry alone is questionable, and it has been suggested that it serves only to prime the immune system via exposure to a molecular mimic of a CNS self-antigen, which is later followed by a non-specific immunological challenge (Libbey *et al.*, 2007).

1.2.6 Pathology

In MS, multiple sharply demarcated lesions, or plaques, of variable size are found randomly distributed within the CNS, predominantly in the white matter, but grey matter

can also be involved. Although the distribution of lesions is random, they are particularly common in areas such as the optic nerve, spinal cord, brainstem and periventricular regions, and they are associated with post-capillary venules and larger veins (Akenami *et al.* 2000). Blood vessels from the edge of large lesions can have lesional projections extending along them, termed 'Dawson's fingers'. New plaques exhibit ongoing inflammation and lipid breakdown as myelin is destroyed, with early acute plaques containing mainly lymphocytes. Chronic, older plaques reveal established gliosis, and fewer inflammatory cells such as lymphocytes and macrophages, but greater numbers of plasma cells than acute lesions (Hickey, 1999).

At the microscopic level, plaques reveal activation of ECs, infiltration of macrophages and lymphocytes, myelin swelling, and a reduction in OLGs. T cells and macrophages are common, whilst plasma cells are not. Chronic active plaques reveal foamy macrophages digesting myelin, and lymphocytes both in perivascular areas and at the advancing edge of myelin loss. Axonal damage can be seen, but typically, axons are preserved in chronic active plaques. Astrocytes in the demyelinated area are reactive. Active demyelination of the frontal white matter is thought to be associated with the fatigue experienced in MS (Lassmann, 1998). Chronic-inactive plaques are thought of as glial scars, where reactive astrocytes demonstrate extensive gliosis, OLGs are severely reduced or absent, myelin loss is clearly marked, and a few macrophages and lymphocytes are seen. Axon loss may be dramatic in older plaques, and is often the cause of persistent neurological disability in MS (Claudio *et al.*, 1995). Bo and colleagues (1994) examined actively demyelinating lesions and reported high levels of MHC class II on microglia and macrophages, but none on astrocytes and ECs. Zeinstra *et al.* (2003), however, reported that astrocytes in active lesions of MS post-mortem brain tissue expressed both MHC class II (induced by IFN-γ) and the B7 co-stimulatory molecules necessary for astrocytes to function as APCs. Cells associated with lesions show changes in size and shape, suggestive of transformation from microglia into phagocytic macrophages that may be involved in demyelination.

Lesions contain not only evidence of injury (involving axonal damage, myelin loss, and apoptotic OLGs), and the presence of immune cells, but molecular components can also be seen, such as Igs, proinflammatory cytokines, chemokines, and adhesion molecules (Hickey, 1999). It is important to consider that the pathology of MS is heterogeneous, with significant variations between patients. This is demonstrated by the occurrence of contrasting events, such as either destruction or proliferation of OLGs (Baranzini and Oksenberg 2005).

1.2.7 Pathogenesis of MS

The pathogenesis of MS is best summarised as damage to axons and destruction of myelin, caused by inflammatory events. Myelin forms a sheath that coats axons, protecting them, and facilitating efficient saltatory conduction of nerve impulses. Axonal loss originates from failure of the myelin-producing OLGs to remyelinate (Compston, 2004). It is well debated as to what initiates the inflammatory reaction that leads to lesion formation, and a full understanding of the pathogenesis still presents a challenge.

There is substantial evidence for an autoimmune pathogenesis. The structure of myelin is in part maintained by MBP, and it is residues 84-102 and 143-168 of MBP that are targets of the T cell response in MS (Ota *et al.*, 1990). High levels of flexibility of T cell receptors (TCRs) on autoreactive cells may assist T cell sensitisation to myelin antigens in the peripheral blood due to molecular mimicry (Fig. 1.6, inset). Myelin-reactive $CD4^+$ T cells are considered critical in triggering autoimmune responses in MS and it has been demonstrated that they have lower activation thresholds, independent of co-stimulation, which may lead to breakdown of self-tolerance and the resultant autoimmune response (Bielekova *et al.*, 2000). Myelin-reactive T cells are present in healthy individuals as well as in MS patients, indicating it is the high frequency of *activated* autoreactive T cells that is significant (Markovic-Plese *et al.* 2004). $CD4^+$ T cells are considered pivotal in initiating inflammation, but neuropathological findings suggest changes in OLGs may also be important in initiation of MS - a 'neurodegenerative' hypothesis (Prat and Antel, 2005). Recent evidence derived from MRI suggests that normal-appearing white matter is also altered in the MS brain, in that MBP suffers a loss of positive charge, rendering it more susceptible to proteolytic attack (Mastronardi and Moscarello, 2005).

It is generally accepted that activated peripheral blood lymphocytes are chemoattracted to the BBB, where upregulation of adhesion molecules on ECs leads to increased binding to their ligands on PBMCs (Prat and Antel, 2005). Interactions of adhesion molecules with PBMCs slow their passage along the blood vessel and facilitate the rolling and adhesion process required for transmigration across ECs. In MS, the BBB is disrupted by proteases, which allows excessive infiltration into the brain parenchyma of T cells, B cells, and macrophages (Fig. 1.6). These immune cells thereby form the perivascular cuffs detected histologically in MS lesions (Markovic-Plese *et al.* 2004). Myelin-reactive T cells are reactivated by neural antigens presented by MHC class II molecules on ECs and microglia, and autoantibody production, demyelination and axonal damage result from the myriad of changes that ensue (Fig. 1.6). Astrocytes are also capable of processing autoantigens and may be involved in antigen presentation

and activation of $CD4^+$ T cells (Soos *et al.*, 1998). Many cellular functions contribute to this pathology, with cytokines, adhesion molecules, chemokines, proteases, complement, NO, and glutamate, all playing a part (Fig. 1.6) (Prat and Antel, 2005). The persistent and recurrent nature of MS may indicate that an expanded immune response has been raised following distribution of neural antigens to lymph nodes, or due to contributions from endogenous cells, such as microglia and astrocytes.

1.2.7.1 Breakdown of the BBB

A key process in the pathogenesis of MS lesions is recruitment of peripheral blood mononuclear cells (PBMCs) across the BBB. Breakdown of the BBB is an initial step in the development of inflammatory demyelinating lesions. This can be demonstrated by the use of gadolinium-diethylenetriamine penta-acetic acid (Gd-DTPA), which acts as an MRI contrast agent, revealing BBB dysfunction (Kraus and Oschmann, 2006). The mechanism of BBB breakdown in MS is not fully known, but is thought to involve both direct inflammatory events and indirect non-inflammatory effects. Soluble mediators, such as the cytokines IFN-γ, TNF, and IL-1β (Minagar *et al.*, 2004), metalloproteinases (Cossins *et al.*, 1997), NO (Hill *et al.*, 2004), and mast-cell-derived histamine (Kruger, 2001), all act as inflammatory mediators in the breakdown of the BBB. In addition, alterations in the microenvironment of the brain ECs, such as loss, or functional alterations, of glial cells, may contribute indirectly to BBB breakdown (Lassmann, 1991).

1.2.7.2 Cell migration into the CNS

Leukocyte infiltration occurs in several disorders of the CNS, including intracerebral haemorrhage (Gong *et al.*, 2000), hyperglycemia following transient ischaemia (Lin *et al.*, 2000) and autoimmune diseases such as MS (Wong *et al.*, 2007). The exact mechanisms involved in cell migration across the BBB have not been fully described, but it is known that endothelial adhesion molecules play a key role (Wong *et al.*, 2007). Movement of cells through the vascular endothelium is preceded by leukocyte tethering, rolling, activation, and firm adhesion. Extravasation follows adhesion, although adherence can occur without migration (Greenwood *et al.*, 2002).

An increase in the permeability of the BBB is an early and pivotal event in the development of CNS inflammatory diseases. Inflammatory cytokines, such as TNF, are thought to contribute to the decreased integrity of the BBB by changing the distribution of junctional proteins (Wong *et al.*, 2004). Without cytokine stimulation of ECs, very few PBMCs are thought to adhere, and the basal expression of cerebral EC adhesion molecules is low (Wong and Dorovini-Zis, 1996). The physical process of migration of inflammatory cells may also increase the permeability of tight junctions.

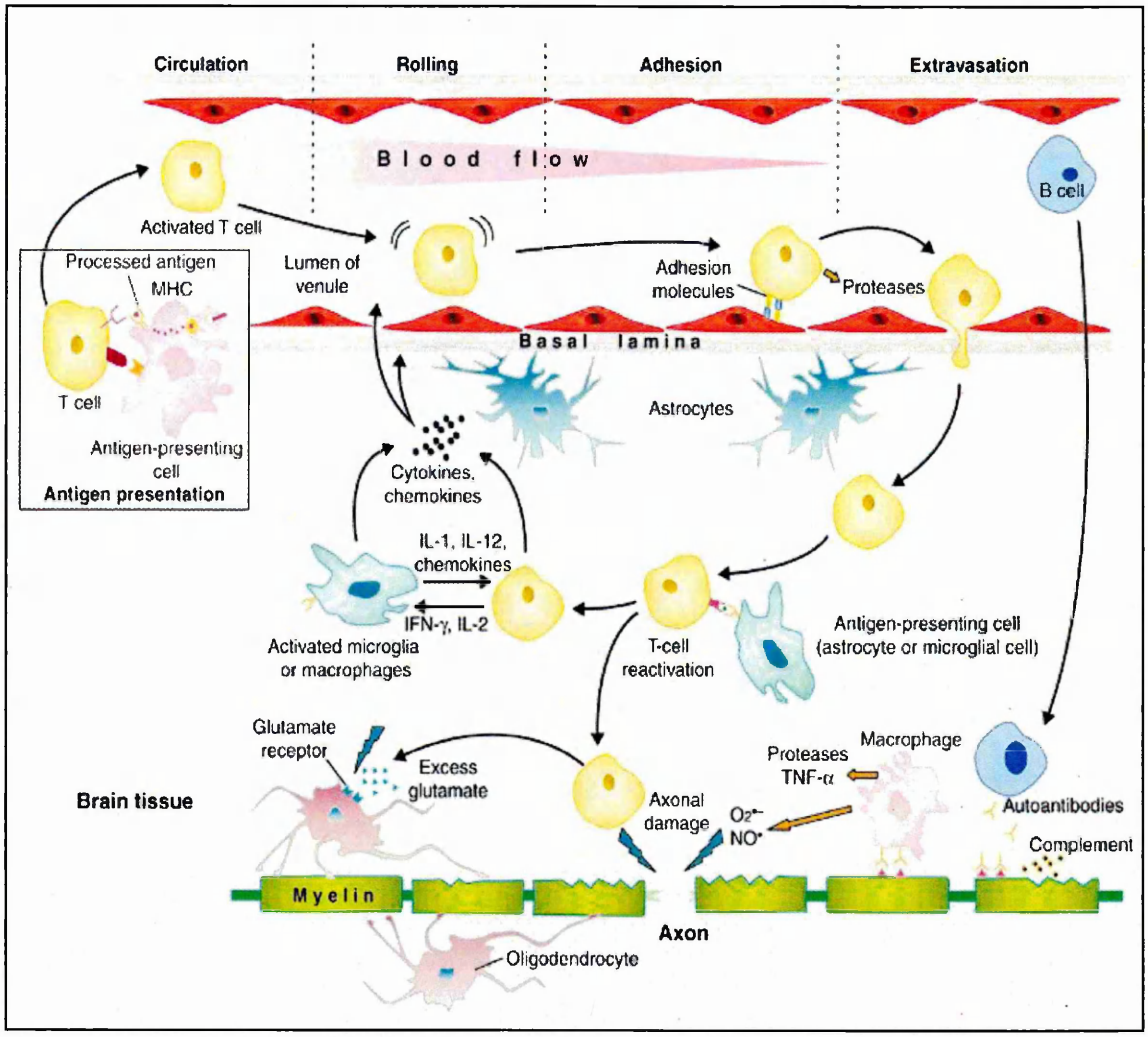

Reprinted from (Markovic-Plese *et al.* 2004) © (2004), with permission from Elsevier.

Figure 1.6 Schematic of cellular events occurring in the pathogenesis of multiple sclerosis

Initiation is thought to involve CD4+ T cells becoming activated in the peripheral blood by peptides which possibly mimic the epitopes of CNS antigens (see inset). Chemoattraction, mediated by chemokines and chemokine receptor interactions, draws the activated cells to the CNS. The increased expression of adhesion molecules and proteases on the T cells leads to their adhesion to, and passage through, the basal lamina of capillaries of the BBB. Once in the brain parenchyma, microglial cells present CNS antigens which activate these T cells further, triggering an inflammatory response involving production of cytokines, chemokines, NO, glutamate, and free radicals. Positive feedback loops maintain the response, which eventually causes damage to myelin, OLGs, and neurons.

For a cell to migrate across the BBB, it must first adhere to the endothelium. PBMCs adhere by extending pseudopodia to the EC surface. Once attached, they arrange themselves so that they are at a contact point between two ECs, where they become flattened and extravasate between them (Wong *et al.*, 2007). Adhesion is possible due to the expression by ECs of the adhesion molecules E-selectin, intercellular adhesion molecule-1 (ICAM-1), and vascular cell adhesion molecule-1 (VCAM-1), which interact with ligands on PBMCs, namely carbohydrate epitopes, leukocyte function antigen-1 (LFA-1), and very late antigen-4 (VLA-4), respectively (Wong *et al.*, 2007). Lymphocyte adhesion to brain ECs utilises VCAM-1 and ICAM-1, and is regulated by chemokines (Quandt and Dorovini-Zis, 2004). Following adhesion, the migration of T cells also involves interactions between ICAM-1 and lymphocyte function-associated antigen-1 (LFA-1) (Laschinger *et al.*, 2002).

1.2.7.3 Inflammation

Once immune cells are in the CNS, antigen presentation is required for the initiation and perpetuation the inflammatory response. Under inflammatory conditions, MHC class II and co-stimulatory molecules (CD80 and CD86), are upregulated on microglia and macrophages, rendering them capable of presenting antigen (Markovic-Plese and McFarland, 2001). Astrocytes are also capable of stimulating memory T cells by presenting antigen in a manner independent of co-stimulation (Cornet *et al.*, 2000).

The exact pathogenic mechanisms are not completely clear, and whether inflammation is the foremost event in MS pathology, or not, remains a source of debate. Some researchers have suggested that levels of tissue degeneration and neuronal injury are independent of the number of actively demyelinating lesions, resulting instead from diffuse inflammation throughout the brain, which is accentuated in lesions (Lassmann, 2003).

There is evidence from MRI studies that extensive axonal damage is present in the early stages of MS, and that relapse severity and the subsequent disability do not always correlate with the inflammatory activity of lesions (Filippi *et al.*, 2003). Lesions without $CD4^+$ T cells or leaked plasma proteins have been found in normal-appearing tissue obtained from early MS cases, suggesting that they occurred prior to disruption of the BBB. These 'pre-demyelinating' lesions have depleted numbers of OLGs and may indicate a pathology involving the presence of an antigen derived from CSF, which is toxic for OLGs and axons, such as a bacterial toxin (Gay, 2006).

The type of inflammation seen in MS may vary depending on the stage of disease. It is

thought that adaptive immune responses are more important in the relapsing-remitting stage, and innate immunity is more prominent in the progressive stage (Vaknin-Dembinsky and Weiner, 2007).

1.2.7.4 Humoral immune response in MS

The humoral immune response was identified as a major contributor to the pathogenesis of MS when research by Kabat *et al.*, approximately 60 years ago, revealed raised levels of Igs in the CSF of over 90% of patients (reviewed in Reindl *et al.*, 2006). OCB can be detected when intrathecal synthesis of IgM is present, and the correlation of this, with disease relapse activity, in MS has proved useful for monitoring purposes. Production of OCB may result from either B cell stimuli leading to increased IgG in the CSF, or from autoantigen immune complexes being triggered by an infectious agent (Sharief and Thompson, 1991).

B cells are important in MS on two counts, and probably play an active role throughout the disease process. Firstly, autoreactive B cells produce autoantibodies (with plasma cells doing this constantly), replicate memory B cells, and secrete cytokines. Secondly, they activate autoreactive T cells by acting as APCs (Nikbin *et al.*, 2007). Ectopic lymphoid structures containing proliferating B cells and plasma cells have been found in the meninges of some patients with SPMS, indicating B cell differentiation can occur in the CNS (Serafini *et al.*, 2004). Cytokines and chemokines most probably drive this homing and proliferation of B cells in secondary lymphoid organs (Corcione *et al.*, 2005). The CSF of MS patients has been found to contain large numbers of B cells with a memory phenotype, compared to peripheral blood, which may contribute to MS pathogenesis, once they have matured into antibody-secreting cells (Cepok *et al.*, 2001).

The complement system comprises nearly 40 soluble proteins and receptors that function as regulators and effectors, with a role in the innate immune system in protecting the host against pathogens (Fujita *et al.*, 2004). In adaptive immune responses, complement is associated with regulation of B and T cells, such as cell activation, signalling and differentiation (Carroll, 2004). The complement system is thought to play both pro-inflammatory and neuroprotective roles in MS pathogenesis (Rus *et al.*, 2006). Complement acts via a cascade that is initiated by either the classical, alternative, or lectin pathways, depending on what factors activate it. The classical and alternative pathways are important in MS, as they are mainly activated by antigen-antibody complexes, and LPS, respectively (Barnum and Szalai, 2006). Activation of all pathways leads to the generation of C3 and C5 convertases. C3 and

C5 cleavage generate the anaphylatoxins C3a and C5a, with C5a having chemotactic properties. C3a and C5a contribute to CNS inflammation by attracting and activating leukocytes. C5b initiates assembly of the C5b-9 membrane attack complex (MAC), which forms pores and lyses cells, and is implicated in demyelination (Ramm *et al.*, 1985). Lysis of OLGs and neurons by the MAC is thought to be responsible for complement-mediated demyelination (Barnum and Szalai, 2006). Myelin prepared from CNS tissue has been shown to activate C1 and is vulnerable to attack from C5b-9 (Vanguri and Shin, 1986).

Complement can be neuroprotective, as C5a can protect against glutamate-induced neurotoxicity (Osaka *et al.*, 1999), and C3a can protect against neuronal cell death normally induced by the excitotoxin N-methyl-D-aspartic acid (NMDA) (van Beek *et al.*, 2001). C3a and C5a have also been shown to induce nerve growth factor (NGF) mRNA expression in astrocytes, suggesting a role for them in neuronal survival (Jauneau *et al.*, 2006).

1.3 Chemokines

Chemokines derive their name from *chemo*attractant cyto*kines*, and are low molecular weight proteins (8-14 kDa), with chemotactic properties that attract immune cells to sites of inflammation, such as is seen in MS pathogenesis. They were highly conserved during evolution, and are present in many vertebrates, assisting in directing immune responses when the host is threatened by pathogens. An increasing number of chemokine functions are emerging, such as having roles in immune surveillance, angiogenesis, apoptosis, cell adhesion, haematopoiesis, and growth regulation (Cartier *et al.*, 2005). Chemokines act by binding to cell surface G protein-coupled receptors (GPCRs) expressed on many immune cell types. The N-terminus of chemokines is paramount in this receptor binding and in their activation (Forssmann *et al.*, 2004). Their activity is tightly controlled by many factors, including receptor expression and chemokine processing. Situations can arise, however, where chemokines aid the destruction of healthy cells, such as neurons in MS, for example. Chemokines are implicated in the pathogenesis of various diseases, such as asthma and AIDS, and along with their receptors, have sparked the interest of pharmaceutical companies as therapeutic targets (Ribeiro and Horuk, 2005).

1.3.1 Classification and structure of chemokines

In excess of forty chemokines have been identified, which have been characterised into four groups according to the position of the conserved cysteine residues, i.e. CXC (α),

CC (β), C (γ), and CX3C (δ), with X representing an adjacent amino acid (Fig. 1.7(i)). Chemokines from each subfamily contain four conserved cysteines, except for the C family, which only have two (equivalent to the second and fourth cysteines of the other groups). The CXC and CC families are the most common, whilst there are only two C chemokines, and one CX3C chemokine (fractalkine) (Thorpe, 2003).

Chemokine nomenclature was confusing, as several systems were used and many were named according to function, with frequent overlap. They are now named according to the structural subfamily they belong to, followed by "L" for ligand, and then a number that designates the encoding gene - CCL2, for example, previously known as monocyte chemoattractant protein-1 (MCP-1) (Fig. 1.8) (Proudfoot 2002).

A subdivision of CXC chemokines also exists, namely the ELR-CXC chemokines, which possess an amino acid motif of glutamic acid-leucine-arginine (ELR) at the N-terminus. CXCL1 and CXCL8 are examples of ELR chemokines, which are generally strong neutrophil attractants. Non-ELR chemokines, such as CXCL10 and CXCL12, predominantly attract lymphocytes. CC chemokines (e.g. CCL5) predominantly attract monocytes, basophils, eosinophils, and T-cells. The C chemokine, XCL1, is a chemoattractant for T-cells and NK cells (Hedrick *et al.*, 1997). CX3CL1, also known as fractalkine, attracts monocytes and T-cells, and is unique amongst chemokines by being present in both membrane-bound and soluble forms (Bazan *et al.*, 1997).

Observed three-dimensionally, chemokines exhibit the first two cysteines near the N-terminus, followed by an area known as the N-loop, three anti-parallel β-strands which are interspersed with turns called 30s, 40s, and 50s loops, and then the C-terminal α-helix. The third and fourth cysteines (if present) are found in the 30s and 50s loops (Fernandez and Lolis, 2002). The α-helix lies across the β sheet and is involved in the biological activity of chemokines (Fig. 1.7(ii)) (Clore *et al.*, 1990).

Classification according to function characterises chemokines as either inflammatory or homeostatic. Inflammatory chemokines are expressed in response to pathogenic stimulation or proinflammatory cytokines, and serve to recruit monocytes, granulocytes, and T cells to inflammatory sites. Homeostatic chemokines are generally expressed constitutively within secondary lymphoid organs and are involved in immune surveillance by cells of the adaptive immune system (Cartier *et al.*, 2005).

Figure 1.7 Structure of chemokines

(i) Chemokines are grouped according to their structure, dependent on the arrangement of the first two cysteine (shown as 'C') residues. Intervening amino acids are represented with an 'X'. The four groups (C, CC, CXC, and CX3C) all contain disulphide bonds important to their tertiary structure, which typically join the first to third, and the second to fourth cysteine residues. CCL2 is an example of a CC chemokine, with two adjacent cysteines near the N-terminus.

(ii) 3-D schematic of the CXC chemokine CXCL10, demonstrating characteristic features of the chemokine family. The N-terminus connects to three strands of the β-sheet (in blue), stabilised by two pairs of conserved cysteines (9:36 and 11:53), the 30s and 40s loops, and the C-terminal α-helix (in yellow). The corresponding amino acid sequence is colour-coded to indicate secondary structure elements related to the schematic (Fernandez and Lolis, 2002).

(i) The four chemokine classes

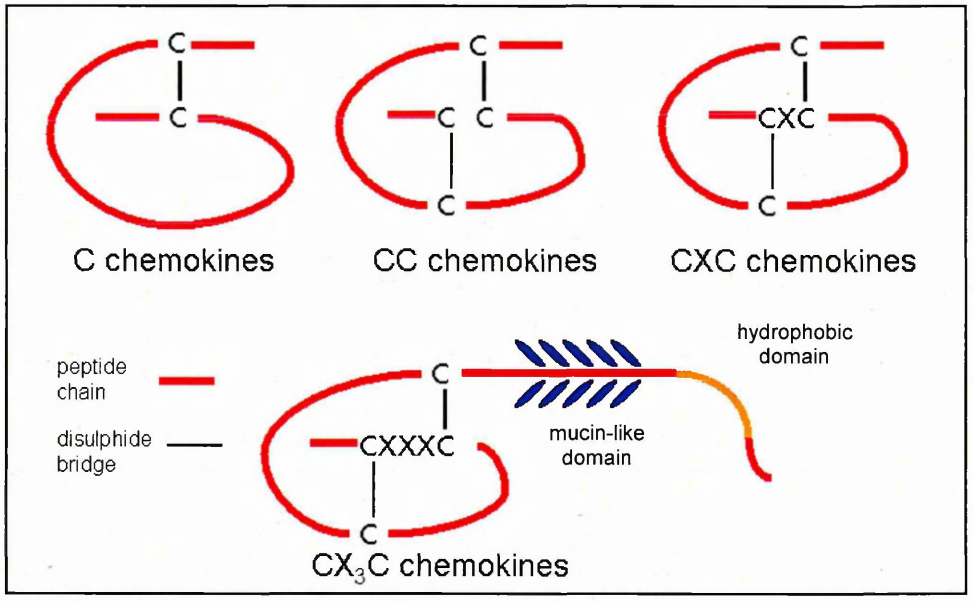

Image source: http://en.wikipedia.org/w/index.php?title=Chemotaxis&oldid=196092071

(ii) Three-dimensional structure of CXCL10

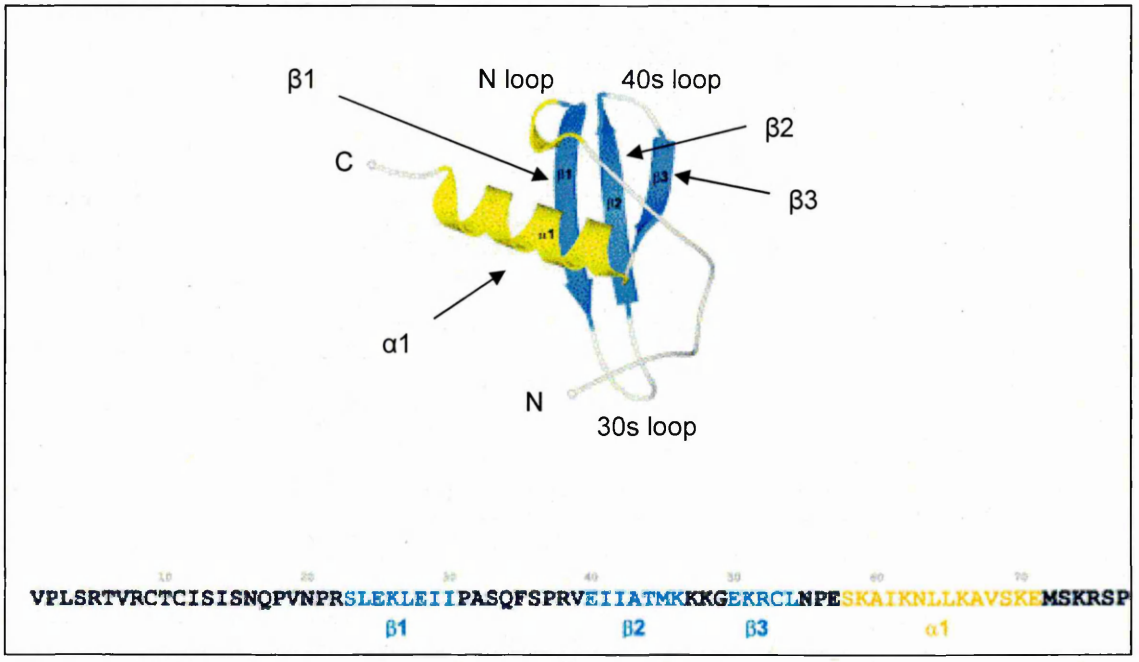

Adapted from (Swaminathan *et al.*, 2003), © (2003), with permission from Elsevier.

1.3.2 Chemokine receptors

Chemokines bind to GPCRs, which belong to the extensive family of seven-transmembrane domain receptors that transmit intracellular signals via heterotrimeric guanosine triphosphate (GTP)-binding proteins. Once a chemokine has bound to its receptor, the G protein heterotrimer dissociates into the α and βγ subunits, and several cascades of intracellular events occur. Effects of these signalling pathways include mobilisation of intracellular calcium, activation of chemotaxis and other functions in leukocytes, such as degranulation, phagocytosis and an increase in the respiratory burst (Cartier *et al.*, 2005).

Chemokine receptors have been named according to the chemokine class that activates them, followed by "R" for receptor, and then a number assigned according to their chronological identification – CXCR1, for example. The majority of the 19 receptors characterised so far belong to the CC family (Fig. 1.8) (Proudfoot 2002). Each chemokine receptor family shows approximately 50% sequence homology amongst their members. Structural similarities exist for all chemokine receptors, such as the polypeptide chain being approximately 350 amino acids long, with a relatively short and acidic N-terminal domain containing cysteine residues, and an intracellular C-terminal domain containing serine and threonine residues that are phosphorylated on receptor activation. Redundancy exists in the chemokine receptor system, in that chemokines can activate more than one receptor, and receptors can respond to several different chemokines (Fig. 1.8). Homeostatic chemokines tend to be more specific in their interactions, e.g. CXCL12 binds exclusively to CXCR4 (Cartier *et al.*, 2005).

Chemokine receptor expression is controlled by basal levels of transcription, and can be increased by calcium levels, cyclic AMP, cytokines such as IL-2, IL-4, IL-7, IL-10, transforming growth factor-1β (TGF-β1) (Jourdan *et al.*, 2000), and growth factors such as basic fibroblast growth factor (bFGF), vascular endothelial growth factor (VEGF) (Salcedo *et al.*, 1999), and epidermal growth factor (Phillips *et al.*, 2005). Conversely, inflammatory cytokines, such as TNF, IFN-γ, and IL-1β, can reduce chemokine receptor transcription (Gupta *et al.*, 1998). CCR2 expression by monocytes is rapidly inhibited by IFN-γ, rendering the cells less responsive to chemokines, and perhaps serving to retain monocytes at inflammatory sites and engage in feedback in regulating cell recruitment from blood (Penton-Rol *et al.*, 1998). Inflammatory cytokines can first induce chemokine expression, and later on, suppress chemokine receptor expression, which would help to end an acute inflammatory response, such as during wound healing (Devalaraja and Richmond, 1999).

Figure 1.8 Chemokine receptors and their ligands

Chemokines are categorised according to the spacing of the N-terminal cysteine residues. Receptors for the CXC subclass are shown in blue; the CC subclass in red; and minor subclasses C and CX3C in green, all paired to their chemokine ligands. The common names for chemokines derive from their function, or from the cell type that produced them, but have been replaced with a simpler, systematic system. Note receptors can have multiple ligands, and chemokines can bind to several receptors.

Abbreviations: ***BCA-1****, B-cell-attracting chemokine 1;* ***CTACK****, cutaneous T-cell-attracting chemokine;* ***ELC****, Epstein–Barr-virus-induced gene 1 ligand chemokine;* ***ENA78****, epithelial-cell-derived neutrophil-activating peptide 78;* ***GCP-2****, granulocyte chemotactic protein 2;* ***Gro****, growth-regulated oncogene;* ***IL-8****, interleukin 8;* ***IP-10****, interferon-inducible protein 10;* ***I-TAC****, interferon-inducible T-cell α-chemoattractant;* ***MCP****, monocyte chemoattractant protein;* ***MDC****, macrophage-derived chemokine;* ***MEC****, mucosae-associated epithelial chemokine;* ***MIG****, monokine induced by interferon-γ;* ***MIP****, macrophage inflammatory protein;* ***NAP-2****, neutrophil-activating peptide 2;* ***RANTES****, regulated on activation, normal T-cell expressed and secreted;* ***SDF-1****, stromal-cell-derived factor 1;* ***SLC****, secondary lymphoid-tissue chemokine;* ***TARC****, thymus and activation-regulated chemokine;* ***TECK****, thymus-expressed chemokine.*

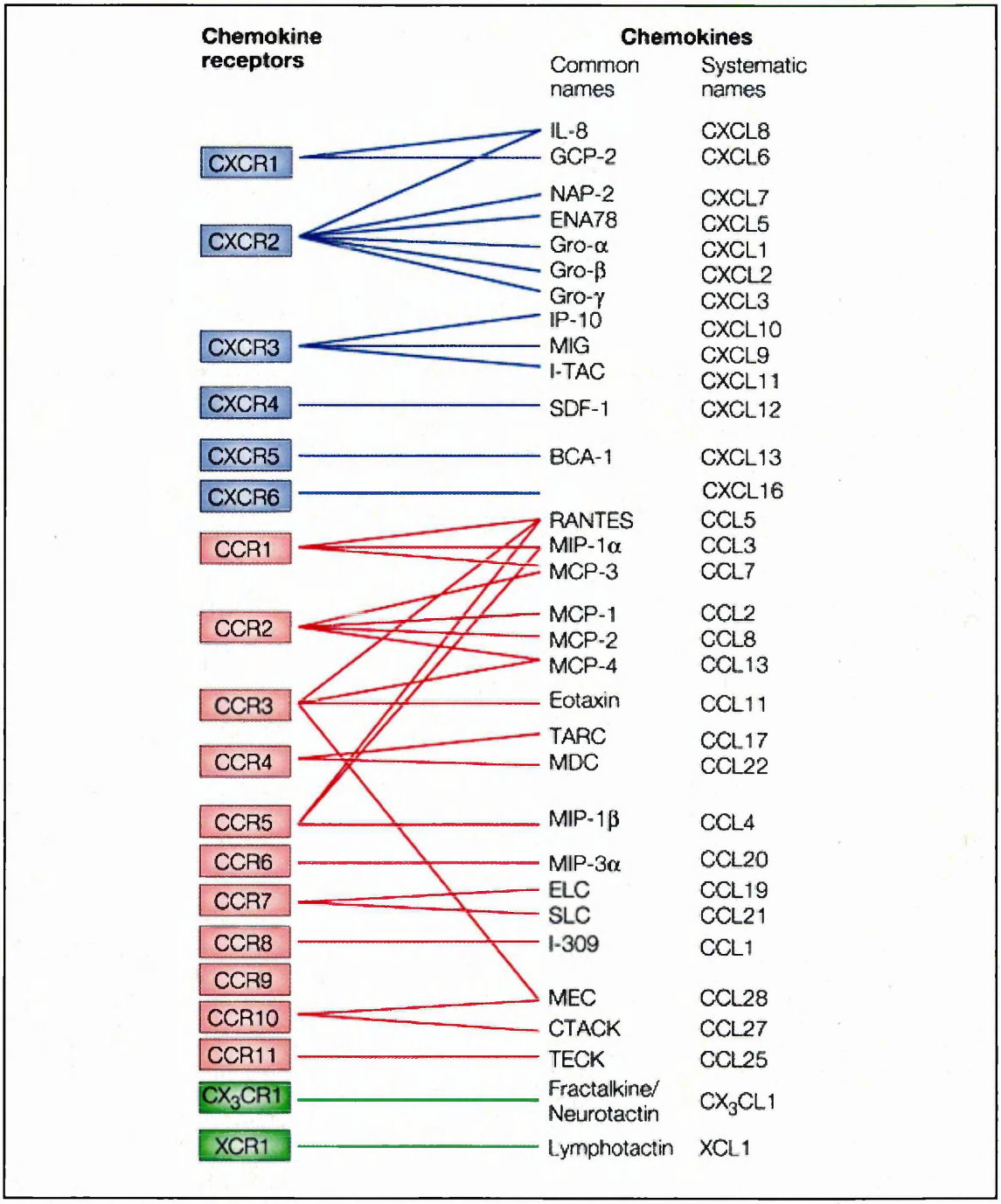

Reprinted by permission from Macmillan Publishers Ltd: Nature Reviews Immunology (Proudfoot, 2002), © (2002)

1.3.3 Chemokine – chemokine receptor interaction

Amino acid residues of chemokines interact with the N-terminal residues of receptors. It is thought that this results in a conformational change of the receptor that exposes a binding pocket and allows interactions of this with specific chemokine amino acids. Proteases released during inflammatory responses can alter chemokine activity by cleaving residues important in this interaction (Huang *et al.*, 2003).

Many chemokines form dimers. The organisation of dimers varies according to the structural class of chemokine. Dimers of CC chemokines tend to be elongated and involve the N-termini but no contact of the C-termini, whereas CXC dimers are compact and have critical interactions of the C-termini of the monomeric subunits. The ability to form dimers has been shown to be vital for the activity of some chemokines *in vivo*, but not *in vitro* (Proudfoot *et al.*, 2003).

Chemokines can also interact with glycosaminoglycans (GAGs), such as heparin sulphate. This may facilitate gradient formation *in vivo*, by immobilising chemokines, and it may also induce oligomerisation of chemokines (Hoogewerf *et al.*, 1997). High concentrations of chemokine also promote oligomerisation, which may then encourage receptor oligomerisation and enhanced function (Fernandez and Lolis, 2002). Dimers are likely to be involved in binding cell surface sugars, thereby facilitating chemokine localisation prior to receptor binding (Proudfoot *et al.*, 2003).

1.3.4 Chemokine signalling

Once a chemokine has bound to its cell surface receptor, cytoskeletal rearrangements can occur, along with regulation of adhesion (dependent on integrin), and binding or detachment of cells via extensions and retractions of pseudopodia. This enables co-ordinated, directional migration (Curnock *et al.*, 2002). The precise mechanics of a cell's response to a chemotactic gradient is yet to be clarified, but most chemokines activate G-protein sensitive phospholipase C (PLC) isoforms, which generates IP3 and results in elevated intracellular calcium. Chemotaxis has been observed without detection of calcium mobilisation, suggesting other mechanisms can be employed (Turner *et al.*, 1995). In addition to calcium influx, kinase activation is also associated with chemokine receptor engagement (Davis *et al.*, 2003). Chemokines can activate multiple signalling pathways that regulate cell growth and transcriptional activation, in addition to migration. This is achieved by chemokine inhibition or activation of various signalling molecules, such as inhibition of adenylate cyclase, activation of mitogen/extracellular signal-regulated kinase (MEK)-1 and/or extracellular signal-

regulated kinase (ERK)-1/2, upregulation of nuclear factor-kappa B (NF-κB), and signal transducer and activator of transcription (STAT)1 and STAT3 transcriptional activity (Curnock *et al.*, 2002).

GPCRs are known to form homo- and heterodimers (e.g. CXCR4 with CCR2 and CD4) although the functional consequences of this have not been fully elucidated (Angers *et al.*, 2002). It has been suggested that homodimerisation might be necessary in G-protein independent activation of JAK/STAT, for example, and heterodimerisation could facilitate additional receptor regulation. Receptors may homodimerise when prompted by their ligands, or in their absence, and enhance the receptor response to the ligand (Busillo and Benovic, 2007). Specialised microdomains of the plasma membrane called lipid rafts, enriched in sphingolipids and cholesterol, have also been implicated in enhancing the response of some receptors to chemokines (Wysoczynski *et al.*, 2005).

Chemokine receptor desensitisation via continued chemokine stimulation is well documented, and leukocytes exposed to chemokines rapidly become unresponsive to repeated stimulation (Baggiolini *et al.*, 1994). Desensitisation is linked to phosphorylation of serine residues in the C-terminal region of the receptor, and is a process which could regulate migration along a chemotactic gradient (Giannini *et al.*, 1995). GPCR signalling can also be regulated via internalisation of the receptor (following phosphorylation induced by ligand activation), recycling of the GPCR back to the plasma membrane, and degradation via lysosomes (Marchese *et al.*, 2003).

1.3.5 Chemokines and receptor expression in normal CNS and diseased states

Constitutive chemokine expression in the CNS principally involves CX3CL1 by neurons and CXCL12 by astrocytes, but evidence is mounting that many others are upregulated in various diseased states. Several chemokine receptors have also been detected in the CNS by immunohistochemistry, including CCR1 through to CCR6, all members of the CXCR family, and CX3CR1. Most of these receptors were detected in diseased CNS tissue, but CCR2, CCR3, CCR5, CXCR2, CXCR3, and CXCR4 have been reported as constitutively expressed in healthy human adult brain (Cartier *et al.* 2005). It is thought that chemokines and their receptors are expressed in healthy CNS tissue to influence the migration of neurons and their progenitors, to contribute to glial cell proliferation during development, and to modulate synaptic activity. During neurological diseases, such as MS and Alzheimer's disease, the presence of these chemokines and their receptors becomes closely linked with the pathogenesis.

Chemokine receptors are not only expressed by leukocytes, but also by microglia, astrocytes, oligodendrocytes, and neurons in the CNS, and there is increasing evidence that they are involved in neuronal death (Cartier *et al.*, 2005).

1.3.6 Chemokines in MS

In MS, chemokines are key targets for further investigation, as they contribute to inflammation and destruction by attracting T cells and macrophages to the CNS, and may be involved in communication between inflammatory cells and neurons (Cartier *et al.*, 2005). Chemokines also act to increase expression of adhesion molecules and activate recruited and resident cells of the CNS (Haringman *et al.*, 2004). Studies using detection by immunohistochemistry have revealed elevated levels of CCL2, CCL8, and CCL7 in acute and chronic MS lesions compared to no immunoreactivity in normal controls (Mc Manus *et al.*, 1998; Van Der Voorn *et al.*, 1999). These chemokines were detected on astrocytes and inflammatory cells, linked to areas where inflammation was evident, indicating a role in the pathogenesis of MS. In post-mortem brain tissue, CCL2, CCL3, CCL4, and CCL5 have been detected in actively demyelinating inflammatory plaques (Simpson *et al.*, 1998). Elevated chemokine levels tended to be linked with specific cells, with CCL2 associated with astrocytes and macrophages.

Chemokines need to engage with their receptors for chemotaxis to occur. Chemokine receptors CCR1, CCR2, CCR3, and CCR5 have been detected on macrophages and microglia within chronic active lesions containing the corresponding chemokine ligands (Fig. 1.8) (Simpson *et al.*, 2000a). Detection of CCR2 is of particular interest to this study, given it is the receptor for CCL2. Similarly, T cells and astrocytes within lesions express CXCR3, the receptor for CXCL10 (Cartier *et al.*, 2005).

In addition to these four receptors, CCR8 has been found on activated microglia and phagocytic macrophages in actively demyelinating lesions (Trebst *et al.*, 2003). A further discovery involved detection of the receptor CXCR3 on T cells and astrocytes within active lesions, together with its ligands CXCL10 and CXCL9, located on macrophages in the plaque, and astrocytes in the parenchyma (Simpson *et al.*, 2000b). Expression of chemokines and their receptors on cells in the CSF of MS patients has also been scrutinised, as there is growing evidence that increased CSF chemokine and receptor levels are associated with neurological dysfunction and relapses (Bartosik-Psujek and Stelmasiak, 2005). CXCL9, CXCL10, and CCL5 have been found to be consistently elevated in the CSF of MS patients, together with an increase in T cells in the CSF, bearing the corresponding receptors CXCR3 and CCR5 (Teleshova *et al.*, 2002). The CSF from MS patients suffering an acute relapse was analysed, and increased levels of CCL3 were found, along with decreased CCL2 levels (Miyagishi *et*

al., 1995). Decreased levels of CCL2 in the CSF of relapsing MS patients was also found in a different study, along with a rise in CXCL8 and CCL5 (Bartosik-Psujek and Stelmasiak, 2005). It has been suggested that this decrease in CCL2 observed in CSF occurs because large numbers of migrating cells are consuming CCL2 during lesion formation (Mahad *et al.*, 2006). It is also possible that CCL2 is being sequestered by astrocytes and microglia due to receptor internalisation, resulting in high levels in lesions, but with limited secretion destined for the CSF. Increased CXCL10 (correlating with CXCR3 expression on CSF $CD4^+$ cells) and decreased CCL2 concentrations in the CSF have been associated with relapses (Mahad *et al.*, 2002). Studies on post-mortem brain tissue, however, show a population of astrocytes and microglia in MS lesions with significantly increased expression of CCL2 (Van Der Voorn *et al.* 1999; Simpson *et al.*, 2000a). A study using blood and CSF from MS patients found little evidence that CCL2 and CCR2 were of much significance in the early active form of the disease (Sorensen *et al.*, 2004).

1.3.6.1 Chemokines in EAE

Studies on chemokine expression pertinent to MS have also used the animal model, experimental autoimmune encephalomyelitis (EAE). EAE is a $CD4^+$ T cell-mediated, inflammatory demyelinating condition, induced by immunisation with PLP, MBP, or MOG, or by transfer of CNS antigen-specific autoreactive T cells (Kuerten and Angelov, 2008). In EAE: CCL3 production has been found to correlate with increasing disease severity; CCL2 was observed late, in acute disease, correlated with relapses and anti-CCL2 treatment during relapsing EAE reduced CNS macrophage accumulation; and CCL5 was observed throughout, with seemingly little importance to the disease course (Kennedy et al., 1998). CCL2 and CCR2 (-/-) knockout mice are resistant to EAE and show significantly reduced CNS mononuclear infiltration (Mahad and Ransohoff, 2003). Levels of CXCL10 have been linked to relapses in mice with EAE (Fife *et al.*, 2001).

1.4 Matrix metalloproteinases (MMPs)

Matrix metalloproteinases (MMPs), or matrixins, comprise a growing family of endopeptidases that contain zinc and are capable of degrading extracellular matrix (ECM) components such as collagens, proteoglycans, elastin, laminin, and fibronectin (Table 1.1). Many other MMP substrates have been identified, such as proteinases and their inhibitors, growth factors, cell surface receptors, adhesion molecules, clotting factors, and chemokines (Szabo *et al.*, 2004). MMPs are synthesised as preproenzymes and predominantly secreted from cells as proenzymes, which are

activated in the extracellular compartment, by MMPs, or proteases of the serine family, such as plasmin. Proteolytic activity involving hydrolysis of the internal bonds of their protein substrates can then begin, if a neutral pH and calcium ions are available. These enzymes play important roles in both normal physiological processes and in pathological events (Gingras *et al.*, 2000).

1.4.1 Classification of MMPs

In excess of 25 MMPs have been described to date (Table 1.1), which originate from different genes but show significant homology due to their domain structure (Fig. 1.9). Certain domains characterise the substrate affinities that categorises MMPs into subgroups. The four main groups of MMPs based on substrate specificity are gelatinases, collagenases, stromelysins, and membrane-type (MT) (Table 1.1). Most MMPs are secreted, apart from MT-MMPs, which are anchored to the membrane via their unique C-terminal sequence (Liu and Rosenberg, 2005).

1.4.2 Structure of MMPs

Differences or similarities in the structure of MMPs facilitate additional classification, as members of each group have distinguishing conserved domains. The propeptide and N-terminal catalytic domains are shared by many MMPs, and it is the C-terminus haemopexin-like domains, fibronectin-like repeats, and transmembrane domains that correspond to the four main substrate-specific groups (Yong *et al.*, 1998). A pre-domain effectively labels the MMP for secretion and is absent in the latent enzyme form. Inactive MMPs possess a pro-domain, or N-terminal domain (Borkakoti, 1998). The "metallo" in their name derives from the two zinc ions in their core domain, one of which contributes to the catalytic activity of the enzyme. The zinc-binding site is a conserved sequence of the catalytic domain (Baramova and Foidart, 1995). At the C-terminus of all MMPs except matrilysin, a haemopexin domain is found, which is a haem-binding peptide involved in substrate specificity. Gelatinases have an additional domain, namely the fibronectin domain, responsible for collagen-binding (Fig.1.9) (Matrisian, 1992).

1.4.3 Activation of MMPs

MMPs can be activated in a number of ways, such as by organomercurial compounds, but endogenous activation must be tightly controlled given their potential for protein destruction (Leppert *et al.*, 2001).

Table 1.1 Matrix metalloproteinase (MMP) nomenclature & substrates

Group	Number	Trivial name	Main physiological substrates
Collagenases	MMP-1	Interstitial/fibroblast collagenase	Interstitial (=fibrillar) collagens,
	MMP-8	Neutrophil collagenase/collagenase-2	(Types I, II, III, VI, X)
	MMP-13	Collagenase-3	
	MMP-18[c]	Collagenase-4	?
Gelatinases	MMP-2	72 kDa-gelatinase/gelatinase A	Basement membrane (=non-fibrillar)
	MMP-9	92 kDa-gelatinase/gelatinase B	Collagens (types IV, V) FN[b]
Stromelysins	MMP-3	Stromelysin-1/transin	FN, LN, various collagens
	MMP-10	Stromelysin-2/transin-2	Other MMPs (?)
	MMP-11	Stromelysin-3	α-1-Protease inhibitor
Membrane-type MMPs	MMP-14	MT1-MMP	Pro-MMP-2
	MMP-15	MT2-MMP	Pro-MMP-2
	MMP-16	MT3-MMP	Pro-MMP-2
	MMP-17	MT4-MMP	Pro-MMP-2
	MMP-24	MT5-MMP	Pro-MMP-2
	MMP-25	MT6-MMP, leukolysin	?
Matrilysins	MMP-7	Matrilysin/pump	FN, LN, vitronectin
	MMP-26	Matrilysin-2	Collagen IV, FN, FG, pro-MMP-9
Other MMPs	MMP-12	Metalloelastase/macrophage elastase	Elastin
	MMP-19	(Initially called MMP-18 [8])	Collagen IV, LN, NG, TC, FN
	MMP-20	Enamelysin	Amelogenin
	MMP-23[d]	Femalysin	?
	MMP-27	–	Collagen I, gelatin, casein
	MMP-28	Epilysin	Casein

Reprinted from (Leppert *et al.* 2001) © (2001), with permission from Elsevier.

MMPs have descriptive names that often refer to their substrates, as well as an MMP number. Those named MMP-4, -5, and -6 were eliminated once it was discovered they were already described. Substrate preference and domain content have been used to categorise MMPs into groups such as gelatinases, stromelysins, collagenases, and membrane-type (MT)-MMPs.

NB: MMP18 is found in Xenopus and not humans; MMP23 is identical to the obsolete MMP21 and MMP22

Abbreviations: ***FN****, fibronectin;* ***LN****, laminin;* ***FG****, fibrinogen;* ***NG****, nidogen;* ***TC****, tenascin C*

The catalytic domain of MMPs contains an active site with a zinc ion bound to three conserved histidines. The N-terminal propeptide sequence has a cysteine residue that chelates the zinc ion in the catalytic site, thereby keeping the enzyme in its latent proform (Fig. 1.9). Intermediate activation of MMPs is achieved by conformational changes that disrupt the cysteine-zinc binding, exposing the catalytic site. Full activation requires ensuing autocatalytic cleavage of the propeptide from the core protein, a process known as the cysteine switch, which results in a decrease in mass of the enzyme. Once activated, MMPs can act synergistically by activating other MMPs (Fu et al., 2001).

Stimulating a coculture of astrocytes and microglia with LPS has been shown to produce active MMP-2 and -9 (Liu and Rosenberg, 2005), which are dependent on interactions with the plasmin/plasminogen system, with plasmin being involved in the activation of proMMP-9 (Lijnen *et al.*, 1998). The activation mechanism of MMP-2 is more complicated than for MMP-9, as MT-MMP and the endogenous MMP inhibitor, tissue inhibitor of metalloproteinase-2 (TIMP2), form a trimolecular complex with proMMP-2, producing the active form close to the cell surface (Sato *et al.*, 1996). This MT-MMP/MMP-2/TIMP2 complex is often used by cancer cells during metastasis and is also important in ischaemic injury (Liu and Rosenberg, 2005).

1.4.4 Function and expression of MMPs

MMPs facilitate cell migration and tissue remodelling by degradation of the ECM during both normal and pathological processes. Tissue alterations during menstruation, morphogenesis, growth, and wound repair are some examples of the many processes that involve MMPs (Page-McCaw *et al.*, 2007). In the CNS, MMPs facilitate beneficial activities such as angiogenesis, myelinogenesis, axonal growth, and migration of neuronal precursors (Yong *et al.*, 2001). The function of MMPs is controlled by regulation of their gene expression and translation, inhibition by TIMPs, and secretion of them as inactive forms that require activation (Opdenakker *et al.*, 2001).
MMPs can be expressed constitutively at a certain level in most cell types, but the majority are induced and tissue-specific (Agapova *et al.*, 2001). ECs, leukocytes, tumour cells, astrocytes, and trophoblasts are all examples of cells that express MMP2 constitutively, and MMP9 is found in large amounts in neutrophils (Rooprai and McCormick, 1997). All types of brain cells produce MMPs, with each cell type having an MMP profile associated with it. MMPs can either be secreted into the ECM or expressed as a plasma membrane bound form. MMPs are not stored for future use, with their secretion being stimulated when needed by multiple factors (Nagase, 1997).

Figure 1.9 Structure of MMPs

(i) All MMPs share three domain structures in common: a pre-domain which assists in extracellular secretion; a pro-domain which preserves the MMP in an inactive state and must be removed for activation; and a catalytic domain containing the proteolytically active zinc ion chelated by three histidine residues. Most MMPs have a haemopexin domain, involved in substrate and inhibitor binding. Other possible domains include the: furin domain which provides an alternative cleavage site for activation; fibronectin and type V collagen (col V) domains involved in substrate recognition; transmembrane domain, which provides a region for transmembrane localisation.

(ii) The crystal structure of recombinant MMP2 (a) is shown alongside a hypothetical 3-D model of intact MMP9 (b). The 3 fibronectin repeats are shown in blue and the Zn^{2+} ions as white spheres. MMP9 has several glycosylation sites, and a collagen V-like spacer, lacked by MMP2. MMP9 is the most complex MMP identified to date.

(i) Schematic of domain structure

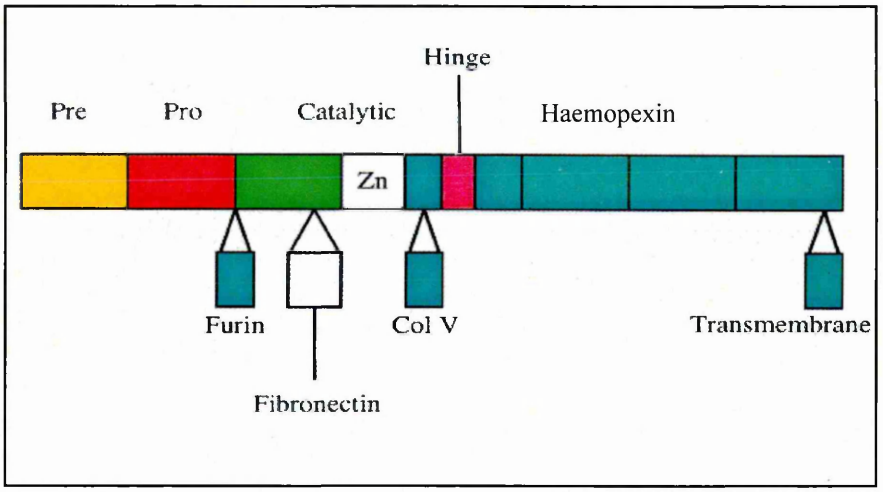

Reprinted from (Leppert *et al.* 2001) © (2001), with permission from Elsevier.

(ii) 3-D structures of (a) MMP2 and (b) MMP9

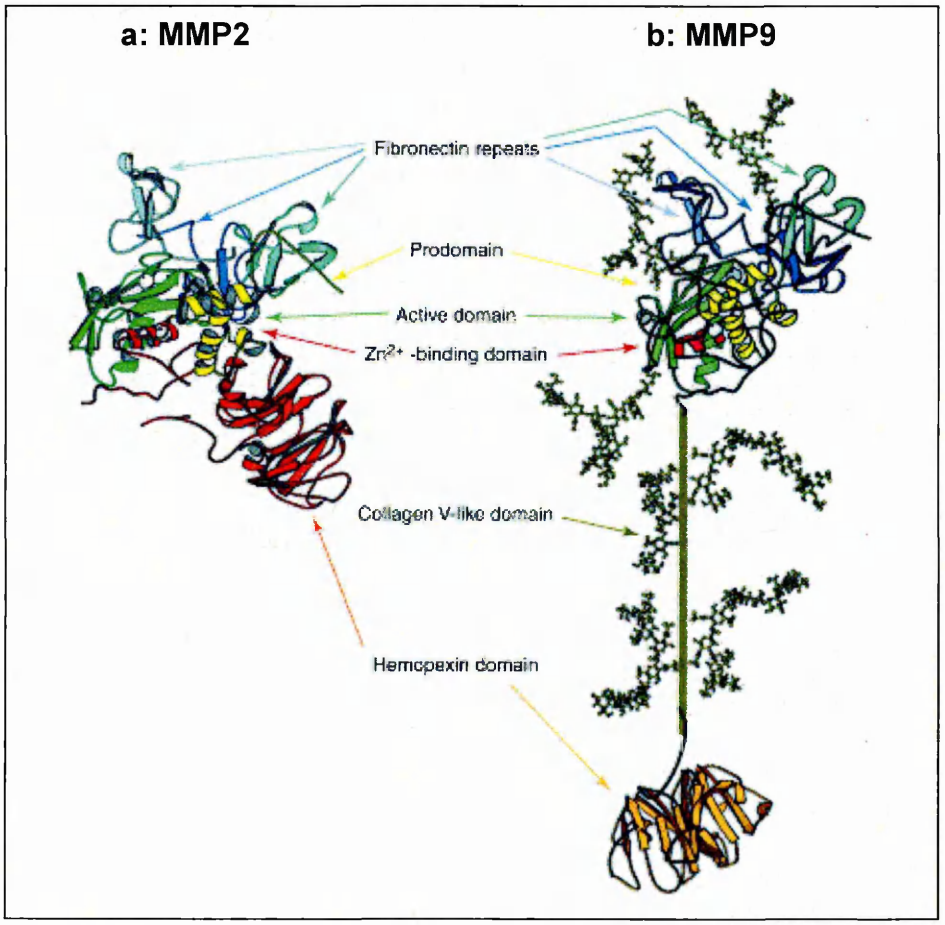

Reprinted from (Opdenakker *et al.*, 2001) © (2001), with permission from Elsevier.

Proinflammatory cytokines, such as IL-1β and TNF, can modulate the expression and regulation of MMPs. Conversely, MMPs can function as sheddases or convertases by transforming membrane-bound cytokines, cytokine receptors, and adhesion molecules to soluble forms (Leppert *et al.*, 2001). MMP production can be stimulated by oncogenes, LPS, and growth factors, such as epidermal growth factor. Prostaglandin E2 has been shown to both inhibit and enhance transcription of MMPs, depending on the cell type and inflammatory state (Ruwanpura *et al.*, 2004). Free radicals are known to activate and interact with MMPs. Direct effects of free radicals include oxidation or nitrosylation of MMPs, thereby activating them. Indirectly, transcription factors integral to the MMP transcription process, such as NF-κB, can be affected by free radicals (Gu *et al.*, 2002).

1.4.5 Inhibition of MMPs by TIMPs

Tight regulation of MMPs to prevent excessive proteolytic activity is greatly assisted by endogenous proteins known as TIMPs. TIMPs comprise four members (TIMPs 1-4) which form complexes with pro- and activated MMPs, blocking their activity. The four TIMPs have similar structures, but their tissue distribution and regulation are varied and they have other complex functions aside from inhibiting MMPs. TIMP1 complexes with MMP9 and inhibits apoptosis (Guedez *et al.*, 1998). TIMP2 assists in the activation of MMP2 by MT-MMP, but inhibits MMP2 at higher concentrations (Strongin *et al.*, 1995). TIMP3 has several cell surface activities, including: inhibition of MMP3, MMP7 and MT-MMPs; blocking of the VEGF receptor-2, thereby inhibiting angiogenesis (Qi *et al.*, 2003); and promotion of cell death by blocking the shedding of cell surface death receptors via inhibition of a disintegrin and metalloprotease 17 (ADAM17) (Ahonen *et al.*, 2003).

1.4.6 MMPs in MS

MMPs can contribute to disease pathogenesis when they are over-expressed. Much has been documented about the role of MMPs in inflammatory diseases, including neurological disorders, such as MS. Astrocytes, microglia, and ECs of the CNS, together with macrophages and T cells, secrete various MMPs that contribute to MS pathogenesis. It is likely that MMPs are involved in BBB damage, brain oedema, lymphocyte infiltration, degradation of myelin, and axonal damage (Fig. 1.10) (Yong *et al.*, 2001). The increased MMP production seen in patients with CNS disorders is often viewed as a target for inhibitory drugs. MMP inhibitors have been proposed as a treatment for MS, but careful use of a highly specific drug would be necessary, to avoid eliminating the useful role of MMPs in tissue repair, particularly as MS is likely to require protracted therapy.

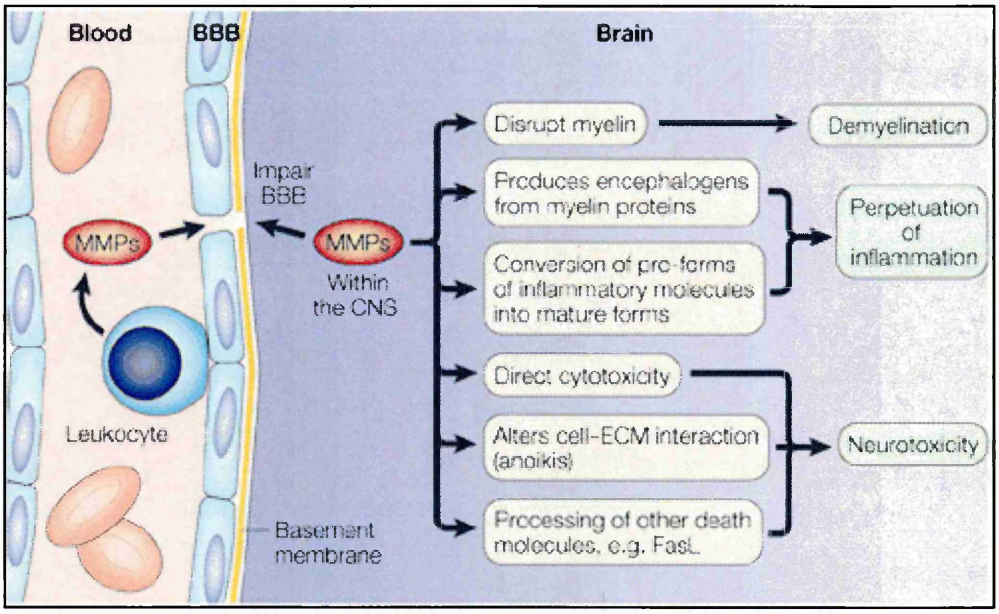

Figure 1.10 MMP involvement in the neuropathology of MS

Leukocytes express MMPs, which help them to enter the CNS. The basement membrane surrounding blood vessels is disrupted and consequently the BBB is disrupted. The CNS contains significant levels of MMPs that are widely distributed, leading to perpetuation of an inflammatory response. This results in demyelination, destruction of OLGs, and axonal damage.

Development of inhibitors for specific MMPs has proved difficult, but it is hoped that the use of a relatively selective MMP inhibitor that does not penetrate the BBB will be possible in MS, with minimal side effects. As leukocyte MMP activity is a target of MMP inhibition, an agent that is not CNS diffusible could still inhibit cell migration into the CNS (Yong *et al.*, 2007a).

In the brain, gelatinases, stromelysins, and MT-MMPs make up the majority of MMPs present, with MMPs 2, 3, and 9, being the most significant (Muir *et al.*, 2002). MMP3 is known to activate MMP9, as is NO, by causing removal of the peptides that maintain the inactivity of the zinc binding site (Gu *et al.*, 2002). MMP2 and 9 act on less ECM substrates than MMP3, but process important constituents of the basal lamina (Yong *et al.*, 1998). It has been suggested that over-expression of MMPs and a relative decrease in their TIMP inhibitors, may produce persistent proteolysis, resulting in the neuronal loss that represents the steady advancement of symptoms of secondary chronic progression in MS (Lindberg *et al.*, 2001). The serum, CSF, and brain tissue of MS patients all demonstrate an increase in MMPs 1, 2, 3, 7, 9, and 12 (Kurzepa *et al.* 2005). MMP9 in particular, is thought to assist with T cell migration into the CNS. High levels of MMP9 are detected in astrocytes and macrophages in demyelinating lesions, and in the CSF of MS patients (Szabo *et al.*, 2004).

Latent MMP9 is found in vesicles within neutrophils, and this can be released during inflammation (Ramos-DeSimone *et al.*, 1999). A 10 month study of 21 RRMS patients revealed high serum levels of MMP9 during relapses, which correlated with increasing numbers of lesions detected by MRI (Lee et al., 1999). The ratio of MMP9 and its inhibitor, TIMP1, has been suggested as a useful indicator in assessing potential BBB destruction in MS. Patients with RRMS often have a high CSF MMP9/TIMP1 ratio, which was found to decrease after 6 months of IFN-β therapy (Boz et al., 2006). Microglia and astrocytes produce MMP9 when stimulated with LPS *in vitro* (Gottschall and Deb, 1996), and MMP2 has been detected in the foot processes surrounding blood vessels as it is produced constitutively by astrocytes (Liu and Rosenberg, 2005).

1.5 Dipeptidylpeptidase IV (CD26)

The cell surface ectopeptidase dipeptidyl peptidase IV (DPPIV) has the Enzyme Commission (EC) number 3.4.14.5 and is identical to the CD26 antigen (Kahne *et al.*, 1999). CD26 was first described in 1966, and has long been known to cleave dipeptides from peptides or proteins with either a proline or alanine in the penultimate position. As substrate size increases, CD26 has been found to lose proline specificity and increase the speed of hydrolysis (Demuth *et al.*, 2005). Proteins with the cyclic

amino acid proline in the N- or C-terminal penultimate position are normally protected from proteolytic attack, so the discovery of this peptidase provoked much interest (Mentlein, 1999).

1.5.1 Structure of CD26

CD26 is a type II integral membrane protein of 110 kDa, possessing a large extracellular domain, a transmembrane domain, and a cytoplasmic tail of six amino acids (Fig. 1.11) (Tanaka *et al.*, 1992). The short, intracellular, hydrophillic N-terminus is followed by a hydrophobic membrane anchor comprised of 22 amino acids, and then 738 residues, containing potential glycosylation sites, located extracellularly. The C-terminus contains the catalytic region, which is fully conserved between human and rat sequences (Mentlein, 1999).

1.5.2 Function of CD26

The function of CD26 eluded discovery for many years, as its unique specificity implicated it in collagen metabolism, but the glycine-proline sequence, frequently seen in collagen, is often followed by a proline-proline bond, which CD26 cannot cleave. In the 1990's, studies focused on the role of CD26 in immune responses, such as T cell activation and proliferation (Mentlein, 1999). It is now known that this peptidase can inactivate many extracellular proteins of biological significance, including neuropeptides, hormones, cytokines, and chemokines, but information about *in vivo* substrates is still limited (Mentlein, 1999). CD26 is not thought to have a unique physiological role, as little difference in phenotype is seen in Fischer rats that lack it (Tiruppathi *et al.*, 1993).The cell type and conditions in which it is expressed affect the functionality of CD26, which includes acting as an enzyme, receptor, and potent co-stimulatory protein. CD26 can bind to a variety of proteins, including an association with adenosine deaminase (ADA) and it has been shown to be identical to the ADA binding protein (Kameoka *et al.*, 1993). On the surface of T cells, CD26 also interacts with CD45, a transmembrane protein with tyrosine phosphatase activity, which has been suggested to result in increased tyrosine kinase activity and T cell activation (Torimoto *et al.*, 1991). Controversy remains as to whether the enzymatic activity of CD26 is required for its signalling role (Kahne *et al.*, 1999).

CD26 is important in immune responses, is involved in apoptosis, acts as an adhesion molecule for collagen and fibronectin, and has been implicated in the pathogenesis of autoimmune diseases, cancer, and human immunodeficiency virus (HIV)-related diseases (Boonacker and Van Noorden, 2003).

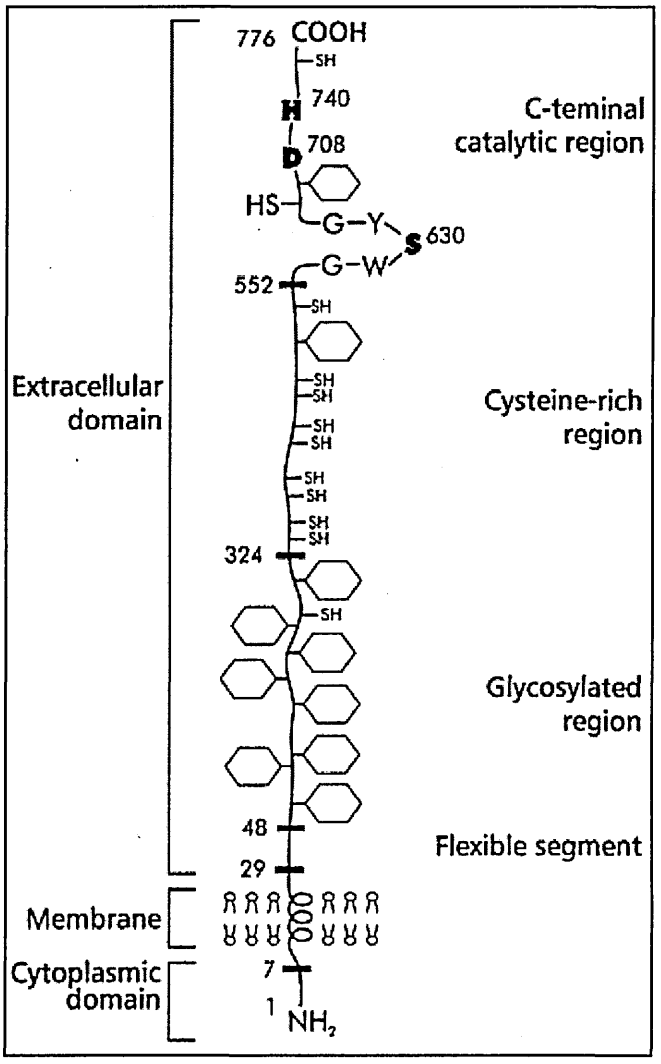

Reprinted from (Mentlein *et al.*, 1999), © (1999), with permission from Elsevier.

Figure 1.11 Structure of human CD26 (DPP IV)

CD26 is a type II transmembrane protein with a cytoplasmic hydrophilic N-terminus composed of 6 amino acids, a 22 amino acid hydrophobic membrane anchor, and a large extracellular domain containing a flexible segment, regions rich in sugars and cysteines, and a C-terminal catalytic domain with a serine-protease type centre. The serine at residue position 630 forms a catalytic triad with the aspartate at position 708, and histidine at 740. CD26 is inhibited by metal ions (e.g. Pb^{2+} and Zn^{2+}) and compounds that covalently modify the active site, such as di-isopropyl fluorophosphates (Puschel et al., 1982), or non-covalent reversible inhibitors.

CD26 has diverse functions in T cells and in regulating peptides, and is found both intracellularly and extracellularly (Tanaka *et al.*, 1993). (See also 4.1 and Fig. 4.1).

1.5.3 CD26 expression

Many cell types express this cell surface glycoprotein. In humans, epithelial cells of liver, intestine, and kidney express membrane-bound CD26 constitutively, and a soluble form is present in the blood and CSF. In particular, tissues and fluids of the body involved in nutrition and excretion, such as the intestinal lumen, urine, bile, and pancreatic fluid, are rich in CD26, where it most likely serves a digestive function by degrading peptides (Brandsch *et al.*, 1995). ECs express CD26, it is found at the capillary epithelia of endocrine organs, and in specialised fibroblasts, as in the mammary gland (Atherton *et al.*, 1992), or skin (Raynaud *et al.*, 1992). The concentration found in the blood is very high compared to other enzymes, with an estimated lower limit of 3μM (Demuth *et al.*, 2005). On T cells, CD26 expression occurs late in thymic differentiation and is thought to be limited to the helper/memory CD4+ population (Morimoto *et al.*, 1989). Other immune cells expressing CD26 include some subsets of macrophages (Jackman *et al.*, 1995).

In the CNS, CD26 is found in the CSF, particularly in the circumventricular organs (Mitro and Lojda, 1988). Capillaries of the brain and some ependymal cells express high levels, and in the peripheral nervous system, CD26 is expressed by the perineurium and Schwann cells (Haninec and Grim, 1990). Neuronal cells of the embryonic brain express abundant CD26 (Bernstein *et al.*, 1987). The location of this peptidase facilitates proteolytic attack on bioactive peptides in body fluids, and it is often found at sites considered to be physiological barriers, such as the BBB.

1.5.4 CD26 in MS

In inflammatory disorders, migrating T cells have been shown to be those which express high levels of CD26 (Mackay, 1996). Studies have demonstrated large numbers of CD26+ T cells in the circulation of patients with MS (Hafler *et al.*, 1985), and rheumatoid arthritis (Nakao *et al.*, 1989), suggesting CD26 might play a role in chemokine-induced migration of T cells. $CD4^+$ T memory cells with high CD26 expression have been found to correlate with disease severity and activity in MS (Krakauer *et al.*, 2006). Peripheral blood $CD8^+$ cells positive for CD26 decreased following treatment of MS patients with IFN-β (Jensen *et al.*, 2006). Expression of CD26 on six MBP-specific $CD4^+$ T cell clones from MS patients was examined, and found to be high, with a 3-4 fold increase in enzymatic activity compared to resting T cells from peripheral blood. In addition, CD26 inhibitors suppressed IFN-γ, IL-4, and

TNF production of antigen-stimulated T cell clones. It is possible that CD26 is involved in regulating activity of autoreactive T cells (Reinhold *et al.*, 1998). (See also 4.1).

1.6 Chemokine Processing

Due to the extensive connections and frequent colocalisation of cytokines and proteases, cleaved forms of chemokines have come under scrutiny. Chemokines are capable of acting as powerful stimuli of MMP and DPPIV expression in various cell types. In return, proteases can cleave chemokines, producing receptor agonists with greater, lesser, or no activity as a result. Numerous examples of chemokine-protease interactions have been reported, yet it remains virtually impossible to predict the outcome in terms of biological activity. Redundancy in the chemokine and receptor system, local or systemic processing (i.e. inducible proteases and chemokines acting at cellular or tissue-specific locations, or proteolysis in the circulation), speed of proteolysis (Lambeir *et al.*, 2001), and involvement of numerous other molecules, all add to the uncertainty of the results of chemokine truncation. Loss of the disulphide bridges of chemokines is generally accepted as loss of biological activity through GPCRs, whereas angiostatic properties mediated by GAG binding of the C-terminus appear to occur independently of chemokine tertiary structure. Limited N-terminal cleavage of inflammatory chemokines can produce dramatic results. N-terminal deletion of ELR^+ CXC chemokines can lead to enhanced chemotactic potency and might produce an increase in angiogenic activity, but the angiostatic ability of ELR^- CXC chemokines does not appear to be affected (Van Damme *et al.*, 2004).

Much has been documented about the relationship between structure and activity of CCL2 (Clark-Lewis *et al.*, 1995). The ten N-terminal amino acids of CC chemokines are thought to be critical in receptor activation, binding and specificity (Iwata *et al.*, 1999). It has been demonstrated that a CCL2 analogue lacking three N-terminal residues had lowered binding affinity and activity than intact CCL2 (Gong *et al.*, 1996). CCL5 lacking eight N-terminal residues is inactive in chemotaxis and is a potent inhibitor of HIV infection (Arenzana-Seisdedos *et al.*, 1996). This blocking of HIV infection serves to illustrate how structural modification of chemokines can produce variants lacking in chemotactic activity, but retaining the ability to bind to their receptor(s). These modified chemokines thereby act as antagonists, with the potential to be utilised therapeutically as anti-inflammatory agents (Struyf et al., 2003).

1.6.1 Cleavage of chemokines by MMPs

Reports of chemokine cleavage have documented N-terminal processing at position 4-5 of CXCL12 by MMP2, and also cleavage of CCL7 at the same position, resulting in a

loss of binding to the receptor (McQuibban *et al.*, 2001). MMP2 and MMP9 are known to truncate CXCL8 and CXCL7 at the N-terminus. MMP2 appears particularly potent, cleaving CCL2, CCL8, CCL13, and CCL7 to complete inactivation (McQuibban *et al.*, 2002). MMP9, however, was found to cleave CXC and not CC chemokines members (Van den Steen *et al.*, 2000). It is not always the case that truncation of chemokines results in inactivity, as unpredictably it can sometimes result in a more potent ligand for the receptor. Reports on chemokine activity following C-terminal truncation are scarce, but one study found enhanced receptor activation following C-terminal processing of CXCL7 (Ehlert *et al.* 1998). Amino-terminal cleavage of CXCL8 by MMP9 has been shown to produce a ten-fold increase in activity (Van den Steen *et al.*, 2000). MMPs 8 and 9 have also been shown to process CXCL9 and CXCL10 at the carboxy-terminus (Van den Steen *et al.*, 2003).

1.6.2 Cleavage of chemokines by CD26

CD26 has a diverse range of substrates, including substance P, growth hormone releasing factor, neuropeptides, the fibrin α-chain, and several chemokines (Boonacker and Van Noorden, 2003). CD26 has been shown to process CCL4 at the N-terminus, in addition to other CC chemokines such as CCL5 (Guan *et al.* 2004). CCL5 is not only a substrate for CD26, but when combined with it, can augment the normal chemotactic response of T cells (Iwata *et al.*, 1999). As CD26 alone was not shown to provoke chemotaxis, it has been suggested that CD26 activity is needed for enhancement of T cell migration across endothelia. This is in keeping with findings that T cells highly positive for CD26 have the greatest migratory capacity and prevalence at chronic inflammatory sites *in vivo* (Brezinschek *et al.*, 1995). In contrast, monocyte migration did not occur to the cleaved form of CCL5, and simultaneous incubation of intact CCL5 with CD26 reduced migration (Iwata *et al.*, 1999).

1.6.3 Implications of chemokine processing for multiple sclerosis pathogenesis

The processing of chemokines by MMPs, or other enzymes such as membrane-anchored CD26, is an interesting consideration when examining the pathogenesis of MS. Since in MS pathology there is a considerable body of evidence for simultaneous and colocalised production of MMPs and chemokines, the role of chemokine processing in the initiation and termination of the immune response is of great interest.

In addition to truncation of chemokines (which results in their inactivation, enhancement, or antagonism), MMPs also regulate chemokines by cleaving chemokine ligands. Chemokines can be bound, retained, and concentrated by ligands designed to create chemotactic gradients that contribute to immune cell influx (Parks *et*

al., 2004). Inflammatory processes involve the recruitment of cells by chemokines, but this must be halted if cessation of inflammation and subsequent tissue recovery is to occur. Identifying proteinases that cleave chemokines is currently inadequately characterised, and yet may serve as an important mechanism for quelling chemoattractant signals.

1.7 Treatment of Multiple Sclerosis

Most treatment offered to patients with MS involves long-term immunological therapy targeting the peripheral immune response, on the assumption that MS is an autoimmune disorder. Acute attacks are treated with high doses of glucocorticoid (Frohman *et al.*, 2007). Although disease-modifying treatments (DMTs) have progressed significantly, their efficacy in preventing disease progression is questionable, and common symptoms such as fatigue, cognitive impairment, pain, and depression are often not alleviated by immune-based therapies (Chaudhuri and Behan, 2005). It is likely that combination therapies will develop, particularly given the complex nature of MS. Current DMTs approved for long-term treatment of MS include three interferon-beta (IFN-β) drugs, and glatiramer acetate (GA)(Neuhaus *et al.*, 2006).

IFN-β is a polypeptide predominantly produced by fibroblasts, with both the intramuscular and subcutaneously administered pharmaceutical versions of IFN-β1a being glycosylated in line with the natural form, but IFN-β1b differing from it slightly, and lacking glycosylation of the asparagine at position 80 in the amino acid chain (Neuhaus *et al.*, 2006). IFN-β exerts many immune effects, but is thought to act mainly by reducing the secretion of MMPs (with MMP9 being of central importance), thereby minimising the destruction of the BBB and migration of T cells into the CNS (Stuve *et al.*, 1996). In addition, it is thought that IFN-β also downregulates MHC class II expression on APCs (Hall *et al.*, 1997), suppresses T cell proliferation (Rep *et al.*, 1996), induces Th2 cytokine expression (e.g. IL-10) and decreases that of Th1 cytokines (e.g. IFN-γ) (Rep *et al.*, 1999), and inhibits monocyte activation (Van Weyenbergh *et al.*, 1998). IFN-β1a and IFN-β1b are thought to differ in their effects on cytokine profiles, with the former enhancing production of anti-inflammatory IL-4 and IL-10, and the latter decreasing secretion of pro-inflammatory IFN-γ (Sega *et al.*, 2004).

Recombinant IFN-β and intravenous Igs can reduce the frequency and severity of attacks in some patients, but others fail to respond. Treatment with IFN-β often leads to production of anti-IFN-β antibodies, which cause a decline in treatment efficacy through neutralising the drug over time (Gibbs and Oger, 2007).

GA, known as Copaxone, induces upregulation of $CD8^+$ T cells with regulatory or suppressing roles, with untreated patients showing a deficit in $CD8^+$ suppression. $CD8^+$ T cells from patients receiving GA also show potent cytotoxicity, restricted to HLA Class I, which can destroy $CD4^+$ cells in a GA-specific manner (Tennakoon *et al.*, 2006). The immunomodulatory effects of GA apply to cells specific for MBP and possibly other myelin antigens, and it has been postulated to exert neuroprotective effects (Farina *et al.*, 2005).

1.7.1 Other treatments

Mitoxantrone causes cross-linking and strand breaks in DNA by interacting with an enzyme called topoisomerase-2, involved in the breaking and rejoining of DNA (Smith, 1983). It is known to have cytotoxic, immunosuppressive, immunomodulatory, antiviral, and antibiotic effects (Neuhaus *et al.*, 2004). Mitoxantrone is used as a second line drug for progressive and worsening MS that is not controlled by IFN-β or GA (Edan *et al.*, 2004).

T cell vaccination (TCV) involves isolation of T cells that react to either MBP or MOG, inactivation by irradiation, and injection as a vaccine to sensitise the immune system to recognise these autoreactive cells, with the goal of eliminating them from the blood. Clinical trials using a small number of patients have confirmed the safety and efficacy of TCV, as relapse rates and neurological disability progression were reduced, suggesting it may be of use in patients who do not respond to treatment with IFN-β (Achiron *et al.*, 2004).

In the quest for improved therapies, the use of stem cell therapies to repair brain lesions appeared an attractive proposition, but recent information gleaned on the pathogenesis of MS, and the risk of producing tumours from transplanted cells, rendered this approach less feasible than first thought (Lassmann 2005). Therapy involving intense immunodepletion, followed by an autologous haematopoietic stem cell transplant (HSCT), is currently being assessed worldwide as a potential therapy for patients unresponsive to other treatments. Although evidence suggests that allogenic HSCT is more effective at eliminating the host's aberrant immune system, the mortality risk is 15-35%, compared to 3-5% for autologous. HSCT currently remains an experimental approach with many uncertainties, and results from the 300 patients treated so far cannot confirm if it is effective in modifying disease progression as randomised controlled trials were not used (Silani and Cova, 2008).

Cannabis is considered beneficial in controlling muscle stiffness, pain, and spasms,

and may even offer neuroprotection as cannabinoids affect oxidative responses, glutamate and ion influxes (Jackson *et al.* 2005). A cannabis-based oral spray called Sativex is available on prescription to MS patients in Canada. UK regulators, however, have decided that further data is required before Sativex is available for MS patients in this country (Pryce and Baker, 2005). Sativex contains delta-9-tetrahydrocannabinol and cannabidiol, and was found to improve pain and sleep disturbance and demonstrated maintenance of the analgesic effect, in a randomised trial of 66 patients, lasting a mean duration of 463 days (Rog *et al.*, 2007).

Drugs targeting specific sections of the inflammatory response are being developed, such as the humanised monoclonal antibody anti-VLA-4, and immunomodulators, such as statins. Natalizumab (Tysabri) is an antagonist, which binds to α4-integrins on leukocytes, preventing them from interacting with adhesion molecules on ECs. Several studies have reported decreases in relapse rates and lesion development following treatment with natalizumab, but when used in combination with IFN-β1a, two MS patients developed progressive multifocal leukoencephalopathy (PML), and dosing was suspended in 2005. It has recently been reintroduced as a monotherapy for patients with RRMS (Kappos et al., 2007).

Chemokine antagonists may prove helpful in curbing the infiltration of inflammatory cells across the BBB (Galimberti *et al.* 2004). Several pharmaceutical companies are involved in the development of antagonists to chemokine receptors, including CCR1 and CCR5, as high numbers of monocytes expressing both of these have been found in perivascular cuffs (PVCs) and at demyelinating edges of MS lesions (Ribeiro and Horuk, 2005).

The antibiotic, minocycline, is a potent inhibitor of gelatinases (MMPs 2 and 9) and was found to reduce MRI Gd-enhancing lesions and relapse frequency in a 2 year study of 10 patients with RRMS, further supporting a substantial role for these MMPs in the disease process (Zabad et al., 2007)

There is pressure to produce DMTs that address the demyelination and axonal loss problems central to MS. Neuroprotective agents and ion channel blockers are currently under investigation to prevent some of this damage (Kappos *et al.* 2004). Disruption of ion channels expressed by T cells, for example, can lead to immune suppression by preventing their response to antigenic challenge (Panyi *et al.*, 2004). Neuroregenerative approaches to treating MS remain speculative, and the principal therapeutic aim persists to reduce neural and glial tissue damage by targeting key aspects of the immunological cascade using DMTs.

1.8 Aims of thesis

It is apparent that the interactions between MMPs and chemokines are complex and not fully understood. A greater comprehension of the chemokine substrates of MMPs and CD26, and the effect cleavage has on their chemotactic activity, is needed to identify potential therapeutic targets amongst chemokines or their receptors, such as an antagonistic cleavage product. This thesis aims to contribute to this knowledge. Four major aims were addressed in the research undertaken in this thesis:

- To investigate the proteolytic processing of recombinant human chemokines (CCL2 and CXCL10) by enzymes (MMP2, MMP9, and CD26), using gel electrophoresis and mass spectrometry to characterise the cleavage products (Chapter 2)
- To assess primary human astrocyte supernatants for the presence of cleaved chemokines using western blotting and mass spectrometry, and astrocyte lysate samples for the whole spectrum of MMPs and TIMPs using RT-PCR (Chapter 3)
- To investigate MS brain tissue by dual-labelling immunofluorescence to identify cell types expressing CD26, and compare expression to that in normal control brain (Chapter 4)
- To assess the migration of T cells and monocytes using cell lines and PBMCs to the cleaved isoforms of CCL2 and CXCL10 (obtained after proteolytic processing by MMP2, MMP9, and CD26) compared to migration to the intact forms (Chapter 5)

Chapter 2

Chemokine cleavage: truncation of CCL2 and CXCL10 by MMP2, MMP9 and CD26

2.1 Introduction

Chemokines play a pivotal role in regulating migration of leukocytes, both during immune surveillance and in inflammatory states. Precise control of leukocyte trafficking is vital to health, and chemokines are regulated at four levels. Firstly, gene expression and protein secretion regulate chemokine expression, including storage in granules of leukocytes or ECs, or being exported as inactive membrane-bound forms (Von Hundelshausen *et al.*, 2007). Chemokine activity can also be altered by interactions with GAGs, leading to retention on cell surfaces at high concentrations and possible protection from processing. Thirdly, chemokines can be bound by non-signalling receptors, known as decoy receptors, such as D6, or the Duffy antigen receptor for chemokines (DARC), and lastly, they can be processed by proteases to forms with different activities, which allows rapid changes in their activity without transcription (Comerford and Nibbs, 2005).

Most chemokines are secreted proteins composed of 67-127 amino acids, which can be isolated in both intact and truncated forms from supernatants obtained from cells stimulated with cytokines *in vitro* (Struyf *et al.*, 2001). Cytokines can induce both chemokine and protease production, so simultaneous upregulation of these is likely to be a natural phenomenon occurring in organ, or cellular compartments *in vivo*, during episodes of inflammation. Positive feedback loops can contribute to conditions where protease-cytokine interactions abound. Interleukin-1β, for example, is a potent inducer of other cytokines (e.g. IL-6) (Musso *et al.*, 1990), chemokines (e.g. CCL2) (Harkness *et al.*, 2003), and MMPs (e.g. MMP9) (see 1.4) (Yoo *et al.*, 2002) from several cell types. Secreted proteases induced by IL-1β can then convert inactive forms of cytokines to active ones (e.g. MMP9 processing of pro-IL-1β to active IL-1β) (Chauvet *et al.*, 2001), or cleave active cytokines to produce more potent versions (e.g. N-terminal cleavage of CXCL8 by MMP9) (Van den Steen *et al.*, 2003).

The results of processing by proteases can also result in negative feedback, as is the case with truncation of some chemokines. In addition to inactivating chemokines, as is seen with proteolysis of CXCL1 by MMP9 (Proost *et al.*, 2006), processing can also generate chemokine antagonists that bind to their receptor but are unable to evoke chemotaxis (e.g. CCL7 cleaved by MMP2) (Van Lint and Libert, 2007). These examples demonstrate that a single protease, such as MMP9, can act upon cytokines and/or chemokines to render them either more or less active. Chemokines reported to be prone to attack from MMPs include CCL2, CCL7, CCL8, CCL13, CXCL8 and CXCL12 (reviewed in Wolf et al., 2008).

Cytokine-protease-chemokine interactions are not limited to MMPs as the protease. Interleukin-12, for example, induces CD26 expression on T cell membranes (see 1.5) (Salgado *et al.*, 2000). CD26 has many substrates, including several chemokines, with potentially wide-reaching effects, due to the soluble form of this protease being present in the circulation (Mentlein, 1999). CD26 highly selectively cleaves a dipeptide from substrates with a proline or alanine residue at the penultimate position of the N-terminus. Some chemokines that possess this sequence are modified by a pyroglutamate, which protects them from truncation by CD26 (Proost *et al.*, 1999). CD26 can induce MMP9 expression (Gonzalez-Gronow *et al.*, 2001), which is of interest in MS given both enzymes are implicated in the pathogenesis.

Cathepsin G, elastase and proteinase-3 are enzymes that can be released from neutrophil and monocyte granules when the cell is activated. As these cells can also secrete CC and CXC chemokines, there is great potential for cleavage. Other enzymes known to engage in proteolysis of chemokines include CD13, uPA, plasmin and thrombin (Tables 2.1, 2.2, 2.3) (reviewed in Wolf *et al.*, 2008).

Truncation of proteins may be pertinent to many diseases, impacting on activities such as inflammation, tumour development and metastasis, and infection with HIV. Indeed, it was the observations of tumour-derived proteases assisting in cellular invasion that led to further investigations of interactions between proteases, cytokines, and chemokines (Chang and Werb, 2001). Chemokine cleavage is a complex area of study, due to the unpredictable nature of how the pathology of diseases is affected, the excessive number of factors involved, and the technical skills required to detect cleavage products in tissue (Van Damme *et al.*, 2004). The last decade has seen numerous reports of proteolytic chemokine processing, but *in vitro* studies may not tally with results in a physiological environment, where greater control of protease and chemokine expression exists.

2.1.1 N-terminal truncation of chemokines

Studies on chemokine cleavage have been focused on the N-terminus, due to N-terminally truncated forms being isolated from natural sources, and the importance of this region for receptor binding and activity (Proost et al., 2006). Chemokine receptors, and all chemokines except XCL1, possess 2 disulphide bridges likely to be involved in stabilising the structural conformation to enable binding, which if lost, frequently results in failure to act via GPCRs (Oppermann, 2004). The N-terminal region, before the first cysteine residue, is exposed with a disordered conformation, making it prone to processing. Minor losses at the N-terminus can lead to drastic alterations in the

chemotactic activity of many chemokines (Table 2.1 and 2.2) (reviewed in Wolf *et al.*, 2008). CXCL7 is a special case, in that to become active in attracting neutrophils, 7 residues from the N-terminus must first be removed by chymotrypsin or cathepsin G (Von Hundelshausen *et al.*, 2007).

N-terminal cleavage of CC chemokines commonly reduces their chemotactic potential, but can also increase activity (Table 2.1). Truncation of CXC chemokines can effect not only their chemotactic potential, but also angiogenesis, due to the angiogenic activities of chemokines with an ELR motif, and angiostatic properties of CXC chemokines without this motif (Lentsch, 2002). In contrast to CC chemokines, removal of N-terminal amino acids from CXC chemokines with an ELR motif often leads to enhanced inflammatory activity due to a greater chemotactic potential, and possibly also an increase in angiogenesis (Table 2.2). Chemokines with an ELR motif exhibit many naturally occurring truncated forms, and it appears that possession of the ELR motif in the aminoterminus is linked to high susceptibility of cleavage in this region by some MMPs (Van Damme *et al.*, 2004). Truncation of the N-terminus of CXC chemokines lacking an ELR motif, such as CXCL10, produces little effect on the angiostatic potential of these chemokines, in contrast to ELR-bearing chemokines. CXCR3 ligands (CXCL9, -10, and -11) are more likely to be cleaved C-terminally but are prone to N-terminal attack by CD26 (Proost *et al.*, 2001). CD26 truncation of CXCR3 ligands at the N-terminus has been shown to result in loss of binding and chemotaxis of these chemokines, yet maintenance of their angiostatic properties, emphasising the need to evaluate the effects of cleavage on chemotaxis and angiogenesis independently *in vivo* (Proost *et al.*, 2001).

CD26 is of particular importance in N-terminal truncation of chemokines (Table 2.1 and 2.2). Research into HIV has revealed that N-terminal truncation by CD26 of the ligands of CXCR4 and CCR5 *in vitro* impacted on susceptibility to infection (Proost *et al.*, 1998a).

2.1.2 C-terminal truncation of chemokines

Reports of chemokine cleavage at the carboxy-terminus are rare compared to the greater susceptibility observed at the N-terminus, and much remains to be discovered (Table 2.3) (Edwards *et al.*, 2005). The leucine residue is highly conserved in CXC chemokines, and when it occurs as the C-terminal amino acid, studies on CXCL8 suggest that it may render the residues next to it, as more prone to proteolysis (Ehlert *et al.*, 1998).

Table 2.1 N-terminal processing of CC chemokines by proteases and effects on activity

Reports of N-terminal truncations of CC chemokines following interactions with enzymes are shown. N-terminal cleavage of CC chemokines often reduces their chemotactic potential, but can also increase it. Several different proteases are able to cleave CC chemokines at the N-terminus, but it can be seen that MMPs and CD26 play highly significant roles. CD26 is highly selective for substrates with a proline or alanine at position two of the N-terminus, a sequence possessed by approximately one-third of human chemokines. The characteristic N-terminal dipeptide removal by CD26 is frequently observed. The most common truncation observed by MMPs is removal of four residues, but this is variable (Van Damme et al., 2004). Chemokines investigated in this study are highlighted in bold.

** Amino acids remaining after processing detailed in brackets*

↑ = increased, ↓ = decreased, uPA = urokinase-plasminogen activator

CHEMOKINE ISOFORM *	PROTEASE(S) INVOLVED	EFFECT ON ACTIVITY AND RECEPTOR AFFINITY
CCL2 (5-76)	**MMPs 1, 3, 8**	**↓ chemotaxis in *in vivo* inflammatory model**
CCL3L1 (3–70)	CD26	↑ monocyte chemotaxis and affinity for CCR1,5; ↓ affinity for CCR3; anti-HIV activity
CCL5 (3–68)	CD26	↓ chemotaxis and affinity for CCR1,3; ↑ affinity for CCR5; ↑ anti-HIV activity
CCL5 (4-68)	Cathepsin G	↓activity
CCL7 (5–76)	MMPs 1,2,3,13,14	↓chemotaxis and affinity for CCR1,2,3
CCL8 (5-76)	MMP3	CCR2 antagonist
CCL11 (3-74)	CD26	↓chemotaxis for $CCR3^+$ cells; Unchanged anti-HIV activity
CCL13 (4-75)	MMP1, 3	↓migration in an *in vivo* inflammatory model; CCR2 and CCR3 antagonist
CCL13 (5-75)	MMP1, 3	↓migration in an *in vivo* inflammatory model; CCR2 and CCR3 antagonist
CCL13 (8-75)	MMP1	↓migration in an *in vivo* inflammatory model; CCR2 and CCR3 antagonist
CCL14 (9–74)	uPA, plasmin	↑ chemotaxis and affinity for CCR1,3,5, but plasmin further degrades active product; Anti-HIV activity
CCL15 (22-92)	Elastase	↑ activity for $CCR1^+$ cells
CCL15 (24-92) (27-92)	Cathepsin G	↑ activity for monocytes and $CCR1^+$ cells
CCL15 (29-92)	Cathepsin G, Chymase	↑ activity for $CCR1^+$ cells
CCL22 (3-69) (5–69)	CD26	↓activity for lymphocytes but not monocytes; ↓ affinity for CCR4
CCL23 (27-99)	Cathepsin G Chymase	↑ activity for $CCR1^+$ cells
CCL23 (30-99)	Elastase	↑ activity for $CCR1^+$ cells

Adapted from (Van Damme *et al.*, 2004), © (2004), and (Wolf *et al.*, 2008) © (2008), with permission from Elsevier.

Table 2.2 N-terminal processing of CXC chemokines by proteases and effects on activity

Reports of N-terminal truncations of CXC chemokines following interactions with enzymes are shown. Several different proteases are able to cleave CXC chemokines at the N-terminus, but it can be seen that MMPs and CD26 play highly significant roles. N-terminal cleavage of CXC chemokines more commonly increases their activity, especially when the substrate has an ELR motif, as shown with those that bind to CXCR1 or 2. For CXC chemokines lacking an ELR motif, the most common outcome is a reduction in activity, or no change. MMP processing most commonly removes 4 or 5 residues from the N-terminus of CXC chemokines, but this can be seen to vary, yet there are no deviations from the dipeptide removal when CD26 is the protease. Chemokines investigated in this study are highlighted in bold.

** Amino acids remaining after processing detailed in brackets*

↑ = increased, ↓ = decreased, uPA = urokinase-plasminogen activator

CHEMOKINE ISOFORM *	PROTEASE(S) INVOLVED	EFFECT ON ACTIVITY AND RECEPTOR AFFINITY
CXCL5 (8-78)	MMP8, 9	↑ activity
CXCL5 (9-78)	Cathepsin G	↑ activity for neutrophils
CXCL5 (10-78)	MMP1	No information
CXCL6 (3–77)	CD26	Unchanged chemotaxis and affinity for CXCR1,2
CXCL6 (5-77) (6-77)	MMP8, 9	No changes
CXCL6 (7-77)	MMP9	No changes
CXCL8 (6–77)	MMP8,13,14	↑ chemotaxis and affinity for CXCR1,2
CXCL8 (6–77)	Plasmin, thrombin, Cathepsin L	↑ activity for neutrophils
CXCL8 (7–77)	MMP1, 9	No information
CXCL8 (8-77)	Proteinase-3	↑ activity
CXCL8 (9-77)	Plasmin	↑ activity for neutrophils
CXCL9 (3-103)	CD26	↓activity
CXCL10 (3–77)	**CD26**	**↓activity; CXCR3 antagonist**
CXCL11 (3-73)	CD26	↓activity; CXCR3 antagonist
CXCL11 (3-73) (5-73) (7-73)	CD13	↓activity for lymphocytes and $CXCR3^+$ cells; antagonistic effects
CXCL12 (3–68)	CD26	↓activity; CXCR4 antagonist
CXCL12 (4-67)	Elastase	No activity
CXCL12 (5–67)	MMP1,3, 9,13,14	No activity
CXCL12 (5–67)	MMP2	CXCR3-mediated neurotoxicity
CXCL12 (6-67)	Cathepsin G	No activity

Adapted from (Van Damme *et al.*, 2004), © (2004), and (Wolf *et al.*, 2008) © (2008), with permission from Elsevier.

Table 2.3 C-terminal and core processing of chemokines by proteases and effects on activity

CHEMOKINE ISOFORM *	PROTEASE(S) INVOLVED	EFFECT ON ACTIVITY AND RECEPTOR AFFINITY
CCL20 (1-19)	Cathepsin D	No information
CCL20 (1-52) (1-55)	Cathepsin D	No activity
CCL20 (59-70)	Cathepsin D	Antimicrobial activity
CCL20 (1-66)	Cathepsin B	No change
CCL21 (1-58) (59-111)	Cathepsin D	No activity
CXCL9 (1-90) (1-93) (1-94)	MMP9	No information
CXCL10 (1-68)	**MMP9**	**No information**
CXCL10 (1-71) (1-73)	**MMP8**	**No information**
Met-CXCL10 (1-76)	Furin	No change
CXCL12 (1–67) (NB Intact was 1-68)	Carboxypeptidase N	↓activity

Adapted from (Wolf *et al.*, 2008) © (2008), with permission from Elsevier.

Reports of C-terminal and core truncations of chemokines following interactions with enzymes are shown. Several different proteases, including MMPs, but not CD26, are able to cleave chemokines at the C-terminus, although the numbers of known interactions are markedly fewer than at the N-terminus. Little is known about the effects of C-terminal processing on chemokine activity. Processing in the core region can also occur, as illustrated by processing of CCL20 by cathepsin D, resulting in inactivation (Wolf et al., 2008). Chemokines investigated in this current study are highlighted in bold.

** Amino acids remaining after processing detailed in brackets*

Using chemically synthesised analogues, truncation beyond the leucine of CXCL8 was found to cause a tenfold reduction in binding to, and activation of, PBMCs (Clark-Lewis *et al.*, 1991). This could be explained by a role of leucine in maintenance of the α-helical structure, without which, CXC chemokine structure might be disturbed. The C-terminal α-helix is thought to be involved in the dimeric structure of CXCL8, a chemokine which attracts monocytes and neutrophils. Serum levels and secretion from PBMCs of CXCL8 are elevated in MS, and are reduced following IFN-β1a treatment (Lund *et al.*, 2004). The bacteria *Streptococcus pyogenes* secretes an enzyme that has been shown to cleave CXCL8 within the α-helix of the C-terminus, resulting in reduced neutrophil migration (Edwards *et al.*, 2005). This reduced activity is explained by impairment in interactions of the C-terminus with GAGs, which usually help to anchor CXCL8 to the EC surface, where it assists with neutrophil slowing, prior to transmigration (Middleton *et al.*, 1997). GAG binding of the C-terminus of a chemokine mediates angiostatic activities that appear to operate independently of chemokine tertiary structure (Van Damme *et al.*, 2004).

The three-dimensional arrangement of the C-terminal residues affects their susceptibility to proteolytic attack. Dimeric CXCL7, for example, has terminal residues that form mobile 'fraying ends' as opposed to helical structures, thereby representing easy targets for proteolysis (Ehlert *et al.*, 1998). Analyses of C-terminal truncation of CXCL7 have indicated that changes in activity accompanying cleavage, are linked more to the nature of the missing residues than the number of them. By performing an increasing number of deletions from the C-terminus, Ehlert and colleagues (1998) showed that a CXCL7 isoform lacking 4 residues showed a three-fold increase in activity above the full-size form, and removal of 5, 6 or 7 amino acids yielded versions all with approximate five-fold potency above the intact form. These results supported the conclusion that negatively charged C-terminal residues are vital for the neutrophil-stimulating activity of CXCL7, but loss of uncharged residues has little effect (Ehlert *et al.*, 1998).

Interestingly, studies on CXCL8 have also shown an increase in activity when acidic residues were removed from the C-terminus, and a decrease in activity if basic residues are lost (Clark-Lewis *et al.*, 1991). The charge distribution of residues at the C-terminus of CXC chemokines may well be involved in receptor binding, with clusters of acidic residues (as seen on the N-terminus of CXCR1 and CXCR2), interacting with groups of basic residues (as found on C-terminal helices of CXC chemokines with an ELR motif) (Baggiolini *et al.*, 1994). If the cluster of basic residues found on the C-terminus of CXCL7 is broken up by acidic residues, the full force of receptor binding

may not be seen, accounting for the increased potency observed with the loss of some C-terminal residues. C-terminal truncation can lead to changes in activity of chemokines by preventing binding to their receptors, as is thought to be the case if C-terminal basic residues are removed from CXCL10 (Campanella *et al.*, 2003).

MMP8 has been shown to process the C-terminus of CXCL10, by cleaving it at positions 71 and 73, but the effects on activity are unknown. Similarly, MMP9 has been reported to degrade CXCL10, and process CXCL9 at 3 sites in the carboxyterminal region, and was considered more effective than MMP8 at degrading these chemokines (Van den Steen *et al.*, 2003). C-terminally truncated CXCL9 exhibited a 30-fold decrease in its biological activity, possibly due to loss of the immobilised chemokine gradient formation due to a failure of the highly basic C-terminus to interact with ECM GAGs (Clark-Lewis *et al.*, 2003).

2.2 Aims and objectives

The chemokines CCL2 and CXCL10 were selected for analysis because several studies have pointed to their involvement in the pathogenesis of MS (Mahad et al., 2002; Simpson et al., 1998 and 2000b; Moreira *et al.*, 2006). MMP2 was investigated as it is implicated in MS, with elevated levels marking the chronic stages of the disease. Activated T cells express MMP9 (Rosenberg, 2005), and increased serum and CSF levels of MMP9 are associated with RRMS (see 1.4.6) (Avolio *et al.*, 2003). Changes in the expression of CD26 on T cells are thought to correlate with disease activity in MS (Selleberg *et al.*, 2005), and this molecule is known to cleave several chemokines (see 1.5.4) (Ludwig *et al.*, 2002). Gathering data from *in vitro* investigations may help to identify possible isoforms of CCL2 and CXCL10 that could be generated *in vivo* in MS, as it is highly likely that these chemokines are exposed to MMP2, MMP9, and CD26 during the pathogenesis of the disease. Thus, the aims of the work in this chapter were to:

- Assess the *in vitro* cleavage of CCL2 and CXCL10 by MMP2, MMP9, and CD26, using gel electrophoresis and mass spectrometry
- Provide a chemokine/protease digestion sample that can subsequently be processed for use in migration experiments (see Chapter 5)

2.3 Materials and Methods

All chemicals used throughout were obtained from Sigma (Dorset, UK). Pipettes used were manufactured by Gilson and obtained from Anachem (Luton, UK). Experiments were repeated at least 3 times, unless otherwise stated.

2.3.1 *In vitro* digestion of recombinant chemokines

To assess the proteolytic effects of MMP2, MMP9, and CD26 on CCL2 and CXCL10, chemokines were incubated *in vitro* with enzymes in appropriate buffers. Samples were taken at various time points (Table 2.4) for analysis by gel electrophoresis (see 2.3.2) and mass spectrometry (MSpec) (see 2.3.4), to identify any cleavage products present, and for use in migration experiments in Chapter 5.

CCL2 and CXCL10 recombinant proteins (from *E.coli*) were obtained from Peprotech EC (London, UK). Human CCL2 was an 8.6 kDa protein containing 76 amino acids, and human CXCL10 was an 8.5 kDa protein consisting of 77 amino acids.

MMP2, MMP9 and CD26 recombinant proteins were obtained from R&D Systems (Abingdon, UK). MMP2 originated from a DNA sequence encoding the human pro-MMP2 enzyme (EC 3.4.24.24) (~71 kDa) expressed in Chinese Hamster ovary (CHO) cells, MMP9 from a DNA sequence encoding the human MMP9 enzyme (EC 3.4.24.35) (~77 kDa) expressed in CHO cells, and CD26 from a construct of human CD33 Signal Peptide (Met 1 - Ala 16) + mature human DPPIV/CD26 (Asn 29 - Pro 766, expressed with a C-terminal His tag in a mouse myeloma cell line, NS0) (EC 3.4.14.5) (~115 kDa).

2.3.1.1 Reconstitution of chemokines and enzymes

Recombinant chemokines CCL2 (20µg) and CXCL10 (25µg) were reconstituted from lyophilised stock in 200µl and 250µl ultrapure water, respectively, giving final concentrations of 100µg/ml (~11.6µM of CCL2 and ~11.7µM CXCL10). The recombinant enzyme MMP2 was provided in a liquid form and was diluted with TCN buffer (50mM Tris-HCl, 10mM $CaCl_2$, 150mM NaCl, pH 7.5) to give a final concentration of 100µg/ml (~1.4µM). Recombinant MMP9 was supplied lyophilised, and was reconstituted in 100µl TCN buffer to yield 100µg/ml (~1.3µM). Recombinant CD26 was supplied at a concentration of 0.5mg/ml in a filtered solution of 25mM 2-(*N*-morpholino) ethanesulfonic acid (MES), 0.7 M NaCl, pH 4.9, and was further diluted with 25mM Tris base, pH 8 to give a final concentration of 100µg/ml (0.87µM).

2.3.1.2 Activation of MMPs using aminophenyl mercuric acetate (APMA)

APMA is an organomercurial compound that activates MMPs by catalysing removal of the pro-domain, thereby allowing the substrate to access the catalytic site, necessary for enzymatic activity (Von Bredow *et al.*, 1998). Recombinant MMPs were activated by incubation with 1mM APMA in assay buffer (100mM Tris-HCl, 100mM NaCl, 10mM $CaCl_2$, 0.01% Tween® 20), for 1h with MMP2, and 2h with MMP9, at 37˚C. A 10mM solution of APMA was made by dissolving 0.0176g APMA in 3ml dH_2O with 1 drop of 6M NaOH. This was vortexed, and 1M HCl added until the solution just turned cloudy, then 0.1M NaOH was added until the solution was clear again. The volume was made up to 5ml with dH_2O, the pH was adjusted to 10-11, and the solution used immediately or stored for up to 48h at 4˚C.

2.3.1.3 Co-incubation of chemokines with enzymes

Each chemokine was incubated seperately with each enzyme in Eppendorf tubes for up to 72h at 37°C. Samples (2 x 5µl) were taken from each of these 6 different mixtures, at various time points, from the total volume of 10-130µl for each tube (see Table 2.4), for analysis by gel electrophoresis and MSpec. Final concentrations of 0.4µM MMP2 and 9 were each incubated with 4µM each of CCL2 and CXCL10 in assay buffer, giving an enzyme to substrate ratio of 1:10. This ratio was adopted from a published method (Van den Steen *et al.*, 2003).

To establish a suitable concentration of CD26, final concentrations of 0.04, 0.2, and 0.4µM CD26 were tested in preliminary experiments, combined with 4µM of CCL2 and CXCL10 separately in 25mM Tris base. Data from exploratory experiments indicated that 0.04µM gave identical results to 0.2µM (data not shown), so the lowest concentration of 0.04µM was used, giving an enzyme to substrate ratio of 1:100.

The time course for each incubation mixture was determined using information from a published method (Van den Steen *et al.*, 2003), together with preliminary experiments using MSpec analysis of samples after 3, 6 and 24h for all chemokine:protease incubation mixtures (data not shown).

2.3.1.4 Control samples for chemokine digestion experiment

It is possible that the chemokines or enzymes could degrade, irrespective of enzymatic activity, when kept in solution at 37°C. To control for this, all chemokines and enzymes were incubated separately in the appropriate assay buffer. MMPs were activated using APMA, which was not subsequently removed, so this was included in the control

chemokine and MMP solutions to account for any degradative effects it may have on the recombinant proteins. To show that cleavage products resulted from proteolytic actions of the enzyme on the chemokine, the enzymes were first inactivated before being incubated with chemokines. MMPs were found to resist heat-inactivation (data not shown) and thus were inhibited by addition of a final concentration of 20mM ethylenediaminetetraacetic acid (EDTA). CD26 was heat-inactivated (HI) by heating to 95°C for 5min. Samples were taken from these controls at the timepoints detailed in Table 2.4, for analysis by gel electrophoresis and Mspec.

2.3.1.5 Stopping the proteolytic reaction following sample collection

Samples taken at various time points for analysis by gel electrophoresis had the proteolytic reaction stopped by conducting the sample preparation procedure used for gel electrophoresis. This entailed adding 2.5µl NuPAGE® lithium dodecyl sulfate (LDS) sample buffer (Invitrogen, Paisley, UK), 1µl NuPAGE® reducing agent (Invitrogen), and 1.5µl dH_2O to 5µl of sample, and heating at 70°C for 10min. Samples destined for MSpec analysis were mixed with an equal volume of sample preparation solution (0.5% trifluoroacetic acid (TFA) in dH_20) to stop the reaction. All samples were then stored at -80°C before gel electrophoresis or MSpec analysis were performed.

2.3.1.6 Preparation of digested chemokine samples for use in migration assays

Endpoint samples (6-72h, depending on the chemokine and protease involved) of each chemokine with each enzyme, and of CCL2 and CXCL10 incubated with APMA and assay buffer alone, were collected for use in migration assays (Chapter 5). These samples were passed through Microcon® YM50 centrifugal filter units (Millipore, UK) as soon as the digestion was completed. This procedure removed the enzyme, thereby leaving the separated chemokine, for use in migration assays, and is described in full in 5.3.8.1. To ensure that the Microcon® ultrafiltration had not removed chemokine cleavage products in addition to the enzyme, samples passed through were also examined by gel electrophoresis.

2.3.2 Sodium dodecyl sulphate-polyacrylamide gel electrophoresis (SDS-PAGE)

2.3.2.1 Principles of SDS-PAGE

SDS-PAGE separates proteins by electrophoresis, using sodium dodecyl sulphate (SDS) to denature the proteins, and polyacrylamide gel as a support and separation medium.

Table 2.4 Chemokine/protease and control samples taken during digestion investigations

TIME (H) / SAMPLE	0	0.5	3	6	24	48	72	TOTAL VOLUME µL
*MMP2 + CCL2			✓	✓				120
EDTA + MMP2 + CCL2				✓				10
*MMP9 + CCL2			✓	✓				120
EDTA + MMP9 + CCL2				✓				10
*CD26 + CCL2		✓	✓	✓				130
HI CD26 + CCL2				✓				10
*CCL2 + APMA + buffer	✓			✓				120
*MMP2 + CXCL10					✓	✓	✓	130
EDTA + MMP2 + CXCL10					✓			10
*MMP9 + CXCL10					✓	✓	✓	130
EDTA + MMP9 + CXCL10						✓		10
*CD26 + CXCL10		✓	✓	✓				130
HI CD26 + CXCL10				✓				10
*CXCL10 + APMA + buffer	✓					✓		120
MMP2 + APMA + buffer	✓					✓		20
MMP9 + APMA + buffer	✓					✓		20
CD26 + buffer	✓			✓				20

Samples were taken at the time points indicated and processed for mass spectrometry, gel electrophoresis, or migration assays accordingly. Final concentrations were as follows: CCL2/CXCL10 = 4µM; MMPs = 0.4µM; CD26 = 0.04µM

HI = heat-inactivated; EDTA = ethylenediaminetetraacetic acid

**Indicates endpoint samples were collected for use in migration assays in Chapter 5*

As SDS is an anionic detergent, it possesses a net negative charge within a wide pH range, which virtually destroys the complex tertiary structure of proteins that would otherwise have affected their migration through a gel matrix. Polypeptides bind to SDS in a manner proportional to their molecular mass, with approximately 1g of protein binding to 1.4g of SDS, resulting in proteins that possess an almost identical charge to mass ratio. SDS imparts a large negative charge to the linearised proteins, making them strongly attracted to an anode in an electric field, where their separation in the gel depends solely on differences in their mass (Schagger and Von Jagow, 1987).

Most protein samples are denatured further by the use of a reducing agent, such as beta-mercaptoethanol or dithiothreitol (DTT), and heat. This reduces disulphide bridges involved in tertiary structure, and breaks up oligomeric subunits related to quaternary structure. To determine the accurate molecular weight of a protein in a gel, the sample should be denatured. Non-reducing SDS-PAGE omits the use of these agents and facilitates further investigations where structure is important (Laemmli, 1970).

The polymer of acrylamide monomers that the gel is composed of forms a meshwork of pores of different diameters, dependent upon the percentage of acrylamide present, which allows the movement of different sized proteins at different rates. Large proteins encounter more resistance than smaller ones, and remain closer to the loading well. The smaller, uppermost 'stacking' portion of the gel, with a lower percentage of acrylamide, allows compression of proteins into thin layers before they enter the lower resolving gel, which separates the proteins by size. A tracking dye is normally added to the samples so that progression of proteins through the gel can be visualised. Separated proteins are seen as distinct bands once the gel has been stained with either Coomassie Brilliant Blue, or silver stain (Sorensen *et al.*, 2002a; Rabilloud et al., 1994).

The buffer used during electrophoresis allows an ion gradient to form during the initial 'stacking' of the proteins in the gel region with larger pores, thereby focussing the proteins into sharp bands. As electrophoresis continues, the ion gradient is removed so that proteins are then separated by their size, and thus weight, in the resolving gel. To enable determination of the weight of unknown proteins, the distance they travel is compared relative to a marker consisting of proteins of known molecular weights, by using a graph of the relative migration distance against the logarithm of the relative molecular mass (M_r) of the standards (Laemmli, 1970).

Precast NuPAGE® bis(2-hydroxyethyl)iminotris(hydroxymethyl)methane (Bis-Tris) gels (invitrogen, UK) were used in this project, and do not contain SDS, but were designed

for denaturing electrophoresis. They utilised Bis-Tris chloride as the gel buffer at neutral pH, and 50mM MES with 50mM Tris at pH 7.2, as the running buffer. This meant that during electrophoresis, MES, instead of the more conventional glycine, was the ion running behind chloride towards the anode, and Tris in the tank buffer, migrated to displace the Bis-Tris that moved towards the cathode (Hachmann and Amshey, 2005). Maintenance of approximately neutral conditions using this system reduced the reactivity of amino acid side chains during electrophoresis, thereby minimising protein modifications and making Bis-Tris gels a good choice for subsequent MSpec applications that require protein integrity (Haebel *et al.*, 1998).

2.3.2.2 Pre-cast gels

All equipment and reagents used with pre-cast gels were from Invitrogen (Paisley, UK). Pre-cast, 1 mm thick, 12-well, 12% Bis-Tris gels were found to give the best results for resolution of chemokines. These were used in an XCell SureLock™ Mini-Cell II tank apparatus, with MES running buffer. NuPAGE® running buffer (20X) was diluted to 1X with dH_2O, and 500µl of NuPAGE® antioxidant was added to the 200ml running buffer destined for the central chamber, comprising the electrode encased by the gel(s). Running buffer without antioxidant was added to the outer region of the tank until it was two-thirds full. Samples (10µl), prepared as described in 2.3.1.5, were pipetted into the wells of the gel, which was run at a constant 200 volts for ~ 1h. Once the dye front had almost reached the bottom, gels were removed from their plastic cassettes.

2.3.3 Silver staining of gels

2.3.3.1 Principles of silver staining

Silver staining is a highly sensitive technique, due to the autocatalytic nature of the reduction of silver ions, capable of detecting nanogram quantities of protein, in either histological sections or gels. Silver ions from the staining solution bind to protein, where they are later reduced to metallic silver by the developing solution, and appear as black deposits. Typically, either silver nitrate is used in silver stains together with formaldehyde, in an alkaline carbonate solution as the developer, or a silver-ammonia complex is developed by formaldehyde in dilute citric acid (Rabilloud *et al.*, 1994).

In order to have the option of subsequent analysis by mass spectrometry of silver-stained bands of interest in a gel, a modified silver-staining kit was used. Sensitising solution is normally aldehyde-based, but the one used in this method did not contain glutaraldehyde or formaldehyde, which would otherwise modify lysine residues and prevent complete digestion of the band by trypsin (Matsumura *et al.*, 1999). Trypsin is used in MSpec analysis to generate peptide fragments of a protein band within the gel.

The fragments can then have their masses determined by matrix assisted laser desorption ionisation (MALDI) MSpec and the protein identified using database searches (Hurkman and Tanaka, 2007).

The silver staining process used in this method involved fixation to remove interfering ions and detergent, and to immobilise the proteins in the gel matrix. A sensitising step followed, designed to increase the contrast of the stain. The ensuing staining step bound silver ions to the protein, before they were reduced to metallic silver by the developer. The reduction reaction was stopped when the desired staining intensity was reached, by addition of a further solution, which formed complexes with any free silver ions. Appropriate alcohol or water washes were used after each step to remove the previous solution.

Silver staining was used instead of Coomassie blue, as it is up to 100-fold more sensitive (Budowle, 1984), which would assist with detection of low levels of protein, such as minor cleavage products.

2.3.3.2 Silver staining technique

Following a brief rinse in ultrapure H_2O after SDS-PAGE (see 2.3.2.2), gels were stained using reagents from a SilverQuest™ kit (Invitrogen), following the manufacturer's recommended protocol. Ultrapure water (>18 megohm/cm resistance) was used throughout the staining procedure, each step was performed on an orbital shaker at 50rpm, and the volume of solutions used per gel at each stage was 100ml. Gels were immersed in 100ml fixative (10% v/v glacial acetic acid, 40% v/v ethanol, in water) for at least 20min. Following fixation, gels were washed in 30% ethanol for 10min, before being placed in sensitising solution (30% ethanol, and10% sensitiser [10-30% w/v MES and 7-13% w/v N,N-dimethylformamide] in water) for 10min. A 10min wash in water preceded 15min incubation in staining solution (1% stainer [10-30% w/v silver nitrate] in water). Gels were then rinsed for 20-60 seconds in water, and left in developing solution (10% developer [15% w/v carbonic acid, dipotassium salt], 1 drop developer enhancer [30-60% w/v formaldehyde], in water) for 4-8min until the required band intensity was reached, when 10ml of stopper (10-30% w/v Tris base, 10-30% EDTA) was added directly to the gel and left to shake for a further 10min. Finally, gels were rinsed with water, scanned using an Epson flatbed scanner, and images obtained using Corel Photo Paint 8 software.

2.3.3.3 Calculating the relative molecular mass of samples in silver-stained gels

A graph was plotted of the log of the M_r of the bands from the molecular weight standard, against the the relative distance (%) travelled by each band, compared to the total distance run by the gel, using the dye front distance. The equation of the trendline was rearranged to allow the approximate M_r of the unknown bands to be calculated, based on their relative distance travelled.

2.3.4 Mass Spectrometry

Mass spectrometry is used to measure the molecular mass of a sample to within approximately 0.01-0.2% of the total mass, which enables detection of minor mass changes such as post-translational modifications or amino acid substitutions. Potentially, sub-picomole levels of a sample with a M_r of up to 300 kDa can be used. Apart from M_r measurement, mass spectrometers can be used for amino acid and/or oligonucleotide sequencing, to monitor reactions, such as protein digestion, and to provide information about protein structure (Karas *et al.*, 1990).

2.3.4.1 Principles of MALDI mass spectrometry

Matrix assisted laser desorption ionisation (MALDI) is a useful tool for analysis of non-volatile organic compounds of high M_r. It is reasonably tolerant, compared to other ionisation techniques, to the additives that are found in some samples, and offers a reliable and straightforward method of analysing proteins, peptides, glycoproteins, oligosaccharides, and oligonucleotides (Yan *et al.*, 2000).

A mass spectrometer has 3 main parts: the ionisation source, the analyser and the detector. Samples are mixed with an organic compound with strong absorption at the laser wavelength, i.e. a matrix solution, and spotted onto a stainless steel target plate numbered with 100 circles. The solvent evaporates and the matrix crystallises, and once in the mass spectrometer, the pulses of light from the laser irradiate the sample on the target. UV lasers are commonly used in MALDI, particularly nitrogen lasers with excitation at 337nm. The laser pulses excite the matrix molecules and energy is transferred to the sample within the matrix, and both sample and matrix desorb from the condensed state and enter the vapour phase. Proton transfer from the matrix to the sample can now occur, thereby resulting in ion formation (Fig. 2.1(i)). The transformation of laser energy to sample excitation energy is efficient and avoids the sample decomposition that could occur if it received excessive direct energy. A high potential is applied to accelerate the ions down a drift tube, which contains a vacuum to prevent any impediment to their journey. The ions are passed through a series of

extraction and focusing electrodes and lenses in the analyser region, where separation according to mass (m) -to-charge (z) ratios (m/z) occurs, before the ions are detected (Fig. 2.1 (ii)) (Schiller *et al.*, 2004).

MALDI is a soft ionisation technique that limits fragmentation and produces singly-charged ions, even with large proteins. This means mass analysers with high m/z capabilities are used in conjunction with MALDI, such as the time-of-flight (TOF) analyser. Other analysers are available, such as quadrupoles, with different m/z range coverage, accuracy, or resolution, but they all serve to separate the ions formed, according to m/z ratios (Schiller et al., 2004). The TOF mass analyser measures the time for ions to travel between the accelerator electrode and the detector, i.e. along the drift tube, and uses this data to determine the m/z value, with heavier particles taking longer to reach the detector.

The laser pulses produce discrete groups of ions intermittently, which facilitates measurement of the flight time. If a series of electrodes at different potentials, called a reflectron, is present, the energy spread of ions is more focused and the resolution of the TOF analyser increased (Fig. 2.1(ii)). Reflectrons are repelling devices that cause ions to change direction and accelerate back towards the detector. This effectively reduces the differences in kinetic energy distribution between ions, as higher energy ions will travel further into the reflectron and have a longer flight path, with an end result of all ions of a specific m/z arriving at the detector in a narrower time span. If a pulsed orthogonal beam pusher is incorporated into the instrument, ions are introduced into the analyser in focused groups perpendicular to their flight path (Ens and Standing, 2005).

Tandem (MS-MS) mass spectrometers have more than one analyser and are useful in acquiring structural and sequence data. If the analysers are of different types, the instrument is classed as a hybrid mass spectrometer, such as the quadrupole-time-of-flight version (Ens and Standing, 2005).

MALDI can be used in either positive or negative ion mode, depending on whether the sample either gains or loses a proton respectively, i.e. $(M+H)^+$ or $(M-H)^-$, where M represents the molecular ion. Positive mode is generally used for protein and peptide analysis, and negative mode for oligonucleotides and oligosaccharides. In positive mode, other species commonly identified are $(M+NH_4)^+$ and salt adducts such as $(M+Na)^+$. Traces of doubly charged molecular ions at half the m/z value, or dimers at twice the m/z value, can sometimes be identified (Schiller *et al.*, 2004).

Figure 2.1 Schematic diagrams illustrating the main processes involved in MALDI-TOF mass spectrometry and a TOF mass spectrometer

(i) Prior to MALDI MSpec analysis, samples are mixed with matrix and spotted onto a target plate. When dry, the matrix crystallises and forms co-crystals with the sample. In the mass spectrometer, an electrical field is applied, and a pulsed laser fired onto the sample. Desorption occurs as the matrix absorbs the laser energy, causing rapid heating and subsequent sublimation of matrix molecules. Matrix and analyte clusters expand into the vapour phase, and are ejected from the target surface. Excited matrix molecules are stabilised by proton transfer to the analyte, and cation attachment to the analyte occurs, such as addition of H^+, Na^+, or K^+. The matrix evaporates away to leave free analyte ions.

(ii) Singly charged ions generated from the desorption-ionisation process pass through a charged grid, and are accelerated into the TOF drift tube, which is under a high vacuum. The length of this tube is typically 0.5-3 m long and determines the possible mass resolution. To improve resolution, a reflector can be incorporated to reflect ions at the end of the flight tube to reach a "reflector-detector", thereby lengthening the field-free path travelled. Low mass ions reach the end of the flight tube in a shorter time than high mass ions, and as they are equally charged, separation based on mass is achieved. A detector at the end of the tube produces a signal upon impact of each ion, and m/z spectra are produced from this signal as a function of time.

$[M+H]^+$ = Ion formed by interaction of a molecule with a proton; TOF = time-of-flight

(i) The ionisation process

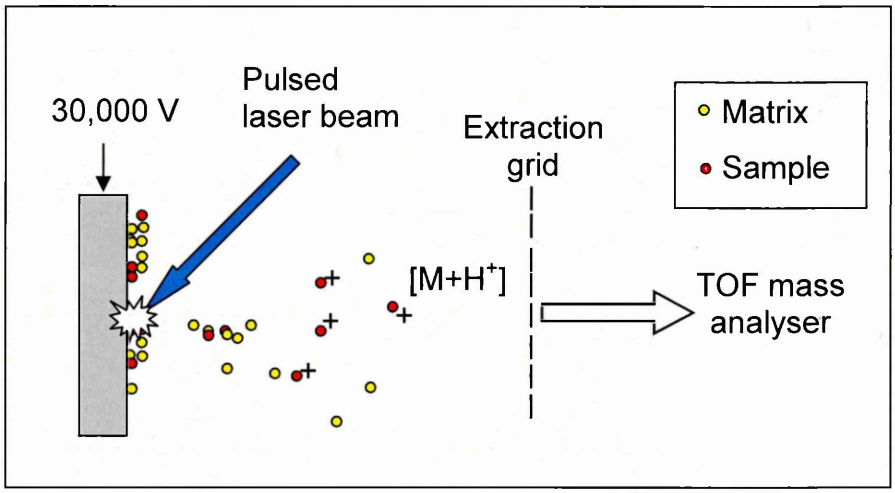

(ii) TOF mass spectrometer

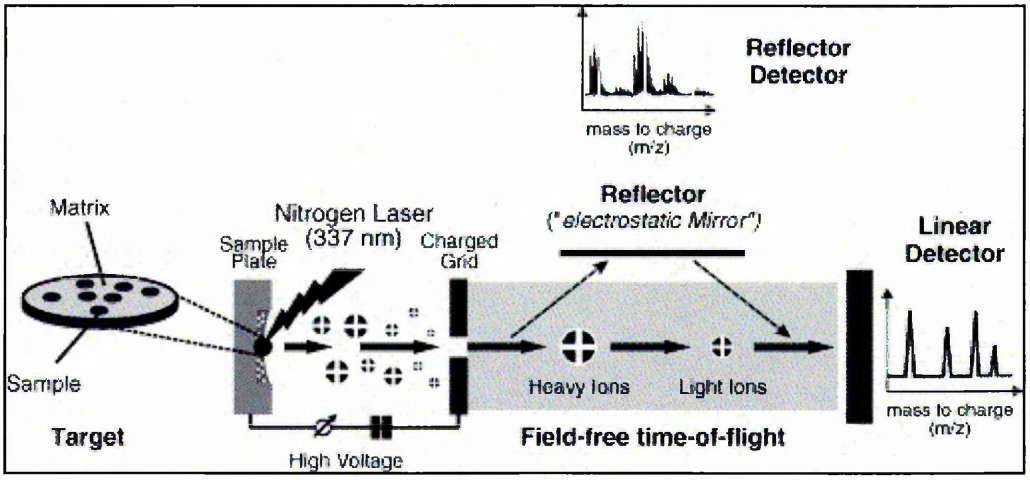

Reprinted from (Schiller et al., 2004), © (2004), with permission from Elsevier.

In positive ion operation, ionisation of the sample is often assisted by the inclusion of 0.1% trifluoroacetic acid (TFA) in the matrix, but this is not used in negative ion MALDI, where it suppresses the formation of sample ions (Schiller *et al.*, 2004).

The detector must suit the type of analyser used in the instrument, and is commonly of a photomultiplier, electron multiplier, or micro-channel type. The ion current is monitored by the detector, which also amplifies it and transmits signals to the data system, which records it as mass spectra. The m/z values are plotted against their intensities, and the resulting spectra show the molecular mass of the sample components and their relative abundance (Barnes and Hieftje, 2004).

2.3.4.2 Matrix requirements for MALDI mass spectrometry

The matrix used in MALDI MSpec has a significant impact on the results obtained and must be selected according to the sample being analysed. Matrices consist of small organic compounds, which absorb the laser energy strongly at the applied wavelength, and separate the analyte molecules, to avoid cluster formation. MALDI preparations should ideally have a low concentration of analyte molecules and an excess of matrix on the target plate, which helps to prevent fragmentation of the analyte. Typically, a sample concentration of 10pmol/µl is mixed with an equal volume of matrix of around 10 mg/ml, but these concentrations can vary depending on the samples being analysed. Small volumes (0.5 – 2µl) of the analyte/matrix mix are used for spotting onto the target plate (Groos and Strupat, 1998). Table 2.5 summarises different matrices and the sample types they are commonly used for. Most importantly, a matrix should be selected that has good absorption properties with the laser used, and that mixes well with the analyte to give homogeneous co-crystalisation (Schiller *et al.*, 2004).

2.3.5 Analysis by mass spectrometry of chemokine/enzyme incubation samples

2.3.5.1 Choice and application of matrix

Both α-CHCA and sinapinic acid (20mg/ml, 50% v/v acetonitrile, 0.1% v/v TFA) were assessed with recombinant chemokine samples to determine which gave the greatest sensitivity. A stock solution of α-CHCA was prepared (25mg/ml, 0.1% v/v TFA, in methanol) and due to low solubility, it was sonicated for 5min in a Branson 1210 sonicator bath (Branson Power Company, USA) to increase dissolution. When Zip Tips® were used (see 2.3.5.2), the final concentration of α-CHCA was 12.5mg/ml, as the matrix solution was mixed with an equal volume of acetonitrile (ACN) + 0.1% TFA, for elution of the sample.

Table 2.5 Matrices used in MALDI-TOF mass spectrometry

MATRIX	SAMPLE
α-cyano-4-hydroxycinnamic acid (α-CHCA)	Peptides, proteins
3,5-dimethoxy-4-hydroxycinnamic acid (sinapinic acid)	Proteins
2,5-dihydroxybenzoic acid (DHB)	Sugars, nucleotides, peptides
Hydroxypicolinic acid (HPA)	Oligonucleotides, glycopeptides
Dithranol	Synthetic polymers, large organics, lipids

Several matrix compounds used in MALDI-TOF mass spectrometry are shown, together with the sample type they are most commonly used for. Proteins with a mass of less than 10 kDa are often used with α-CHCA, whilst sinapinic acid is better suited to proteins larger than 10 kDa. DHB is a useful matrix when the samples are polar. HPA is frequently used with oligonucleotides, with masses greater than 3.5 kDa (Schiller et al., 2004).

Preliminary experiments were performed to investigate the most effective method of sample addition to the target plate, matrix alone was spotted and allowed to dry, before the sample was spotted on to the top of this, or the sample was pre-mixed with matrix and applied in a one-step method).

2.3.5.2 Use of Zip Tips® in sample preparation for analysis by MSpec

Mass spectrometry is often complicated by the presence of salts and contaminants in the sample, which can obscure the protein of interest, particularly when it is present at low concentrations (Monroe *et al.*, 2007). To concentrate and purify samples for optimal results with MALDI-quadrupole/TOF (MALDI-QTOF) analysis, Zip Tips® (Millipore) were used prior to spotting samples onto the target plate. Zip Tips® are 10µl pipette tips that contain chromatography media. Various resins are available for different applications, and for concentrating small proteins such as chemokines, Zip Tips® with 0.6µl of a C_{18} resin were used, composed of 15µm silica with 20nm pores.

Chemokine/protease digestion samples were analysed by MALDI-QTOF both with, and without, the use of Zip Tips® in the sample preparation stage. It was expected that Zip Tips® should desalt and concentrate the samples, but it was necessary to eliminate the possibility that artefacts could result from their use. Preliminary experiments were thus conducted where samples were compared after being mixed with matrix and spotted onto the target plate, or first passed through a Zip Tip® according to the following protocol, which is hereafter called "zip tipping".

The chemokine/protein digest sample was first mixed with an equal volume (5µl) of sample preparation solution (see 2.3.1.5). The Zip Tip® was wetted twice with 10µl acetonitrile (ACN), which was then expelled before two equilibration steps involving slow uptake and expulsion of 10µl equilibration/wash solution (0.1% TFA in dH_20). The digest sample was cycled slowly through the Zip Tip® 7 – 10 times in an Eppendorf tube, and finally expelled. Three x 10µl of wash solution (0.1% TFA in dH_20) were then drawn up and ejected, before 2µl of elution solution (0.1% v/v TFA, 50% v/v ACN, 50% v/v methanol,12.5mg/ml α-CHCA) was aspirated and cycled 3 – 4 times into a clean Eppendorf tube before being spotted directly onto the target plate.

2.3.5.3 MALDI-QTOF of cleavage products

Preliminary data supported the use of Zip Tips® in preparation for MSpec, and this was performed as detailed above in 2.3.5.2. Samples were analysed using an Applied Biosystems/MDS Sciex API "Q-Star" Pulsar i hybrid quadrupole time-of-flight mass

spectrometer. This was fitted with an orthogonal MALDI ion source, and an neodymium-doped yttrium aluminium garnet (Nd:YAG) laser, which was used at an energy of 20-30%, and a repetition rate of 500Hz – 1kHz. The instrument was governed by "o-MALDI Server 4.0" software, and was used in positive ionisation mode. Analysis was performed for 5min for each sample. Mass spectra showing m/z values, with their intensity, were acquired using Analyst QS software (Applied Biosystems, Warrington, UK).

2.3.5.4 Interpretation of mass spectra

The m/z value for intact CCL2 and CXCL10 was obtained by MSpec analysis of the recombinant proteins. Peaks obtained after digestion were then compared to this value, and differences in the m/z values matched to losses of amino acids, based on the known average masses of the residues, and the sequence supplied by the manufacturer of the chemokines (Peprotech EC).

2.4 Results

2.4.1 Gel electrophoresis of CCL2 incubated with MMP2 or MMP9

A downward shift of bands from all samples involving incubation of CCL2 with either MMP2 or MMP9 for 3-6h (Fig. 2.2) was detected, compared to intact CCL2 (where the MMPs were inhibited with EDTA). Bands seen after 3h incubations of CCL2 with MMPs 2 and 9, appeared at a slightly higher position and were blurred, compared to bands involving 6h exposure to enzyme, suggesting digestion was still ongoing. The approximate M_r of intact CCL2 was calculated to be 7.7 kDa, 3h incubation with MMP2 reduced this by ~0.2 kDa to ~7.5 kDa, and at 6h, a total loss of ~0.5 kDa reduced it to ~7.2 kDa. MMP9 reduced the mass of CCL2 even further overall, yielding ~7.3 kDa at 3h (a loss of ~0.4 kDa), and ~7.1 kDa at 6h (a total loss of ~0.6 kDa). Controls of CCL2 and MMP2 incubated separately in buffer indicated that no spontaneous breakdown of either CCL2 or MMP2 occurred. Inhibition of MMPs 2 and 9 with EDTA prevented the shift in bands of CCL2 to a lower M_r, leaving it unprocessed (Fig. 2.2).

2.4.2 Gel electrophoresis of CXCL10 incubated with MMP2 or MMP9

All samples involving incubation of CXCL10 with either MMP2 or MMP9 for 24-48h resulted in multiple bands being observed, compared to intact CXCL10 (where the MMPs were inhibited with EDTA) (Fig. 2.3). Where multiple bands occurred, the uppermost band corresponded to the band for intact CXCL10. The upper two bands at 24h incubations of CXCL10 with MMPs 2 and 9, situated close to each other, were of a greater density than comparable upper bands from the 48h samples. The lower 2 bands, of lanes with multiple bands, were of a lower density than the upper 2 bands in all cases. When CXCL10 is incubated with MMP9 for 48h, it is still being processed after 24h, confirmed by the reduction in density of the uppermost band at 48h compared to 24h. The approximate M_r of intact CXCL10 was calculated to be 6.7 kDa, and 24-48h incubation with either MMP2 or MMP9 produced bands with M_r s of ~6.7, 6.1, 4.1 and 3.5 kDa, representing intact CXCL10, and losses of ~0.6, 2.6 and 3.2 kDa. Control samples of CXCL10 in buffer and MMP9 in buffer, did not produce any unexplained bands, and confirmed that the recombinant proteins did not auto-degrade during the incubation (Fig. 2.3).

2.4.3 Gel electrophoresis of CCL2 and CXCL10 incubated with CD26

A slight downward shift of bands from all samples involving incubation of CCL2 or CXCL10 with CD26 for 0.5-6h was detected, compared to the intact chemokines (where CD26 was heat-inactivated) (Fig. 2.4).

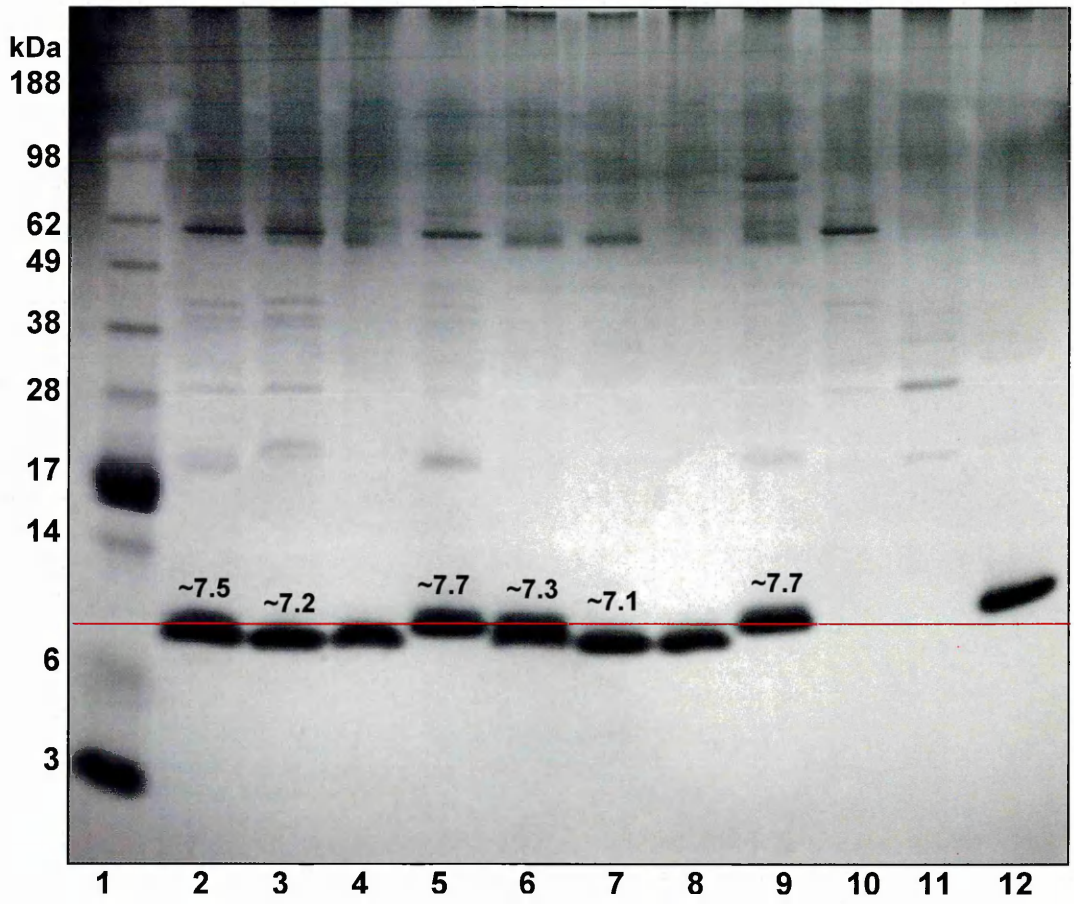

Figure 2.2 Chemokine cleavage: electrophoresis using Bis-Tris 12% silver-stained gel of CCL2 at 3 and 6h incubation with MMPs 2 or 9

CCL2 (4μM) was incubated with either MMP2 or MMP9 (0.4μM) in assay buffer (100mM Tris-HCl, 100mM NaCl, 10mM $CaCl_2$, 0.01% Tween® 20) for 6h at 37˚C. Samples were taken at 3 and 6h, and some were passed through YM50 Microcons® to remove the enzyme. LDS sample buffer and reducing agent were added to the samples, which were denatured by heating at 70˚C for 10min. SDS-PAGE was performed using MES running buffer, and the gel was silver-stained. Downward shifts of the bands in lanes 2, 3, 4, 6, 7, and 8, can be detected following cleavage of CCL2 by either MMP2 or MMP9.

Lanes shown above had 10μl of the following samples loaded:
***(1)** SeeBlue Plus 2 marker; **(2)** MMP2/CCL2 3h; **(3)** MMP2/CCL2 6h;*
***(4)** MMP2/CCL2 6h after passing through a YM50; **(5)** MMP2/EDTA/CCL2 6h;*
***(6)** MMP9/CCL2 3h; **(7)** MMP9/CCL2 6h; **(8)** MMP9/CCL2 6h after passing through a YM50; **(9)** MMP9/EDTA/CCL2 6h; **(10)** MMP2/APMA/buffer 0h;*
***(11)** MMP2/APMA/buffer 48h; **(12)** CCL2/buffer control 6h*

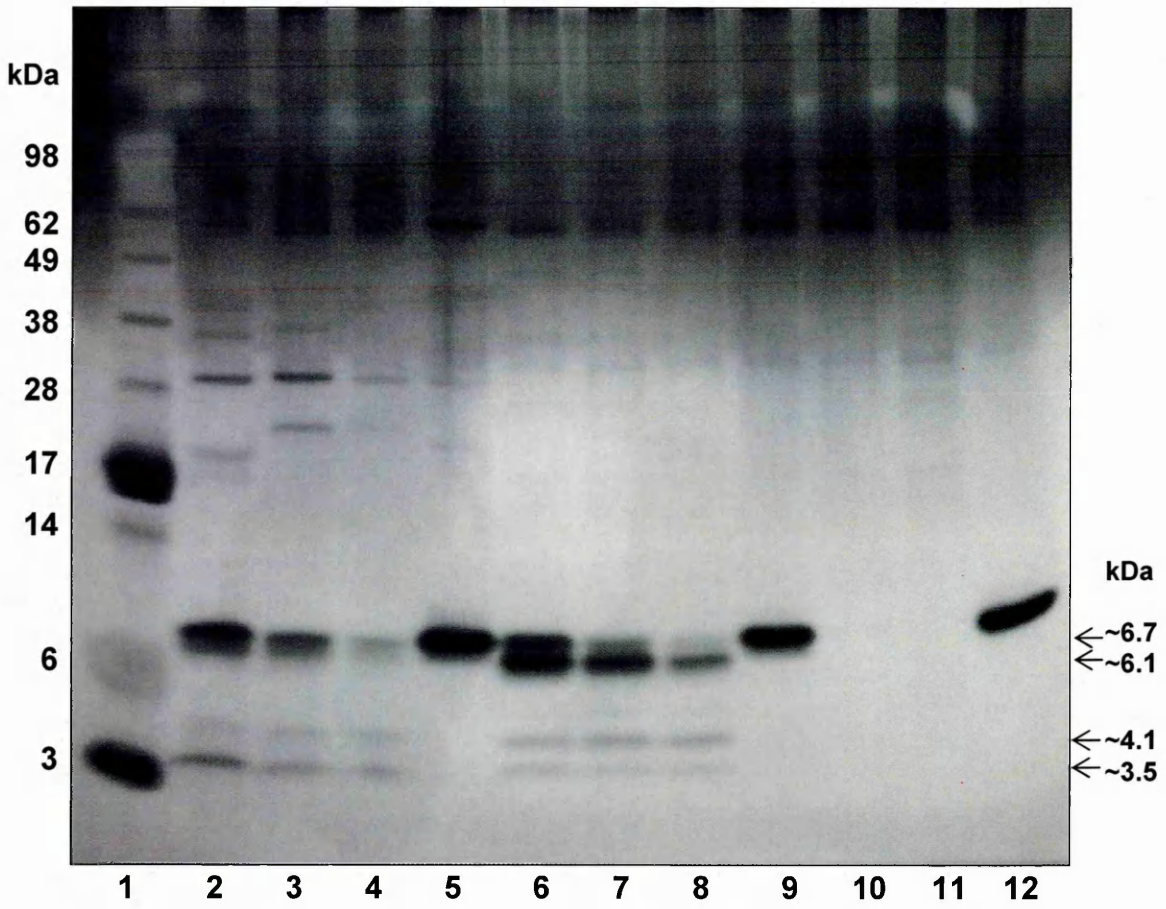

Figure 2.3 Chemokine cleavage: electrophoresis using Bis-Tris 12% silver-stained gel of CXCL10 at 24 and 48h incubation with MMPs 2 or 9

CXCL10 (4μM) was incubated with either MMP2 or MMP9 (0.4μM) in assay buffer (100mM Tris-HCl, 100mM NaCl, 10mM $CaCl_2$, 0.01% Tween® 20) for 72h at 37˚C. Samples were taken at 24 and 48h, and some passed through YM50 Microcons® to remove the enzyme. LDS sample buffer and reducing agent were added, and the samples denatured by heating at 70˚C for 10min. SDS-PAGE was performed using MES running buffer, and the gel was silver-stained. Multiple bands can be detected following cleavage of CXCL10 by both MMP2 and MMP9, but not in controls involving EDTA inhibition of MMPs.

Lanes shown above had 10μl of the following samples loaded:

***(1)** SeeBlue Plus 2 marker; **(2)** MMP2/CXCL10 24h; **(3)** MMP2/CXCL10 48h; **(4)** MMP2/CXCL10 48h after passing through a YM50; **(5)**MMP2/EDTA/CXCL10 24h; **(6)** MMP9/CXCL10 24h; **(7)** MMP9/CXCL10 48h; **(8)** MMP9/CXCL10 48h after passing through a YM50; **(9)** MMP9/EDTA/CXCL10 24h; **(10)** MMP9/APMA/buffer 0h; **(11)** MMP9/APMA/buffer 48h; **(12)** CXCL10/buffer control 48h*

After 30min incubations of CCL2 and CXCL10 with CD26, no further shift is seen with the corresponding bands where the time was extended to 6h. The approximate M_r for CCL2 was calculated to be 8.5 kDa, which was decreased by ~0.6 kDa to ~7.9 kDa, following 0.5-6h incubation with CD26. The approximate M_r for intact CXCL10 was calculated to be 7 kDa, which was reduced by ~0.2 kDa to ~6.8 kDa, following 0.5-6h incubation with CD26 (Fig. 2.4). Control samples of CD26 alone in buffer revealed that the enzyme did not degrade products during 6h incubation (data not shown).

2.4.4 Optimisation of MALDI-QTOF mass spectrometry for use in identification of chemokine cleavage products

The visual representation of chemokine cleavage products obtained with the use of silver-stained gels was supported by an accurate determination of their masses using MALDI-QTOF MSpec. MSpec was optimised for analysis of chemokine-protease samples by investigating aspects of sample preparation and application to the target plate. The use of Zip Tips® to concentrate and desalt samples prior to analysis was found to dramatically improve results by increasing peak intensity, reducing background, and removing salt adducts (Fig. 2.5). Premixing samples with matrix prior to spotting onto the target was found to give substantially better results than applying samples onto dried matrix already on the target (data not shown). The matrix selected for use in analysis of chemokines and their cleavage products was α-CHCA, as this resulted in mass spectra with greater intensity, lower background, and no salt adducts (Fig. 2.6).

2.4.5 MALDI-QTOF mass spectrometry of CCL2 incubated with MMP2

Mass spectra of Zip tipped samples of CCL2 incubated with activated MMP2 for 3h showed that the intact CCL2 molecule was no longer present. The dominant peak had an m/z of 8263 (Fig. 2.7a), representing a reduction in mass of 411. This difference in mass is equal to the sum of the average masses of the 4 N-terminal residues of CCL2. The mass spectrum obtained after CCL2 was incubated with MMP2 for 6h confirmed that 8263 m/z remained as the dominant peak and had not been processed further (Fig. 2.7b). When MMP2 was inhibited by 20mM EDTA, the only peak seen at 6h was that of 8674 m/z, corresponding to intact CCL2 (Fig. 2.7c). Matrix salt adducts (401, 524, and 568 m/z), and contaminants (8452 and 8641 m/z), were observed in 3h samples.

2.4.6 MALDI-QTOF mass spectrometry of CCL2 incubated with MMP9

Mass spectra of zip tipped samples of CCL2 incubated with activated MMP9 gave identical results as with MMP2 (see 2.4.5).

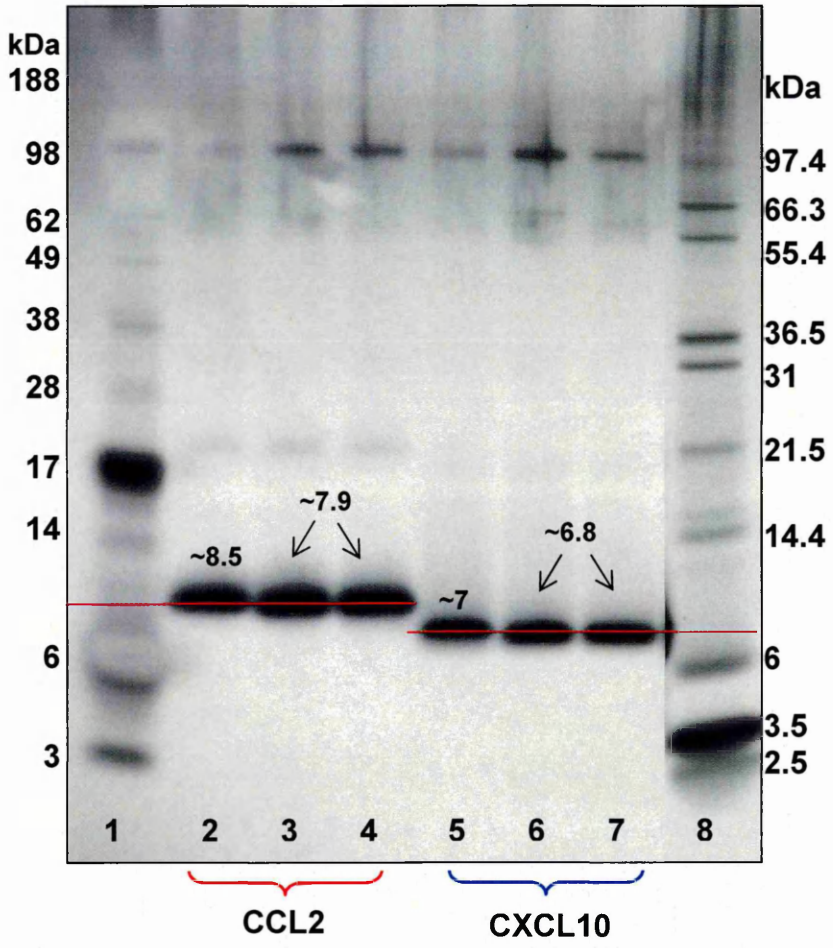

Figure 2.4 Chemokine cleavage: electrophoresis using Bis-Tris 12% silver-stained gel of CCL2 and CXCL10 at 0.5 and 6h incubation with CD26

CCL2 or CXCL10 (4μM) were incubated with CD26 (0.04μM) in assay buffer (25mM Tris) for 6h at 37˚C. Samples were taken at 30min and 6h, LDS sample buffer and reducing agent were added, and samples denatured by heating at 70˚C for 10min. SDS-PAGE was performed using MES running buffer, and the gel was silver-stained. Slight downward shifts in the bands in lanes 3, 4, 6, and 7 can be seen, compared to lanes 2 and 5.

Lanes shown above had 10μl of the following samples loaded:
***(1)** SeeBlue Plus2 MW marker; **(2)** Heat-inactivated CD26/CCL2 6h;*
***(3)** CD26/CCL2 30min; **(4)** CD26/CCL2 6h;*
***(5)** Heat-inactivated CD26/CXCL10 6h; **(6)** CD26/CXCL10 30min;*
***(7)** CD26/CXCL10 6h; **(8)** Mark12 MW marker*

Figure 2.5 Optimisation of mass spectrometry: mass spectra showing the effects of zip tipping a chemokine-protease sample prior to MALDI-QTOF analysis

CCL2 was incubated at 37˚C with MMP2, without activation with APMA, and samples were taken at 15min. Samples were analysed by MALDI-QTOF MSpec, using α-CHCA as the matrix, and were either mixed with matrix and spotted onto the target plate directly, or were first zip tipped, before analysis.

(a) Mass spectrum of CCL2, with a peak at 8682.9 m/z. The peak intensity was relatively low, at a maximum of 200 counts, and the background noise was quite high. The peaks seen to the left of the spectrum at ~1000-1600 m/z, with a dominant peak at 1600 m/z, derive from clusters of matrix molecules with potassium and sodium ions (Neubert et al., 2004).

(b) Mass spectrum of the same sample analysed in (a), but incorporating zip tipping before analysis by MSpec. The CCL2 peak at 8682 m/z is clearly dominant, with a much stronger intensity of 1392 counts. Background is minimal, and matrix cluster peaks are barely seen.

(a) Without zip tipping, CCL2 and MMP2, 15min incubation

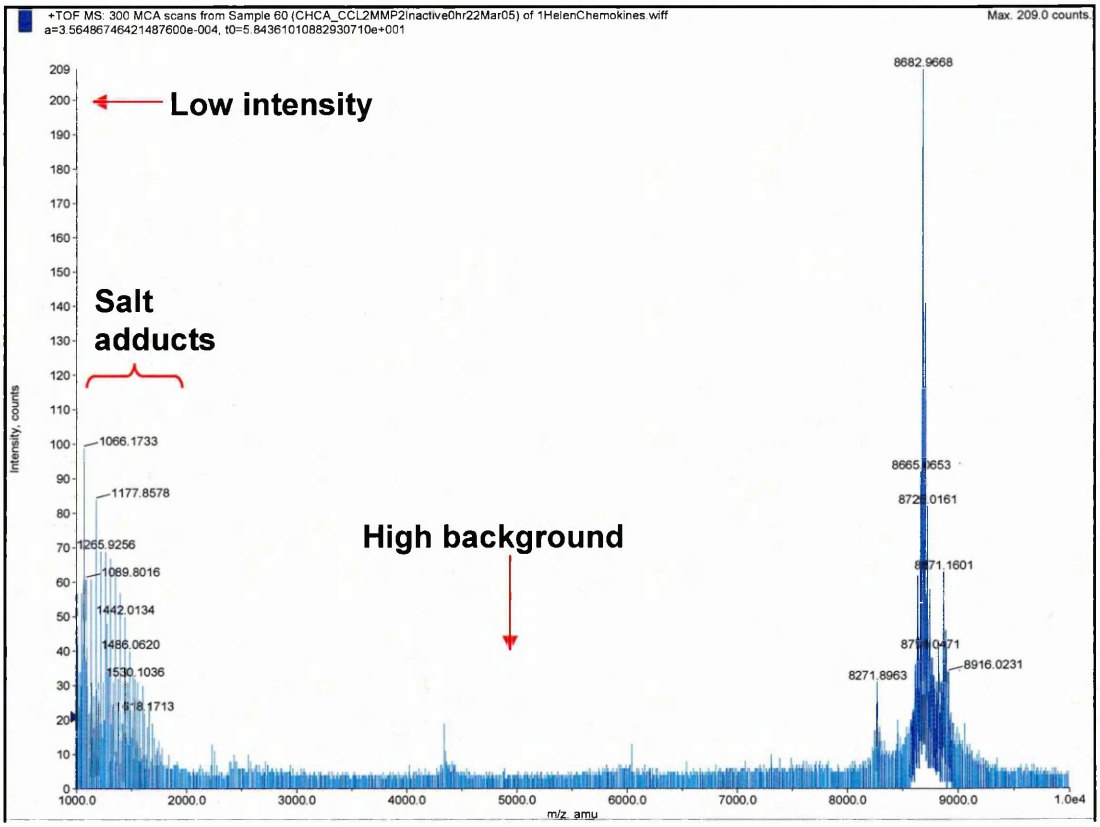

(b) With zip tipping, CCL2 and MMP2, 15min incubation

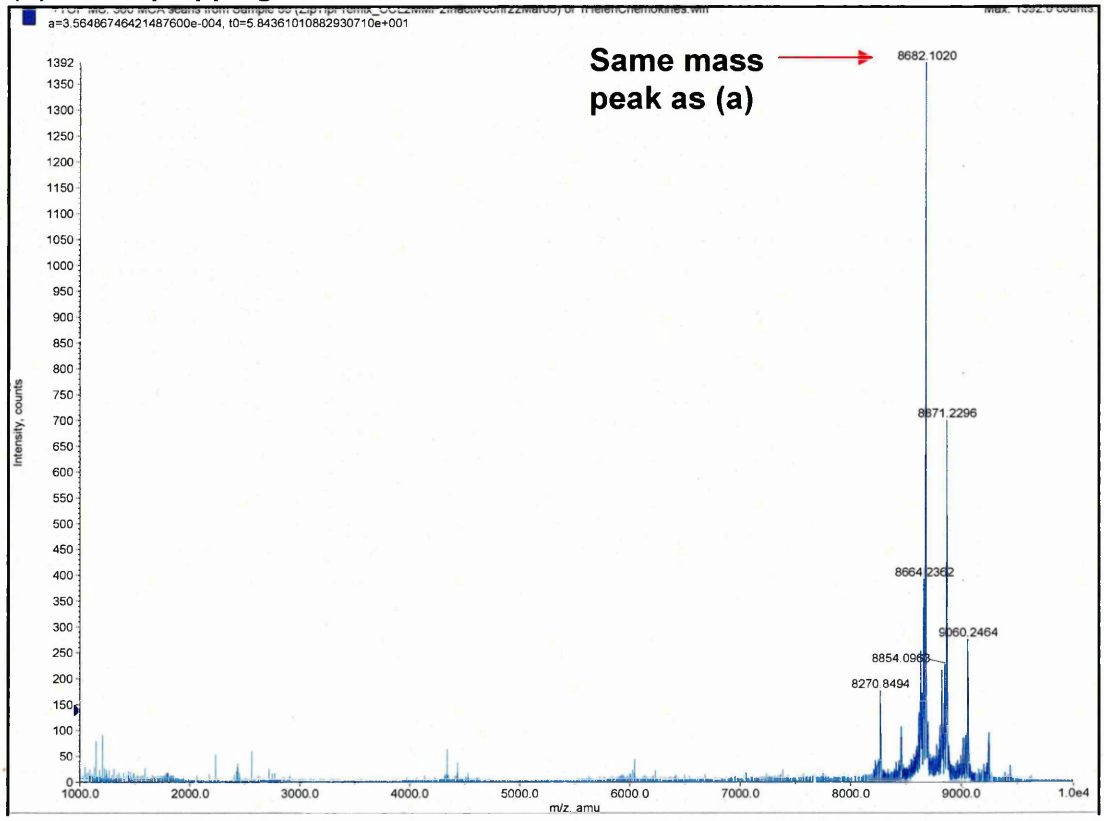

Figure 2.6 Optimisation of mass spectrometry: mass spectra comparing sinapinic acid and α-CHCA as the matrix prior to MALDI-QTOF analysis of a zip tipped chemokine-protease sample

Two matrices were tested with samples from the chemokine-protease incubation experiment to establish which one gave the greatest sensitivity. CCL2 was incubated at 37˚C with MMP2, that had not received prior treatment with APMA, and samples were taken at 6h. Samples were prepared for MALDI-QTOF MSpec analysis by zip tipping, follwed by mixing with either sinapinic acid, or α-CHCA, as the matrix.

(a) Mass spectrum of CCL2 from the incubation mixture, using sinapinic acid as the matrix. The dominant peak is that of CCL2, seen at 8682 m/z. The peak intensity was relatively low, at a maximum of 119 counts, and the background noise was high. The peaks seen to the left of the spectrum at ~1000-1600 m/z are likely to derive from the matrix.

(b) Mass spectrum of the same sample analysed in (a), but using α-CHCA as the matrix. The dominant peak is that of CCL2, seen at 8682 m/z, with a very high intensity of 1723 counts. Background was low, and clustered matrix-associated peaks to the left of the spectrum are not seen.

(a) CCL2 & MMP2 at 6h, zip tipped, and premixed with sinapinic acid matrix

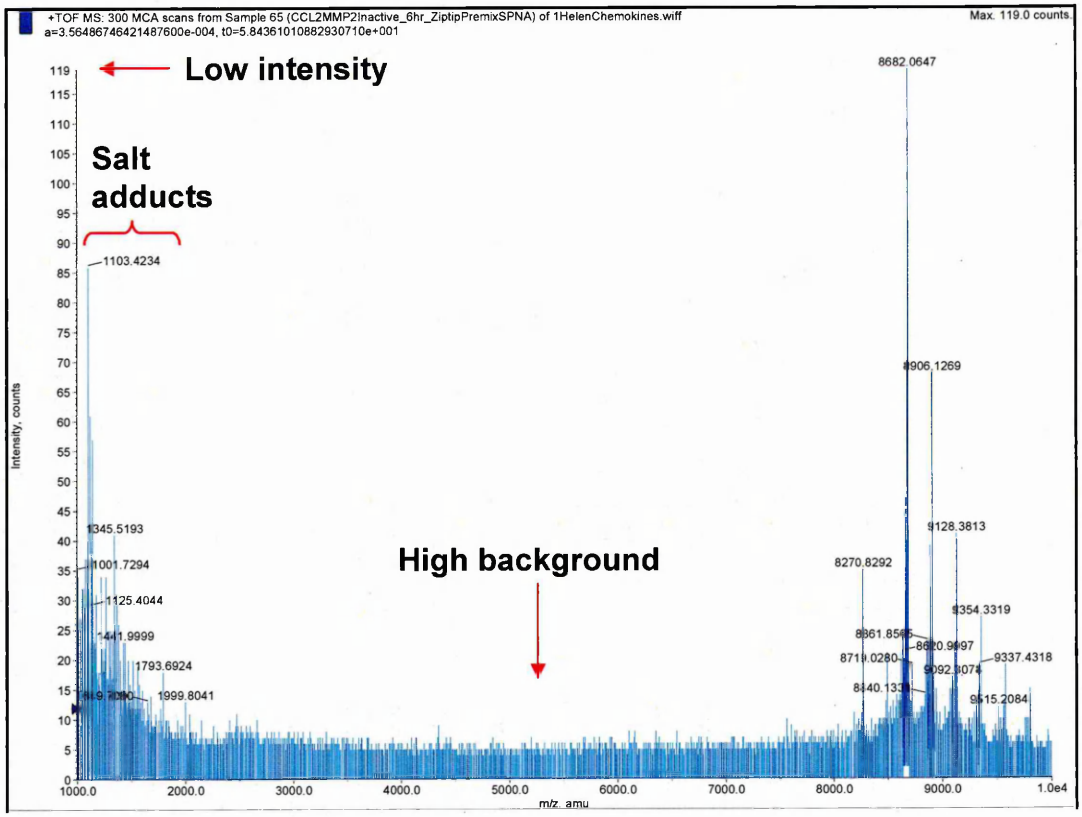

(b) CCL2 & MMP2 at 6h, zip tipped, and premixed with α-CHCA Matrix

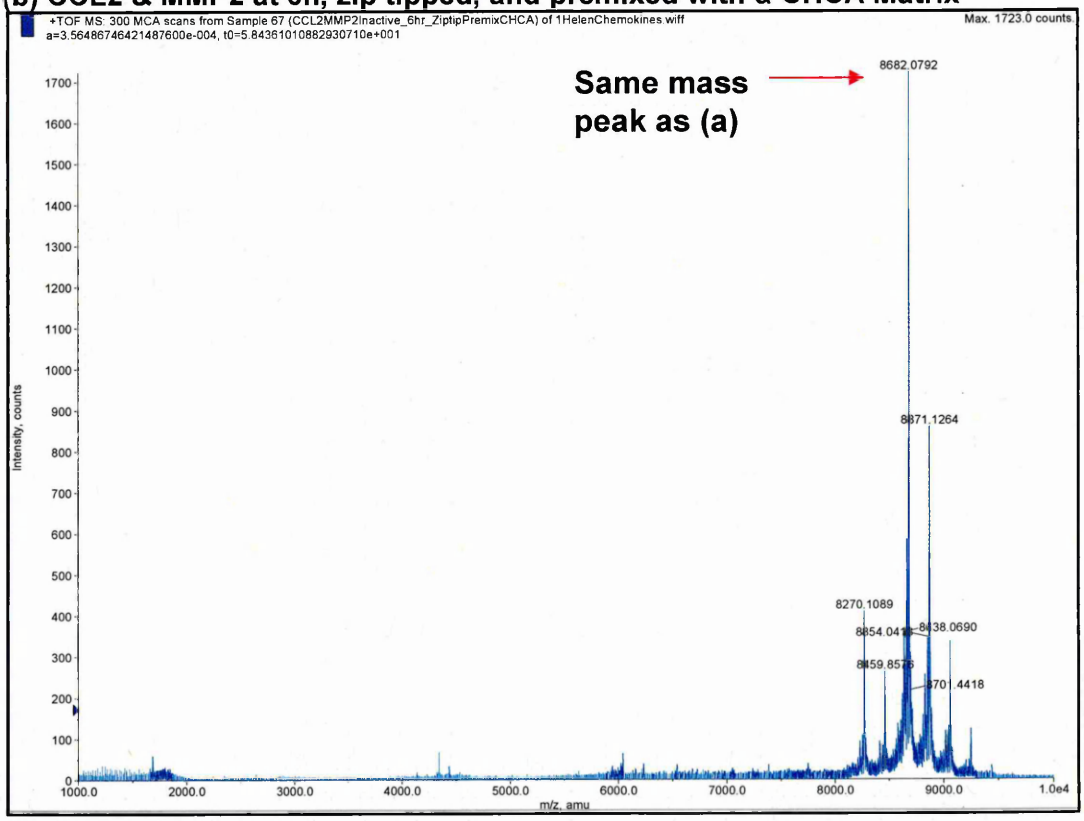

Figure 2.7 Chemokine cleavage: mass spectra from MALDI-QTOF analysis of CCL2 incubated with MMP2 for 3 and 6h, and with inhibited MMP2

Recombinant human CCL2 (4μM) and MMP2 (0.4μM) were incubated in assay buffer (100mM Tris-HCl, 100mM NaCl, 10mM $CaCl_2$, 0.01% Tween® 20) for 6h at 37˚C. Samples were taken at 3 and 6h and the reaction stopped by addition of an equal volume of 0.5% TFA and freezing at -80˚C. Samples were zip tipped, mixed with α-CHCA matrix, spotted onto a target plate and analysed by MALDI-QTOF MSpec.

(a) 3h incubation resulted in no peak being present that corresponded to the m/z of intact CCL2. The dominant peak was 8263, which represented a reduction of 411 from intact CCL2. This difference in mass was equal to the sum of the average masses of the 4 N-terminal amino acids of CCL2. N.B. Major peaks representing matrix salt adducts were also seen (401, 524, and 568 m/z), and contaminants (8452.7 and 8641.8 m/z) in the spectra shown, but not in repeat analyses.

(b) 6h incubation resulted in an absence of peaks in the 400-600 m/z range, but a single dominant peak of 8263 m/z was seen.

(c) 6h incubation in the presence of 20mM EDTA resulted in a single peak of 8674 m/z, corresponding to intact CCL2

(a) 3h

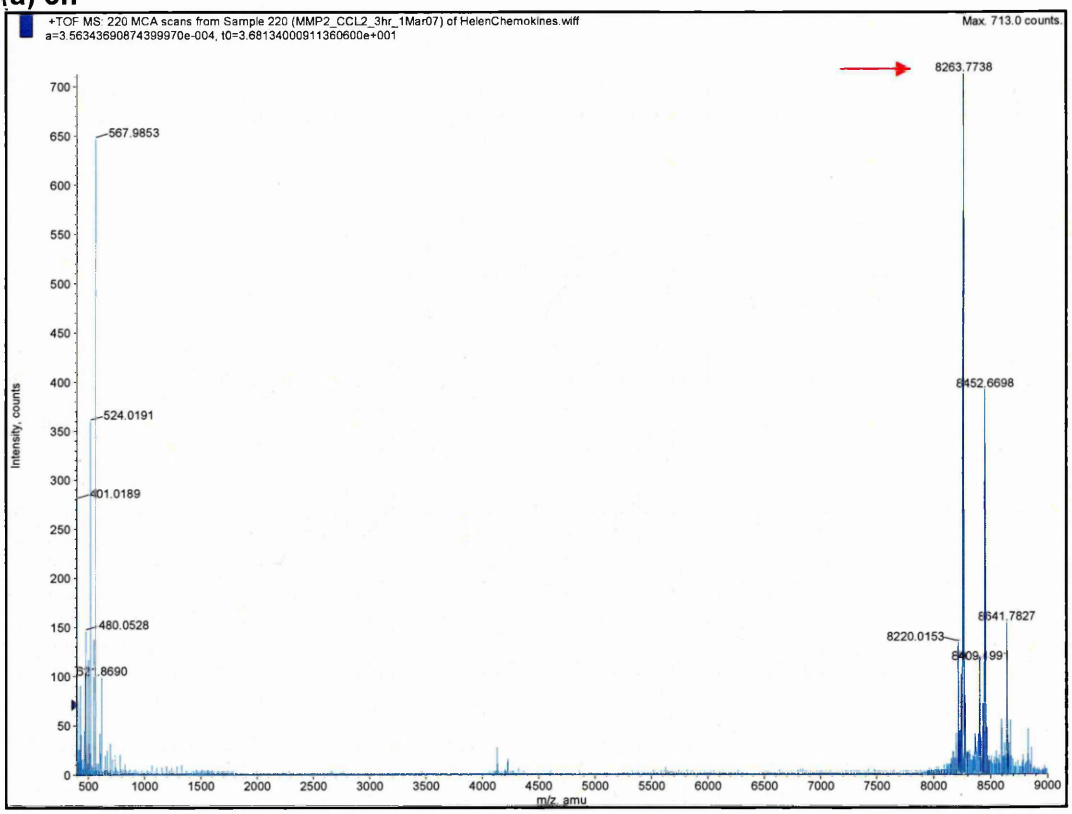

(b) 6h

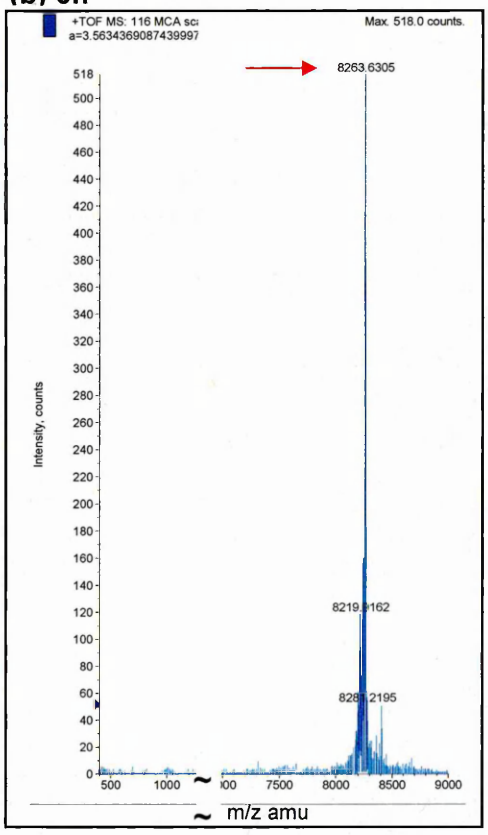

(c) 6h with inhibited MMP2

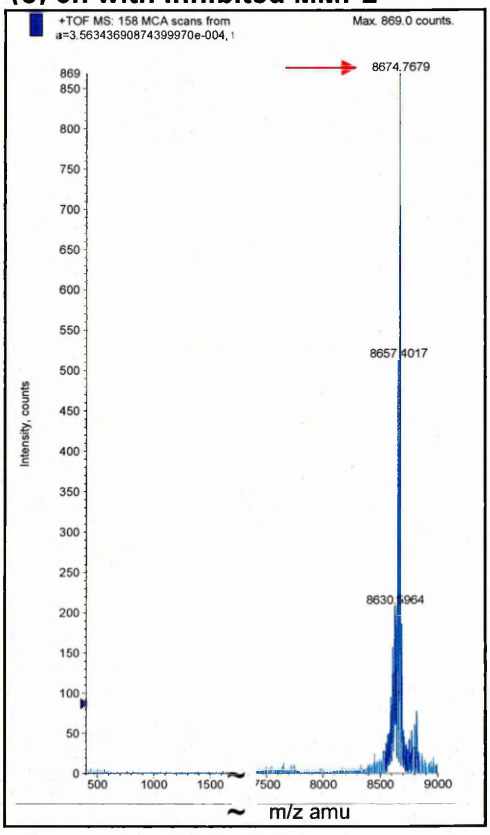

Briefly, at 3h intact CCL2 was not seen and the dominant peak had an m/z of 8263 (Fig. 2.8a), representing a reduction in mass of 411 (equal to the sum of the masses of the 4 N-terminal residues). Longer incubation (6h) did not reveal any changes (Fig. 2.8b). When MMP9 was inhibited by 20mM EDTA, the only peak seen at 6h was that of 8674 m/z, corresponding to intact CCL2 (Fig. 2.8c).

2.4.7 MALDI-QTOF mass spectrometry of CCL2 incubated with CD26

Mass spectra of zip tipped samples of CCL2 incubated with CD26 for 30min showed that the intact CCL2 molecule was present at half the intensity of a product of 8449.8 m/z (Fig. 2.9a). The dominant peak represented a rapid reduction in mass of 225. This difference in mass is equal to the sum of the average masses of the 2 N-terminal residues of CCL2. The mass spectrum obtained for 6h showed a single peak of 8449.8 m/z, representing the cleaved form, with no further processing (Fig. 2.9b). Heat-inactivating CD26 prior to use resulted in a single peak of intact CCL2 at 8674.7 (Fig. 2.9c).

2.4.8 MALDI-QTOF mass spectrometry of CXCL10 incubated with MMP2

Mass spectra of zip tipped samples of CXCL10 incubated with activated MMP2 for 24h showed that the intact CXCL10 molecule was the dominant peak. Minor peaks at less than 25% the intensity of this were noted at 437.1 and 926.2 (matrix salt adducts), and 8058.9 and 8144.5 m/z (Fig. 2.10a). The total mass of the first 5 N-terminal residues of CXCL10 equals 552, which corresponded to the reduction of intact CXCL10 to the minor peak seen at 8058.9 m/z. In addition, the peak at 8144.5 represents a loss of 467 from intact CXCL10, which is very similar to 468, the total mass of the first 4 C-terminal amino acids. At 48h, intact CXCL10 still dominates, but the relative intensities of the peaks at 8059.1 and 8143.3 m/z have increased. Peaks representing matrix salt adducts (437.1 and 962.2 m/z) have also increased from 24h to 48h (Fig. 2.10b). At 72h, the only non-matrix peak visible was that of 8062.7 m/z, at a very low intensity of 7 counts (Fig. 2.10c). As the intensity was much reduced compared to earlier spectra, the accuracy was reduced, and this was most likely the same peak as 8059 m/z seen at 24 and 48h, deemed to represent a loss of 5 N-terminal residues. It is possible that by 72h, CXCL10 has been almost completely degraded by activity at other cleavage sites within the molecule. Inhibiting MMP2 with EDTA abrogated the production of cleavage products, producing only a single peak at 24h pertaining to intact CXCL10 (Fig. 2.10d).

Figure 2.8 Chemokine cleavage: mass spectra from MALDI-QTOF analysis of CCL2 incubated with MMP9 for 3 and 6h, and with inhibited MMP9

Recombinant human CCL2 (4μM) and MMP9 (0.4μM) were incubated in assay buffer (100mM Tris-HCl, 100mM NaCl, 10mM $CaCl_2$, 0.01% Tween® 20) for 6h at 37˚C. Samples were taken at 3 and 6h and the reaction stopped by addition of an equal volume of 0.5% TFA and freezing at -80˚C. Samples were zip tipped, mixed with α-CHCA matrix, spotted onto a target plate and analysed by MALDI-QTOF MSpec.

(a) 3h incubation resulted in no peak being present that corresponded to the m/z of intact CCL2 (8674 m/z, determined by analysis of CCL2 alone). The dominant peak was 8263, which represented a reduction of 411 from intact CCL2. This difference in mass was identical to the reduction found with MMP9 and is equal to the sum of the average masses of the first 4 N-terminal amino acids. N.B. Major peaks representing matrix salt adducts were also seen (401, 505, and 568 m/z), and contaminants (8452.8 and 8641.5 m/z) in the spectra shown, but not in repeat analyses.

(b) 6h incubation resulted in an absence of peaks in the 400-600 m/z range, but a single dominant peak of 8263 m/z was seen.

(c) 6h incubation in the presence of 20mM EDTA resulted in a single peak of 8674 m/z, corresponding to intact CCL2

(a) 3h

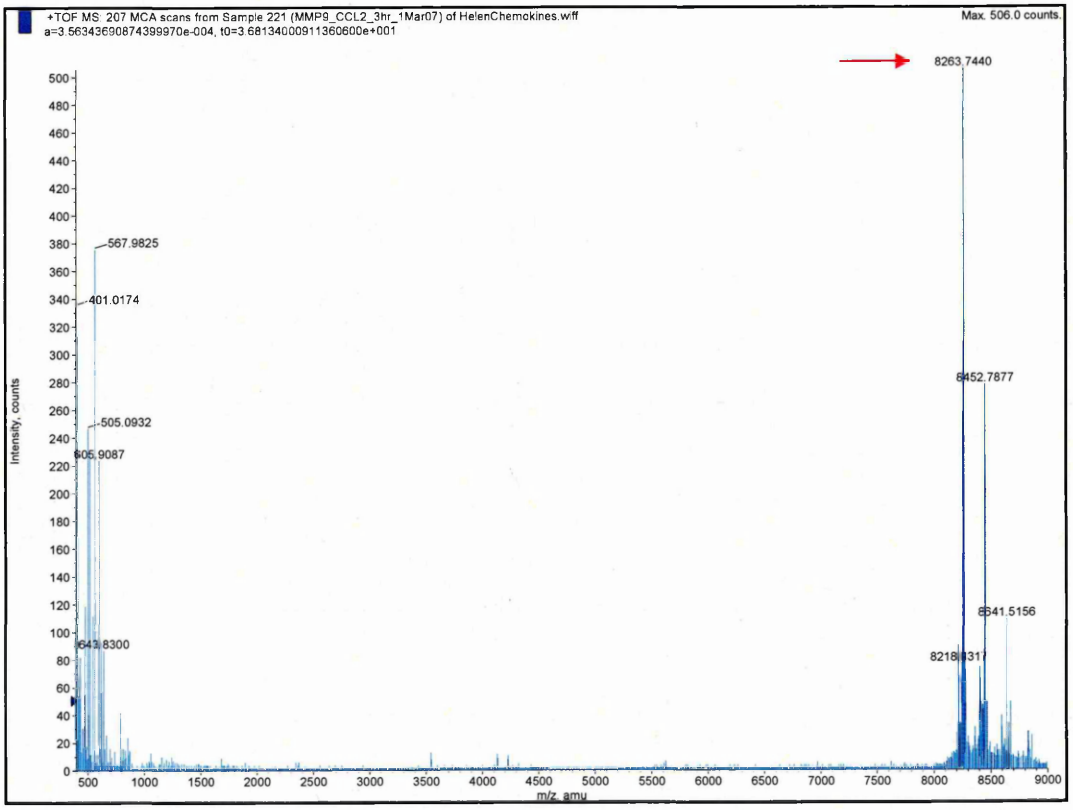

(b) 6h

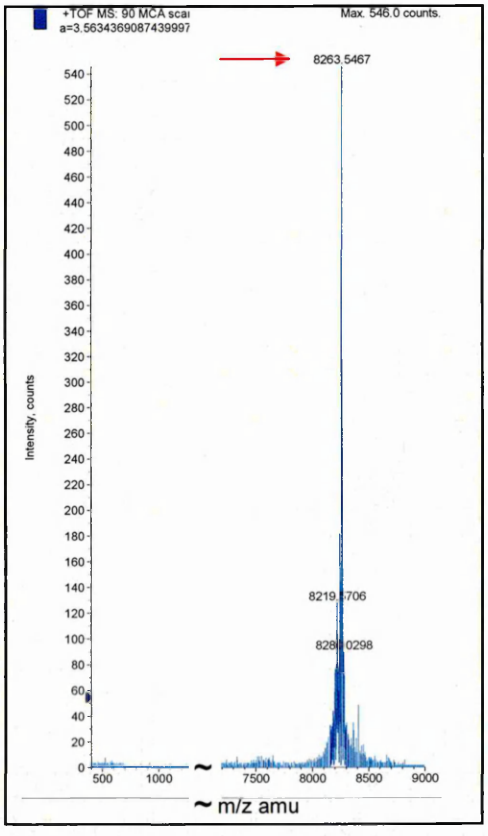

(c) 6h with inhibited MMP9

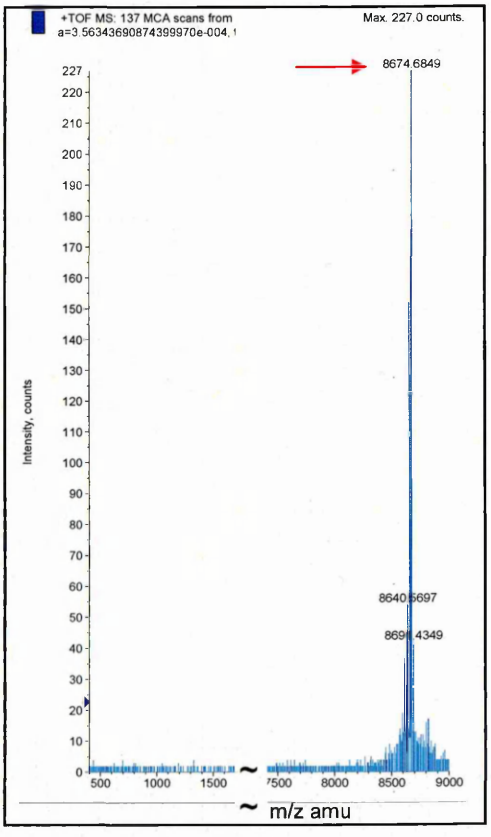

Figure 2.9 Chemokine cleavage: mass spectra from MALDI-QTOF analysis of CCL2 incubated with CD26 for 30min, 6h and with inactivated CD26

Recombinant human CCL2 (4μM) and CD26 (0.04μM) were incubated in assay buffer (25mM Tris) for 6h at 37˚C. Samples were taken at 30min, 3h (not shown) and 6h, and the reaction stopped by addition of an equal volume of 0.5% TFA and freezing at -80˚C. Samples were zip tipped, mixed with α-CHCA matrix, spotted onto a target plate and analysed by MALDI-QTOF MSpec.

(a) 30min incubation resulted in a peak at 8675 m/z that corresponded to the m/z of intact CCL2, but this was less than half the intensity of the dominant peak of 8449.8 m/z. The peak at 8449.9 m/z represented a reduction of 225 from intact CCL2, which equals the sum of the average masses of the first 2 N-terminal amino acids.

(b) 6h incubation resulted in a single dominant peak of 8449.8 m/z being seen, which equals the mass of intact CCL2 minus an N-terminal dipeptide.

(c) 6h incubation with CD26 being first heat-inactivated, resulted in a single peak of 8674.7 m/z, corresponding to intact CCL2.

(a) 30min

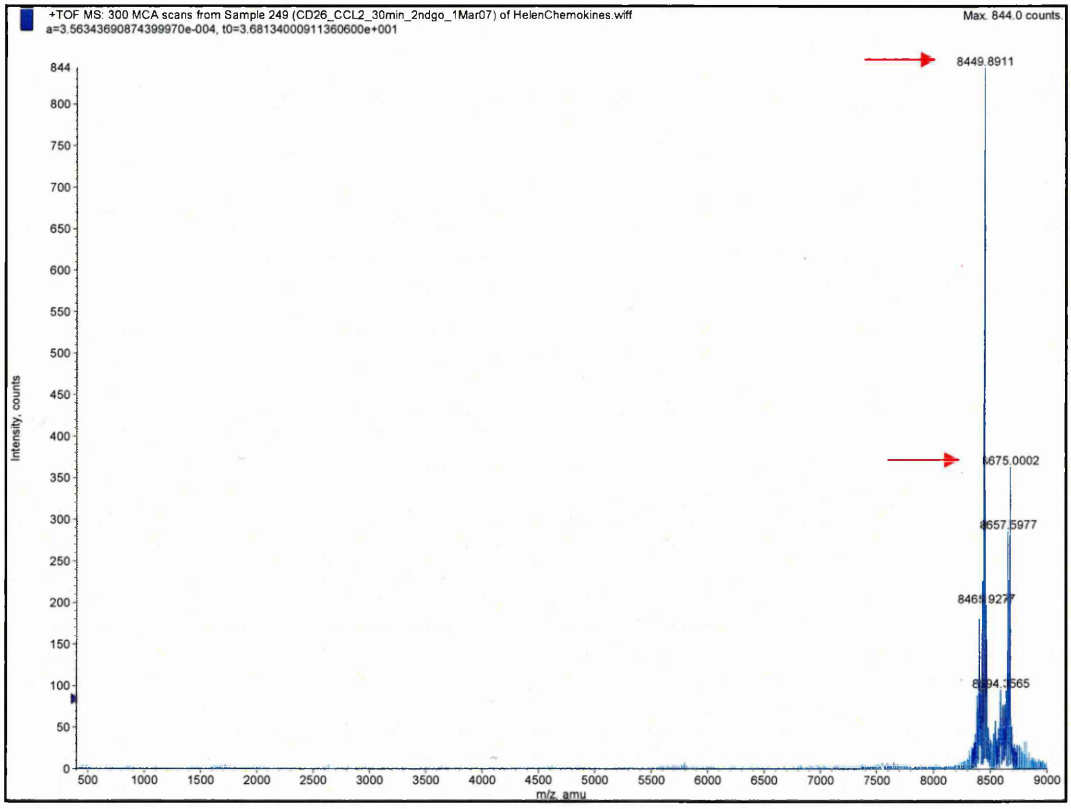

(b) 6h

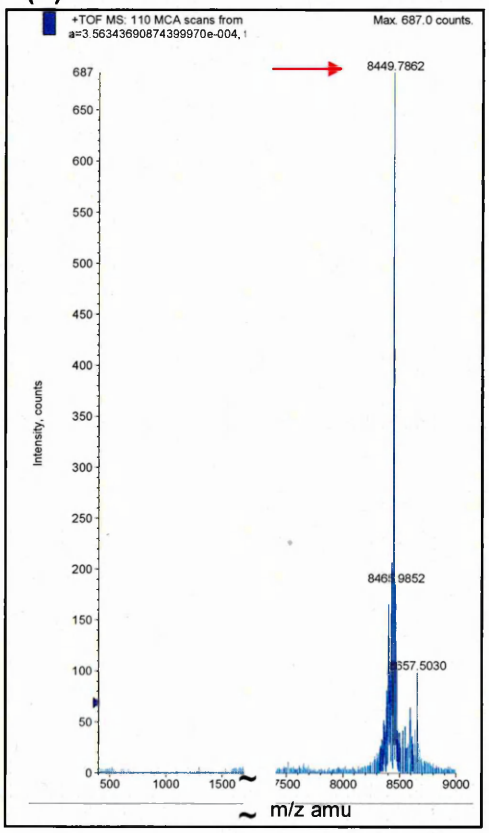

(c) 6h with heat-inactivated CD26

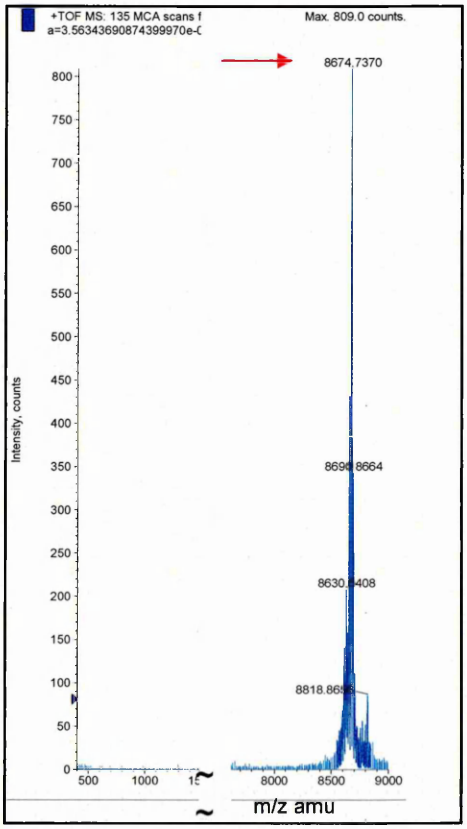

Figure 2.10 Chemokine cleavage: mass spectra from MALDI-QTOF analysis of CXCL10 incubated with MMP2 for 24, 48 and 72h, and with inhibited MMP2

Recombinant human CXCL10 (4μM) and MMP2 (0.4μM) were incubated in assay buffer (100mM Tris-HCl, 100mM NaCl, 10mM $CaCl_2$, 0.01% Tween® 20) for 72h at 37˚C. Samples were taken at 24, 48 and 72h, and the reaction stopped by addition of an equal volume of 0.5% TFA, and freezing at -80˚C. Samples were zip tipped, mixed with α-CHCA matrix, spotted onto a target plate and analysed by MALDI-QTOF MSpec.

(a) 24h incubation resulted in observation of the dominant peak at 8611 m/z, which corresponded to the m/z of intact CXCL10. Several minor peaks of less than 25% intensity of the major peak were seen, notably matrix salt adducts (437.1 and 926.2 m/z), and cleavage products at 8058.9 and 8144.5 m/z. The peak at 8058.9 m/z represented a reduction of 552 from intact CXCL10, which equals the sum of the average masses of the first 5 N-terminal amino acids. The peak at 8144.5 involved a loss of 467 from intact CXCL10, closely resembling 468, which is the sum of the average masses of the first 4 C-terminal amino acids.

(b) 48h incubation revealed the dominant peak remained that of intact CXCL10 at 8611 m/z, but relative to this, the intensity of the peak at 8059.1 m/z, representing a loss of 5 N-terminal amino acids, had increased to ~37 %. The peak at 8143.3 m/z had also increased relative to the dominant peak, and this loss of 468 was indicative of removal of the first 4 C-terminal amino acids.

(c) 72h incubation resulted in a very low intensity peak of 8062.7 m/z, of only 7 counts, suggesting that CXCL10 has been completely degraded.

(d) 24h incubation in the presence of 20mM EDTA produced no evidence of cleavage, with a single high intensity peak of intact CXCL10 at 8611 m/z.

(a) 24h

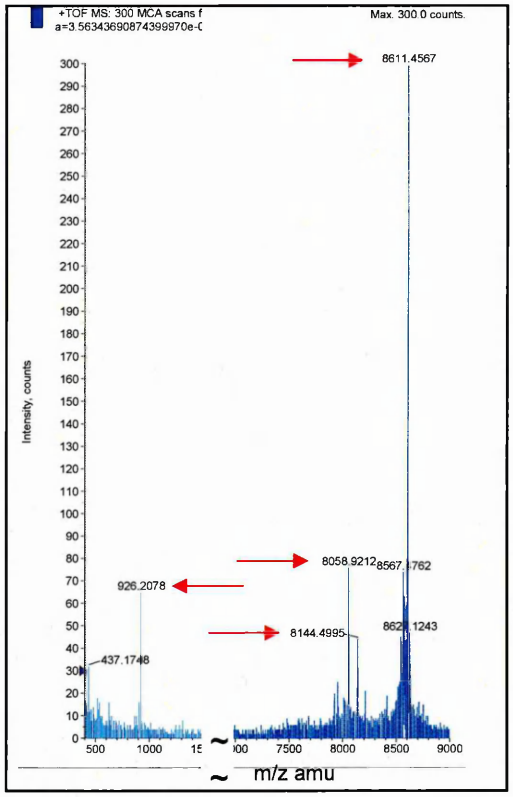

(b) 48h

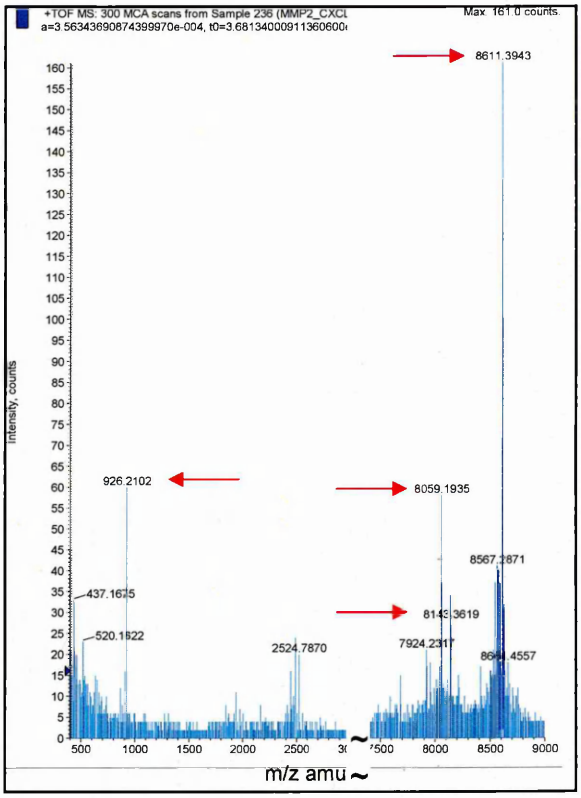

(c) 72h

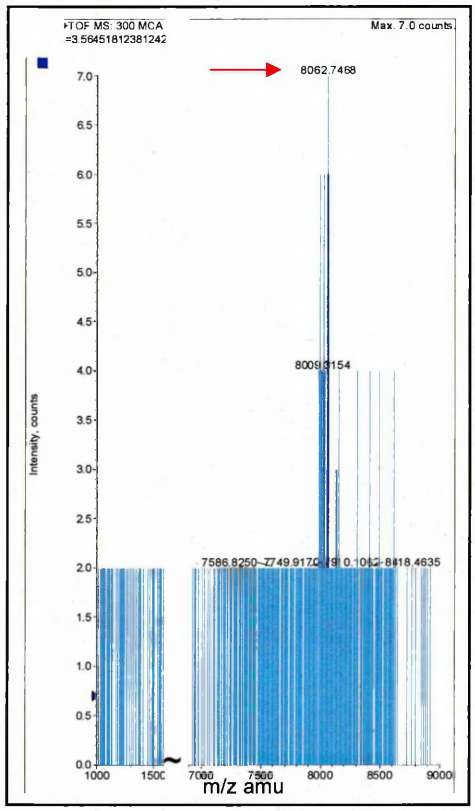

(d)24h with inhibited MMP2

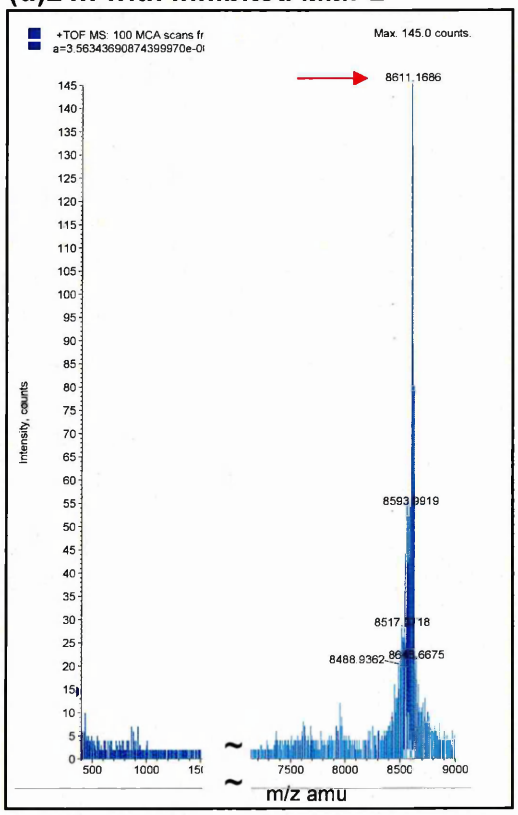

2.4.9 MALDI-QTOF mass spectrometry of CXCL10 incubated with MMP9

Mass spectra of zip tipped samples of CXCL10 incubated with activated MMP9 for 24h showed that intact CXCL10 is present in large amounts, but does not represent the dominant peak, which is seen at 8143.3 m/z. This peak was also seen to a lesser extent with CXCL10 and MMP2, and represents a loss of 468 Da, the same mass as the first 4 C-terminal residues. Minor peaks at ~15% intensity of the major peak were visible, including 7748.8 and 8215 m/z peaks (Fig. 2.11a). The sum of the average masses of the first 4 N-terminal residues is 396 Da, the loss of which, from CXCL10, yields the peak seen at 8215 m/z. Combining the mass of this N-terminal loss with the mass of the first 4 C-terminal residues equals 864, which reflects the same reduction of CXCL10 to produce a peak at 7747 m/z. Intact CXCL10 was still present at 48h, but its intensity had reduced somewhat, compared to the major product of 8143.4 m/z. The minor peak of 7748.8 m/z had almost doubled in relative intensity by 48h (Fig. 2.11b). Peaks at 72h were only of very low intensity (18 counts or less), apart from matrix peaks. The masses of 8145.87 and 7749.8 m/z were present, representing peaks seen at 48h plus a mass of 2 Da. A third peak at 8216 m/z was seen, consistent with the peak at 8215 m/z seen at 24h (Fig. 2.11c). Inhibition of MMP9 with EDTA prevented formation of cleavage products (Fig. 2.11d).

2.4.10 MALDI-QTOF mass spectrometry of CXCL10 incubated with CD26

Mass spectra of zip tipped samples of CXCL10 incubated with CD26 for 30min were striking in that intact CXCL10 had already been completely processed, resulting in a single peak of 8415.4 m/z (Fig. 2.12a). This represented a reduction in mass of 196, which is the same as the total average masses of the 2 N-terminal residues of CXCL10, and indicates that CD26 processed both CCL2 and CXCL10 by removing a dipeptide from this region. The mass spectrum obtained for 6h was identical, indicating no further processing occurred (Fig. 2.12b). Heat-inactivating CD26 prior to use resulted in a single peak of intact CXCL10 at 8611.4 (Fig. 2.12c).

2.4.11 MALDI-QTOF mass spectrometry of control samples from chemokine-protease digestion

All recombinant chemokines and enzymes were tested for spontaneous degradation by incubation at 37˚C in assay buffer for 24-48h. No degradation products were found (Fig. 2.13), which supported the gel electrophoresis results.

Figure 2.11 Chemokine cleavage: mass spectra from MALDI-QTOF analysis of CXCL10 incubated with MMP9 for 24, 48 and 72h, and with inhibited MMP9

Recombinant human CXCL10 (4μM) and MMP9 (0.4μM) were incubated in assay buffer (100mM Tris-HCl, 100mM NaCl, 10mM $CaCl_2$, 0.01% Tween® 20) for 72h at 37˚C. Samples were taken at 24, 48 and 72h, and the reaction stopped by addition of an equal volume of 0.5% TFA, and freezing at -80˚C. Samples were zip tipped, mixed with α-CHCA matrix, spotted onto a target plate and analysed by MALDI-QTOF MSpec.

(a) 24h incubation resulted in observation of a dominant peak at 8143.3 m/z, representing a loss of 468 from intact CXCL10, which corresponded to the sum of the average masses of the first 4 C-terminal amino acids. Intact CXCL10 is shown in the high intensity peak at 8611.5 m/z. Minor peaks of ~15% intensity, or less, of the dominant peak were seen, notably at 7748.8 m/z (equal to CXCL10 with 4 residues cleaved from both N- and C-termini) and 8215 m/z (equal to CXCL10 minus 4 residues at N-terminus).

(b) 48h incubation revealed the dominant peak to remain that of 8143.4 m/z, representing CXCL10 lacking 4 C-terminal amino acids. Intact CXCL10 was still visible as a peak at 8612 m/z, but the peak intensity relative to the dominant peak was reduced from that seen at 24h. The minor peak of 7747.4 m/z had almost doubled in relative intensity compared to levels at 24h, potentially indicating an increase in cleavage of 4 residues from both the N- and C-termini.

(c) 72h incubation resulted in very low intensity peaks (maximum of 18 counts) at 8145.87 and 7749.8 m/z, representing the peaks seen at 24 and 48h, plus a mass of 2 Da. A peak of 8216 m/z is visible, most likely consistent with the peak at 8215 m/z seen at 24h, as accuracy will have reduced in line with the intensity, suggesting that the majority of CXCL10 has been degraded.

(d) 24h incubation in the presence of 20mM EDTA produced no evidence of cleavage, with a single high intensity peak at 8611 m/z.

(a) 24h

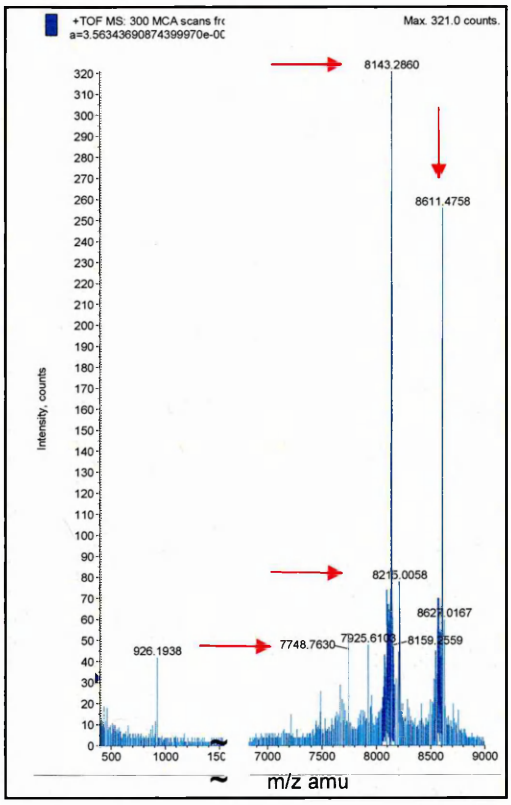

(b) 48h

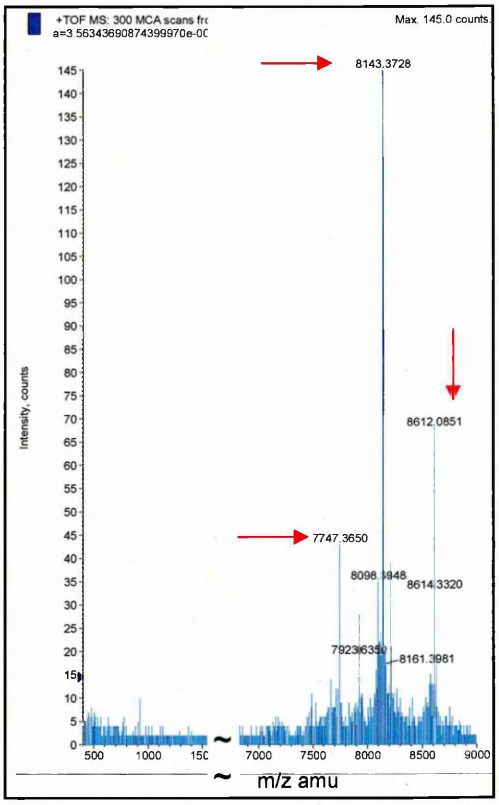

(c) 72h

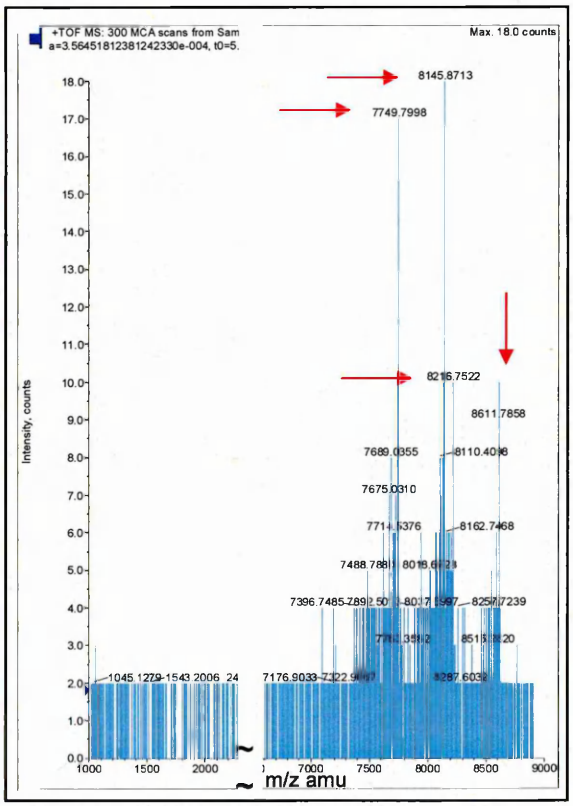

(d) 24h with inhibited MMP9

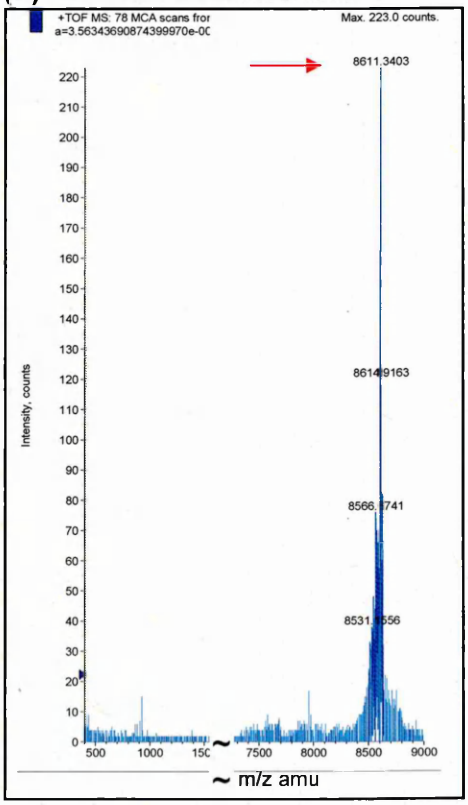

Figure 2.12 Chemokine cleavage: mass spectra from MALDI-QTOF analysis of CXCL10 incubated with CD26 for 0.5 and 6h, and with inactivated CD26

Recombinant human CXCL10 (4μM) and CD26 (0.04μM) were incubated in assay buffer (25mM Tris) for 6h at 37˚C. Samples were taken at 30min, 3h (not shown) and 6h, and the reaction stopped by addition of an equal volume of 0.5% TFA and freezing at -80˚C. Samples were zip tipped, mixed with α-CHCA matrix, spotted onto a target plate and analysed by MALDI-QTOF MSpec.

(a) 30min incubation resulted in a single peak at 8415.4 m/z that was a loss of 196 from intact CXCL10, and corresponded to the sum of the average masses of the first 2 N-terminal amino acids. No intact CXCL10 was seen.

(b) 6h incubation resulted in no change from 0.5h, with a single peak at 8415.2 m/z.

(c) 6h incubation with the CD26 being first heat-inactivated, resulted in a single peak of 8611.4 m/z, corresponding to intact CXCL10.

(a) 0.5 h

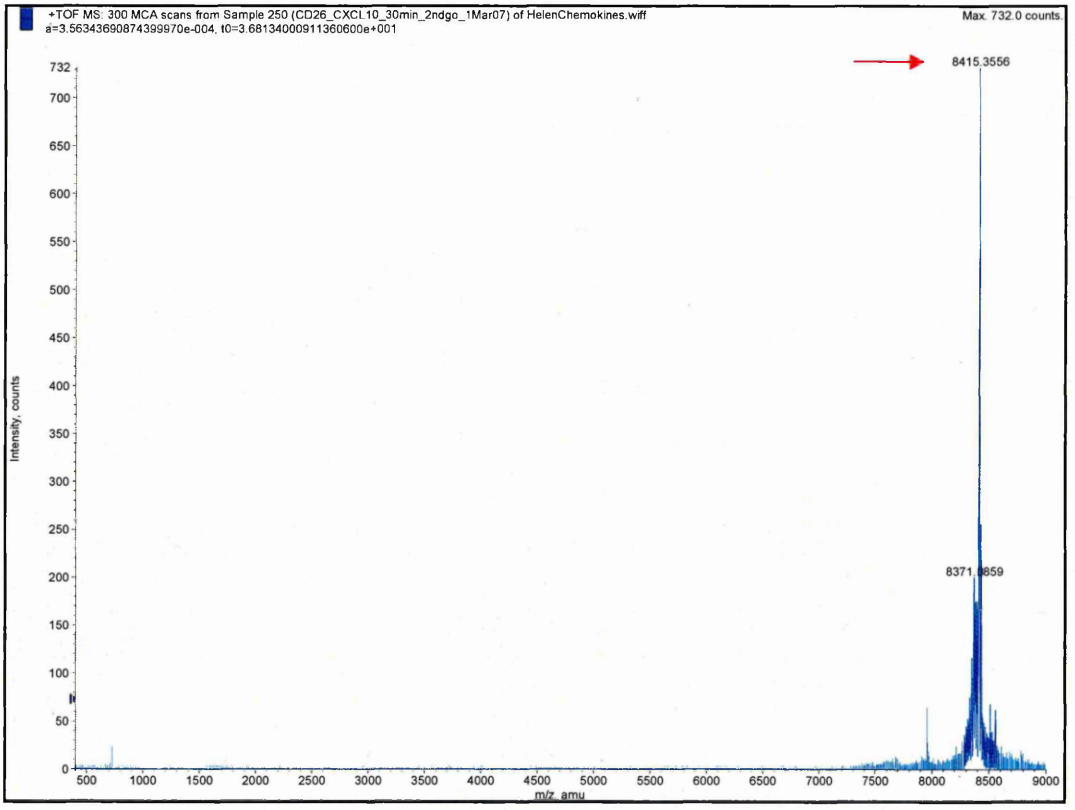

(b) 6h

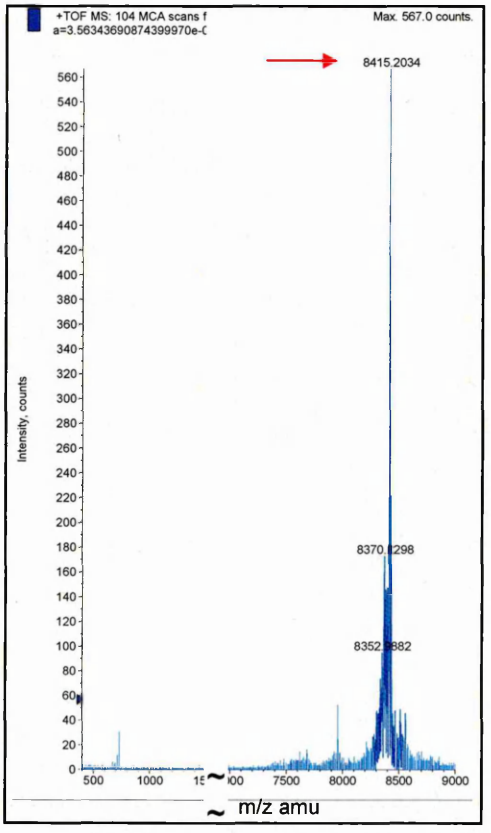

(c) 6h with heat-inactivated CD26

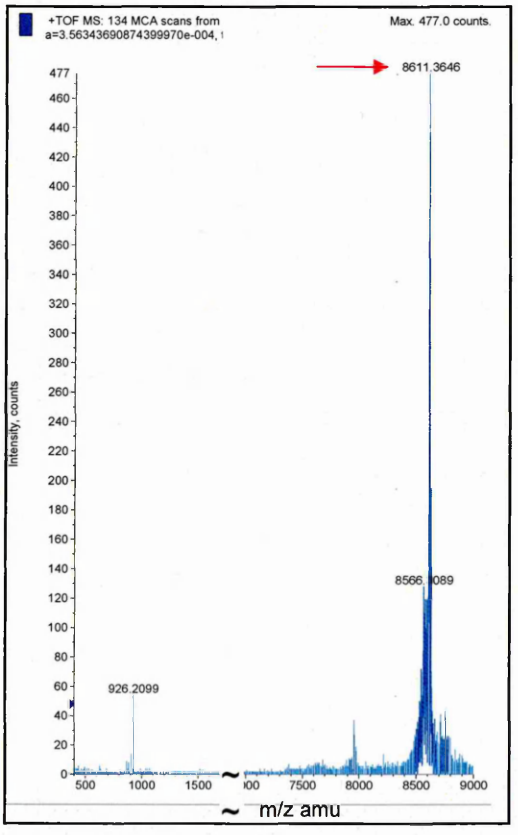

Figure 2.13 Chemokine cleavage controls: mass spectra from MALDI-QTOF analysis of CCL2 and CXCL10 incubated with APMA and assay buffer for 6h and 48h respectively

Recombinant human CCL2 (4μM) and CXCL10 (4μM) were incubated in assay buffer (100mM Tris-HCl, 100mM NaCl, 10mM $CaCl_2$, 0.01% Tween® 20) + APMA for 6 and 48h respectively at 37˚C. This was to control for degradation of chemokines in the absence of enzymes. At the end of the incubation period, samples were added to an equal volume of 0.5% TFA and stored at -80˚C. Samples were zip tipped, mixed with α-CHCA matrix, spotted onto a target plate and analysed by MALDI-QTOF MSpec.

(a) 6h incubation of CCL2 in assay buffer resulted in observation of a single peak at 8674 m/z, representing the intact molecule. No degradation products were found.

(b) 48h of incubation of CXCL10 in assay buffer resulted in observation of a dominant peak at 8611 m/z, representing the intact molecule. No significant degradation products were found.

(a) CCL2 after 6h

(b) CXCL10 after 48h

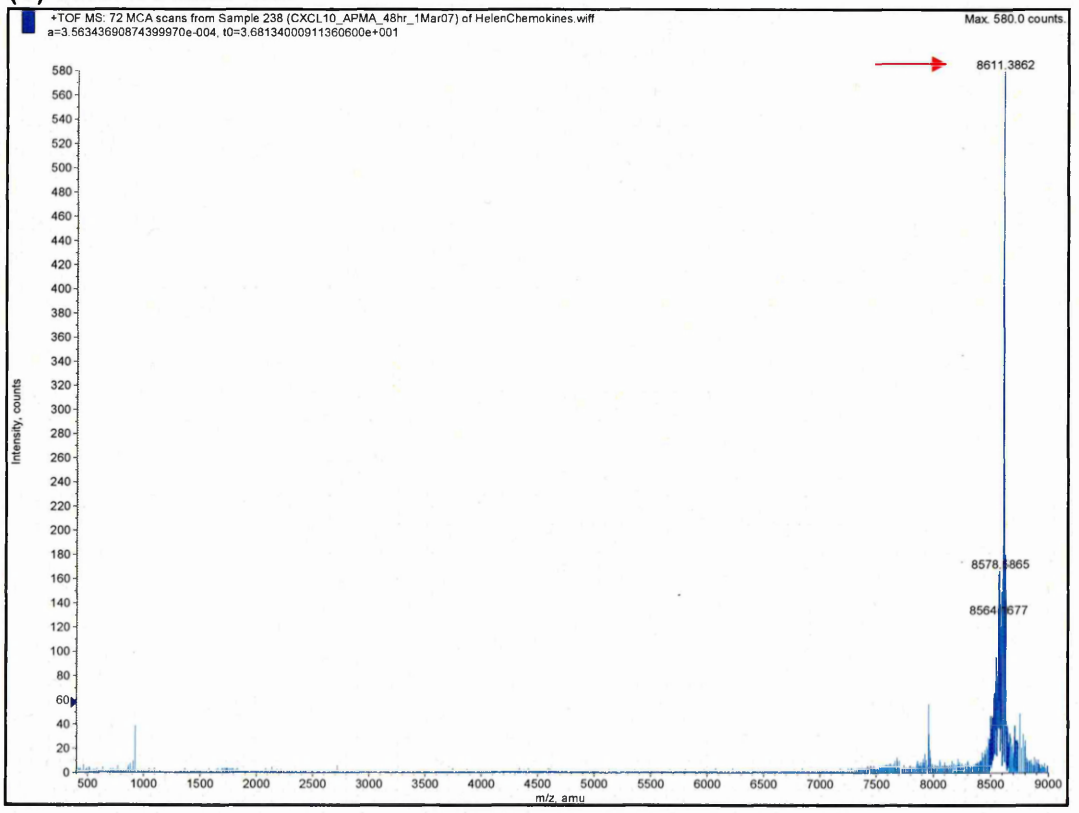

2.5 Discussion

Incubation of recombinant CCL2 and CXCL10 independently with MMPs 2 and 9 and CD26 produced a variety of truncated chemokine forms that were detected both by gel electrophoresis and MALDI-QTOF MSpec. Both chemokines were processed by each of the enzymes, with cleavage sites pertaining to the N- and C- termini being involved. Results are summarised in Table 2.6 and Figure 2.14. Data obtained using gel electrophoresis was consistent with MALDI-QTOF MSpec findings, giving enough sensitivity to detect even minor losses, such as removal of 2 residues by CD26. Accurate determination of the masses of chemokines and their cleavage products was only possible using MSpec, however, but the gels proved useful as visual evidence. The multiple bands seen in the gel showing CXCL10 incubated with MMP2 or MMP9 support the MSpec findings that this chemokine is cleaved in more than one place by these MMPs, and that cleavage is incomplete at 48h. The gel showing CCL2 incubated with enzymes demonstrated a simple downward shift of the bands, indicating the less complicated nature of the processing that occurred, which was confirmed by the 'cleaner' spectra with few peaks obtained by MSpec. Thus, gel electrophoresis and MSpec were found to complement each other well, for a study of this kind.

The cleavage by MMP2 of CCL2 found in the work in this thesis is in disagreement with previous studies, where MMP2 was found unable to process CCL2. The same study found, however, that CCL2 was processed between residues 4 and 5 by MMPs 1, 3 and 8, which is in agreement with the cleavage site found here (McQuibban *et al.*, 2002). The identical processing of CCL2 by several members of the MMP family is not an unexpected finding, as MMPs exhibit considerable overlap in their substrate specificity. MMP2 and 9 in particular have a preference for similar primary sequences, in that they commonly cleave proteins at sites with a hydrophobic residue in the first position upstream (P1') of the scissile bond. MMP2 demonstrates a preference for hydroxyproline at P5' and P5, and a proline (P/Pro) separated from a glycine (G/Gly) by one residue on the N-terminal side of the scissile bond (Seltzer *et al.*, 1990). MMP9 preferentially processes bonds with a small amino acid immediately downstream (P1), and a Pro as the third residue downstream (P3) (Netzel-Arnett *et al.*, 1993).

With this evidence in mind, it was not surprising that the bond between the alanine (A/Ala) and isoleucine (I/Ile) of CCL2 was cleaved by both MMPs 2 and 9, as Ala is a small amino acid, and Ile is very hydrophobic (Urry, 2004). Also consistent with the preference of MMP9 for a small amino acid in the P1 position, were the bonds found to be processed in CXCL10, i.e. between serine (S/Ser) and arginine (R/Arg) at the N-terminus, and Ser and lysine (K/Lys) at the C-terminus.

Table 2.6 Summary of principal findings following the incubation of recombinant human CCL2 and CXCL10 with MMP2, MMP9 or CD26

	CCL2	CXCL10
MMP2	Removal of residues 1-4 from N-terminus (411 Da) within 3h	Slow and partial removal of residues 1-5 from N-terminus (552 Da) and 1-4 from C-terminus (468 Da), incomplete at 48h. Possible degradation by 72h
MMP9	Removal of residues 1-4 from N-terminus (411 Da) within 3h	Slow and partial removal of residues 1-4 from C-terminus (468 Da), and to a lesser extent, 1-4 from N-terminus (396 Da), incomplete at 72h
CD26	Rapid removal of dipeptide from N-terminus (225 Da) almost complete within 30min	Very rapid removal of dipeptide from N-terminus (196 Da), complete within 30min

Recombinant human CCL2 and CXCL10 (4μM) were incubated separately with MMP2, MMP9 (0.4μM) and CD26 (0.04μM), for up to 72h (see Table 2.4), and the resultant cleavage products were analysed by MALDI-QTOF mass spectrometry. MMP2 and MMP9 both cleaved CCL2 at the same N-terminal position, and in addition, processed CXCL10 between residues 4 and 5 of the C-terminus. MMPs 2 and 9 also processed CXCL10 at the N-terminus, but in different locations. CD26 rapidly removed a dipeptide from both CCL2 and CXCL10.

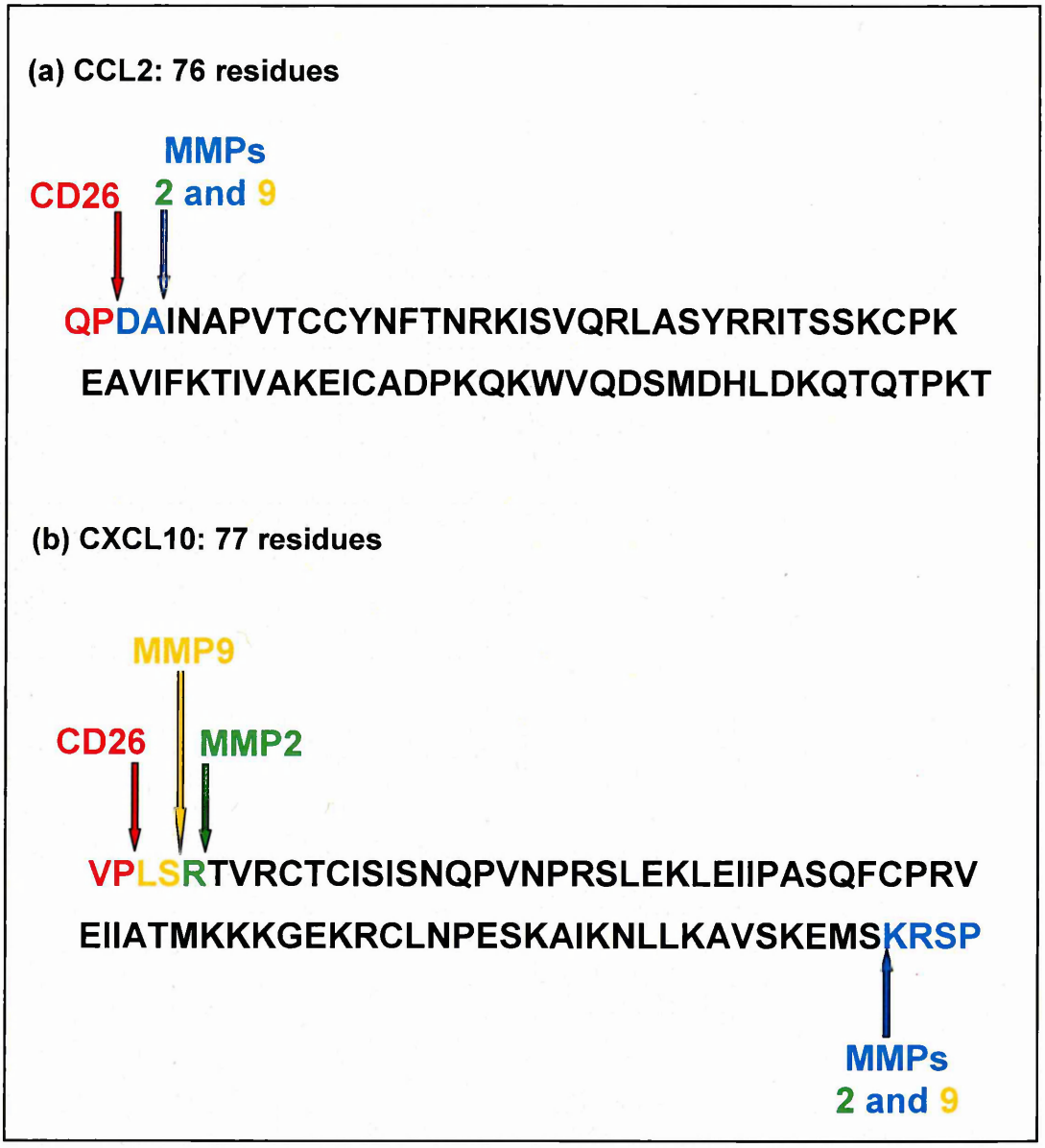

Figure 2.14 Amino acid sequences of CCL2 and CXCL10 indicating the sites where MMP2, MMP9 and CD26 were found to cleave

Cleavage sites within the amino acid sequences of CCL2 and CXCL10 and the enzyme(s) involved are shown, based on incubation at 37˚C of recombinant human proteins for up to 72h (see Table 2.4), followed by MALDI-QTOF mass spectrometric analysis. Sequences start with the N-terminus. CCL2 is cleaved in 2 positions at the N-terminus: MMPs 2 and 9 both cut between residues 4 and 5, and CD26 removed a dipeptide. CXCL10 was cleaved in 4 positions: by MMPs 2 and 9 at different positions at the N-terminus and the same position at the C-terminus, and CD26 removed 2 residues from the N-terminus.

Interestingly, these cleavage sites contradict the strong preference for a hydrophobic residue at P1', as both Arg and Lys are strongly hydrophilic. The preference of MMP9 for cleaving bonds where P3 is a Pro is upheld in cleavage of both CCL2 and CXCL10 at the N-termini, but not with C-terminal cleavage of CXCL10. It can be seen, therefore, that sequence preferences are not rigid, and it is difficult to predict exactly where an enzyme will cleave.

MMP2 and MMP9 have preferences for cleavage at similar sequences, yet differ in their processing of chemokines. The reason for this is not fully understood, but may be due to the location of the haemopexin domain, which is located further from the catalytic site in MMP9 due to its extended collagen type V domain (Mattu *et al.*, 2000). Positioning of the haemopexin domain is considered important, as it is known to serve as a secondary binding site for chemokine substrates of MMP2 (Van den Steen, 2003).

Comparing previous studies of chemokine cleavage to the findings reported here reveals many discrepancies. Results from this study are not in agreement with the frequent opinion that MMP9 processes CXC, but not CC chemokines. C-terminal truncation of CXCL10 by MMP9 was documented elsewhere as producing a product lacking 9 residues (1-68), before it was fully degraded within 24h (Van den Steen et al., 2003), whereas cleavage detailed in this thesis involved loss of 4 C-terminal amino acids, coupled with additional N-terminal processing by MMP9, with the reaction being slow and incomplete at 72h. It is important to consider differences in technique, however, as in Van den Steen's study, the MMP9 used was natural, being derived from human neutrophils. The authors also conceded that the 1-68 isoform of CXCL10 was only detected as a very low intensity fragment and several more heterogeneous cleavages were thought to contribute to its degradation. Comparing gel electrophoresis results with this study also flagged differences, as whilst multiple bands were found here, Van den Steen reported a single band representing CXCL10 cleavage by MMP9. An isoform of CXCL10 lacking 4 C-terminal amino acids has been reported, along with a further variant lacking 6 C-terminal residues, following incubation with MMP8 (Van den Steen et al., 2003).

It is well established that CD26 cleaves several chemokines with a Pro or Ala as the penultimate residue at the N-terminus. Ligands for CXCR3, including CXCL10, have been shown elsewhere to lose an N-terminal dipeptide when exposed to this enzyme (Proost *et al.*, 2001), which is in agreement with findings documented here. Iwata and colleagues (1999) have shown that CD26 cleaved a dipeptide from CCL5 in accordance with enzyme specificity, but under identical experimental conditions, failed to observe any cleavage of CCL2, using a form identical to that used in this current

study, with glutamine as the N-terminal residue. This conflicts with data reported here, where CD26 was found to rapidly process CCL2. It is known that despite possessing a sequence prone to N-terminal attack by CD26, CCL2 is normally protected by a pyroglutamatic acid residue, which was replaced by a glutamine in the recombinant form used in this current study (Van Coillie *et al.*, 1998). Discrepancies may have arisen due to different sources of CCL2 being used in different studies, and it should be noted that CCL2 used here originated from production in *E.coli.*

The speed with which cleavage can occur is pivotal in affecting the outcome *in vivo*, and the relevance of some chemokine:protease interactions may be questionable if they take several days to occur. CD26 exhibited strikingly rapid activity, cleaving all of CXCL10, and most of CCL2, within 30min. Noteworthy also is that CD26 was used at a ten-fold lower molarity than the MMPs, and did not process the chemokines any further when incubated for 6h, suggesting it is highly specific.

The physiological significance of chemokine processing is potentially a very important regulator of their function. Results obtained in this study and previously indicate that the interactions of chemokines with proteases are numerous and often complicated. N-terminal residues of chemokines have been shown to be important in receptor binding and chemotaxis. In addition, the basic residues at the C-terminus of CXCL10 have been shown to be critical for binding to CXCR3, but less important in binding polysaccharides (Campanella *et al.*, 2003). If the *in vitro* results documented here prove to be applicable to the *in vivo* situation and two or more of the enzymes tested here are co-expressed, it is possible that an isoform of CXCL10, cleaved at both termini, would result.

Previous studies indicate that an intact N-terminus is necessary for the receptor binding and signalling properties of CCL2 (Proost et al., 1998b; McQuibban *et al.*, 2002), and thus it was expected that all cleaved CCL2 isoforms identified in this current study would exhibit severely impaired chemotactic potential. Similarly, on the basis of previous reports, it was anticipated that CXCL10 cleaved by MMP2, MMP9, and CD26, would exhibit reduced chemotactic potential due to removal of N-terminal residues (Proost *et al.*, 2001). MMP9 cleaved CXCL10 more extensively at the C-terminus than the N-terminus, making it possible that the CXCL10 isoform isolated from this incubation was more likely to remain unaltered in its *in vitro* chemotactic activity, in line with previous findings. Furin cleaved 4 C-terminal residues from CXCL10, which did not alter the activity on CXCR3 (Hensbergen *et al.*, 2004), and these 4 residues are not thought critical for binding to CXCR3 or GAGs (Campanella *et al.*, 2003).

2.6 Summary

Proteolytic processing of chemokines is a complex area of study that can have dramatic effects on their activity. Results from gel electrophoresis and MALDI-QTOF MSpec using recombinant CCL2 and CXCL10, incubated individually with MMPs 2 and 9 and CD26, are summarised in Table 2.6 and indicate that each chemokine is cleaved by each enzyme. Processing often involved removal of 2-5 amino acids from the N-terminus, but C-terminal cleavage of CXCL10 was also observed with MMPs 2 and 9. CXCL10 was cleaved at both termini by MMPs 2 and 9. The speed of the reaction was enzyme-dependent, with CD26 completing cleavage of an N-terminal dipeptide from CXCL10 within 30min, whereas activity of the MMPs on CXCL10 remained incomplete at 48h. The effects on biological function, particularly on chemotactic potential, of cleavage of CCL2 and CXCL10 warranted further investigation, which was undertaken using *in vitro* migration assays in Chapter 5.

Chapter 3

Astrocyte expression of chemokines CCL2 and CXCL10, and MMPs, and TIMPs

3.1 Introduction

3.1.1 Astrocytes

Astrocytes constitute approximately half of all cells in the human brain and spinal cord, making them the most abundant glial cell in the CNS (Carroll-Anzinger and Al-Harthi, 2006). The human brain has the highest ratio of glia to neurons of >10:1 (Araque *et al.*, 2001). During brain development, astrocytes originate from neuroepithelial cells following the generation of neurons (Namihira *et al.*, 2004). Astrocytes form a mesh throughout the brain, with their distinctive star-shape comprising processes that connect with neurons and blood vessels, providing perfect morphology for sensing parenchymal disturbances (Banaclocha, 2007).

It is thought that there are two main types of astrocytes, differentiated by their morphology and distribution, but not function. Protoplasmic astrocytes have short, thick, highly branched processes, and are common in grey matter, whereas fibrous astrocytes have long, thin, less branched processes, and typically exist in white matter. Interlaminar astrocytes, and polarised astrocytes are unique to humans and primates, and represent additional populations (Oberheim *et al.*, 2006).

Astrocytes contribute indirectly to CNS leukocyte trafficking by their involvement in maintenance of the BBB, but they also affect it directly, by expressing cytokines, chemokines, and their receptors, thereby influencing adhesion molecule expression in brain ECs, and creating chemotactic gradients (Ostrow and Sachs, 2005). In response to cytokines and other stimuli, astrocytes secrete a variety of chemokines, including CCL2 and CXCL10, (Huang *et al.*, 2000), MMPs, such as MMPs 2 and 9 (Yin *et al.*, 2006) and TIMPs 1 and 2 (Leveque et al., 2004).

Inflammatory conditions can activate astrocytes, causing proliferation, cytoskeletal remodelling, migration, and an increased production of cytokines. These functional, structural, and biochemical changes constitute *reactive gliosis*, and are significant early responses to CNS injury (Ostrow and Sachs, 2005). Reactive astrocytes show rapid enhanced expression of the intermediate filament, glial fibrillary acidic protein (GFAP), and engage in astrogliosis, where they exhibit hypertrophy of their cell bodies and cytoplasmic processes, proliferate, and accumulate between intact and damaged tissue, leading to glial scar formation. This scar tissue has been implicated in failure to remyelinate and regenerate axons in MS (Zhang *et al.*, 2006). Interestingly, proliferation of astrocytes *in vitro* occurs in response to CCL2 (Rezaie *et al.*, 2002) and also CXCL10 (Flynn *et al.*, 2003), which might contribute to the astrogliosis seen in MS.

3.1.2 Astrocyte specific cell markers

Astrocytes exhibit considerable phenotypical plasticity both *in vivo* and *in vitro*, with primary cultures being very heterogeneous in terms of receptor expression and calcium signalling, even within the same cell culture. This is exemplified by the ability of two astrocytes derived from a single mitosis of the parent cell to differ in their response to neuroligands (Shao and Mc Carthy, 1994). To help identify astrocytes, two markers are commonly used: glial fibrillary acidic protein (GFAP) and S100-β.

3.1.2.1 Glial fibrillary acidic protein (GFAP)

Glial fibrils of astrocytes are mainly composed of the protein GFAP, a class III intermediate filament protein of approximately 50 kDa (Rutka *et al.*, 1997), involved in maintenance of the shape of astrocytes, and is a specific marker that differentiates mature astrocytes from other glial cells (Patanow *et al.*, 1997). In utero, GFAP production in human astrocytes can commence at 25 weeks after conception (Cohen and Rossmann, 1994), with activation of the transcription factor STAT3 being necessary for GFAP expression in neural precursor cells (Takizawa *et al.*, 2001). GFAP is important in neuronal migration due to its involvement in the formation of fibres from astrocytic processes, along which neurons move (Liesi *et al.*, 1992). Whilst GFAP is primarily associated with maintenance of astrocyte cell shape, it may also operate with other cytoskeletal components, the ECM, and kinases, to form a dynamic cell-signalling apparatus (Rutka *et al.*, 1997). This suggestion is supported by findings that intermediate filaments might be used as 'docking sites' for kinases, and that GFAP assists in linking microfilaments, integrin receptors, and the ECM (Tsujimura *et al.*, 1994).

3.1.2.2 S100-β

S100-β is considered to be a marker of immature astrocytes, and is expressed earlier in development than GFAP (Namihira *et al.*, 2004). S100 proteins are small (10-12 kDa) and acidic, exhibiting high specificity in their cell and tissue expression patterns (Marenholz *et al.*, 2004). S100 protein was first isolated from the CNS in 1965, and is found in the cytoplasm and nuclei of astrocytes, OLGs, and Schwann cells. The S100 family consists of 20 proteins in humans, possessing 22 – 57% sequence homology (Marenholz *et al.*, 2004). Members of the S100 protein family are calcium-binding proteins, which also have zinc and copper-binding sites, and participate in regulation of protein phosphorylation in the CNS via inhibition of protein kinase C (Steiner *et al.*, 2007). S100 proteins are multifunctional signalling molecules, thought to be involved in cell differentiation, cell cycle progression, and the structure and function of the cytoskeleton (via regulation of assembly of components such as GFAP, microtubules,

or vimentin) (Bianchi *et al.*, 1993). Altered levels of S100 have been associated with neurodegenerative disorders, cancer, and lowered expression has been observed in cardiomyopathies (Marenholz *et al.*, 2004).

S100 proteins are composed of two differentially expressed subunits (α and β) produced by separate genes. The beta subunit (S100-β) is highly conserved in the brains of vertebrates, and its expression has been localised to astrocytes (Friend *et al.*, 1992), where it is found diffusely in the cytoplasm, and associated with membranes and cytoskeletal components (Adami *et al.*, 2001). In addition to its role in regulating intracellular processes, S100-β is also secreted. The secreted form mediates the interactions of glial cells with other glial cells and neurons, partly via involvement of S100-β with the cell surface receptor for advanced glycation end products (RAGE), found on inflammatory cells and neurons (Donato, 2001). Brain trauma leads to an increase of S100-β levels in blood, as is also seen in chronic disorders, such as MS and Alzheimer's disease (Sheng *et al.*, 1994). Nanomolar concentrations of S100-β encourage neuron growth, whereas micromolar levels promote apoptosis (Huttenen *et al.*, 2000).

3.2 Aims and objectives

Astrocytes are a source of both chemokines and MMPs in the brain, and are thus of key importance in view of the effects of these enzymes on chemokines, as described in the previous chapter. The aim of the work in this chapter was to determine whether astrocytes express the truncated forms of CCL2 and CXCL10 *in vitro,* thus supporting the likelihood that they are of significance in MS. Accordingly, the following objectives were addressed:

- To characterise primary human astrocytes used in this project by immunofluorescence and western blotting
- To identify the presence of CCL2, CXCL10, and chemokine cleavage products detailed in Chapter 2, in astrocyte supernatants by western blotting and MALDI-QTOF MSpec
- To determine the expression profile of MMPs and TIMPs by TaqMan® real-time polymerase chain reaction (PCR) in astrocytes, thereby identifying MMPs which may play important roles in chemokine cleavage in the CNS

3.3 Materials and Methods

3.3.1 Primary human astrocytes

3.3.1.1 Source of primary human astrocytes and ethical approval

Astrocytes were a gift from Dr I. Romero of the Open University (OU), Milton Keynes, UK. Non-MS astrocytes were derived from adult human brain tissue obtained from patients with epilepsy who underwent temporal lobe resection surgery at King's College Hospital to control their seizures. Tissue is most commonly removed from the anterior or mesial portions of the temporal lobe during this procedure, and was used for astrocyte isolation in accordance with the approval and guidelines of the Local Ethics Committee of King's College Hospital, London. Astrocytes from MS patients were prepared by Dr. Romero's research group at the OU (Flynn *et al.*, 2003), using brain tissue supplied by the UK MS Tissue Bank. Reciprocal ethical approval is in place between the UK MS Tissue Bank, the OU, and Sheffield Hallam University, which enables their use at both sites.

3.3.1.2 Cell culture of primary human astrocytes

All cell culture techniques were conducted using sterile materials and conditions in a high efficiency particulate air (HEPA)-filtered class II laminar flow cabinet (Heraeus, Germany). Sterile plasticware was obtained from BD Falcon (BD Biosciences, UK) and all constituents of growth media were from Invitrogen, UK, unless otherwise stated.

Cells derived from 5 epileptic patients (EP14, EP15, B73, B327/01, and 668/01), and 3 patients with MS (SMS12, MS16, MS21) were used in various experiments, up to passage 8. SMS12 was obtained from normal appearing white matter (NAWM) of an MS patient, and MS16 and MS21 were from MS lesions. Cells were stored in cryovials (Nalgene, Hereford, UK) kept in a dewar (Forma Scientific Inc., Ohio) containing liquid nitrogen until required, by slow-freezing at 1°C per minute in a 'Cryo Freezing Container' (Nalgene), in astrocyte culture media containing 10% v/v dimethyl sulphoxide (DMSO) (Sigma). Cells were cultured in either 25 or 75 cm^2 filter-cap flasks (Nunc, UK) in an incubator (Heraeus, Germany) providing a humid environment at 37°C, containing 95% air and 5% CO_2. Astrocyte medium was composed of a 1:1 nutrient mixture of MEM-α and F-10, supplemented with 250U/ml fungizone, 100U/ml penicillin/100µg streptomycin (1% v/v), 10% v/v heat-inactivated foetal calf serum (HI-FCS) (56°C for 30min) and 1% v/v human AB serum (Sigma, UK). Medium was changed twice weekly and the astrocytes passaged when almost confluent. Passaging was performed by removal of medium, cells were rinsed briefly with phosphate buffered

saline (PBS) without calcium and magnesium, and then 5ml of trypsin/EDTA (0.5g/L trypsin, 0.2g/L EDTA) was applied at 37°C for no more than 5min.

3.3.1.3 Cytokine treatment of astrocytes to increase chemokine expression

In order to increase expression of CCL2 and CXCL10 and to mimic the inflammatory environment of the CNS in MS, astrocytes were treated with pro-inflammatory cytokines. It is known that TNF and IL-1β induce expression of CCL2, and IFN-γ induces CXCL10 expression (Oh *et al.*, 1999). Astrocytes were plated at 1 x 10^5 cells/well into a 24-well plate, in 1ml per well of media without FCS and human serum, i.e. serum-free media (SFM), containing 0, 1, 10 or 100ng/ml of IFN-γ, IL-1β, or TNF (Peprotech, EC), for 24-48h. Cytokine treatment was performed prior to selected western blotting and MSpec procedures, and astrocytes were treated with 100ng/ml of TNF, IL-1β, or IFN-γ prior to RNA extraction for RT-PCR experiments.

3.3.2 Immunocytochemistry for detection of GFAP and S100-β to assess astrocyte purity

3.3.2.1 Principles of immunocytochemistry

Immunostaining was first devised in the 1930s but it took until 1942 for the first study to be reported, which used fluorescently-labelled antibodies to localise pneumococcal antigens in tissues. Immunocytochemistry is based on the affinity of an antibody for an antigen in a cell, whereas immunohistochemistry applies to the same process, but in tissue sections. The antigen and antibody form a complex, held together by forces such as ionic interaction, hydrogen bonding, and hydrophobic interaction. The part of the antigen that is recognised by the antibody is known as the epitope, and many epitopes can exist on the same protein molecule. Polyclonal antibodies bind to more than one epitope, whereas monoclonal antibodies recognise a single epitope. Antibodies only form complexes with the specific antigen that stimulated their production, but some cross-reactivity can occur, however, whereby one antibody can recognise two similar proteins, as the epitope may be a short amino acid sequence common to both proteins (Ramos-Vara, 2005).

As antibodies are large molecules, with IgG having a molecular weight of 150,000, for example, the amino acid side chains can be conjugated with fluorochromes (e.g. fluorescein isothiocyanate (FITC)) or enzymes (e.g. horseradish peroxidase (HRP)). This antibody-labelling allows antigen-antibody complexes to be detected, a process which forms the basis of immunocytochemistry (Fig. 3.1) (Ramos-Vara, 2005).

In order to test the specificity of the antibodies used, immunoglobulins of the same class, namely isotype controls, can be used under the same experimental conditions. Optimal conditions for each antigen-antibody reaction must be determined, as antigen and antibody availability, antigen-antibody affinity, and detection methods will vary.

3.3.2.2 Direct immunofluorescence

The simplest form of antibody detection is the direct fluorescent method, where antigens are localised by combination with a fluorescently-labelled antibody (Fig. 3.1(i)). Direct immunofluorescence was applied in flow cytometry, in Chapter 5. Direct fluorescent antibody methods lack sensitivity, however, and if the antigen concentration is low, the density of bound fluorochrome molecules may be insufficient to be detected.

3.3.2.3 Indirect immunofluorescence

Indirect immunofluorescence techniques are more commonly employed, as they offer greater sensitivity due to the increase in potential binding sites for the fluorescently-labelled antibody (Fig.3.1(ii)). Indirect methods involve incubation of the sample with an unlabelled primary antibody, followed by washes, and addition of a labelled secondary antibody. The secondary antibody is directed against the species that the primary antibody was raised in, and is able to bind to Fc segments of bound primary antibody, as these are identical within the same species. In this way, the antigenic sites of the sample are identified by the fluorochromes of the secondary antibody, which binds to the primary antibody attached to the antigen (Fig. 3.1(ii)).

3.3.2.4 Detection of cell antigens using antibodies with enzyme conjugates

Antibodies can also be labelled by conjugation with enzymes, such as HRP or alkaline phosphatase. Detection of the antibody-bound antigen is dependent upon the production of a precipitating or intensely coloured product after the enzyme label has reacted with its substrate, or by chemiluminescence, where light is produced at the target sites, as seen in the reaction of HRP with luminol (Ramos-Vara, 2005).

3.3.2.5 Use of biotinylated antibodies in immunocytochemistry

Primary antibodies used in direct immunocytochemistry, and secondary antibodies used in the indirect method, can be biotinylated to generate increased amplification of signal. Biotin is a water-soluble B-complex vitamin which binds very strongly, and almost irreversibly, to avidin, strepatavidin, or extravidin. Avidin, strepatavidin, or extravidin, conjugated to either a fluorochrome or an enzyme, are added after

application of a biotinylated antibody, and are capable of binding to multiple sites on the biotinylated antibody. This amplifies the signal that can be detected and is more sensitive than simply using enzyme or fluorochrome-conjugated antibodies alone (Ramos-Vara, 2005) (Fig. 3.1(iii)).

3.3.2.6 Blocking of non-specific binding in immunofluorescent staining

A blocking step is usually included prior to antibody application, particularly with tissue sections, most commonly involving incubation with a 3% solution of the serum of the species that the secondary antibody was raised in, thereby occupying non-specific binding sites, such as Fc receptors. Blocking was not found to be necessary for immunocytochemistry of the astrocytes.

3.3.2.7 Use of human astrocytomas (U373MG) as a positive control in immunocytochemistry for detection of GFAP and S100-β in astrocytes

The human glioblastoma astrocytoma (grade III) cell line (U373MG) (European Collection of Cell Cultures (ECACC), Wiltshire, UK), derived from a 61 year old Caucasian male (Ponten and Mackintyre, 1968), was used as a positive control for astrocyte characterisation by immunocytochemistry. U373 cells were cultured in MEM media containing 10% v/v HI-FCS, 2mM (1% v/v) L-glutamine, 1% v/v penicillin/streptomycin, 1% v/v non-essential amino acids, and 1mM sodium pyruvate. These cells were passaged and frozen down as described for the astrocytes (3.3.1.2).

3.3.2.8 Cell culture preparation prior to immunocytochemistry

Astrocytes were plated into 8-well chamber slides (Fisher Scientific, Loughborough, UK), 400µl per well, with a seeding density of 1 x 10^5 cells per ml, and left overnight to attach. Media was removed and 2 rinses in PBS, of 5min each, were performed to remove media.

3.3.2.9 Fixation of astrocytes

Cells were fixed prior to use to preserve their structure by preventing autolysis. Fixatives also stabilise specimens so that they can withstand subsequent processing. Formaldehyde and paraformaldehyde are often used when the antigen of interest is a protein of low molecular weight. Acetone, ethanol and methanol (often pre-cooled to -20°C) are commonly used with larger protein antigens, and offer fixation by a different means, namely denaturing the protein by coagulation (Ramos-Vara, 2005).

Figure 3.1 Schematic diagram of immunocytochemistry methods

i) Direct immunofluorescent staining of a cell involves using an antibody with a fluorescent dye attached, which binds to antigens it has been raised against, expressed by cells or tissue. This simple and quick technique allows the location of the antigen to be observed using a fluorescent microscope, but it lacks sensitivity, and is less commonly used than indirect methods.

ii) Indirect immunofluorescence involves binding of an unlabelled primary antibody to the antigen it is specific for. After careful washing following binding of the primary antibody, a secondary antibody is applied, which is directed against the Ig of the species the primary antibody is raised in. This secondary antibody is conjugated with a fluorophore, and will bind to Fc domains of the primary antibody, thereby linking indirectly to the antigen and enabling detection by fluorescent microscopy. Several secondary antibody molecules can bind to one primary antibody molecule, resulting in signal amplification and greater sensitivity.

iii) The streptavidin-biotin method uses a secondary antibody with a biotin conjugate, which binds to the primary antibody, using the same principles as in (ii). A third reagent of labelled streptavidin is used, which binds firmly to large numbers of biotin molecules, giving increased sensitivity. The label can be an enzyme, such as peroxidase (detected by formation of an insoluble product after reaction with a substrate), or a fluorophore.

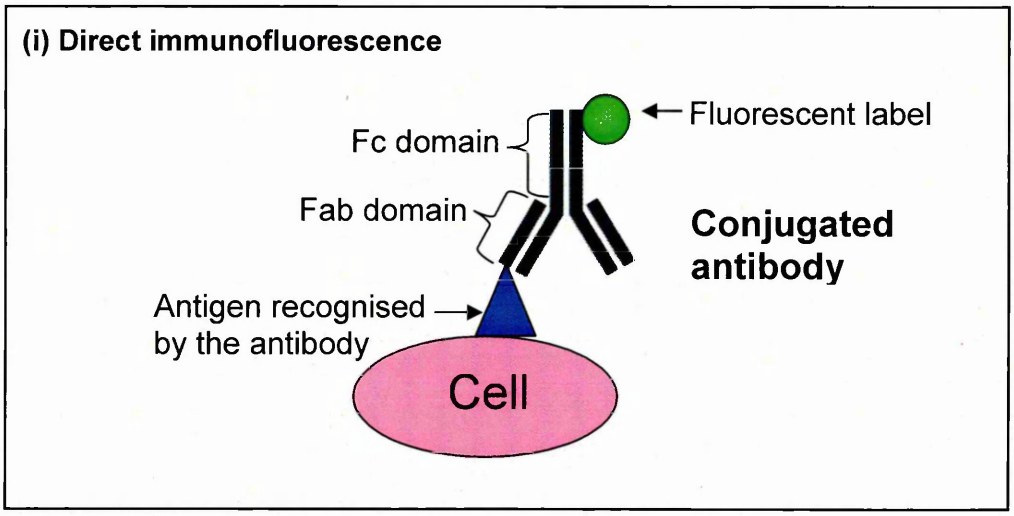
(i) Direct immunofluorescence
Fluorescent label
Fc domain
Fab domain
Conjugated antibody
Antigen recognised by the antibody
Cell

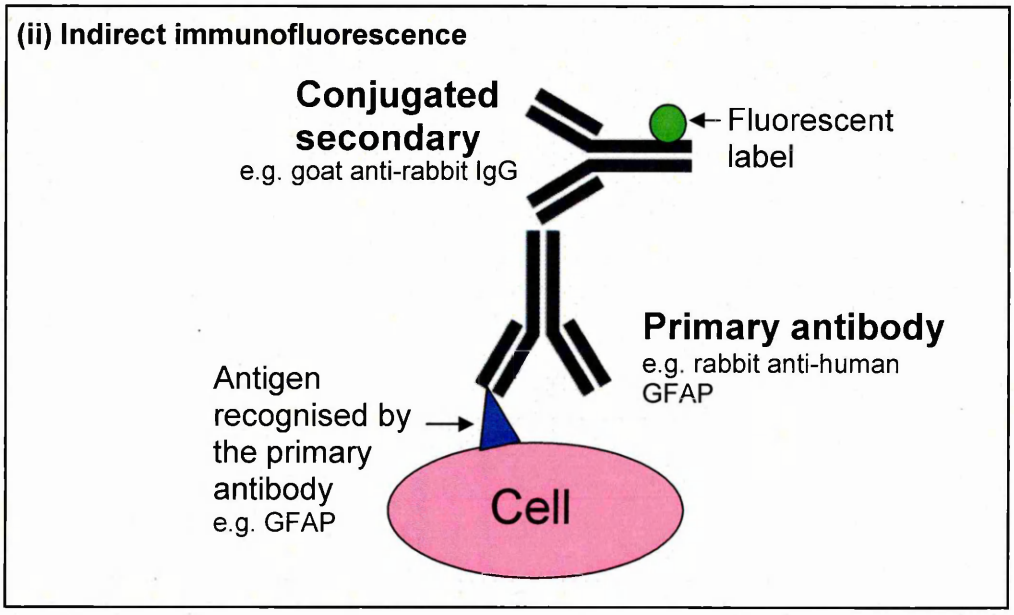
(ii) Indirect immunofluorescence
Conjugated secondary
e.g. goat anti-rabbit IgG
Fluorescent label
Primary antibody
e.g. rabbit anti-human GFAP
Antigen recognised by the primary antibody
e.g. GFAP
Cell

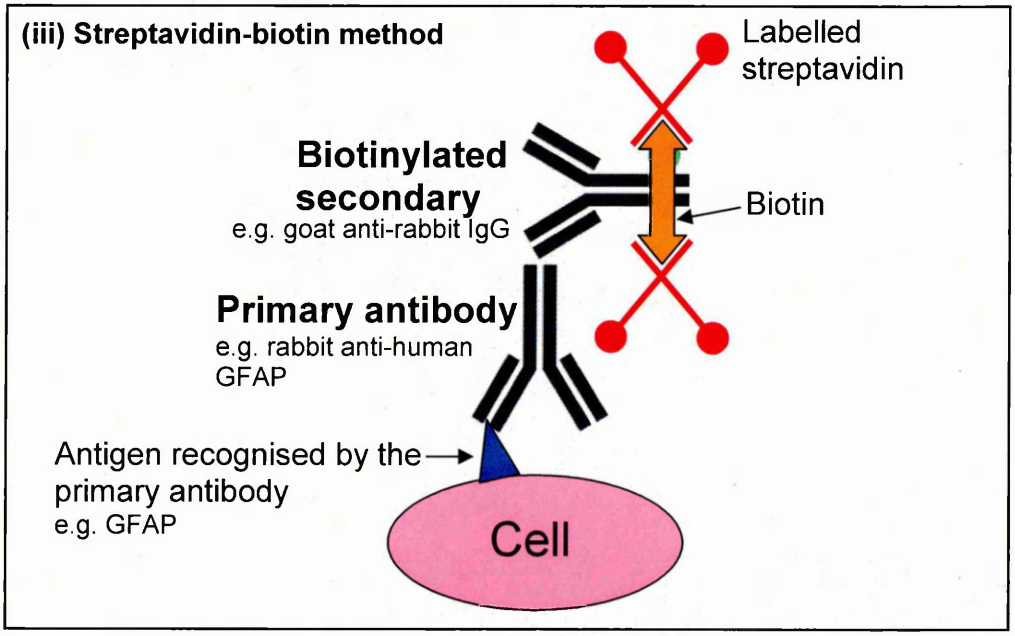
(iii) Streptavidin-biotin method
Labelled streptavidin
Biotinylated secondary
e.g. goat anti-rabbit IgG
Biotin
Primary antibody
e.g. rabbit anti-human GFAP
Antigen recognised by the primary antibody
e.g. GFAP
Cell

Experimenting with different fixatives, and fixation times, was undertaken to optimise cellular structure but minimise epitope masking or destruction. Astrocytes were fixed using 4% paraformaldehyde (PFA) (see Appendix I) for 5min at RT, followed by 3 consecutive 5min PBS washes prior to incubation in primary antibody. Alternatively, ice-cold acetone for 5 – 10min at RT, followed by air drying for 15min, was used for comparative purposes in some preliminary experiments.

3.3.2.10 Detection of GFAP and S100-β antigens in astrocytes by indirect immunofluorescence

The optimal working concentration of each antibody was determined for each set of experimental conditions using a series of dilutions, to obtain a positive result with minimal background staining. Temperature, pH, incubation times, and buffer composition were also optimised, as they can all affect antibody binding.
The plastic upper part of the chamber slide was removed prior to antibody application, leaving the rubber gasket in place. Following fixation, primary antibodies (Table 3.1) (100µl per well, diluted in PBS + 0.5% Triton® X-100) were applied to cells in each well, apart from the negative controls, where PBS + 0.5% Triton® X-100 alone was used. Addition of non-ionic detergent helped to reduce hydrophobic interactions between the reagent proteins and the cells and permeabilise the membranes (Stuart and Oorschot, 1995). Slides were incubated in a humid chamber for between 90-120min at RT, or, alternatively, overnight at 4˚C (Table 3.1). Slides were transferred to Coplin jars and unbound primary antibodies washed off in PBS, in 3 consecutive 5min washes on an orbital shaker (Stuart Scientific, Staffordshire, UK). Secondary antibodies (Table 3.1) were then applied to the slides, for 90-120min, in the dark, and were subsequently removed as for the primary antibodies.

3.3.2.11 Mounting and final processing of slides

Rubber gaskets on the slides were removed, and the slides were mounted with 22 x 50 mm coverslips with 4',6-diamidino-2-phenylindole (DAPI) mountant (Vector Laboratories, Peterborough, UK), which forms blue fluorescent complexes with DNA, thereby labelling cell nuclei (Degtyareva *et al.*, 2007). The mountant also contained anti-fading agents to prolong the viewing time by limiting the fading of fluorescence under UV light. The edges of the coverslip were sealed with nail varnish to prevent the slides from drying out. Slides were protected from light by wrapping in foil, and stored at 4˚C until required for viewing.

Table 3.1 Antibodies used in detection of GFAP and S100-β to assess astrocyte purity

PRIMARY ANTIBODY	SPECIES RAISED IN	DILUTION	INCUBATION TIME (S)	SUPPLIER
α-human GFAP (polyclonal)	Rabbit	1:1000	2h at RT	Abcam, Cambridge, UK
α-human GFAP (monoclonal)	Mouse	1:400	2h at RT	Sigma, Dorset, UK
α-human S100-β (monoclonal)	Mouse	1:500	90min at RT	Sigma, Dorset, UK
SECONDARY ANTIBODY				
α-rabbit IgG Alexa Fluor 488	Goat	1:500	90min at RT	Molecular Probes, Invitrogen, UK
α-mouse FITC	Rabbit	1:50	90min at RT	Dako, Ely, UK

Primary antibodies against GFAP and S100-β were detected by the appropriate fluorescently labelled secondary antibody.

3.3.2.12 Use of confocal microscopy to detect fluorescently-labelled antibodies

A confocal laser scanning microscope (CLSM) works by systematically illuminating single points of a specimen, usually with focused laser beams to excite the fluorophore in the sample, followed by use of a photodetector, such as a photomultiplier tube or charge-coupled device (CCD), to capture the emitted light that has passed through a pinhole aperture from the point of focus. Light originating away from the point of focus is eliminated by the use of a pinhole aperture. The detector pinhole is positioned to be in a conjugate plane with both the point of excitation of the laser defined by the excitation pinhole and the plane of focus of the microscope objective (Fig. 3.2). In confocal microscopy, the sequential scanning of the specimen and assembly of the final image are controlled by a computer. A single laser point beam of a specific wavelength is scanned across the sample using oscillating mirrors. The emitted light, of a longer wavelength, is separated from the excitation light by a dichroic mirror and passed through the pinhole aperture to the detector, which then transmits the data for each individual point to the computer (Fig. 3.2) (Cox, 2002).

3.3.2.13 Image acquisition using the confocal microscope

The confocal microscope used throughout this project was a Zeiss LSM 510 (Germany), equipped with argon (450-530nm) and helium-neon lasers (543 and 633nm). It was linked to a Fujitsu Siemens computer, running Windows 2000, with LSM 510 software installed, and the use of 2 monitors. Single track images of 512 x 512 pixel resolution were obtained of the FITC or Alexa 488 green fluorescence, and overlaid with images of the DAPI fluorescence before being exported as JPEGs.

3.3.3 Western blotting for detection of GFAP to assess astrocyte purity

3.3.3.1 TRI Reagent® method for extracting protein from astrocytes

Protein was extracted from both the supernatant of cultured astrocytes, using TRI Reagent LS® (Sigma) designed for liquid samples, and from the cells, with TRI Reagent® (Sigma). Both types of TRI Reagent® were used according to the manufacturer's protocol (Appendix II). TRI Reagent® is a mixture of guanidine thiocyanate and phenol in a mono-phase solution used for homogenising or lysing samples. Addition of chloroform causes the mixture to separate into 3 phases which can each be isolated: RNA is found in the aqueous phase, DNA in the interphase, and protein in the organic phase (Siebert and Chenchik, 1993). Extracted protein samples were stored in 1% SDS at -20˚C until required.

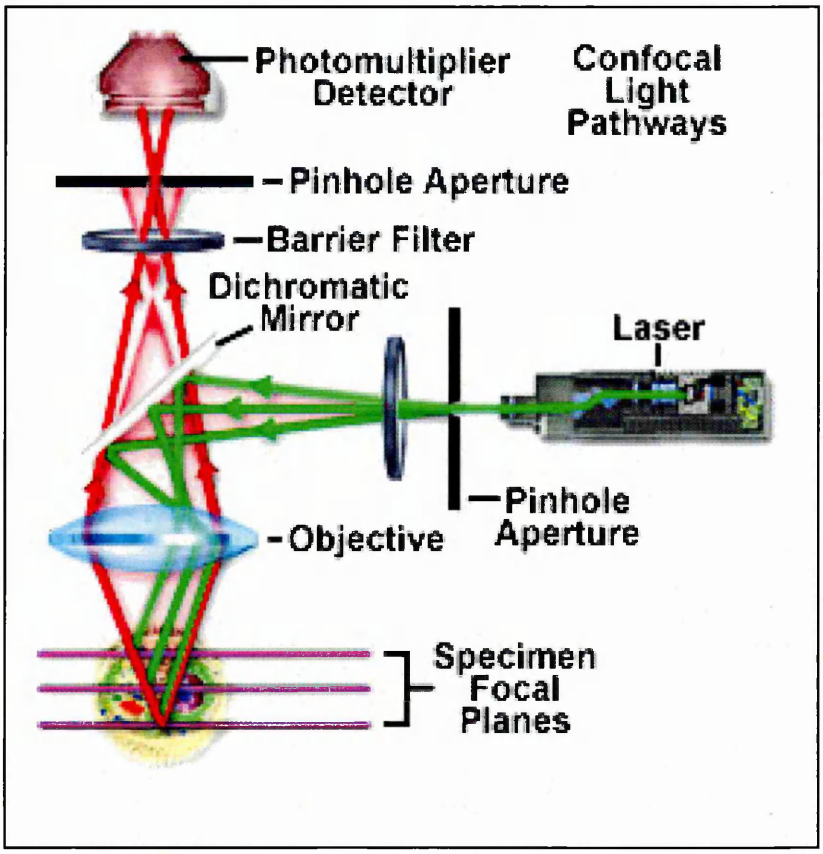

(Image source: http://www.microscopyu.com/articles/confocal/confocalintrobasics.html)

Figure 3.2 Schematic diagram of the optics of a confocal microscope

In confocal microscopes, light from a laser passes through a pinhole before being reflected by a dichroic mirror and focused through the objective onto a single spot of the specimen on the microscope slide, as represented by the green path in the figure. The excitation of the specimen from the laser results in emitted light in random directions, a selection of which passes through the objective and then through a pinhole to the detector, as seen in red. The detector pinhole prevents out-of focus emissions from the sample from reaching the detector, ensuring three-dimensional resolution is possible. Only a single point of the sample is imaged at one time, so to obtain the whole image, the laser beam systematically scans across the sample, and the image is built up in layers or 'optical slices'.

3.3.3.2 Alternative method for extracting protein from astrocytes

When protein yields were low using TRI Reagent®, the following method, suitable for cell monolayers, was used as an alternative. Sample and extraction buffers were made the day before use (Appendix I), and stored at 4˚C.

A protease inhibitor tablet (Roche, East Sussex, UK), containing mannitol (80-90%), 4-(2-aminoethyl)-benzenesulphonyl fluoride hydrochloride (AEBSF) (1-5%), EDTA (5-10%), polyvinylpyrrolidone (1-5%) and polyethylene glycol (1-5%), which inhibits serine proteases, cysteine proteases, and metalloproteases, was added to 10ml extraction buffer (Appendix I) just before use, and 500µl of this added per 25cm^2 flask of cells that had been previously washed in PBS. Cells were detached using a scraper (BD), transferred to a tube, homogenised using a grinding action with a glass rod, 495µl cell homogenate transferred to an Eppendorf tube, and 5µl (1%) Triton® X-100 was added. This mixture was incubated for 1h at 4˚C, and was vortexed for 3min every 7min. It was then spun in a 'Mini Spin Plus' micro-centriguge (Eppendorf, Cambridge, UK) at 11337*g* for 10min at 4˚C. The supernatant was removed to a clean tube and the pellet resuspended in 500µl dH_2O. 2X sample buffer (Appendix I) was added in an equal volume to both the pellet and supernatant, heated to 85˚C for 2.5min, and protein samples stored at -80˚C until required.

3.3.3.3 Bicinchoninic acid (BCA) assay to assess the concentration of protein extracted from astrocytes

BCA assays were performed to determine the protein concentration of the samples obtained from the cell extractions. It is based on the reaction of protein with Cu^{2+} ions in an alkaline environment, producing cuprous (Cu^+) ions. Cu^+ ions are then detected by the interaction of 2 molecules of BCA to each Cu^+ ion, forming a soluble purple product which absorbs strongly at 570nm.

Dilutions for a standard curve were prepared using bovine serum albumin (BSA). A stock solution of 20mg/ml BSA was prepared in dH_2O (or 1% SDS, if this was used as a diluent for the samples), and further diluted to yield concentrations of 10, 8, 6, 4, 2, 1, 0.8, 0.6, 0.4, 0.2, and 0.1 mg/ml. 20µl aliquots of the BSA standards, samples, and appropriate blanks (dH_2O and extraction buffer) were added in triplicate to wells of a 96-well plate. BCA reagent was prepared by adding 10ml BCA to 200µl 4% (w/v) copper sulphate solution, and 200µl of this was added to each well. The plate was incubated at RT for 30min, and then read at 570nm using a Wallac Victor^2 plate reader (PerkinElmer, USA). A mean value was calculated for all triplicate readings and a

standard curve plotted for mean absorbance of the BSA standards at each concentration. The protein concentration of the samples was then derived from the standard curve using the linear equation $y = mx + c$, rearranged to give $x = (y - c) / m$, where x is the concentration (mg/ml), y is the absorbance of each sample minus the blank, m is the gradient, and c is the y intercept. Once the sample protein concentration was derived, the volume required to load a set amount of protein (usually 4µg) for use in SDS-PAGE was calculated.

3.3.3.4 Gel electrophoresis of protein samples extracted from astrocytes

Gel electrophoresis was performed as described in 2.3.2.2, loading up to 20µl (containing ~4µg protein) of each astrocyte cell lysate and supernatant sample into lanes of a 12-well, 1 mm thick, precast 12% Bis-Tris gel. SeeBlue Plus2 pre-stained standard (7µl), with bands in the 4-250 kDa range, was run in the end lane of the gel to enable visualisation of molecular weight bands and confirm blotting transfer efficiency.

3.3.3.5 Principles of western blotting

When detection of a specific protein in a complex mixture is required, western blotting is used, after separation of proteins by gel electrophoresis. Electrophoresis is also used to transfer the proteins from the gel to a support membrane, with the electrodes being parallel to the plane of the gel so that uniform voltage is applied across the whole surface. Transfer can either be performed in a tank with a buffer containing methanol to increase the membrane binding capacity, or in a semi-dry system, which uses minimal buffer and low voltages. Proteins migrate from the gel and are immobilised on the membrane in the same pattern as in the gel. Membranes are typically nitrocellulose, offering good sensitivity, or polyvinylidene difluoride (PVDF), giving high protein binding capacity. Non-specific antibody binding is prevented by incubating the membrane with reagents such as non-fat dried milk or BSA, to block excess protein-binding sites. Proteins of interest are located by exposing the membrane, or 'blot', to appropriate antibodies, in a similar process as described for immunocytochemistry, with chemiluminescence being a popular detection method (3.3.2). Working with a membrane instead of a gel offers several advantages, as low antigen densities are more readily detected due to increased accessibility, and membranes are easier to handle.

3.3.3.6 Protein transfer from separating gel to the membrane

Gloves were worn throughout the procedure to prevent keratin proteins being transferred to the membrane. After separation of proteins from cytokine-treated and untreated astrocyte supernatant and lysate samples by gel electrophoresis, the gel was rinsed for 5-10min in 100ml NuPAGE® transfer buffer (Invitrogen) (5% v/v 20X transfer buffer, 10% v/v methanol, 85% v/v upH_2O). Porous components of the western blot assembly were pre-soaked in cooled transfer buffer, arranged as in Figure 3.3, using a Hybond C nitrocellulose membrane (Amersham, UK) and slotted into a transfer tank, with the black plate nearest to the negative electrode. The tank was filled with cold transfer buffer, and placed in a large container filled with ice to prevent over-heating. The transfer was conducted at 150 volts for approximately 90min, or overnight at 35 volts at 4˚C.

3.3.3.7 Blocking of non-specific binding to the membrane

Tris buffered saline (TBS) (20mM Tris, 0.9% NaCl w/v, pH of 7.5) had 0.05% v/v Tween® 20 freshly added, to yield TBST. The membrane was removed from the assembly apparatus and blocked in 5% non-fat milk powder in TBST, either overnight at 4˚C, or for 1h at RT, on an orbital shaker.

Blocking was later assessed using 5% 'Marvel' non-fat milk powder (Premier Brands Ltd., Birmingham, UK) in TBS, during optimisation of the technique. Blocking was followed by 3 consecutive, 10min washes at RT in TBST, on an orbital shaker.

3.3.3.8 Antibody application for detection of GFAP by western blotting

Primary antibody solutions were made in TBST and included monoclonal mouse anti-human GFAP at 1:5000 (0.2µg/ml) (Chemicon), and polyclonal rabbit anti-human GFAP at 1:2500 (Dako). Membranes were incubated with primary antibody (or TBST for the negative control) for either 90min at RT, or overnight at 4˚C, on an orbital shaker. During optimisation, primary antibodies were initially applied in TBST containing 5% non-fat milk powder.

Primary antibodies were washed off with 3 consecutive, 10min TBST washes. Mouse anti-GFAP (Chemicon) primary was detected with a polyclonal rabbit anti-mouse HRP-conjugated secondary antibody (Dako), used at 1:1000, for 90min at RT. The rabbit anti-GFAP (Dako) primary was detected using a goat anti-rabbit HRP-conjugated secondary antibody (Sigma), used at 1:40,000 for 90min at RT.

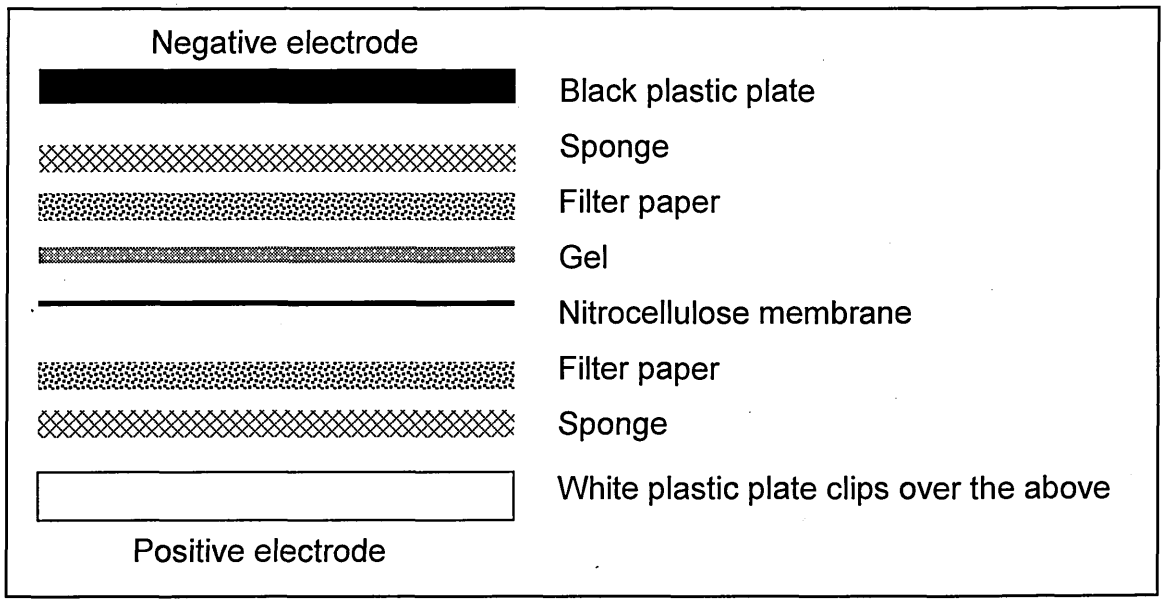

Figure 3.3 Schematic of assembly order of western blotting equipment

All components of the above assembly were pre-soaked in transfer buffer before use. The outer plates, sponges, and filter paper sheets were used to sandwich the gel against the nitrocellulose membrane, in the order detailed above, carefully avoiding introduction of air bubbles. The black plate was postioned nearest to the negative electrode, and the electrophoretic transfer of proteins from the gel to the membrane achieved at 4 ˚C in a tank filled with buffer. The electric current 'pulls' proteins from the gel to the membrane, whilst maintaining their arrangement, so that a replica pattern, or 'blot', is achieved on the membrane. Proteins bind to the membrane, and can be detected by the use of antibodies.

Secondary antibody was washed off with 3 consecutive, 5min TBST washes with orbital shaking, followed by 3 consecutive, 5min TBS washes.

3.3.3.9 Detection of bound antibody using chemiluminescence

Enhanced chemiluminescence (ECL) reagent ECL Plus (Amersham Biosciences) was prepared immediately before use by mixing 2ml of Solution A with 50µl of Solution B and storing in the dark until required. Approximately 1ml of this was applied to each membrane for 5min at RT. This was then tapped off by handling the membranes with forceps, and the membrane was transferred to the inside of a washed clear plastic wallet. Light emitted from areas where the primary and secondary antibodies were bound was detected using an EpiChemi II Darkroom UVP system (BioImaging Systems), and images of the membrane obtained using LabWorks image acquisition and analysis software. To increase visibility of the SeeBlue Plus 2 rainbow marker bands, they were highlighted in pencil on the membrane prior to detection in the UVP system.

3.3.4 Detection of astrocyte expression of CCL2 and CXCL10

To assess the feasibility of isolating intact and truncated forms of CCL2 and CXCL10 from astrocytes, cell supernatants and lysates were investigated for the presence of these chemokines by western blotting and MALDI MSpec. To test the detection levels of these techniques, known concentrations of CCL2 and CXCL10 were prepared using recombinant proteins, and run alongside astrocyte-derived samples.

3.3.4.1 Western blotting for detection of CCL2 and CXCL10 in astrocyte samples and determination of detection limit

CCL2 and CXCL10 standards (Peprotech, EC) were prepared by dilution of recombinant proteins with dH_2O and LDS sample buffer (4X) to give final protein amounts of 15, 10, 7.5, 5, 2.5, 2, 1, 0.5, and 0.25ng, and 1X sample buffer, for loading onto a gel. These amounts were chosen to reflect a range within which CCL2 and CXCL10 had been previously found in astrocyte cell supernatants (Suliman *et al.*, 2006). Chemokine standards were run alongside supernatant and lysate samples from SMS12 astrocytes, treated with 0, 10, and 100ng/ml IL-1β, TNF and IFN-γ for 24 and 48h.

Western blotting was performed as described above, using a mouse monoclonal anti-human CCL2 primary antibody (Abcam) at 1:500 (0.2µg/ml) for either 90min at RT or overnight at 4˚C, and a polyclonal rabbit anti-mouse HRP-conjugated secondary

antibody (Dako), used at 1:1000, for 90min at RT. Biotinylated primary antibodies against CCL2 and CXCL10 (R&D Systems) were also used in western blotting at 0.2µg/ml, with detection of biotin by extravidin-peroxidase (Sigma), applied at 1:2000 for 1h at RT, prior to ECL detection as described above.

3.3.4.2 Detection of CCL2 and CXCL10 in astrocyte supernatant by MALDI-QTOF mass spectrometry

Supernatant from primary human astrocytes (EP15 P8) treated with 0, 1, 10, and 100ng/ml IFN-γ for 24h, was collected, the protein extracted using TRI Reagent®, and the protein pellet dissolved in 10µl dH_2O. This was mixed with 3µl α-CHCA (25mg/ml) matrix, and 1.5µl spotted onto a target plate and analysed by MALDI mass spectrometry using an Applied Biosystems/MDS Sciex "QStar" hybrid quadrupole mass spectrometer. A laser power of 40 - 60% and a pulse rate of 1000Hz were used for this analysis. This process was repeated, with zip tipping (see 2.3.5.2) of the samples, prior to analysis.

3.3.4.3 Assessment of the detection limit of CCL2 and CXCL10 by MALDI-QTOF mass spectrometry

To assess the MALDI detection limit for CCL2 and CXCL10, SF media was spiked with recombinant chemokine and analysed by MALDI mass spectrometry. Serial dilution of CCL2 was done to prepare concentrations of 1000, 800, 400, 200, 100, and 50pg/ml. CXCL10 concentrations prepared were 1000, 240, 120, 60, 30, and 15pg/ml, as expression of this chemokine was lower than for CCL2 in previous *in vitro* experiments with human adult astrocytes (Suliman *et al.*, 2006). 1µl of the various concentrations were mixed with 4µl of αCHCA matrix and 1.5µl spotted onto a target plate. A laser power of 15% and a pulse rate of 500Hz were used during MALDI analysis. This process was repeated, with zip tipping (see 2.3.5.2) of the chemokine solutions, prior to analysis.

3.3.4.4 Concentration of chemokine-spiked media by freeze drying

The effect of concentrating astrocyte supernatants for detection of chemokine by MSpec was investigated, since there were concerns that chemokines in the supernatant would be present at a range below the detection limit. 20ml SFM was spiked with 1µl of 0.1mg/ml CCL2 or CXCL10 to give 5000pg/ml, which contained approximately 581 femtomoles (fmoles) of chemokine. 1ml of this was serially diluted by adding 1ml of SF media to produce concentrations of 2500, 1250, 625, and

312.5pg/ml (containing ~290, 145, 73, and 36 fmoles of chemokine respectively). Samples were stored frozen at -80°C for 2 days. For the freeze-drying process, these samples were transferred to15ml conical tubes with holes pierced in the lids, and placed in a pre-cooled glass vessel which was fitted to a ModulyoD freeze-drier (Thermo Electron Corporation, Cheshire, UK). The freeze-drier had been turned on 30min before to reduce the temperature. Once the glass vessel was in place, a vacuum was applied, and the tubes left to dry overnight. Dried samples were resuspended in 80µl dH_2O + 20µl sample preparation solution (0.5% TFA) before being zip-tipped and 2µl spotted onto a target plate for MALDI analysis. These spots were analysed using 20% laser power, and a pulse rate of 1000Hz.

3.3.5 Detection of MMPs expressed by astrocytes using TaqMan® polymerase chain reaction (PCR)

To determine the range of MMPs and TIMPs that chemokines might be exposed to *in vivo*, and to investigate if any particular MMPs were more abundant than others, their RNA expression profiles were investigated in astrocytes.

3.3.5.1 Principles of TaqMan® PCR

TaqMan® PCR is a real-time PCR method that utilises a probe with attached fluorescent tags, namely a reporter dye such as VIC®, or 6-carboxy-fluorescein (FAM), which has its emission spectra suppressed due to the proximity of a quencher dye, such as TAMRA (6-carboxy-tetramethylrhodamine) (Osgood-McWeeney *et al.*, 2000). Forward and reverse primers anneal to particular sequences of the target DNA, and then extend. The TaqMan® probe hybridises to target DNA, internal to the primer sequences. The forward primer displaces the TaqMan® probe, and the 5' exonuclease activity of Taq DNA polymerase then hydrolyses it during the extension phase of PCR, thus liberating the reporter dye from the quencher, resulting in fluorescence (Fig 3.4). After several amplification cycles, sufficient reporter dye is released through this cleavage, enabling detection of fluorescence, proportional to the quantity of PCR product formed, using a laser-coupled spectrophotometer. The cycle threshold (Ct) represents the cycle number at which a positive result above background fluorescence is obtained, illustrated by the level at which amplification entered the exponential phase (Fig. 3.5). Lower Ct values indicated a higher quantity of target RNA initially in the sample (Vega *et al.*, 2005).

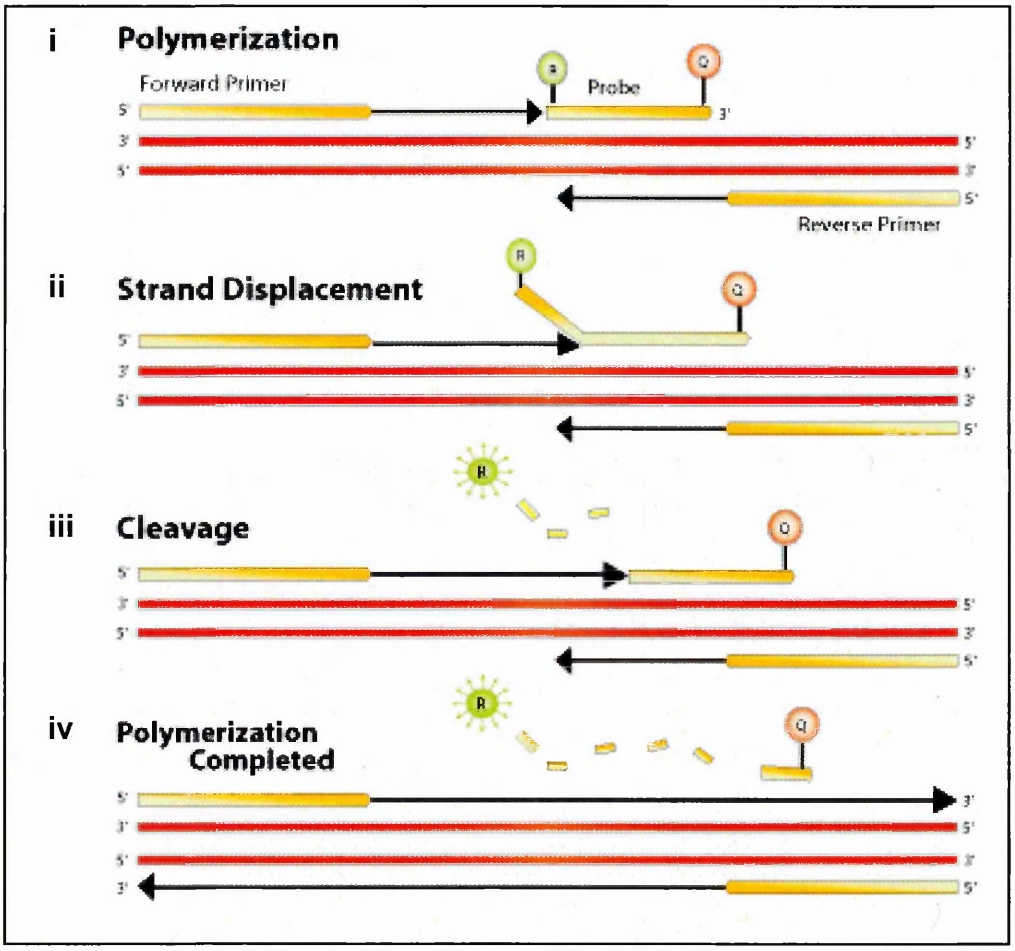

(Image source: http://www.servicexs.com/plaatjes/TaqMan_RT-PCR_assay.jpg)

Figure 3.4 Principles of TaqMan® PCR

A cDNA copy of the RNA template of interest is used in TaqMan® PCR. The TaqMan® probe contains a quenching molecule (orange circle labelled 'Q' above) at the 3' end, which, when it is close by, prevents observation of fluorescent signal from the reporter dye (green circle labelled 'R' above) at the 5' end. After denaturation, both probe and primer bind to the target cDNA. During the polymerisation step (i), Taq polymerase creates a complementary strand via its 5' nuclease activity, which displaces (ii) and cleaves the probe (iii). Disruption of the probe results in fluorescence from the reporter molecule, in a directly proportional manner to the number of molecules released during that cycle, so that accumulation of PCR product is detected by measuring the increase in fluorescence (iv).

3.3.5.2 Preparation of cDNA samples

RNA extracted from astrocytes (cytokine-treated and untreated) using TRI Reagent®, following the manufacturer's protocol (Appendix II), was used in the preparation of cDNA samples, which were stored at -20˚C for 2 days and then transported to the University of East Anglia (UEA) for analysis by TaqMan® PCR.

RNase-free filter tips (Fisher Scientific, Loughborough, UK) and tubes (Sigma) were used throughout the preparation of cDNA. RNA was incubated in a mix containing deoxynucleotide triphosphates (dNTPs), which carry the bases adenine (dATP), guanine (dGTP), cytosine (dCTP), and thymine (dTTP), from which DNA is constructed. The primers in the mix bind to the RNA randomly, and the reverse transcriptase (RT) inserts dNTPs into the gaps to complete the cDNA strand, which represents all the transcribed RNA. Control samples of RNA without RT, and the negative with no RNA + RT were included. For each 1µl sample of RNA in dH_2O (kept at -20˚C until required), the following 'mastermix' was added:

4µl	5 x 1st strand buffer	} Provided with the enzyme (Invitrogen)
2µl	0.1M dithiothreitol (DTT)	
1µl	Deoxynucleotide triphosphates (dNTPs) (Bioline, London, UK)	
0.5µl	RNase inhibitor (Invitrogen)	
0.5µl	Random Hexamers (Invitrogen)	
9µl	Molecular grade H_2O (Sigma)	
1µl	Super Script II reverse transcriptase (RT) (Invitrogen)	

The RT was added last and was kept frozen until required. It was pipetted gently to avoid degradation. After the mastermix and RNA were combined, mineral oil was added to prevent evaporation on the heat block. The samples were heated to 42˚C for 1 hour, and then 95˚C for 5min to inactivate the enzyme, using a Biometra 'Trio-Thermoblock' heating block (Biometra, Hamburg, Germany). The samples were then stored at -20˚C.

3.3.5.3 TaqMan® PCR method for detecting MMPs and TIMPs using cDNA from astrocytes

TaqMan® PCR was performed at the UEA, in the laboratory of Prof. D. Edwards, under the supervision of Dr. R. Nuttall. Samples were analysed only once due to high costs, which precluded statistical analysis of the results. By screening astrocytes for the entire range of MMPs and TIMPs, however, it was hoped that detection of specific mRNAs at

high levels following treatment with pro-inflammatory cytokines might indicate which MMPs are likely to play important roles in chemokine processing in the inflamed CNS. Trends in MMP expression revealed by this pilot investigation could then be considered in future investigations of chemokine processing.

All pipetting procedures were conducted in a designated clean area, and water used was molecular grade (Sigma). Preliminary experiments were conducted with 18S and GAPDH housekeeping genes to establish which one gave the least variation in expression between the samples. The gene for 18S ribosomal RNA (rRNA) was selected and used as a control to normalise for variations in the amount of total RNA in each sample by using 18S rRNA primers and probe (Applied Biosystems, Warrington, UK) alongside each set for the target genes.

All reagents were from Applied Biosystems, unless otherwise specified. 4µl of each cDNA sample was diluted 1:100 with 396µl water. Each well of a 96-well plate had 10µl cDNA sample, 8.5µl TaqMan® mastermix, 0.5µl forward primer, 0.5µl reverse primer, 0.5µl probe, and 5µl water added. Reverse pipetting was used for greater accuracy. For each well containing the housekeeping gene, 2µl cDNA, 8.5µl TaqMan® mastermix, 0.125µl forward primer, 0.125µl reverse primer, and 0.125µl probe, were added.

Five RNA standards (S1 – S5) of known amounts (4, 2, 1, 0.5, and 0.25ng), kindly provided by Dr. R. Nuttall (obtained from U251 human glioblastoma cells), were run for each gene. A negative control sample (no RNA), and a sample with no reverse transcriptase, were run for each MMP. Plates were sealed with an adhesive film and placed in the ABI Prism 7700 sequence detector (Applied Biosystems).

The PCR program was operated using Sequence Detection System (SDS) V1.9 software, using the 'FAM' setting for all genes, except the housekeeping gene 18S, where the 'VIC' setting was used, according to the reporter dyes present. Plates were run using a 2-step PCR process incorporating 40 cycles, which heated the plates to 60°C for 1min, and then 94°C for 15 seconds. Ct values for each MMP and TIMP were obtained from plots generated by the software, once the threshold had been set manually. Comparing gene expression using Ct alone is imprecise, so Ct levels were converted to quantitative relative expression levels. This was done by preparing standard curves (see Fig. 3.11) for each reaction using the standards S1-S5, which had also been subjected to PCR. Standard curves for Ct versus RNA level were used to determine relative starting RNA levels within the sample, which were then normalised to 18S rRNA levels of the same sample.

3.3.5.4 Primer and probe sequences

Sequences for the primers and probes used (of the TIMPs only) are given below, in the 5' to 3' orientation. MMP primer and probe sequences are not shown, as they remain the property of Applied Biosystems (Warrington, UK). The 5' end of the probes contained a FAM fluorescent reporter, and the 3' end had a TAMRA quencher.

TIMP-1

Forward primer: GACGGCCTTCTGCAATTCC

Reverse primer: GTATAAGGTGGTCTGGTTGACTTCTG

Probe: ACCTCGTCATCAGGGCCAAGTTCGT

TIMP-2

Forward primer: GAGCCTGAACCACAGGTACCA

Reverse primer: AGGAGATGTAGCACGGGATCA

Probe: CTGCGAGTGCAAGATCACGCGC

TIMP-3

Forward primer: CCAGGACGCCTTCTGCAA

Reverse primer: CCCCTCCTTTACCAGCTTCTTC

Probe: CGACATCGTGATCCGGGCCA

TIMP-4

Forward primer: CACCCTCAGCAGCACATCTG

Reverse primer: GGCCGGAACTACCTTCTCACT

Probe: CACTCGGCACTTGTGATTCGGGC

3.4 Results

3.4.1 Characterisation of astrocytes by immunocytochemistry

All primary astrocytes showed positive staining results using both monoclonal and polyclonal anti-GFAP antibodies (Figs 3.5 a-f and 3.6 a–f), but the pattern of staining was grainy, and diffuse in appearance with both antibodies, and of a weak intensity. The monoclonal antibody gave stronger staining overall than the polyclonal, and this was particularly noticeable with the astrocyte preparation 668/01. These astrocytes exhibited the poorest GFAP expression out of the 6 preparations examined (Figs 3.5d and 3.6d), and were only very weakly positive with the polyclonal antibody (Fig 3.6d). 668/01 astrocyte cells also appeared to have a small and round morphology, whereas all the other astrocytes had irregular processes. Thus, 668/01 cells were not used in further experiments. The fibrillary staining pattern characteristic of GFAP was clearly demonstrated by U373 astrocytoma cells (Figs 3.5g and 3.6g), which gave a strongly positive result. The negative control revealed no detectable background staining (Figs. 3.5h and 3.6h).

Primary astrocytes gave strongly positive results with the S100-β antibody, with all but B73 cells, giving clear and extensive fibrillary staining patterns (Fig. 3.7 a, b, c, e, f). B73 cells gave a more limited and grainy staining pattern, and demonstrated a smaller, rounded morphology (Fig. 3.7d), and were thus not selected for further analysis. Cellular processes were well defined with the S100-β antibody on U373 astrocytoma cells (Fig.3.7g), but staining was weaker in appearance than with the primary astrocytes. Interestingly, this contrasts with the GFAP staining patterns, where U373 cells gave stronger, more fibrillary staining, than primary astrocytes. The negative control involved omission of the primary anti-s100-β antibody, and revealed no detectable background staining (Fig. 3.7h).

3.4.2 Characterisation of astrocytes by western blotting for detection of GFAP

Optimal conditions for western blotting were obtained by conducting the transfer at 4˚C using 150 volts for 90min, blocking for 90min at RT without Tween® 20, removing the milk from the TBST containing the primary antibody, and incubating overnight at 4 ˚C. Blots demonstrating evidence of GFAP in the astrocytes were obtained (Fig. 3.8) under these conditions. The Triton® X-100 protein extraction method (3.3.3.2) was found to be the optimal choice for obtaining protein from astrocytes (data not shown).

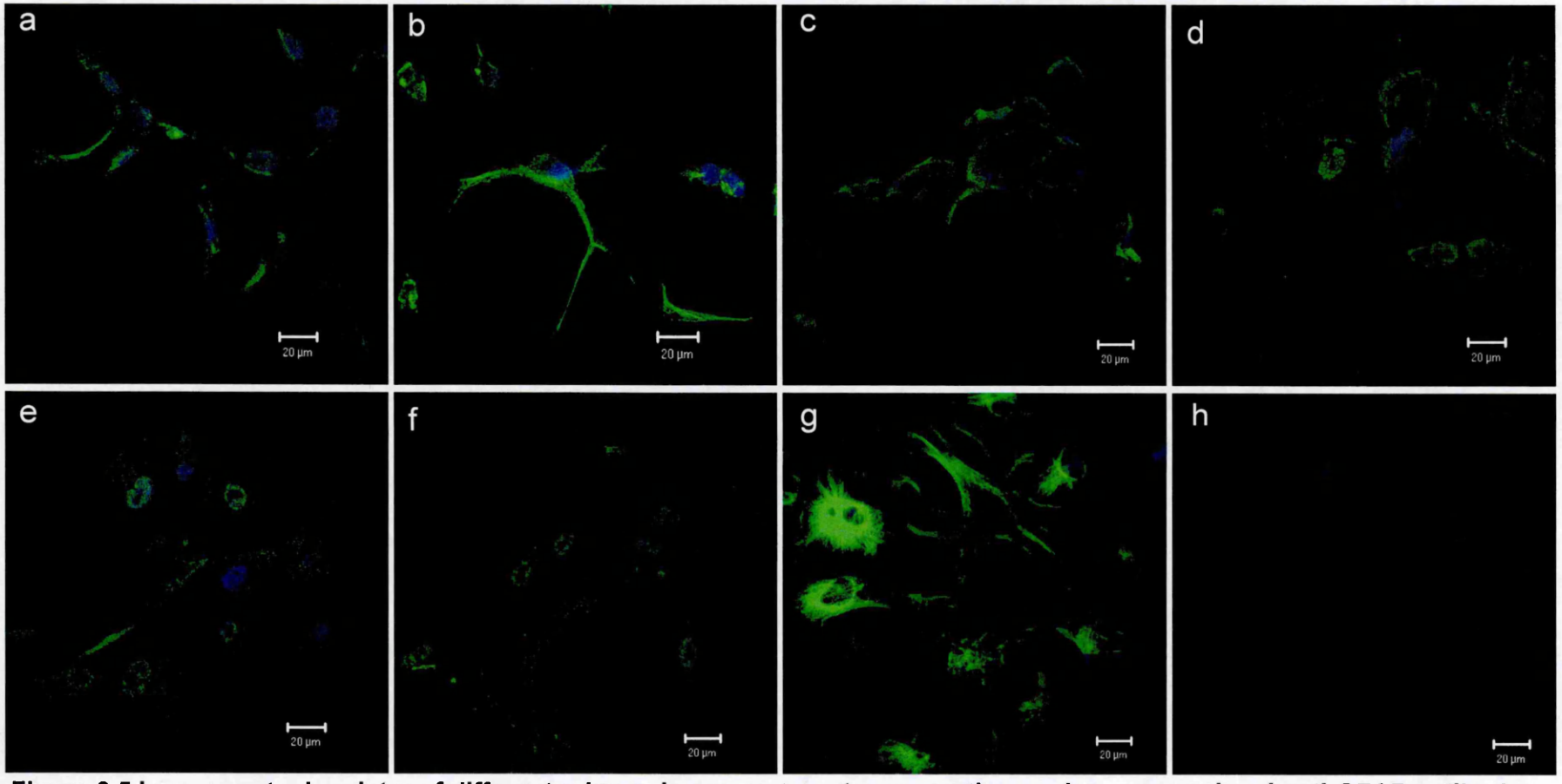

Figure 3.5 Immunocytochemistry of different primary human astrocyte preparations using a monoclonal anti-GFAP antibody
a = EP14 p8, b = EP15 p8, c = B327 p6, d = 668/01 p8, e = MS16 p5, f = MS21 p6, g = U373 astrocytoma cells (positive control), h = primary astrocyte negative control (EP14). Primary antibody = mouse α-human GFAP (1:400, 2hr at RT) (Sigma), secondary antibody = rabbit α-mouse- FITC (1:50, 90 min at RT) (Dako). Nuclei were counterstained with DAPI (blue) and images obtained using a confocal microscope.

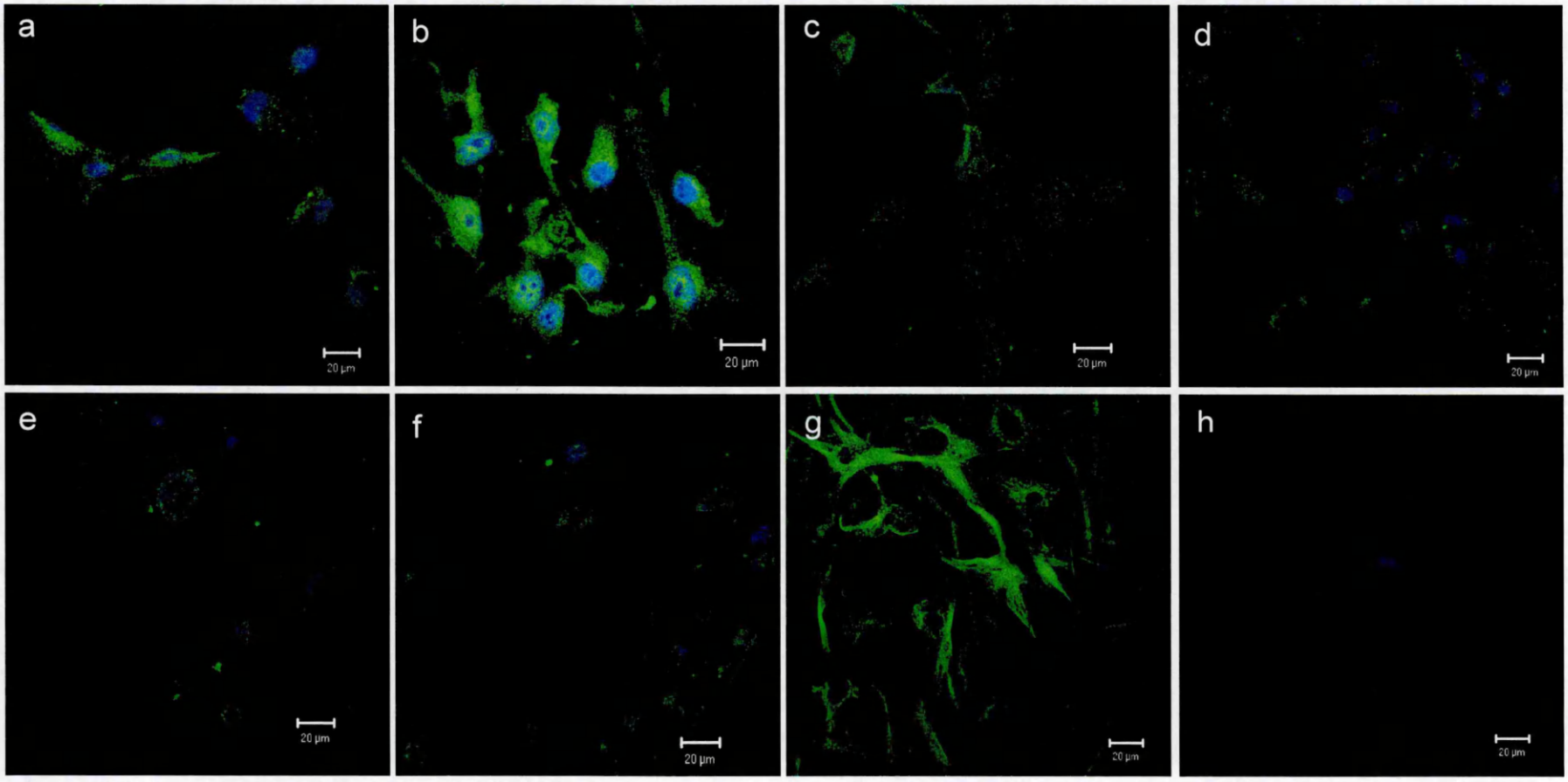

Figure 3.6 Immunocytochemistry of different primary human astrocyte preparations using a polyclonal anti-GFAP antibody
a = EP14 p8, b = EP15 p8, c = B327 p6, d = 668/01 p8, e = MS16 p5, f = MS21 p6, g = U373 astrocytoma cells (positive control), h = primary astrocyte negative control (EP14). Primary antibody = rabbit α-human GFAP (1:1000, 2hr at RT) (Abcam), secondary antibody = goat α-rabbit – AlexaFluor 488 (1:500, 90 min at RT) (Invitrogen). Nuclei were counterstained with DAPI (blue) and images obtained using a confocal microscope.

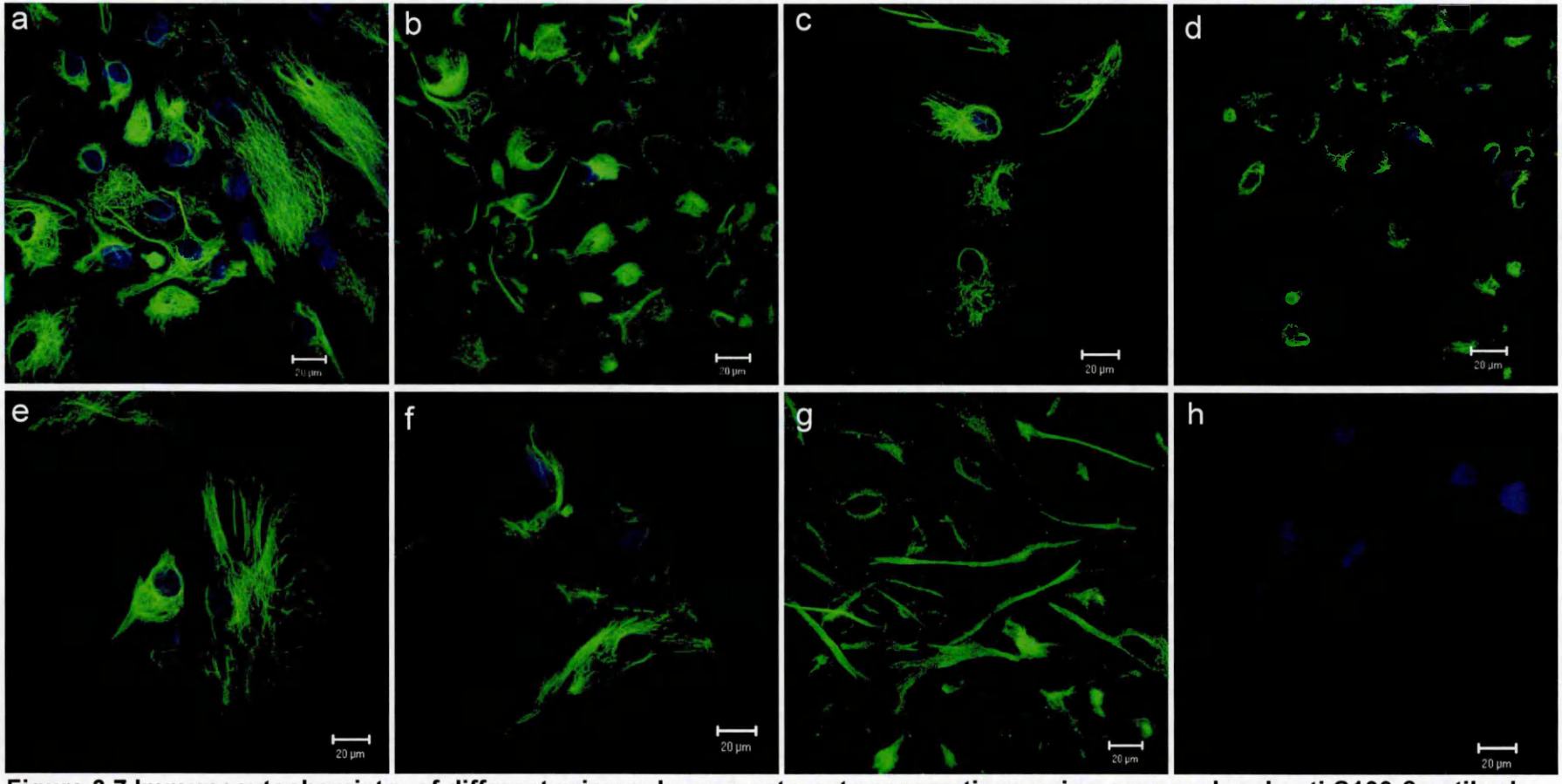

Figure 3.7 Immunocytochemistry of different primary human astrocyte preparations using a monoclonal anti-S100-β antibody
a = EP14 p8, b = EP15 p8, c = B327/01 p6, d = B73 p8, e = MS16 p5, f = MS21 p6, g = U373 astrocytoma cells (positive control), h = primary astrocyte negative control (EP14). Primary antibody = mouse α-human S100-β (1:500, 90 min at RT) (Sigma), secondary antibody = rabbit α-mouse- FITC (1:50, 90 min at RT) (Dako). Nuclei were counterstained with DAPI (blue) and images obtained using a confocal microscope.

Primary astrocyte lysate samples from SMS12, EP15, MS16, and B327/01 gave clear bands at ~50kDa, which indicated the presence of GFAP (Reeves et al., 1989). MS21 gave weaker expression in comparison (Fig. 3.8a). Astrocyte supernatants (Fig. 3.8a) showed no significant GFAP expression as expected, although some reactivity at ~62kDa was seen on the negative blot. Astrocyte lysate samples showed no reactivity in the negative control blot (Fig. 3.8b).

Using protein extracted from lysate and supernatant samples from astrocyte preparations EP14 and EP15, revealed very clear bands for the lysate samples at ~50kDa (Fig. 3.8c), indicating the presence of GFAP. Supernatant samples showed minimal reactivity (Fig. 3.8c), and no reactivity was seen in the negative control blot (Fig. 3.8d).

3.4.3 Detection of CCL2 and CXCL10 by western blotting

Recombinant human CCL2 and CXCL10 standards were detected at all concentrations in western blots using biotinylated antibodies and Extravidin (Fig. 3.9). The lowest level of standard seen was 2.5ng, which was just evident for CCL2 (Fig. 3.9a), and clearly visible for CXCL10 (Fig. 3.9b), suggesting the anti-CXCL10 antibody was the most sensitive. The negative controls showed no reactivity in the 8-9kDa region.

No CCL2 or CXCL10 could be detected in either astrocyte lysate preparations or cell supernatant samples, with or without cytokine treatment (Fig. 3.9). Non-specific bands were seen at ~64kDa in all the astrocyte preparations, with both anti-CCL2 and anti-CXCL10 antibodies, and were more prominant in lysate samples. These non-specific bands were also seen in the negative controls, which indicated that they were not due to non-specific binding of the primary antibody (Fig. 3.9). Thus, levels of these 2 chemokines present in the astrocyte lysate and supernatant samples were below the detection limit (2.5ng).

3.4.4 Detection of CCL2 and CXCL10 by MALDI-QTOF mass spectrometry

3.4.4.1 MALDI-QTOF analysis of serum-free media spiked with chemokine to assess detection limits

SFM spiked with 50-1000pg/ml recombinant CCL2 or CXCL10 did not produce any peaks, other than matrix peaks, when analysed by MALDI MSpec, without prior zip tipping of the samples (data not shown). By zip tipping the same chemokine samples, 1000pg/ml CCL2 (Fig. 3.10) could be detected, but not 1000pg/ml CXCL10 (data not shown).

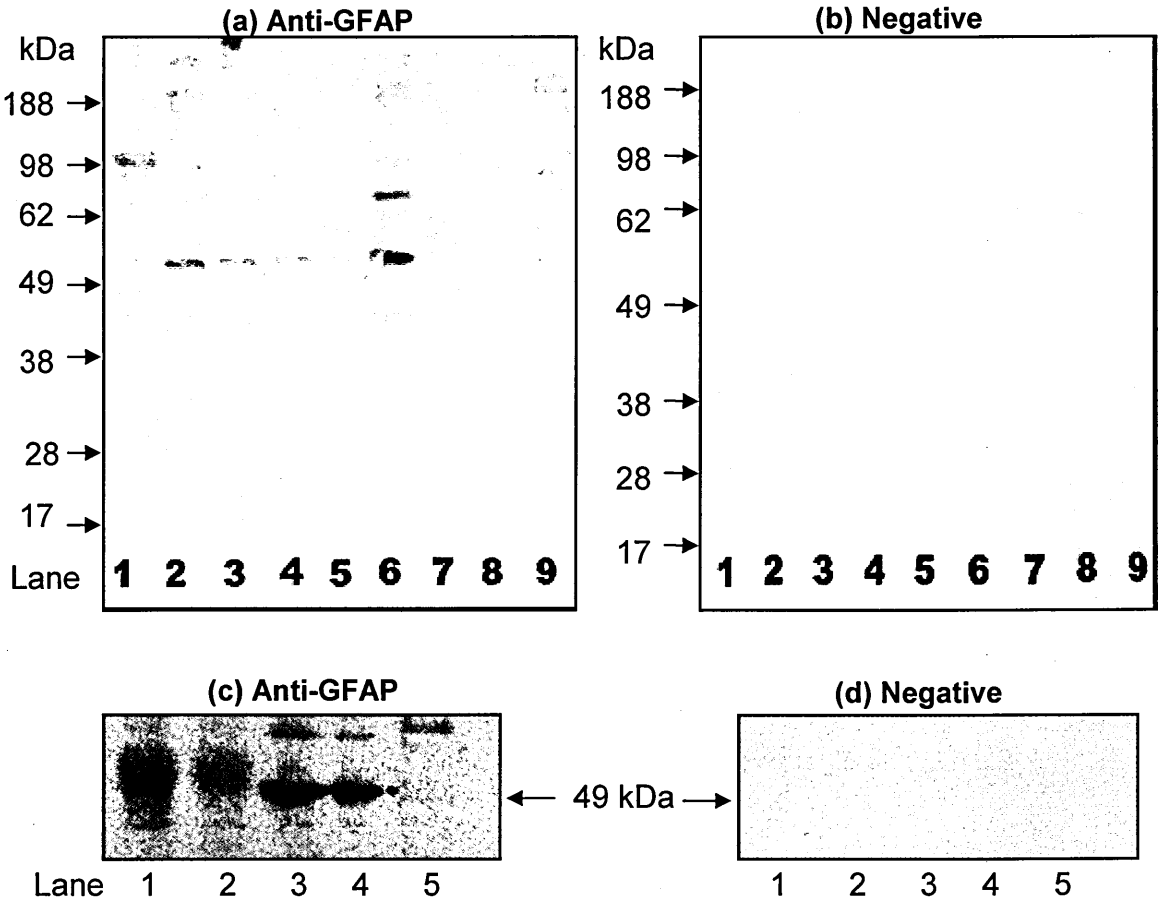

Figure 3.8 Detection by western blotting of GFAP in six preparations of primary human astrocytes to assess astrocyte purity

Western blots of 6 different primary human astrocyte lysate (L) and supernatant (S) preparations, using α-GFAP primary antibody (1:1000, rabbit α-human, Dako) ***(a)*** *and* ***(c),*** *and goat α-rabbit IgG HRP secondary antibody (1: 50,000, Sigma).*

(b) *Negative (omission of primary) corresponding to gel in* ***(a)***

(d) *Negative corresponding to gel in* ***(c)***

In ***(a)*** *and* ***(b)****, samples represented in lanes 1-9 are:* ***(1)*** *SeeBlue Plus 2 MW marker;* ***(2)*** *SMS12 (L);* ***(3)*** *EP15 (L);* ***(4)*** *MS16 (L);* ***(5)*** *MS21 (L);* ***(6)*** *B327/01 (L);* ***(7)*** *MS16 (S);* ***(8)*** *MS21 (S);* ***(9)*** *B327/01 (S)*

In ***(c)*** *and* ***(d)****, samples represented in lanes 1-9 are:* ***(1)*** *EP15 (S);* ***(2)*** *EP14 (S);* ***(3)*** *EP15 (L);* ***(4)*** *EP14 (L);* ***(5)*** *SeeBlue Plus 2 MW marker*

A distinct band can be seen at the expected molecular weight of GFAP at ~ 50kDa for each astrocyte lysate preparation.

Figure 3.9 Western blot analysis for detection of CCL2 and CXCL10 in primary human astrocytes (SMS12) to assess detection limit using chemokine standards

(i) *Western blot of CCL2 standards and primary human astrocyte (SMS12) lysate (L) and supernatant (S) samples, using anti-CCL2 biotinylated antibody (1:250) (R&D Systems), followed by Extravidin (1:2000), and detection by chemiluminescence. The negative control involved omission of the primary antibody.*

Lanes 1-12 represent the following samples: ***(1)*** *Negative - SMS12 (L) 24h treatment with 10ng/ml TNF;* ***(2)*** *15ng;* ***(3)*** *10ng;* ***(4)*** *7.5ng ;* ***(5)*** *5ng;* ***(6)*** *2.5ng;* ***(7)*** *SMS12 (L) 24h treatment with 10ng/ml TNF;* ***(8)*** *SMS12 (S) 24h treatment with 10ng/ml TNF;* ***(9)*** *SMS12 (L) untreated;* ***(10)*** *SMS12 (S) (untreated);* ***(11)*** *SeeBlue Plus 2 MW marker*

(ii) *Western blot of CXCL10 standards and primary human astrocyte (SMS12) lysate (L) and supernatant (S) samples, using anti-CXCL10 biotinylated antibody (1:250) (R&D Systems), followed by Extravidin (1:2000), and detection by chemiluminescence. The negative control involved omission of the primary antibody.*

Lanes 1-12 represent the following samples: ***(1)*** *Negative - SMS12 (L) 24h treatment with 100ng/ml IFN;* ***(2)*** *15ng;* ***(3)*** *10ng;* ***(4)*** **7.5ng;* ***(5)*** **5ng;* ***(6)*** *2.5ng;* ***(7)*** *SMS12 (L) 24h treatment with 100ng/ml IFN;* ***(8)*** *SMS12 (S) 24h treatment with 100ng/ml IFN;* ***(9)*** *SMS12 (L) untreated;* ***(10)*** *SMS12 (S) untreated;* ***(11)*** *SeeBlue Plus 2 MW marker.*
** not visible as obscured by air bubble.*

Bands for CCL2 and CXCL10 standards can be detected at the 2.5ng level.
No bands at ~ 8-9kDa are visible with the astrocyte lysate or supernatant samples, but non-specific bands are seen in all the astrocyte preparations at ~65kDa.

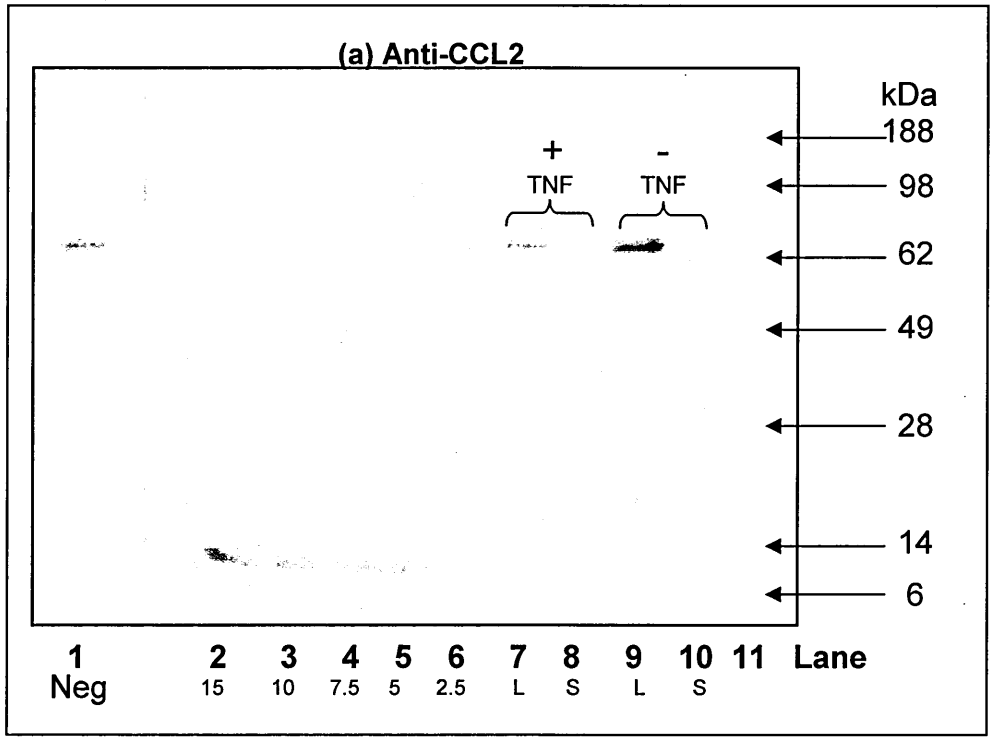
(a) Anti-CCL2
kDa
188
98
62
49
28
14
6
+
TNF
-
TNF
1 2 3 4 5 6 7 8 9 10 11 Lane
Neg 15 10 7.5 5 2.5 L S L S

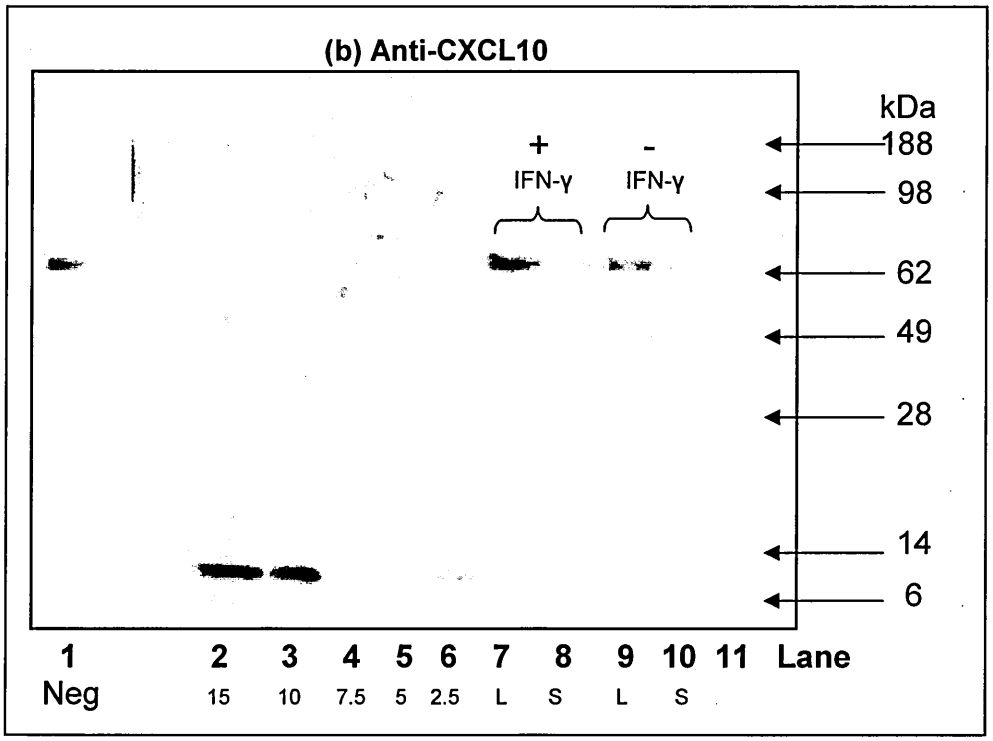
(b) Anti-CXCL10
kDa
188
98
62
49
28
14
6
+
IFN-γ
-
IFN-γ
1 2 3 4 5 6 7 8 9 10 11 Lane
Neg 15 10 7.5 5 2.5 L S L S

Figure 3.10 MALDI-QTOF mass spectrometric analysis of serum free media spiked with 1000pg/ml of CCL2 to assess detection levels

Recombinant human CCL2 (Serotec, Oxford, UK) was added to serum-free media (SFM), to give a final concentration of 1000pg/ml. Samples (10µl) were zip tipped to concentrate and desalt them, spotted onto a MALDI target plate, and analysed by MALDI-QTOF mass spectrometry. Mass spectra shown are as follows:

***(a)** SFM spiked with 1000pg/ml CCL2 (equivalent to a maximum of 10pg eluted on to the target). A peak was only just evident on the spectra at around 8600 m/z in the region circled.*

***(b)** Detailed spectra of region circled in (a), showing m/z values of 8400 – 8950. A low intensity peak of 8680 m/z was visible, which corresponded to the m/z value previously obtained for CCL2 (Chapter 2), indicating it was possible to detect 1000pg/ml CCL2.*

The dominant peak at 1329 m/z was seen in all spectra, including media spiked with CXCL10, and was likely to have originated from a component of the media.

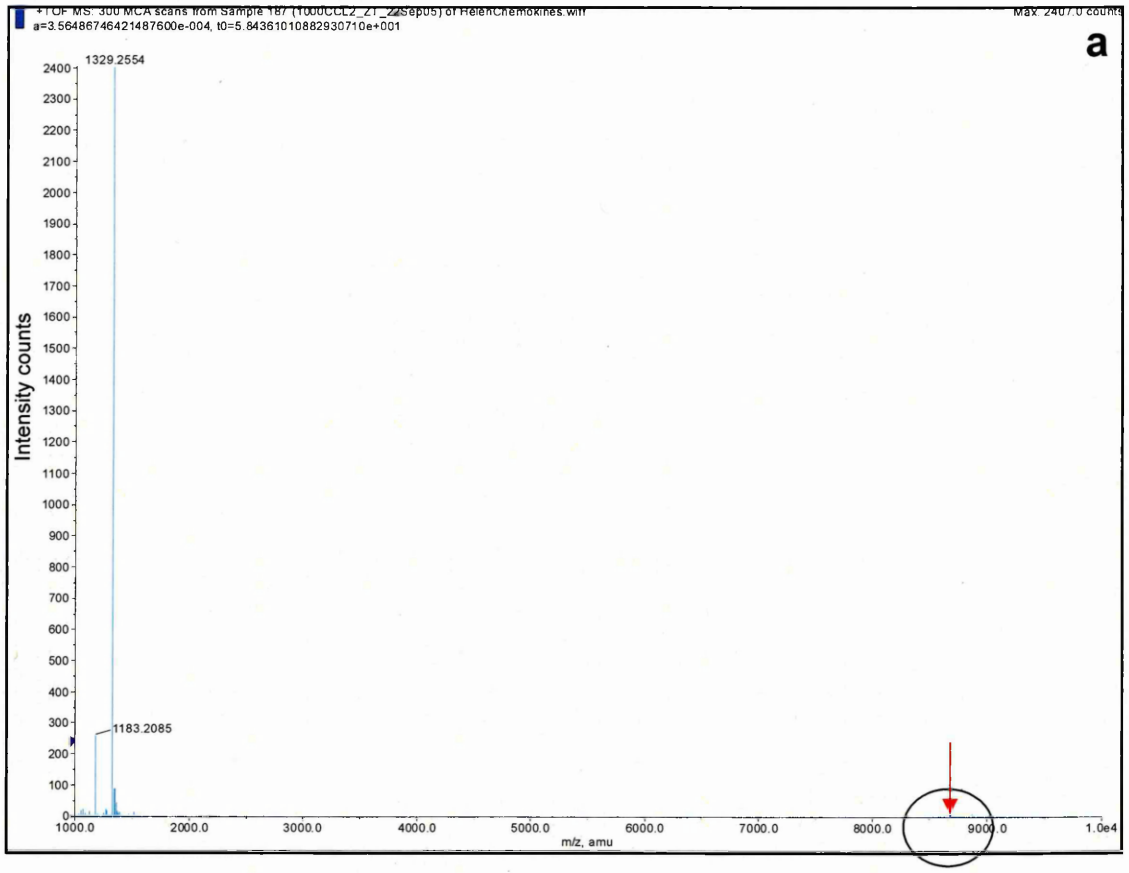
a
a=3.56486746421487600e-004, t0=5.84361010882930710e+001
Max: 2407.0 counts
1329.2554
1183.2085
Intensity counts
m/z, amu

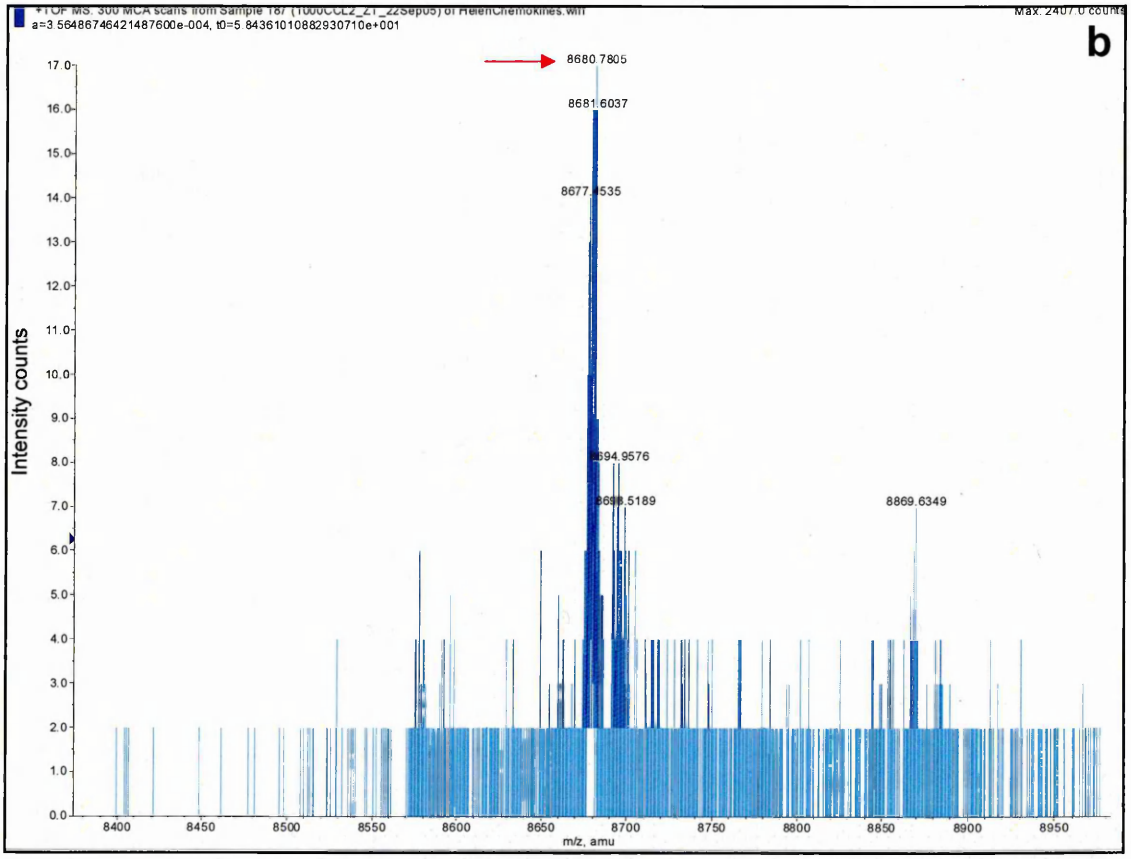
b
a=3.56486746421487600e-004, t0=5.84361010882930710e+001
Max: 2407.0 counts
8680.7805
8681.6037
8677.4535
8694.9576
8698.5189
8869.6349
Intensity counts
m/z, amu

As 10µl of the 1000pg/ml solution was zip tipped, this bound a maximum of 10pg of CCL2 for elution onto the target plate.

Freeze drying of SFM spiked with recombinant chemokine did not improve the detection of chemokines by MALDI-QTOF MSpec. The dried samples were too rich in salts and required too large a volume for reconstitution to be suitable (data not shown).

3.4.4.2 MALDI-QTOF analysis of supernatant from astrocytes (EP15) with and without cytokine treatment

MALDI MSpec results did not reveal any CCL2 or CXCL10 in the supernatant of either IFN-γ-treated or untreated primary human astrocytes EP15 (data not shown), suggesting that these chemokines were present at concentrations below 1000pg/ml.

3.4.5 TaqMan® PCR Detection of MMPs and TIMPs mRNAs

3.4.5.1 Expression of housekeeping genes

The housekeeping gene18S was found to be more suitable than *GAPDH* for use with the astrocyte lysate samples in TaqMan® PCR. 18S gave the most stable expression in the samples investigated, at adequate levels, with little variation in Ct values between samples. A standard curve for 18S expression by the RNA standards (S1-S5) is shown in Figure 3.11.

3.4.5.2 TaqMan® PCR detection of MMPs mRNAs expression by astrocytes

Results of the expression of MMPs in astrocytes are summarised in Table 3.2, and in Figures 3.12 and 3.13. Key findings included: high expression of MMP2 in treated and untreated astrocytes; high expression of MMPs 1, 3, and 10, in SMS12 astrocytes when treated with IL-1β; an increase in MMP9 expression when astrocytes were treated with either TNF or IL-1β; a reduction in MMP11, following treatment with cytokines; and no expression of MMPs-7, -8, -20, -21, and -26 (Figs. 3.12 and 3.13).

3.4.5.3 TaqMan® PCR detection of TIMPs mRNAs expression in primary human astrocyte cell cultures

Results of the expression of TIMPs in astrocytes prepared from control brain (EP15), and MS NAWM (SMS12) are summarised in Table 3.3, and displayed in more detail in Figure 3.14. TIMP3 mRNA was found to be the most abundant, and TIMP4, the least expressed.

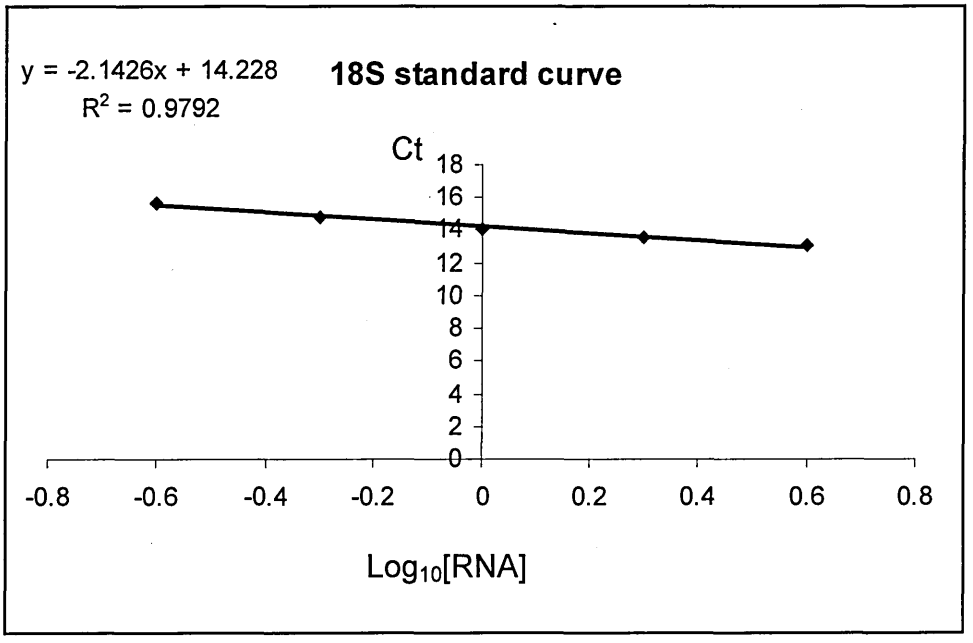

Figure 3.11 Standard curve for expression of the housekeeping gene 18S using RNA standards obtained from U251 human glioblastoma cells

The log of the concentration of each RNA standard (S1-S5), was plotted against the Ct value, resulting in a standard curve for the housekeeping gene 18S. The equation generated by the curve was used to calculate the log of relative expression of 18S RNA in each astrocyte and tissue sample, by subtracting the y-intercept (14.228) from the Ct value, and dividing this value by the gradient of the curve (-2.1426). An inverse log was then used to obtain a value for relative mRNA expression. Standard curves were created for each of the MMP and TIMP target genes in the same way, and used in the calculation of their relative RNA levels, which were then normalised to 18S levels by dividing by the corresponding relative RNA level of 18S.

All samples showed some expression of all 4 TIMPs, with SMS12 astrocytes generally expressing higher TIMP levels than EP15 astrocytes, particularly when treated with cytokines. TNF treatment appeared to decrease expression of TIMP2 in both SMS12 and EP15 astrocyte cells (Fig. 3.14b). Results from cytokine treatment were variable, but IL-1β generally created the largest increase in TIMP mRNA expression in astrocytes, particularly SMS12.

3.4.5.4 Effects of cytokine treatment on primary human astrocyte expression of MMPs and TIMPs mRNAs, as detected by TaqMan® RT PCR

Of the 3 cytokines used to treat astrocytes from control (EP15), and MS NAWM (SMS12), IL-1β increased the expression of the majority of MMPs, with notable exceptions being MMP11, and MMP25. IL-1β exerted its most dramatic effects on SMS12, particularly with MMP1 relative mRNA expression, which increased from ~100 to 2300, when astrocytes were treated with 100ng/ml IL-1β (Fig. 3.12a). MMPs 3, 10, and 12 mRNAs were not expressed in untreated astrocytes, but appeared with both SMS12 and EP15 astrocytes that had received 24h of 100ng/ml IL-1β. This enhancement in expression was particularly marked with MMP10 mRNA in SMS12 astrocytes, increasing from 0 to ~2200 (Fig. 3.12e). TIMPs 1 and 4 showed no less than two-fold increases in their relative mRNA levels following IL-1β treatment on SMS12 astrocytes (Fig. 3.14a and d).

Treatment with TNF increased relative mRNA levels of MMP9 in both SMS12 and EP15 astrocytes, and had the opposite effect on expression of MMP11 and MMP14 (Fig. 3.12). TNF treatment appeared to decrease expression of all four TIMPs, particularly TIMP1 and TIMP3 (Fig. 3.14).

IFN-γ treatment decreased expression of MMPs 11, 14, and19 (Figs. 3.12 and 3.13) mRNAs, with little effect on other MMP mRNAs. IFN-γ induced an increase in TIMP2 (Fig. 3.14b) mRNA expression, however.

Figure 3.12 Relative mRNA levels detected by TaqMan® RT PCR of MMPs 1, 2, 3, 9, 10, 11, 12, 13, 14, and 15, in two primary human astrocyte preparations from either control or MS NAWM

Relative RNA levels of each MMP detected in astrocytes isolated from MS white matter (SMS12) and control brain (EP15) are shown, expressed in arbitrary units as a ratio to 18S RNA. Colour coding is used to indicate the cytokine treatment status of the astrocytes prior to RNA extraction, with either no treatment (blue), or 100ng/ml IL-1β (purple), TNF (red), or IFN-γ (green). Levels for MMP-7 and -8 were below detection levels in all samples. Notably, high RNA levels were seen for MMPs -1 and -10 after treatment with IL-1β, and MMP2 RNA was detected at moderately high levels, with and without cytokine treatment.

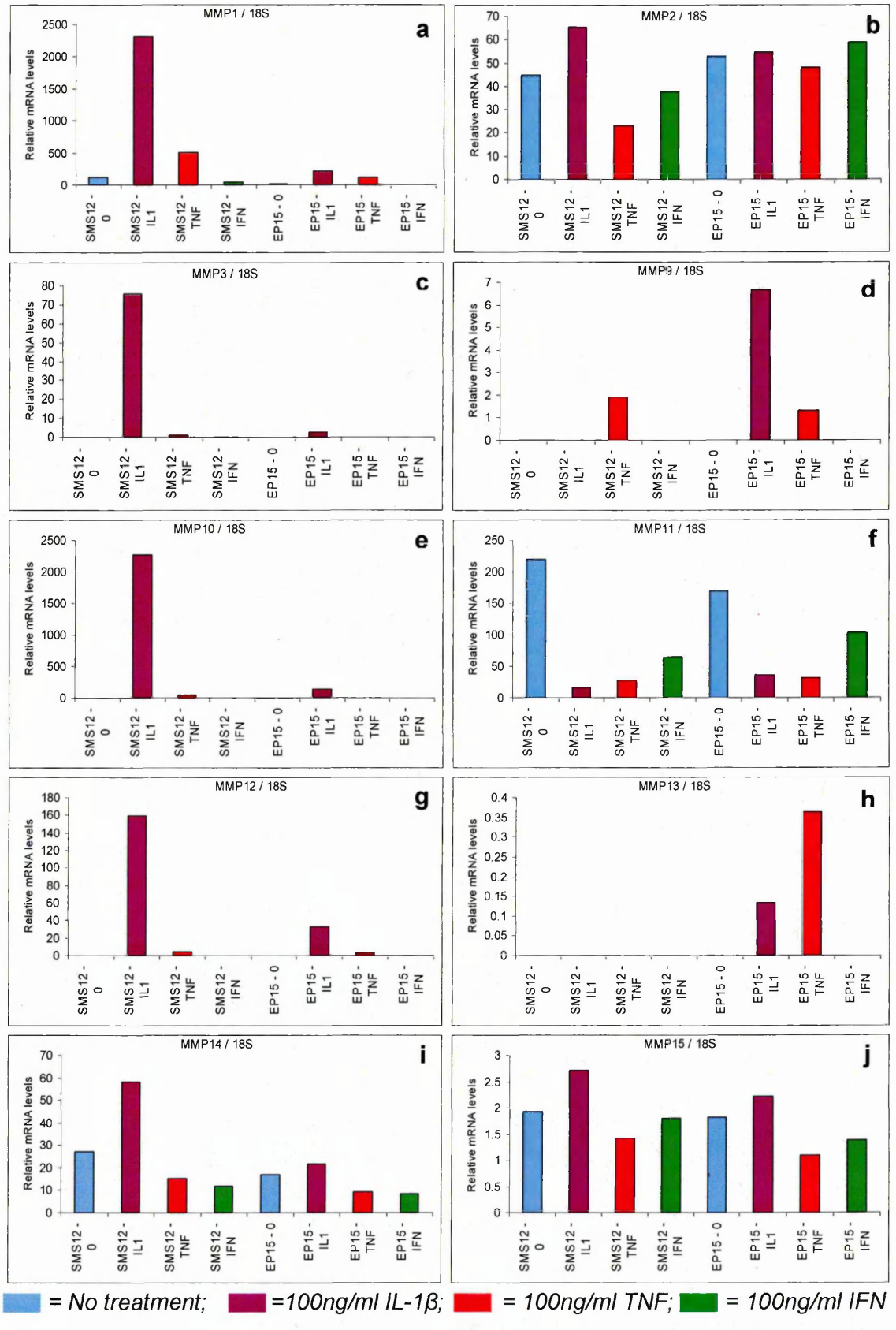
MMP1 / 18S
a
MMP2 / 18S
b
MMP3 / 18S
c
MMP9 / 18S
d
MMP10 / 18S
e
MMP11 / 18S
f
MMP12 / 18S
g
MMP13 / 18S
h
MMP14 / 18S
i
MMP15 / 18S
j
Relative mRNA levels
SMS12 - 0
SMS12 - IL1
SMS12 - TNF
SMS12 - IFN
EP15 - 0
EP15 - IL1
EP15 - TNF
EP15 - IFN
= No treatment;
=100ng/ml IL-1β;
= 100ng/ml TNF;
= 100ng/ml IFN

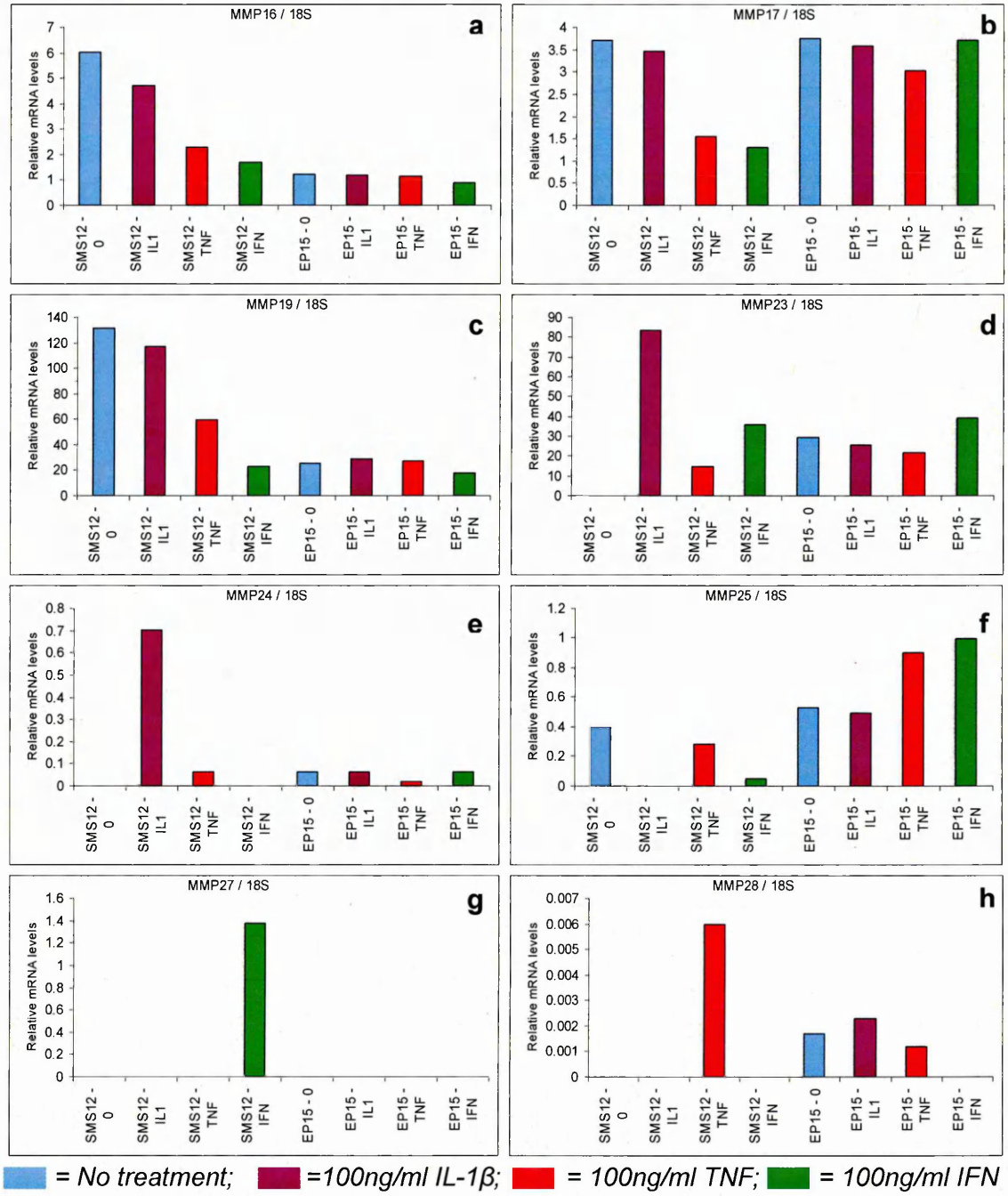

Figure 3.13 Relative mRNA levels detected by TaqMan® RT PCR of MMPs 16, 17, 19, 23, 24, 25, 27, and 28, in two primary human astrocyte preparations from either control or MS NAWM

Relative RNA levels of each MMP detected in astrocytes isolated from MS white matter (SMS12) and control brain (EP15) are shown, expressed in arbitrary units as a ratio to 18S RNA. Colour coding is used to indicate the cytokine treatment status of the astrocytes prior to RNA extraction, with either no stimulation (blue), or 100ng/ml IL-1β (purple), TNF (red), or IFN-γ (green). Levels for MMP-20, -21, and -26, were below detection levels in all samples.

Table 3.2 Summary of TaqMan® RT PCR results of MMPs mRNAs expression in primary human astrocyte cell cultures and effects of cytokine treatment

MMP	RELATIVE mRNA EXPRESSION IN ASTROCYTES (Figs. 3.12 and 3.13)
1	IL-1β↑ expression, and to very high levels in SMS12. SMS12 > EP15. TNF also↑ expression to lesser extent
2	High expression ± treatment. TNF↓ expression slightly
3	IL-1β↑ expression, and to high levels in SMS12. SMS12>EP15. None seen ±IFN
7	None
8	None
9	TNF↑ expression; IL-1β↑ expression in EP15. None seen ± IFN
10	IL-1β induced very high expression in SMS12. None seen ± IFN
11	All treatment↓ expression, especially IL-1β and TNF. Untreated cells showed high expression
12	IL-1β↑expression; SMS12>EP15. None seen ± IFN
13	Very low expression, and only with TNF and IL-1β
14	IL-1β↑ expression, TNF and IFN slightly↓ amount. SMS12>EP15
15	Low expression. IL-1β↑ and TNF ↓ expression very slightly
16	Low expression. Treatment ↓ expression in SMS12. SMS12>EP15
17	Low expression
19	IFN and TNF↓ expression in SMS12. SMS12>EP15
20	None
21	None
23	IL-1β↑expression in SMS12 None in untreated SMS12
24	Very low expression. IL-1β↑ expression in SMS12
25	Low expression None with IL-1β in SMS12
26	None
27	Only induced by IFN in SMS12 and very low expression
28	Very low expression None seen with IFN

↑ = *increase;* ↓ = *decrease;* > = *higher overall expression than*

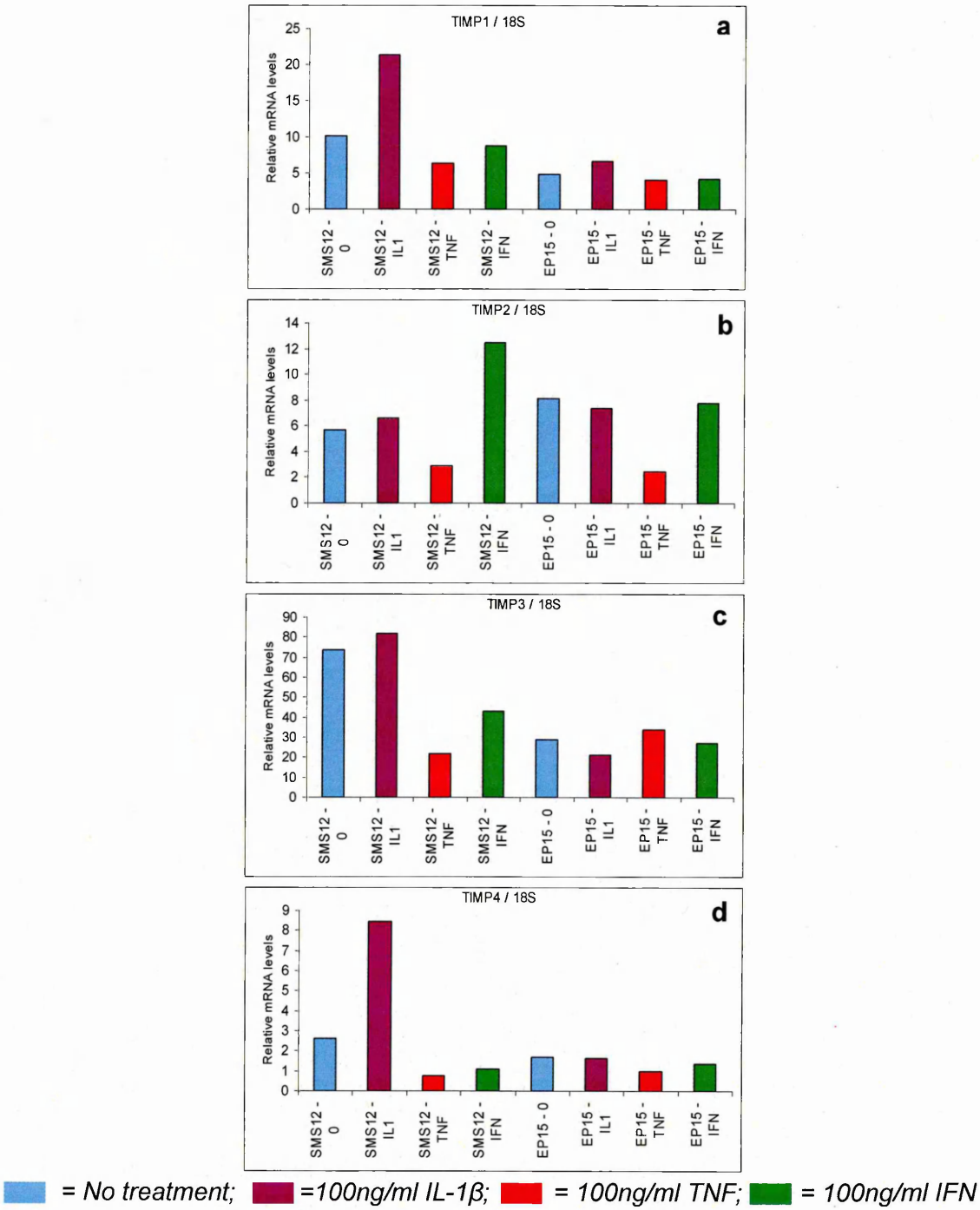

Figure 3.14 Relative mRNA levels detected by TaqMan® RT PCR of TIMPs 1,2, 3, and 4, in primary human astrocytes from control and MS NAWM

Relative RNA levels of each TIMP detected in astrocytes isolated from MS white matter (SMS12) and control brain (EP15) are shown, expressed in arbitrary units as a ratio to 18S RNA. Colour coding is used to indicate the cytokine treatment status of the astrocytes prior to RNA extraction, with either no treatment (blue), or 100ng/ml IL-1β (purple), TNF (red), or IFN-γ (green).

Table 3.3 Summary of TaqMan® RT PCR results of TIMPs mRNAs expression in primary human astrocyte cell cultures and effects of cytokine treatment

TIMP	RELATIVE mRNA EXPRESSION IN ASTROCYTES (Fig. 3.14)
1	↑ seen with IL-1β SMS12>EP15
2	No treatment gave similar levels as IL-1β. TNF↓ expression. IFN↑ expression in SMS12
3	Most highly expressed. Untreated similar to treated in EP15. IL-1β and untreated showed higher levels than TNF and IFN in SMS12
4	Low level of expression. Treated and untreated similar, except for↑ seen with IL-1β in SMS12

↑ = *increase;* ↓ = *decrease;* > = *higher overall expression than*

3.5 Discussion

3.5.1 Characterisation of primary human astrocytes

Adult human brain tissue has been used to produce *in vitro* cell cultures since the 1960s (Ponten and Macintyre, 1968), but the exact cellular composition of these cultures is often questionable. Purity of cell cultures is essential for meaningful results, as astrocyte responses to stimuli will vary greatly if neurons are present, and other contaminating cell types, such as fibroblast-like cells, that can proliferate rapidly and dominate after several passages (Lee *et al.*, 1994). Astrocytes commonly have their purity assessed by measuring reactivity for GFAP (Gibbons *et al.*, 2007). GFAP immunoreactivity often diminishes with successive passages (Lue *et al.*, 1996), and cultured astrocytes are known to modulate GFAP synthesis in response to growth media composition (Morrison *et al.*, 1985), and cell density (Goldman and Chiu, 1984). GFAP expression is not considered to be a definitive astrocytic marker by some, who argue that astrocytes *in situ* exhibit very little (Walz, 2000). In addition, low GFAP expression can escape detection depending on the fixative and antibodies used (Eng *et al.*, 2000). To attempt to confirm the GFAP staining pattern observed with astrocytes used in this project, both a change of fixative, and the use of different antibodies was tried. PFA gave better results than acetone, possibly due to the protein coagulation actions of acetone producing grainy staining patterns (Farmilo and Stead, 1989).

S100-β was used an additional astrocytic marker to support results obtained with GFAP. The differences in GFAP and S100-β staining seen between primary astrocytes and the astrocytoma cells might result from a higher level of maturity of astrocytomas, and/or alterations acquired during cell culture. The stronger GFAP staining seen in the astrocytoma cells (U373) supports the suggestion that U373 cells express more of the marker GFAP than S100-β, compared to astrocytes, due to their immortality giving a greater level of maturity. S100-β is less specific for astrocytes than GFAP, and has been localised by immunohistochemistry to many neural cell types in humans, including OLGs, ependymal cells, ECs, lymphocytes, neurons, and the choroid plexus epithelium (Steiner *et al.*, 2007).

Brightfield microscopy examinations and immunofluorescent results suggest that EP14 and EP15 had a fibrous morphology, whereas B327, 668/01, MS16 and MS21 showed more of a protoplasmic structure. Protoplasmic astrocytes tend to be considerably less GFAP immunoreactive than fibrous cells (Lue *et al.*, 1996).

Collectively, results from immunocytochemistry and western blotting indicated that EP14, EP15 and SMS12 astrocytes demonstrated a morphology and positivity for

GFAP and S100-β highly consistent with that of astrocytes. Thus, the study was restricted to use of these 3 cultures for assessment of astrocyte MMP expression, and detection of truncated chemokines in astrocyte supernatant.

3.5.2 Detection of CCL2 and CXCL10 in primary human astrocyte cell culture supernatants

It has previously been reported that astrocytes *in vivo* and *in vitro* express CCL2 and CXCL10, particularly when exposed to inflammatory stimuli (Farina *et al.*, 2007). CCL2 is considered one of the most abundant chemokines produced within the brain, predominantly by astrocytes, and plays a key role in leukocyte recruitment (Guillemin *et al.*, 2003). CXCL10 has been shown to be expressed by a subpopulation of both resting and reactive astrocytes in control brain (Xia et al., 2000), and is associated with reactive astrocytes around inflamed lesions in MS (Sorensen et al., 1999). Aside from their inflammatory roles, CCL2 and CXCL10 are involved in CNS tissue regenerating roles, such as regulation of myelination and migration of microglia (Farina *et al.*, 2007). Astrocytes have been shown to have a central role in regulating neuroinflammation, which corresponded to their expression of these two chemokines. Transgenic mice with selective inactivation in astrocytes of the transcription factor NF-κB, showed a reduction in lesion volume and white matter damage following injury. This corresponded to decreased leukocyte recruitment into the lesion, due to reduced NF-κB-dependent expression of CCL2 and CXCL10 (Brambilla *et al.*, 2005).

Human foetal astrocyte secretion of CCL2 has been reported to be greatly increased by 24-72h treatment with TNF, IL-1β, TNF/IFN-γ, IFN-γ/IL-1β, and TNF/IL-6, with a maximum CCL2 concentration of 201ng/ml detected by enzyme-linked immunosorbent assay (ELISA) after 72h (Guillemin *et al.*, 2003). In adult primary human astrocytes, chemokine expression was much lower. An increase (~5-fold) in CCL2 secretion by primary adult human astrocytes was detected by ELISA following treatment with IL-1β and TNF for 48h, thereby yielding ~9ng/ml. Similarly, astrocyte CXCL10 secretion increased (~2-fold) to ~1.9ng/ml after 48h exposure to IFN-γ (Fouillet *et al.*, 2005). Thus, IL-1β, TNF, and IFN-γ were used to maximise secretion of these chemokines and reflect the elevated cytokine expression demonstrated in MS lesions.

Since astrocytes also secrete MMPs (Leveque *et al.*, 2004), the cleavage of CCL2 and CXCL10 that occurs *in vitro*, as detailed in Chapter 2, could take place *in vivo*. Thus, astrocyte supernatants were investigated for the presence of chemokine cleavage products. Initial experiments using recombinant chemokines, performed to assess the detection limits of CCL2 and CXCL10, revealed that western blotting detected 2.5ng

chemokine, and MSpec was able to identify a very low intensity peak from a zip tipped solution of 1000pg/ml CCL2, equivalent to a maximum of 10pg of protein. No chemokine could be detected in astrocyte supernatant or lysate samples by either method, despite treatment with IL-1β (for CCL2) or IFN-γ (for CXCL10). Difficulties arose due to the small volumes needed for analysis, and concentrating supernatants by freeze-drying created a sample with a very high salt concentration, that would interfere with MALDI MSpec and prevent detection of the chemokine. As chemokines are close to the upper range of ~10 kDa capable of detection by MALDI on the QStar instrument, this may add further to the difficulties in detection. It was calculated that 1000pg/ml chemokine only contains ~1.16 fmoles CCL2 and ~1.17 fmoles CXCL10, when the volume applied to the MALDI target plate is considered. The level of detection of the instrument was given as ~50 fmoles, so it would not be possible to detect anything less than had already been achieved, without additional concentrating and desalting steps. This indicated that detection of basal expression of CCL2 and CXCL10 in astrocyte supernatant, and their reported levels following cytokine treatment, is beyond the sensitivity of the instrument with the current method. Previous reports of isolation and purification of chemokines from cell supernatants involve concentrating several litres of medium (Proost *et al.*, 1996), which was beyond the scope of the current study.

3.5.3 Detection of MMPs and TIMPs mRNAs in primary human astrocytes

Results from TaqMan® PCR tend to be reliable and reproducible due to low inter-assay variation (Bustin and Mueller, 2005). The accuracy of the standards is responsible for the accuracy of the quantification used for comparison, and using a standard curve generally gives highly reproducible results (Bustin and Mueller, 2005). Caution must be employed when comparing samples with each other, as although results are normalised to expression of the housekeeping genes, real-time PCR involves amplification, so small differences in the amount of cDNA loaded from each sample, will lead to much larger fluctuations of product amount (Bubner at al., 2004). Screening for expression of MMPs in astrocytes served useful, however, to help identify MMPs worthy of further investigation into the chemokine cleavage that might occur in the inflamed CNS. Protein expression does not always mirror that of mRNA, but a good correlation was found by Anthony and colleagues (1998), who examined expression of both for a range of MMPs, in a rat model of MS.

MMP9 is thought to be particularly important in MS as studies consistently find increases in brain tissue, serum, and CSF (Yong *et al.*, 2007b). Both astrocyte preparations assessed here by TaqMan® PCR showed an increase of MMP9 mRNA

following TNF treatment, and the largest increase resulted from IL-1β treatment of EP15 astrocytes. TaqMan® data from the astrocytes is in agreement with previous findings, in that basal expression of mRNAs of MMP2, TIMP1, and TIMP2, are seen, but little, if any secretion of MMP9 (Leveque *et al.*, 2004). In the current study, relative mRNA expression of MMP2 was approximately 10 times greater than maximal MMP9 expression.

TIMP3 was found to be the most abundant inhibitor mRNA expressed in astrocytes, which contrasts with reports of TIMP2 and TIMP4 being the most prevalent in normal brain (Nuttall *et al.*, 2003). Observations that TIMPs -1, -2, and -3, mRNA are expressed in substantial quantities in astrocytes, is consistent with the findings of Muir *et al.* (2002), however.

Following cytokine treatment of human astrocytes, IL-1β was found to produce the most dramatic increases in expression of many of the MMPs. This finding is in agreement with that of Muir and colleagues (2002), who found upregulation of MMP2 and MMP9 with IL-1β treatment, and also TNF-induced increases in MMP9. MMP11 appeared to be down-regulated in astrocytes by all the cytokine treatments tried. Previous studies have reported a reduction in TIMP3 expression in astrocytes following TNF and IFN-γ treatment, but an upregulation of TIMP1 after TNF treatment (Bugno *et al.*, 1999). The results with SMS12 are consistent with this decrease in TIMP3, but those from the EP15 astrocytes are not. Moreover, EP15 and SMS12 astrocytes did not follow this increase reported for TIMP1 expression after TNF treatment.

MMP expression in MS lesions has received much attention. A study using PCR to investigate the expression of MMPs -2, -3, -7, -8, -9, -12 , and the TIMPs, in MS brain tissue, detected strong induction of MMP7 and MMP9 in lesions and NAWM (Lindberg *et al.*, 2001). MMP7 and MMP9 were also reported by Cossins *et al.*, (1997) to be elevated in active lesions in MS. Using immunohistochemistry, Anthony and colleagues (1997) detected increased expression of MMP2, MMP7, and MMP9 in microglia and macrophages of acute MS lesions. The upregulation of MMP7 in chronic lesions was associated with macrophages within PVCs, which might explain the lack of detection of MMP7 mRNA in astrocytes, in the current study. MMP7 and MMP2 were located in the active borders of active-chronic MS lesions and are likely to have major roles in MS pathogenesis, including breakdown of the BBB, particularly as levels of MMP2 and MMP7 were low in control brain (Anthony et al., 1997). Kouwenhoven *et al.* (2001) used *in situ* hybridisation to look at RNA levels of MMPs -1, -3, -7, -9, -14 and TIMP1 in monocytes from peripheral blood of MS patients and healthy controls, and detected elevations in MS, compared to controls, of all MMPs, except MMP14.

It is apparent that in addition to MMPs 2 and 9 investigated in this study, previous studies suggest a role for MMP7, which could also be implicated in interactions with chemokines in MS. TaqMan® PCR data presented here showed very high relative MMP1 mRNA expression in astrocytes treated with IL-1β, compared to other MMPs. This may also be of significance in MS, particularly as MMP1 has been shown to destroy the chemotactic activity of CXCL12 (by cleaving 4 residues from the N-terminus) (McQuibban *et al.*, 2001), and elevated levels of CXCL12 protein have been demonstrated on astrocytes and blood vessels of active and chronic inactive MS lesions (Krumbholz et al., 2006).

Anthony *et al.* (1997) concluded that MMP expression patterns in CNS lesions were dependent on the nature of the lesion, given the considerable variation between MS and stroke. Astrocyte MMP expression data obtained in the current study supports this, as expression patterns varied significantly depending on cytokine treatment, and also between individual astrocyte cultures. Further work to follow up data obtained here could include detection of cleavage products generated after incubation of recombinant chemokine with astrocyte supernantants.

3.6 Summary

The primary astrocyte preparations used in this project were not all identical in their GFAP expression, and cells with appropriate morphology and clear GFAP expression were selected to obtain high purity of the astrocyte cell cultures used in investigations of chemokine and MMP expression. CCL2 and CXCL10 were not be detected by western blotting, dot blotting (data not shown), or MALDI MSpec, in astrocyte supernatants, either with or without cytokine treatment. Expression of mRNA of MMPs and TIMPs was detected by TaqMan® real- time PCR, in both cytokine-treated and untreated astrocytes. MMP2 mRNA was expressed in all astrocyte samples, and MMP9 was expressed in astrocytes treated with TNF or IL-1β. The expression patterns were partially, but not fully, in agreement with previous studies, depending on the MMP or TIMP in question.

Chapter 4

CD26 expression in control and MS CNS white matter

4.1 Introduction

The structure and function of CD26, and its potential role in MS is discussed in section 1.5, and its ability to cleave chemokines detailed in section 1.6.2.

4.1.1 Lymphocyte expression of CD26

The lymphocyte cell surface antigen CD26, associated with an effector phenotype, is increased during T cell activation, and exhibits serine protease activity (Abbott *et al.*, 1994). CD26 is expressed on all lymphocytes and is considered to play a critical role in regulating the immune response via regulation of cytokine and chemokine expression, and T cell activation and proliferation (Ansorge and Reinhold, 2006). CD26 is also expressed by a minority (0-5%) of resting B cells isolated from peripheral blood, which is increased to 51% following stimulation with pokeweed mitogen, suggesting an involvement of CD26 in B cell activation (Buhling et al., 1995).

4.1.2 CD26 expression in tissues

The human CD26 gene on chromosome 2 encodes mRNA of 4.2 kilobases (kb), and also one of 2.8 kb, both of which are expressed at high levels in kidney and the placenta, and to a lesser extent in liver and lung (Abbott *et al.*, 1994). Little is known about CD26 expression in the human brain, but the 4.2 kb mRNA has been detected at low levels. In goldfish, the protein has been found in several neuronal populations, and in the radial glia of the visual processing area, known as the optic tectum (Beraudi *et al.*, 2003).

4.1.3 CD26 activity

CD26 is a multifunctional molecule involved in various physiological processes throughout the body (Fig. 4.1). The enzymatic activity of CD26 was first shown to be involved in the regulation of DNA synthesis of immune cells in 1985, when a CD26 inhibitor suppressed the proliferation of mitogen-stimulated PBMCs (Schon *et al.*, 1987). CD26 is inhibited by HIV-1 Tat protein, the N-terminal peptide Tat (1-9), and synthetic inhibitors e.g. Lys[Z(NO2)]-pyrrolidide (I40) (Lorey *et al.*, 2003).

The ability of CD26 to cleave chemokines can lead to unpredictable results on chemotactic activity. Truncation of CCL5 by CD26, for example, reduces signalling through two of its receptors, CCR3 and CCR1, but generates a more potent ligand for CCR5, compared to intact CCL5.

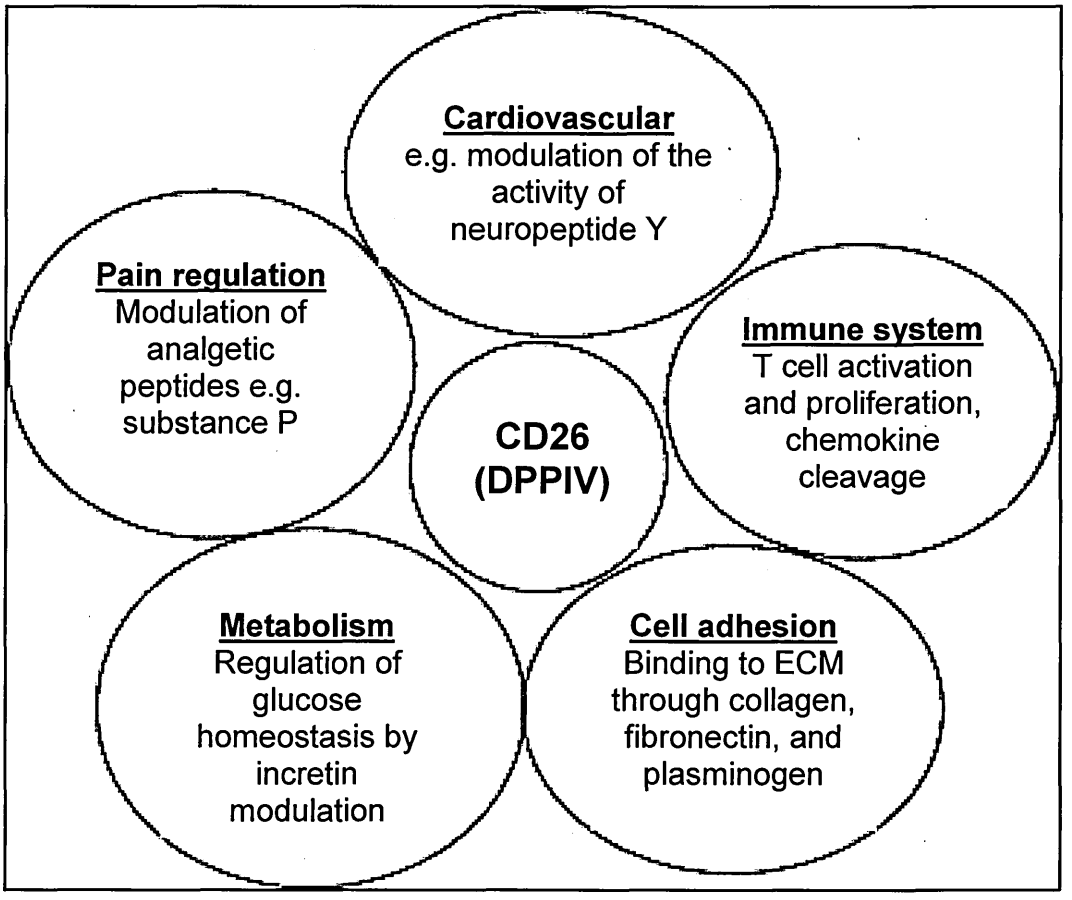

Adapted from (Demuth *et al.*, 2005) © (2005), with permission from Elsevier.

Figure 4.1 CD26 as a multifunctional protein with proteolytic and binding activity in physiological processes

CD26 has diverse effects on several physiological processes, as shown, with no known tissue-specific differences in enzymatic activity. Substrates of CD26 include cytokines, chemokines, hormones, and peptides associated with glucagon homeostasis. The use of enzyme inhibitors to modulate CD26 activity has been investigated as a potential therapy in various pathological conditions, such as for Type 2 diabetes.

ECM = extracellular matrix

Monocyte and eosinophil chemotactic activity was lost due to this increased specificity for CCL5, but lymphocyte chemotaxis was retained (Struyf *et al.*, 1998).

Inhibition of CD26 was shown to be effective as a therapy in EAE, through induction of autocrine production of the anti-inflammatory cytokine, TGF-β1, and suppression of T cell proliferation and proinflammatory cytokine secretion in response to myelin antigens (Reinhold *et al.*, 2006). The immunosuppressive effects of TGF-β1 are proposed to arise because it maintains the expression of the cell cycle regulator p27kip, thereby encouraging arrest of the cell cycle in G1 (Kahne *et al.*, 1999).

Other studies also support the potential role of CD26 inhibitors as therapeutic agents in T cell-mediated inflammatory diseases of the CNS (Steinbrecher *et al.*, 2001). T cell clones taken from MS patients and stimulated with MBP expressed high levels of CD26 and exhibited reduced production of IFN-γ, IL-4, and TNF in a dose-dependent manner when exposed to CD26 inhibitors, suggesting CD26 is involved in regulation of activation of autoreactive T cells. Inhibiting the catalytic activity of CD26 has several consequences, including p38 MAP kinase activation, tyrosine phosphorylation, suppression of DNA synthesis, and reduced production of TGF-β1 (Reinhold *et al.*, 1998).

Preller and colleagues (2006), however, have shown that deletion of CD26 genes in mice resulted in deregulation of Th1 immune responses and an increase in clinical EAE scores, by reduction *in vivo* and *in vitro* of T cell production of TGF-β1 in response to myelin antigens, although IFN-γ and TNF were elevated. In addition, ligands of CD26 induced TGF-β1 production from T cells in wild-type mice, but failed to do so in CD26(-/-) mice. EAE scores were increased in CD26 knockout mice immunised with MOG peptides. These results thus led to CD26 being viewed as an inhibitory receptor controlling T cell activation and Th1-driven autoimmune responses, with potentially important implications in the treatment of MS (Preller *et al.*, 2006).

CD26 has attracted great interest as a target for development of anti-inflammatory therapy, after successfully being targeted in animal models of rheumatoid arthritis (Tanaka *et al.*, 1997), transplantation (Korom *et al.*, 1997), and MS (Steinbrecher *et al.*, 2001). In MS, CD26 was found to be expressed on myelin-reactive T cells (Reinhold *et al.*, 1998). In a study of 35 MS patients, a markedly elevated percentage of effector CD4+ T cells in the peripheral blood were $CD26^+$, compared to 27 healthy controls (Jensen *et al.*, 2004). In a study of 15 RRMS patients and 14 healthy controls, $CD4^+$ $CD45R0^+$ memory T cells with high CD26 expression were increased in MS and cell counts of this subset correlated with disease severity (Krakauer *et al.*, 2006).

4.2 Aims and objectives

Results from Chapter 2 have shown that CD26 cleaves a dipeptide from the N-terminus of both recombinant CCL2 and CXCL10 with dramatic rapidity, but little is known about the distribution of CD26 in the human brain. To investigate the potential significance of this chemokine cleavage within the brain in MS, it must be established whether CD26 is expressed in human white matter, and the cell type expressing it. Since CD26 has been shown to be involved in EAE (Reinhold *et al.*, 2006), and two small studies have suggested a role for expression of CD26 on T cells in MS (Constantinescu *et al.*, 1995; Krakauer *et al.*, 2006), further investigation of this protein in the CNS in MS was vital. The objectives, therefore, of Chapter 4 were to:

- Determine CD26 expression in frozen human brain sections using immunohistochemistry
- Identify the cell types within the brain associated with CD26 expression, using dual staining immunohistochemistry
- Investigate levels of CD26 expression in MS brain tissue, compared to levels in control brain

4.3 Materials and Methods

Unless otherwise stated, all reagents used were purchased from Sigma, UK.

4.3.1 Human brain tissue

The UK MS Tissue Bank, situated in the Imperial College School of Medicine at Charing Cross Hospital in London, was established in 1998 by the Multiple Sclerosis Society to co-ordinate the collection of tissue from donors, and distribute high quality CNS tissue samples to MS researchers.

Snap-frozen brain blocks (~20 x 20 x 10 mm) of lesions from MS patients, and control (non-neurological) white matter (Table 4.1) were obtained from the Tissue Bank (UK Multicentre Research Ethics Committee), and transported on dry ice, before being stored in a -80˚C freezer until required. Control tissue was matched to MS tissue as closely as possible, in terms of corresponding areas of the brain, cause of death, age and sex of the donor.

4.3.2 Histopathology of frozen brain tissue

4.3.2.1 Haematoxylin and eosin staining

Brain blocks were mounted on a chuck by embedding the base in Cryo-M-bed mounting medium (Bright Instrument Co. Ltd., Huntingdon, UK), 10µm sections were cut on a cryostat (Leica Microsystems, Germany) at -20˚C, and collected onto polysine microscope slides (VWR International, Lutterworth, UK). Slides were air-dried for ~30min, and stored at -80˚C until required, or fixed in 4% PFA for 5min at RT and used immediately for staining.

Haematoxylin and eosin (H&E) is a routine histological stain that uses the basic dye haematoxylin to colour basophilic structures, such as ribosomes, the nucleus, and RNA-rich cytoplasmic regions, a blue/purple shade, and the acidic dye, eosin Y, to stain eosiniphilic structures, typically the cytoplasm, connective tissue, and collagen, bright pink (Ross and Pawlina, 2006).

Slides were immersed in filtered Harris's haematoxylin for 1min, rinsed in tap water until it ran clear, immersed in eosin Y for 2min, and rinsed in tap water until it ran clear. Slides were then dehydrated by immersing them in 50%, 70%, 80% and 95% ethanol consecutively, for 2min at each concentration. Four changes of xylene were applied to the slides in a fume hood for 1min each time, to clear them, before the slides were mounted by application of a 22 x 50 mm coverslip with DPX mountant.

Table 4.1 Case details of the subjects used in the study of CD26 expression in control brain and MS lesions

CASE NUMBER (BLOCK NUMBER)	AGE (YRS)	SEX	PMD (H)	BRAIN WEIGHT (G)	DIAGNOSIS	CAUSE OF DEATH
C11 **(A1B5)**	77	M	26	1375	Normal	Carcinoma of the lung (metastasised)
C14 **(P2C3)**	64	F	18	1431	Normal	Cardiac failure
MS74 **(A1C6: lesion)** **(A1E7: lesion)**	64	F	7	889	SPMS	Gastrointestinal bleed/ obstruction, aspiration pneumonia
MS90 **(P2E3: lesion)**	62	M	17	1127	SPMS	MS
MS130 **(P2D3: lesion)** **(P2F4: lesion)**	57	F	22	1150	SPMS	MS

Snap-frozen brain blocks of lesions from MS patients, and control (non-neurological) white matter were kindly provided by the UK MS Tissue Bank. Control blocks were selected from donors that were age and sex-matched to MS donors, and from similar brain regions, identified by the 4 digit block code. Brains were cut coronally through mamillary bodies into anterior (A) and posterior (P) halves, and 1 cm slices were numbered towards frontal and occipital poles, respectively. Slices were divided into blocks, with the grid co-ordinates of the block (letters for the rows, and numbers for columns) listed after the anterior/posterior slice number.

PMD = post-mortem delay (death to tissue preservation interval)
M = male, F = female
SPMS = secondary progressive MS

Slides were allowed to harden in the fume hood and examined using light microscopy with an Olympus BX60 microscope with a CoolSNAP-Pro (Media Cybernetics) imaging system.

4.3.2.2 Oil Red O staining

ORO is a red, fat-soluble dye used to stain neutral triglycerides and lipids on frozen sections (Ross and Pawlina, 2006). ORO solution was prepared by adding 1g of ORO powder to 60ml of triethyl phosphate (TEP) and 40ml of dH_2O, heating to 100˚C for 5min whilst stirring continuously. The ORO solution was filtered through filter paper (Whatman, UK) whilst hot, and again, when cold.

Frozen sections were prepared for Oil Red O (ORO) staining by fixation in 4% PFA at 4˚C for 1h. After fixation, slides were washed in tap water, briefly rinsed in 60% TEP, and stained in filtered ORO solution for 10-15min at RT. Stained slides were then briefly rinsed in 60% TEP, and given a further rinse in tap water. Nuclei were stained with Harris's haematoxylin (diluted with dH_2O to 20% v/v), the slides washed in dH_2O, and mounted using 22 x 50 mm coverslips containing the aqueous mountant glycerol gelatin.

4.3.2.3 Characterisation of tissue blocks

The pathological state of the blocks used in this study was investigated by observation of sections stained with H&E, and ORO.

To examine levels of inflammation, H&E stained slides were graded according to the extent of perivascular cuffing observed, being given scores of 0, 1+, 2+, 3+, or 4+, ranging from none, to severe immune cell infiltration (see Fig. 4.2).

Sections stained with ORO were used to assess the extent of myelin loss, and were given scores of 0 for absence of staining, 1+ for evidence of scattered ORO-positive cells, 2+ for clusters of ORO-positive cells, and 3+ for evidence of ORO staining throughout the section (see Fig. 4.3). Blocks positive for ORO which showed inflammation were classified as containing chronic active plaques.

4.3.3 Immunohistochemistry of normal and MS brain

4.3.3.1 Single labelling immunofluorescence for CD26

Prior to immunofluorescence, sections used in single and dual labelling were fixed in ice-cold acetone in Coplin jars for 10min at RT, and air-dried at RT for 20min.

Each antibody used in dual labelling was first optimised individually by changing the primary and secondary antibody dilutions (see Table 4.2), incubation times (1h at RT, or overnight at 4 °C), and washing medium (PBS + 0.5% Tween® 20, or PBS). The primary antibodies used were goat anti-CD26 (R&D Systems), mouse anti-GFAP (Chemicon), mouse anti-CD3 (BD), mouse anti-HLA-DR (Novocastra), and mouse anti-von Willebrand factor (VWF) (Dako). Alexa 488 (green) donkey anti-goat antibody (Invitrogen) was used as the secondary antibody with the anti-CD26 primary, and Alexa 568 (red) rabbit ant-mouse (Invitrogen) with all of the other primary antibodies. Appropriate isotype controls were used to confirm specificity of the primary antibodies to the target antigens, which involved using myeloma proteins of the same isotype and concentration as the primary antibodies to establish the amount of non-specific staining. Details of the primary and secondary antibodies, and the experimental conditions used during and after optimisation, are given in Table 4.2. Negative controls with omission of the primary antibodies were also performed.

After fixation, the tissue area of the slide was defined to contain the antibody solution by drawing a wax circle around it with an "ImmEdge" pen (Vector Labs, Peterborough, UK). Primary antibodies (180µl) were applied in PBS + 0.5% Tween® 20, and the slides incubated in a moist chamber for 1h at RT. Antibody was removed by 3 x 5min PBS + 0.5% Tween® 20 washes, on an orbital shaker. Secondary antibodies (180µl per slide, in PBS + 0.5% Tween® 20) were then added for 1h at RT, whilst the slides were incubated in a moist chamber in the dark. Secondary antibodies were washed off in the same way as primary antibodies, and then Sudan Black B (SBB) staining was performed as described in 4.3.2.2, prior to mounting in DAPI medium.

4.3.3.2 Sudan Black B

Brain tissue is prone to autofluorescence caused by the fluorescent pigment lipofuscin, present in the cytoplasm of cells of the CNS. This becomes more pronounced when dealing with aged tissues, as lipofuscin accumulates over time, and creates problems due to its broad emission and excitation spectra (Schnell *et al.*, 1999). It is, therefore, often necessary to treat sections of CNS tissue to reduce lipofuscin-like autofluorescence to enable detection of specific fluorescence from bound antibody.

SBB is a fat-soluble dye that stains neutral triglycerides and lipids a blue-black colour by readily dissolving in lipids, thereby concealing them (Yao *et al.*, 2003). SBB has been used successfully to eliminate autofluorescence without significantly reducing the intensity of fluorescent labels associated with antibodies (Schnell *et al.*, 1999).
SBB (1% w/v) was prepared by dissolving 1g in 100ml 70% ethanol.

Table 4.2 Details of the primary and secondary antibodies used in single and dual immunofluorescence for detection of CD26 expression in human CNS

ANTIBODY	SPECIES RAISED IN & ISOTYPE	DILUTION/ CONCENTRATION (µg/ml)	INCUBATION TIME	SUPPLIER
α-CD26 Polyclonal	Goat IgG	**1:10 (10)** 1:20 (5) 1:40 (2.5)	**1h at RT** O/N at 4°C	R&D Systems, UK
α-GFAP Monoclonal	Mouse IgG1	1:200 (5) **1:500 (2)** 1:1000 (1)	**1h at RT** O/N at 4°C	Chemicon, UK
α-CD3 Monoclonal	Mouse IgG1	1:25 (20) **1:50 (10)**	**1h at RT** O/N at 4°C	BD, UK
α-HLA-DR Monoclonal	Mouse IgG2b	1:25 (1) **1:50 (0.5)**	**1h at RT** O/N at 4°C	Novocastra
α-VWF Monoclonal	Mouse IgG1	1:50 (6.3) **1:100 (3.15)**	**1h at RT** O/N at 4°C	Dako, UK
2° Alexa 488	Donkey α goat	1:400 **1:500** 1:1000	1h at RT	Molecular Probes, Invitrogen, UK
2° Alexa 568	Rabbit α mouse	1:400 **1:500** 1:1000	1h at RT	Molecular Probes, Invitrogen, UK
IgG isotype control	Goat IgG	Same as for CD26 1:100 (10)	**1h at RT** O/N at 4°C	Pro Sci Inc., USA
IgG1 isotype control	Mouse IgG1	Same as for: GFAP (2) CD3 (10) VWF (3.15)	**1h at RT** O/N at 4°C	Sigma, UK
IgG2b isotype control	Mouse IgG2b	Same as for HLA-DR (0.5)	**1h at RT** O/N at 4°C	Sigma, UK

Antibodies were optimised to investigate expression of CD26 in the human brain. Dilutions and incubation times shown in bold represent those that were found to be optimal, which were used for dual immunofluorescence.

2° = secondary antibody, α = anti, RT = room temperature, O/N = overnight

The solution was stirred in the dark for 2h at RT, filtered, and stored at 4°C for a maximum of 2 months. SBB staining was performed on all brain tissue sections, after the final PBS wash of the immunofluorescence procedure. Slides were immersed in 1% SBB in the dark for 5min at RT, rinsed briefly 8-10 times in PBS, and mounted using DAPI mountant on a 22 x 50mm coverslip.

4.3.3.3 Dual labelling immunofluorescence

To identify the cellular location of CD26 in the human brain, dual labelling immunofluorescence was performed. The procedure for single labelling was used (4.3.2.1), incubating the sections with the polyclonal anti-CD26 and Alexa 488 antibodies first, followed by sequential addition of the monoclonal antibody and Alexa 568 secondary. After the final secondary antibody had been washed off, slides were treated with SBB (4.3.2.2) to quench autofluorescence of the tissue, and mounted using DAPI mountant.

Various controls were performed alongside the slides that were dual labelled, including single labelling, omission of the first or second primary antibodies in turn, omission of the first or second secondary antibodies, incubation of one primary antibody with both secondary antibodies, and the use of isotype controls as primary antibodies.

4.3.3.4 Image acquisition

Images were acquired using a Zeiss LSM510 confocal scanning laser microscope (see 3.3.2.13). Multi-track acquisition was used, to enable collection of dual-labelling data. Filter sets for 488 and 568nm were selected, which loaded predefined parameters for data acquisition. In continuous scan mode, and using the range indicator of the palette setting, detector gain and amplifier offset were adjusted, so that only a few red and blue pixels were visible on the screen, to optimise scanning conditions. The pinhole was set to 1 Airy unit, and the optical slice to 2, for both red and green channels. Composite 'Z-stack' images were then obtained by scanning from the manually selected deepest focal point to the highest focal point, of ~15 optical slices in the Z-plane. Colocalisation was detected using the histogram function of the LSM510 software, with pixels detected in both fluorescent channels at >100 intensity appearing white. Images were saved, overlaid with images of the DAPI staining of nuclei if required, and exported as JPEG files, without further manipulation. The detector gain setting used during image acquisition was also applied for visualisation and image capture of the negative control slides (isotype controls), to enable direct comparison of visible fluorescence levels.

4.4 Results

4.4.1 Characterisation of tissue blocks by H&E and ORO for the extent of inflammation and demyelination

H&E staining was used to detect areas of inflammatory perivascular cuffs, within the brain tissue used for this study, and ORO used to identify areas of demyelination. No inflammation or demyelination was seen in control brain tissue, although a few immune cells were observed associated with blood vessels, indicative of routine surveillance of the CNS (Xiao and Link, 1998). Minimal perivascular cuffing was seen in MS block MS74 A1E7, but some ORO staining was evident. All other lesion blocks showed extensive inflammation, perivascular cuffing (Fig. 4.2), and ORO staining (Fig. 4.3). Results of characterisation of the blocks used, based on grading illustrated in Figs. 4.2 and 4.3, are summarised in Table 4.3.

4.4.2 CD26 expression in control brain tissue

Frozen brain sections were dual labelled for CD26 with either GFAP, VWF, CD3, or HLA-DR. In control, non-neurological white matter, diffuse CD26 staining was evident on the abluminal surface of blood vessels, which was not colocalised with VWF expression (Fig. 4.5). Staining was quite extensive around some blood vessels, which may indicate CD26 secreted by ECs binding to connective tissue components. Some colocalisation of CD26 was seen with CD3 (Fig. 4.6) and also HLA-DR (Fig. 4.7), but not with GFAP (Fig. 4.4).

4.4.3 CD26 expression in chronic active MS lesions in block MS74 A1E7

Block MS74 A1E7 showed minimal levels of inflammation and moderate demyelination. In demyelinating lesions, CD26 was expressed at higher levels than in control brain, and appears to be associated with infiltrating perivascular cells. The diffuse CD26 staining surrounding blood vessels appeared to be diminished (Figs. 4.8, 4.9, 4.10 and 4.12) compared to control brain. Colocalisation of CD26 and CD3 was seen, with a subset of T cells surrounding the blood vessel appearing as $CD3^{+}CD26^{+}$ (Fig. 4.10). Cells staining positive for HLA-DR were common throughout the parenchyma, and also surrounding blood vessels (Fig. 4.11). Colocalisation of CD26 and HLA-DR was observed in several cells in the parenchyma, but there were approximately equal numbers of cells that stained positive for either CD26 or HLA-DR alone (Fig. 4.11 and 4.12). Colocalisation of CD26 and HLA-DR around blood vessels was also seen (Fig. 4.12), but to a lesser extent than in the parenchyma (Fig. 4.11). Co-expression of CD26 and GFAP was insignificant (Fig. 4.8), and colocalisation with VWF was not observed (Fig. 4.9).

Table 4.3 Characterisation of tissue blocks used in this study by H&E and ORO staining

BLOCK NUMBER	H&E: INFLAMMATION	ORO: DEMYELINATION	CLASSIFICATION	COMMENTS
C11 A1B5	0	1+	Control brain	Minimal ORO
C14 P2C3	0	0	Control brain	No inflammation / demyelination seen
MS74 A1C6	2+	2+	Lesion (Chronic active)	Large part of block is grey matter; few and small PVCs
MS74 A1E7	1+	2+	Lesion (Chronic active)	Minimal T cell infiltrate and PVCs
MS90 P2E3	2+	3+	Lesion (Chronic active)	Clear plaque border; extensive cellular infiltrate
MS130 P2D3	2+	2+	Lesion (Chronic active)	Large part of block is grey matter; moderate cellular infiltrate
MS130 P2F4	4+	2+	Lesion (Chronic active)	Plentiful and large PVCs

H&E and ORO staining was performed on snap-frozen, PFA-fixed, 10µm sections of human brain, obtained from the UK MS Tissue Bank from MS and control tissue blocks. Blocks were graded according to the amount of inflammation/perivascular cuffing identified by H&E, ranging from 0-4+ with increasing abundance, and the extent of demyelination, ranging from 0-3+. All lesions were classified as chronic active, due to the presence of both plaques and ORO+ staining.

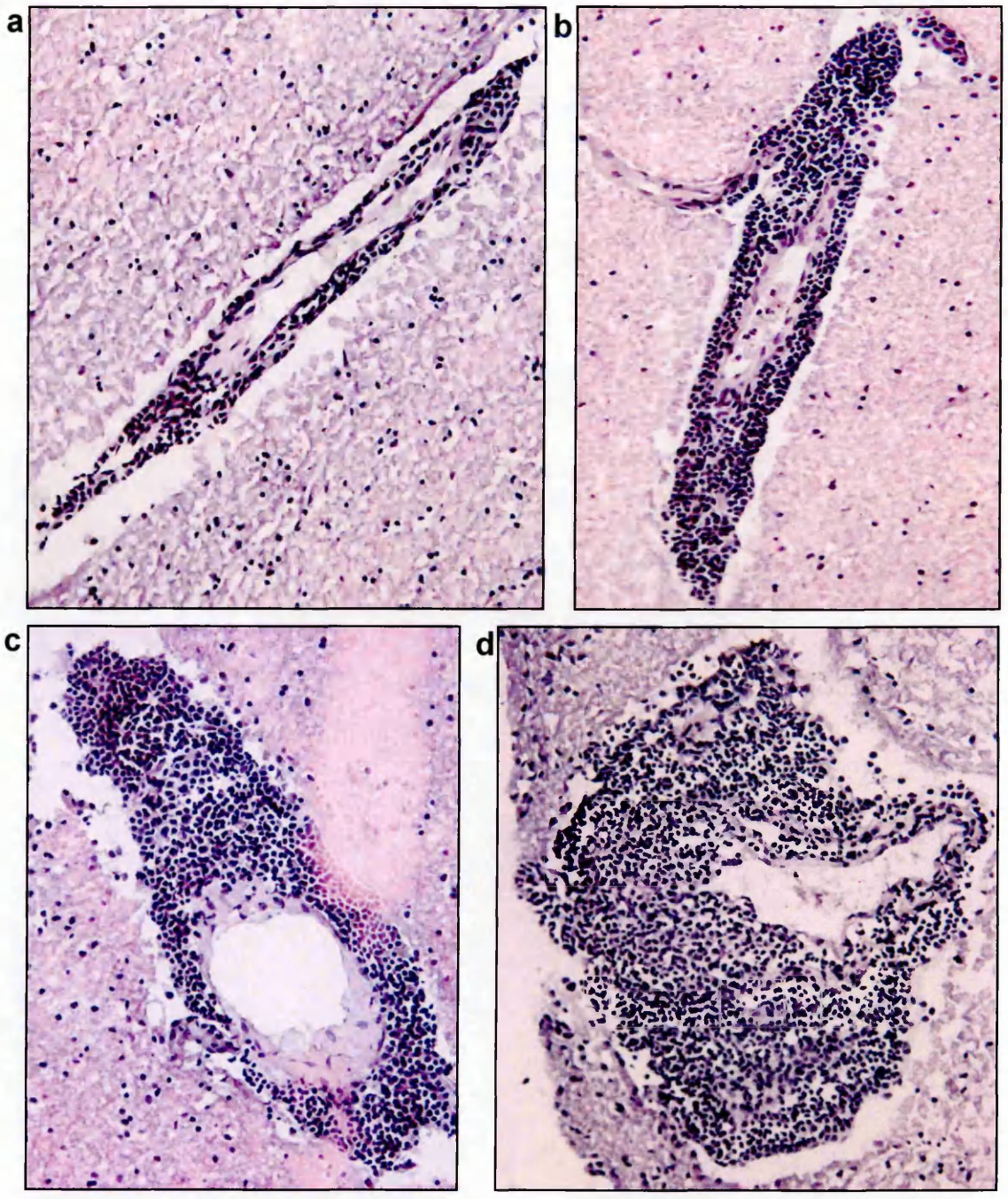

Figure 4.2 Grading of levels of inflammation in white matter MS lesions detected by H&E staining

Snap-frozen human MS brain tissue from an area containing lesions (MS130 P2F4) was stained using H & E, and various stages of inflammation were identified by the degree of perivascular cuffing observed: ***a****=1+,* ***b****=2+,* ***c****=3+, and* ***d****=4+ (200X). The grading of inflammation around blood vessels was used to characterise the blocks used in this study.*

Figure 4.3 Grading of levels of demyelination in white matter MS lesions detected by ORO staining

ORO staining of snap-frozen human MS brain tissue from: ***(a)*** *an area with minimal infiltrate (MS74 A1E7); and* ***(b and c),*** *lesions showing substantial infiltrate (MS90 P2E3). Nuclei were subtly counterstained pale blue using 20% Harris's haematoxylin. ORO stains lipids red and can be used to identify areas of myelin loss, and phagocytic macrophages. White matter in* ***(a)*** *stained positive (1+) with ORO (200X). The blood vessel in* ***(b)*** *shows extensive perivascular macrophage staining, and also significant ORO staining (3+) in the surrounding tissue (100X).* ***(c)*** *shows the edge of the lesion (arrowheads), defined by an area of pallor on the right, where macrophages phagocytosing myelin have stained red. Pink tissue on the left indicates the presence of myelin, but contains blood vessels with some perivascular ORO staining (arrows) (40X). The grading of ORO staining was used to characterise the extent of demyelination seen in the tissue blocks used in this study.*

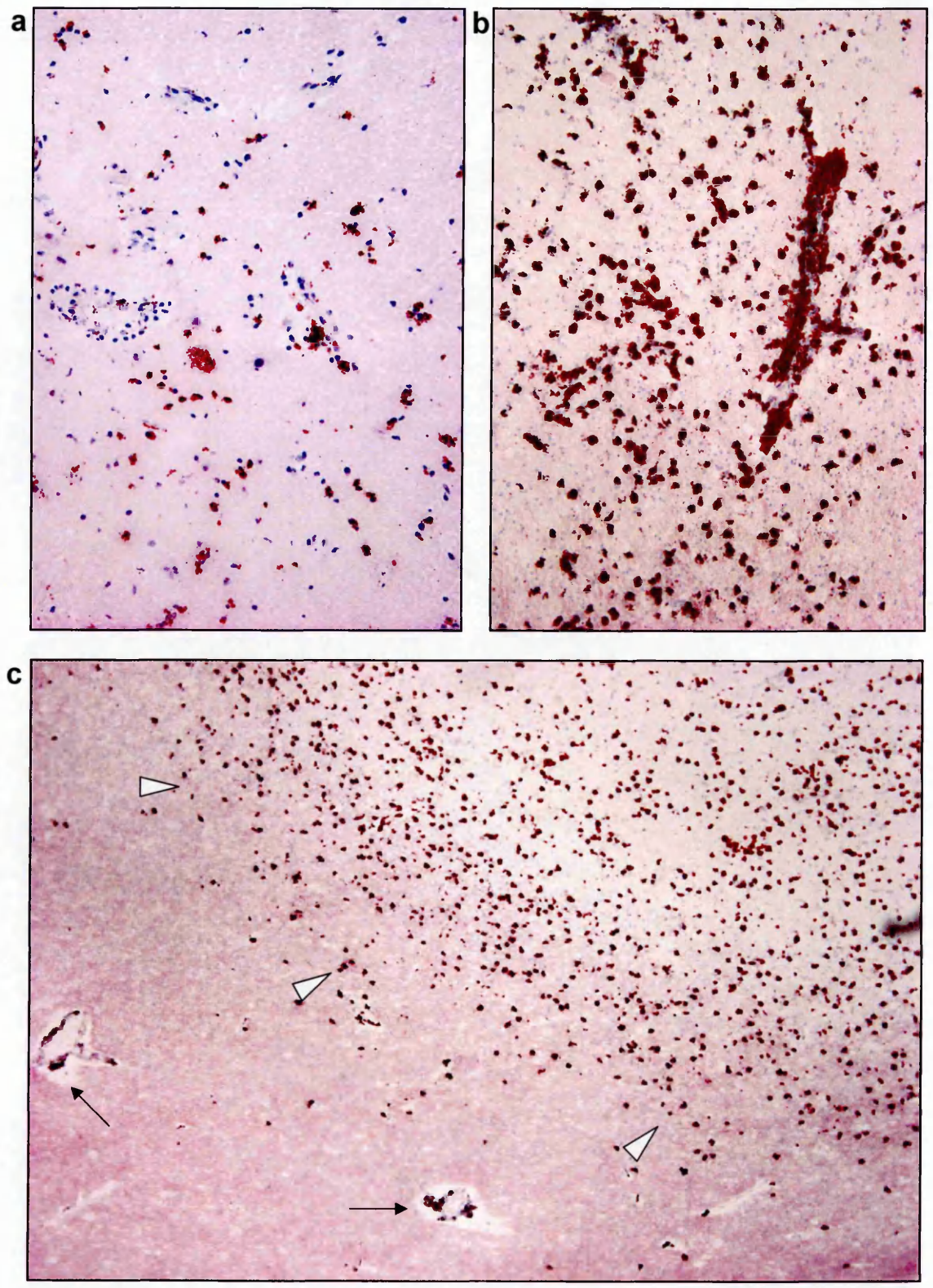
a
b
c

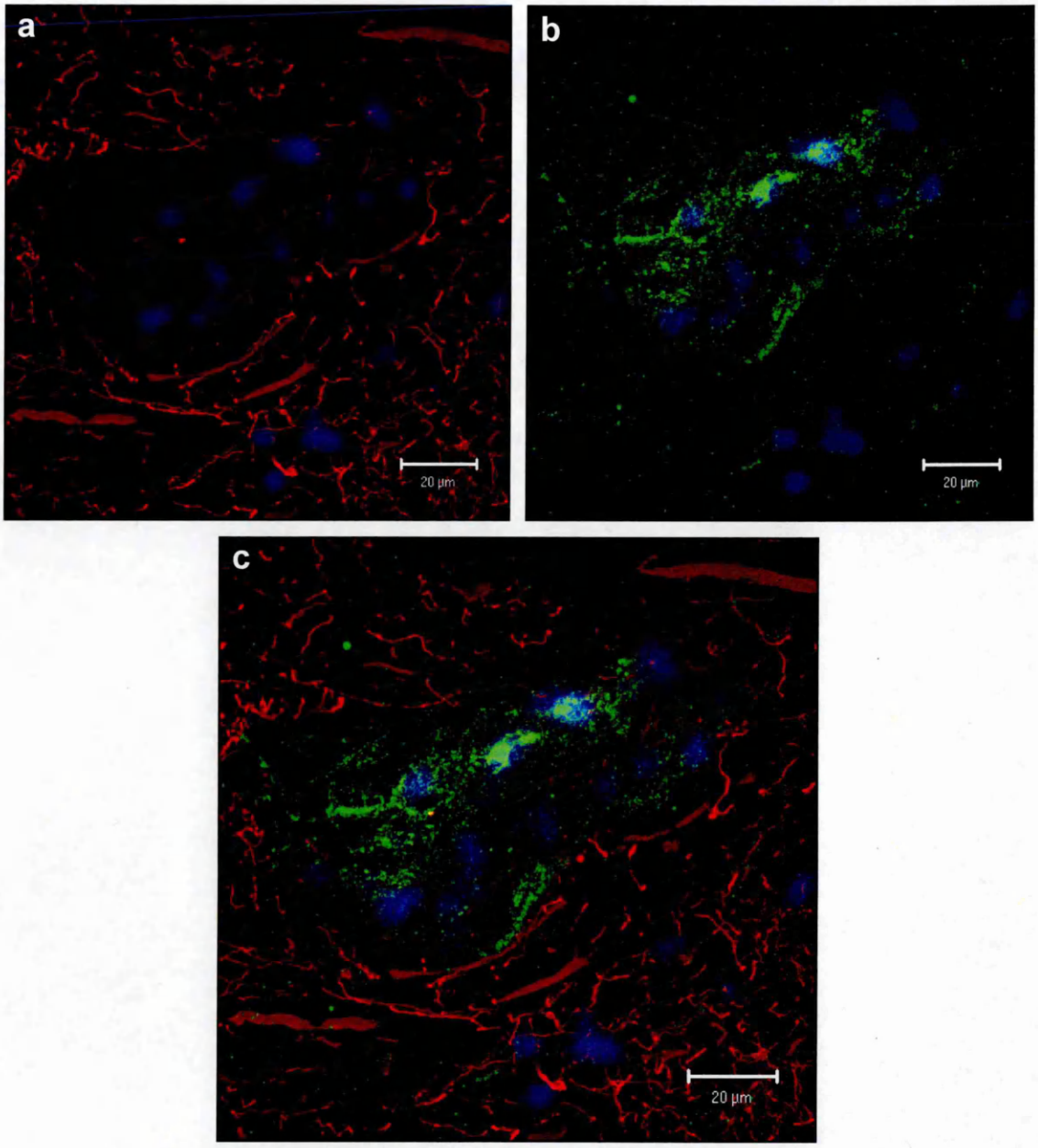

Figure 4.4 Dual-label immunofluorescence of GFAP and CD26 in control brain

Snap frozen, non-neurological, control human brain tissue (C14 P2C3) was fixed in acetone and dual-labelled for ***(a)*** *GFAP (red) and* ***(b)*** *CD26 (green) expression, using Alexa 568, and 488, fluorescent antibodies, respectively. Nuclei were counterstained with DAPI and appear blue. The dual-labelled image* ***(c)*** *was screened for areas of colocalisation of GFAP and CD26 using LSM510 software; none was evident.*

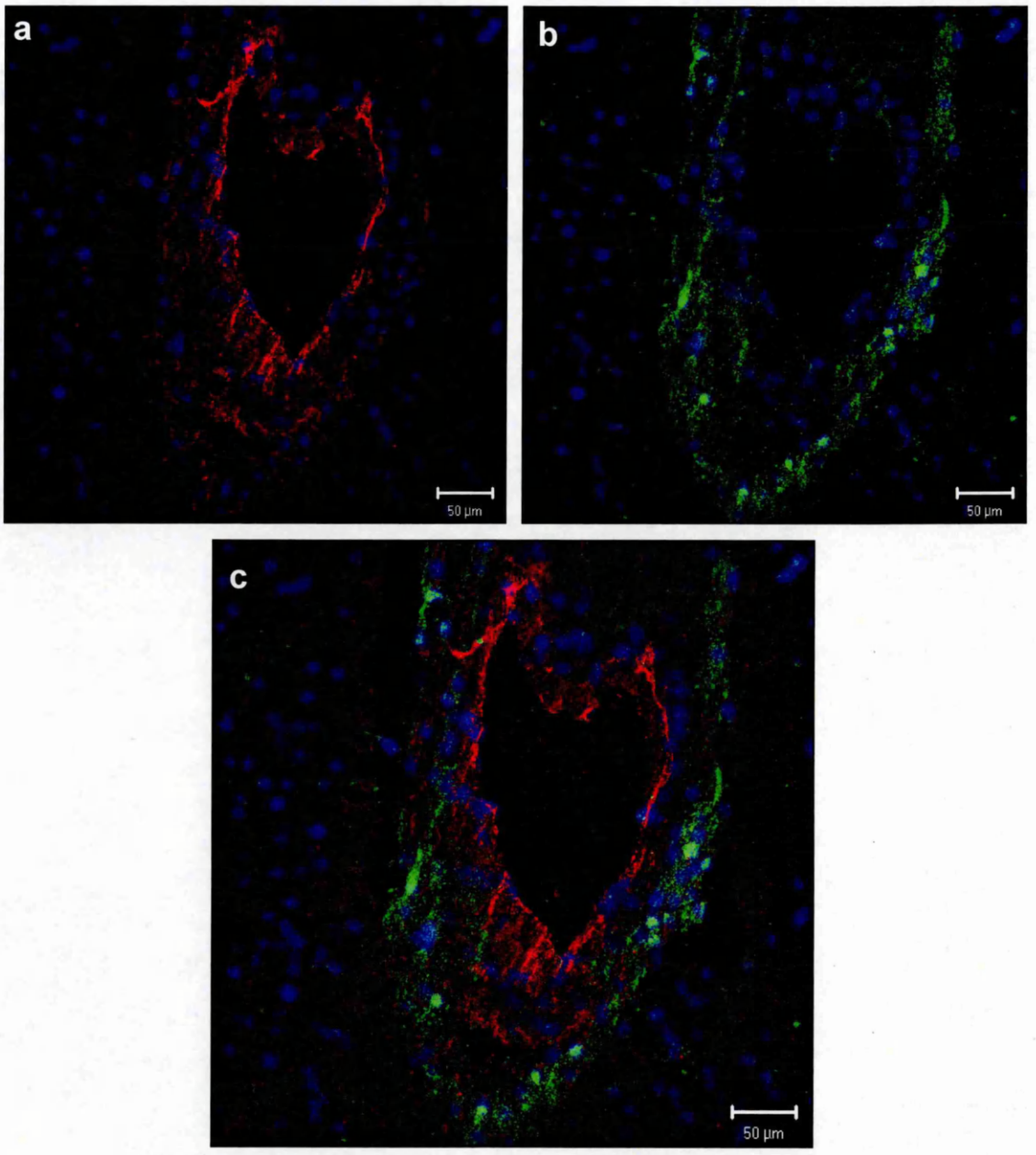

Figure 4.5 Dual-label immunofluorescence of VWF and CD26 in control brain

Snap frozen, non-neurological, control human brain tissue (C11 A1B5) was fixed in acetone and dual-labelled for ***(a)*** *VWF (red) and* ***(b)*** *CD26 (green) expression, using Alexa 568, and 488, fluorescent antibodies, respectively. Nuclei were counterstained with DAPI and appear blue. The dual-labelled image* ***(c)*** *was screened for areas of colocalisation of VWF and CD26 using LSM510 software; none was detected.*

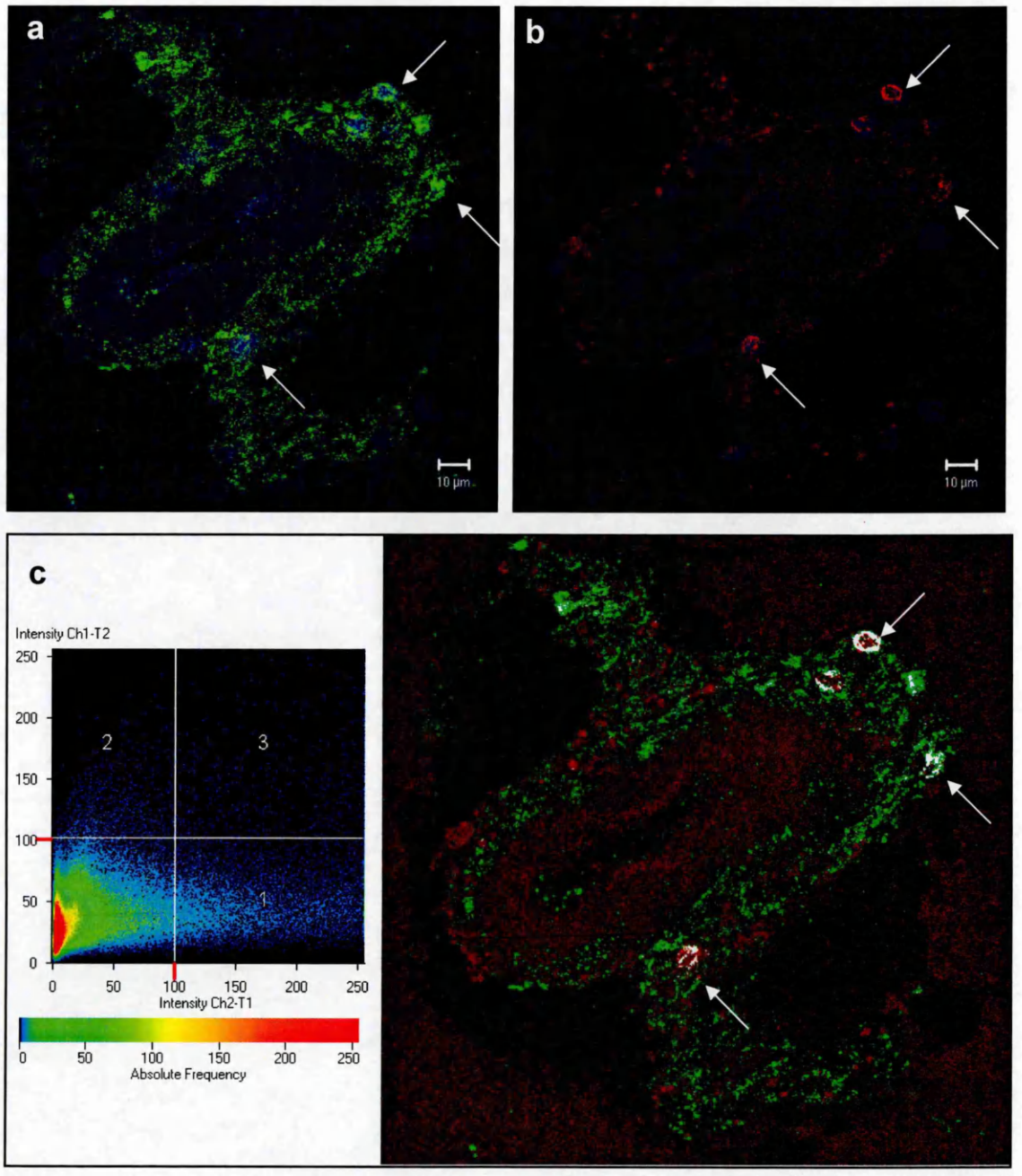

Figure 4.6 Dual-label immunofluorescence of CD3 and CD26 in control brain

Snap frozen, non-neurological control human brain tissue (C11 A1B5) was fixed in acetone and dual-labelled for ***(a)*** *CD3 (red) and* ***(b)*** *CD26 (green) expression, using Alexa 568, and 488, fluorescent antibodies, respectively. Nuclei were counterstained with DAPI and appear blue. Areas of colocalisation of CD3 and CD26 were identified by the presence of pixels in quadrant 3 of the intensity grid in* ***(c),*** *and appear as white areas on the image. Arrows indicate colocalisation of CD3 and CD26 on a few T cells.*

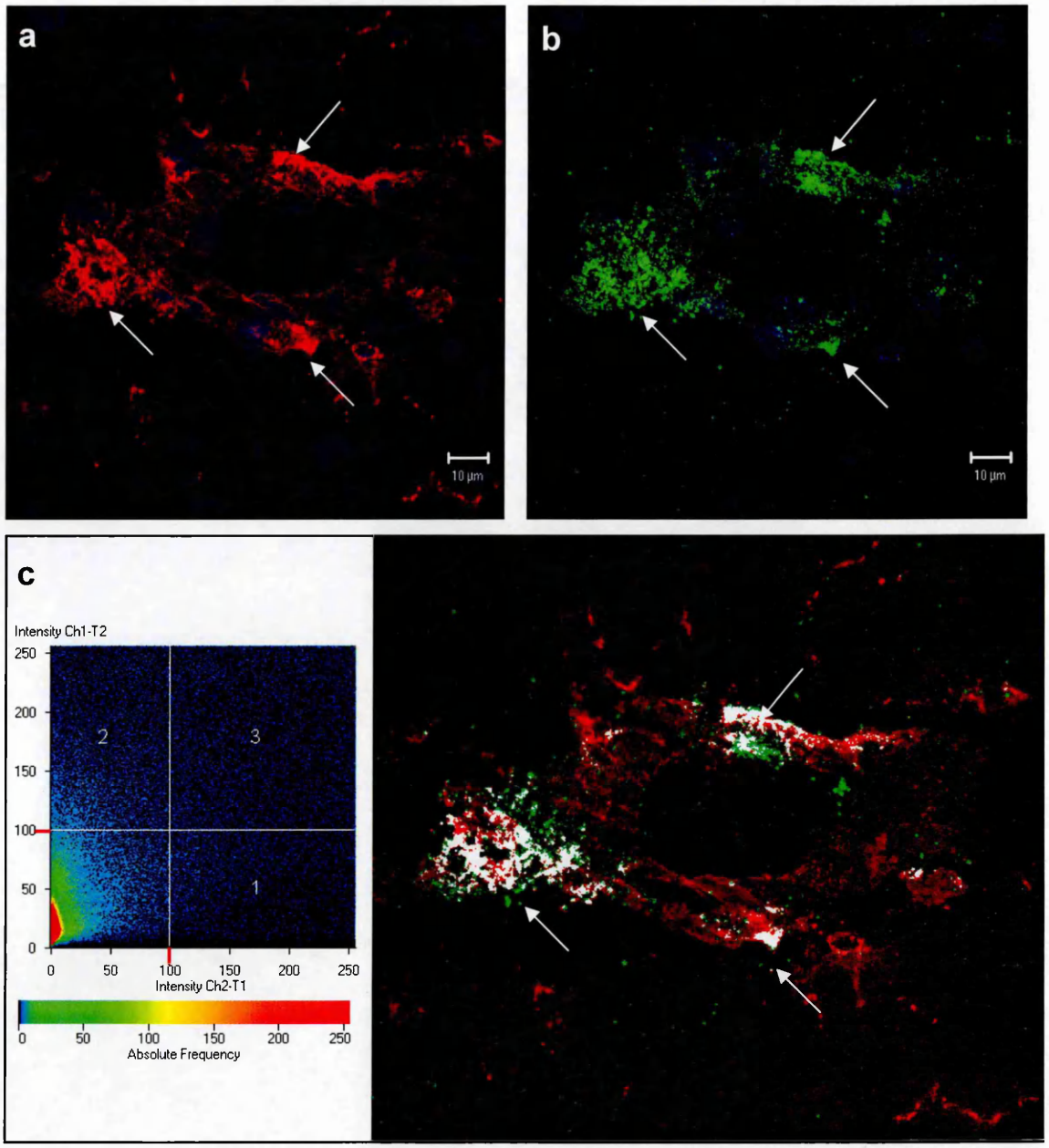

Figure 4.7 Dual-label immunofluorescence of HLA-DR and CD26 in control brain

Snap frozen, non-neurological control human brain tissue (C14 P2C3) was fixed in acetone and dual-labelled for ***(a)*** *HLA-DR (red) and* ***(b)*** *CD26 (green) expression, using Alexa 568, and 488, fluorescent antibodies, respectively. Nuclei were counterstained with DAPI and appear blue. Areas of colocalisation of HLA-DR and CD26 were identified by the presence of pixels in quadrant 3 of the intensity grid in* ***(c),*** *and appear as white areas on the image. Arrows indicate the colocalisation of HLA-DR and CD26 of several cells, possibly perivascular macrophages.*

4.4.4 CD26 expression in chronic active MS lesions in block MS74 A1C6

Block MS74 A1C6 showed moderate levels of inflammation and demyelination. Increased levels of CD26 and the presence of PVCs were seen in the white matter, compared to control brain. GFAP expression was increased in lesions, compared to control, as is commonly seen with reactive astrocytes, but colocalisation of GFAP with CD26 was an insignificant rarity (Fig. 4.13). Similar to control tissue, no colocalisation was seen with CD26 and VWF in lesions with extensive PVCs (Fig. 4.14). The diffuse CD26 staining seen around blood vessels in control brain was reduced in lesional tissue (Fig. 4.15). $CD26^+$ cells were seen in the parenchyma, a proportion of which were colocalised with either CD3, or HLA-DR (Fig. 4.16). A marked increase was seen in HLA-DR^+ cells (Fig. 4.16) compared to control brain. Although lesions in block MS74 A1C6 gave staining patterns consistent with abundant activated microglia that were HLA-DR^+CD26^- (Fig. 4.15), significant numbers of $CD26^+$HLA-DR^+ cells were also detected (Fig. 4.16).

4.4.5 CD26 expression in chronic active MS lesions in block MS90 P2E3

Block MS90 P2E3 showed moderate levels of inflammation and extensive demyelination. Increased numbers of $CD26^+$ cells (Fig. 4.17) were seen, compared to control brain. Significant colocalisation of CD3 and CD26 was seen in PVCs, although some $CD3^+CD26^-$ and $CD3^-CD26^+$ cells were also seen (Fig. 4.18). Only relatively small numbers of $CD26^+$HLA-DR^+ cells were seen surrounding blood vessels in some lesions (Figs. 4.17 and 4.19). The edge of a lesion was evident by ORO staining, which showed abundant macrophages in an area of myelin pallor (Fig. 4.19a). Dual-labelled immunofluorescent images from serial sections, showing the same blood vessel from this area (Figs. 4.19b-f), demonstrated that CD26 was primarily associated with T cells around the blood vessel, rather than elsewhere in the parenchyma. Selected lesions in this block demonstrated a staining pattern consistent with foamy macrophages that were HLA-DR^+CD26^-, suggesting that CD26 had not contributed to MS pathogenesis at the edge of these actively demyelinating lesions. No colocalisation of CD26 was seen with either GFAP or VWF.

4.4.6 CD26 expression in chronic active MS lesions in block MS130 P2F4

Block MS130 P2F4 showed extensive inflammation and moderate demyelination. A grade 4+ PVC (Fig. 4.2d) was identified as having $CD3^+CD26^+$ cells throughout. HLA-DR^+CD26^+ cells were also evident, to a lesser extent than $CD3^+CD26^+$ cells, and were mainly focused near the periphery of the PVC, further from the lumen of the blood vessel (Fig. 4.20). No colocalisation of CD26 was seen with either GFAP or VWF.

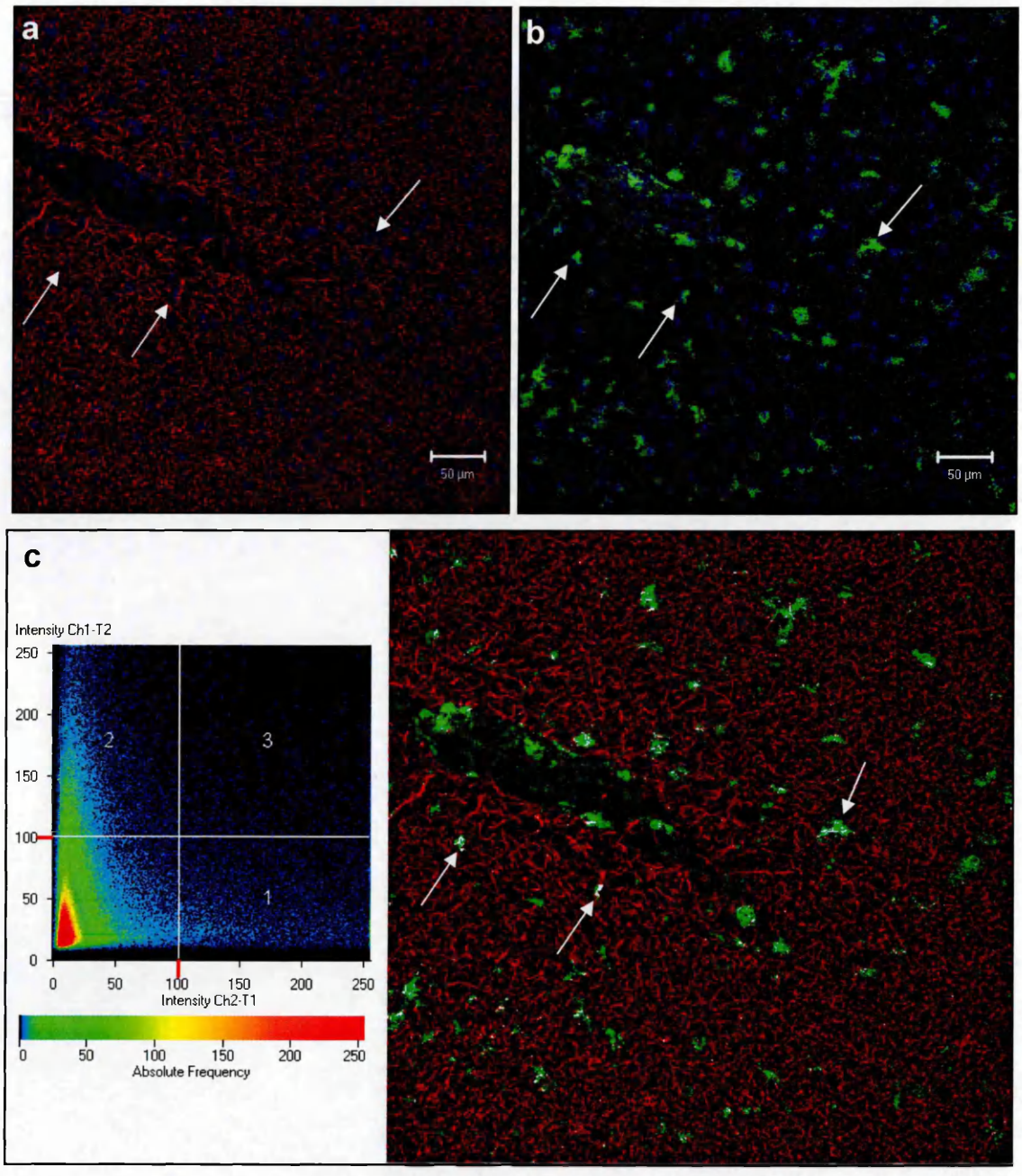

Figure 4.8 Dual-label immunofluorescence of GFAP and CD26 in MS brain (MS74 A1E7)

Snap frozen, white matter from an MS brain was fixed in acetone and dual-labelled for ***(a)*** *GFAP (red) and* ***(b)*** *CD26 (green) expression, using Alexa 568, and 488, fluorescent antibodies, respectively. Nuclei were counterstained with DAPI and appear blue. Areas of colocalisation of GFAP and CD26 were identified by the presence of pixels in quadrant 3 of the intensity grid in* ***(c),*** *and appear as white areas on the image. Small areas of colocalisation of GFAP and CD26 above are identified by arrows.*

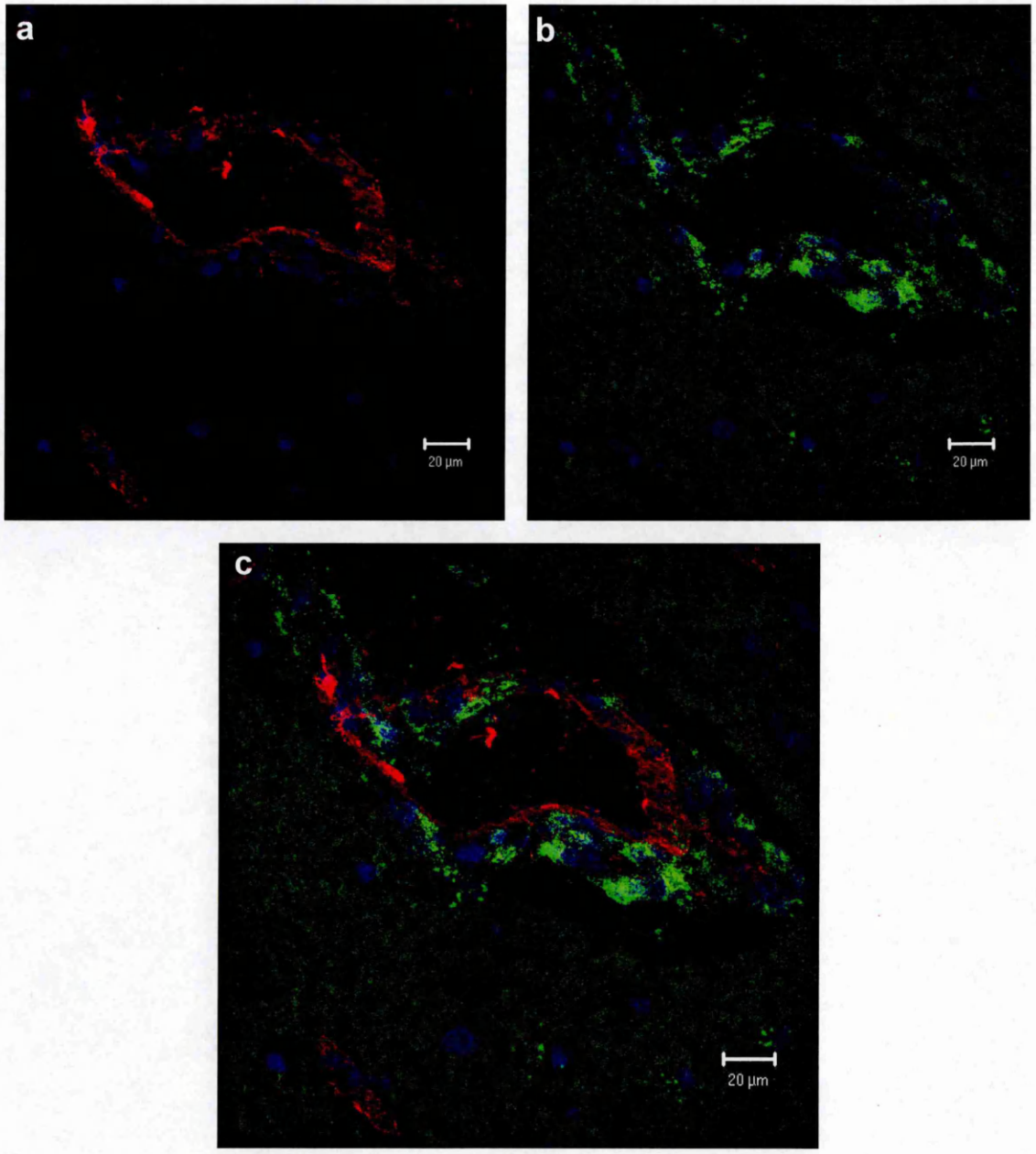

Figure 4.9 Dual-label immunofluorescence of VWF and CD26 in MS brain (MS74 A1E7)
Snap frozen, white matter from an MS brain was fixed in acetone and dual-labelled for ***(a)*** *VWF (red) and* ***(b)*** *CD26 (green) expression, using Alexa 568, and 488, fluorescent antibodies, respectively. Nuclei were counterstained with DAPI and appear blue. The dual-labelled image* ***(c)*** *was screened for areas of colocalisation of VWF and CD26 using LSM510 software; none were evident.*

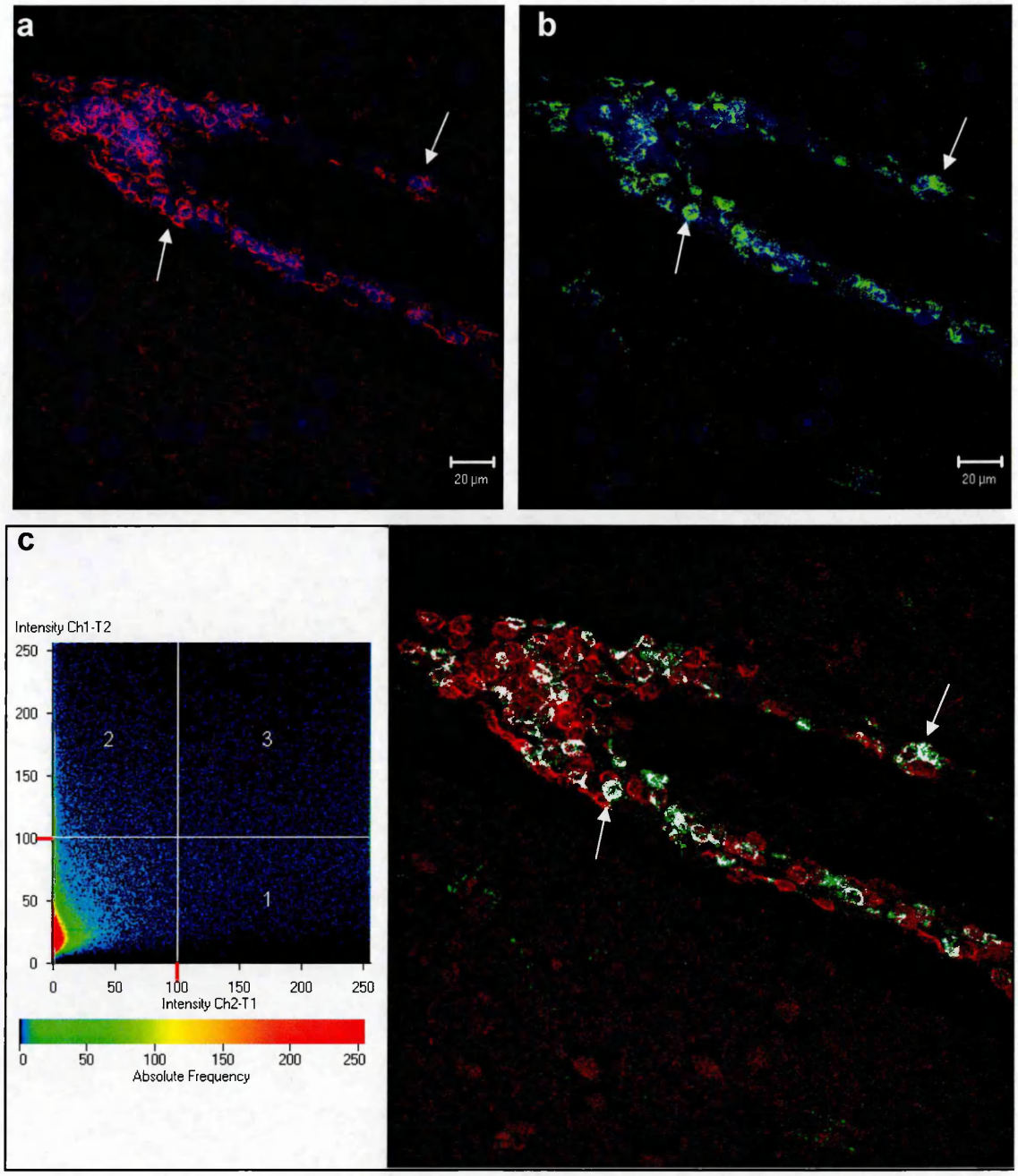

Figure 4.10 Dual-label immunofluorescence of CD3 and CD26 in MS brain (MS74 A1E7)

Snap frozen, white matter from an MS brain was fixed in acetone and dual-labelled for ***(a)*** *CD3 (red) and* ***(b)*** *CD26 (green) expression, using Alexa 568, and 488, fluorescent antibodies, respectively. Nuclei were counterstained with DAPI and appear blue. Areas of colocalisation of CD3 and CD26 were identified by the presence of pixels in quadrant 3 of the intensity grid in* ***(c),*** *and appear as white areas on the image. Colocalisation of CD3 and CD26 of several, but not all, T cells is seen above, with arrows showing a few examples.*

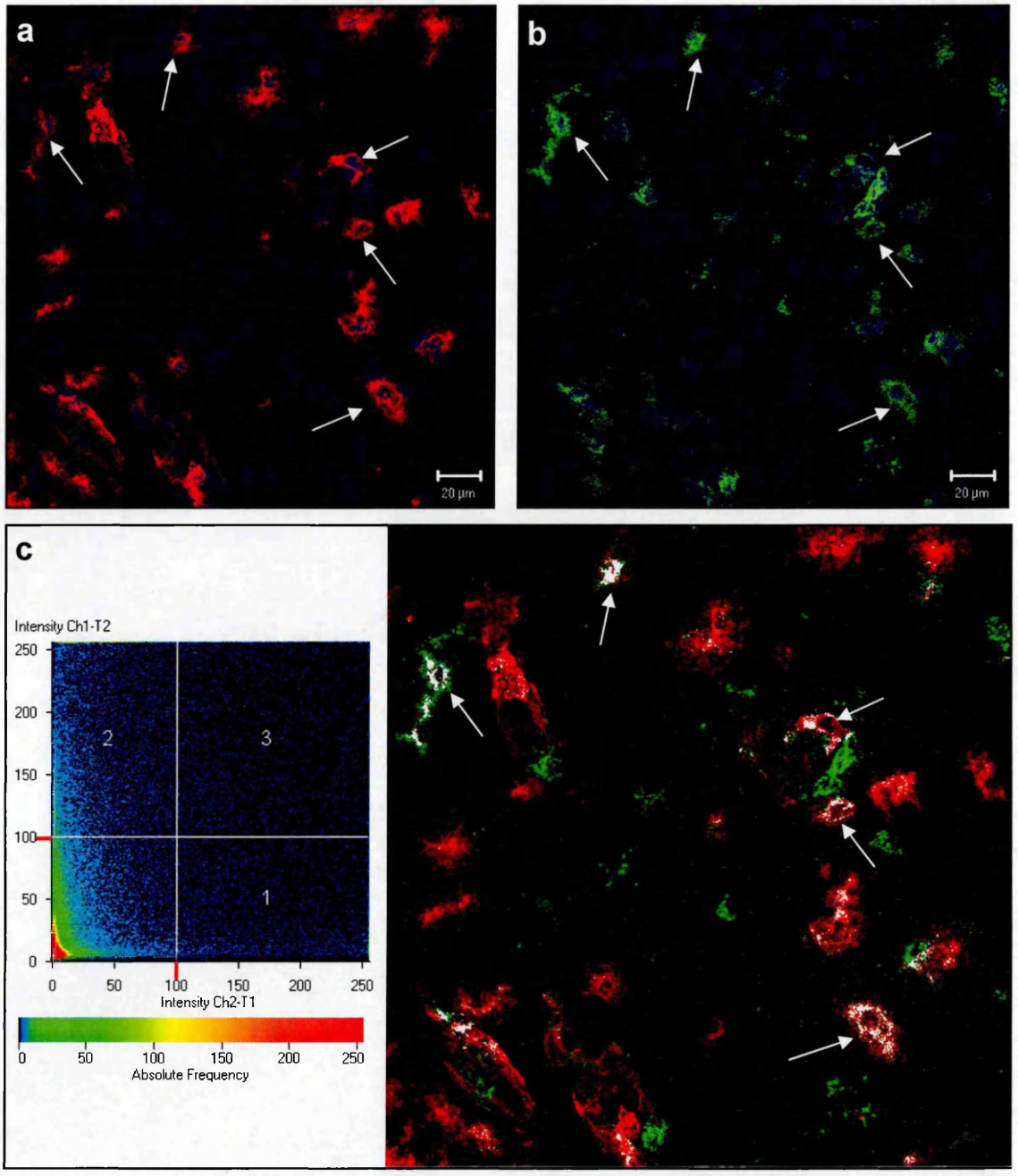

Figure 4.11 Dual-label immunofluorescence of HLA-DR and CD26 distant from blood vessels in MS brain (MS74 A1E7)

Snap frozen, white matter from an MS brain was fixed in acetone and dual-labelled for ***(a)*** *HLA-DR (red) and* ***(b)*** *CD26 (green) expression, using Alexa 568, and 488, fluorescent antibodies, respectively. Nuclei were counterstained with DAPI and appear blue. Areas of colocalisation of HLA-DR and CD26 were identified by the presence of pixels in quadrant 3 of the intensity grid in* ***(c),*** *and appear as white areas on the image. Arrows show colocalisation of HLA-DR and CD26 of several, but not all, immune cells (morphologically identified as microglia/macrophages), distant from blood vessels.*

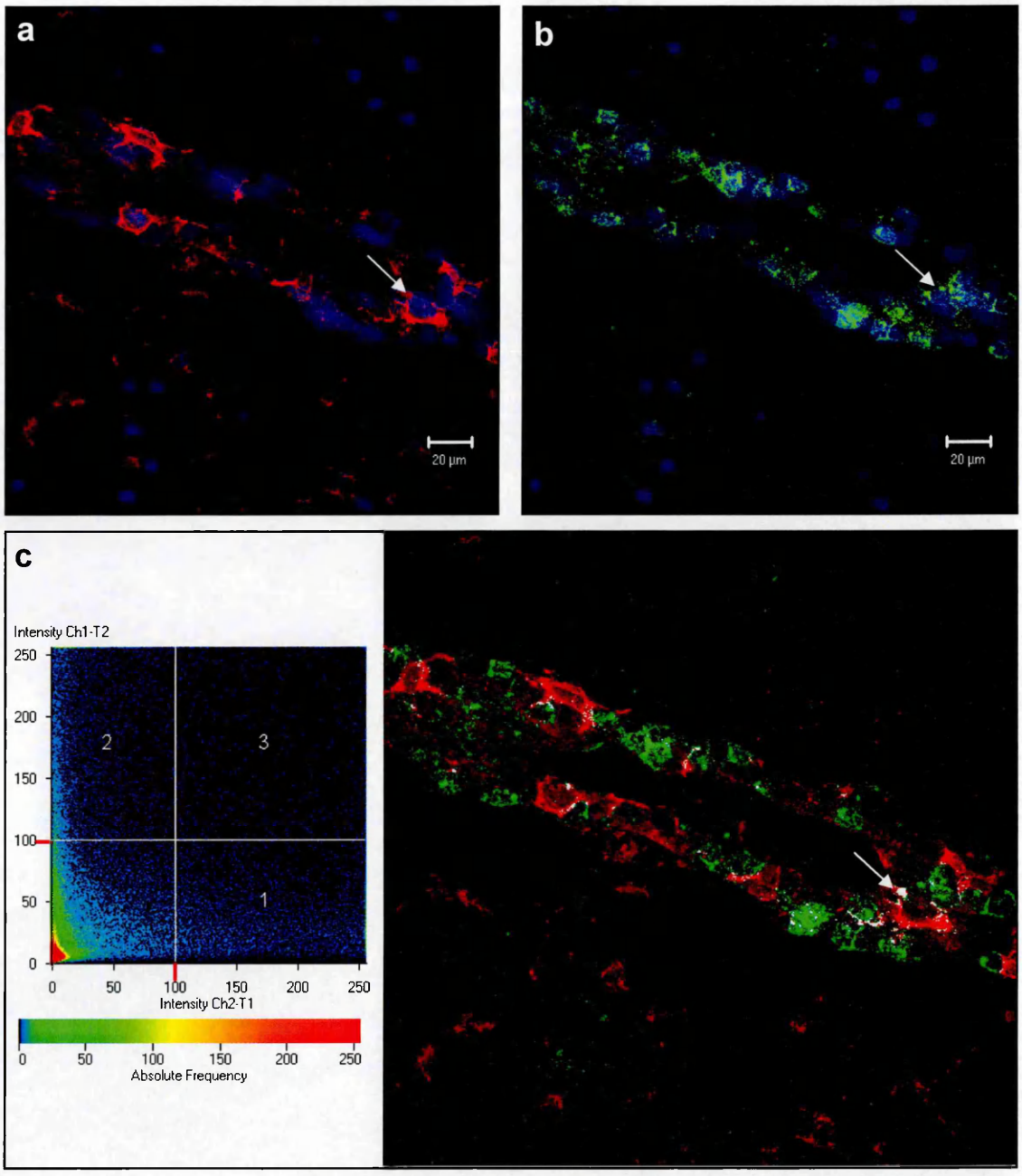

Figure 4.12 Dual-label immunofluorescence of HLA-DR and CD26 associated with a blood vessel in MS brain (MS74 A1E7)

Snap frozen, white matter from an MS brain was fixed in acetone and dual-labelled for ***(a)*** *HLA-DR (red) and* ***(b)*** *CD26 (green) expression, using Alexa 568, and 488, fluorescent antibodies, respectively. Nuclei were counterstained with DAPI and appear blue. Areas of colocalisation of HLA-DR and CD26 were identified by the presence of pixels in quadrant 3 of the intensity grid in* ***(c),*** *and appear as white areas on the image. The arrow shows some colocalisation of HLA-DR and CD26 on a minority of immune cells, around the blood vessel.*

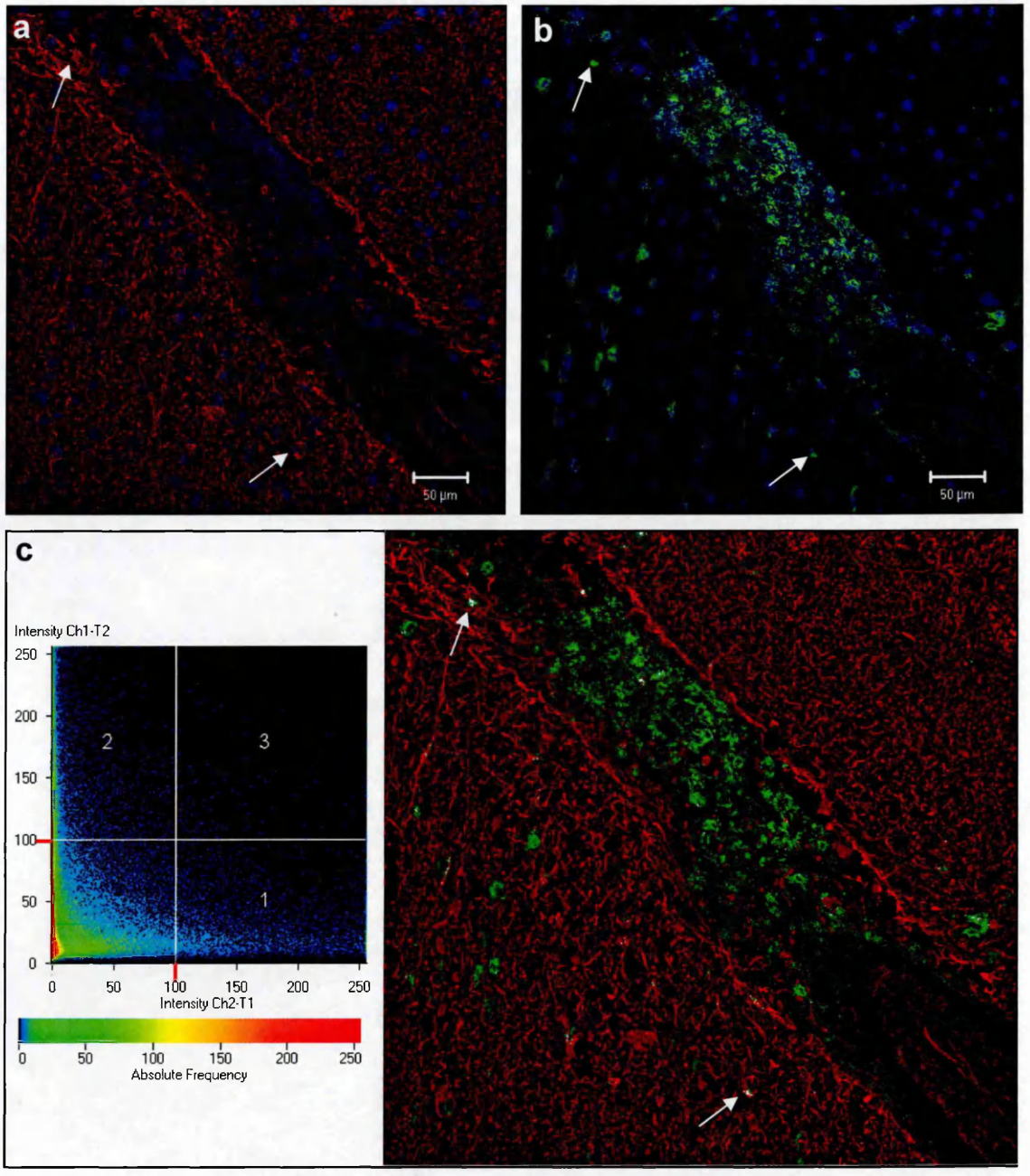

Figure 4.13 Dual-label immunofluorescence of GFAP and CD26 in lesions from MS brain (MS74 A1C6)

Snap frozen, lesional tissue from an MS brain was fixed in acetone and dual-labelled for ***(a)*** *GFAP (red) and* ***(b)*** *CD26 (green) expression, using Alexa 568, and 488, fluorescent antibodies, respectively. Nuclei were counterstained with DAPI and appear blue. Areas of colocalisation of GFAP and CD26 were identified by the presence of pixels in quadrant 3 of the intensity grid in* ***(c),*** *and appear as white areas on the image. Arrows indicate the barely significant colocalisation seen of GFAP and CD26.*

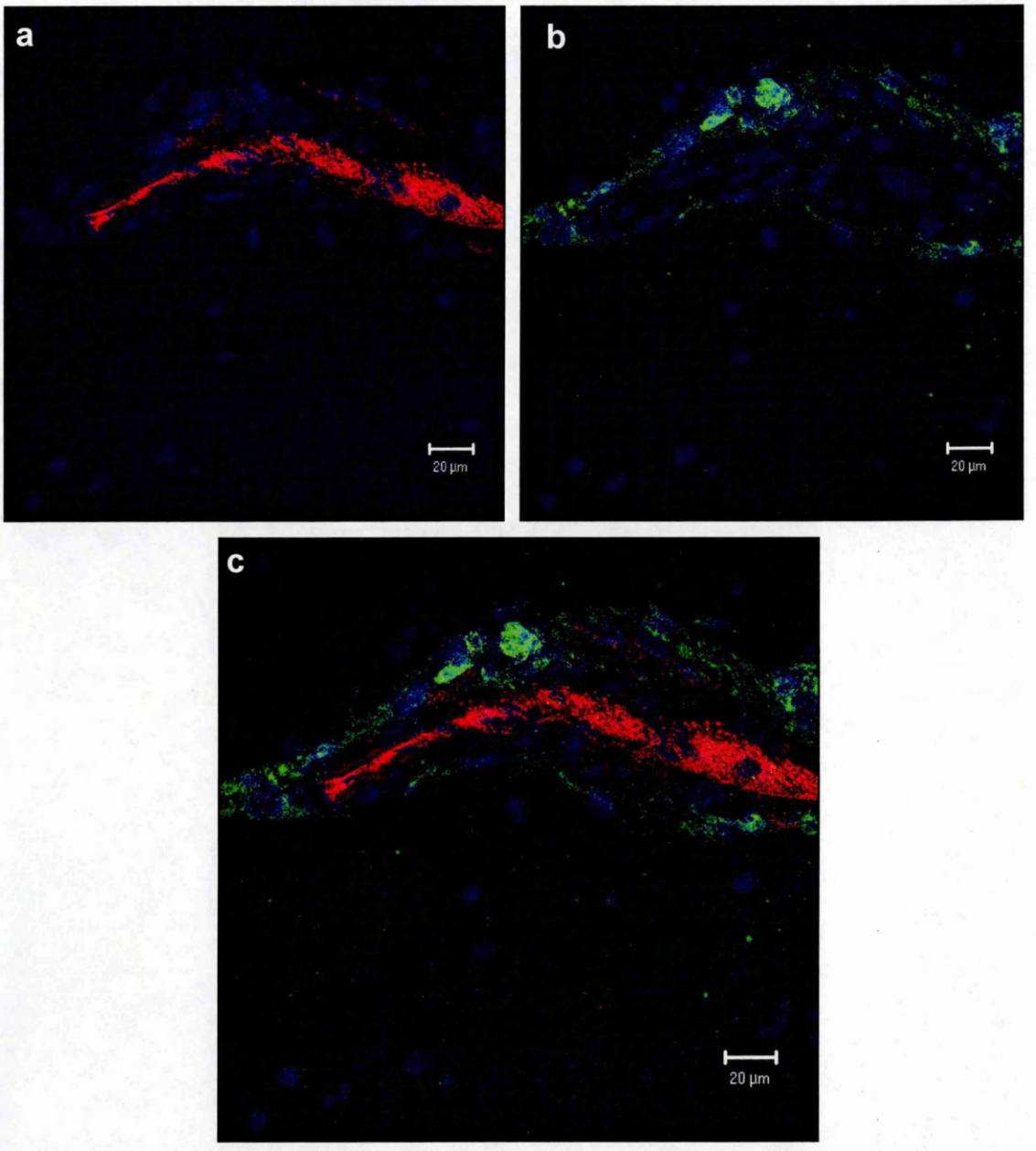

Figure 4.14 Dual-label immunofluorescence of VWF and CD26 in MS brain (MS74 A1C6)
Snap frozen, lesional tissue from an MS brain was fixed in acetone and dual-labelled for ***(a)*** *VWF (red) and* ***(b)*** *CD26 (green) expression, using Alexa 568, and 488, fluorescent antibodies, respectively. Nuclei were counterstained with DAPI and appear blue. The dual-labelled image* ***(c)*** *was screened for areas of colocalisation of VWF and CD26 using LSM510 software; none was evident.*

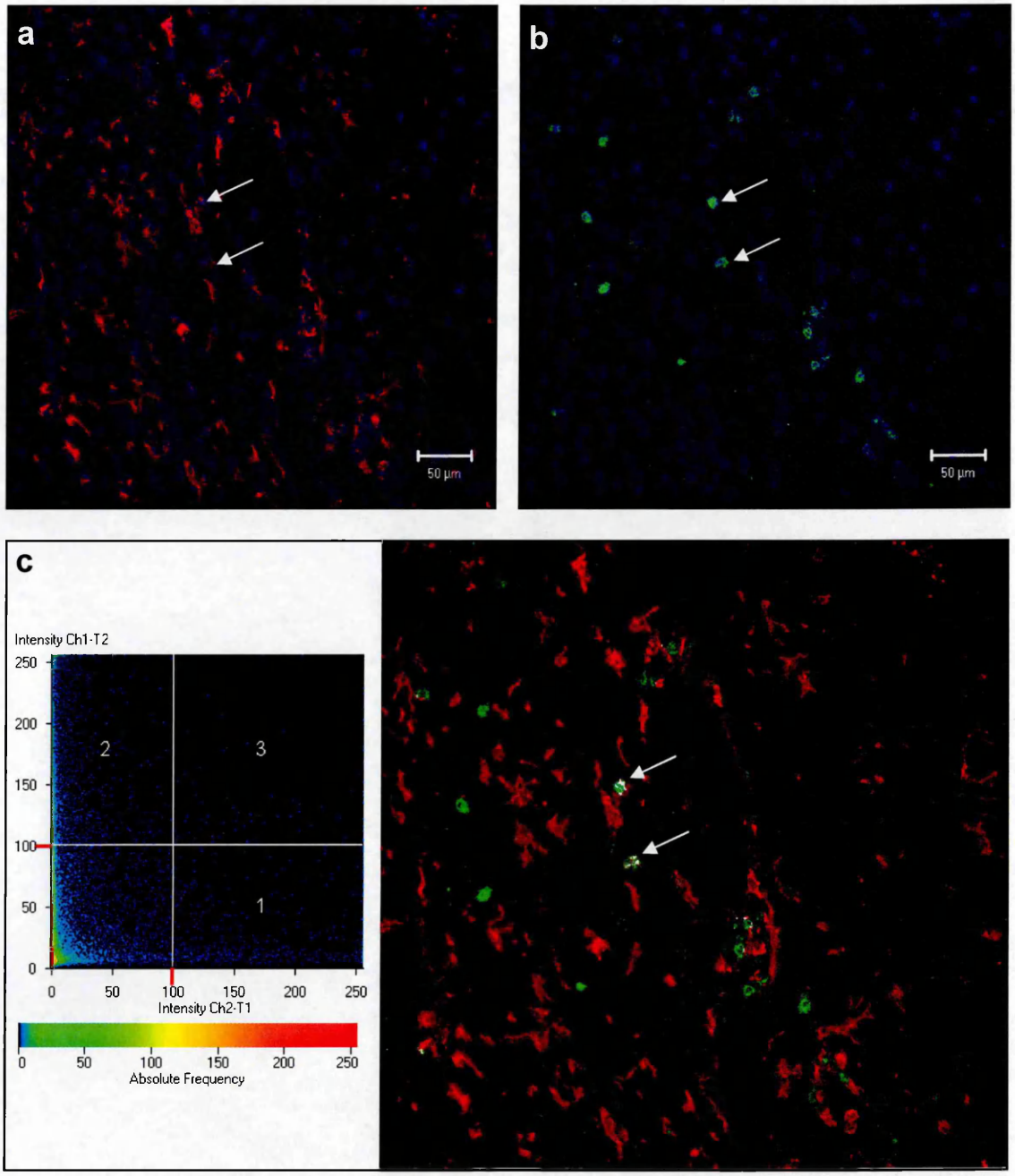

Figure 4.15 Dual-label immunofluorescence in MS brain (MS74 A1C6) of HLA-DR and CD26 in lesions with activated microglia/macrophages

Snap frozen, lesional tissue from an MS brain was fixed in acetone and dual-labelled for ***(a)*** *HLA-DR (red) and* ***(b)*** *CD26 (green) expression, using Alexa 568, and 488, fluorescent antibodies, respectively. Nuclei were counterstained with DAPI and appear blue. Areas of colocalisation of HLA-DR and CD26 were identified by the presence of pixels in quadrant 3 of the intensity grid in* ***(c),*** *and appear as white areas on the image. Arrows indicate colocalisation of HLA-DR and CD26 by a minority of cells. CD26+ cells are less abundant.*

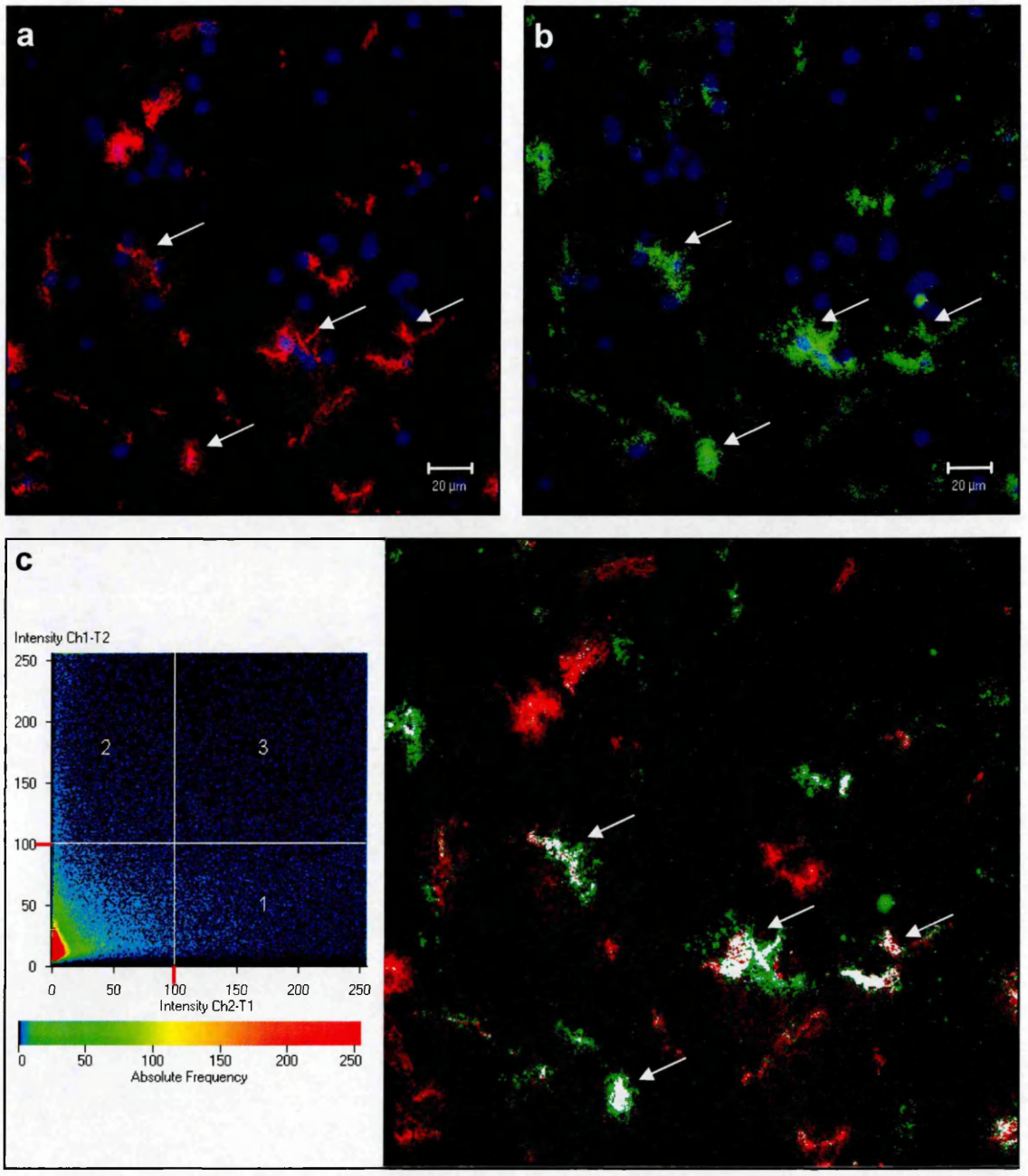

Figure 4.16 Dual-label immunofluorescence of HLA-DR and CD26 distant from blood vessels in MS lesions (MS74 A1C6)

Snap frozen, lesional tissue from an MS brain was fixed in acetone and dual-labelled for ***(a)*** *HLA-DR (red) and* ***(b)*** *CD26 (green) expression, using Alexa 568, and 488, fluorescent antibodies, respectively. Nuclei were counterstained with DAPI and appear blue. Areas of colocalisation of HLA-DR and CD26 were identified by the presence of pixels in quadrant 3 of the intensity grid in* ***(c),*** *and appear as white areas on the image. Arrows indicate significant colocalisation of HLA-DR and CD26 in the parenchyma, on cells with a macrophage/microglial cell morphology.*

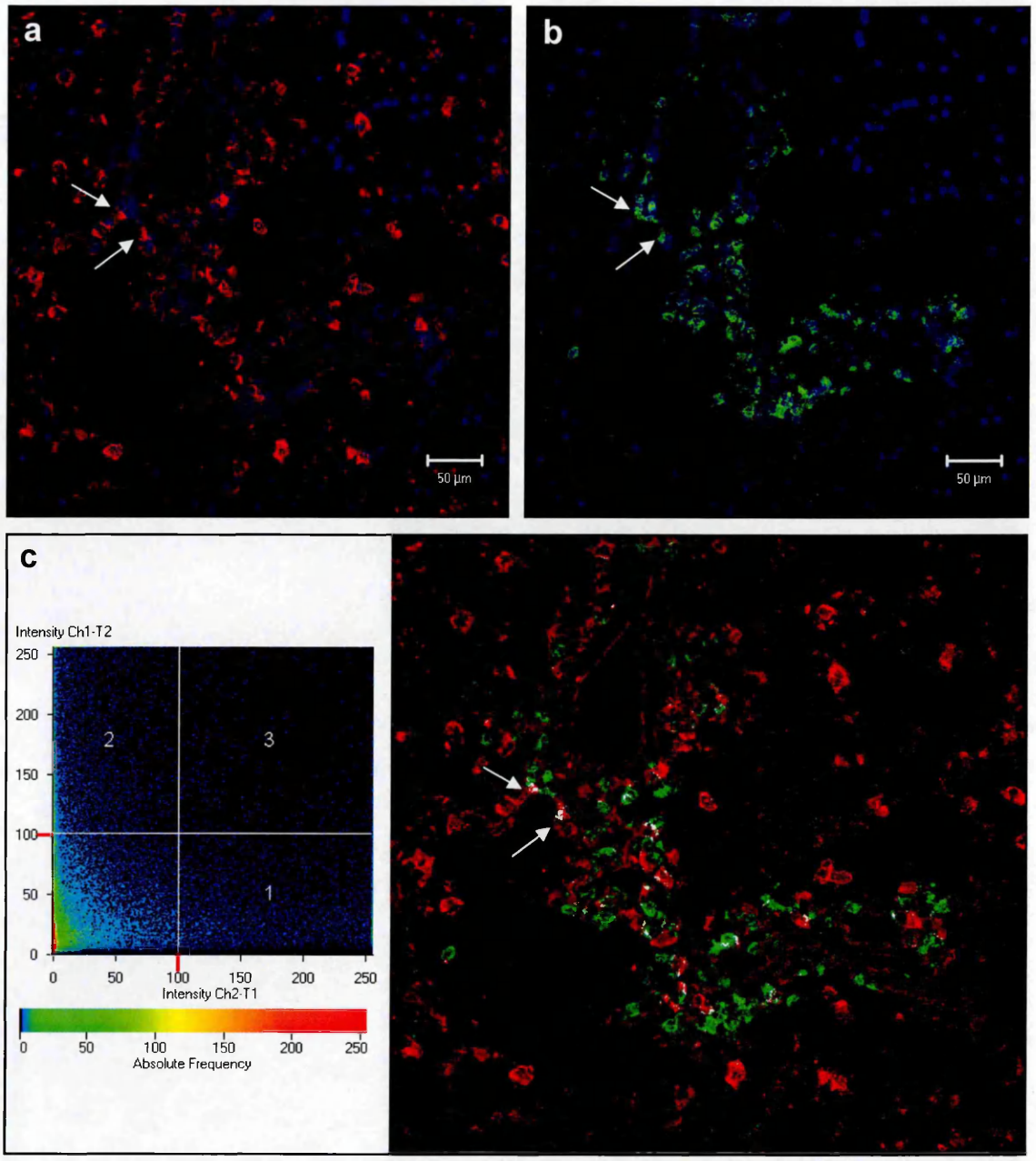

Figure 4.17 Dual-label immunofluorescence of HLA-DR and CD26 in MS brain (MS90 P2E3)

Snap frozen, lesional tissue from an MS brain was fixed in acetone and dual-labelled for ***(a)*** *HLA-DR (red) and* ***(b)*** *CD26 (green) expression, using Alexa 568, and 488, fluorescent antibodies, respectively. Nuclei were counterstained with DAPI and appear blue. Areas of colocalisation of HLA-DR and CD26 were identified by the presence of pixels in quadrant 3 of the intensity grid in* ***(c),*** *and appear as white areas on the image. Arrows show a minority of cells with colocalisation of HLA-DR and CD26. CD26+ cells are less diffusely spread.*

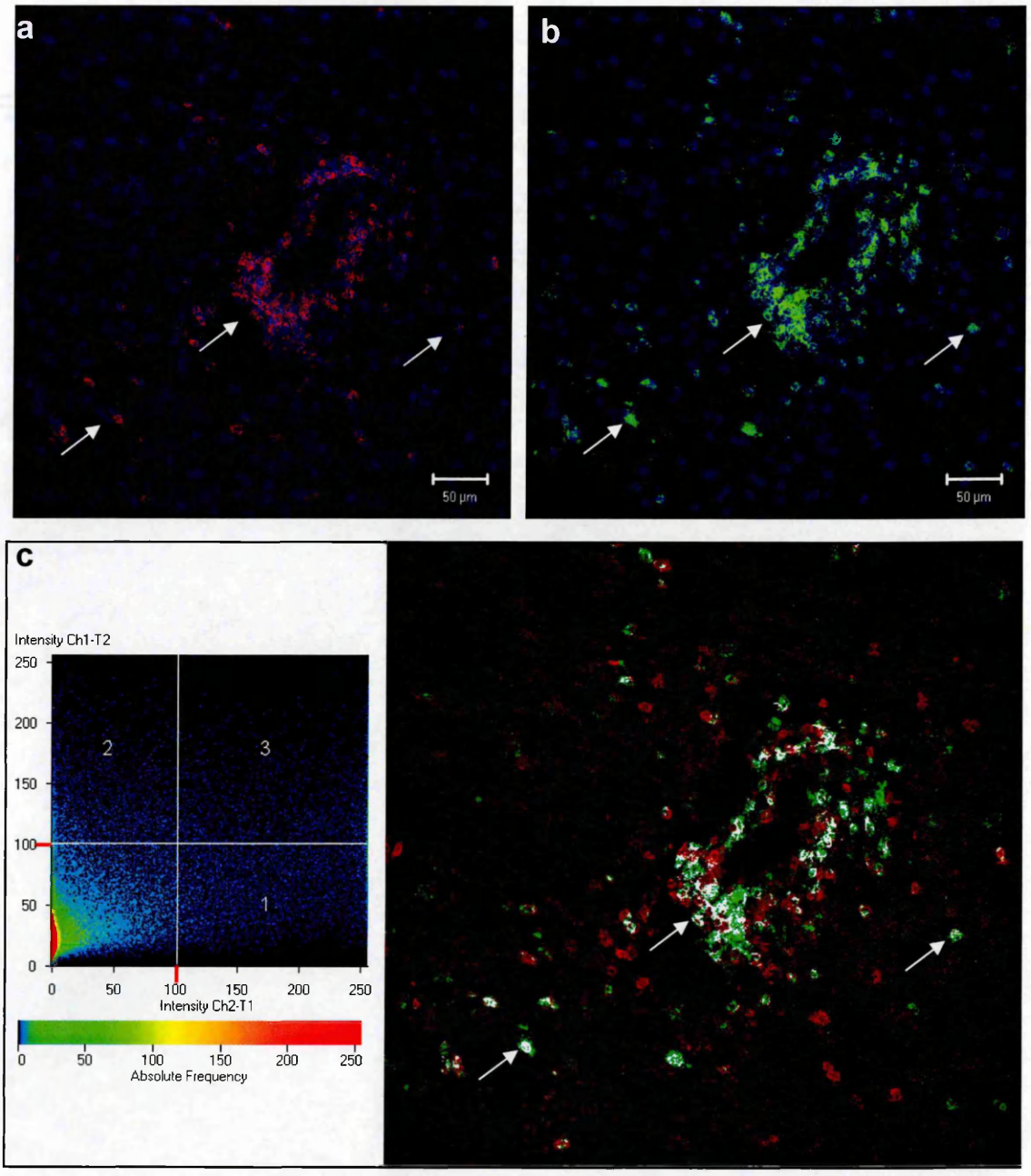

Figure 4.18 Dual-label immunofluorescence of CD3 and CD26 in MS brain (MS90 P2E3)

Snap frozen, lesional tissue from an MS brain was fixed in acetone and dual-labelled for ***(a)*** *CD3 (red) and* ***(b)*** *CD26 (green) expression, using Alexa 568, and 488, fluorescent antibodies, respectively. Nuclei were counterstained with DAPI and appear blue. Areas of colocalisation of CD3 and CD26 were identified by the presence of pixels in quadrant 3 of the intensity grid in* ***(c),*** *and appear as white areas on the image. Arrows indicate that colocalisation of CD3 and CD26 occurs with many, but not all, T cells, both around the blood vessel, and distant from it.*

Figure 4.19 ORO of lesion edge, and dual-label immunofluorescence of CD26 and GFAP, HLA-DR, or CD3, in a blood vessel in MS lesions (MS90 P2E3)

Snap frozen, lesional tissue from an MS brain was fixed in acetone and dual-labelled for CD26 (green) and GFAP, HLA-DR, or CD3 (red) expression, using Alexa 488, and 568, fluorescent antibodies. Images of the same blood vessel near the lesion edge were obtained using serial 10μm sections for ORO staining (nuclei counterstained with 20% Harris's haematoxylin), and each dual-label antibody combination ***(a)*** *ORO staining; arrows indicate the lesion edge (100X),* ***(b)*** *CD26 + GFAP,* ***(c)*** *CD26,* ***(d)*** *CD26 + HLA-DR, showing a staining pattern consistent with foamy macrophage morphology,* ***(e)*** *CD3,* ***(f)*** *CD26 + CD3. Nuclei (in b-e) were counterstained with DAPI (blue). Areas of colocalisation of CD3 + CD26 (f) were identified by the presence of white pixels on the image, obtained using LSM510 software. Arrows indicate significant colocalisation of CD26 and CD3 associated with the cells around the blood vessel, but not in the parenchyma. No colocalisation of CD26 and GFAP, or CD26 and HLA-DR, was evident.*

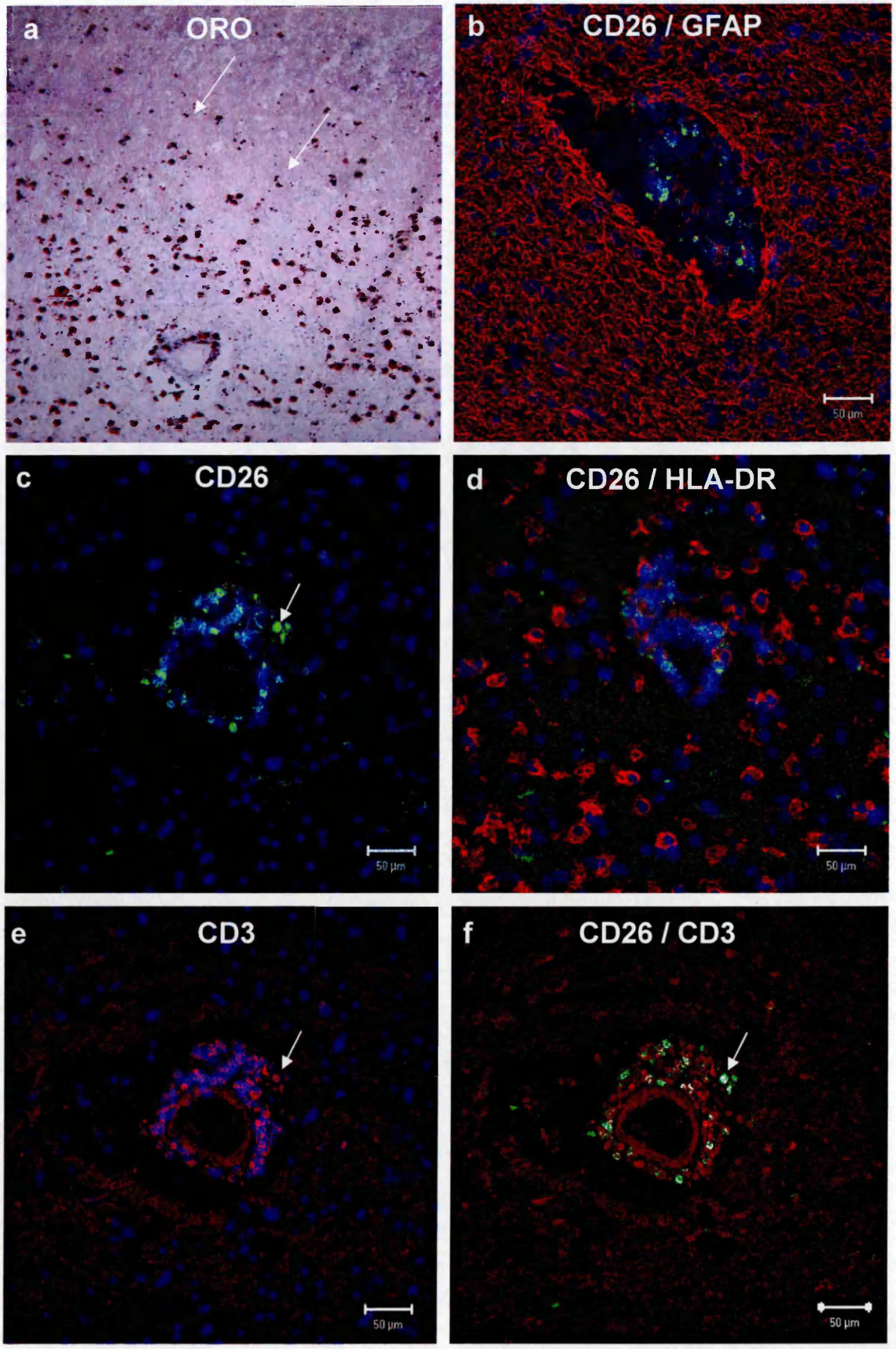
a
ORO
b
CD26 / GFAP
50 µm
c
CD26
50 µm
d
CD26 / HLA-DR
50 µm
e
CD3
50 µm
f
CD26 / CD3
50 µm

Figure 4.20 Dual-label immunofluorescence of CD26 and VWF, CD3, or HLA-DR, in a grade 4+ perivascular cuff in MS lesions (MS130 P2F4)

Snap frozen, lesional tissue from an MS brain was fixed in acetone and dual-labelled for CD26 (green) and VWF, CD3, or HLA-DR (red) expression, using Alexa 488, and 568, fluorescent antibodies. Images of the same PVC were obtained using serial 10μm sections for each dual-label antibody combination ***(a)*** *CD26* ***(b)*** *CD26 + VWF, with nuclei counterstained with DAPI (blue),* ***(c)*** *CD3,* ***(d)*** *CD26 + CD3,* ***(e)*** *HLA-DR,* ***(f)*** *CD26 + HLA-DR. Areas of colocalisation of CD3 + CD26 (d), and HLA-DR + CD26 (f), were identified by the presence of white pixels on the image, obtained using LSM510 software. Arrows indicate significant colocalisation of CD26 and CD3 throughout the PVC, and to a lesser extent, colocalisation of CD26 and HLA-DR. No colocalisation of CD26 and VWF was evident.*

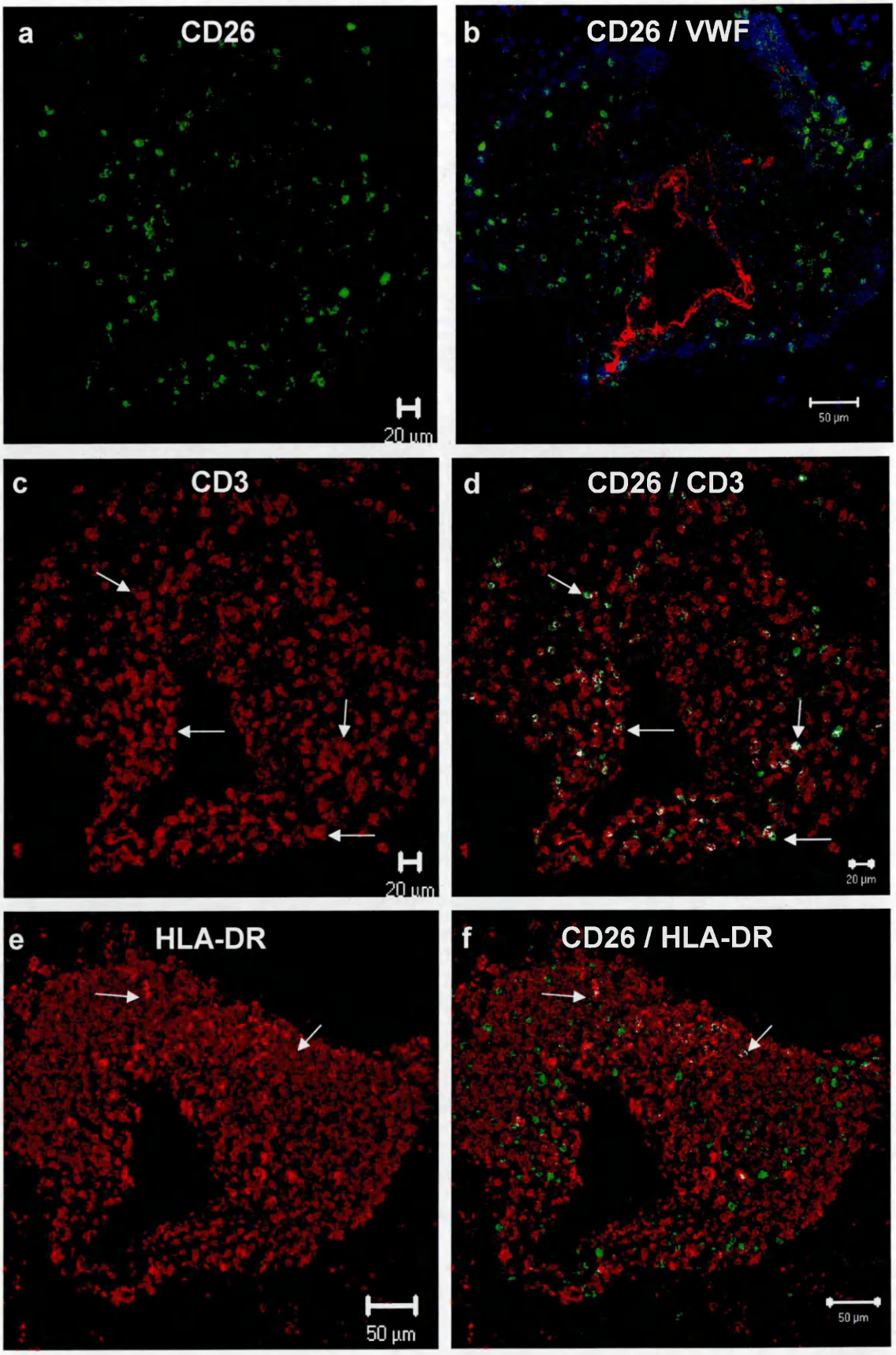
a
CD26
20 µm
b
CD26 / VWF
50 µm
c
CD3
20 µm
d
CD26 / CD3
20 µm
e
HLA-DR
50 µm
f
CD26 / HLA-DR
50 µm

4.5 Discussion

CD26 is a multifunctional molecule, that is implicated in the pathology of MS, as aside from its enzymatic activity which cleaves chemokines, it exhibits several relevant properties linked to autoimmunity, as it is known to have co-stimulatory effects on T cells, and function as a receptor for some ECM proteins (Iwata and Moromoto, 1999). The discovery of a high expression of CD26 on activated T cells led to increased interest in targeting this ectopeptidase immunopharmacologically, for treatment of a number of autoimmune diseases. Indeed, CD26 inhibitors tested *in vitro* on human PBMCs reduced T cell activation and function (Reinhold *et al.*, 2006). Inhibition of CD26 suppressed T-cell proliferation *in vitro*, suppressed production of IL-2, IL-10, and IFN-γ, whilst increasing TGF-β1 levels, and decreased antibody production in mice immunised with BSA (Kubota *et al.*, 1992). Following organ transplantation, inhibition of the enzymatic activity of CD26 is thought to diminish early humoral responses to alloantigens (Korom *et al.*, 1999). Collectively, the effects of CD26 inhibition strongly indicate a role for CD26 in immune regulation.

The expression of CD26 on the surface of immune cells is regulated by their differentiation and activation states, with induction upon stimulation (Bauvois *et al.*, 1999). Activated B cells and NK cells express CD26, and a small population of resting T cells, with specific characteristics, express a high surface density of CD26 ($CD26^{bright}$ T cells). These $CD26^{bright}$ T cells are memory ($CD45R0^{+}$) T cells responsible for most IL-2 production, with important roles in the proliferative response to antigens and CTL activity against antigens present in different allelic forms depending on the individual (alloantigens) (Morimoto and Schlossman 1998). $CD26^{bright}$ T cells are also responsible for the helper function of recruiting T-cell assistance for B-cell antibody synthesis. Th1-type cells are associated with CD26 expression (Cordero *et al.*, 1997).

Substrates of CD26 include an abundance of cytokines, haematopoietic growth factors, neuropeptides, and hormones, which possess either a proline or alanine as the penultimate amino acid at the N-terminus, with the proline conferring protection against non-specific proteolysis (Van Hoof *et al.*, 1995). Synthetic N-terminal oligopeptides of IL-1α, IL-1β, and IL-2 are cleaved by CD26, unlike their intact and mature counterparts, which led to suggestions that only small molecules are natural substrates for CD26 (Hoffmann *et al.*, 1993). It is known, however, that peptides of at least 40 amino acids can be processed *in vivo* by CD26 (De Meester *et al.*, 2003).

The precise cellular mechanisms involved in the formation of demyelinating plaques in MS remain largely unknown. Little is also known about the changes that occur in pre-plaque tissue, considered the NAWM, which could lead on to lesion formation in MS. Myelin-reactive Th1 cells express CD26 at high levels, and when CD26 inhibitors are used, their activity and Th1 cytokine production are blocked (Reinhold *et al.*, 1998). EAE induction is also prevented by inhibition of CD26 (Steinbrecher *et al.*, 2001). It was thus considered important to examine the CD26 expression in the white matter of MS brain, particularly as this has not been previously investigated.

Several studies on CD26 expression in MS have focused on PBMCs in the circulation and CSF. Constantinescu and colleagues (1995) conducted a 12 month study, measuring T cell activation molecules in peripheral blood, and their correlation with disease progression in 14 patients with chronic MS. They found that CD26 showed consistent patterns of expression, was elevated in MS, and unlike HLA-DR expression, correlated significantly with patients' disability scores. The increase in CD26 compared to controls was not statistically significant, however, and many inconsistencies exist concerning the expression of this marker when examining results from other studies.

No increase in CD26 in peripheral blood in MS patients, or correlation with disease activity, was found in one study (Chapel *et al.*, 1990), and another research group also failed to find an increase in $CD26^+$ cells in MS (Crockard *et al.*, 1988). Hafler and colleagues (1985), however, detected increased CD26 levels on T cells in peripheral blood, in the majority of their 35 patients studied. In a study of 40 MS patients, a correlation was observed between the increased CD26 expression by peripheral $CD4^+$ T cells, and clinical and MRI activity (Khoury *et al.*, 2000). A more recent study of 44 patients with clinically isolated syndromes, which is frequently the first manifestation of MS, found elevated levels of peripheral $CD4^+CD26^+$ T cells which correlated with MRI disease activity (Jensen *et al.*, 2004).

The soluble form of CD26 is normally found at low levels in CSF, moderate levels in plasma, and high levels in seminal fluid (De Meester *et al.*, 2000). In MS, increased CD26 expression on PBMCs from CSF has been found compared to both non-neurological controls and patients with other inflammatory neurological diseases (Hafler *et al.*, 1985). During T cell activation, different isoforms of CD26 are found, which might result from its ability to engage in a cycle of endocytosis/exocytosis, with glycosylation changes resulting from re-entry into the Golgi apparatus (Kahne *et al.*, 1996). Inconclusive results from the aforementioned investigations of peripheral blood CD26 levels might reflect wide genetic variation of CD26 expression, inclusion of

patients in remission, or use of an antibody reactive with a CD26 isoform not expressed at high levels, which emphasises the need for examination of more MS cases in our study before firm conclusions can be drawn.

It would be interesting to discover if an increased proportion of a subpopulation of T cells are $CD26^+$. In patients with AIDS, for example, there is a decrease in CD26 expression, with a selective loss of $CD4^+CD26^+$ cells (Blazquez *et al.*, 1992). Our dual immunofluorescent staining results on MS lesions certainly show that not all T cells are $CD26^+$. Consistently in MS, $CD8^+$ suppressor/cytotoxic T cells are reduced, or there is an increase in the $CD4^+/CD8^+$ ratio, and a loss of the $CD4^+$ $CD45R^+$ subset (Constantinescu *et al.*, 1995). The $CD45R0^+$ cells are antigen-experienced memory $CD4^+$ T-cells, whereas the naive equivalent $CD4^+$ helper T-cells are $CD45R0^-$, and positive for L-selectin (Krakauer *et al.*, 2006). $CD45R0^+$ cells can be further divided according to their homing location, with central memory cells homing to secondary lymphoid organs, or effector memory cells, which traffic to inflammatory sites (Sallusto *et al.*, 2004). A study of 15 patients with RRMS revealed a subset of $CD4^+$ $CD45R0^+$ $CD26^{bright}$ memory T cells, whose numbers correlated with disease severity, and which exhibited high levels of markers of Th1 effector functions, activation, and migratory potential (determined by expression levels of: CCR5; CXCR3; CXCR6; L-selectin; VLA-4; Fas ligand, which can induce apoptosis in T cells; and the receptor for IL-12, crucial for the development of Th1 cells) (Krakauer *et al.*, 2006). This subset, therefore, had enhanced expression of markers previously linked to MS disease activity, as it is known that expression of CCR5 (Misu *et al.*, 2001) and CXCR3 (Mahad *et al.*, 2003) by $CD4^+$ Th1 cells is elevated in peripheral blood. $CD4^+$ Th1 cells from MS patients during relapse express high levels of the adhesion molecule VLA-4, which is important in transmigration, and the target of the drug natalizumab (Barrau *et al.*, 2000). Interestingly, high-dose treatment of another drug used in MS, methylprednisolone, produces a decrease in CD26 expression on $CD4^+$ cells (Sellebjerg *et al.*, 2000).

CD26 is implicated in immune deficiency syndromes, such as severe combined immunodeficiency (SCID), involving a deficit of the enzyme adenosine deaminase (ADA). ADA is possibly involved in the initial stages of T cell activation, and is important in cellular and humoral immunity (Iwata and Morimoto, 1999). On the surface of T cells, expressed CD26 is known to form complexes with ADA, thereby preserving the enzymatic activity of both molecules, which is thus reduced when CD26 is under-expressed (De Meester *et al.*, 1999). It is conceivable, therefore, that the opposite situation of increased immune activity, as is seen in MS, could be associated with greater T cell activation due to higher levels of CD26 (Constantinescu *et al.*, 1995).

Using dual immunofluorescent staining, we found that CD26 was present in control and MS brain tissue, and was often associated with cells that expressed either CD3 or HLA-DR. No significant colocalisation of CD26 with GFAP or VWF was observed, indicating astrocytes and endothelial cells do not show significant CD26 expression in the white matter examined. The anti-CD26 antibody also stained areas associated with the BM, which is consistent with previous findings of connective tissue staining (Seitzer *et al.*, 1998). This staining was diminished in MS lesions, compared to control, indicative of the enzymatic activity that occurs as part of the breakdown of the BBB.

The high expression level of HLA-DR seen in white matter of MS brains compared to control brain, is consistent with the findings of previous studies, which reported the presence of activated macrophages/microglia throughout the white matter of all cases examined (Graumann *et al.*, 2003; Woodroofe *et al.*, 1986). This suggests that macrophage/microglial activity is common in MS brain, and may be a precursor to lesion formation. Previous findings have identified cells that co-express HLA-DR and CD26 as mature macrophages (Watkins *et al.*, 1996) and monocytes (Ellingsen *et al.*, 2007). Based on morphological examination, our results indicate that a proportion of monocytes in PVCs, and macrophages or microglia in the parenchyma, stained positive for both HLA-DR and CD26.

Active phases of autoimmune diseases are associated with higher numbers of $CD26^{bright}$ T cells and/or CD26 density, with corresponding decreases during immunosuppression. Results reported here are consistent with previous findings of the presence of high numbers of $CD26^{+}$ cells at sites of inflammation, and of significance to this study is that $CD26^{bright}$ T cells have a high transendothelial migration capacity (Mizokami *et al.*, 1996). High levels of $CD26^{+}$ cells in, and around, PVCs in MS tissue shown in this study are likely to play a crucial role in the regulation of local immune responses due to the rapid and specific enzyme activity of CD26, shown in data from Chapter 2. In chronic active MS lesions, CCL2 staining has predominantly been localised to the inner rim of the edge, adjacent to the hypercellular leading edge (Van der Voorn *et al.*, 1999), and within hypertrophic astrocytes, adjacent to chronic active lesions (McManus et al., 1998). Binding experiments using isolated human brain microvessels led to reports of binding sites for CCL2 on the parenchymal surface of brain microvessels (Andjelkovic *et al.*, 1999), which corresponds to an area where this current study identified CD26 expression in both control brain and MS lesions. Thus, CCL2 and CD26 are highly likely to be expressed within the same microenvironment, offering great scope for CCL2 regulation via cleavage. Similarly, in post-mortem brain tissue, CXCL10 is expressed within areas of demyelination, particularly around blood

vessels, and by hypertrophic astrocytes at the edge of active MS lesions (Sorensen *et al.*, 2002b). This CXCL10 expression pattern overlaps with results reported here for CD26 expression, which strongly suggests CXCL10 cleavage by CD26 could occur *in vivo* in MS, due to the rapid truncation detected in Chapter 2.

It has been suggested that the ability of $CD26^+$ cells to migrate across endothelium to inflammatory sites might be due to the known coexpression of CD26 with CCR5 and leukocyte function-associated (LFA-1) (Sallusto *et al.*, 1998), which could be investigated in further immunofluorescent studies. CD26 is known to interact with fibronectin and collagen of the ECM (De Meester *et al.*, 1999). The role of CD26 in cell adhesion is unclear, but via its ligation with fibronectin on the surface of breast cancer cells, it has been shown to act as an adhesion receptor on rat lung capillary endothelia for metastasising tumour cells (Cheng *et al.*, 1998). High expression of CD26 in MS may be of pathological significance due to its ability to bind to fibronectin, thereby mediating adhesion of $CD26^+$ T cells to the basal lamina. CD26 also plays a role in promoting MMP2 activity, thereby facilitating degradation of collagen and gelatin, and the ensuing passage across the BBB (Kumagai *et al.*, 2005). This could help to explain the reduction in what appeared to be connective tissue staining, which was observed in MS lesions in our study.

It is possible that in MS, increased CD26 expression by immune cells is first linked to systemic activation of Th1 cells, including myelin-reactive T-cells, which then cross the BBB in significant numbers. Passage into the CNS may be assisted by increased adhesion due to the CD26 expressed by immune cells binding to fibronectin, and also by enhancement via CD26 of the ability of MMP2 to degrade the BBB. Once inside the CNS, cleavage of chemokines by CD26 may cause either further inflammation, by enhancing chemotactic potential, or reduce immune cell infiltration by diminishing or destroying the functional activity of chemokines. CD26 has also been shown to inhibit mobilisation and attachment of fibroblasts to components of the ECM, thereby interfering with the healing process after inflammation (Kumagai *et al.*, 2005). Despite the confusion surrounding the precise effects of CD26, it is clear that CD26 is a multifunctional molecule that is very likely to play a pathological role in the progression of MS, and future studies on its expression in human brain, and the effect on activity of its chemokine substrates, should yield interesting results.

4.6 Summary

CD26 is a multifunctional glycoprotein that can truncate a number of substrates within the CNS, with implications for the immune, nervous, and endocrine systems of the body. Expression of CD26, particularly by peripheral blood T cells, has been linked to disease activity in MS. We have identified CD26 expression in human control brain and in MS lesions. In control brain, CD26 staining was principally associated with the BM region of blood vessels, and occasional T cells performing surveillance. In MS lesions showing predominantly demyelination, CD26 staining was increased and principally associated with cells in the parenchyma that expressed HLA-DR, and a subset of T cells in PVCs. In MS lesions with extensive inflammation, CD26 was further increased, and most commonly associated with T cells both in the parenchyma and in PVCs, but BM staining was reduced. Some dual staining of CD26 and HLA-DR was also observed in inflammatory lesions, predominantly in the parenchyma.

Chapter 5

In vitro chemokine-induced cell migration to intact and cleaved CCL2 and CXCL10

5.1 Introduction

5.1.1 Cell rolling, adhesion and extravasation

PBMC migration into tissues involves a series of events, starting with selectin-mediated cell rolling on the endothelium, followed by firm adhesion and arrest mediated by leukocyte integrins, and culminating in extravasation via rearrangements of cell-cell contacts, and chemotaxis up a chemokine gradient (Butcher and Picker, 1996). Selectins mediate both the capture of free-flowing PBMCs and their rolling activity along the endothelium (Bianchi *et al.*, 1997). Selectin bonds are unique in that their strength increases up to a point under pulling forces, thereby locking when blood flows over the cell (Fujiwara and Hamaoka, 2001).

Chemokines bound to the endothelium via interactions with GAGs interact with receptors expressed on leukocytes, leading to activation of leukocyte integrins and the cell then becomes firmly adhered, and arrests (Sperandio *et al.*, 2006). Leukocyte transmigration into tissue follows this cell arrest, mediated by additional adhesion and signalling molecules (Fig. 5.1) (Muller, 2003). Small GTPases, such as RhoA and Rac1, are proteins which bind GTP, and are implicated in the process of transmigration. RhoA regulates adhesion receptor function in response to chemokine activation, and Rac1 induces cytoskeletal changes resulting in lamellipodia formation during extravasation, as well as activating phosphoinositide 3-kinase (PI3K), involved in cell motility regulation (Bianchi *et al.*, 1997). It has been suggested that leukocyte binding promotes signals in ECs that encourage opening of EC contacts and junctions, facilitating leukocyte passage (Vestweber, 2000). A transcellular route for leukocyte migration across the BBB has also been proposed, via membrane invagination and transcellular pore formation (Greenwood *et al.*, 2002).

Protease-mediated digestion of junctional proteins is not considered essential for transmigration, as protease inhibitors do not prevent it, but proteases from ECs and stromal cells are often involved, nonetheless (Wolf *et al.*, 2003). Indeed, engagement of $\alpha_1\beta_1$ integrin on T-cells with VCAM-1 on ECs, induces transcriptional regulation of MMP2 (Bianchi *et al.*, 1997). Inflammatory microenvironments often result in substances such as thrombin being produced, that can destabilise junctions between cells by their action on the EC cytoskeleton, thereby creating intercellular gaps that facilitate transmigration (Chapman, 2006). Chemokines contribute to the process of cell adhesion, prior to their role in migration, through their activation of integrin adhesiveness via their solid-phase immobilisation on the EC surface (Vestweber, 2002).

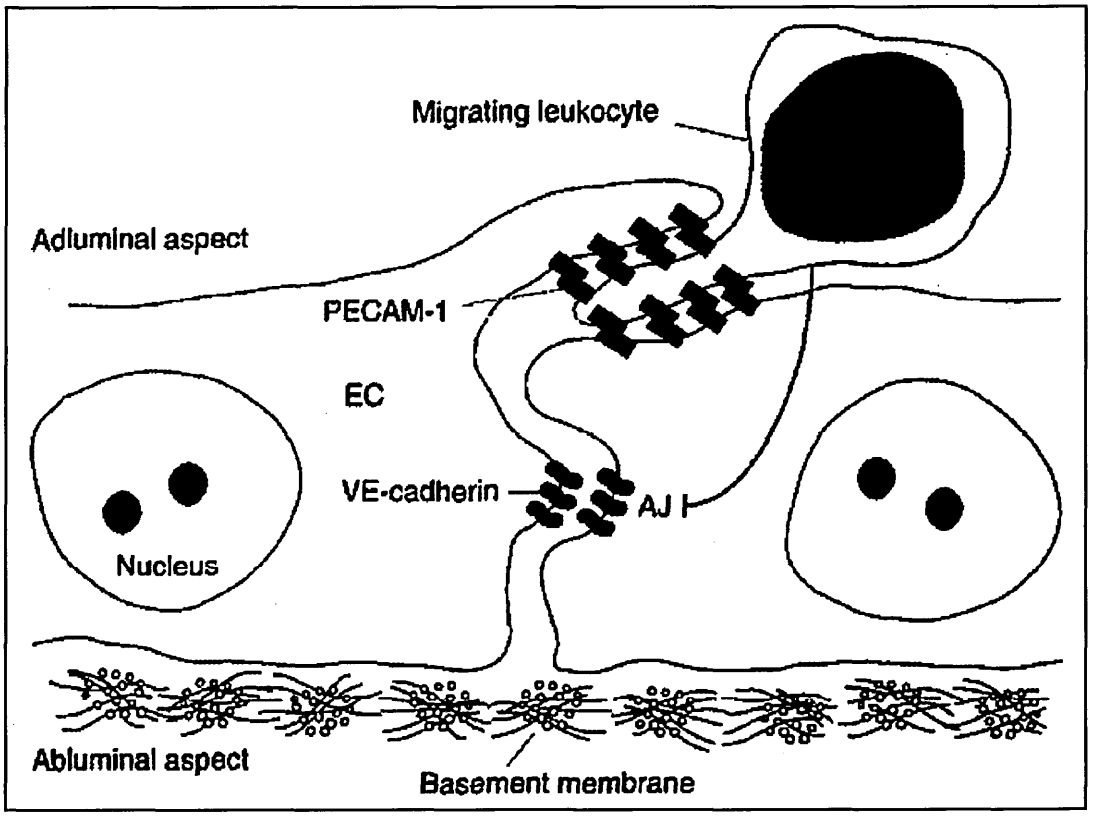

Reprinted from (Bianchi *et al.*, 1997), © (1997), with permission from Elsevier

Figure 5.1 Transendothelial cell migration

Leukocytes and endothelial cells (ECs) express platelet/endothelial cell adhesion molecule-1 (PECAM-1), mainly in interdigitating EC projections near to the lumen, which is implicated in the early stages of cell transmigration. A 'molecular zipper' arrangement of PECAM-1 molecules may facilitate leukocyte progression through the junction between ECs, by helping to effectively pull them towards the BM. Leukocytes bound to ECs can promote disassembly of adherens junctions (AJ), thus assisting with separation of ECs to allow passage. Vascular endothelial (VE)-cadherin is the main transmembrane protein of AJs, which interacts with identical molecules on opposing cells.

5.1.2 Mechanisms of cell migration

Recruitment of PBMCs to sites of inflammation requires directional migration in a chemotactic gradient via a complex process of adhesion, cytoskeletal rearrangements, movement and detachment. Actin polymerisation within the cell drives its movement forward (Wells, 2003). Chemotactic agents trigger cells to polarise into a forward moving leading edge, and a retracting rear portion. Polarisation of a cell involves atypical protein kinase C (aPKC), partitioning defective (PAR) proteins, and production at the leading edge of phosphatidylinositol triphosphate (PIP3) via the action of PI3K (Vicente-Manzanares *et al.*, 2005). In many cell types, cellular architecture is reorganised, such as positioning of the nucleus behind the microtubules, microtubule organising centre, and the Golgi apparatus. Polarisation is maintained by feedback loops involving PI3K, microtubules, Rho GTPases, integrins, and vesicular transport (Gomes *et al.*, 2005).

Several integrated processes converge at the leading edge of a migrating leukocyte, with receptors for adhesion molecules, proteases, and chemokines establishing various associations with one another. Transient interactions between adhesion receptors and membrane proteases or their receptors, for example, are involved in directed migration where the subendothelial matrix is loosened or digested. The invasion of leukocytes through the interstitial matrix and across an extravascular space is co-ordinated by adhesion-dependent upregulation of proteases and their receptors, with a carefully regulated balance between adhesive and proteolytic activity being essential for migration (Bianchi *et al.*, 1997).

In the cytoplasm of a cell, actin filaments are fast-growing at one end, and slow-growing at the other, which facilitates the production of cellular protrusions. Protrusions can take the form of spike-like filopodia used to explore the environment, or broad lamellipodia, which provide a foundation for forward motion (Pollard and Borisy, 2003). The actin-related proteins (Arp)-2/3 complex is involved in the induction of new actin filaments in lamellipodia (Weaver *et al.*, 2003).

Traction is required if a cell is to move forward, which is achieved by attachment of protrusions to the surroundings via integrins. Tractional force is created by the interactions of actin filaments, linked via adaptor proteins to integrins at adhesion sites, with the contractile properties of myosin II (Vicente-Manzanares *et al.*, 2005). Adhesion assembly and disassembly mechanisms are poorly understood, but it is known that forward motion requires precise regulation to enable assembly at the front, with simultaneous disassembly at the rear. Myosin II is essential for retraction of the back

end of the cell, and for development of sufficient tension to open calcium-channels and lead to activation of the protease calpain. Calpain cleaves integrins and other adhesion proteins, and the release of rear adhesions then provides positive feedback for the migration cycle (Franco *et al.*, 2004). The cellular morphology and style of movement exhibited during migration varies according to the cell type. Leukocytes show an amoeba-like morphology and movement, have few integrin clusters, and adhesions that allow rapid movement (Gunzer *et al.*, 2000).

5.1.3 Degradation of the extracellular matrix

In addition to movement, cells often engage in degradation of extracellular matrix (ECM) proteins to reach their destination (Patel *et al.*, 2001). Once past the EC barrier, the BM and connective tissue must be overcome (Fig. 5.1). MMPs play a key role in this, with T-cell migration, for example, being shown to be assisted across an *in vitro* BM by secretion of MMP2 and MMP9 (Bianchi *et al.*, 1997). Leukocytes not only secrete proteases that promote breakdown of the ECM, but also contribute to degradation by converting plasminogen to plasmin, via activation of urokinase-type plasminogen activator (uPA) (Bianchi *et al.*, 1997). The binding of uPA to its receptor, uPAR, catalyses the formation of plasmin, and initiates pericellular proteolysis and cell migration (Bruse *et al.*, 2005). Macrophages and activated leukocytes produce uPA, and also express uPAR, which increases their adhesion in culture (Ossowski and Aguirre-Ghiso, 2000). In a study by Gyetko and colleagues (1994), the localisation of uPARs at the leading migratory edge of human monocytes exposed to a chemotactic gradient, was required for chemotaxis. Interestingly, uPARs also have high affinity for integrins, and are thought to be regulators of integrin activity during leukocyte adhesion (Ossowski and Aguirre-Ghiso, 2000). Thus, uPARs play a role in cell-surface proteolysis, cell adhesion, and migration.

5.1.4 Chemotactic gradients

The roles of chemokines and their receptors in cell migration is discussed in 1.3. Chemotactic gradients can be very complex, as they arise from solid-phase, and soluble-phase, chemokines. Chemokines have diverse abilities to form solid-phase gradients *in situ* by binding to the ECM via interactions with GAGs, but this ability is restricted in the extravascular space (Patel *et al.*, 2001). When chemokines are immobilised on endothelial cells, unlike chemokines in solution, they can act to direct rolling leukocytes expressing the appropriate chemokine receptor to adhere to the endothelium, and are essential for firm adhesion (Vestweber, 2002). Activation of G-protein signals via GPCRs on tethered leukocytes, following brief contact with immobilised endothelial chemokines, leads to integrin clustering (Cinamon *et al.*, 2001).

Membrane-bound chemokines are, therefore, functionally different from their soluble counterparts. Chemotactic gradients, with important roles in extravasation of cells into tissue, are formed by both soluble and immobilised chemokines (Patel *et al.*, 2001). To be able to sense chemokine gradients and engage in directional cell migration, rapid receptor internalisation and redistribution is essential (Loetscher *et al.*, 1996).

Cytokines can have a dramatic effect on cellular chemokine production and chemotaxis, such as the rapid inhibition of CCR2 expression by monocytes when exposed to IFN-γ, rendering them less responsive to chemokines, and perhaps serving to retain monocytes at inflammatory sites and engage in feedback in regulating cell recruitment from blood (Penton-Rol *et al.*, 1998).

CCL2 is implicated in the arrest of rolling monocytes on endothelial cells expressing E-selectin, and this effect appears to be independent of chemotaxis (Gerszten *et al.*, 1999). CCL2 is also thought to be involved in the spreading and alterations in the shape of monocytes, attached to the endothelium under inflammatory and flow conditions, and subsequent transendothelial migration. As the shape change and migration were rarely seen under static conditions, it was suggested that a diffusible gradient of soluble CCL2 is required for these effects (Weber *et al.*, 1999). Endothelial cells activated with TNF have been shown to upregulate expression of both CXCL1 and CCL2, which bind to receptors CXCR2 and CCR2 respectively, expressed by monocytes. CCL2 was secreted as a soluble form, but CXCL1 was immobilised to the endothelium via interactions with proteoglycans, and thus contributed substantially to the firm adhesion of monocytes. The differential presentation of chemokines in either a solid-phase or soluble form may determine functional specialisations required for the sequential steps of monocyte migration (Weber *et al.*, 1999).

CCL2 is presented on the apical endothelial cell surface, focused into discrete regions by interactions with heparan sulphate. This apical chemokine presentation pattern is thought to provide a means for concentrating small quantities of chemokines produced by subendothelial tissues, thereby promoting activation and recruitment of leukocytes from the blood (Hardy *et al.*, 2004). Rapid, regulated secretion of chemokines from ECs is thought to occur via two distinct compartments. CXCL8, for example, has been observed in rod-like compartments called Weibel-Palade bodies (WPB), whereas CCL2 was mainly localised to small granules (distinct from WPB), throughout the EC cytoplasm. CXCL10 was not observed in either compartment, and was thus not considered to be stored for subsequent regulated secretion in ECs (Oynebraten *et al.*, 2004).

It is thought that CXCL10 recruits activated effector T cells under inflammatory conditions, and that CXCR3 is upregulated during effector T cell generation in secondary lymphoid tissues. IL-2 links acquisition of chemotactic capability with T cell expansion (Moser and Loetscher, 2001).

5.1.5 *In vitro* models of migration

Most *in vitro* migration has traditionally been performed using a Boyden chamber, i.e. a chamber composed of 2 compartments separated by a microporous membrane, with 3-8μm pore size. A chemotactic gradient develops across the membrane when a chemotactic agent is placed in the lower compartment, and cells in the upper compartment migrate through the membrane for a set incubation time. The membrane is fixed and stained, and the number of migrated cells counted (Boyden, 1962). Many modifications of this technique exist, and it has also been described as a trans-well, or filter membrane, migration assay.

Transendothelial chemotaxis is often studied using filters coated with ECM proteins, with an overlying EC monolayer. The EC monolayer can be pre-treated with inflammatory cytokines in an attempt to mimic inflamed vessels and induce adhesion (Roth *et al.*, 1995a). There is doubt, however, as to whether chemotactic gradients established *in vitro* mimic the endothelial chemokine distribution through which leukocytes would extravasate *in vivo* (Middleton *et al.*, 1997). A further problem with the application of Boyden chamber assays to study transendothelial migration is the time frame commonly used, as *in vivo* studies have suggested leukocyte extravasation in post capillary venules of inflamed tissue occurs in a few minutes, yet migration assays are commonly left for 1-4h before readings are taken (Roth *et al.*, 1995a). The prolonged time frame of an assay compared to the relatively short time of contact of PBMCs with the endothelium *in vivo* cannot give a true indication of the ability of adhered leukocytes to sense chemokine gradients, particularly as the shear forces of blood flow are missing (Cinamon and Alon, 2003). Shear forces are important as they may transfer strong pro-migratory signals to adherent leukocytes (Cinamon *et al.*, 2001). The use of an EC monolayer may slow and reduce transendothelial migration, as leukocytes that have traversed the monolayer may become trapped between ECs and the filter. In addition, once past the filter pores, lymphocytes have been observed to move along the lower side of the filter for a considerable time, before detachment into the lower chamber. It is also possible that ECs may form an additional layer on the underside of the filter, creating a further obstacle for migrating leukocytes (Mackarel *et al.*, 1999). The measurement of leukocytes collected from the lower chamber, therefore, is no guarantee of a true reflection of the entire transmigrated population, and the

migration rates are often lengthened compared to those observed for *in vivo* endothelial migration (Cinamon and Alon, 2003).

5.2 Aims and objectives

Truncated CCL2 and CXCL10 could be important regulators of cell trafficking across the BBB in MS, and may result from local exposure to MMP2, MMP9, or CD26 *in vivo*, which are localised at the BBB or on inflammatory cells migrating into the CNS. Thus, the main objectives of this chapter were to:

- Develop and optimise a quantitative method for measuring cell migration over time with minimal manipulation
- Separate cleaved CCL2 and CXCL10 from the enzymes responsible for their truncation in the digestion mixtures detailed in Chapter 2
- Assess migration of THP-1 cells to intact and cleaved CCL2
- Assess migration of Jurkat cells to intact and cleaved CXCL10
- Comparatively assess migration of PBMCs to intact and truncated CCL2 and CXCL10 in an *in vitro* assay

5.3 Materials and Methods

5.3.1 Cell culture of THP-1 monocytic cell line and Jurkat T cell line

THP-1 cells, a human monocytic leukaemia cell line derived from a 1 year old male, were obtained from ECACC, Wiltshire, UK. Cells were cultured at 37°C and 5% CO_2 in 75 cm^2 flasks in RPMI 1640 medium (Sigma) containing 2mM L-glutamine (Invitrogen), 10% v/v HI-FCS, 50U/ml penicillin, and 50µg/ml streptomycin. Stocks of THP-1 cells were maintained by freezing overnight at -80°C in 90% v/v HI-FCS with 10% v/v glycerol (Sigma), before being transferred to a dewar containing liquid nitrogen. When cells were thawed from a frozen cryovial, they were added to 5ml medium, centrifuged at 150*g* for 5min, the medium removed, and cells resuspended in medium as above, but with 20% v/v HI-FCS. The serum concentration was reduced to 10% v/v after 5-7 days.

5.3.2 Cell culture of Jurkat T cell line

Jurkat cells, a human lymphoblastic leukaemic T cell line, were obtained from ECACC. Cells were cultured in medium as described for THP-1 cells above, but were frozen down in medium containing 10% v/v DMSO. Jurkat cells were recovered from frozen storage using their standard culture medium.

5.3.3 Treatment of lymphocytes and Jurkat cells with IL-2 and phytohaemagglutinin

Treatment with IL-2 has previously been shown to increase the migratory capacity of human lymphocytes, and their ability to adhere to endothelial cells (Pankonin *et al.*, 1992). Phytohaemagglutinin (PHA) has also been shown to increase the rate of migration of human lymphocytes (Shiu and Schor, 1987), and activates T cells by binding to glycoproteins on the cell membrane (Kay, 1991). To enhance the migratory potential of lymphocytes derived from peripheral blood, they were thus cultured in THP-1 medium with 1µg/ml PHA (Sigma) and 20ng/ml IL-2 (R&D Systems) for 7 days. Jurkat cells were treated with 10ng/ml IL-2 for 6 days to assess the effects of short-term IL-2 treatment.

5.3.4 Separation of whole blood to obtain peripheral blood mononuclear cells

Whole blood (10ml) was obtained from healthy volunteers using venepuncture performed by qualified personnel, and processed within 2h. Blood was injected into glass tubes coated with K_2EDTA (BD Biosciences, Oxford, UK), and the tube inverted

8-10 times to mix the blood with the anticoagulant coating. An equal volume of PBS without calcium and magnesium was mixed with the whole blood in 15ml conical tubes.

The following procedure was performed in a HEPA-filtered class II laminar flow cabinet (Heraeus, Germany). Histopaque-1077 (Sigma) was brought to RT and 5ml placed in each of 4 x 15ml conical tubes. An equal volume (5ml) of the blood/PBS mixture was gently pipetted down the side of the conical tube onto the Histopaque-1077, and care was taken to avoid mixing the 2 liquids. Histopaque-1077 contains polysucrose and sodium diatrizoate, adjusted to a density of 1.077 ± 0.001 g/ml, and is designed to facilitate rapid recovery of viable mononuclear cells via density centrifugation. Tubes were centrifuged (with the brake off) at 400*g* for 30min at RT, during which time, erythrocytes and granulocytes sediment due to aggregation by polysucrose, leaving mononuclear cells at the plasma-Histopaque interface. After centrifugation, the upper plasma layer was carefully removed with a Pasteur pipette, to within 5mm of the opaque layer containing mononuclear cells. The opaque layer was transferred to a conical tube using a Pasteur pipette, mixed with 10ml PBS without calcium or magnesium, and centrifuged at 250*g* for 10min at RT. The supernatant was discarded, and the cell pellet resuspended in 5ml PBS without calcium or magnesium, and centrifuged at 250*g* for 10min at RT. This last centrifugation step was then repeated. The majority of platelets were removed by these 3 centrifugation steps.

5.3.5 Separation of lymphocytes and monocytes

The washed pellet of mononuclear cells obtained from 5.3.4 above, was resuspended in 7ml PBS with cations and transferred to a 100mm petri dish (Sarstedt, Leicester, UK). This was incubated at 37°C and 95% air/5% CO_2 for 1h to allow the monocytes to adhere to the plastic. The dish was rinsed three times with 5ml PBS, and these were pooled with the cell suspension, to collect lymphocytes. Monocytes were removed from the dish by adding PBS without cations, pre-cooled to 4°C, and employing a cell scraper (BD), if necessary. Cells were counted using a haemocytometer (Sigma) to ensure sufficient numbers were present for experimentation.

5.3.6 Cell viability determination by Trypan Blue exclusion

Trypan blue is an acid stain containing a negatively charged chromophore that only reacts with cells if the membrane is damaged (Green, 1990). Live cells do not take up the blue stain, whereas dead ones do. To test for cell viability, 10µl cell suspension was mixed with 10µl 0.4% Trypan Blue solution (Sigma), left to stand for 5min at RT, and then viable and non-viable cells counted using a haemocytometer. The number of

viable cells was then expressed as a percentage of the total number of cells counted. This procedure was repeated to ensure accuracy. Cells were tested for viability both before and after migration assays.

5.3.7 Flow cytometry to investigate cell phenotype and chemokine receptor expression

5.3.7.1 Principles of flow cytometry

Flow cytometry utilises measurements of the light-scattering ability, fluorescence, and absorbance of single cells as they flow past excitation sources in a liquid medium. These measurements are used for either quantitative analysis of a wide range of cellular characteristics, such as size, and levels of DNA, protein, and surface receptors, or for use in cell separation in a cell sorter (Rieseberg *et al.*, 2001).

Flow cytometers encompass 5 main operating units (Fig. 5.2b): a light source, typically a laser; a flow cell; optical filter units for detection of different wavelengths; a photodiode or photomultiplier tube for signal detection; and an operating and data processing unit. Cells in suspension individually pass the light source positioned orthoganally to the flow (Fig. 5.2a), and excitation light is scattered in forward and sideways directions by the presence of the cells. Forward-scattered light provides information about the size of the cell and is detected by the forward-scatter sensor (Fig. 5.2b). Sideways-scattered light is influenced by the granularity and morphology of the cell.

The use of specific fluorescent labelling facilitates the analysis of selective cell components. Direct labelling of cells with antibodies coupled to fluorophores enables detection of specific antigens by flow cytometry, and multiple lasers on one platform allow simultaneous analysis of several fluorophores with different emission spectra. Fluorescent light is processed through the PMT to the data processing unit (Rieseberg *et al.*, 2001). Scattering and fluorescence can be combined to allow observation of all subpopulations of cells. Commonly, dual parameter dot plots are used to represent flow cytometry data, and frequency histograms (Davey *et al.*, 1999).

Following separation of mononuclear cells from whole blood, as described in 5.3.4, flow cytometry was performed to investigate the proportion of cells that were monocytes or lymphocytes. The cell pellet obtained after the final rinse in 5.3.4 was resuspended in 3ml of PBS without cations, and 25µl used for each flow cytometry investigation.

Figure 5.2 Fluid dynamics and optics of a flow cytometer

(a) *Cells in suspension are focused into a single column by laminar flow and hydrodynamic forces, using sheath fluid. The diameter of the laminar streams of sheath fluid and sample are gradually restricted until a single file of cells is achieved.*

(b) *The flow cell described above allows introduction of cells into a flow cytometer, where they are interrogated by a laser, and the scattered light measured at a low angle (forward scatter or FSC), and also a high angle (side scatter, or SSC). These measurements provide information about the physical properties of a cell, with side scatter representing the internal complexity. If cells have been labelled with fluorescent markers, high angle light, or side scatter, also contains fluorescent emission from cells, which is separated into different wavelengths by dichroic mirrors and band filters, for measurement by multiple fluorescent detectors. Photons detected by a photomultiplier tube (PMT) and photodiodes are converted to analogue voltages in the photodetector. The analogue signal is later digitalised into numerical files, displayed on a computer screen. The sensitivity of the instrument can be altered by adjusting the gain (Tarrant, 2005).*

a

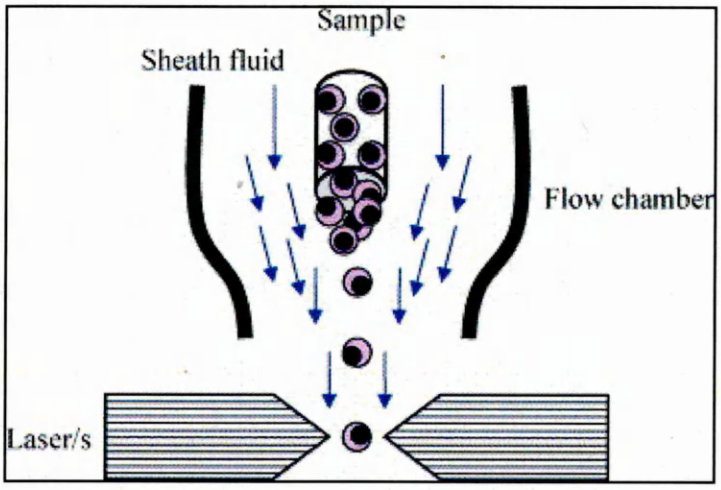

b

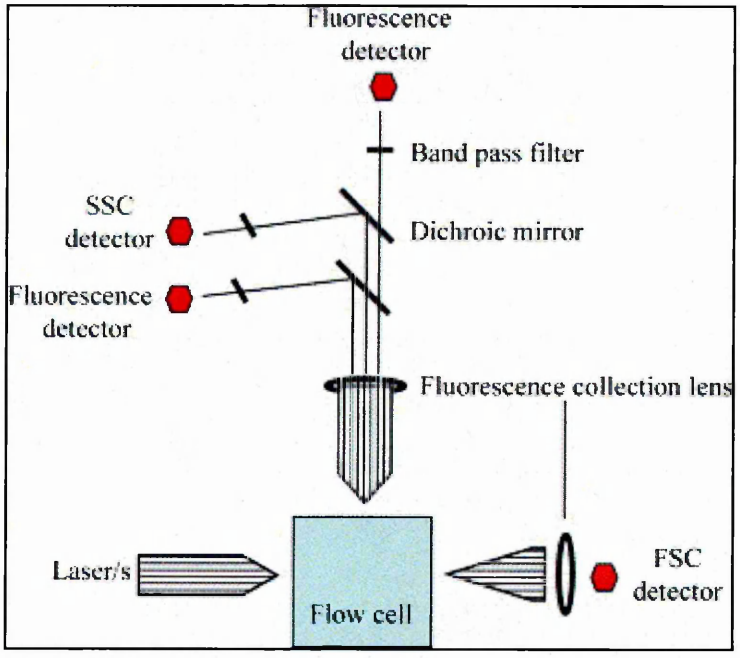

Reprinted from (Tarrant, 2005), © (2005), with permission from Elsevier

All antibodies and isotype controls used in flow cytometry were obtained from R & D Systems (UK).

5.3.7.2 Analysis of mononuclear cell populations by flow cytometry

Unlabelled cells were kept on ice with 10µl PBS, alongside cells incubated for 1.5h at 4°C in the dark with 10µl of either anti-$CD4^+$ or $CD8^+$ fluorescein-conjugated monoclonal antibody, anti-$CD14^+$ phycoerythrin-conjugated monoclonal antibody (to detect monocytes), or their respective isotype controls of mouse IgG2a or mouse IgG1. The samples then had 1ml PBS without cations added, and were centrifuged at 500*g* for 5min at 4°C. The supernatant was discarded, cells resuspended in 300µl PBS without cations, and analysed using a FACS Calibur flow cytometer (BD).

The flow cytometer was flushed through with distilled water, and the unlabelled cells were used for optimisation of the flow settings, assisted by altering the voltage and amplifier gain, to obtain the population of cells displayed in approximately the centre of the x-axis, and in the lower half of the y-axis. The isotype control samples served as negative controls and were run next. Instrument settings were optimised so that the histogram plot for the negative control was aligned to the left for the whole of its normal distribution curve (Fig. 5.5b). The cells labelled with anti-$CD4^+$, $CD8^+$, or $CD14^+$ antibodies were analysed last, and if sufficient antibody was bound to the selected cell antigen, the histogram plot appeared to the right of that of the isotype control. For each sample, a gate was drawn around the dot plot of the cells of interest, and 10,000 events within the gate were analysed by the flow cytometer. The percentages of cells positive for $CD4^+$, $CD8^+$, or $CD14^+$ expression were calculated by performing analysis with CellQuest software (BD) on an Apple Mac computer.

5.3.7.3 Analysis of THP-1 expression of CCR2 by flow cytometry

THP-1 cells were centrifuged at 200*g*, the medium removed, and the cell pellet resuspended in PBS without cations to give 1×10^7 cells per ml. Duplicate samples of 25µl of cell suspension were incubated for 1.5h in the dark at 4°C with 10µl of either anti-CCR2 phycoerythrin (PE)-conjugated monoclonal antibody, mouse PE-IgG2B isotype control, or PBS without cations. The samples were then washed and analysed by flow cytometry, as above (see 5.3.7.2).

5.3.7.4 Analysis of Jurkat expression of CXCR3 by flow cytometry

Jurkat cells were processed similarly to THP-1 cells above (see 5.3.7.3), using an anti-CXCR3 PE-conjugated monoclonal antibody, and a mouse PE-IgG1 isotype control.

5.3.8 Preparation of cleaved chemokines for use in migration assays

5.3.8.1 Separation of cleaved chemokine from enzyme following digestion

Mixtures of chemokine, enzyme, and assay buffer, obtained from the digestion detailed in 2.2.1.3, were passed through Microcon® centrifugal filter units (Millipore, UK) to separate the chemokine from the larger M_r enzymes. Microcons® have an ultrafiltration membrane composed of regenerated cellulose acetate that enables collection of proteins in solution below the nominal molecular weight limit (NMWL) of the membrane, and concentration of proteins above the NMWL. Membranes with a NMWL of 30, and 50 kDa, were assessed.

Mixtures of chemokines and enzymes from 2.3.1.3 were pipetted into the upper chamber of the Microcon® filter unit, positioned in the accompanying tube. The lid was fastened onto the top of the filter unit, and the Microcons® centrifuged at 503*g* for 10min at RT. A further identical centrifugation step was performed if a substantial volume remained above the filter, although care was taken not to centrifuge to dryness. The filter was removed and inverted into a clean tube, and 10µl of the filtrate in the original tube processed for gel electrophoresis (see 2.3.2.2), whilst the remainder had 10% HSA added, to create a final chemokine solution containing 0.1% HSA. To recover the concentrated enzyme, the inverted filter was pulsed briefly in the centrifuge, the enzyme solution collected in the tube. Separated enzyme and chemokine solutions were stored at -80˚C.

The above procedure for using Microcons® to separate chemokines from enzymes was optimised, comparing CCL2 and CXCL10 standards in different volumes (2µg protein in total volumes of either 65, 200, or 400µl assay buffer - 2.3.1.2), and flushing chemokine:enzyme mixtures (2µg chemokine + 2µg MMP2 in assay buffer + 1mM APMA) by adding 100µl assay buffer after centrifugation, and again after a further spin. Initially, centrifugation at 9447*g* for 10min was undertaken and the enzyme solution was recovered by inverting the filter and centrifuging at 503*g* for 3min.

5.3.8.2 Calculation of concentrations of cleaved chemokines using densitometry

Samples from the Microcon® separation (see 5.3.8.1) were used in gel electrophoresis with 12% Bis-Tris gels, alongside CCL2 and CXCL10 standards, with 20µl samples loaded per well. Chemokine standards were made by adding dH_2O to recombinant chemokines to give concentrations of 2.5, 5, 7.5, 10, 15, 20, 30, and 40µg/ml. Each digestion experiment performed in 2.3.1.3 utilised 33µg/ml chemokine, so it was

concluded that this would be the maximum possible concentration obtained after separation using Microcons®.

Gels were silver-stained, as described in 2.3.3.2, images captured using a UVP Bioimaging Systems instrument, running Lab Works (version 4) software, and used in densitometry. Using the single protein band analysis setting, each band was selected, background correction ('joining valleys') was applied, and the integrated optical density (IOD) calculated for each band using the software. The IOD of the standards were plotted against their known concentrations to generate a standard curve, from which concentrations of the cleaved chemokines, collected after filtration through Microcons®, were calculated. The appropriate volume of each cleaved chemokine could then be used to generate a concentration of 200ng/ml for the migration assay to compare intact and truncated chemokines.

5.3.9 *In vitro* cell migration assay

5.3.9.1 Labelling of cells with calcein AM

Acetoxymethyl ester of calcein (calcein AM) is an esterified fluorescein derivative that is membrane-permeant, and can be introduced into cells by incubation. Within the cell, calcein AM is hydrolysed by endogenous esterases into the negatively charged, green fluorescent calcein, which is retained in the cytoplasm of live cells. Calcein has excitation and emission wavelengths of 490nm and 515nm, respectively, and is rapidly lost under conditions that cause cell lysis (Weston and Parish, 1990). Calcein AM is not thought to interfere with cellular functions, such as lymphocyte proliferation or chemotaxis (Weston and Parish, 1990).

After the final PBS wash of PBMCs following separation from whole blood, or removal of media from THP-1 or Jurkat cells, the supernatant was discarded and the cell pellet resuspended in Hank's Balanced Salt Solution (HBSS) (PAA Laboratories, Somerset, UK), without calcium, magnesium, or phenol red. Calcein AM (50µg vial) (Invitrogen, UK) was dissolved in 10µl DMSO, and mixed with the cell suspension in HBSS. The volume of HBSS was varied during optimisation of the labelling technique, with 8, 12, 33, and 44ml assessed, to give final molarities of calcein AM of 6.2, 4.1, 1.5, and 1µM respectively. Cells were incubated with calcein AM at 37°C in an incubator with 95% air/5% CO_2 for either 30min, or 1h for comparison. Labelled cells were centrifuged at 200*g* for 5min, supernatant removed, and cells washed twice in HBSS, before being used in migration assays.

5.3.9.2 Comparison of cell number versus fluorescence

To ensure measurement of fluorescent values of calcein AM-labelled cells accurately reflected cell numbers, various experiments were performed to assess this. Lymphocytes (10.2×10^5 per ml) and monocytes (3×10^4 per ml) from whole blood were labelled independently for 30min with 4.12µM calcein AM in HBSS without cations or phenol red, and then washed as before. Increasing volumes (50, 100, 200, 300, 400, 500, 600, 700, 800, 900µl, and 1ml) of labelled cells were aliquoted into a 24-well plate, and made up to 1ml with HBSS. The plate was read at 530nm using a Wallac Victor^2 1420 plate reader, and graphs plotted of cell number versus fluorescence value.

The above comparison of cell number with fluorescence value was repeated using a mixed monocyte:lymphocyte population labelled with 4.12µM calcein AM in RPMI medium without phenol red (PAA Laboratories) for 30min. Fluorescence was measured on the Wallac plate reader at 530nm from the top, and also on the GENios Plus plate reader (Tecan, Reading, UK) at 535nm from the bottom.

Following optimisation of the calcein AM concentration, the above procedure was repeated using THP-1 cells labelled with 1.5µM calcein AM in RPMI medium without phenol red + 0.1% human serum albumin (HSA) for 30min, and fluorescence was measured on the GENios Plus plate reader at 535nm, from the bottom.

5.3.9.3 Optimisation of settings of the fluorescent plate reader

When trans-well inserts were used that had a fluorescent-blocking membrane (BD), it was essential that fluorescence was measured from the bottom of the plate using the GENios Plus plate reader, to enable detection of migrated cells alone, a feature not possible with the Wallac plate reader. Companion plates (BD) used with the inserts were not of regular dimensions for a 24-well plate, so a plate definition file was created by inputting the specific dimensions of the plate (Appendix III). Using Xfluor4 software, a program was designed to read the plate from the bottom, with excitation and emission wavelengths of 485 and 535nm respectively, using a manual gain setting of 60, 3 flashes from a high energy Xenon flash lamp per well, a lag time of 0µs, an integration time of 20µs, and a 2x2 read formation in a square pattern per well. Gain settings of 50, 60, 80, and 'optimal' (derived by the instrument from assessment of the range of fluorescence in all wells) were tried, as were different read patterns (e.g. single central spot, or 4 circles). Plates were read with the lid off, as it autofluoresced.

5.3.9.4 Migration of THP-1 cells to human serum albumin

As HSA was used in both the upper and lower chambers of the migration apparatus, the effects on migration of various HSA concentrations were analysed.

THP-1 cells were labelled with 1.5μM calcein AM for 30min. Cells were washed twice with HBSS without cations or phenol red, resuspensed in RPMI without phenol red + 0.1% HSA, and placed in migration inserts. FluoroBlok™ inserts (BD) have a polyethylene terephthalate (PET) membrane as their base, which blocks light transmission within the 490-700nm range. The membrane had 3μm pores, which allowed labelled cells to migrate to the underlying chamber (Fig. 5.3). The inserts had a human fibronectin coating to promote attachment of cells to the amino acid sequence, RGD, which interacts with integrin receptors, thereby facilitating migration. Inserts were used in a 24-well companion plate, and 500,000 cells placed in each well. RPMI + 0, 0.1, 1, and 5% HSA, or RPMI + 10^{-8} M N-formyl-methionyl-leucyl-phenylalanine (fMLP) (Sigma) were placed in the lower chamber, and migration investigated by measuring the fluorescence from the bottom of the plate, every 15min for 3h at 37˚C, to detect cells that had passed through the filter. The non-specific chemoattractant fMLP is a synthetic peptide that mimics bacterially-derived peptides, which activates phagocytic leukocytes, causing chemotaxis and other responses (Prossnitz and Ye, 1997). It was included to serve as a positive control for migration.

5.3.9.5 Migration to CCL2 using THP-1 cells and monocytes

THP-1 cells or monocytes, labelled with either 1 or 1.5μM calcein AM, were used in migration assays to 0, 10, 25, 35, 50, 75, 100, 200, 400ng/ml recombinant human CCL2 (Peprotech, EC). Preliminary experiments were performed using a range of CCL2 concentrations to determine the optimum, in terms of generating maximum migration. The optimum cell density for use in migration assays was also investigated, by seeding 200μl of the cell types used at different concentrations, including 0.2, 1, 1.2, 2.5, 3.85, and 4 million cells/ml, per trans-well insert.

RPMI + 0.1% HSA containing CCL2, or a control of RPMI + 0.1% HSA only, were pipetted into wells of a 24-well companion plate (BD), with 800μl added per well. Samples were run in duplicate or triplicate. The plate was incubated at 37˚C for 5-10min to warm the contents. Inserts were positioned into wells of the companion plate, and 200μl of labelled cells (resuspended in RPMI + 0.1% HSA) were added to the insert. The plate was read immediately, using a GENios Plus plate reader, by measuring fluorescence at 535nm from the bottom of the plate. Subsequent readings were taken every 15min, up to 3h.

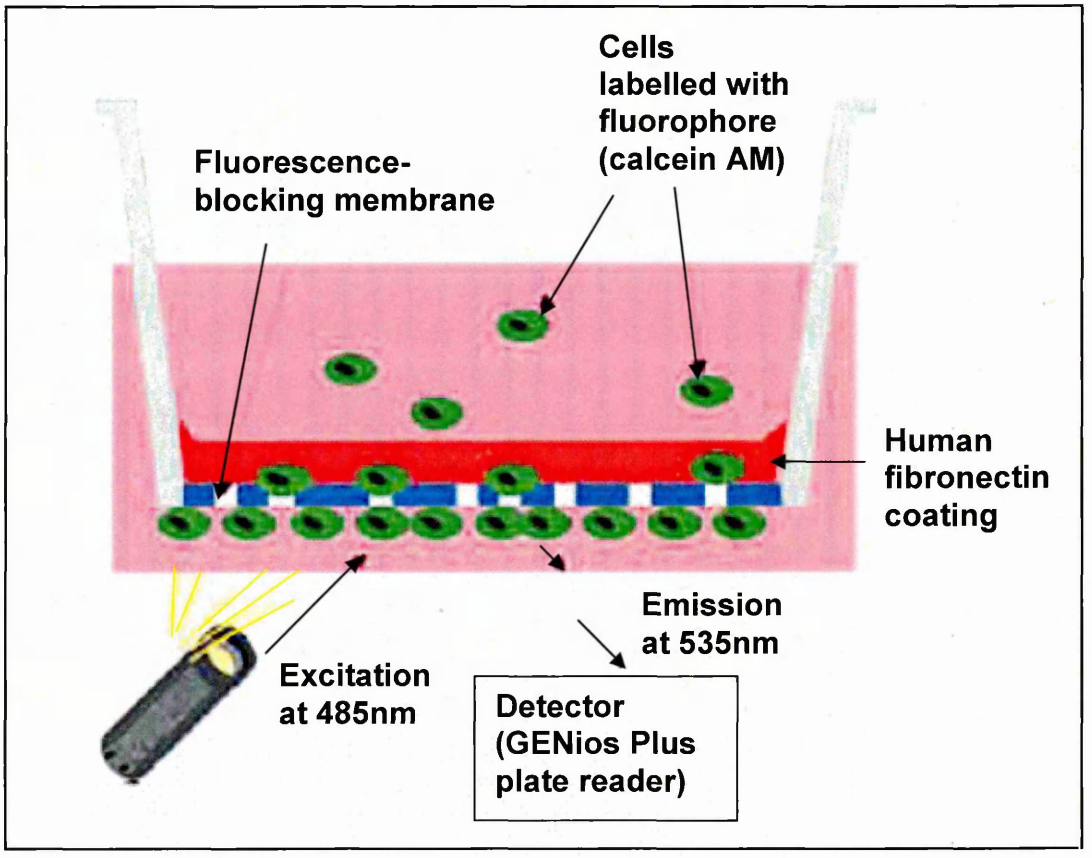

Adapted from www.bdbiosciences.ca/image_library/cell_mig.jpg

Figure 5.3 Schematic of the *in vitro* migration assay using fluorescent-blocking inserts and cells labelled with calcein AM

Cells were labelled with calcein AM. Labelled cells were counted and the required density placed in FluoroBlok™ inserts, which have a membrane (3µm pores) that blocked light transmission within the range of 490-700nm, so that cells in the insert were not detected from below. Inserts were positioned in a 24-well plate, containing chemoattractants or control solutions. Plates were incubated for up to 5h (depending on the cell type), and fluorescence quantitated as required from the bottom of the plate using a GENios Plus plate reader at 485nm excitation and 535nm emission.

5.3.9.6 Migration to CXCL10 with Jurkat cells and lymphocytes

Jurkat cells or lymphocytes, labelled with either 1 or 1.5μM calcein AM, were used in migration assays to: 0; 10; 12.5; 25; 50; 100; 200; 250; 400; 500ng/ml; and 1μg/ml, recombinant human CXCL10 (Peprotech, EC). Preliminary experiments were performed using a range of CXCL10 concentrations to determine the optimum in terms of generating maximum migration. The migration assays were conducted as described in 5.3.10.5.

Jurkat cells and lymphocytes were used without prior treatment, and also following exposure to IL-2 (see 5.3.3) for 6 days, as this has been shown to increase CXCR3 expression (Reckamp *et al.*, 2007) and the migration response of cells to CXCL10 (Beider *et al.*, 2003).

5.3.9.7 Use of cleaved forms of CCL2 and CXCL10 in migration assays

To assess the effects on the chemotactic ability of CCL2 and CXCL10 following cleavage by MMP2, MMP9, and CD26, truncated chemokines were used alongside intact forms at the same concentration of 200ng/ml, in migration assays. Cleaved chemokines were generated as described in 2.3.1.3 and prepared for use in migration assays (see 5.3.8).

5.3.9.8 Blocking the activity of CCL2

Intact CCL2 was blocked using an antibody prior to use in migration assays, to indicate that increased movement of cells to CCL2 was due to chemotaxis, and not chemokinesis. Polyclonal goat IgG anti-CCL2 blocking antibody (R&D Systems) was incubated at a 1:7.5 dilution (267μg/ml) with 200ng/ml CCL2 in 2.5ml RPMI + 0.1% HSA, for 30min at RT.

5.3.10 Analysis of migration data

The mean fluorescence, and the standard error of the mean (SEM), for the number of inserts (normally n=3) used with each of the chemoattractant or control solutions in the plate wells were calculated. Statistical tests used were the analysis of variance (ANOVA) with Bonferroni's test, or the unpaired, 2-tailed Student's *t*-test, to look for statistically significant differences between various chemoattractant conditions (such as cleaved and intact CCL2), with a p-value of <0.05 being considered significant, illustrated by *, $P<0.01$ as **, and highly significant $P<0.001$ symbolised by *** (Wallenstein *et al.*, 1980). Statistical tests were performed in Microsoft Excel, and using

GraphPad Prism version 4.00 for Windows, (GraphPad Software, San Diego, California USA).

The migration index of cells was calculated by dividing the mean fluorescence value of cells migrated to chemokine by the mean fluorescence value of the control (cells not exposed to chemokine), at the same time point.

5.4 Results

5.4.1 Analysis by flow cytometry of PBMCs obtained after Histopaque separation of whole blood

Analysis of PBMCs, conducted with Dr Omer Suliman (BMRC), revealed that 60% were positive for $CD4^+$ / $CD8^+$ (T cells), and 22% were positive for $CD14^+$ (monocytes) (data not shown). Monocytes isolated from whole blood express CCR2 (Opalek *et al.*, 2007), the receptor for CCL2, and ~40% resting lymphocytes express CXCR3, the receptor for CXCL10 (Loetscher *et al.*, 1998), so separation of these 2 cell types was undertaken in order to assess migration to each chemokine individually with an appropriate cell type. Following plastic adhesion to separate monocytes and lymphocytes, a significant reduction in the number of cells was observed, most likely caused by the washing steps, precluding the use of monocytes alone in migration assays. The enriched lymphocyte population was cultured in the presence of IL-2 and PHA and used in migration assays to CXCL10.

5.4.2 Surface expression of CCR2 by THP-1 cells analysed by flow cytometry

THP-1 cells were analysed by flow cytometry to confirm their surface expression of CCR2, and thus, the suitability of using THP-1 cells in migration assays to CCL2. CCR2 was found to be highly expressed by THP-1 cells, with a total of 83.6% of cells analysed by flow cytometry found positive (Fig. 5.4d), compared to only 2.62% of cells in the same specified region (M1) labelled with the isotype control (Fig. 5.4b).

5.4.3 Surface expression of CXCR3 by Jurkat cells analysed by flow cytometry

Jurkat cells were analysed by flow cytometry to confirm their expression of CXCR3, and thus, the suitability of using Jurkat cells in migration assays to CXCL10. CXCR3 was strongly expressed by Jurkat cells, with a total of 90.45% of cells positive, (Fig. 5.5d), compared to only 5.68% labelled with the isotype control in the same region (M1) (Fig. 5.5b).

Figure 5.4 Flow cytometry of THP-1 cells for surface expression of CCR2

THP-1 cells were labelled with anti-CCR2 antibody, without prior fixation or permeabilisation, enabling surface receptor expression to be analysed by flow cytometry. Dot blots ***a*** *and* ***c*** *show forward scatter peak height (FSC-H), indicating cell size, and side scatter peak height (SSC-H), indicative of cell granularity. The gates used are shown, R1 for THP-1 cells labelled with the isotype control, and R2 for CCR2 labelling. Histograms of fluorescence from labelled cells in R1 and R2 gate regions are shown in* ***b*** *and* ***d****, respectively, with an overlay of negative control and CCR2-positive results in* **e***. Flow cytometry channel 2 (FL2) was used to detect levels of phycoerythrin-labelled anti-CCR2 antibody, and the isotype control. Marker M1 was placed to the right of the isotype control result. The mean fluorescence intensity (MFI), and percentage of gated cells positive for CCR2, within the M1 zone, are given.*

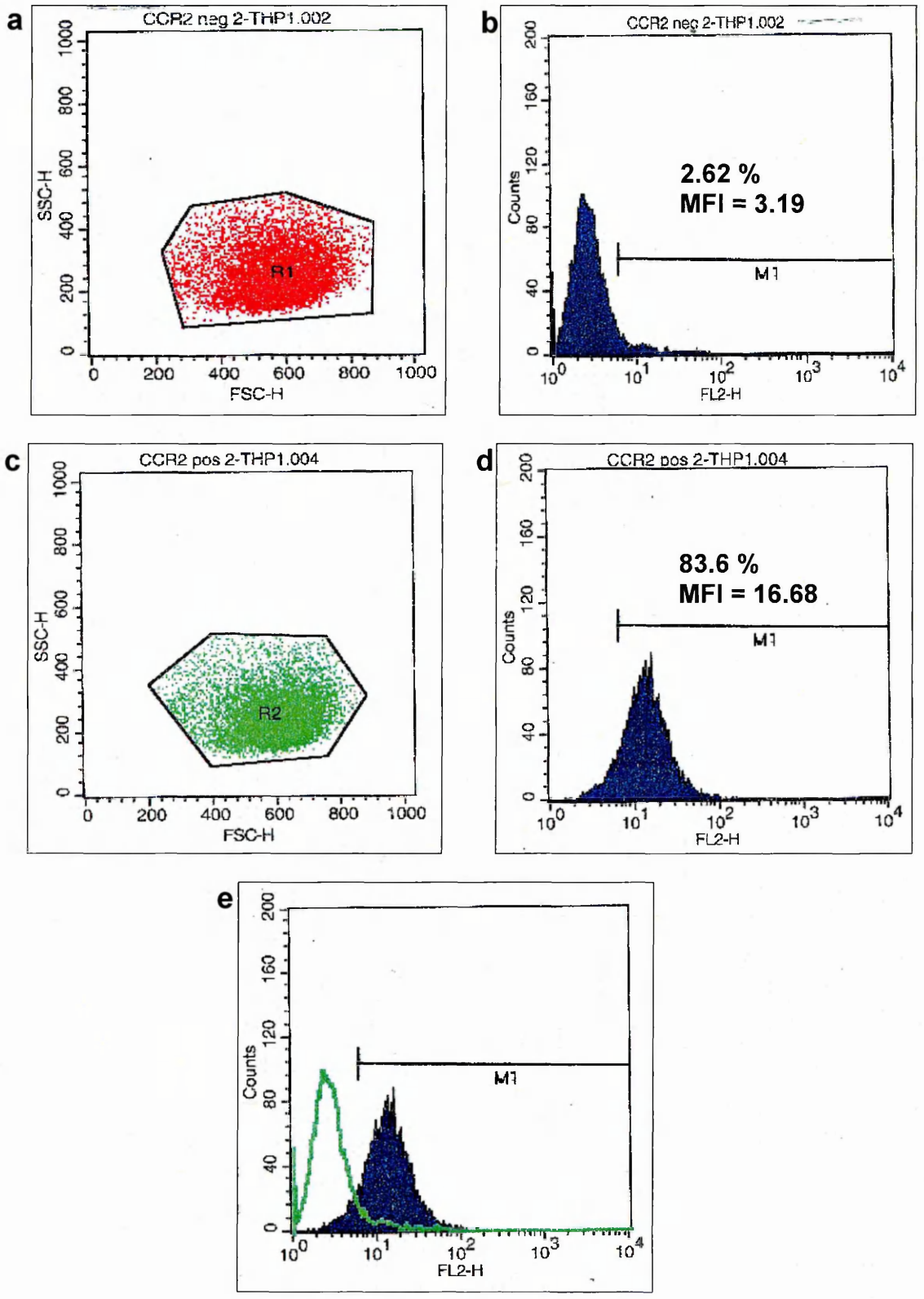
a
CCR2 neg 2-THP1.002
SSC-H
FSC-H
R1
b
CCR2 neg 2-THP1.002
Counts
FL2-H
2.62 %
MFI = 3.19
M1
c
CCR2 pos 2-THP1.004
SSC-H
FSC-H
R2
d
CCR2 pos 2-THP1.004
Counts
FL2-H
83.6 %
MFI = 16.68
M1
e
Counts
FL2-H
M1

Figure 5.5 Flow cytometry of Jurkat cells for surface expression of CXCR3

Jurkat cells were labelled with anti-CXCR3 antibody, without prior fixation or permeabilisation, enabling surface receptor expression to be analysed by flow cytometry. Dot blots ***a*** *and* ***c*** *show forward scatter peak height (FSC-H), indicating cell size, and side scatter peak height (SSC-H), indicative of cell granularity. The gates used are shown, R1 for Jurkat cells labelled with the isotype control, and R2 for CXCR3 labelling. Histograms of fluorescence from labelled cells in R1 and R2 gate regions are shown in* ***b*** *and* ***d****, respectively, with an overlay of negative control and CXCR3-positive results in* ***e****. Flow cytometry channel 2 (FL2) was used to detect levels of phycoerythrin-labelled anti-CXCR3 antibody, and the isotype control. Marker M1 was placed to the right of the isotype control result. The mean fluorescence intensity (MFI), and percentage of gated cells positive for CXCR3, within the M1 zone, are given.*

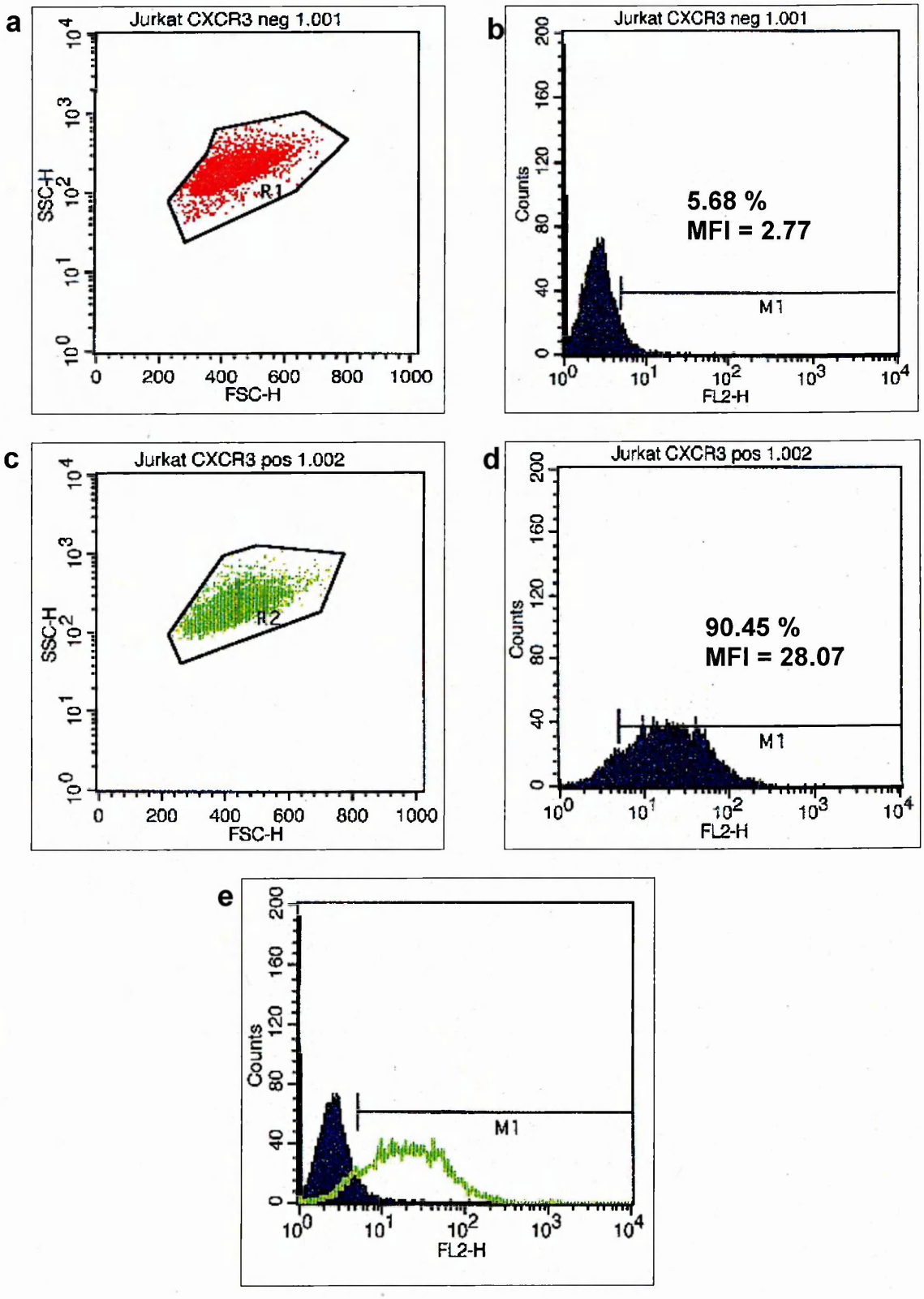
a
Jurkat CXCR3 neg 1.001
SSC-H
FSC-H
R1
b
Jurkat CXCR3 neg 1.001
Counts
FL2-H
5.68 %
MFI = 2.77
M1
c
Jurkat CXCR3 pos 1.002
SSC-H
FSC-H
R2
d
Jurkat CXCR3 pos 1.002
Counts
FL2-H
90.45 %
MFI = 28.07
M1
e
Counts
FL2-H
M1

5.4.4 Optimisation of the migration assay

5.4.4.1 Optimisation of the use of Microcon® filter devices to separate recombinant chemokines from enzymes in the digestion mixture

It was necessary to remove the enzymes from the cleaved chemokines generated in 2.3.1.3, as enzymes were not present in the intact chemokine solutions, and directly comparable solutions of cleaved and intact chemokines were required for cell migration assays.

Microcons® with 2 different cut offs were compared, to obtain the maximum chemokine yield with effective enzyme removal. Use of Microcons® was optimised by altering the centrifuge speed and volume, and flushing through with buffer. CCL2 was retained to a lesser extent than CXCL10.

Microcons® with a cut off of 30 kDa (YM30) were shown by gel electrophoresis to retain all of CCL2 and CXCL10 if 0.1% HSA was present in solution (data not shown), and the majority of chemokine in its absence. Flushing the Microcons® through with additional buffer reduced chemokine retention on the membrane. YM30s were completely effective at removing enzymes (Fig. 5.6a). Comparing YM30 Microcons® directly with YM50s by gel electrophoresis indicated that YM50s gave better recovery of CCL2 and CXCL10, whilst remaining effective at removing enzymes (Fig. 5.6b). YM50s were thus selected for removal of enzymes from the chemokine digestion mixtures.

Decreasing the centrifugation speed from 9447*g* to 503*g* increased recovery rates of chemokine in the filtrate, although it was necessary to repeat the centrifugation 1 or 2 times at the lower speed. Microcons® are suitable for volumes of 50-500µl, and larger starting volumes were found to facilitate the ultrafiltration process, but this had to be balanced with the chemokine concentration required for migration experiments.

5.4.4.2 Comparison of cell number and fluorescence of calcein AM-labelled cells

The fluorescence values of known numbers of calcein AM-labelled cells were measured using both plate readers, to ensure that a good correlation existed between fluorescence and cell number, thereby validating the use of fluorescence values as a measure of the number of migrated cells.

Figure 5.6 Optimisation of separation of enzyme and chemokine mixtures: gel electrophoresis of samples separated using Microcon® ultrafiltration devices

Silver-stained 12% Bis-Tris gels were used to assess separation of recombinant chemokine from enzyme using Microcon® ultrafiltration devices YM30 and YM50.

***(a)** YM30, used with different sample volumes, and with and without flushing through with buffer. Lanes 1-12 represent 10µl of the following samples: **(1)** CXCL10 (400µl) retentate; **(2)** CXCL10 (400µl) filtrate; **(3)** CXCL10 (65µl) retentate; **(4)** CXCL10 (65µl) filtrate; **(5)** CCL2/MMP9 retentate; **(6)** CCL2/MMP9 filtrate; **(7)** CXCL10/MMP9 retentate; **(8)** CXCL10/MMP9 filtrate; **(9)** Flushed CCL2/MMP9 retentate; **(10)** Flushed CCL2/MMP9 filtrate; **(11)** Flushed CXCL10/MMP9 retentate; **(12)** Flushed CXCL10/MMP9 filtrate. Flushing the Microcon® membrane was shown to improve the yield of chemokine in the filtrate.*

***(b)** YM30 and YM50. Lanes 1-9 representing 10µl of the following samples: **(1)** Mark12 MW marker; **(2)** CCL2 retentate from YM30; **(3)** CCL2 filtrate from YM30; **(4)** CXCL10 retentate from YM30; **(5)** CXCL10 filtrate from YM30; **(6)** CXCL10/MMP2 retentate from YM50; **(7)** CCL2/MMP2 filtrate from YM50; **(8)** CCL2/MMP2 retentate from YM50; **(9)** CXCL10/MMP2 filtrate from YM50. YM50s gave a greater yield of chemokine in the filtrate, compared to YM30s.*

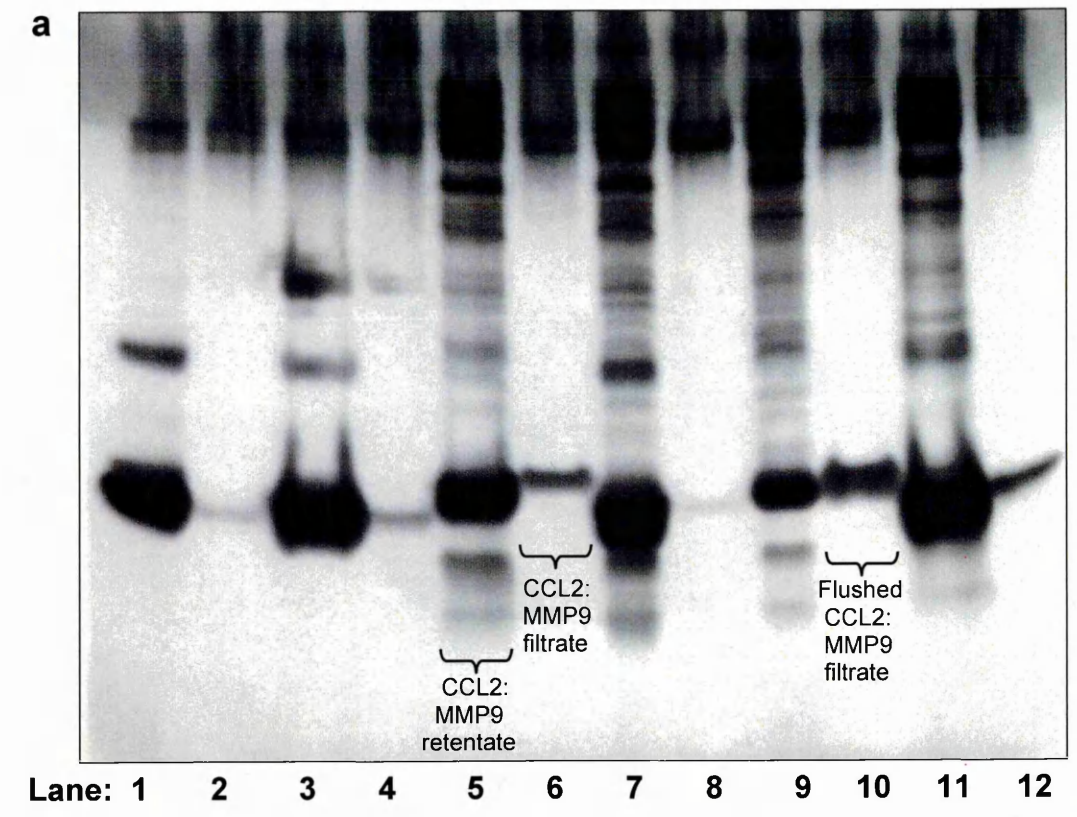
a
CCL2:
MMP9
retentate
CCL2:
MMP9
filtrate
Flushed
CCL2:
MMP9
filtrate
Lane: 1 2 3 4 5 6 7 8 9 10 11 12

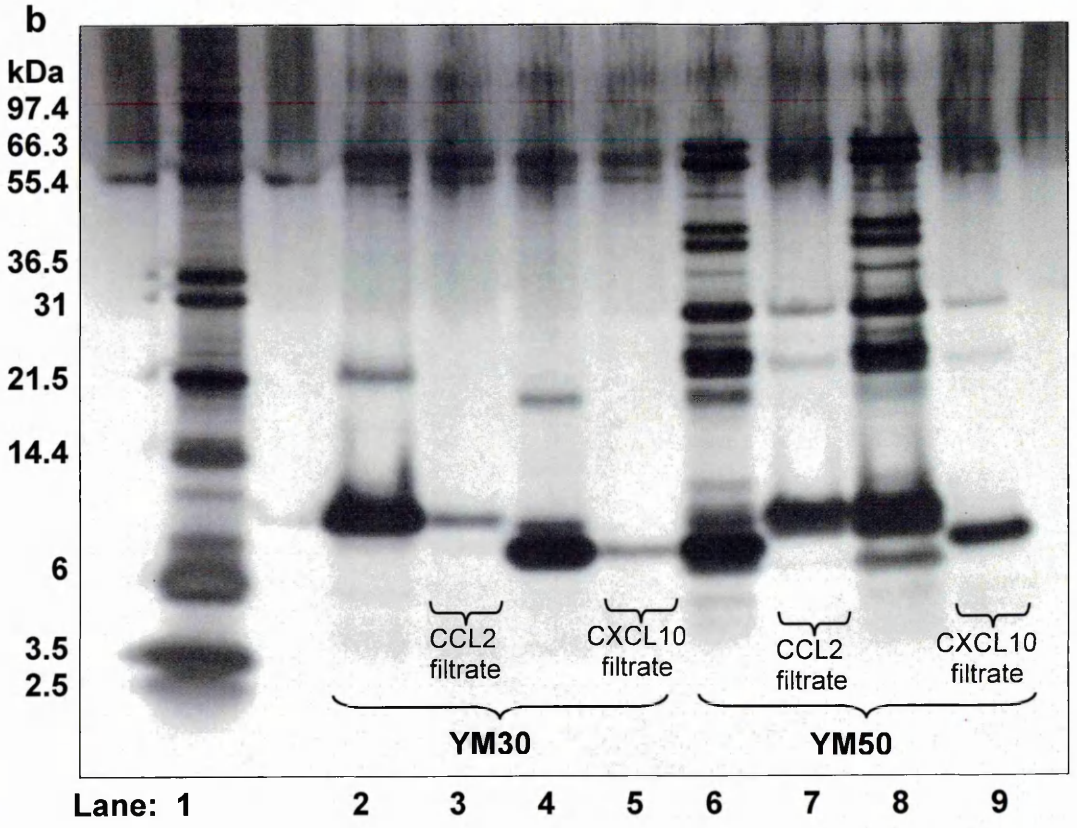
b
kDa
97.4
66.3
55.4
36.5
31
21.5
14.4
6
3.5
2.5
CCL2
filtrate
CXCL10
filtrate
CCL2
filtrate
CXCL10
filtrate
YM30
YM50
Lane: 1 2 3 4 5 6 7 8 9

Fluorescence values achieved with both the Wallac Victor^2 and GENios Plus plate readers correlated very well (R^2 values typically of 0.99) with the number of labelled PBMCs (Fig. 5.7a), monocytes, lymphocytes, THP-1 cells (Fig. 5.7b and c), and Jurkat cells. Very low numbers of cells proved difficult to measure, however, particularly with the Wallac Victor^2 plate reader. This is an important consideration, as only a fraction of the total number of cells used in migration assays will migrate. Figure 5.7c shows a standard curve generated from fluorescence of THP-1 cell numbers of 0-901, which showed some discrepancies for cell numbers less than 200, and gave a lower R^2 value of 0.93. Above 200 cells, correlation was excellent, which indicated measuring fluorescence of cells labelled with 1.5µM calcein AM achieves a good representation of cell number for the range expected to be relevant to migration assays. The linear relationship between fluorescence and cell number also remained constant for the duration of the assay for all cell types used, as no significant difference was observed in measurements taken immediately after labelling with calcein AM (Fig. 5.7b), and 4h 25min, afterwards (Fig. 5.7a).

5.4.4.3 Optimal cell density per insert for migration assays

Optimal cell density for use in migration assays was assessed and found to vary depending on the cell type. A seeding density of THP-1 cells of 2-5 x 10^5 cells per insert gave good results in migration assays to CCL2 (data not shown).

5.4.4.4 Comparison of the migration of unlabelled PBMCs to cells labelled with calcein AM

Effects of calcein AM labelling of cells on their migratory capacity were investigated by comparing the migration of unlabelled and labelled PBMCs to 1 and 10% BSA. Labelling with 6µM calcein AM did not interfere with the migratory capacity of PBMCs to BSA. Similar results were seen with labelled and unlabelled PBMCs, as they both showed migration after 18h to 1% BSA that was significantly greater (P>0.001) than migration to the control, HBSS (Fig. 5.8).

Migration to 10% BSA was significantly increased compared to control (P<0.01) when using unlabelled cells, but this significant difference was not evident with calcein AM-labelled cells (Fig. 5.8). This difference was not considered a cause for concern, as an increase in background fluorescence could account for the failure to find a significant difference between 0 and 10% BSA with labelled cells, particularly as a high molarity of calcein AM, and a long time course, were used.

Figure 5.7 Correlation of number of calcein AM-labelled cells with fluorescence value at 535nm

(a) *PBMCs were isolated from human blood by density gradient centrifugation, labelled with 4.1μM calcein AM, counted and further diluted with RPMI to give known cell numbers, and fluorescence measured at 535nm using a GENios Plus plate reader. The* R^2 *value of 0.9949 illustrates that the relationship between the number of PBMCs and the associated fluorescence value is a linear one, and that fluorescence can be accurately correlated with cell number, 265min after labelling with calcein AM.*

(b) *THP-1 cells were labelled with 1.5μM calcein AM and known cell numbers plotted against fluorescence measured at 535nm using a GENios Plus plate reader. The plot generated for the whole range of 0-568,000 cells gave an* R^2 *value of 0.9979, which illustrates that the relationship between the number of cells and the associated fluorescence value is a linear one, and that fluorescence can be accurately correlated with cell number immediately after labelling with calcein AM.*

(c) *The plot for low THP-1 cell numbers (from* ***b****) between 0-901 cells gave an* R^2 *value of 0.9374 and showed a reduced correlation between cell number and fluorescence for cell numbers below 200.*

(a) PBMCs, 4.1μM calcein AM, 265min after labelling

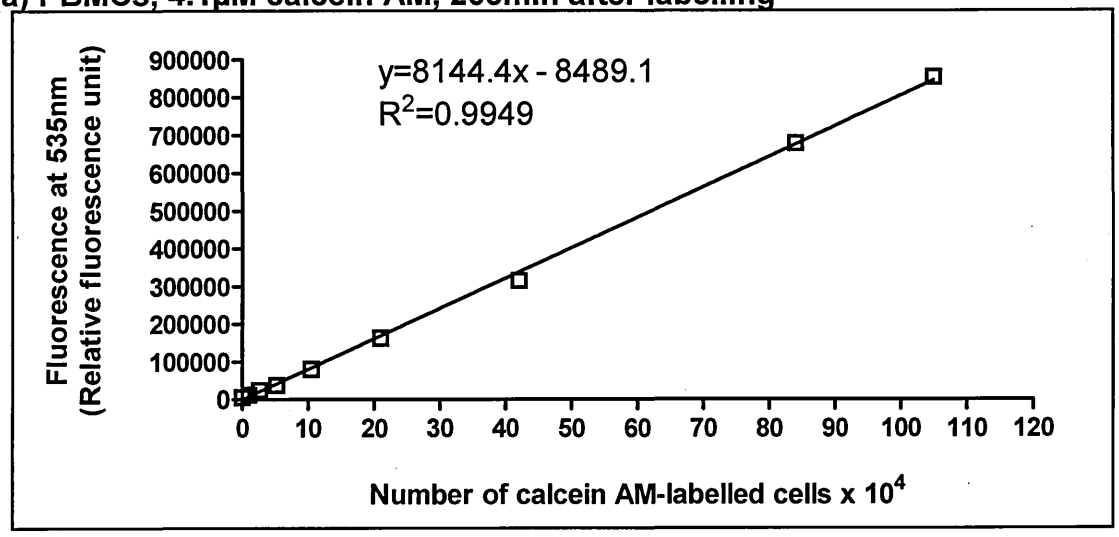

(b) THP-1 cells, 1.5μM calcein AM, immediately after labelling

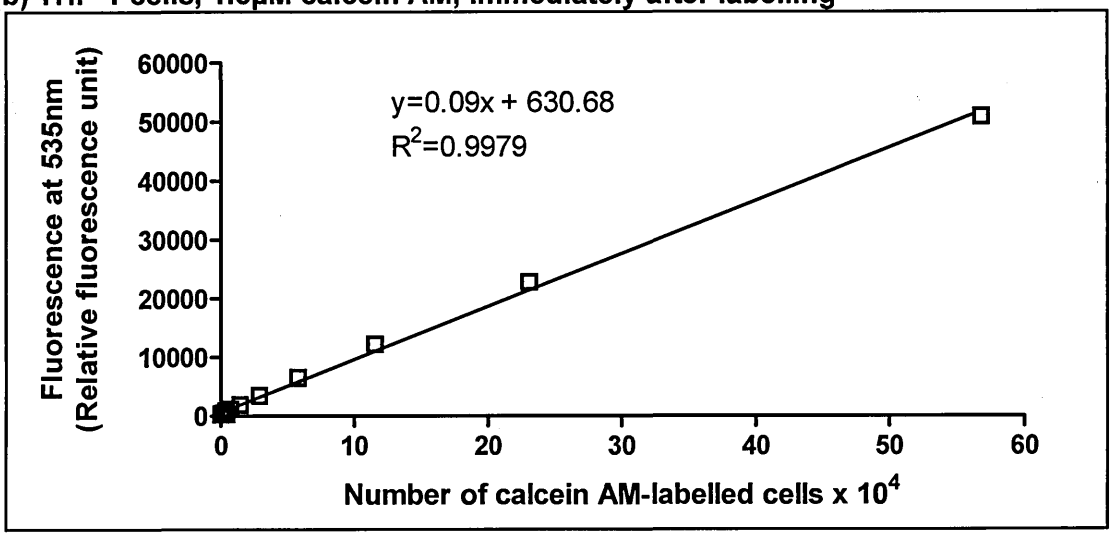

(c) Low THP-1 cell number, 1.5μM calcein AM, immediately after labelling

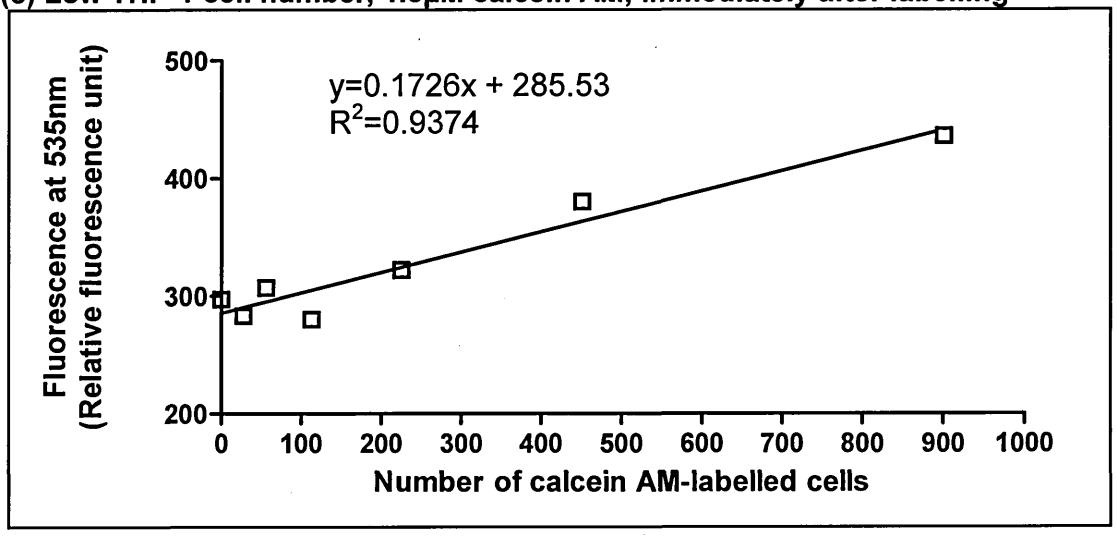

Figure 5.8 Comparison of the migration of unlabelled and calcein AM-labelled PBMCs to 1% and 10% BSA at 18h

*Effects of calcein AM labelling of PBMCs on migration was assessed by using labelled and unlabelled PBMCs in a migration assay with uncoated inserts with 3μm pores. Each insert received 8 x 10^5 cells, suspended in HBSS, and HBSS, 1%, or 10% BSA were placed in the lower chambers. Cell migration into the lower chamber was measured after 18h at 37˚C and 5% CO_2. Data are presented as mean ± SEM (n=2 inserts); one-way ANOVA with Bonferroni's post test indicate differences from HBSS control, with **= P<0.01, and ***= P<0.001.*

(a) *Cells were not labelled prior to migration. After 18h, cells adherent to the filter underside were removed with trypsin-EDTA solution, pooled with cells in the lower chamber, and counted using a haemocytometer*

(b) *Cells were labelled with 6μM calcein AM for 30min at 37˚C and 5% CO_2, and washed twice, prior to use in the migration assay. After 18h, the inserts were removed after gentle scraping of adherent cells into the lower chamber, and the level of fluorescence in the lower chamber measured at 535nm using a Wallac Victor^2 plate reader.*

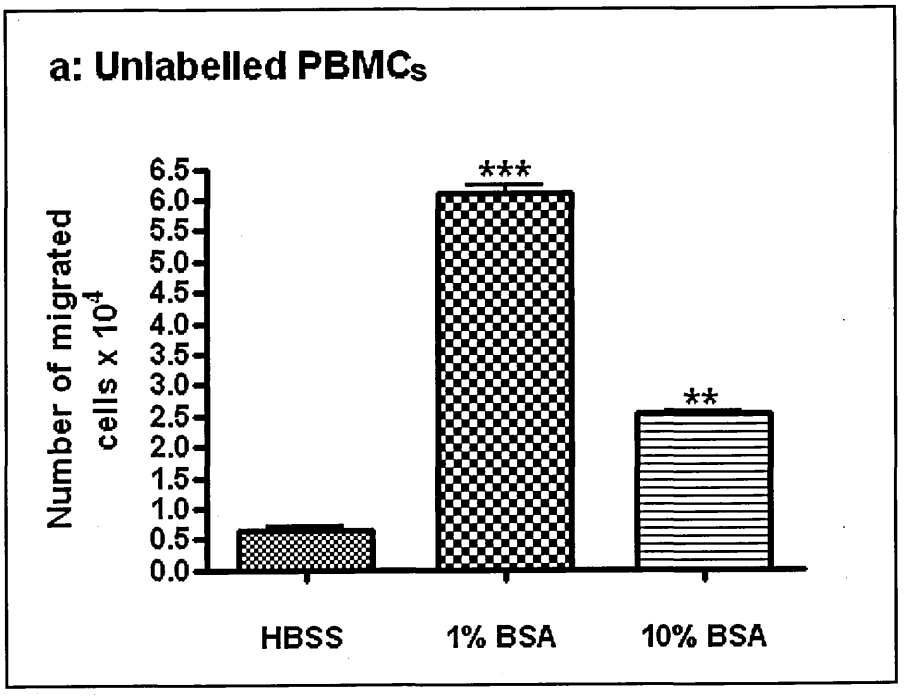
a: Unlabelled PBMCs
Number of migrated cells x 10^4
6.5
6.0
5.5
5.0
4.5
4.0
3.5
3.0
2.5
2.0
1.5
1.0
0.5
0.0
***
**
HBSS
1% BSA
10% BSA

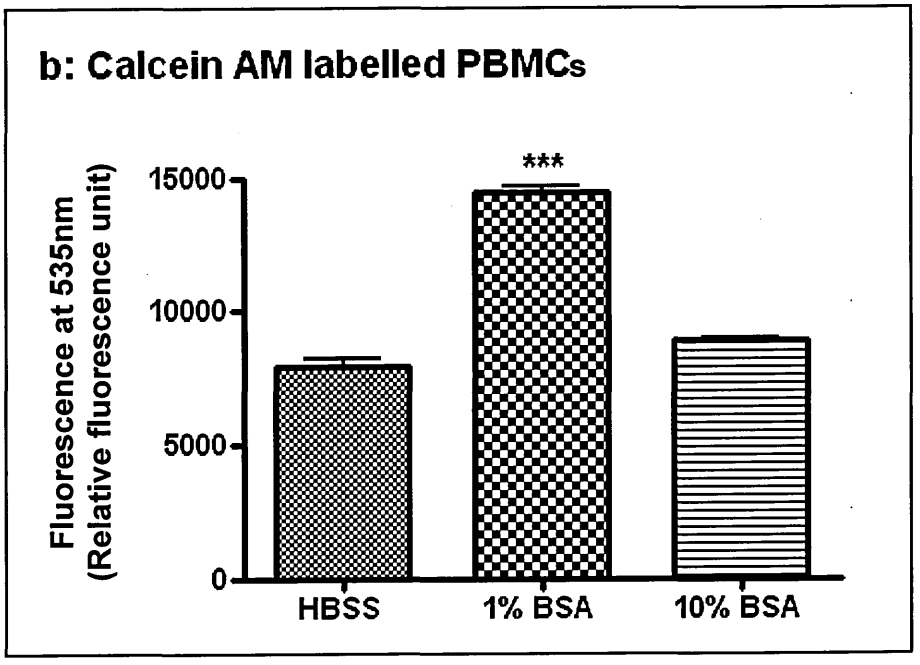
b: Calcein AM labelled PBMCs
Fluorescence at 535nm (Relative fluorescence unit)
15000
10000
5000
0
***
HBSS
1% BSA
10% BSA

5.4.4.5 Optimal calcein AM concentration for labelling cells

The molarity of the calcein AM used to label cells was optimised, to ensure the lowest effective molarity was used, thereby reducing the likelihood of effects on the cells arising from calcein AM. Very high levels of fluorescence exceeded the upper detection limit of the GENios Plus plate reader, so lower molarities of calcein AM were used, with 1 and 1.5μM giving good results (data not shown). A low calcein AM concentration also reduced the possibility of the dye interfering with cellular function, or being released from the cell. All cell types used gave a viability result of greater than 99% as determined by Trypan Blue exclusion, both before labelling, and after labelling. This remained the case for the duration of the migration assays.

5.4.4.6 THP-1 cell migration to various concentrations of human serum albumin and fMLP

HSA was used in both the upper and lower chambers of the migration apparatus during assays using chemokines, so the effects on migration of THP-1 cells to various HSA concentrations were analysed to see if small deviations in HSA concentration between assays would affect results attributed to chemokines. Significant migration to 5% HSA, compared to the control of 0% HSA, was first observed at 105min, and then maintained at similar levels at 120, 135, 150, and 165min, assessed using unpaired, 2-tailed, Student's *t*-tests (Fig. 5.9). Significant migration to 5% HSA, compared to 0.1% HSA, and fMLP, was also observed. No significant migration to 0.1% or 1% HSA, or 10^{-8} M fMLP, compared to the control of no HSA, was seen (Fig. 5.9), indicating that the 0.1% HSA used in migration assays to chemokines is not responsible for the migratory response.

5.4.5 Cell migration to CCL2

5.4.5.1 THP-1 cell migration to various concentrations of CCL2

Significant migration was observed to 100, 200, and 400ng/ml CCL2, compared to no CCL2 (RPMI + 0.1% HSA) (Fig. 5.10). CCL2 concentrations of 200 and 400ng/ml induced the highest level of migration, with $P<0.001$, compared to $P<0.01$ for 100ng/ml, when one-way ANOVA and Bonferroni's multiple comparison post-test were performed. Migration peaked early on in the assay for all CCL2 concentrations, with high levels observed at 30min, with no further increase in cell migration for the remaining 90min. A more rapid initial migratory response was observed with 400ng/ml CCL2, as this appeared to peak at 15min (Fig. 5.10).

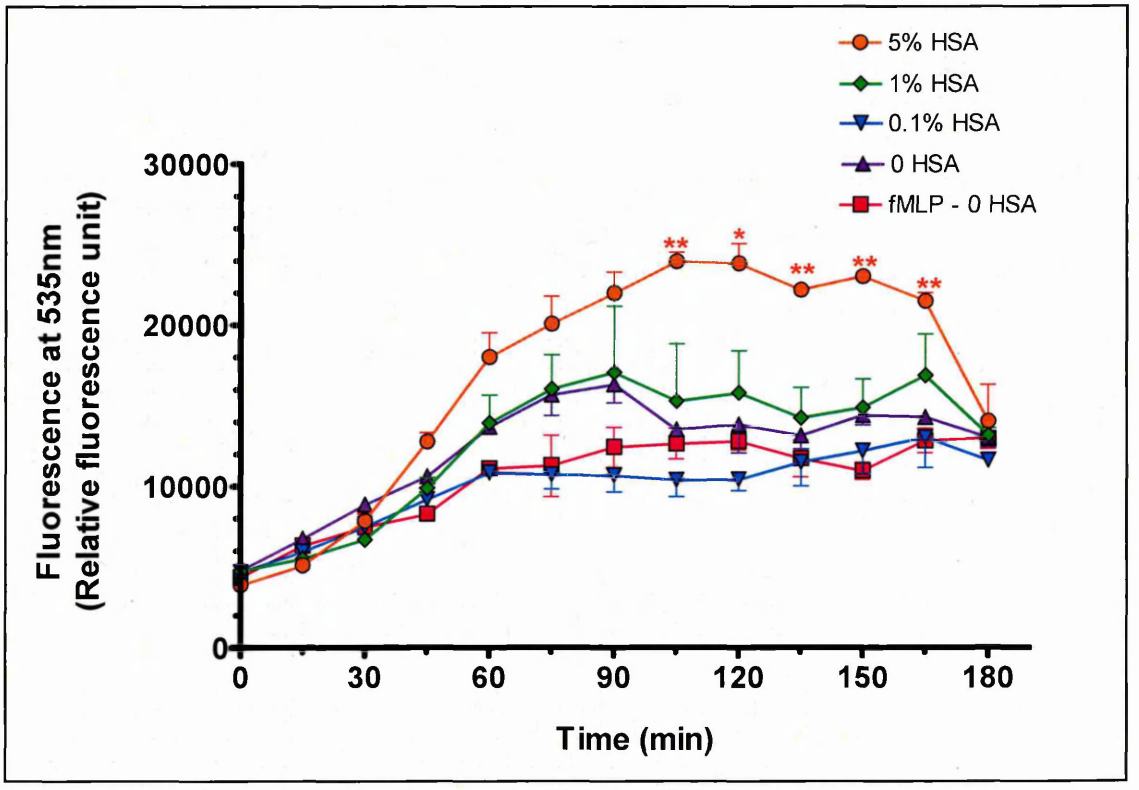

Figure 5.9 Effect of HSA concentration on THP-1 cell migration

*THP-1 cells labelled with 1.5μM calcein AM were placed in fluorescent-blocking inserts with 3μm pores (8.30 x 10^5 cells / insert), and exposed to RPMI + 0, 0.1, 1, and 5% HSA, or RPMI + 10^{-8} M fMLP (used as a positive control), in the lower chamber. Migration was measured every 15min for 3h at 37˚C, to detect cells that had passed through the filter to the lower chamber. Mean fluorescence (n=2) at 15min intervals, for each concentration of HSA is shown, and the error bars represent SEM. Results from unpaired, 2-tailed, Student's t-tests, comparing fluorescence values of migration to 5% HSA to 0% HSA are shown for each time point, with *= P<0.05, and **= P<0.01. No significant difference was seen between 0.1% and 1% HSA, compared to 0% HSA.*

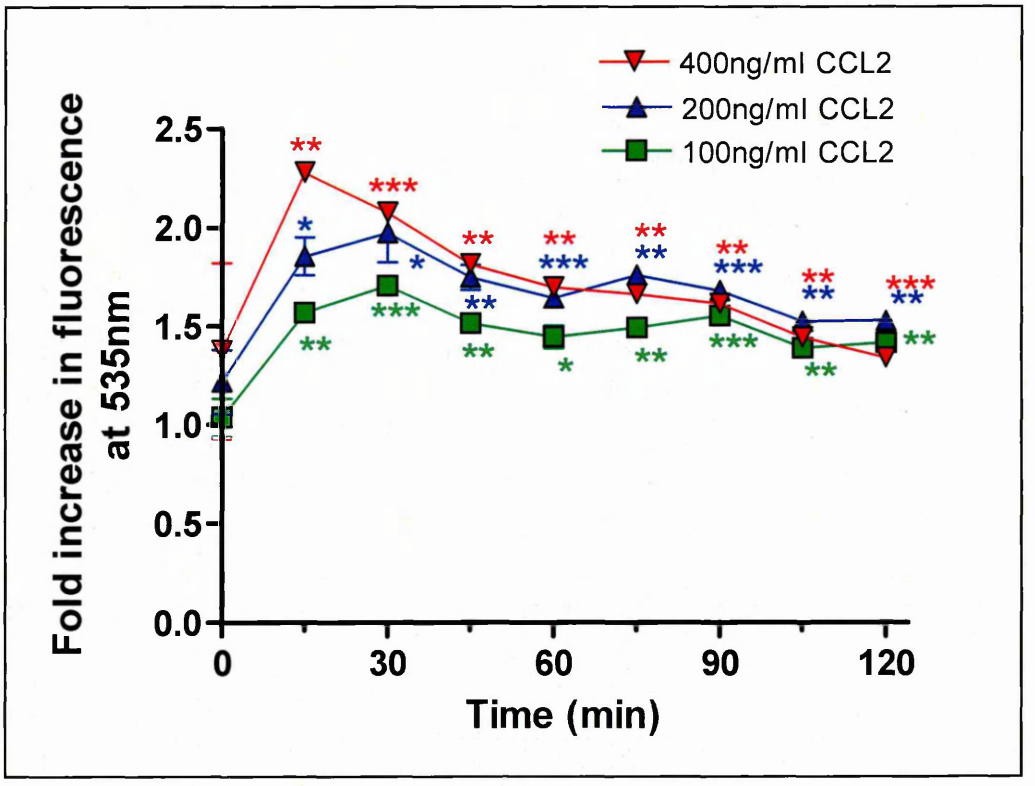

Figure 5.10 Effect of CCL2 concentration on THP-1 cell migration

THP-1 cells labelled with 1.5μM calcein AM were placed in fluorescent-blocking trans-well filters with 3μm pores (2.4 x 10^5 cells / insert), and exposed to RPMI + 0, 100, 200, and 400ng/ml CCL2, in the lower chamber. Migration to CCL2 was measured by reading the fluorescence from the bottom of the plate, every 15min for 3h at 37˚C, to detect cells that had passed through the filter to the lower chamber. Mean fluorescence (n=2) values (MFVs) for each concentration of CCL2 were divided by the MFVs of no CCL2 at each timepoint to give the fold increase. Error bars represent SEM. Results from Student's t-tests (unpaired, 2-tailed) for each time point, comparing MFVs of CCL2 concentrations to no CCL2 are shown.

5.4.5.2 Comparison of migration to intact and cleaved CCL2 by THP-1 cells

Truncated CCL2 (from 2.3.1.3) was used to compare the migratory response of THP-1 cells to intact and cleaved CCL2.

Cleavage of CCL2 by either MMP2, MMP9 or CD26 significantly reduced the rate of THP-1 migration, as fold increases (~1.4-1.9) in migration to cleaved CCL2 at 15min, above that seen with no CCL2, were approximately half of the fold increase seen with intact CCL2 (~3.8 fold increase). CCL2 blocked by an antibody resulted in negligible migration (~1.4 fold increase) (Fig. 5.11). Performing one-way ANOVA with Bonferroni's post-test indicates that overall significant differences ($P<0.01$), exist between migration to CCL2 cleaved by MMP2 and CD26, compared to migration to intact CCL2 incubated with APMA alone. MMP9-cleaved CCL2 induced a more marked reduction in migration ($P<0.001$). Analyses by Student's t-tests at each time point indicate that the differences are not maintained over time, however. At 45min, migration to MMP2-cleaved CCL2 compared to APMA-incubated CCL2 does not show any significant reduction ($P>0.05$), whereas MMP9-cleaved CCL2 exhibits reduced migration ($P<0.01$), and CD26-cleaved CCL2 demonstrates significant differences ($P<0.05$). By 75min, the reduced migration to cleaved chemokines has been eradicated, compared to intact CCL2 (Fig. 5.11).

5.4.6 Migration to CXCL10

5.4.6.1 Lymphocyte migration to CXCL10

Treatment of lymphocytes with 1µg/ml PHA and 20ng/ml IL-2 for 7 days in culture, did not induce significant migration (7.7×10^5 cells per insert) to 250ng/ml CXCL10 (data not shown), as determined by an unpaired, 2-tailed, Student's t-test. Difficulties associated with low lymphocyte recovery (following separation from monocytes and washing steps after calcein AM-labelling), and the need for pre-treatment with IL-2, precluded repetition of the migration assay.

5.4.6.2 Jurkat cell migration to CXCL10

No significant migration of Jurkat cells was observed at 0.25-2µg/ml CXCL10, either with, or without, prior treatment with 10ng/ml IL-2 for 6 days (data not shown).

Figure 5.11 Fold increase in mean migration of THP-1 cells to cleaved and intact CCL2

*Migration of THP-1 cells was measured to intact CCL2, with and without a CCL2 blocking antibody, and CCL2 incubated for 48hr with either APMA, MMP2, MMP9, or with CD26 for 6h, and then passed through Microcon® YM50 filters. All CCL2 samples were diluted to 200ng/ml in RPMI + 0.1% HSA, and tested in triplicate in a 24-well plate, using calcein AM (1μM)-labelled THP-1 cells (in RPMI + 0.1% HSA), in fibronectin-coated inserts for 3h duration, at 37˚C. Fluorescence was measured at 535nm from the bottom of the 24-well plate every 15min, and the migration indices of each chemoattractant calculated. Error bars represent SEM. Results from Student's t-tests comparing cleaved, blocked, and control CCL2 to intact CCL2 (incubated with APMA) are shown for each timepoint, where *=P<0.05, **=P<0.01 and ***=P<0.001. Compared to intact CCL2, by the first 15min, migration was significantly reduced to CCL2 cleaved by MMP2 (P<0.01), MMP9 (P<0.001) and CD26 (P<0.01). Significant differences were eradicated by 45min for CCL2 cleaved by MMP2, by 60 min for migration to CD26-cleaved CCL2, and by 75min for MMP9-cleaved CCL2.*

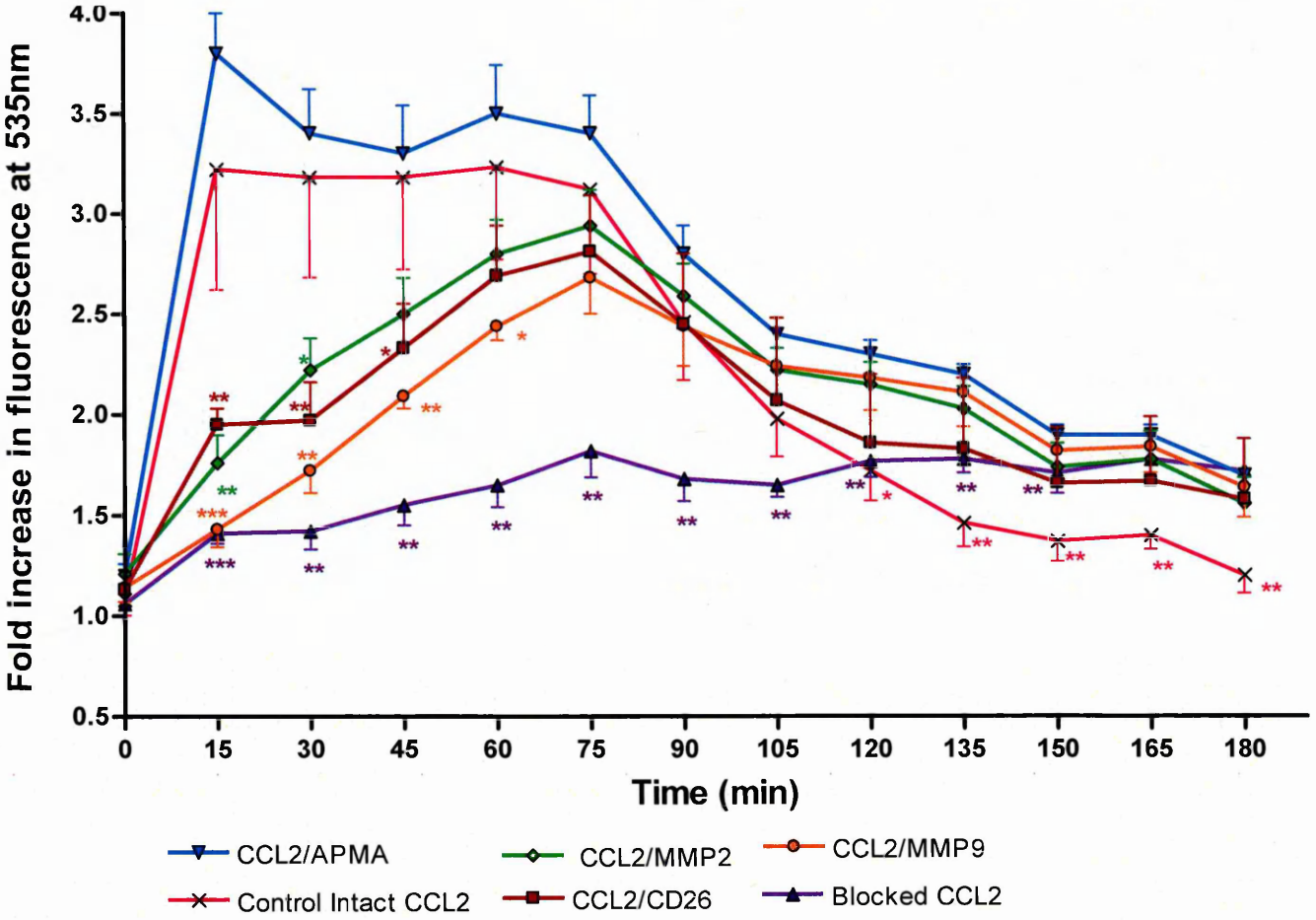
Fold increase in fluorescence at 535nm
4.0
3.5
3.0
2.5
2.0
1.5
1.0
0.5
0
15
30
45
60
75
90
105
120
135
150
165
180
Time (min)
CCL2/APMA
CCL2/MMP2
CCL2/MMP9
Control Intact CCL2
CCL2/CD26
Blocked CCL2

5.5 Discussion

5.5.1 Optimisation of the migration assay

Trans-well inserts are widely used in the study of chemotaxis of cells, for research into metastasis and inflammation, amongst others. These assays are time-consuming, and prone to operator error due to the manual fixation, staining, and counting of cells required. In addition, they do not allow measurement at more than one time point due to destruction of the sample. Detection of cells by fluorescence offers easy analysis, but is not easy to incorporate in traditional migration assays. The migration assay using FluoroBlok™ fluorescence-blocking inserts, optimised as part of this project, proved successful at measuring cell migration in real time, enabling comparison of enzymatically-cleaved CCL2 with the intact form. It offered a number of advantages over traditional Boyden chamber methods, as data acquisition was rapid, it offered good sensitivity with low cell numbers, and variation and errors were minimised as the inserts did not have to be manipulated to allow collection of data at various time points. The use of real-time monitoring proved a very useful tool, as the kinetics of migration vary according to the cell type, and choosing a single time point could give misleading results. *In vitro* models of migration can be used to demonstrate directional migration of leukocytes in response to a soluble chemotactic gradient, but it is important to remember that conditions *in vivo* include shear flow forces that normally prohibit formation of stable chemokine gradients within the vascular lumen.

Fibronectin-coated inserts were used in migration assays, as this glycoprotein promotes cell adhesion and motility (Yamada, 2000). Enzymatic digestion of fibronectin can yield a 120 kDa fragment, which has been shown to induce monocyte chemotaxis (Clark *et al.*, 1988). Potential variation caused by fibronectin digestion in trans-well inserts emphasised the need to remove enzymes from the cleaved chemokines used in assays, which was achieved by the use of ultrafiltration using Microcons®.
Of particular interest in this current study are the findings of Sobel and Mitchell (1989), who identified a significant increase in fibronectin in blood vessel walls of active, but not inactive, MS plaques. The degree of inflammation in MS was seen to correlate with fibronectin levels, active plaques possessed extracellular fibronectin, and the fibronectin receptor was found on macrophages (Sobel and Mitchell, 1989). Fibronectin is not typically a membrane protein, and normally forms cell surface fibrillary networks between adjacent cells and substrata (Hynes *et al.*, 1979). In MS, fibronectin may be secreted by, or deposited on, ECs and macrophages in the CNS, and might encourage PBMC migration (Sobel and Mitchell, 1989). Accordingly, it is highly relevant to include

fibronectin in a migration assay whose findings will be considered in the context of potential effects in MS.

Very recently, Czepluch and colleagues (2007) reported that pre-labelling monocytes with calcein AM (5μM) decreased their adherence to plastic and reduced overall migration to TGF-β1 and fMLP, although size and viability were not affected. This conflicts with previous reports that claim calcein AM has only negligible effects on cellular functions (Weston and Parish, 1990), but effects on chemotaxis (Abbitt *et al.*, 2000) and adhesion (De Clerck *et al.*, 1994) were assessed for lymphocytes or neutrophils, rather than monocytes. Abbitt and colleagues tested various fluorescent dyes for their effects on adhesion and migration of leukocytes, and concluded that whilst acridine orange interfered with adhesion, and rhodamine 6G inhibited mononuclear cell migration, calcein AM was not found to significantly affect the capture and migration phases of any leukocytes. Preliminary comparisons of unlabelled and labelled PBMC migration to BSA performed as part of this project suggest that even relatively high concentrations (6μM) of calcein AM used in labelling do not significantly hinder the migration process. Moreover, a low concentration of calcein AM (1.5μM) was used in migration assays in the present study. This warrants further investigation using THP-1 and Jurkat cells, however, as dyes can cause concentration-dependent alterations on the different stages of adhesion and migration, which vary according to the cell type and receptors involved.

Calcein AM was considered suitable for use in this study as it labels cells to high fluorescence intensity, in a persistent fashion, and it has previously been used for migration studies (Chiba *et al.*, 1998). In the current study, numbers of labelled cells correlated well with fluorescence values, demonstrating a linear relationship, thereby enabling calculation of the numbers of migrated cells from a standard curve. Increases in fluorescence with time were seen for all samples, however, and in the absence of chemokine, this could be explained by random chemokinesis of cells. It is also possible that small amounts of calcein were released from cells with time, particularly if they were dying, but cell viability was found to be well maintained during the time course of the assay.

It was initially thought that fMLP would be useful as a positive control in migration experiments, which would demonstrate the assay was working. Surprisingly, no migration was observed to fMLP, as fluorescence values generated by migrated THP-1 cells were lower when exposed to this, than to RPMI alone. This might be explained by the findings of Resnati and colleagues (2002), that fMLP inhibits THP-1 migration by

interfering with the uPA-associated chemotactic response in THP-1 cells and human monocytes.

5.5.2 *In vitro* cell migration assays to CCL2 and CXCL10

Results from this chapter are summarised in Table 5.1. Migration of THP-1 cells to CCL2 occurred rapidly, with maximum migration demonstrated at 15min when intact CCL2 was assessed. This result is considerably faster than the migration of monocytes across a model endothelial monolayer, observed by Hardy and colleagues (2004), where a significant level occurred within 60min of addition of CCL2. Results from migration assays described in this chapter demonstrate a significant delay in achieving the maximum fold increase in migration of THP-1 cells when cleaved CCL2 was assessed, as this occurred at 75min for all truncated isoforms present, compared to 15min for full-length CCL2. At 15min, the fold increases in migration to all truncated CCL2 isoforms were approximately half that seen with the full-length version. All significant differences between cleaved and intact forms of CCL2 were eliminated at 75min, suggesting that proteolytic processing may be most important in regulating the initial stages of cellular infiltration *in vivo.* As CD26 was shown to cleave CCL2 almost completely within 30min (Chapter 2), this enzyme stands out as being instrumental in rapidly reducing the chemotactic potential of CCL2.

Results using THP-1 cells in migration assays to cleaved and intact CCL2 reported here (Table 5.1) are in agreement with previous findings that loss of residues from the N-terminus of CC chemokines often reduces their chemotactic potential (reviewed in Wolf *et al.*, 2008). Moreover, McQuibban *et al.* (2002) reported that injection of the 5-76 isoform of CCL2 demonstrated reduced cell migration in an inflammatory *in vivo* model, by inducing a 66% reduction in the increase of oedema in rat paws following injection with carrageenan. They also reported a similar reduction in paw volume following injection of an engineered form of CCL2 (9-76). It is interesting to note that McQuibban concluded that MMP2 failed to cleave CCL2, reporting instead production of the 5-76 isoform following processing by MMPs 1, 3, and 8, although the CCL2 in their study was generated using chemical synthesis and folded via air oxidation.

The striking similarity in THP-1 cell migration patterns seen in the current study (Table 5.1) in response to CCL2 cleaved by MMPs 2 and 9, and CD26, suggest that chemotactic ability is reduced by the same extent, irrespective of whether 2 or 4 N-terminal residues are lost.

Table 5.1 Summary of results from cell migration assays to cleaved and intact CCL2 and CXCL10

	INTACT CCL2	MMP2-CLEAVED CCL2 *5-76	MMP9-CLEAVED CCL2 *5-76	CD26-CLEAVED CCL2 *3-76
THP-1 cells	3-3.5 fold ↑ in migration within 15min, reducing gradually after 75min, to no detected migration at 3h	Significant ↓ in migration from 15-75min, compared to intact CCL2. Greatest ↓ seen at 15min (~50% ↓ in migration, compared to intact CCL2)	As for MMP2-cleaved CCL2	As for MMP2-cleaved CCL2
	INTACT CXCL10	**MMP2-CLEAVED CXCL10 *6-73**	**MMP9-CLEAVED CXCL10 *5-73**	**CD26-CLEAVED CXCL10 *3-77**
Lymphocyte-enriched population from PBMCs	No significant migration after short-term IL-2 + PHA treatment (data not shown)	NT	NT	NT
Jurkat cells	No significant migration after short-term IL-2 treatment (data not shown) Preliminary data (after long-term IL-2 treatment) indicated slight ↑ in migration (data not shown)	Preliminary data (after long-term IL-2 treatment) indicated slight ↑ in migration compared to intact CXCL10 (data not shown)	Preliminary data (after long-term IL-2 treatment) indicated slight ↑ in migration compared to intact CXCL10 (data not shown)	Preliminary data (after long-term IL-2 treatment) indicated no change in migration compared to intact CXCL10 (data not shown)

NT = not tested; ↑ *= increase;* ↓ *= decrease*

** Amino acids remaining after processing*

Preliminary data obtained following long-term treatment of Jurkat cells with IL-2 indicated that cleavage of CXCL10 by CD26 does not alter its chemotactic potential, but MMP2 or MMP9 truncation of CXCL10 may lead to a slight increase in Jurkat cell migration after 1h and 4h respectively, compared to intact CXCL10 (data not shown). This warrants further investigation, and may be linked to loss of residues from the C-terminus of CXCL10, as truncation of both the N- and C- termini were reported with MMPs 2 and 9, whereas CD26 cleaved solely at the N-terminus (reported in Chapter 2). Previously, N-terminal cleavage of CXCL10 by CD26 was reported to result in a 30-fold decrease in lymphocyte chemotaxis, generating a CXCR3 antagonist (Proost *et al.*, 2001). Due to the extremely rapid and highly specific processing of CXCL10 by CD26 (see Chapter 2), it is prudent that the effects of this truncation are investigated further.

Assessment of Jurkat cell migration to CXCL10 proved to be problematic, despite utilisation of several chemokine concentrations, pre-treatment of cells with PHA and IL-2, demonstration using flow cytometry of a high CXCR3 receptor density on the membrane of Jurkat cells, and extension of the assay length to account for potentially slower migration than was demonstrated using THP-1 cells to CCL2.

When lymphocyte-enriched cell populations from PBMCs were used in migration assays, it was possible that CXCR3 receptor expression was low, a factor that warrants further investigation. Resting and short-term TCR-activated (e.g. with PHA) T cells have been reported to lack expression of transcripts for CXCR3 and other inflammatory receptors, in contrast to homeostatic chemokine receptors, such as CXCR5. I*n vitro* investigations demonstrated that receptor expression and responses to inflammatory chemokines were strongly dependent on IL-2 (Loetscher *et al.*, 1996). IL-2 has been shown to enhance the cytotoxicity and antigen-specific proliferation of T cells (Waldmann *et al.*, 1993). Resting lymphocytes constitutively express the β- and γ-chains of the IL-2 receptor, but the α-chain, necessary for formation of the high-affinity receptor, is evident only after T cell activation (Waldmann, 1991).

IL-2 is considered a major regulatory factor of lymphocyte migration *in vivo*, and it is thought it activates and expands $CD45RO^+$ T cells for recruitment to inflammatory sites (Loetscher *et al.*, 1996). Loetscher and colleagues (1996) reported that IL-2 was essential for lymphocyte migration and receptor expression involving CC chemokines, and that their migratory responsiveness was lost if IL-2 was removed. Their research also demonstrated that use of PHA when culturing lymphocytes delayed the effects of IL-2, as migration to CCL2 and CCL5 was only observed after 9 days of culture, instead of 4 days. If the same delay after PHA/IL-2 treatment occurs with lymphocyte

migration to CXCL10, Loetscher's findings could explain why the assay described in this thesis, performed after 6 days of dual treatment, failed to demonstrate any significant migration in lymphocytes. The situation is further complicated, as prolonged administration of IL-2 stimulates apoptosis of activated T cells (Lenardo *et al.*, 1999). Reports of the duration of lymphocyte culture with IL-2 necessary for maximal CXCR3 expression vary, from 10 days (Loetscher *et al.*, 1998), to 3 weeks (Cheeran *et al.*, 2003), and further work is needed to optimise the use of IL-2 treatment prior to the migration assays used here.

There is substantial evidence that migrating lymphocytes respond to CC rather than CXC chemokines, and that a $CD45RO^+$ phenotype of T cell are predominantly involved (Carr *et al.*, 1994). Indeed, Roth and colleagues (1995b) found that CC chemokines stimulated transendothelial chemotaxis of lymphocytes, but CXC chemokines (including CXCL10), did not. It would, therefore, be of interest to extend the current study to include Jurkat cell and lymphocyte migration assays to intact and cleaved CCL2.

It is possible that each combination of experimental conditions using Jurkat cells or lymphocytes contained some prohibitive element, such as a cell density that was too high, or too low. Cell migration is affected by many parameters in an *in vitro* system, with cell concentration being a very important factor. Fibroblasts, for example, have demonstrated migration behaviour that depended on their distance to surrounding cells, with increases in both speed and distance travelled when seeded at a low density (Raeber *et al.*, 2007). It is thought that high cell densities can be inhibitory for a number of reasons, including an increase in cytokines, blocking of adhesion sites by integrin fragments remaining from previously migrated cells, and cell-cell contacts causing contact inhibition (Huttenlocher *et al.*, 1998).

A further factor that may account for the lack of cell migration to CXCL10 reported in the current study is the absence of shear stress in the assay system used. Cinamon and colleagues (2001) found that lymphocytes only engaged in transendothelial migration to CXCL12 or CCL19 when continuous exposure to shear forces was applied. They deduced that the shear stress triggered mechanoresponsive elements on lymphocytes, which combined with chemokine signals to facilitate migration. Under shear flow conditions, stimulation of leukocyte integrins by apical chemokines was shown to be essential for cell adhesion. *In vivo*, apical immobilised chemokines may act alone, or with subendothelial chemokines, to promote transendothelial migration.

Chapter 6

General discussion

6.1 Chemokines in MS pathogenesis

MS is often described as an inflammatory demyelinating disease, characterised by the formation of plaques in the white matter of the CNS. Mechanisms involved in the pathogenesis of MS are complex and varied, resulting in a wide assortment of clinical manifestations. Current treatments have very limited benefit once the disease has entered the progressive phase, necessitating closer scrutiny of the pathology and immunology in an attempt to identify new targets for therapeutic intervention (Lassmann, 2007). The present study attempted to elucidate the involvement of cleavage of the chemokines, CCL2 and CXCL10, in the inflammatory process in MS, which may warrant further investigation as potential targets for drug development.

The extensive chemokine system is responsible for cell homing during homeostasis and inflammation, and contributes to regulation of many functions, such as angiogenesis, tumour growth, and haematopoiesis. The diverse actions of chemokines, and the redundancy that exists in the receptor and ligand system, emphasise the need for strict regulation of chemokine activity. Proteolytic cleavage can control chemokine activity by increasing or reducing the chemotactic response, and also by altering receptor selectivity (reviewed in Wolf *et al.*, 2008). Proteases such as MMPs and CD26 are known to cleave chemokines, and are often induced by the same stimuli, and produced in the same microenvironment as chemokines. This simultaneous production of chemokines and proteases may be designed to facilitate rapid regulation of chemokine activity. It is important to remember that proteolytic processing of chemokines is only one method of regulating chemokine activity, existing alongside control via gene expression, variations in chemokine secretion and storage (Catalfamo *et al.*, 2004), interactions with GAGs (that create elevated local chemokine levels and offer potential protection from digestion) (Proudfoot, 2006), binding to non-signalling decoy receptors, such as D6 (Comerford *et al.*, 2007), and regulation of chemokine receptor expression (e.g. via internalisation) (Marchese *et al.*, 2003).

CCL2 is principally involved in recruiting monocytes and T cells (Conti and Rollins, 2004), and CXCL10 attracts T cells (Flier *et al.*, 2001), with both cell types being major contributors to MS pathogenesis. Previous studies have revealed the expression of CCL2 and CXCL10 by astrocytes, and detected them in abundance in MS lesions (Simpson *et al.*, 1998 and 2000b), but not in normal control brain, strongly indicating that these chemokines are very important in the disease process. Indeed, chemokines and their receptors have often been considered as potential therapeutic targets to reduce leukocyte trafficking in MS and other inflammatory disorders (Proudfoot *et al.*, 2003). As CXCL10 is induced by a cytokine profile indicative of chronically inflamed

lesions (e.g. by IFN-γ), it is possible that CXCL10 exerts its maximum effects during the later stages of MS pathogenesis, when rapid recruitment of immune cells is no longer pivotal (Oynebraten *et al.*, 2004). Understanding the precise mechanisms of how the inflamed CNS recruits PBMCs in MS is particularly important, as preventing normal leukocyte trafficking pharmacologically can have unforeseen consequences. This was demonstrated by the development of progressive multifocal leukoencephalopathy (PML), a lethal infection of the CNS, in three MS or Crohn's patients treated with natalizumab, a monoclonal antibody against integrins on PBMCs (Berger and Koralnik, 2005).

Secretion of CCL2 by astrocytes has previously facilitated use of astrocyte supernatant as the chemoattractant source in THP-1 cell migration assays (Lehmann et al., 2006). In Chapter 2, truncated forms of CCL2 and CXCL10 were identified using mass spectrometry and gel electrophoresis, following processing by recombinant enzymes. The same techniques were then applied to assess primary human astrocytes for the presence of truncated chemokines, in a quest to subsequently utilise supernatants containing cleaved chemokines in monocytic and T cell migration assays. Since a concentration of 200ng/ml CCL2 was found to be optimal for THP-1 cell migration assays (Chapter 5), the levels of CCL2 (~9ng/ml) and CXCL10 (~1.9ng/ml) (Suliman *et al.*, 2006) in astrocyte supernatant following cytokine treatment were too low to be assessed for chemotactic potential. In addition, sample volumes used in mass spectrometry were not sufficient to enable detection of either intact or cleaved CCL2 in astrocyte supernatant (Chapter 3).

6.2 Proteases in multiple sclerosis

Enzymes such as MMPs are found at elevated levels in patients with MS (Agrawal *et al.*, 2008). They are important in MS pathogenesis as they contribute to the breakdown of the BBB, can cause neuronal death and axonal damage, and can cleave chemokines (Yong *et al.*, 2007b). MMP2 and MMP9 received particular focus in this investigation, as previous studies have consistently demonstrated their upregulation in MS, especially MMP9 (Yong *et al.*, 2007b). Increased expression of MMP2 and MMP9 has been reported in lymphocytes and macrophages around PVCs, and high MMP9 levels have been found in lesions (Lindberg *et al.*, 2001). Brain ECs also express MMPs 2 and 9 (Harkness et al., 2000). The current analysis of mRNA expression of MMP2 and MMP9 by TaqMan® PCR (Chapter 3) found high levels of MMP2 mRNA in all astrocyte samples analysed, consistent with constitutive MMP2 expression (Leveque *et al.*, 2004), and an increase in MMP9 mRNA expression in astrocytes

following treatment with TNF and IL-1β, which is in agreement with reports that MMP9 is increased in the pro-inflammatory environment of MS lesions (Yong *et al.*, 2007b).

The T cell activation molecule, CD26, which possesses ectopeptidase activity and is known to cleave dipeptides from polypeptides with a proline or alanine at the penultimate position, is also implicated in the pathogenesis of MS (Aytac *et al.*, 2001). Levels of CD26 in the peripheral blood and CSF have been shown to correlate with disease activity in MS (Krakauer *et al.*, 2006), and as chemokines can be cleaved by CD26, this molecule warranted investigation in this study. Information about CD26 expression in the human brain is scarce, but using immunohistochemistry, it was present in all white matter samples examined (Chapter 4). Increased CD26 levels were found in MS brain, compared to control brain. This increase is in agreement with findings detailing higher levels in MS of peripheral $CD26^+CD4^+$ T cells (Krakauer *et al.*, 2006) and $CD26^+CD8^+$ T cells (Jensen *et al.*, 2006), but it was clear in the current study that not all T cells present in lesions were $CD26^+$, and some HLA-DR^+ cells (macrophage/microglia) were also $CD26^+$. Previous studies in MS have shown that the majority of T cells in the CSF and the perivascular space are $CD4^+$, whereas those that infiltrate tissue are $CD8^+$ (Woodroofe *et al.*, 1986). $CD26^+$ cells were found in PVCs and also in the parenchyma of white matter from MS brains.

6.3 Chemokine and protease interactions

Recruitment of immune cells to inflammatory sites is dependent on the interactions of chemokines with their receptors. Alterations in the structure of a chemokine can dramatically affect its ability to bind to receptors, and thus functional activity, particularly if amino acids at the N-terminus of the chemokine are involved (Fig. 6.1). This study has focussed on chemokine processing by MMP2, MMP9, and CD26, but it is important to remember that numerous other enzymes may produce truncated forms. Elastase, for example, is released from activated monocytes (Wolf *et al.*, 2008). In addition, chemokines can be cleaved in their core regions, such as the inactivation of CCL20 when exposed to cathepsin B (Hasan *et al.*, 2006).

The effects of chemokine processing are largely unpredictable, rendering it important to investigate the effects on activity of each enzymatic cleavage individually. In addition to effects on receptor activation, truncated chemokines can occasionally exhibit unexpected biological responses that are independent of chemokine receptors (Zhang *et al.*, 2003).

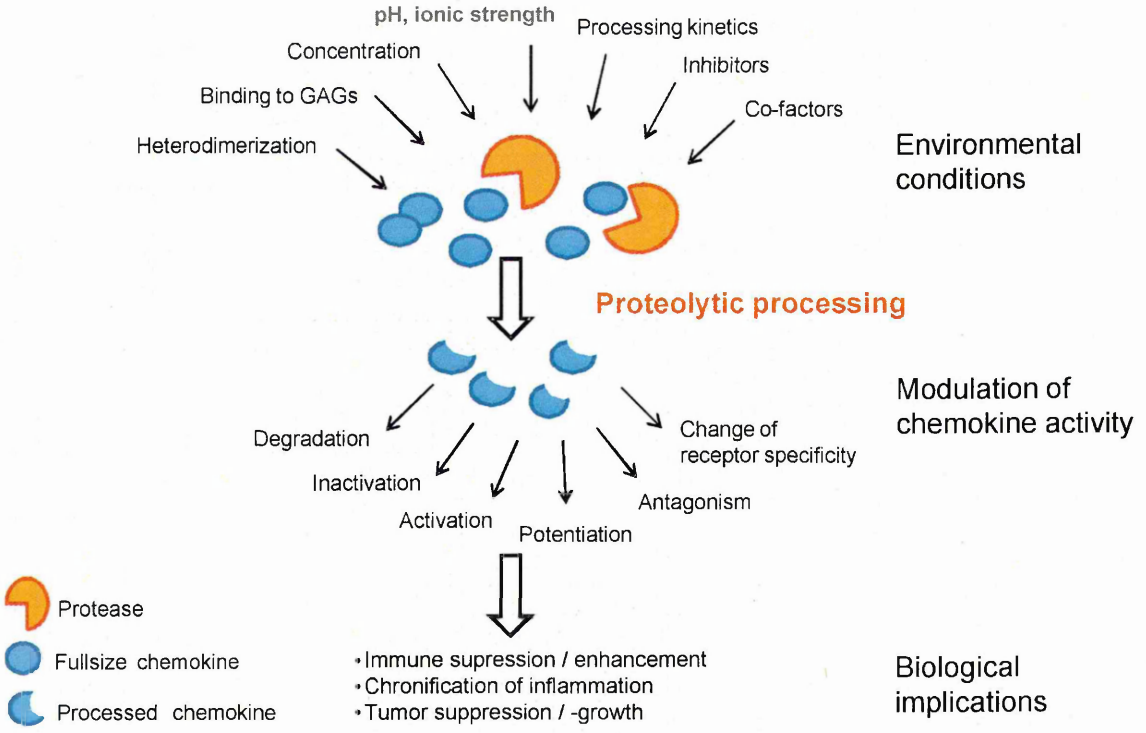

Reprinted from (Wolf *et al.*, 2008) © (2008), with permission from Elsevier.

Figure 6.1 Proteolytic processing of chemokines

Many factors influence the cleavage of chemokines by proteases such as MMPs and CD26. Truncated chemokines can have decreased or enhanced activity, and altered receptor specificity. The altered function of proteolytically processed chemokines can influence the outcome of the biological response, and potentially affect the disease process.

MMP2 processing of CXCL12 at the N-terminus, for example, generates a highly neurotoxic form involved in neuronal apoptosis, resulting in neurodegeneration (Zhang *et al.*, 2003).

Interactions between chemokines and proteases should not be considered as one-way processes. Chemokines can modulate protease expression, as is seen by the stimulation by CCL2 of MMP9 expression in macrophages (Balkwill, 2004), and its regulation of MT1-MMP expression in ECs (Son *et al.*, 2006). Other protease activities, such as shedding of GAGs bound to the ECM, will affect chemokine actions by abolishing their ability to be retained on cell surfaces at high local concentrations (Proudfoot, 2006).

Protease-chemokine interactions warrant further investigation, as their complexities may reveal details pivotal in understanding the disease process, and the immune response might be substantially heightened or dampened depending on the activation or inactivation of chemokines processed by proteases released from infiltrating immune cells and surrounding cells. Chemokine cleavage has implications in many disease processes. It has been hypothesised, for example, that proteases upregulated in cancer might selectively cleave chemokines, thereby inactivating them and driving a preferred route of metastasis (Mohamed and Sloane, 2006).

This present study has expanded the current knowledge of truncated forms of these chemokines that might be formed naturally by enzymatic processing in the inflammatory environment of MS, and investigated the potential effects of this truncation on the ability to attract monocytes and T cells.

6.3.1 N-terminal processing of chemokines

Forms of chemokines truncated at the N-terminus have been found naturally, which focussed the earliest studies of proteolytic processing of chemokines on this region. Indeed, CXCL7 and CCL14 need to be N-terminally truncated to become active. N-terminal processing is common due to the exposed and conformationally disordered nature of this terminus of chemokines (reviewed in Wolf *et al.*, 2008).

Approximately one third of human chemokines have a proline in the penultimate position at the N-terminus, making them candidate substrates for CD26. This region is not considered to be available for processing in many such chemokines, however, due to modification by pyroglutamate (Struyf *et al.*, 2003). Indeed, this pyroglutamatic acid residue protection from N-terminal cleavage by CD26 has been observed with CCL2

(Van Coillie *et al.*, 1998). In the current study, CCL2 was susceptible to CD26 cleavage as the recombinant CCL2 utilised had a glutamine as the N-terminal residue. This demonstrates that discrepancies may arise when considering chemokine substrates occurring *in vivo*, and recombinant forms obtained from *E.coli*.

Several CC chemokines, including CCL2, have been shown to have strict requirements for an intact N-terminus for their biological activities to be fulfilled (Proost *et al.*, 2006). This study supports this result for CCL2, as MMP2 and MMP9 cleaved 4 residues from the N-terminus, and CD26 cleaved a dipeptide, with all truncated forms showing a reduction in their ability to attract THP-1 cells. In addition to the reduced receptor binding and signalling capabilities that often result from N-terminal truncation of CC chemokines, the shortened forms can act as chemotaxis antagonists (McQuibban *et al.*, 2002). The negative regulatory effects of N-terminal processing of CCL2, for example, contrast with the more commonly minor effects on biological activity created by C-terminal truncation, or glycosylation (Proost *et al.*, 1998c).

Results from the current study confirmed that cleavage at the N-terminus is a regular occurrence, as CCL2 was processed by all three enzymes used. MMP2, MMP9, and CD26, removed five, four, and two residues, respectively, from the N-terminus of CXCL10. Truncated forms of CXCL10 lacking two and five N-terminal residues have been found naturally (Hensbergen *et al.*, 2004). N-terminal cleavage of CXCL10 by MMPs 2 and 9 has not previously been reported elsewhere. The mass spectrometric finding of this study indicated that the cleavage of an N-terminal dipeptide from CXCL10 by CD26 is in agreement with previous findings (Proost *et al.*, 2001), although the impaired activity and role of this truncated form as a CXCR3 antagonist remains to be established.

Cleavage at the N-terminus of inflammatory CXC chemokines with an ELR motif often results in an increase in their activity (Proost *et al.*, 2006). Contrastingly, removal of amino acids from the N-terminus of CXC chemokines without an ELR motif, such as CXCL10, has been shown to reduce chemotactic potential (Proost *et al.*, 2001). Impaired receptor binding and signalling properties of CXCR3 ligands truncated by CD26 have been shown, together with simultaneous retention of the anti-angiogenic activity of CXCL10 *in vivo* (Proost *et al.*, 1993). It is important to consider that MMPs 2 and 9 appeared to simultaneously cleave 4 amino acids from the C-terminus of CXCL10 in the current study, generating a form of CXCL10 altered at both termini.

6.3.2 C-terminal processing of chemokines

Few studies have reported proteolytic processing of chemokines at the C-terminus, but it is generally considered to have minimal effects on activity (Hensbergen *et al.*, 2004). The C-terminus plays an essential role in direct antibacterial activity exhibited by some chemokines, such as CXCL7 (Krijgsveld *et al.*, 2000). CXCL10 has also been shown to have microbicidal activity independent of activation of CXCR3, but C-terminal truncation does not appear to affect this response (Cole *et al.*, 2001).

Analysis of mass spectrometric data from this study revealed that MMP2 and MMP9 cleaved 4 amino acids from the C-terminus of CXCL10. The C-terminally truncated form of CXCL10 was identical to one previously reported following processing by the enzyme furin, which has been isolated from natural sources (Hensbergen *et al.*, 2004). Previous studies have not confirmed the C-terminal cleavage of CXCL10 by MMP2 that was observed here.

This study found that MMPs 2 and 9 cleaved CXCL10 at both the N- and C-termini, and it would make an interesting comparison to assess the effects of processing of CXCL10 at both termini, with effects on chemotactic activity arising from truncation by CD26 at the N-terminus alone.

6.4 Implications of cleavage of CCL2 or CXCL10 in MS

There is no shortage of chemokines identified as substrates for proteases, but the relevance of their processing often remains undiscovered. The true situation *in vivo* can be difficult to establish, as chemokine availability and protease activity in a physiological environment will differ significantly from conditions created in *in vitro* digestion experiments. Chemokines can be completely degraded *in vitro*, for example, whereas tighter regulation *in vivo* would prevent this (Wolf *et al.*, 2008). By assessing the chemokines and proteases that have key roles in MS pathogenesis and are expressed in the same milieu, however, the results from this study may add to the understanding of cellular events that occur in the inflamed CNS.

This study has demonstrated the expression of CD26 in MS lesions, and the expression of MMPs 2 and 9 by astrocytes. All three of these enzymes have the ability to cleave CCL2 (with glutamine as the N-terminal amino acid), and CXCL10. Mass spectrometric detection of the processing of CCL2 and CXCL10 by CD26 indicated that it occurred very rapidly, taking only a few minutes, suggesting potential physiological significance. Previous studies indicate that CCL2 *in vivo* would be protected from cleavage by CD26 due to the N-terminal pyroglutamic acid residue (Van Coillie *et al.*,

1998), but this residue is thought to derive from glutamine and be formed just prior to cellular protein secretion, or as a post-translational event. Moreover, enzymes capable of removing pyroglutamic acid have been isolated from mammalian cells, where they have a ubiquitous distribution (Abraham and Podell, 1981). It is not improbable, therefore, that CCL2 can be cleaved by CD26, or MMPs 2 and 9, *in vivo*, as isoforms of CCL2 may exist with glutamine as the N-terminal residue, or the pyroglutamic acid may be removed by endogenous enzymes. N-terminal processing of CCL2 by MMPs 2 and 9, and CD26, produced a truncated form with a severely restricted ability to attract monocytic cells, and thus CCL2 cleavage would contribute to abrogation of the damaging inflammatory response. This is of particular relevance in MS, as CCL2 attracts both monocytes and T cells. Pharmacological inhibition of MMP2, MMP9, or CD26, could, therefore, eliminate this beneficial effect of CCL2 truncation, but administration of a drug based on N-terminally cleaved CCL2 could be advantageous in reducing overall immune cell infiltration across the BBB, and further inflammation in lesions, by competing with native intact CCL2 for CCR2.

Similarly for CXCL10, once the effects of proteolytic processing are confirmed, implications and possible therapeutic targets could be identified. As CXCL10 was processed even more rapidly than CCL2 by CD26, and at both termini by MMPs 2 and 9, perhaps regulation of CXCL10 activity is more relevant, particularly as MS is considered a T cell-driven disease.

6.5 Summary

Chemokines are implicated in the pathogenesis of MS both through their induction of protease release, and their ability to attract immune cells across the BBB. Proteases can then process the chemokines that induced them, with N-terminal processing altering chemokine receptor interaction, with ensuing increases or decreases of biological activity. The principal findings of this study concerning chemokine-protease interactions are summarized in Figure 6.2.

The role reversals that can occur as a result of chemokine cleavage demonstrates the importance of simultaneously detecting proteases and chemokines when considering the pathogenesis of diseases. Proteases not only assist with leukocyte migration across the BBB in MS, but also regulate this infiltration of the CNS by modifying chemokine activity. The presence of chemokine antagonists that occur naturally following their proteolytic cleavage provide interesting avenues for exploration in drug design to treat not just inflammatory diseases such as MS, but also AIDS and cancer.

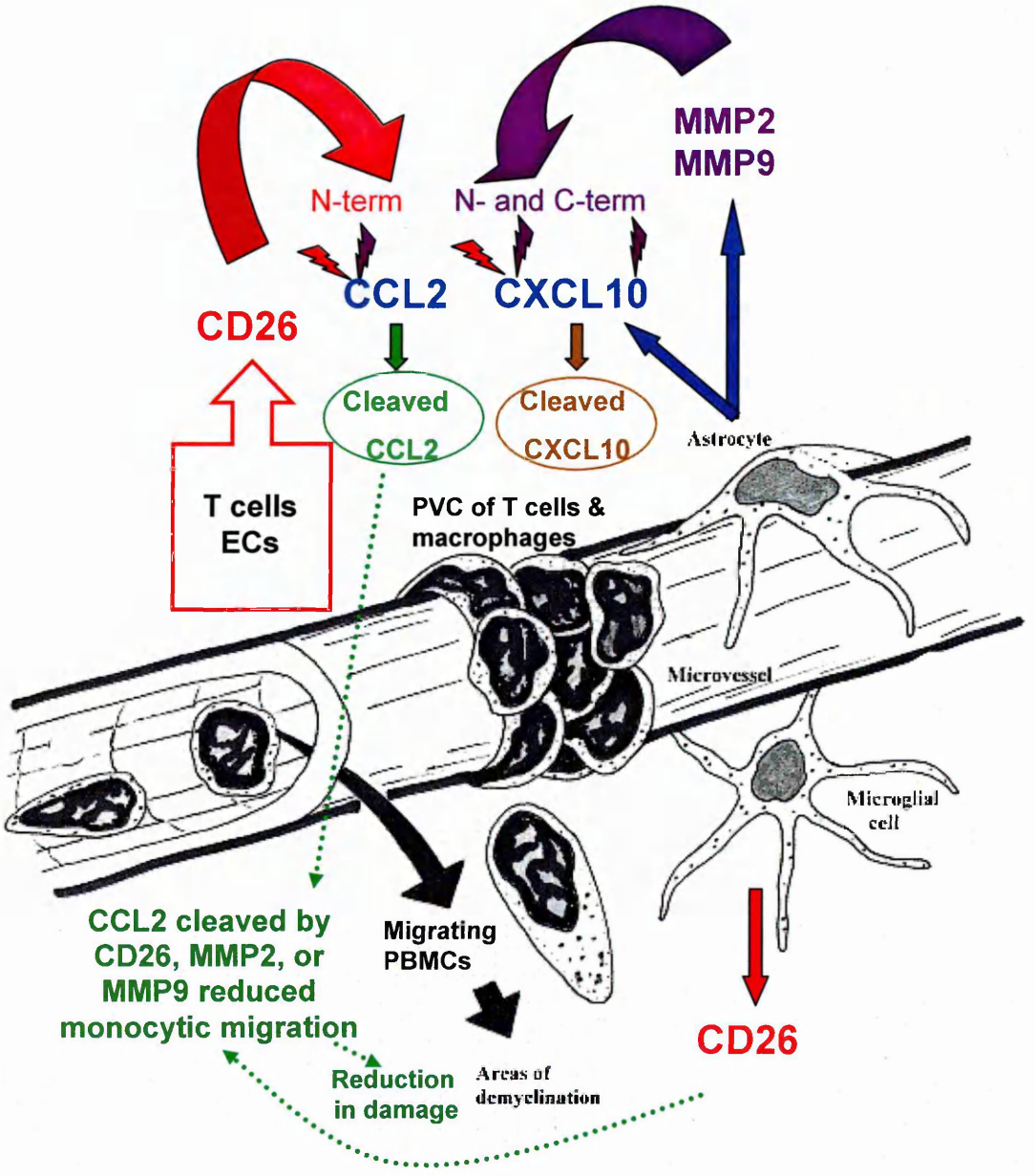

Adapted from (Alun Brown., 2001), © (2001), with permission from Elsevier 2001

Figure 6.2 Schematic summarising principal findings of this study and potential implications for MS pathogenesis

Chemokines CCL2 and CXCL10, and the proteases MMP2 and MMP9, are expressed by astrocytes in contact with CNS blood vessels. CD26 is expressed as a cell-surface peptidase on activated T cells in peripheral blood, and was demonstrated on T cells and microglia/macrophages in PVCs and the parenchyma of MS lesions. Each enzyme cleaved CCL2 and CXCL10 at the N-terminus. CXCL10 was also cleaved by MMPs 2 and 9 at the C-terminus. Cleaved CCL2 reduced migration of THP-1 cells, which may have implications for the in vivo inflammatory environment in MS.

Proteolytic processing by CD26 ( ) or MMP2/9 ( )

6.6 Further work

Astrocytes are known to express CCL2 (Simpson *et al.*, 1998), CXCL10 (Simpson *et al.*, 2000b), and MMPs -2 and -9 (Gottschall and Deb, 1996), with implications for MS pathogenesis. This formed the rationale for investigating the effects of proteolytic processing on these two chemokines, as the loss of only a few residues has previously been demonstrated to radically alter chemokine activity (reviewed in Wolf *et al.*, 2008). CD26 has also been implicated in MS, and is known to cleave several chemokines (Mentlein, 1999), and was thus similarly examined. Experiments were performed using recombinant proteins purchased externally. Further studies could involve the use of expression vectors and protein purification to generate the chemokines and proteases required, thereby producing a greater supply at lower cost.

Previous reports led to an expectation that CCL2 would not be cleaved by MMP2 (McQuibban *et al.*, 2002), and the effect of MMP9 was unknown. Both MMP2 and MMP9 preferentially cleave proteins at sites with a hydrophobic residue immediately upstream, which suggested that CCL2 might be a substrate of these MMPs, however, due to possessing Ile as the fifth residue at the N-terminus (Seltzer *et al.*, 1990). As CCL2 has a proline as the penultimate residue, it was a likely substrate for cleavage by CD26, although previous reports have shown this not to be the case *in vivo* due to a protective pyroglutamic acid as the N-terminal residue (Iwata *et al.*, 1999). Results from this current *in vitro* study revealed that CCL2 was cleaved at the N-terminus by MMP2, MMP9, and CD26. The effects of this processing were expected to substantially reduce chemotactic activity, as the isoform of CCL2 generated following N-terminal removal of four residues by MMPs 1, 3, and 8, had previously been shown to lack activity when used in trans-well migration assays with THP-1 cells (McQuibban *et al.*, 2002). Results from the current study concurred with this reduction in chemotactic potential of cleaved CCL2, although activity was not completely lost. Further work could be done to assess whether the reduction in chemotaxis was due to reduced receptor binding of cleaved CCL2, or if the truncated form acts as a receptor antagonist.

CXCL10 has previously been shown to be a substrate of CD26 (Proost *et al.*, 2001), with the loss of an N-terminal dipeptide also being demonstrated in this study. Van den Steen *et al.* (2003) demonstrated C-terminal processing of CXCL10 by MMP9, which resulted in degradation after prolonged exposure. Results from the current study confirmed C-terminal processing of CXCL10 by MMP9, but also revealed limited N-terminal cleavage, and contrastingly, some intact CXCL10 remained after a comparable duration of MMP9 exposure. The effects of MMP2 on CXCL10 were

previously unknown, but results presented here suggest that MMP2 processes CXCL10 at both the N- and C-termini, and may culminate in complete degradation of the chemokine after 72h. It was anticipated that cleaved CXCL10 would demonstrate reduced activity, based on evidence from previous studies (Van Damme *et al.*, 2004), but problems encountered in the current study prevented conclusions as to the effect of processing of CXCL10 on chemotaxis.

The activity of cleaved forms of chemokines was assessed using an *in vitro* migration assay, which lacked the shear forces provided by blood flow *in vivo*. It has been argued that shear stress is required for facilitation of cell migration (Cinamon *et al.*, 2001), which may partially account for some of the negative results described here. There were particular difficulties associated with investigating the chemotactic activity of CXCL10, however, such as the requirement to culture cells for several days in the presence of IL-2 to achieve high levels of functional expression of the receptor CXCR3 (Loetscher *et al.*, 1998), and the consideration that *in vivo*, oligomerisation of CXCL10 is necessary for its retention on the endothelium, and resulting chemotactic gradient (Campanella *et al.*, 2006). Further work could be done to optimise the migration assay performed in this study for use with CXCL10, such as perfecting the IL-2 treatment of the cells. Alternatively, a different T cell chemoattractant, such as CCL5, could be selected for further investigation, particularly as this is known to play a significant role in MS pathogenesis (Szczuciński and Losy, 2006). The long time course required to obtain significant levels of cleaved CXCL10 following incubation with MMPs -2 and -9 must also be considered critically, as such prolonged exposure is unlikely to be of relevance to the *in vivo* situation, in MS brain. CD26 processed CXCL10 within a few minutes, however, and it might be prudent to focus further studies of the significance of chemokine processing on rapid and highly specific interactions of this nature.

The use of natural forms of chemokines and proteases, derived from cells known to secrete them in the CNS, would be likely to yield results about chemokine processing that were highly relevant to the inflamed CNS. Mass spectrometry was used in the current study in an attempt to detect truncated chemokines in astrocyte supernatant. Difficulties encountered during sample preparation, whereby concentrating supernatant created a sample very rich in salts, limited the effectiveness of this approach. Ultracentrifugation or ultrafiltration techniques could be investigated for concentration of several litres of astrocyte supernatant (Russell *et al.*, 2007), followed by purification using high-performance liquid chromatography (HPLC) to obtain chemokines. Chemokines derived in such a way could then be used in cell migration assays, and also in digestion experiments with proteases derived from astrocyte supernatants or

MS brain tissue extracts. Further studies could also include the use of microglia for isolation of chemokines, and to screen for MMP expression. The use of chemokines derived from cell supernatants would help to minimise discrepancies that may occur between the processing of chemokines that occur naturally in the CNS, and recombinant forms derived from *E.coli*.

ELISA has traditionally been used to detect serum proteins, a method that requires appropriate monoclonal antibodies. Alternative techniques are being developed, which use surface-enhanced laser desorption ionisation (SELDI)-TOF MSpec, with protein chip arrays containing immobilised polyclonal antibodies (Favre-Kontula *et al.*, 2006). A study using a variant of CCL5 found that the SELDI-TOF method was able to detect protein modifications that would be missed by ELISA, namely being processed twice to truncated forms, and being oxidised in serum (Favre-Kontula *et al.*, 2006). The use of SELDI-TOF to detect cleaved chemokines in astrocyte supernatant could be explored.

The pilot data generated by screening astrocyte lysate samples for MMP mRNAs could be utilised to identify MMPs worthy of further investigation in chemokine processing experiments. Microglia express IL-1β (reviewed by Stock *et al.*, 2006), which may increase expression of some MMPs in the brain, as was suggested by results from the current study which showed an increase in the mRNAs of several MMPs, notably MMPs -1, -10, and -12, following treatment of astrocytes with IL-1β. The RT PCR investigations could be repeated several times, with a focus on only the MMPs found to be of interest in preliminary results, thereby enabling statistical analysis to be performed to identifiy significant differences in MMP mRNA expression that occur with cytokine treatment. Brain tissue samples, from both control and MS donors, could also be examined similarly for MMP mRNAs.

CD26 definitely warrants further investigation as to its role in MS pathogenesis. The study described in Chapter 4 could be extended to include more tissue blocks and NAWM from MS brains, in addition to dual labelling for T cell subsets, to further characterise the cellular distribution of CD26 in relation to MS lesions. Quantitative investigations of individual lesions would provide valuable information, whereby the number of $CD26^+$ T cells could be expressed as a percentage of the total number of T cells observed. It would also be interesting to perform dual label immunofluorescence to detect potential co-localisation of CD26 and the basal lamina, using an anti-laminin antibody.

Cell migration experiments could be expanded to incorporate culture of ECs and astrocytes on opposite sides of trans-well inserts (allowing astrocytic processes to contact ECs via 3μm pores), to more closely resemble the three-dimensional nature of the BBB (Eugenin *et al.*, 2006).

Appendix I

Fixation in paraformaldehyde (PFA)

0.2M Phosphate buffer

0.2M phosphate buffer was made by mixing solutions A and B below (pH to 7.2 once mixed).

Solution A: 11.36g Na_2HPO_4 was dissolved in 400ml dH_2O

Solution B: 3.2g $NaH_2PO_4.2H_2O$ in 100ml dH_2O

4% Paraformaldehyde

In a fume hood, 16g PFA was added to 100ml dH_2O and heated to 60°C. Drops of 2M NaOH were added until the PFA dissolved. dH_2O was added to give a total volume of 200ml and then 200ml 0.2M phosphate buffer was added and a pH of 7.2 reached. This solution was filtered prior to use and stored at 4°C for 2 weeks only.

Protein extraction buffers

2X Sample buffer

2.5ml 0.5M Tris-HCl pH6.8; 4ml 10% SDS; 2ml glycerol; 0.2ml β-mercaptoethanol; 0.2mg bromophenol blue; made up to 10ml with dH_2O and stored at 4°C.

Extraction Buffer

0.1475g Tris base; 0.7938g Tris-HCl; 0.09305g EDTA; in 250ml dH_2O

Appendix II

Protein and RNA extraction using TRI Reagent®

The following manufacturer's protocol from Sigma was used for extraction of RNA and protein from cells:

0.75ml of TRI Reagent® was mixed with 0.25ml of sample and the cells lysed (or cellular debris) by passing the suspension several times through a pipette. At least 0.75ml of TRI Reagent® per 5-10 x 10^6 cells was used. Samples were then stored at -80°C for up to one month if necessary, before completing the protocol below.

Phase Separation: To ensure complete dissociation of nucleoprotein complexes, samples were allowed to stand for 5min at RT. Chloroform (0.2ml of per 0.75ml of TRI Reagent® used) was added, the sample covered, shaken vigorously for 15 seconds and left to stand for 2-15min at RT. The resulting mixture was centrifuged at 12,000*g* for 15min at 4°C. Centrifugation separated the mixture into 3 phases: a lower red organic phase (containing protein), an interphase (containing DNA), and a colourless upper aqueous phase (containing RNA). The volume of the aqueous phase was about 70% of the volume of TRI Reagent® used for homogenisation.

RNA Isolation

Note: The organic phase was stored at 4°C for subsequent isolation of proteins.

1. RNA Precipitation: The aqueous phase was transfered to a fresh tube and isopropanol (0.5ml per 0.75ml of TRI Reagent® used for the initial homogenisation) added. The sample was allowed to stand for 5-10min at RT, centrifuged at 12,000*g* for 8min at 4-25°C and the RNA precipitate formed a pellet on the side and bottom of the tube.

2. RNA Wash: The supernatant was removed and the RNA pellet washed by adding 1ml (minimum) of 75% ethanol per 0.75ml of TRI Reagent® used for the initial homogenisation. The sample was vortexed and centrifuged at 7,500*g* for 5min at 4-25°C.

(Notes: If the RNA pellet floated or accumulated on the side of the tube, the wash was performed in 75% ethanol at 12,000*g*; samples were stored in ethanol at 4°C for up to 1 year at -20°C).

3. RNA Solubilisation: the RNA pellet was dried for 5-10min by air-drying or under a

vacuum, but not allowed to dry completely, as this greatly decreases its solubility. An appropriate volume of dH_2O was added to the RNA pellet, the solution mixed by repeated pipetting and incubated at 55-60°C for 10-15min, if necessary to aid dissolution.

Protein Isolation

1. DNA removal: the remaining aqueous phase overlaying the interphase was discarded. To precipitate the DNA from the interphase and organic phase, 100% ethanol (0.3ml per 0.75ml of TRI Reagent® used in sample preparation) was added, the sample mixed by inversion, left to stand for 2-3min and centrifuged at 2,000*g* for 5min at 4°C. The supernatant was removed and stored at 4°C, if necessary, prior to the procedure below.

2. Protein precipitation: proteins were precipitated (see note below) from the phenol-ethanol supernatant with 1.5ml of isopropanol per 0.75ml of TRI Reagent® used in the initial sample preparation. Samples were left to stand for at least 10min at RT and centrifuged at 12,000*g* for 10min at 4°C.

3. Protein wash: the supernatant was discarded and the pellet washed 3 times in 0.3M guanidine hydrochloride/ 95% ethanol solution, using 2ml per 0.75ml of TRI Reagent® used in the initial sample preparation. During each wash, samples were stored in wash solution for 20min at RT prior to centrifugation at 7,500*g* for 5min at 4°C. After the 3 washes, 2ml of 100% ethanol was added, the protein pellet vortexed, left to stand for 20min at RT and centrifuged at 7,500*g* for 5min at 4°C.

Note: Protein samples suspended in 0.3M guanidine hydrochloride/95% ethanol solution or 100% ethanol were stored for up to 1 month at 4°C or 1 year at -20°C, if necessary.

4. Protein solubilisation: the protein pellet was air-dried for 5-15min and dissolved in 1% SDS, aided by pipetting up and down. Some protein pellets required incubation at 50°C for complete solubilisation. Any insoluble material was removed by centrifugation at 10,000*g* for 10min at 4°C. The supernatant protein solution was transferred to a new tube and was used immediately for western blotting or stored at -20°C.

Appendix III

The plate dimensions for BD 24-well companion plates (for use with migration inserts) are not symmetrical and a plate definition file was created as follows in Xfluor4.xls for use with the GENios Plus plate reader:

1. The 'Xfluor4' menu tab was selected, and then the 'Edit PlateDefinition...' tab.
2. The plate parameters shown below were entered, then 'Update' and 'Close' (this did not save the file).
3. Under 'File' menu 'Save PlateDef as...' was selected and the Plate Definition File named and saved.

Measurement parameters for BD companion plates for use with FluoroBlok™ 24- multiwell insert	
Columns	6
Rows	4
Well Form	Round
Well Diameter	6.5
Upper Left Well	X-1560
Start Position	Y 2812
Lower Right Well	X 94825
End Position	Y 60937
Unlidded Plate Height	22500µm
Plate Height with Cover	24500µm

To use fluorescence-based detection of migration using the GENios Plus plate reader, 'Xfluor4.xls' software was opened (macros were enabled) and a connection made to the reader. The 'Edit Measurement Parameter...' menu item was opened, and in the 'General' tab in the drop down menu, 'Fluorescence' detection mode was selected. The plate definition created via the above procedure was selected from the 'Plate' tab; 'Multiple reads per well' was selected, with a square pattern and 2 x 2 for the number of replicates. The 485nm excitation and 535nm emission filters were selected from the 'Meas. Params' tab (drop down menu); and 'Bottom' selected as the read mode. A manual Gain setting method was selected, and integration parameters of a zero time lag, and 20µsec integration time were used. The 'Edit Measurement Parameter...' menu item was closed, and 'Start' selected to commence the reading.

Appendix IV

Publications and presentations

Published abstracts

DENNEY, H., CLENCH, M., and WOODROOFE, M.N. (2005).
Investigations into the significance of the truncation of chemokines CCL2 and CXCL10 by MMP2, MMP9, and CD26, in multiple sclerosis.
Immunology, **116** (Supplement 1) p. 42.

DENNEY, H., BUNNING, R.A.D., CLENCH, M. AND WOODROOFE, M.N. (2007).
Expression of CD26/DPPIV in normal CNS and MS lesions: Implications for pathogenesis via cleavage of chemokines CCL2 and CXCL10.
Poster presented at Multiple Sclerosis Society "MS Frontiers" event, London, UK.

Oral presentations

Mar. 2006 "Truncation of chemokines CCL2 and CXCL10 by MMP2, MMP9 and CD26: implications for multiple sclerosis" at the British Society of Immunology 50th Anniversary Regional Meeting, Sheffield, UK.

Jun. 2007 "Cell migration *in vitro* in response to chemoattractant proteins: a model system for assessing immunomodulatory treatments in MS" at the National Multiple Sclerosis Society Meeting, Sheffield, UK

Poster presentations

Sep. 2005 British Mass Spectrometry Society, Annual Meeting, York, UK.

Dec. 2005 British Society of Immunology Congress, Harrogate, UK.

May 2006 Yorkshire BioEnterprise Networking Event, Wakefield, UK.

References

ABBITT, K.B., RAINGER, G.E. and NASH, G.B., (2000). Effects of fluorescent dyes on selectin and integrin-mediated stages of adhesion and migration of flowing leukocytes. *Journal of Immunological Methods,* **239**(1-2), pp. 109-119.

ABBOTT, C.A., MCCAUGHAN, G.W., BAKER, E. and SUTHERLAND, G.R., (1994). Genomic organization, exact localization, and tissue expression of the human CD26 (dipeptidyl peptidase IV) gene. *Immunogenetics,* **40**(5), pp. 331-338.

ABBOTT, N.J., RONNBACK, L. and HANSSON, E., (2006). Astrocyte-endothelial interactions at the blood-brain barrier. *Nature Reviews: Neuroscience,* **7**(1), pp. 41-53.

ABELLA-CORRAL, J., PRIETO, J.M., DAPENA-BOLANO, D., IGLESIAS-GOMEZ, S., NOYA-GARCIA, M. and LEMA, M., (2005). Seasonal variations in the outbreaks in patients with multiple sclerosis. *Revista de Neurologia,* **40**(7), pp. 394-396.

ABRAHAM, G.N. AND PODELL, D.N., (1981). Pyroglutamic acid. *Molecular and Cellular Biochemistry*, **38**(1), pp. 181-190.

ACHIRON, A., LAVIE, G., KISHNER, I., STERN, Y., SAROVA-PINHAS, I., BEN-AHARON, T., BARAK, Y., RAZ, H., LAVIE, M. and BARLIYA ET, A., (2004). T cell vaccination in multiple sclerosis relapsing-remitting nonresponder patients. *Clinical Immunology,* **113**(2), pp. 155-160.

ADAMI, C., SORCI, G., BLASI, E., AGNELETTI, A., BISTONI, F. and DONATO, R., (2001). S100b expression in and effects on microglia. *Glia,* **33**(2), pp. 131-142.

AGAPOVA, O.A., RICARD, C.S., SALVADOR-SILVA, M. and HERNANDEZ, M.R., (2001). Expression of matrix metalloproteinases and tissue inhibitors of metalloproteinases in human optic nerve head astrocytes. *Glia,* **33**(3), pp. 205-216.

AGRAWAL, S.M., LAU, L. and YONG, V.W., (2008). MMPs in the central nervous system: Where the good guys go bad. *Seminars in Cell & Developmental Biology,* **19**(1), pp. 42-51.

AHONEN, M., POUKKULA, M., BAKER, A.H., KASHIWAGI, M., NAGASE, H., ERIKSSON, J.E. and KAHARI, V., (2003). Tissue inhibitor of metalloproteinase-3 induces apoptosis in melanoma cells by stabilization of death receptors. *Oncogene,* **22**(14), pp. 2121-2134.

AKENAMI, F.O.T., KOSKINIEMI, M. and VAHERI, A., (2000). Plasminogen activation in multiple sclerosis and other neurological disorders. *Fibrinolysis and Proteolysis,* **14**(1), pp. 1-14.

AL-ARAJI, A. and MOHAMMED, A.I., (2005). Multiple sclerosis in Iraq: Does it have the same features encountered in Western countries? *Journal of the Neurological Sciences,* **234**(1-2), pp. 67-71.

ALLT, G. and LAWRENSON, J.G., (2001). Pericytes: Cell biology and pathology. *Cells Tissues Organs,* **169**(1), pp. 1-11.

ALOISI, F., RIA, F. and ADORINI, L., (2000). Regulation of T-cell responses by CNS antigen-presenting cells: different roles for microglia and astrocytes. *Immunology Today,* **21**(3), pp. 141-147.

ALTMANN, D.M. and BOYTON, R.J., (2004). Models of multiple sclerosis. *Drug Discovery Today: Disease Models,* **1**(4), pp. 405-410.

ALUN BROWN, K., (2001). Factors modifying the migration of lymphocytes across the blood–brain barrier. *International Immunopharmacology*, **1**(12), pp. 2043-2062.

ANDJELKOVIC, A.V., SPENCER, D.D. and PACHTER, J.S., (1999). Visualization of chemokine binding sites on human brain microvessels. *Journal of Cell Biology*, **145**(2), pp. 403-412.

ANGERS, S., SALAHPOUR, A. and BOUVIER, M., (2002). Dimerization: an emerging concept for G protein-coupled receptor ontogeny and function. *Annual Review of Pharmacology and Toxicology,* **42**, pp. 409-435.

ANSORGE, S. and REINHOLD, D., (2006). Immune peptides related to dipeptidyl aminopeptidase IV/CD26. In: ABBA J. KASTIN, ed, *Handbook of Biologically Active Peptides,* Burlington: Academic Press, pp. 567-572.

ANTEL, J.P. and BAR-OR, A., (2006), Roles of immunoglobulins and B cells in multiple sclerosis: From pathogenesis to treatment. *Journal of Neuroimmunology,***180**(1-2), pp. 3-8.

ANTEL, J.P. and OWENS, T., (1999). Immune regulation and CNS autoimmune disease. *Journal of Neuroimmunology,* **100**(1-2), pp. 181-189.

ANTHONY, D.C., FERGUSON, B., MATYZAK, M.K., MILLER, K.M., ESIRI, M.M. & PERRY, V.H. (1997), Differential matrix metalloproteinase expression in cases of multiple sclerosis and stroke. *Neuropathology and Applied Neurobiology,* **23**(5), pp. 406-415.

ANTHONY, D.C., MILLER, K.M., FEARN, S., TOWNSEND, M.J., OPDENAKKER, G., WELLS, G.M.A., CLEMENTS, J.M., CHANDLER, S., GEARING, A.J.H. & PERRY, V.H. (1998), Matrix metalloproteinase expression in an experimentally-induced DTH model of multiple sclerosis in the rat CNS. *Journal of Neuroimmunology,* **87**(1-2), pp. 62-72.

ARAQUE, A., CARMIGNOTO, G. and HAYDON, P.G., (2001). Dynamic signaling between astrocytes and neurons. *Annual Review of Physiology,* **63**(1), pp. 795-813.

ARENZANA-SEISDEDOS, F., VIRELIZIER, J., ROUSSET, D., CLARK-LEWIS, I., LOETSCHER, P., MOSER, B. and BAGGIOLINI, M., (1996). HIV blocked by chemokine antagonist. *Nature,* **383**(6599), pp. 400-400.

ATHERTON, A.J., MONAGHAN, P., WARBURTON, M.J., ROBERTSON, D., KENNY, A.J. and GUSTERSON, B.A., (1992). Dipeptidyl peptidase IV expression identifies a functional sub-population of breast fibroblasts. *International Journal of Cancer*, **50**, pp. 15-19.

AURRAND-LIONS, M., JOHNSON-LEGER, C., WONG, C., DUPASQUIER, L. and IMHOF, B.A., (2001). Heterogeneity of endothelial junctions is reflected by differential expression and specific subcellular localization of the three JAM family members. *Blood,* **98**(13), pp. 3699-3707.

AVOLIO, C., RUGGIERI, M., GIULIANI, F., LIUZZI, G., LEANTE, R., RICCIO, P., LIVREA, P. and TROJANO, M., (2003). Serum MMP-2 and MMP-9 are elevated in different multiple sclerosis subtypes. *Journal of Neuroimmunology,* **136**(1-2), pp. 46-53.

AYTAC, U., CLARET, F., HO, L., SATO, K., OHNUMA, K., MILLS, G.B., CABANILLAS, F., MORIMOTO, C. and DANG, N.H., (2001). Expression of CD26 and its associated dipeptidyl peptidase IV enzyme activity enhances sensitivity to doxorubicin-induced cell cycle arrest at the G2/M checkpoint. *Cancer Research,* **61**(19), pp. 7204-7210.

BAGGIOLINI, M., DEWALD, B. and MOSER, B., (1994). Interleukin-8 and related chemotactic cytokines--CXC and CC chemokines. *Advances in Immunology.* **55**, pp. 97-179.

BAKSHI R., (2003). Fatigue associated with multiple sclerosis: diagnosis, impact, and management. *Multiple Sclerosis,* **9**, pp. 219-227.

BALKWILL, F., (2004). Cancer and the chemokine network. *Nature Reviews Cancer,* **4**(7), pp. 540-550.

BALLABH, P., BRAUN, A. and NEDERGAARD, M., (2004). The blood-brain barrier: an overview: structure, regulation, and clinical implications. *Neurobiology of disease,* **16**(1), pp. 1-13.

BANACLOCHA, M., (2007). Neuromagnetic dialogue between neuronal minicolumns and astroglial network: A new approach for memory and cerebral computation. *Brain Research Bulletin,* **73**(1-3), pp. 21-27.

BANWELL, B., GHEZZI, A., BAR-OR, A., MIKAELOFF, Y. and TARDIEU, M., (2007). Multiple sclerosis in children: clinical diagnosis, therapeutic strategies, and future directions. *The Lancet Neurology,* **6**(10), pp. 887-902.

BARAMOVA, E. and FOIDART, J., (1995). Matrix metalloproteinase family. *Cell Biology International,* **19**(3), pp. 239-242.

BARANZINI, S.E. and OKSENBERG, J.R., (2005). Genomics and new targets for multiple sclerosis. *Pharmacogenomics,* **6**(2), pp. 151-161.

BARNES IV, J.H. and HIEFTJE, G.M., (2004). Recent advances in detector-array technology for mass spectrometry. *International Journal of Mass Spectrometry,* **238**(1), pp. 33-46.

BARNETT, M.H., WILLIAMS, D.B., DAY, S., MACASKILL, P. and MC LEOD, J.G., (2003). Progressive increase in incidence and prevalence of multiple sclerosis in Newcastle, Australia: a 35-year study. *Journal of the Neurological Sciences,* **213**(1-2), pp. 1-6.

BARNUM, S. and SZALAI, A., (2006). Complement and demyelinating disease: no MAC needed? *Brain Research Reviews,* **52**(1), pp. 58-68.

BAR-OR, A., OLIVEIRA, E.M.L., ANDERSON, D.E. and HAFLER, D.A., (1999). Molecular pathogenesis of multiple sclerosis. *Journal of Neuroimmunology,* **100**(1-2), pp. 252-259.

BARRAU, M.A., MONTALBAN, X., SÁEZ-TORRES, I., BRIEVA, L., BARBERÀ, N. and MARTÍNEZ-CÁCERES, E.M., (2000). CD4+CD45RO+CD49d high cells are involved in the pathogenesis of relapsing–remitting multiple sclerosis. *Journal of Neuroimmunology,* **111**(1-2), pp. 215-223.

BARTOSIK-PSUJEK, H. and STELMASIAK, Z., (2005). The levels of chemokines CXCL8, CCL2 and CCL5 in multiple sclerosis patients are linked to the activity of the disease. *European Journal of Neurology,* **12**(1), pp. 49-54.

BATINAC, T., PETRANOVIC, D., ZAMOLO, G., PETRANOVIC, D. and RUZIC, A., (2007). Lyme borreliosis and multiple sclerosis are associated with primary effusion lymphoma. *Medical Hypotheses,* **69**(1), pp. 117-119.

BAUMANN, N. and PHAM-DINH, D., (2001). Biology of oligodendrocyte and myelin in the mammalian central nervous system. *Physiological Reviews,* **81**(2), pp. 871-927.

BAUVOIS, B., DE MEESTER, I., DUMONT, J., ROUILLARD, D., ZHAO, H.X. and BOSMANS, E., (1999). Constitutive expression of CD26/dipeptidylpeptidase IV on peripheral blood B lymphocytes of patients with B chronic lymphocytic leukaemia. *British Journal of Cancer* **79**, pp. 1042–1048.

BAZAN, J.F., BACON, K.B., HARDIMAN, G., WANG, W., SOO, K., ROSSI, D., GREAVES, D.R., ZLOTNIK, A. and SCHALL, T.J., (1997). A new class of membrane-bound chemokine with a CX3C motif. *Nature,* **385**(6617), pp. 640-644.

BECHMANN, I., MOR, G., NILSEN, J., ELIZA, M., NITSCH, R. and NAFTOLIN, F., (1999). FasL (CD95L, Apo1L) is expressed in the normal rat and human brain: evidence for the existence of an immunological brain barrier. *Glia,* **27**(1), pp. 62-74.

BECHMANN, I., GALEA, I. and PERRY, V.H., (2007). What is the blood–brain barrier (not)? *Trends in Immunology,* **28**(1), pp. 5-11.

BEIDER, K., NAGLER, A., WALD, O., FRANITZA, S., DAGAN-BERGER, M., WALD, H., GILADI, H., BROCKE, S., HANNA, J., MANDELBOIM, O., DARASH-YAHANA, M., GALUN, E. and PELED, A., (2003). Involvement of CXCR4 and IL-2 in the homing and retention of human NK and NK T cells to the bone marrow and spleen of NOD/SCID mice. *Blood,* **102**(6), pp. 1951-1958.

BELLINGER, S., (2005). Modeling calcium wave oscillations in astrocytes. *Neurocomputing,* **65-66**, pp. 843-850.

BERAUDI, A., TRAVERSA, U., VILLANI, L., SEKINO, Y., NAGY, J.I. and POLI, A., (2003). Distribution and expression of A1 adenosine receptors, adenosine deaminase and adenosine deaminase-binding protein (CD26) in goldfish brain. *Neurochemistry International,* **42**(6), pp. 455-464.

BERGER, A., (2000). Science commentary: Th1 and Th2 responses: what are they? *British Medical Journal,* **321**(7258), pp. 424.

BERGER, J.R. and KORALNIK, I.J., (2005). Progressive Multifocal Leukoencephalopathy and Natalizumab - Unforeseen Consequences. *The New England Journal of Medicine,* **353**(4), pp. 414-416.

BERNSTEIN, H.G., SCHON, E., ANSORGE, S., ROSE, I. DORN, A., (1987). Immunolocalization of dipeptidyl aminopeptidase (DAP IV) in the developing human brain. *International Journal of Developmental Neuroscience*, **55**, pp. 237-42.

BIANCHI, E., BENDER, J., BLASI, F. and PARDI, R., (1997). Through and beyond the wall: late steps in leukocyte transendothelial migration. *Immunology Today,* **18**(12), pp. 586-591.

BIANCHI, R., GIAMBANCO, I. and DONATO, R., (1993). S-100 protein, but not calmodulin, binds to the glial fibrillary acidic protein and inhibits its polymerization in a Ca(2+)-dependent manner. *Journal of Biological Chemistry,* **268**(17), pp. 12669-12674.

BIELEKOVA, B., GOODWIN, B., RICHERT, N., CORTESE, I., KONDO, T., AFSHAR, G., GRAN, B., EATON, J., ANTEL, J., FRANK, J.A., MCFARLAND, H.F. and MARTIN, R., (2000). Encephalitogenic potential of the myelin basic protein peptide (amino acids 83-99) in multiple sclerosis: Results of a phase II clinical trial with an altered peptide ligand. *Nature Medicine,* **6**(10), pp. 1167-1175.

BIGNER, D.D., BIGNER, S.H., PONTEN, J., WESTERMARK, B., MAHALEY, M.S., RUOSLAHTI, E., HERSCHMAN, H., ENG, L.F. and WIKSTRAND, C.J., (1981). Heterogeneity of genotypic and phenotypic characteristics of fifteen permanent cell lines derived from human gliomas. *Journal of Neuropathology and Experimental Neurology*, **40**, pp. 201–229.

BLAZQUEZ, M., MADUENO, J., GONZALEZ, R., JURADO, R., BACHOVCHIN, W., PENA, J. and MUNOZ, E., (1992). Selective decrease of CD26 expression in T cells from HIV-1-infected individuals. *Journal of Immunology,* **149**(9), pp. 3073-3077.

BO, L., MORK, S., KONG, P.A., NYLAND, H., PARDO, C.A. and TRAPP, B.D. (1994). Detection of MHC class II-antigens on macrophages and microglia, but not on astrocytes and endothelia in active multiple sclerosis lesions. *Journal of Neuroimmunology,* **51**(2), pp. 135-146.

BOLTON, S.J., ANTHONY, D.C. and PERRY, V.H., (1998). Loss of the tight junction proteins occludin and zonula occludens-1 from cerebral vascular endothelium during neutrophil-induced blood–brain barrier breakdown in vivo. *Neuroscience,* **86**(4), pp. 1245-1257.

BOONACKER, E. and VAN NOORDEN, C.J.F., (2003). The multifunctional or moonlighting protein CD26/DPPIV. *European Journal of Cell Biology,* **82**(2), pp. 53-73.

BORKAKOTI, N., (1998). Matrix metalloproteases: variations on a theme. *Progress in Biophysics and Molecular Biology,* **70**(1), pp. 73-94.

BOYDEN, S., (1962). The chemotactic effect of mixtures of antibody and antigen on polymorphonuclear leucocytes. *Journal of Experimental Medicine,* **115**(3), pp. 453-466.

BOZ, C., OZMENOGLU, M., VELIOGLU, S., KILINC, K., OREM, A., ALIOGLU, Z. and ALTUNAYOGLU, V., (2006). Matrix metalloproteinase-9 (MMP-9) and tissue inhibitor of matrix metalloproteinase (TIMP-1) in patients with relapsing–remitting multiple sclerosis treated with interferon beta. *Clinical Neurology and Neurosurgery,* **108**(2), pp. 124-128.

BRAMBILLA, R., BRACCHI-RICARD, V., HU, W., FRYDEL, B., BRAMWELL, A., KARMALLY, S., GREEN, E.J. and BETHEA, J.R., (2005). Inhibition of astroglial nuclear factor kappa-B reduces inflammation and improves functional recovery after spinal cord injury. *Journal of Experimental Medicine*, **202**(1), pp. 145-156

BRANDSCH, M., GANAPATHY, V. and LEIBACH, F.H., (1995). Role of dipeptidyl peptidase IV (DP IV) in intestinal and renal absorption of peptides, in *Dipeptidyl peptidase IV (CD26) in metabolism and the immune response,* (Fleischer, B., ed.), pp. 111–130, Springer, New York.

BREZINSCHEK, R.I., LIPSKY, P.E., GALEA, P., VITA, R. & OPPENHEIMER-MARKS, N., (1995). Phenotypic characterization of CD4+ T cells that exhibit a transendothelial migratory capacity. *Journal of Immunology,***154**(7), pp. 3062-3077.

BRIERE, F., DUBOIS, B., FAYETTE, J., VAN DEN ABEELE, S., CAUX, C. and BANCHEREAU, J. (2001). B cells. *Dendritic Cells (Second Edition),* eds. Michael T. Lotze & Angus W. Thomson, Academic Press, London, pp. 255-261.

BRUSE, C., GUAN, Y., CARLBERG, M., CARLSTRÖM, K. and BERGQVIST, A., (2005). Basal release of urokinase plasminogen activator, plasminogen activator inhibitor-1, and soluble plasminogen activator receptor from separated and cultured endometriotic and endometrial stromal and epithelial cells. *Fertility and Sterility,* **83**(4, Supplement 1), pp. 1155-1160.

BUBNER, B., GASE, K. and BALDWIN, I., (2004). Two-fold differences are the detection limit for determining transgene copy numbers in plants by real-time PCR. *BMC Biotechnology,* **4**(1), pp. 14.

BUDOWLE, B., (1984). Increasing the sensitivity of protein detection of a silver stain for agarose gels. *Electrophoresis,* **5**(3), pp. 174-175.

BUGNO, M., WITEK, B., BERETA, J., BERETA, M., EDWARDS, D.R. and KORDULA, T., (1999). Reprogramming of TIMP-1 and TIMP-3 expression profiles in brain microvascular endothelial cells and astrocytes in response to proinflammatory cytokines. *FEBS Letters,* **448**(1), pp. 9-14.

BÜHLING, F., JUNKER, U., REINHOLD, D., NEUBERT, K., JÄGER, L. and ANSORGE, S., (1995). Functional role of CD26 on human B lymphocytes. *Immunology Letters,* **45**(1-2), pp. 47-51.

BURROWS, J.M., BELL, M.J., BRENNAN, R., MILES, J.J., KHANNA, R. and BURROWS, S.R. (2008). Preferential binding of unusually long peptides to MHC class I and its influence on the selection of target peptides for T cell recognition. *Molecular Immunology,* **45**(6), pp. 1818-1824.

BUSILLO, J.M. and BENOVIC, J.L., (2007). Regulation of CXCR4 signaling. *Biochimica et Biophysica Acta (BBA) - Biomembranes,* **1768**(4), pp. 952-963.

BUSTIN, S. and MUELLER, R., (2005). Real-time reverse transcription PCR (qRT-PCR) and its potential use in clinical diagnosis. *Clinical Science*, **109**(4), pp. 365-79.

BUTCHER, E.C. and PICKER, L.J., (1996). Lymphocyte homing and homeostasis. *Science,* **272**(5258), pp. 60-66.

CAMPANELLA, G.S.V., GRIMM, J., MANICE, L.A., COLVIN, R.A., MEDOFF, B.D., WOJTKIEWICZ, G.R., WEISSLEDER, R. and LUSTER, A.D., (2006). Oligomerization of CXCL10 is necessary for endothelial cell presentation and *in vivo* activity. *Journal of Immunology,* **177**(10), pp. 6991-6998.

CAMPANELLA, G.S.V., LEE, E.M.J., SUN, J. and LUSTER, A.D., (2003). CXCR3 and heparin binding sites of the chemokine IP-10 (CXCL10). *Journal of Biological Chemistry,* **278**(19), pp. 17066-17074.

CARMIGNOTO, G., (2000). Reciprocal communication systems between astrocytes and neurones. *Progress in Neurobiology,* **62**(6), pp. 561-581.

CARR, M.W., ROTH, S.J., LUTHER, E., ROSE, S.S. and SPRINGER, T.A., (1994). Monocyte chemoattractant protein 1 acts as a T-lymphocyte chemoattractant. *Proceedings of the National Academy of Sciences of the U.S.A.,* **91**(9), pp. 3652-3656

CARROLL, M.C., (2004). The complement system in regulation of adaptive immunity. *Nature Immunology,* **5**(10), pp. 981-986.

CARROLL-ANZINGER, D. and AL-HARTHI, L., (2006). Gamma interferon primes productive human immunodeficiency virus infection in astrocytes. *Journal of Virology,* **80**(1), pp. 541-544.

CARTIER, L., HARTLEY, O., DUBOIS-DAUPHIN, M. and KRAUSE, K., (2005). Chemokine receptors in the central nervous system: role in brain inflammation and neurodegenerative diseases. *Brain Research Reviews,* **48**(1), pp. 16-42.

CATALFAMO, M., KARPOVA, T., MCNALLY, J., COSTES, S.V., LOCKETT, S.J., BOS, E., PETERS, P.J. and HENKART, P.A., (2004). Human CD8+ T cells store RANTES in a unique secretory compartment and release it rapidly after TcR stimulation. *Immunity,* **20**(2), pp. 219-230.

CEPOK, S., JACOBSEN, M., SCHOCK, S., OMER, B., JAEKEL, S., BODDEKER, I., OERTEL, W.H., SOMMER, N. and HEMMER, B., (2001). Patterns of cerebrospinal fluid pathology correlate with disease progression in multiple sclerosis. *Brain,* **124**(11), pp. 2169-2176.

CEPOK, S., VON GELDERN, G., GRUMMEL, V., HOCHGESAND, S., CELIK, H., HARTUNG, H. and HEMMER, B., (2006). Accumulation of class switched $IgD^{-}IgM^{-}$ memory B cells in the cerebrospinal fluid during neuroinflammation. *Journal of Neuroimmunology,* **180**(1-2), pp. 33-39.

CHANG, C. and WERB, Z., (2001). The many faces of metalloproteases: cell growth, invasion, angiogenesis and metastasis. *Trends in Cell Biology,* **11**(11), pp. S37-S43.

CHAPEL, H.M., SMALL, M., GREGORY, S. and MATTHEWS, W.B., (1990). Serial studies of evoked potentials and circulating lymphocyte subsets for multiple sclerosis: attempts to monitor progress. *Journal of Neurology,* **237**(5), pp. 303-305.

CHAPMAN, J., (2006). Thrombin in inflammatory brain diseases. *Autoimmunity Reviews,* **5**(8), pp. 528-531.

CHARIL, A., YOUSRY, T.A., ROVARIS, M., BARKHOF, F., DE STEFANO, N., FAZEKAS, F., MILLER, D.H., MONTALBAN, X., SIMON J.H., POLMAN, C. and FILIPPI, M., (2006). MRI and the diagnosis of multiple sclerosis: expanding the concept of "no better explanation". *The Lancet Neurology,* **5**(10), pp. 841-852.

CHAUDHURI, A., (2005). Why we should offer routine vitamin D supplementation in pregnancy and childhood to prevent multiple sclerosis. *Medical Hypotheses,* **64**(3), pp. 608-618.

CHAUDHURI, A. and BEHAN, P.O., (2005). Treatment of multiple sclerosis: beyond the NICE guidelines. *Quarterly Journal of Medicine,* **98**(5), pp. 373-378.

CHAUVET, N., PALIN, K., VERRIER, D., POOLE, S., DANTZER, R. and LESTAGE, J., (2001). Rat microglial cells secrete predominantly the precursor of interleukin-1β in response to lipopolysaccharide. *European Journal of Neuroscience,* **14**(4), pp. 609-617.

CHEERAN, M.C.-., HU, S., SHENG, W.S., PETERSON, P.K. and LOKENSGARD, J.R., (2003). CXCL10 Production from Cytomegalovirus-Stimulated Microglia Is Regulated by both Human and Viral Interleukin-10. *Journal of Virology*, **77**(8), pp. 4502-4515.

CHENG, H-C., ABDEL-GHANY, M., ELBLE, R. and PAULI, B., (1998). Lung endothelial dipeptidyl peptidase IV promotes adhesion and metastasis of rat breast cancer cells via tumor cell surface-associated fibronectin. *Journal of Biological Chemistry,* **273**, pp. 24207–24215

CHIBA, K., YANAGAWA, Y., MASUBUCHI, Y., KATAOKA, H., KAWAGUCHI, T., OHTSUKI, M. and HOSHINO, Y., (1998). FTY720, a novel immunosuppressant, induces sequestration of circulating mature lymphocytes by acceleration of lymphocyte homing in rats. I. FTY720 selectively decreases the number of circulating mature lymphocytes by acceleration of lymphocyte homing. *Journal of Immunology,* **160**(10), pp. 5037-5044.

CINAMON, G., GRABOVSKY, V., WINTER, E., FRANITZA, S., FEIGELSON, S., SHAMRI, R., DWIR, O. and ALON, R., (2001). Novel chemokine functions in lymphocyte migration through vascular endothelium under shear flow. *Journal of Leukocyte Biology,* **69**(6), pp. 860-866.

CINAMON, G. and ALON, R., (2003). A real time in vitro assay for studying leukocyte transendothelial migration under physiological flow conditions. *Journal of Immunological Methods,* **273**(1-2), pp. 53-62.

CLARK, R., WIKNER, N., DOHERTY, D. and NORRIS, D., (1988). Cryptic chemotactic activity of fibronectin for human monocytes resides in the 120-kDa fibroblastic cell-binding fragment. *Journal of Biological Chemistry,* **263**(24), pp. 12115-12123.

CLARK-LEWIS, I., SCHUMACHER, C., BAGGIOLINI, M. and MOSER, B., (1991). Structure-activity relationships of interleukin-8 determined using chemically synthesized analogs. Critical role of NH2-terminal residues and evidence for uncoupling of neutrophil chemotaxis, exocytosis, and receptor binding activities. *Journal of Biological Chemistry,* **266**(34), pp. 23128-23134.

CLARK-LEWIS, I., KIM, K., RAJARATHNAM, K., GONG, J., DEWALD, B., MOSER, B., BAGGIOLINI, M. and SYKES, B. (1995). Structure-activity relationships of chemokines. *Journal of Leukocyte Biology,* **57**(5), pp. 703-711.

CLAUDIO, L., RAINE, C.S. & BROSNAN, C.F., (1995). Evidence of persistent blood-brain barrier abnormalities in chronic-progressive multiple sclerosis. *Acta Neuropathologica,* **90**(3), pp. 228-238.

CLORE, G.M., APPELLA, E., YAMADA, M., MATSUSHIMA, K., and GRONENBORN, A.M., (1990). Three-dimensional structure of interleukin 8 in solution. *Biochemistry,* **29**, pp. 1689-1696.

COHEN, M. and ROSSMANN, U., (1994). In utero brain damage: relationship of gestational age to pathological convergences. *Developmental Medicine and Child Neurology,* **36**, pp. 363–370.

COLE, A.M., GANZ, T., LIESE, A.M., BURDICK, M.D., LIU, L. and STRIETER, R.M., (2001). Cutting edge: IFN-inducible ELR- CXC chemokines display defensin-like antimicrobial activity. *Journal of Immunology,* **167**(2), pp. 623-627.

COMERFORD, I., LITCHFIELD, W., HARATA-LEE, Y., NIBBS, R.J.B. and MC COLL, S.R., (2007). Regulation of chemotactic networks by 'atypical' receptors. *BioEssays,* **29**(3), pp. 237-247.

COMERFORD, I. and NIBBS, R.J.B., (2005). Post-translational control of chemokines: a role for decoy receptors? *Immunology Letters*, **96**(2), pp. 163-174.

COMPSTON, A., (1998). Distribution of MS. *MaCalpines Multiple Sclerosis* (Third Edition), Eds. A. Compston, G. Ebers, H. Lassman and I. McDonald, Churchill Livingstone, London.

COMPSTON, A., (2004). The pathogenesis and basis for treatment in multiple sclerosis. *Clinical Neurology and Neurosurgery,* **106**(3), pp. 246-248.

CONSTANTINESCU, C.S., KAMOUN, M., DOTTI, M., FARBER, R.E., GALETTA, S.L. and ROSTAMI, A., (1995). A longitudinal study of the T cell activation marker CD26 in chronic progressive multiple sclerosis. *Journal of the Neurological Sciences,* **130**(2), pp. 178-182.

CONTI, I. and ROLLINS, B.J., (2004). CCL2 (monocyte chemoattractant protein-1) and cancer. *Seminars in Cancer Biology,* **14**(3), pp. 149-154.

CORCIONE, A., ALOISI, F., SERAFINI, B., CAPELLO, E., MANCARDI, G., PISTOIA, V. and UCCELLI, A., (2005). B-cell differentiation in the CNS of patients with multiple sclerosis. *Autoimmunity Reviews,* **4**(8), pp. 549-554.

CORDERO, O., SALGADO, F., VINUELA, J. and NOGUEIRA, M. (1997). Interleukin-12 enhances CD26 expression and dipeptidyl peptidase IV function on human activated lymphocytes. *Immunobiology*, **197**, pp. 522–533

CORNET, A., BETTELLI, E., OUKKA, M., CAMBOURIS, C., AVELLANA-ADALID, V., KOSMATOPOULOS, K. and LIBLAU, R., (2000). Role of astrocytes in antigen presentation and naive T-cell activation. *Journal of Neuroimmunology,* **106**(1-2), pp. 69-77.

COSSINS, J.A., CLEMENTS, J.M., FORD, J., MILLER, K.M., PIGOTT, R., VOS, W., VAN DER VALK, P. and DE GROOT, C. J. A., (1997). Enhanced expression of MMP-7 and MMP-9 in demyelinating multiple sclerosis lesions. *Acta Neuropathologica,* **94**(6), pp. 590-598.

COX, G., (2002). Biological confocal microscopy. *Materials Today,* **5**(3), pp. 34-41.

CRAYTON, H.J. and ROSSMAN, H.S., (2006). Managing the symptoms of multiple sclerosis: A multimodal approach. *Clinical Therapeutics,* **28**(4), pp. 445-460.

CROCKARD, A.D., MCNEILL, T.A., MCKIRGAN, J. and HAWKINS, S.A., (1988). Determination of activated lymphocytes in peripheral blood of patients with multiple sclerosis. *Journal of Neurology Neurosurgery and Psychiatry,* **51**(1), pp. 139-141.

CURNOCK, A.P., LOGAN, M.K. and WARD, S.G., (2002). Chemokine signalling: Pivoting around multiple phosphoinositide 3-kinases. *Immunology,***105**(2), pp. 125-136.

CZEPLUCH, F., OLIESLAGERS, S.F. and WALTENBERGER, J., (2007). Monocyte function is severely impaired by the fluorochrome calcein acetomethylester. *Biochemical and Biophysical Research Communications,* **361**(2), pp. 410-413.

DAVEY, H.M., JONES, A., SHAW, A.D. and KELL, D.B., (1999). Variable selection and multivariate methods for the identification of microorganisms by flow cytometry. *Cytometry,* **35**(2), pp. 162-168.

DAVIS, C.N., CHEN, S., BOEHME, S.A., BACON, K.B. and HARRISON, J.K., (2003). Chemokine receptor binding and signal transduction in native cells of the central nervous system. *Methods,* **29**(4), pp. 326-334.

DEAN, G., MC LOUGHLIN, H., BRADY, R., ADELSTEIN, A.M. and TALLETT-WILLIAMS, J., (1976). Multiple sclerosis among immigrants in Greater London. *British Medical Journal,* **1**, pp. 861–4.

DE CLERCK, L., BRIDTS, C., MERTENS, A., MOENS, M. and STEVENS, W., (1994). Use of fluorescent dyes in the determination of adherence of human leucocytes to endothelial cells and the effect of fluorochromes on cellular function. *Journal of Immunological Methods,* **172**(1), pp. 115-124.

DEGTYAREVA, N., WALLACE, B., BRYANT, A., LOO, K. and PETTY, J., (2007). Hydration changes accompanying the binding of minor groove ligands with DNA. *Biophysical Journal,* **92**(3), pp. 959-965.

DE MEESTER, I., KOROM, S., VAN DAMME, J. and SCHARPE, S., (1999). CD26, let it cut or cut it down. *Immunology Today,* **20**(8), pp. 367-375.

DE MEESTER, I., DURINX, C., BAL, G., PROOST, P., STRUYF, S., GOOSSENS, F., AUGUSTYNS, K. and SCHARPE, S., (2000). Natural substrates of dipeptidyl peptidase IV. *Advances in Experimental Medicine and Biology,* **477**, pp. 67-87.

DE MEESTER, I., LAMBEIR, A., PROOST, P. and SCHARPE, S., (2003). Dipeptidyl peptidase IV substrates. an update on in vitro peptide hydrolysis by human DPPIV. *Advances in Experimental Medicine and Biology,* **524**, pp. 3-17.

DEMUTH, H., MCINTOSH, C.H.S. and PEDERSON, R.A., (2005). Type 2 diabetes—therapy with dipeptidyl peptidase IV inhibitors. *Biochimica et Biophysica Acta - Proteins & Proteomics,* **1751**(1), pp. 33-44.

DEVALARAJA, M.N. and RICHMOND, A., (1999). Multiple chemotactic factors: fine control or redundancy? *Trends in Pharmacological Sciences,* **20**(4), pp. 151-156.

DIETRICH, D.E., HAUSER, U., PETERS, M., ZHANG, Y., WIESMANN, M., HASSELMANN, M., RUDOLF, S., JUNGLING, O., KIRCHNER, H., MUNTE, T.F., AROLT, V., EMRICH, H.M., JOHANNES, S. and ROTHERMUNDT, M., (2004). Target evaluation processing and serum levels of nerve tissue protein S100B in patients with remitted major depression. *Neuroscience Letters,* **354**(1), pp. 69-73.

DONATO, R., (2001). S100: a multigenic family of calcium-modulated proteins of the EF-hand type with intracellular and extracellular functional roles. *The International Journal of Biochemistry & Cell Biology,* **33**(7), pp. 637-668.

DYMENT, D.A., EBERS, G.C. and DESSA SADOVNICK, A., (2004). Genetics of multiple sclerosis. *The Lancet Neurology,* **3**(2), pp. 104-110.

EDAN, G., MORRISSEY, S. and LE PAGE, E., (2004). Rationale for the use of mitoxantrone in multiple sclerosis. *Journal of the Neurological Sciences,* **223**(1), pp. 35-39.

EDGAR, J.M., MC LAUGHLIN, M., YOOL, D., ZHANG, S., FOWLER, J.H., MONTAGUE, P., BARRIE, J.A., MC CULLOCH, M.C., DUNCAN, I.D., GARBERN, J., NAVE, K.A. and GRIFFITHS, I.R. (2004). Oligodendroglial modulation of fast axonal transport in a mouse model of hereditary spastic paraplegia. *Journal of Cell Biology,* **166**(1), pp. 121-131.

EDWARDS, R.J., TAYLOR, G.W., FERGUSON, M., MURRAY, S., RENDELL, N., WRIGLEY, A., BAI, Z., BOYLE, J., FINNEY, S.J., JONES, A., RUSSELL, H.H., TURNER, C., COHEN, J., FAULKNER, L. and SRISKANDAN, S., (2005). Specific C-terminal cleavage and inactivation of interleukin-8 by invasive disease isolates of Streptococcus pyogenes. *Journal of Infectious Diseases,* **192**(5), pp. 783-790.

EHLERT, J.E., GERDES, J., FLAD, H.D. and BRANDT, E., (1998). Novel C-terminally truncated isoforms of the CXC chemokine beta-thromboglobulin and their impact on neutrophil functions. *Journal of Immunology,* **161**(9), pp. 4975-4982.

ELIAN, M., NIGHTINGALE, S. and DEAN, G., (1990). Multiple sclerosis among United Kingdom-born children of immigrants from the Indian subcontinent, Africa and the West Indies. *Journal of Neurology, Neurosurgery, and Psychiatry,* **53**(10), pp. 906-911.

ELLINGSEN, T., HORNUNG, N., MOLLER, B.K., HJELM-POULSEN, J. and STENGAARD-PEDERSEN, K., (2007). In active chronic rheumatoid arthritis, dipeptidyl peptidase IV density is increased on monocytes and CD4+ T lymphocytes. *Scandinavian Journal of Immunology,* **66**(4), pp. 451-457.

EMBRY, A.F., SNOWDON, L.R. and VIETH, R., (2000). Vitamin D and seasonal fluctuations of gadolinium-enhancing magnetic resonance imaging lesions in multiple sclerosis. *Annals of Neurology,* **48**(2), pp. 271-272.

ENG, L.F., GHIRNIKAR, R.S. and LEE, Y.L., (2000). Glial fibrillary acidic protein: GFAP-thirty-one years (1969-2000). *Neurochemical Research,* **25**(9), pp. 1439-1451.

ENGELHARDT, B. and RANSOHOFF, R.M., (2005). The ins and outs of T-lymphocyte trafficking to the CNS: anatomical sites and molecular mechanisms. *Trends in Immunology,* **26**(9), pp. 485-495.

ENS, W. and STANDING, K.G., (2005). Hybrid quadrupole/time-of-flight mass spectrometers for analysis of biomolecules. *Methods in Enzymology*, Ed. A. L. Burlingame, Academic Press, New York, pp. 49-78.

EUGENIN, E.A., OSIECKI, K., LOPEZ, L., GOLDSTEIN, H., CALDERON, T.M. and BERMAN, J.W., (2006). CCL2/monocyte chemoattractant protein-1 mediates enhanced transmigration of human immunodeficiency virus (HIV)-infected leukocytes across the blood-brain barrier: a potential mechanism of HIV-CNS invasion and neuroAIDS. *Journal of Neuroscience*, **26**(4), pp. 1098-1106.

FARBER, K. and KETTENMANN, H., (2005). Physiology of microglial cells. *Brain Research Reviews,* **48**(2), pp. 133-143.

FARINA, C., WEBER, M., MEINL, E., WEKERLE, H. and HOHLFELD, R., (2005). Glatiramer acetate in multiple sclerosis: update on potential mechanisms of action. *The Lancet Neurology,* **4**(9), pp. 567-575.

FARINA, C., ALOISI, F. and MEINL, E., (2007). Astrocytes are active players in cerebral innate immunity. *Trends in Immunology,* **28**(3), pp. 138-145.

FARMILO A.J. and STEAD, R.H., (2001). Fixation. *Handbook Immunochemical Staining Methods* (3rd edition), p. 18.

FATEMI, S.H., LAURENCE, J.A., ARAGHI-NIKNAM, M., STARY, J.M., SCHULZ, S.C., LEE, S. and GOTTESMAN, I.I., (2004). Glial fibrillary acidic protein is reduced in cerebellum of subjects with major depression, but not schizophrenia. *Schizophrenia Research,* **69**(2-3), pp. 317-323.

FAVRE-KONTULA, L., JOHNSON, Z., STEINHOFF, T., FRAUENSCHUH, A., VILBOIS, F. and PROUDFOOT, A.I., (2006). Quantitative detection of therapeutic proteins and their metabolites in serum using antibody-coupled ProteinChip® Arrays and SELDI-TOF-MS. *Journal of Immunological Methods,* **317**(1-2), pp. 152-162.

FERNANDEZ, E.J. and LOLIS, E., (2002). Structure, function, and inhibition of chemokines. *Annual Review of Pharmacology and Toxicology,* **42**, pp. 469-499.

FIFE, B.T., KENNEDY, K.J., PANIAGUA, M.C., LUKACS, N.W., KUNKEL, S.L., LUSTER, A.D. and KARPUS, W.J., (2001). CXCL10 (IFN-γ-inducible protein-10) control of encephalitogenic CD4+ T cell accumulation in the central nervous system during experimental autoimmune encephalomyelitis. *Journal of Immunology,* **166**(12), pp. 7617-7624.

FILIPPI, M., BOZZALI, M., ROVARIS, M., GONEN, O., KESAVADAS, C., GHEZZI, A., MARTINELLI, V., GROSSMAN, R.I., SCOTTI, G., COMI, G. and FALINI, A., (2003). Evidence for widespread axonal damage at the earliest clinical stage of multiple sclerosis. *Brain,* **126**(2), pp. 433-437.

FLIER, J., BOORSMA, D.M., VAN BEEK, P.J., NIEBOER, C., STOOF, T.J., WILLEMZE, R. and TENSEN, C.P., (2001). Differential expression of CXCR3 targeting chemokines CXCL10, CXCL9, and CXCL11 in different types of skin inflammation. *Journal of Pathology,* **194**(8), pp. 397-404.

FLYNN, G., MARU, S., LOUGHLIN, J., ROMERO, I.A. and MALE, D., (2003). Regulation of chemokine receptor expression in human microglia and astrocytes. *Journal of Neuroimmunology,* **136**(1-2), pp. 84-93.

FORSSMANN, U., HARTUNG, I., BALDER, R., FUCHS, B., ESCHER, S.E., SPODSBERG, N., DULKYS, Y., WALDEN, M., HEITLAND, A. and BRAUN ET, A., (2004). N-nonanoyl-CC chemokine ligand 14, a potent CC chemokine ligand 14 analogue that prevents the recruitment of eosinophils in allergic airway inflammation. *Journal of Immunology,* **173**(5), pp. 3456-3466.

FOUILLET, A., SULIMAN, O., SHARRACK, B., ROMERO, I. and WOODROOFE, M.N., (2005). Cytokine regulation of CXCL10 and CCL2 expression by primary adult human astrocytes *in vitro. Immunology,* **116**(S1), pp. 40.

FRANCO, S.J., RODGERS, M.A., PERRIN, B.J., HAN, J., BENNIN, D.A., CRITCHLEY, D.R. and HUTTENLOCHER, A., (2004). Calpain-mediated proteolysis of talin regulates adhesion dynamics. *Nature Cell biology,* **6**(10), pp. 977-983.

FRIEND, W.C., CLAPOFF, S., LANDRY, C., BECKER, L.E., O'HANLON, D., ALLORE, R.J., MARKS, A., RODER, J. and DUNN, R.J., (1992). Cell-specific expression of high levels of human S100 beta in transgenic mouse brain is dependent on gene dosage. *Journal of Neuroscience,* **12**(11), pp. 4337–4346.

FRITZSCHE, M., (2005). Chronic lyme borreliosis at the root of multiple sclerosis - is a cure with antibiotics attainable? *Medical Hypotheses,* **64**(3), pp. 438-448.

FROHMAN, E.M., SHAH, A., EGGENBERGER, E., METZ, L., ZIVADINOV, R. and STÜVE, O., (2007). Corticosteroids for multiple sclerosis: application for treating exacerbations. *Neurotherapeutics,* **4**(4), pp. 618-626.

FROSSI, B., DECARLI, M., PIEMONTE, M. and PUCILLO, C., (2008). Oxidative microenvironment exerts an opposite regulatory effect on cytokine production by Th1 and Th2 cells. *Molecular Immunology,* **45**(1), pp. 58-64.

FU, X., KASSIM, S.Y., PARKS, W.C. and HEINECKE, J.W. (2001).Hypochlorous acid oxygenates the cysteine switch domain of pro-matrilysin (MMP-7). A mechanism for matrix metalloproteinase activation and atherosclerotic plaque rupture by myeloperoxidase. *Journal of Biological Chemistry,* **276**(44), pp. 41279-41287.

FUJITA, T., MATSUSHITA, M. and ENDO, Y., (2004). The lectin-complement pathway - its role in innate immunity and evolution. *Immunological Reviews,* **198**(1), pp. 185-202.

FUJIWARA, H. and HAMAOKA, T., (2001). Coordination of chemokine and adhesion systems in intratumoral T cell migration responsible for the induction of tumor regression. *International Immunopharmacology*, **1**(4), pp. 613-623.

GALEA, I., BECHMANN, I. and PERRY, V.H., (2007). What is immune privilege (not)? *Trends in Immunology,* **28**(1), pp. 12-18.

GALIMBERTI, D., BRESOLIN, N. and SCARPINI, E., (2004). Chemokine network in multiple sclerosis: role in pathogenesis and targeting for future treatments. *Expert Review of Neurotherapeutics,* **4**(3), pp. 439-453.

GAY, F., (2006). Early cellular events in multiple sclerosis: Intimations of an extrinsic myelinolytic antigen. *Clinical Neurology and Neurosurgery,* **108**(3), pp. 234-240.

GE, S., SONG, L. and PACHTER, J.S., (2005). Where is the blood-brain barrier ... Really? *Journal of Neuroscience Research,* **79**(4), pp. 421-427.

GERSZTEN, R.E., GARCIA-ZEPEDA, E.A., LIM, Y., YOSHIDA, M., DING, H.A., GIMBRONE, M.A., LUSTER, A.D., LUSCINSKAS, F.W. and ROSENZWEIG, A., (1999). MCP-1 and IL-8 trigger firm adhesion of monocytes to vascular endothelium under flow conditions. *Nature,* **398**(6729), pp. 718-723.

GIANNINI, E., BROUCHON, L., and BOULAY, F., (1995). Identification of the major phosphorylation sites in human C5a anaphylatoxin receptor *in vivo. Journal of Biological Chemistry.* **270**, pp. 19166-19172.

GIBBONS, H., HUGHES, S., VANROON-MOM, W., GREENWOOD, J., NARAYAN, P., TEOH, H.H., BERGIN, P., MEE, E., WOOD, P., FAULL, R.M. and DRAGUNOW, M., (2007). Cellular composition of human glial cultures from adult biopsy brain tissue. *Journal of Neuroscience Methods,* **166**(1), pp. 89-98.

GIBBS, E. and OGER, J., (2007). The IgG subclass-specificities of anti-IFN-β antibodies change with time and differ between the IFN-β products in relapsing remitting multiple sclerosis patients. *Journal of Neuroimmunology,* **190**(1-2), pp. 146-50.

GINGRAS, D., PAGE, M., ANNABI, B. & BELIVEAU, R., (2000). Rapid activation of matrix metalloproteinase-2 by glioma cells occurs through a posttranslational MT1-MMP-dependent mechanism. *Biochimica et Biophysica Acta (BBA) - Molecular Cell Research,* **1497**(3), pp. 341-350.

GIUNTI, D., BORSELLINO, G., BENELLI, R., MARCHESE, M., CAPELLO, E., VALLE, M.T., PEDEMONTE, E., NOONAN, D., ALBINI, A., BERNARDI, G., MANCARDI, G.L., BATTISTINI, L. and UCCELLI, A., (2003). Phenotypic and functional analysis of T cells homing into the CSF of subjects with inflammatory diseases of the CNS. *Journal of Leukocyte Biology,* **73**(5), pp. 584-590.

GLEZER, I., SIMARD, A.R. and RIVEST, S., (2007). Neuroprotective role of the innate immune system by microglia. *Neuroscience,* **147**(4), pp. 867-883.

GOLDMAN, J.E. and CHIU, F., (1984). Dibutyryl cyclic AMP causes intermediate filament accumulation and actin reorganization in astrocytes. *Brain Research,* **306**(1-2), pp. 85-95.

GOMES, E.R., JANI, S. and GUNDERSEN, G.G., (2005). Nuclear movement regulated by Cdc42, MRCK, myosin, and actin flow establishes MTOC polarization in migrating cells. *Cell,* **121**(3), pp. 451-463.

GONG, C., HOFF, J.T. and KEEP, R.F., (2000). Acute inflammatory reaction following experimental intracerebral hemorrhage in rat. *Brain Research,* **871**(1), pp. 57-65.

GONG, J., UGUCCIONI, M., DEWALD, B., BAGGIOLINI, M. & CLARK-LEWIS, I., (1996). RANTES and MCP-3 antagonists bind multiple chemokine receptors. *Journal of Biological Chemistry,* **271**(18), pp. 10521-10527.

GONZALEZ-GRONOW, M., GRENETT, H. E.,WEBER,M. R., GAWDI, G., PIZZO, S. V., (2001). Interaction of plasminogen with dipeptidyl peptidase IV initiates a signal transduction mechanism which regulates expression of matrix metalloproteinase-9 by prostate cancer cells. *Journal of Biochemistry,* **355**, pp. 397-407.

GOTTSCHALL, P.E. and DEB, S., (1996). Regulation of matrix metalloproteinase expression in astrocytes, microglia and neurons. *NeuroImmunoModulation,* **3**(2-3), pp. 69-75.

GRANT, W.B., (2006). Epidemiology of disease risks in relation to vitamin D insufficiency. *Progress in Biophysics and Molecular Biology,* **92**(1), pp. 65-79.

GRAUMANN, U., REYNOLDS, R., STECK, A.J. and SCHAEREN-WIEMERS, N., (2003). Molecular changes in normal appearing white matter in multiple sclerosis are characteristic of neuroprotective mechanisms against hypoxic insult. *Brain Pathology*, **13**, pp. 554-573.

GREEN, F.J., Ed., (1990). The Sigma-Aldrich Handbook of Stains, Dyes and Indicators, Aldrich Chemical Co., Milwaukee, WI, pp. 721-722.

GREENWOOD, J., ETIENNE-MANNEVILLE, S., ADAMSON, P. and COURAUD, P., (2002). Lymphocyte migration into the central nervous system: Implication of ICAM-1 signalling at the blood–brain barrier. *Vascular Pharmacology,* **38**(6), pp. 315-322.

GRETER, M., HEPPNER, F.L., LEMOS, M.P., ODERMATT, B.M., GOEBELS, N., LAUFER, T., NOELLE, R.J. and BECHER, B., (2005). Dendritic cells permit immune invasion of the CNS in an animal model of multiple sclerosis. *Nature Medicine,* **11**(3), pp. 328-334.

GROSS, J. & STRUPAT, K., (1998). Matrix-assisted laser desorption/ionisation–mass spectrometry applied to biological macromolecules. *Trends in Analytical Chemistry,* **17**(8-9), pp. 470-484.

GU, Z., KAUL, M., YAN, B., KRIDEL, S.J., CUI, J., STRONGIN, A., SMITH, J.W., LIDDINGTON, R.C. and LIPTON, S.A., (2002). S-nitrosylation of matrix metalloproteinases: signaling pathway to neuronal cell death. *Science,* **297**(5584), pp. 1186-1190.

GUAN, E., WANG, J. and NORCROSS, M.A., (2004). Amino-terminal processing of MIP-1β/CCL4 by CD26/dipeptidyl-peptidase IV. *Journal of Cellular Biochemistry,* **92**(1), pp. 53-64.

GUEDEZ, L., COURTEMANCH, L. and STETLER-STEVENSON, M., (1998). Tissue inhibitor of metalloproteinase (TIMP)-1 induces differentiation and an antiapoptotic phenotype in germinal center B cells. *Blood,* **92**(4), pp. 1342-1349.

GUILLEMIN, G.J., CROITORU-LAMOURY, J., DORMONT, D., ARMATI, P.J. and BREW, B.J., (2003). Quinolinic acid upregulates chemokine production and chemokine receptor expression in astrocytes. *Glia*, **41**(4), pp. 371-381.

GUNZER, M., SCHÄFER, A., BORGMANN, S., GRABBE, S., ZÄNKER, K.S., BRÖCKER, E., KÄMPGEN, E. and FRIEDL, P., (2000). Antigen presentation in extracellular matrix: interactions of T Cells with dendritic cells are dynamic, short lived, and sequential. *Immunity,* **13**(3), pp. 323-332.

GUPTA, S.K., LYSKO, P.G., PILLARISETTI, K., OHLSTEIN, E. and STADEL, J.M., (1998). Chemokine receptors in human endothelial cells. Functional expression of CXCR4 and its transcriptional regulation by inflammatory cytokines. *Journal of Biological Chemistry,* **273**(7), pp. 4282-4287.

GUTTMANN, C.R.G., MEIER, D.S. and HOLLAND, C.M., (2006). Can MRI reveal phenotypes of multiple sclerosis? *Magnetic Resonance Imaging,* **24**(4), pp. 475-481.

GYETKO, M.R., TODD III, R.F., WILKINSON, C.C. and SITRIN, R.G., (1994). The urokinase receptor is required for human monocyte chemotaxis in vitro. *Journal of Clinical Investigation,* **93**(4), pp. 1380-1387.

HACHMANN, J. and AMSHEY, J., (2005). Models of protein modification in Tris–glycine and neutral pH Bis–Tris gels during electrophoresis: Effect of gel pH. *Analytical Biochemistry,* **342**(2), pp. 237-245.

HAEBEL, S., ALBRECHT, T., SPARBIER, K., WALDEN, P., KÖRNER, R., and STEUP, M., (1998). Electrophoresis-related protein modification: alkylation of carboxy residues revealed by mass spectrometry. *Electrophoresis,* **19**(5), pp. 679-686.

HAFLER, D.A., FOX, D.A., MANNING, M.E., SCHLOSSMAN, S.F., REINHERZ, E.L. and WEINER, H.L., (1985). *In vivo* activated T lymphocytes in the peripheral blood and cerebrospinal fluid of patients with multiple sclerosis. *The New England Journal of Medicine*, **312**, pp. 1405– 1411.

HALL, G., COMPSTON, A. and SCOLDING, N., (1997). Beta-interferon and multiple sclerosis. *Trends in Neurosciences,* **20**(2), pp. 63-67.

HANINEC, P. and GRIM, M., (1990). Localization of dipeptidylpeptidase IV and alkaline phosphatase in developing spinal cord meninges and peripheral nerve coverings of the rat. *International Journal of Developmental Neuroscience*, **8**, pp. 175–185.

HARDY, L.A., BOOTH, T.A., LAU, E.K., HANDEL, T.M., ALI, S. and KIRBY, J.A., (2004). Examination of MCP-1 (CCL2) partitioning and presentation during transendothelial leukocyte migration. *Laboratory Investigation,* **84**(1), pp. 81-90.

HARINGMAN, J.J., LUDIKHUIZE, J. and TAK, P.P., (2004). Chemokines in joint disease: the key to inflammation? *Annals of the Rheumatic Diseases,* **63**(10), pp. 1186-1194.

HARKNESS, K.A., ADAMSON, P., SUSSMAN, J.D., DAVIES-JONES, G.A.B., GREENWOOD, J. and WOODROOFE, M.N., (2000). Dexamethasone regulation of matrix metalloproteinase expression in CNS vascular endothelium. *Brain*, **123**(4), pp. 698-709.

HARKNESS, K.A., SUSSMAN, J.D., DAVIES-JONES, G.A.B., GREENWOOD, J. and WOODROOFE, M.N., (2003). Cytokine regulation of MCP-1 expression in brain and retinal microvascular endothelial cells. *Journal of Neuroimmunology,* **142**(1-2), pp. 1-9.

HASAN, L., MAZZUCCHELLI, L., LIEBI, M., MADDALENA LIS, HUNGER, R.E., TESTER, A., OVERALL, C.M. and WOLF, M., (2006). Function of liver activation-regulated chemokine/CC chemokine ligand 20 is differently affected by cathepsin B and cathepsin D processing. *Journal of Immunology,* **176**(11), pp. 6512-6522.

HEDRICK, J.A., SAYLOR, V., FIGUEROA, D., MIZOUE, L., XU, Y., MENON, S., ABRAMS, J., HANDEL, T. and ZLOTNIK, A., (1997). Lymphotactin Is produced by NK cells and attracts both NK cells and T cells *in vivo. Journal of Immunology,* **158**(4), pp. 1533-1540.

HENSBERGEN, P.J., VERZIJL, D., BALOG, C.I.A., DIJKMAN, R., VAN DER SCHORS,ROEL C., VAN DER RAAIJ-HELMER,ELIZABETH M.H., VAN DER PLAS,MARIENA J.A., LEURS, R., DEELDER, A.M., SMIT, M.J. and TENSEN, C.P., (2004). Furin is a chemokine-modifying enzyme: in vitro and in vivo processing of CXCL10 generates a C-terminally truncated chemokine retaining full activity. *Journal of Biological Chemistry,* **279**(14), pp. 13402-13411.

HICKEY, W.F., (1999). The pathology of multiple sclerosis: a historical perspective. *Journal of Neuroimmunology,* **98**(1), pp. 37-44.

HILL, K.E., ZOLLINGER, L.V., WATT, H.E., CARLSON, N.G. and ROSE, J.W., (2004). Inducible nitric oxide synthase in chronic active multiple sclerosis plaques: distribution, cellular expression and association with myelin damage. *Journal of Neuroimmunology,* **151**(1-2), pp. 171-179.

HOFFMANN, T., FAUST, J., NEUBERT, K., and ANSORGE, S., (1993). Dipeptidyl peptidase IV (CD 26) and aminopeptidase N (CD 13) catalyzed hydrolysis of cytokines and peptides with N-terminal cytokine sequences. *FEBS Letters,* **336**(1), pp. 61-64

HOOGEWERF, A.J., KUSCHERT, G.S.V., PROUDFOOT, A.E.I., BORLAT, F., CLARK-LEWIS, I., POWER, C.A. and WELLS, T.N.C., (1997). Glycosaminoglycans mediate cell surface oligomerization of chemokines. *Biochemistry,* **36**(44), pp. 13570-13578.

HUANG, D., HAN Y, RANI, M.R., GLABINSKI, A., TREBST, C., SØRENSEN, T., TANI, M., WANG, J., CHIEN, P., O'BRYAN, S., BIELECKI, B., ZHOU, Z.L., MAJUMDER, S. and RANSOHOFF, R.M., (2000). Chemokines and chemokine receptors in inflammation of the nervous system: manifold roles and exquisite regulation. *Immunological Reviews*, **177**, pp. 52.-67.

HUANG, X., SHEN, J., CUI, M., SHEN, L., LUO, X., LING, K., PEI, G., JIANG, H. and CHEN, K., (2003). Molecular dynamics simulations on SDF-1α: binding with CXCR4 receptor. *Biophysical Journal,* **84**(1), pp. 171-184.

HUIJBREGTS, S.C.J., KALKERS, N.F., DE SONNEVILLE, L.M.J., DE GROOT, V. and POLMAN, C.H., (2006). Cognitive impairment and decline in different MS subtypes. *Journal of the Neurological Sciences,* **245**(1-2), pp. 187-194.

HURKMAN, W. & TANAKA, C., (2007). High-Resolution Two-Dimensional Gel Electrophoresis: A Cornerstone of Plant Proteomics. Springer Berlin Heidelberg. *Plant Proteomics.* pp. 14-28

HUTTENLOCHER, A., LAKONISHOK, M., KINDER, M., WU, S., TRUONG, T., KNUDSEN, K.A. and HORWITZ, A.F., (1998). Integrin and cadherin synergy regulates contact inhibition of migration and motile activity. *Journal of Cell Biology,* **141**(2), pp. 515-526.

HYNES, R.O., DESTREE, A.T., PERKINS, M.E., and WAGNER, D.D., (1979). Cell surface fibronectin and oncogenic transformation. *Journal of Supramolecular Structure,* **11**(1), pp. 95-104.

IKEJIMA, H., FRIEDMAN, H. and YAMAMOTO, Y., (2006). Chlamydia pneumoniae infection of microglial cells in vitro: a model of microbial infection for neurological disease. *Journal of Medical Microbiology,* **55**(7), pp. 947-952.

IMAI, F., SAWADA, M., SUZUKI, H., KIYA, N., HAYAKAWA, M., NAGATSU, T., MARUNOUCHI, T. and KANNO, T., (1997). Migration activity of microglia and macrophages into rat brain. *Neuroscience Letters,* **237**(1), pp. 49-52.

IRANI, D.N., (2005). Immunological mechanisms in multiple sclerosis. *Clinical and Applied Immunology Reviews,* **5**(4), pp. 257-269.

IWATA, S. and MORIMOTO, C., (1999). CD26/Dipeptidyl peptidase IV in context: the different roles of a multifunctional ectoenzyme in malignant transformation. *Journal of Experimental Medicine,* **190**(3), pp. 301-306.

JACKMAN, H., TAN, F., SCHRAUFNAGEL, D., DRAGOVIC, T., DEZSO, B., BECKER, R. and ERDOS, E., (1995). Plasma membrane-bound and lysosomal peptidases in human alveolar macrophages. *American Journal of Respiratory Cell and Molecular Biology,***13**(2), pp. 196-204.

JACKSON, S.J., DIEMEL, L.T., PRYCE, G. and BAKER, D., (2005). Cannabinoids and neuroprotection in CNS inflammatory disease. *Journal of the Neurological Sciences,* **233**(1-2), pp. 21-25.

JAUNEAU, A., ISCHENKO, A., CHATAGNER, A., BENARD, M., CHAN, P., SCHOUFT, M., PATTE, C., VAUDRY, H. and FONTAINE, M., (2006). Interleukin-1β and anaphylatoxins exert a synergistic effect on NGF expression by astrocytes. *Journal of Neuroinflammation,* **3**, p. 8.

JENSEN, J., LANGKILDE, A.R., FENST, C., NICOLAISEN, M.S., ROED, H.G., CHRISTIANSEN, M. and SELLEBJERG, F., (2004). CD4 T cell activation and disease activity at onset of multiple sclerosis. *Journal of Neuroimmunology,* **149**(1-2), pp. 202-209.

JENSEN, J., LANGKILDE, A.R., FREDERIKSEN, J.L. and SELLEBJERG, F., (2006). CD8+ T cell activation correlates with disease activity in clinically isolated syndromes and is regulated by interferon-β treatment. *Journal of Neuroimmunology,* **179**(1-2), pp. 163-172.

JOURDAN, P., VENDRELL, J., HUGUET, M., SEGONDY, M., BOUSQUET, J., PENE, J. and YSSEL, H., (2000). Cytokines and cell surface molecules independently induce CXCR4 expression on CD4+ CCR7+ human memory T cells. *Journal of Immunology,* **165**(2), pp. 716-724.

KAHNE, T., KRONING, H., THIEL, U., ULMER, A., FLAD, H-D. and ANSORGE, S., (1996). Alterations in structure and cellular localization of molecular forms of DP IV/CD26 during T cell activation. *Cellular Immunology,* **170**(1), pp. 63–70

KAHNE, T., LENDECKEL, U., WRENGER, S., NEUBERT, K., ANSORGE, S., and REINHOLD, D., (1999). Dipeptidyl peptidase IV: A cell surface peptidase involved in regulating T cell growth. *International Journal of Molecular Medicine,* **4**, pp. 3–15.

KAMEOKA, J., TANAKA, T., NOJIMA, Y., SCHLOSSMAN, S. and MORIMOTO, C., (1993). Direct association of adenosine deaminase with a T cell activation antigen, CD26. *Science,* **261**(5120), pp. 466-469.

KAPPOS, L., KUHLE, J., GASS, A., ACHTNICHTS, L. and RADUE, E., (2004). Alternatives to current disease-modifying treatment in MS: what do we need and what can we expect in the future? *Journal of Neurology,* **251**(Supplement 5), pp. v57-v64.

KAPPOS, L., BATES, D., HARTUNG, H., HAVRDOVA, E., MILLER, D., POLMAN, C.H., RAVNBORG, M., HAUSER, S.L., RUDICK, R.A., WEINER, H.L., O'CONNOR, P.W., KING, J., RADUE, E.W., YOUSRY, T., MAJOR, E.O. and CLIFFORD, D.B., (2007). Natalizumab treatment for multiple sclerosis: recommendations for patient selection and monitoring. *Lancet Neurology,* **6**(5), pp. 431-441.

KARAS, M., BAHR, U., INGENDOH, A., NORDHOFF, E., STAHL, B., STRUPAT, K. & HILLENKAMP, F., (1990). Principles and applications of matrix-assisted UV-laser desorption/ionization mass spectrometry. *Analytica Chimica Acta,* **241**(2), pp. 175-185.

KAY, J.E., (1991). Mechanisms of T lymphocyte activation. *Immunology Letters,* **29**(1-2), pp. 51-54.

KENNEDY, K.J., STRIETER, R.M., KUNKEL, S.L., LUKACS, N.W. and KARPUS, W.J., (1998). Acute and relapsing experimental autoimmune encephalomyelitis are regulated by differential expression of the CC chemokines macrophage inflammatory protein-1α and monocyte chemotactic protein-1. *Journal of Neuroimmunology,* **92**(1-2), pp. 98-108.

KHOURY, S.J., GUTTMANN, C.R.G., ORAV, E.J., KIKINIS, R., JOLESZ, F.A. and WEINER, H.L., (2000). Changes in activated T cells in the blood correlate with disease activity in multiple sclerosis. *Archives of Neurology,* **57**(8), pp. 1183-1189.

KIIALAINEN, A., HOVANES, K., PALONEVA, J., KOPRA, O. and PELTONEN, L. (2005). DAP12 and TREM2, molecules involved in innate immunity and neurodegeneration, are co-expressed in the CNS. *Neurobiology of Disease*, **18**(2), pp. 314-322.

KNOPF, P.M., HARLING-BERG, C.J., CSERR, H.F., BASU, D, SIRULNICK, E.J., NOLAN, S.C., PARK, J.T., KEIR, G., THOMPSON, E.J. and HICKEY, W.F., (1998). Antigen-dependent intrathecal antibody synthesis in the normal rat brain: tissue entry and local retention of antigen-specific B cells. *Journal of Immunology*, **161**, pp. 692-701.

KORN, T., OUKKA, M., KUCHROO, V. and BETTELLI, E. (2007). Th17 cells: Effector T cells with inflammatory properties. *Seminars in Immunology,***19**(6), pp. 362-371.

KORNEK, B. and LASSMANN, H., (2003). Neuropathology of multiple sclerosis—new concepts. *Brain Research Bulletin,* **61**(3), pp. 321-326.

KOROM, S., DE MEESTER, I., STADLBAUER, T.H.W., CHANDRAKER, A., SCHAUB, M., SAYEGH, M.H., BELYAEV, A., HAEMERS, A., SCHARPÉ, S. and KUPIEC-WEGLINSKI, J.W., (1997). Inhibition of CD26/dipeptidyl peptidase IV activity in vivo prolongs cardiac allograft survival in rat recipients. *Transplantation,* **63**(10), pp. 1495-1500.

KOROM, S., DE MEESTER, I., SCHMIDBAUER, G., PRATSCHKE, J., BRENDEL, M.D., DURINX, C., SCHWEMMLE, K., HAEMERS, A., SCHARPE, S. and KUPIEC-WEGLINSKI, J.W., (1999). Specific inhibition of CD26/DPP IV enzymatic activity in allograft recipients: effects on humoral immunity. *Transplantation Proceedings,* **31**, pp. 778.

KOUWENHOVEN, M., ÖZENCI, V., GOMES, A., YARILIN, D., GIEDRAITIS, V., PRESS, R. and LINK, H., (2001). Multiple sclerosis: elevated expression of matrix metalloproteinases in blood monocytes. *Journal of Autoimmunity,* **16**(4), pp. 463-470.

KRAKAUER, M., SORENSEN, P.S. and SELLEBJERG, F., (2006). CD4+ memory T cells with high CD26 surface expression are enriched for Th1 markers and correlate with clinical severity of multiple sclerosis. *Journal of Neuroimmunology,* **181**(1-2), pp. 157-164.

KRAMER-HAMMERLE, S., ROTHENAIGNER, I., WOLFF, H., BELL, J.E. and BRACK-WERNER, R., (2005). Cells of the central nervous system as targets and reservoirs of the human immunodeficiency virus. *Virus Research,* **111**(2), pp. 194-213.

KRAUS, J. and OSCHMANN, P., (2006). The impact of interferon-β treatment on the blood–brain barrier. *Drug Discovery Today,***11**(15-16), pp. 755-762.

KRIJGSVELD, J., ZAAT, S.A.J., MEELDIJK, J., VAN VEELEN, P.A., FANG, G., POOLMAN, B., BRANDT, E., EHLERT, J.E., KUIJPERS, A.J., ENGBERS, G.H.M., FEIJEN, J. and DANKERT, J., (2000). Thrombocidins, microbicidal proteins from human blood platelets, are C-terminal deletion products of CXC chemokines. *Journal of Biological Chemistry,* **275**(27), pp. 20374-20381.

KRUGER, P.G., (2001). Mast cells and multiple sclerosis: a quantitative analysis. *Neuropathology and Applied Neurobiology,* **27**(4), pp. 275-280.

KRUMBHOLZ, M., THEIL, D., CEPOK, S., HEMMER, B., KIVISAKK, P., RANSOHOFF, R.M., HOFBAUER, M., FARINA, C., DERFUSS, T., HARTLE, C., NEWCOMBE, J., HOHLFELD, R. and MEINL, E., (2006). Chemokines in multiple sclerosis: CXCL12 and CXCL13 up-regulation is differentially linked to CNS immune cell recruitment. *Brain,***129**(12), pp. 200-211.

KUBOTA, T., FLENTKE, G.R., BACHOVCHIN, W.W. and STOLLAR, B.D., (1992). Involvement of dipeptidyl peptidase IV in an *in vivo* immune response. *Clinical and Experimental Immunology,* **89**(2), pp. 192–197.

KUERTEN, S. and ANGELOV, D.N., (2008). Comparing the CNS morphology and immunobiology of different EAE models in C57BL/6 mice – a step towards understanding the complexity of multiple sclerosis. *Annals of Anatomy,* **190**(1), pp. 1-15.

KUMAGAI, Y., YAGISHITA, H., YAJIMA, A., OKAMOTO, T. and KONISHI, K., (2005). Molecular mechanism for connective tissue destruction by dipeptidyl aminopeptidase IV produced by the periodontal pathogen porphyromonas gingivalis. *Infection and Immunity,* **73**(5), pp. 2655-2664.

KURTZKE, J.F., BEEBE, G.W. and NORMAN J.E., J., (1979). Epidemiology of multiple sclerosis in U.S. veterans: 1. Race, sex, and geographic distribution. *Neurology,* **29**(9 I), pp. 1228-1235.

KURZEPA, J., BARTOSIK-PSUJEK, H., SUCHOZEBRSKA-JESIONEK, D., REJDAK, K., STRYJECKA-ZIMMER, M. and STELMASIAK, Z., (2005). Role of matrix metalloproteinases in the pathogenesis of multiple sclerosis. *Polish Journal of Neurology and Neurosurgery,* **39**(1), pp. 63-67.

LAEMMLI, U. K., (1970). Cleavage of structural proteins during the assembly of the head of bacteriophage T4. *Nature* **227**, pp. 680–685.

LAMBEIR, A., PROOST, P., DURINX, C., BAL, G., SENTEN, K., AUGUSTYNS, K., SCHARPE, S., VAN DAMME, J. & DE MEESTER, I., (2001). Kinetic Investigation of Chemokine Truncation by CD26/Dipeptidyl Peptidase IV Reveals a Striking Selectivity within the Chemokine Family. *Journal of Biological Chemistry,* **276**(32), pp. 29839-29845.

LA ROSA, D.F. and ORANGE, J.S. (2008). 1. Lymphocytes, *Journal of Allergy and Clinical Immunology,* **121**(2), Supplement 2, pp. S364-S369.

LASCHINGER, M., VJAKOCZY, P. and ENGELHARDT, B., (2002). Encephalitogenic T cells use LFA-1 for transendothelial migration but not during capture and initial adhesion strengthening in healthy spinal cord microvessels in vivo. *European Journal of Immunology,* **32**(12), pp. 3598-3606.

LASSMANN, H. (1998). Neuropathology in multiple sclerosis: new concepts. *Multiple Sclerosis,* **4**(3), pp. 93-98.

LASSMANN, H., (2003). Brain damage when multiple sclerosis is diagnosed clinically. *The Lancet,* **361**(9366), pp. 1317-1318.

LASSMANN, H., (2005). Stem cell and progenitor cell transplantation in multiple sclerosis: The discrepancy between neurobiological attraction and clinical feasibility. *Journal of the Neurological Sciences,* **233**(1-2), pp. 83-86.

LASSMANN, H., (2007). Multiple sclerosis: Is there neurodegeneration independent from inflammation? *Journal of the Neurological Sciences,* **259**(1-2), pp. 3-6.

LASSMANN, H., WAKSMAN, B. and BROSNAN, C.F., (1991). Mechanisms of vascular and tissue damage in demyelinating diseases : Viterbo, Italy, 3–7 October 1990. *Journal of Neuroimmunology,* **32**(1), pp. 83-85.

LEE, M.A., PALACE, J., STABLER, G., FORD, J., GEARING, A. & MILLER, K., (1999). Serum gelatinase B, TIMP-1 and TIMP-2 levels in multiple sclerosis: A longitudinal clinical and MRI study. *Brain,***122**(2), pp. 191-197.

LEE, S.C., LIU, W., BROSNAN, C.F. and DICKSON, D.W., (1994). GM-CSF promotes proliferation of human fetal and adult microglia in primary cultures. *Glia,* **12**(4), pp. 309-318.

LEHMANN, M.H., MASANETZ, S., KRAMER, S. and ERFLE, V., (2006). HIV-1 Nef upregulates CCL2/MCP-1 expression in astrocytes in a myristoylation- and calmodulin-dependent manner. *Journal of Cell Science,* **119**(21), pp. 4520-4530.

LENARDO, M., CHAN, F.K., HORNUNG, F., MCFARLAND, H., SIEGEL, R., WANG, J. and ZHENG, L., (1999). Mature T lymphocyte apoptosis-immune regulation in a dynamic and unpredictable antigenic environment. *Annual Review of Immunology,* **17**(1), pp. 221-253.

LENTSCH, A.B. (2002). The Duffy antigen/receptor for chemokines (DARC) and prostate cancer. A role as clear as black and white? *FASEB Journal,* **16**(9), pp. 1093-1095.

LEPPERT, D., LINDBERG, R.L.P., KAPPOS, L. and LEIB, S.L., (2001). Matrix metalloproteinases: multifunctional effectors of inflammation in multiple sclerosis and bacterial meningitis. *Brain Research Reviews,* **36**(2-3), pp. 249-257.

LÉVÊQUE, T., LE PAVEC, G., BOUTET, A., TARDIEU, M., DORMONT, D. and GRAS, G., (2004). Differential regulation of gelatinase A and B and TIMP-1 and -2 by TNFα and HIV virions in astrocytes. *Microbes and Infection,* **6**(2), pp. 157-163.

LIBBEY, J.E., MC COY, L.L. and FUJINAMI, R.S., (2007). Molecular mimicry in multiple sclerosis. *International Review of Neurobiology,* Ed. Alireza Minagar, Academic Press, pp. 127-147.

LIESI, P., SEPPÄLÄ, I., TRENKNER, E., (1992). Neuronal migration in cerebellar microcultures is inhibited by antibodies against a neurite outgrowth domain of laminin. *Journal of Neuroscience Research,* **33**(1), pp. 170-176.

LIJNEN, H.R., VAN HOEF, B., LUPU, F., MOONS, L., CARMELIET, P. and COLLEN, D., (1998). Function of the plasminogen/plasmin and matrix metalloproteinase systems after vascular injury in mice with targeted inactivation of fibrinolytic system genes. *Arteriosclerosis, Thrombosis, and Vascular Biology,* **18**(7), pp. 1035-1045.

LIN, B., GINSBERG, M.D., BUSTO, R. and LI, L., (2000). Hyperglycemia triggers massive neutrophil deposition in brain following transient ischemia in rats. *Neuroscience Letters,* **278**(1-2), pp. 1-4.

LINDBERG, R.P., DE GROOT, C.A., MONTAGNE, L., FREITAG, P., VAN DER VALK, P., KAPPOS, L. and LEPPERT, D., (2001). The expression profile of matrix metalloproteinases (MMPs) and their inhibitors (TIMPs) in lesions and normal appearing white matter of multiple sclerosis. *Brain,* **124**(9), pp. 1743-1753.

LIU, J.K. and ROSENBERG, G.A., (2005). Matrix metalloproteinases and free radicals in cerebral ischemia. *Free Radical Biology and Medicine,* **39**(1), pp. 71-80.

LOETSCHER, P., SEITZ, M., BAGGIOLINI, M. and MOSER, B., (1996). Interleukin-2 regulates CC chemokine receptor expression and chemotactic responsiveness in T lymphocytes. *Journal of Experimental Medicine,* **184**(2), pp. 569-577.

LOETSCHER, M., LOETSCHER, P., BRASS, N., MEESE, E. and MOSER, B., (1998). Lymphocyte-specific chemokine receptor CXCR3: regulation, chemokine binding and gene localization. *European Journal of Immunology*, **28**(11), pp. 3696-3705.

LOREY, S., STOCKEL-MASCHEK, A., FAUST, J., BRANDT, W., STIEBITZ, B., GORRELL, M.D., KAHNE, T., MRESTANI-KLAUS, C., WRENGER, S., REINHOLD, D., ANSORGE, S. and NEUBERT, K., (2003). Different modes of dipeptidyl peptidase IV (CD26) inhibition by oligopeptides derived from the N-terminus of HIV-1 Tat indicate at least two inhibitor binding sites. *European Journal of Biochemistry,* 270(10), pp. 2147-2156.

LUBLIN, F.D. and REINGOLD, S.C., (1996). Defining the clinical course of multiple sclerosis: Results of an international survey. *Neurology,* **46**(4), pp. 907-911.

LUDWIG, A., SCHIEMANN, F., MENTLEIN, R., LINDNER, B. and BRANDT, E., (2002). Dipeptidyl peptidase IV (CD26) on T cells cleaves the CXC chemokine CXCL11 (I-TAC) and abolishes the stimulating but not the desensitizing potential of the chemokine. *Journal of Leukocyte Biology,* **72**(1), pp. 183-191.

LUE, L., BRACHOVA, L., WALKER, D. and ROGERS, J., (1996). Characterization of glial cultures from rapid autopsies of Alzheimer's and control patients. *Neurobiology of Aging,* **17**(3), pp. 421-429.

LUND, B.T., ASHIKIAN, N., TA, H.Q., CHAKRYAN, Y., MANOUKIAN, K., GROSHEN, S., GILMORE, W., CHEEMA, G.S., STOHL, W., BURNETT, M.E., KO, D., KACHUCK, N.J. & WEINER, L.P., (2004). Increased CXCL8 (IL-8) expression in Multiple Sclerosis. *Journal of Neuroimmunology,* **155**(1-2), pp. 161-171.

MACKAREL, A.J., COTTELL, D.C., FITZGERALD, M.X. and O'CONNOR, C.M., (1999). Human endothelial cells cultured on microporous filters used for leukocyte transmigration studies form monolayers on both sides of the filter. *In Vitro Cellular and Developmental Biology - Animal,* **35**(6), pp. 346-351.

MACKAY, C.R., (1996). Chemokine receptors and T cell chemotaxis. *Journal of Experimental Medicine,* **184**, pp. 799.

MAHAD, D.J., HOWELL, S.J.L. and WOODROOFE, M.N., (2002). Expression of chemokines in the CSF and correlation with clinical disease activity in patients with multiple sclerosis. *Journal of Neurology, Neurosurgery, and Psychiatry,* **72**(4), pp. 498-502.

MAHAD, D.J., LAWRY, J., HOWELL, S.J. and WOODROOFE, M.N., (2003). Longitudinal study of chemokine receptor expression on peripheral lymphocytes in multiple sclerosis: CXCR3 upregulation is associated with relapse. *Multiple Sclerosis,* **9**(2), pp. 189–198.

MAHAD, D.J. and RANSOHOFF, R.M., (2003). The role of MCP-1 (CCL2) and CCR2 in multiple sclerosis and experimental autoimmune encephalomyelitis (EAE). *Seminars in Immunology,* **15**(1), pp. 23-32.

MAHAD, D.J., CALLAHAN, M.K., WILLIAMS, K.A., UBOGU, E.E., KIVISAKK, P., TUCKY, B., KIDD, G., KINGSBURY, G.A., CHANG, A., FOX, R.J., MACK, M., SNIDERMAN, M.B., RAVID, R., STAUGAITIS, S.M., STINS, M.F. and RANSOHOFF, R.M., (2006). Modulating CCR2 and CCL2 at the blood-brain barrier: relevance for multiple sclerosis pathogenesis. *Brain,* **129**(1), pp. 212-223.

MALIK, O., COMPSTON, D.A.S. and SCOLDING, N.J. (1998). Interferon-beta inhibits mitogen induced astrocyte proliferation in vitro. *Journal of Neuroimmunology,* **86**(2), pp. 155-162.

MANTZOURANI, E., PLATTS, J., BRANCALE, A., MAVROMOUSTAKOS, T. and TSELIOS, T., (2007). Molecular dynamics at the receptor level of immunodominant myelin basic protein epitope 87–99 implicated in multiple sclerosis and its antagonists altered peptide ligands: Triggering of immune response. *Journal of Molecular Graphics and Modelling,* **26**(2), pp. 471-481.

MARCHESE, A., CHEN, C., KIM, Y. and BENOVIC, J.L., (2003). The ins and outs of G protein-coupled receptor trafficking. *Trends in Biochemical Sciences,* **28**(7), pp. 369-376.

MARENHOLZ, I., HEIZMANN, C.W. and FRITZ, G., (2004). S100 proteins in mouse and man: from evolution to function and pathology (including an update of the nomenclature). *Biochemical and Biophysical Research Communications,* **322**(4), pp. 1111-1122.

MARGIS, R., ZANATTO, V., TRAMONTINA, F., VINADE, E., LHULLIER, F., PORTELA, L., SOUZA, D.G., DALMAZ, C., KAPCZINSKI, F. and GONÇALVES, C., (2004). Changes in S100B cerebrospinal fluid levels of rats subjected to predator stress. *Brain Research,* **1028**(2), pp. 213-218.

MARK, B.L. and CARSON, J.A.S., (2006). Vitamin D and autoimmune disease-implications for practice from the multiple sclerosis literature. *Journal of the American Dietetic Association,* **106**(3), pp. 418-424.

MARKOVIC-PLESE, S. and MCFARLAND, H.F., (2001). Immunopathogenesis of the multiple sclerosis lesion. *Current Neurology and Neuroscience Reports,* **1**(3), pp. 257-262.

MARKOVIC-PLESE, S., PINILLA, C. and MARTIN, R., (2004). The initiation of the autoimmune response in multiple sclerosis. *Clinical Neurology and Neurosurgery,* **106**(3), pp. 218-222.

MARRIE, R., (2004). Environmental risk factors in multiple sclerosis aetiology. *Lancet Neurology,* **3**(12), pp. 709-718.

MARTIN, L.J., PARDO, C.A., CORK, L.C. and PRICE, D.L., (1994). Synaptic pathology and glial responses to neuronal injury precede the formation of senile plaques and amyloid deposits in the aging cerebral cortex. *American Journal of Pathology*, **145**, pp. 1358-1381.

MASTRONARDI, F.G. and MOSCARELLO, M.A., (2005). Molecules affecting myelin stability: A novel hypothesis regarding the pathogenesis of multiple sclerosis. *Journal of Neuroscience Research,* **80**(3), pp. 301-308.

MATRISIAN, L.M., (1992). The matrix-degrading metalloproteinases. *BioEssays,* **14**(7), pp. 455-463.

MATSUMURA, I., WALLINGFORD, J.B., SURANA, N.K., VIZE, P.D. and ELLINGTON, A.D., (1999). Directed evolution of the surface chemistry of the reporter enzyme β-glucuronidase. *Nature Biotechnology,* **17**(7), pp. 696-701.

MATTER, K. and BALDA, M.S., (2003). Signalling to and from tight junctions. *Nature Reviews Molecular Cell Biology,* **4**(3), pp. 225-236.

MATTU, T.S., ROYLE, L., LANGRIDGE, J., WORMALD, M.R., VAN DEN STEEN, P.E., VAN DAMME, J., OPDENAKKER, G., HARVEY, D.J., DWEK, R.A. and RUDD, P.M., (2000). O-glycan analysis of natural human neutrophil gelatinase B using a combination of normal phase-HPLC and online tandem mass spectrometry: implications for the domain organization of the enzyme. *Biochemistry,* **39**(51), pp. 15695-15704.

MCGUIGAN, C., MCCARTHY, A., QUIGLEY, C., BANNAN, L., HAWKINS, S.A.. and HUTCHINSON, M., (2004). Latitudinal variation in the prevalence of multiple sclerosis in Ireland, an effect of genetic diversity. *Journal of Neurology, Neurosurgery, and Psychiatry*, **75**(4), pp. 572-576.

MCMANUS, C., BERMAN, J.W., BRETT, F.M., STAUNTON, H., FARRELL, M. and BROSNAN, C.F., (1998). MCP-1, MCP-2 and MCP-3 expression in multiple sclerosis lesions: an immunohistochemical and in situ hybridization study. *Journal of Neuroimmunology,* **86**(1), pp. 20-29.

MCQUIBBAN, G.A., BUTLER, G.S., GONG, J.H., BENDALL, L., POWER, C., CLARK-LEWIS, I. and OVERALL, C.M., (2001). Matrix metalloproteinase activity inactivates the CXC chemokine stromal cell-derived factor-1. *Journal of Biological Chemistry,* **276**(47), pp. 43503-43508.

MCQUIBBAN, G.A., GONG, J., WONG, J.P., WALLACE, J.L., CLARK-LEWIS, I. and OVERALL, C.M., (2002). Matrix metalloproteinase processing of monocyte chemoattractant proteins generates CC chemokine receptor antagonists with anti-inflammatory properties *in vivo. Blood,* **100**(4), pp. 1160-1167.

MENTLEIN, R., (1999). Dipeptidyl-peptidase IV (CD26)-role in the inactivation of regulatory peptides. *Regulatory Peptides,* **85**(1), pp. 9-24.

MERRILL, J.E., IGNARRO, L.J., SHERMAN, M.P., MELINEK, J. and LANE, T.E., (1993). Microglial cell cytotoxicity of oligodendrocytes is mediated through nitric oxide. *Journal of Immunology,* **151**(4), pp. 2132-2141.

MIDDLETON, J., NEIL, S., WINTLE, J., CLARK-LEWIS, I., MOORE, H., LAM, C., AUER, M., HUB, E. and ROT, A., (1997). Transcytosis and surface presentation of IL-8 by venular endothelial cells. *Cell,* **91**(3), pp. 385-395.

MINAGAR, A., TOLEDO, E.G., ALEXANDER, J.S. and KELLEY, R.E., (2004). Pathogenesis of brain and spinal cord atrophy in multiple sclerosis. *Journal of Neuroimaging,* **14**(3), pp. 5S-10S.

MISU, T., ONODERA, H., FUJIHARA, K., MATSUSHIMA, K., YOSHIE, O., OKITA, N., TAKASE, S. and ITOYAMA, Y., (2001). Chemokine receptor expression on T cells in blood and cerebrospinal fluid at relapse and remission of multiple sclerosis: imbalance of Th1/Th2-associated chemokine signaling. *Journal of Neuroimmunology,* **114**(1-2), pp. 207-212.

MITRO, A. and LOJDA, Z., (1988). Histochemistry of proteases in ependyma, choroid plexus and leptomeninges. *Histochemistry,* **88**(3-6), pp. 645-646.

MIYAGISHI, R., KIKUCHI, S., FUKAZAWA, T. and TASHIRO, K., (1995). Macrophage inflammatory protein-1 alpha in the cerebrospinal fluid of patients with multiple sclerosis and other inflammatory neurological diseases. *Journal of the Neurological Sciences,* **129**(2), pp. 223-227.

MIZOKAMI, A., EGUCHI, K., KAWAKAMI, A., IDA, H., KAWABE, Y., TSUKADA, T., AOYAGI, T., MAEDA, K., MORIMOTO, C. and NAGATAKI, S., (1996). Increased population of high fluorescence 1F7 (CD26) antigen on T cells in synovial fluid of patients with rheumatoid arthritis. *Journal of Rheumatology,* **23**(12), pp. 2022–2026.

MOHAMED, M.M. and SLOANE, B.F., (2006). Cysteine cathepsins: multifunctional enzymes in cancer. *Nature Reviews Cancer,* **6**(10), pp. 764-775.

MONROE, E.B., KOSZCZUK, B.A., LOSH, J.L., JURCHEN, J.C. & SWEEDLER, J.V., (2007). Measuring salty samples without adducts with MALDI MS. *International Journal of Mass Spectrometry,* **260**(2-3), pp. 237-242.

MOREIRA, M.A., TILBERY, C.P., MONTEIRO, L.P., TEIXEIRA, M.M. and TEIXEIRA, A.L., (2006). Effect of the treatment with methylprednisolone on the cerebrospinal fluid and serum levels of CCL2 and CXCL10 chemokines in patients with active multiple sclerosis. *Acta Neurologica Scandinavica,* **114**(2), pp. 109-113.

MORIMOTO, C., TORIMOTO, Y., LEVINSON, G., RUDD, C., SCHRIEBER, M., DANG, N., LETVIN, N. and SCHLOSSMAN, S., (1989). 1F7, a novel cell surface molecule, involved in helper function of CD4 cells. *Journal of Immunology,***143**(11), pp. 3430-3439.

MORIMOTO, C. and SCHLOSSMAN, S.F., (1998). The structure and function of CD26 in the T-cell immune response. *Immunological Reviews,* **161**, pp. 55–70.

MORRISON, R.S., DE VELLIS, J., LEE, Y.L., BRADSHAW, R.A. and ENG, L.F., (1985). Hormones and growth factors induce the synthesis of glial fibrillary acidic protein in rat brain astrocytes. *Journal of Neuroscience Research,* **14**, pp. 167-176.

MOSER, B. and LOETSCHER, P., (2001). Lymphocyte traffic control by chemokines. *Nature Immunology*, **2**(2), pp. 123-128.

MUIR, E.M., ADCOCK, K.H., MORGENSTERN, D.A., CLAYTON, R., VON STILLFRIED, N., RHODES, K., ELLIS, C., FAWCETT, J.W. and ROGERS, J.H., (2002). Matrix metalloproteases and their inhibitors are produced by overlapping populations of activated astrocytes. *Molecular Brain Research,* **100**(1-2), pp. 103-117.

MULLER, W.A., (2003). Leukocyte-endothelial-cell interactions in leukocyte transmigration and the inflammatory response. *Trends in Immunology,* **24**(6), pp. 327-334.

MUNGER, K.L., ZHANG, S.M., O'REILLY, E., HERNAN, M.A., OLEK, M.J., WILLETT, W.C. and ASCHERIO, A., (2004). Vitamin D intake and incidence of multiple sclerosis. *Neurology,* **62**(1), pp. 60-65.

MURPHY, S., SIMMONS, M.L., AGULLO, L., GARCIA, A., FEINSTEIN, D.L., GALEA, E., REIS, D.J., MINC-GOLOMB, D. and SCHWARTZ, J.P., (1993). Synthesis of nitric oxide in CNS glial cells. *Trends in Neurosciences,* **16**(8), pp. 323-328.

MUSSO, T., ESPINOZA-DELGADO, I., PULKKI, K., GUSELLA, G., LONGO, D. and VARESIO, L., (1990). Transforming growth factor beta downregulates interleukin-1 (IL-1)- induced IL-6 production by human monocytes. *Blood,* **76**(12), pp. 2466-2469.

NAGASE, H., (1997). Activation mechanisms of matrix metalloproteinases. *Biology and Chemistry,* **378**, pp. 151–160.

NAKAO, H., EGUCHI, K., KAWAKAMI, A., MIGITA, K., OTSUBO, T., UEKI, Y., SHIMOMURA, C., TEZUKA, H., MATSUNAGA, M., MAEDA, K. and NAGATAKI, S., (1989). Increment of Tal positive cells in peripheral blood from patients with rheumatoid arthritis. *Journal of Rheumatology,* **16**(7), pp. 904-910.

NAMIHIRA, M., NAKASHIMA, K. and TAGA, T., (2004). Developmental stage dependent regulation of DNA methylation and chromatin modification in an immature astrocyte specific gene promoter. *FEBS Letters,* **572**(1-3), pp. 184-188.

NETZEL-ARNETT, S., SANG, Q.X., MOORE, W.G.I., NAVRE, M., BIRKEDAL-HANSEN, H. & VAN WART, H.E., (1993). Comparative sequence specificities of human 72- and 92-kDa gelatinases (type IV collagenases) and PUMP (matrilysin). *Biochemistry,* **32**(25), pp. 6427-6432.

NEUBERT, H., HALKET, J.M., FERNANDEZ OCAÑA, M. & PATEL, R.K.P., (2004). MALDI post-source decay and LIFT-TOF/TOF investigation of α-cyano-4-hydroxycinnamic acid cluster interferences. *Journal of the American Society for Mass Spectrometry,* **15**(3), pp. 336-343.

NEUHAUS, O., KIESEIER, B. and HARTUNG, H., (2004). Mechanisms of mitoxantrone in multiple sclerosis–what is known? *Journal of the Neurological Sciences,* **223**(1), pp. 25-27.

NEUHAUS, O., KIESEIER, B.C. and HARTUNG, H., (2006). Therapeutic role of mitoxantrone in multiple sclerosis. *Pharmacology & Therapeutics,* **109**(1-2), pp. 198-209.

NEUMANN, H. and TAKAHASHI, K., (2007). Essential role of the microglial triggering receptor expressed on myeloid cells-2 (TREM2) for central nervous tissue immune homeostasis. *Journal of Neuroimmunology,* **184**(1-2), pp. 92-99.

NIKBIN, B., BONAB, M., KHOSRAVI, F. and TALEBIAN, F., (2007). Role of B cells in pathogenesis of multiple sclerosis. *International Review of Neurobiology,* Ed. Alireza Minagar, Academic Press, pp. 13-42.

NOONAN, C.W., KATHMAN, S.J. & WHITE, M.C., (2002). Prevalence estimates for MS in the United States and evidence of an increasing trend for women. *Neurology,* **58**(1), pp. 136-138.

NOSEWORTHY, J., PATY, D., WONNACOTT, T. and ET, A., (1983). Multiple sclerosis after age 50. *Neurology,* **33**(12), pp. 1537-1544.

NUTTALL, R.K., PENNINGTON, C.J., TAPLIN, J., WHEAL, A., YONG, V.W., FORSYTH, P.A. and EDWARDS, D.R., (2003). Elevated membrane-type matrix metalloproteinases in gliomas revealed by profiling proteases and inhibitors in human cancer cells. *Molecular Cancer Research,* **1**(5), pp. 333-45.

OBERHEIM, N.A., WANG, X., GOLDMAN, S. and NEDERGAARD, M., (2006). Astrocytic complexity distinguishes the human brain. *Trends in Neurosciences,* **29**(10), pp. 547-553.

OH, J.W., SCHWIEBERT, L.M., BENVENISTE, E.N., (1999). Cytokine regulation of CC and CXC chemokine expression by human astrocytes. *Journal of Neurovirology,* **5**(1), pp. 82-94.

OPALEK, J., ALI, N., LOBB, J., HUNTER, M. and MARSH, C., (2007). Alveolar macrophages lack CCR2 expression and do not migrate to CCL2. *Journal of Inflammation,* **4**(1), pp. 19.

OPDENAKKER, G., VAN DEN STEEN, P.E. and VAN DAMME, J., (2001). Gelatinase B: a tuner and amplifier of immune functions. *Trends in Immunology,* **22**(10), pp. 571-579.

OPPERMANN, M., (2004). Chemokine receptor CCR5: insights into structure, function, and regulation. *Cellular Signalling,* **16**(11), pp. 1201-1210.

ORTON, S., HERRERA, B.M., YEE, I.M., VALDAR, W., RAMAGOPALAN, S.V., SADOVNICK, A.D. and EBERS, G.C., (2006). Sex ratio of multiple sclerosis in Canada: a longitudinal study. *Lancet Neurology,* **5**(11), pp. 932-936.

OSAKA, H., MC GINTY, A., HOPKEN, U.E., LU, B., GERARD, C. and PASINETTI, G.M., (1999). Expression of C5a receptor in mouse brain: role in signal transduction and neurodegeneration. *Neuroscience,* **88**(4), pp. 1073-1082.

OSGOOD-MC WEENEY, D., GALLUZZI, J. and ORDOVAS, J., (2000). Allelic discrimination for single nucleotide polymorphisms in the human scavenger receptor class B type 1 gene locus using fluorescent probes. *Clinical Chemistry,* **46**(1), pp. 118-119.

OSSOWSKI, L. and AGUIRRE-GHISO, J.A., (2000). Urokinase receptor and integrin partnership: coordination of signaling for cell adhesion, migration and growth. *Current Opinion in Cell Biology,* **12**(5), pp. 613-620.

OSTROW, L.W. and SACHS, F., (2005). Mechanosensation and endothelin in astrocytes—hypothetical roles in CNS pathophysiology. *Brain Research Reviews,* **48**(3), pp. 488-508.

OTA, K., MATSUI, M., MILFORD, E.L., MACKIN, G.A., WEINER, H.L. and HAFLER, D.A., (1990). T-cell recognition of an immunodominant myelin basic protein epitope in multiple sclerosis. *Nature,* **346**(6280), pp. 183-187.

OYNEBRATEN, I., BAKKE, O., BRANDTZAEG, P., JOHANSEN, F. and HARALDSEN, G., (2004). Rapid chemokine secretion from endothelial cells originates from two distinct compartments. *Blood,* **104**(2), pp. 314-320.

PAGE-MC CAW, A., EWALD, A.J. and WERB, Z., (2007). Matrix metalloproteinases and the regulation of tissue remodelling. *Nature Reviews. Molecular Cell Biology,* **8**(3), pp. 221-233.

PANKONIN, G., REIPERT, B. and AGER, A., (1992). Interactions between interleukin-2-activated lymphocytes and vascular endothelium: binding to and migration across specialized and non-specialized endothelia. *Immunology,* **77**(1), pp. 51-60.

PANYI, G., VARGA, Z. and GASPAR, R., (2004). Ion channels and lymphocyte activation. *Immunology Letters,* **92**(1-2), pp. 55-66.

PARKS, W.C., WILSON, C.L. and LOPEZ-BOADO, Y.S., (2004). Matrix metalloproteinases as modulators of inflammation and innate immunity. *Nature Reviews.Immunology,* **4**(8), pp. 617-629.

PARRATT, J.D.E., O'RIORDAN, J. and SWINGLER, R.J., (2007). 316: Chlamydia pneumoniae infection in patients with multiple sclerosis. *Journal of Clinical Neuroscience,* **14**(10), pp. 1013.

PATANOW, C.M., DAY, J.R. and BILLINGSLEY, M.L., (1997). Alterations in hippocampal expression of SNAP-25, GAP-43, stannin and glial fibrillary acidic protein following mechanical and trimethyltin-induced injury in the rat. *Neuroscience,***76**(1), pp. 187-202.

PATEL, D., KOOPMANN, W., IMAI, T., WHICHARD, L., YOSHIE, O. and KRANGEL, M., (2001). Chemokines have diverse abilities to form solid phase gradients. *Clinical Immunology,* **99**(1), pp. 43-52.

PEDEMONTE, E., MANCARDI, G., GIUNTI, D., CORCIONE, A., BENVENUTO, F., PISTOIA, V. and UCCELLI, A., (2006). Mechanisms of the adaptive immune response inside the central nervous system during inflammatory and autoimmune diseases. *Pharmacology & Therapeutics,* **111**(3), pp. 555-566.

PENTON-ROL, G., POLENTARUTTI, N., LUINI, W., BORSATTI, A., MANCINELLI, R., SICA, A., SOZZANI, S. and MANTOVANI, A., (1998). Selective inhibition of expression of the chemokine receptor CCR2 in human monocytes by IFN-γ. *Journal of Immunology,* **160**(8), pp. 3869-3873.

PHILLIPS, L.M. and LAMPSON, L.A., (1999). Site-specific control of T cell traffic in the brain: T cell entry to brainstem vs. hippocampus after local injection of IFN-γ. *Journal of Neuroimmunology,* **96**(2), pp. 218-227.

PHILLIPS, R.J., MESTAS, J., GHARAEE-KERMANI, M., BURDICK, M.D., SICA, A., BELPERIO, J.A., KEANE, M.P. and STRIETER, R.M., (2005). Epidermal growth factor and hypoxia-induced expression of CXC chemokine receptor 4 on non-small cell lung cancer cells is regulated by the phosphatidylinositol 3-kinase/PTEN/AKT/mammalian target of rapamycin signaling pathway and activation of hypoxia inducible factor-1α. *Journal of Biological Chemistry,* **280**(23), pp. 22473-22481.

PODOJIL, J. and MILLER, S., (2006). Immunopathological mechanisms in multiple sclerosis. *Drug Discovery Today: Disease Mechanisms,* **3**(2), pp. 177-184.

POLLARD, T.D. and BORISY, G.G., (2003). Cellular motility driven by assembly and disassembly of actin filaments. *Cell,* **112**(4), pp. 453-465.

PONTÉN, J. and MACINTYRE, E.H., (1968). Long term culture of normal and neoplastic human glia. *Acta Pathologica et Microbiologica Scandinavica,* **74**(4), pp. 465-486.

PRAT, A. and ANTEL, J., (2005). Pathogenesis of multiple sclerosis. *Current Opinion in Neurology,* **18**(3), pp. 225-230.

PRELLER, V., GERBER, A., TOGNI, M., WRENGER, S., SCHRAVEN, B., ROCKEN, C., MARGUET, D., ANSORGE, S., BROCKE, S. and REINHOLD, D., (2006). CD26/DP IV in T cell activation and autoimmunity. *Advances in Experimental Medicine and Biology*, **575,** pp. 187-93

PROOST, P., DE WOLF-PEETERS, C., CONINGS, R., OPDENAKKER, G., BILLIAU, A. and VAN DAMME, J., (1993). Identification of a novel granulocyte chemotactic protein (GCP-2) from human tumor cells. *In vitro* and *in vivo* comparison with natural forms of GRO, IP-10, and IL-8. *Journal of Immunology,* **150**(3), pp. 1000-1010.

PROOST, P., WUYTS, A., CONINGS, R., LENAERTS, J., PUT, W. & VAN DAMME, J., (1996). Purification and identification of natural chemokines. *Methods,* **10**(1), pp. 82-92.

PROOST, P., DE MEESTER, I., SCHOLS, D., STRUYF, S., LAMBEIR, A.M., WUYTS, A., OPDENAKKER, G., DE CLERCQ, E., SCHARPE, S. and VAN DAMME ET, A., (1998a). Amino-terminal truncation of chemokines by CD26/dipeptidyl-peptidase IV. Conversion of RANTES into a potent inhibitor of monocyte chemotaxis and HIV-1-infection. *Journal of Biological Chemistry,* **273**(13), pp. 7222-7227.

PROOST, P., STRUYF, S., COUVREUR, M., LENAERTS, J., CONINGS, R., MENTEN, P., VERHAERT, P., WUYTS, A. and DAMME, J.V., (1998b). Posttranslational modifications affect the activity of the human monocyte chemotactic proteins MCP-1 and MCP-2: Identification of MCP-2(6-76) as a natural chemokine inhibitor. *Journal of Immunology*, **160**(8), pp. 4034-4041.

PROOST, P., STRUYF, S., SCHOLS, D., DURINX, C., WUYTS, A., LENAERTS, J., DECLERCQ, E., DE MEESTER, I. and VAN DAMME, J., (1998c). Processing by CD26/dipeptidyl-peptidase IV reduces the chemotactic and anti-HIV-1 activity of stromal-cell-derived factor-1α. *FEBS Letters,* **432**(1-2), pp. 73-76.

PROOST, P., STRUYF, S., SCHOLS, D., OPDENAKKER, G., SOZZANI, S., ALLAVENA, P., MANTOVANI, A., AUGUSTYNS, K., BAL, G., HAEMERS, A., LAMBEIR, A., SCHARPE, S., VAN DAMME, J. & DE MEESTER, I., (1999). Truncation of macrophage-derived chemokine by CD26/ dipeptidyl-peptidase IV beyond Its predicted cleavage site affects chemotactic activity and CC chemokine receptor 4 interaction. *Journal of Biological Chemistry,* **274**(7), pp. 3988-3993.

PROOST, P., SCHUTYSER, E., MENTEN, P., STRUYF, S., WUYTS, A., OPDENAKKER, G., DETHEUX, M., PARMENTIER, M., DURINX, C., LAMBEIR, A.., NEYTS, J., LIEKENS, S., MAUDGAL, P.C., BILLIAU, A. and VAN DAMME, J., (2001). Amino-terminal truncation of CXCR3 agonists impairs receptor signaling and lymphocyte chemotaxis, while preserving antiangiogenic properties. *Blood,* **98**(13), pp. 3554-3561.

PROOST, P., STRUYF, S. and VAN DAMME, J., (2006). Natural post-translational modifications of chemokines. *Biochemical Society Transactions,* **34**(6), pp. 997-1001.

PROSSNITZ, E.R. and YE, R.D., (1997). The *N*-formyl peptide receptor: a model for the study of chemoattractant receptor structure and function. *Pharmacology and Therapeutics,* **74**, pp. 73-102.

PROUDFOOT, A.E.I., (2002). Chemokine receptors: multifaceted therapeutic targets. *Nature Reviews. Immunology,* **2**(2), pp. 106-115.

PROUDFOOT, A.E.I., HANDEL, T.M., JOHNSON, Z., LAU, E.K., LI WANG, P., CLARK-LEWIS, I., BORLAT, F., WELLS, T.N.C. and KOSCO-VILBOIS, M.H., (2003). Glycosaminoglycan binding and oligomerization are essential for the *in vivo* activity of certain chemokines. *Proceedings of the National Academy of Sciences,* **100**(4), pp. 1885-1890.

PROUDFOOT, A.E.I., (2006). The biological relevance of chemokine-proteoglycan interactions. *Biochemical Society Transactions,* **34**(3), pp. 422-426.

PRYCE, G., MALE, D., CAMPBELL, I. and GREENWOOD, J., (1997). Factors controlling T-cell migration across rat cerebral endothelium in vitro. *Journal of Neuroimmunology,* **75**(1-2), pp. 84-94.

PRYCE, G. and BAKER, D., (2005). Emerging properties of cannabinoid medicines in management of multiple sclerosis. *Trends in Neurosciences,* **28**(5), pp. 272-276.

PUSCHEL, G., MENTLEIN, R., and HEYMANN, E. (1982). Isolation and characterization of dipeptidyl peptidase IV from human placenta. *European Journal of Biochemistry,* **126**, pp. 359–365.

QI, J.H., EBRAHEM, Q., MOORE, N., MURPHY, G., CLAESSON-WELSH, L., BOND, M., BAKER, A. and ANAND-APTE, B., (2003). A novel function for tissue inhibitor of metalloproteinases-3 (TIMP3): Inhibition of angiogenesis by blockage of VEGF binding to VEGF receptor-2. *Nature Medicine,* **9**(4), pp. 407-415.

QUANDT, J. and DOROVINI-ZIS, K., (2004). The beta chemokines CCL4 and CCL5 enhance adhesion of specific CD4+ T cell subsets to human brain endothelial cells. *Journal of Neuropathology and Experimental Neurology,* **63**(4), pp. 350-362.

RABILLOUD, T., VUILLARD, L., GILLY, C. and LAWRENCE, J., (1994). Silver-staining of proteins in polyacrylamide gels: a general overview. *Cellular and Molecular Biology,* **40**(1), pp. 57-75.

RAEBER, G.P., LUTOLF, M.P. and HUBBELL, J.A., (2007). Mechanisms of 3-D migration and matrix remodeling of fibroblasts within artificial ECMs. *Acta Biomaterialia,* **3**(5), pp. 615-629.

RAMM, L., WHITLOW, M. and MAYER, M., (1985). The relationship between channel size and the number of C9 molecules in the C5b-9 complex. *Journal of Immunology,* **134**(4), pp. 2594-2599.

RAMOS-DE SIMONE, N., HAHN-DANTONA, E., SIPLEY, J., NAGASE, H., FRENCH, D.L. and QUIGLEY, J.P., (1999). Activation of matrix metalloproteinase-9 (MMP-9) via a converging plasmin/stromelysin-1 cascade enhances tumor cell invasion. *Journal of Biological Chemistry,* **274**(19), pp. 13066-13076.

RAMOS-VARA, J.A. (2005). Technical Aspects of Immunohistochemistry. *Veterinary Pathology*, **42**(4), pp. 405-426.

RANSOHOFF, R.M., HOWE, C.L. and RODRIGUEZ, M., (2002). Growth factor treatment of demyelinating disease: at last, a leap into the light. *Trends in Immunology,* **23**(11), pp. 512-516.

RAYNAUD, F., BAUVOIS, B., GERBAUD, P. and EVAIN-BRION, D., (1992). Characterization of specific proteases associated with the surface of human skin fibroblasts, and their moduration in pathology. *Journal of Cellular Physiology,* **151**, pp. 378-385

RECKAMP, K.L., FIGLIN, R.A., MOLDAWER, N., PANTUCK, A.J., BELLDEGRUN, A.S., BURDICK, M.D. and STRIETER, R.M., (2007). Expression of CXCR3 on mononuclear cells and CXCR3 ligands in patients with metastatic renal cell carcinoma in response to systemic IL-2 therapy. *Journal of Immunotherapy.* **30**(4), pp. 417-424.

REEVES, S., HELMAN, L., ALLISON, A. and ISRAEL, M., (1989). Molecular cloning and primary structure of human glial fibrillary acidic protein. *Proceedings of the National Academy of Sciences,* **86**(13), pp. 5178-5182.

REINDL, M., LINNINGTON, C., BREHM, U., EGG, R., DILITZ, E., DEISENHAMMER, F., POEWE, W. and BERGER, T., (1999). Antibodies against the myelin oligodendrocyte glycoprotein and the myelin basic protein in multiple sclerosis and other neurological diseases: a comparative study. *Brain,* **122**(11), pp. 2047-2056.

REINDL, M., KHALIL, M. and BERGER, T., (2006). Antibodies as biological markers for pathophysiological processes in MS. *Journal of Neuroimmunology,* **180**(1-2), pp. 50-62.

REINHOLD, D., HEMMER, B., GRAN, B., BORN, I., FAUST, J., NEUBERT, K., MC FARLAND, H.F., MARTIN, R. and ANSORGE, S., (1998). Inhibitors of dipeptidyl peptidase IV/CD26 suppress activation of human MBP-specific CD4 + T cell clones. *Journal of Neuroimmunology,* **87**(1-2), pp. 203–209.

REINHOLD, D., BITON, A., PIEPER, S., LENDECKEL, U., FAUST, J., NEUBERT, K., BANK, U., TÄGER, M., ANSORGE, S. and BROCKE, S., (2006). Dipeptidyl peptidase IV (DP IV, CD26) and aminopeptidase N (APN, CD13) as regulators of T cell function and targets of immunotherapy in CNS inflammation. *International Immunopharmacology,* **6**(13-14), pp. 1935-1942.

REIPERT, B., (2004). Multiple sclerosis: a short review of the disease and its differences between men and women. *Journal of Men's Health and Gender*, **1**(4), pp. 334-340.

REP, M.G., HINTZEN, R., POLMAN, C. and VANLIER, R.W., (1996). Recombinant interferon-β blocks proliferation but enhances interleukin-10 secretion by activated human T-cells. *Journal of Neuroimmunology,* **67**(2), pp. 111-118.

REP, M.G., SCHRIJVER, H., VANLOPIK, T., HINTZEN, R., ROOS, M.L., ADÈR, H., POLMAN, C. and VANLIER, R.W., (1999). Interferon (IFN)-β treatment enhances CD95 and interleukin 10 expression but reduces interferon-γ producing T cells in MS patients. *Journal of Neuroimmunology,* **96**(1), pp. 92-100.

RESNATI, M., PALLAVICINI, I., WANG, J.M., OPPENHEIM, J., SERHAN, C.N., ROMANO, M. and BLASI, F., (2002). The fibrinolytic receptor for urokinase activates the G protein-coupled chemotactic receptor FPRL1/LXA4R. *Proceedings of the National Academy of Sciences,* **99**(3), pp. 1359-1364.

RIBEIRO, S. and HORUK, R., (2005). The clinical potential of chemokine receptor antagonists. *Pharmacology & Therapeutics,* **107**(1), pp. 44-58.

RIESEBERG, M., KASPER, C., REARDON, K.F. and SCHEPER, T., (2001). Flow cytometry in biotechnology. *Applied Microbiology and Biotechnology,* **56**(3), pp. 350-360.

RISTIC, S., LOVRECIC, L., BRAJENOVIC-MILIC, B., STARCEVIC-CIZMAREVIC, N., JAZBEC, S.S., SEPCIC, J., KAPOVIC, M. and PETERLIN, B., (2005). Mutations in the hemochromatosis gene (HFE) and multiple sclerosis. *Neuroscience Letters,* **383**(3), pp. 301-304.

ROG, D.J., NURMIKKO, T.J., SARANTIS, N.S. and YOUNG, C.A., (2007). Long-term use of sativex in multiple sclerosis central pain; dosing and changes in concomitant analgesia. *European Journal of Pain,* **11**(1, Supplement 1), pp. 136.

ROOPRAI, H.K. and MC CORMICK, D., (1997). Proteases and their inhibitors in human brain tumours: a review. *Anticancer Research,***17**(6 B), pp. 4151-4162.

ROSENBERG, G.A., (2005). Matrix metalloproteinases biomarkers in multiple sclerosis. *The Lancet,* **365**(9467), pp. 1291-1293.

ROSS, M.H. and PAWLINA, W., (2006). Histology: a text and atlas (Fifth edition). Lippincott Williams & Wilkins.

ROTH, S.J., CARR, M.W., ROSE, S.S. and SPRINGER, T.A., (1995a). Characterization of transendothelial chemotaxis of T lymphocytes. *Journal of Immunological Methods,* **188**(1), pp. 97-116.

ROTH, S.J., CART, M.W. and SPRINGER, T.A., (1995b). C-C chemokines, but not the C-X-C chemokines interleukin-8 and interferon-gamma inducible protein-10, stimulate transendothelial chemotaxis of T lymphocytes. *European Journal of Immunology,* **25,** pp. 3482-3488.

RUS, H., CUDRICI, C., NICULESCU, F. and SHIN, M.L., (2006). Complement activation in autoimmune demyelination: Dual role in neuroinflammation and neuroprotection. *Journal of Neuroimmunology,* **180**(1-2), pp. 9-16.

RUSSELL, B.J., VELEZ, J.O., LAVEN, J.J., JOHNSON, A.J., CHANG, G.J. and JOHNSON, B.W., (2007). A comparison of concentration methods applied to non-infectious flavivirus recombinant antigens for use in diagnostic serological assays. *Journal of Virological Methods,* **145**(1), pp. 62-70.

RUTKA, J.T., MURAKAMI, M., DIRKS, P.B., HUBBARD, S.L., BECKER, L.E., FUKUYAMA, K., JUNG, S., TSUGU, A. and MATSUZAWA, K., (1997). Role of glial filaments in cells and tumors of glial origin: A review. *Journal of Neurosurgery,* **87**(3), pp. 420-430.

RUWANPURA, S.M.P.M., NOGUCHI, K. and ISHIKAWA, I., (2004). Prostaglandin E2 regulates interleukin-1β-induced matrix metalloproteinase-3 production in human gingival fibroblasts. *Journal of Dental Research,* **83**(3), pp. 260-265.

SADOVNICK, A.D., ARMSTRONG, H., RICE, G.P.A., BULMAN, D., HASHIMOTO, L., PATY, D.W., HASHIMOTO, S.A., WARREN, S., HADER, W., MURRAY, T.J., SELAND, T.P., METZ, L., BELL, R., DUQUETTE, P., GRAY, T., NELSON, R., WEINSHENKER, B., BRUNET, D. and EBERS, G.C., (1993). A population-based study of multiple sclerosis in twins: Update. *Annals of Neurology,* **33**(3), pp. 281-285.

SALCEDO, R., WASSERMAN, K., YOUNG, H.A., GRIMM, M.C., HOWARD, O.M.Z., ANVER, M.R., KLEINMAN, H.K., MURPHY, W.J. and OPPENHEIM, J.J., (1999). Vascular endothelial growth factor and basic fibroblast growth factor induce expression of CXCR4 on human endothelial cells: *In vivo* neovascularization induced by stromal-derived factor-1alpha. *American Journal of Pathology,* **154**(4), pp. 1125-1135.

SALGADO, F.J., VELA, E., MARTÍN, M., FRANCO, R., NOGUEIRA, M. and CORDERO, O.J., (2000). Mechanisms of CD26/dipeptidyl peptidase IV cytokine-dependent regulation on human activated lymphocytes. *Cytokine,* **12**(7), pp. 1136-1141.

SALLUSTO, F., LANZAVECCHIA, A. and MACKAY, C.R., (1998). Chemokines and chemokine receptors in T-cell priming and Th1/Th2-mediated responses. *Immunology Today,* **19**(12), pp. 568-574.

SALLUSTO, F., GEGINAT, J. and LANZAVECCHIA, A., (2004). Central memory and effector memory T cell subsets: function, generation, and maintenance. *Annual Review of Immunology,* **22**(1), pp. 745-763.

SATO, H., KINOSHITA, T., TAKINO, T., NAKAYAMA, K. and SEIKI, M., (1996). Activation of a recombinant membrane type 1-matrix metalloproteinase (MT1-MMP) by furin and its interaction with tissue inhibitor of metalloproteinases (TIMP)-2. *FEBS Letters,* **393**(1), pp. 101-104.

SCHÄGGER, H. and VON JAGOW, G., (1987). Tricine-sodium dodecyl sulfate-polyacrylamide gel electrophoresis for the separation of proteins in the range from 1 to 100 kDa. *Analytical Biochemistry,* **166**(2), pp. 368-379.

SCHILLER, J., SÜß, R., ARNHOLD, J., FUCHS, B., LEßIG, J., MÜLLER, M., PETKOVIĆ, M., SPALTEHOLZ, H., ZSCHÖRNIG, O. and ARNOLD, K., (2004). Matrix-assisted laser desorption and ionization time-of-flight (MALDI-TOF) mass spectrometry in lipid and phospholipid research. *Progress in Lipid Research,* **43**(5), pp. 449-488.

SCHLAEGER, R., SCHINDLER, C., GRIZE, L., KAPPOS, L. and FUHR, P., (2006). Multimodal visual, motor and somatosensory evoked potentials as markers of clinical disability in primary progressive multiple sclerosis. *Clinical Neurophysiology,* **117**(Supplement 1), pp. 141-142.

SCHNELL, S.A., STAINES, W.A. and WESSENDORF, M.W., (1999). Reduction of lipofuscin-like autofluorescence in fluorescently labeled tissue. *Journal of Histochemistry and Cytochemistry,* **47**(6), pp. 719-730.

SCHON, E., JAHN, S., KIESSIG, S.T., DEMUTH, H.U., NEUBERT, K., BARTH, A., VON BAEHR, R. and ANSORGE, S., (1987). The role of dipeptidyl peptidase IV in human T lymphocyte activation. Inhibitors and antibodies against dipeptidyl peptidase IV suppress lymphocyte proliferation and immunoglobulin synthesis *in vitro*. *European Journal of Immunology,* **17**(12), pp. 1821–1826.

SCHWARZ, M., SPECTOR, L., GORTLER, M., WEISSHAUS, O., GLASS-MARMOR, L., KARNI, A., DOTAN, N. and MILLER, A., (2006). Serum anti-Glc(α1,4)Glc(α) antibodies as a biomarker for relapsing-remitting multiple sclerosis. *Journal of the Neurological Sciences,* **244**(1-2), pp. 59-68.

SEABROOK, T.J., JOHNSTON, M. and HAY, J.B., (1998). Cerebral spinal fluid lymphocytes are part of the normal recirculating lymphocyte pool. *Journal of Neuroimmunology,* **91**(1-2), pp. 100-107.

SEGA, S., WRABER, B., MESEC, A., HORVAT, A. and IHAN, A., (2004). IFN-β1a and IFN-β1b have different patterns of influence on cytokines. *Clinical Neurology and Neurosurgery,* **106**(3), pp. 255-258.

SEITZER, U., SCHEEL-TOELLNER, D., MATTERN, T., HAAS, H., FLAD, H. and GERDES, J., (1998). Staining pattern of seven monoclonal anti-CD26 antibodies in leprosy: implications for the use of CD26 as a surrogate marker of a human Th1-like reaction. *Virchows Archiv,* **432**(4), pp. 343-347.

SELLEBJERG, F., CHRISTIANSEN, M., JENSEN, J. and FREDERIKSEN, J.L., (2000). Immunological effects of oral high-dose methylprednisolone in acute optic neuritis and multiple sclerosis. *European Journal of Neurology,* **7**(3), pp. 281– 289.

SELTZER, J., AKERS, K., WEINGARTEN, H., GRANT, G., MCCOURT, D. & EISEN, A., (1990). Cleavage specificity of human skin type IV collagenase (gelatinase). Identification of cleavage sites in type I gelatin, with confirmation using synthetic peptides. *Journal of Biological Chemistry,* **265**(33), pp. 20409-20413.

SERAFINI, B., ROSICARELLI, B., MAGLIOZZI, R., STIGLIANO, E. and ALOISI, F., (2004). Detection of ectopic B-cell follicles with germinal centers in the meninges of patients with secondary progressive multiple sclerosis. *Brain Pathology,* **14**(2), pp. 164-174.

SERVET-DELPRAT, C., ARNAUD, S., JURDIC, P., NATAF, S., GRASSET, M.F., SOULAS, C., DOMENGET, C., DESTAING, O., RIVOLLIER, A., PERRET, M., DUMONTEL, C., HANAU, D., GILMORE, G.L., BELIN, M.F., RABOURDIN-COMBE, C. and MOUCHIROUD, G., (2002). Flt3+ macrophage precursors commit sequentially to osteoclasts, dendritic cells and microglia. *BMC Immunology*, **3**(1), pp. 15.

SHAO, Y. and MC CARTHY, K.D., (1994). Plasticity of astrocytes. *Glia*, **11,** 147–155.

SHARIEF, M.K. and THOMPSON, E.J., (1991). Intrathecal immunoglobulin M synthesis in multiple sclerosis. Relationship with clinical and cerebrospinal fluid parameters. *Brain,* **114**(1 A), pp. 181-195.

SHARPE, R.J., (1986). The low incidence of multiple sclerosis in areas near the equator may be due to ultraviolet light induced supressor cells to melanocyte antigens. *Medical Hypotheses,* **19**(4), pp. 319-323.

SHARPE, G., PRICE, S., LAST, A. and THOMPSON, R., (1995). Multiple sclerosis in island populations: prevalence in the Bailiwicks of Guernsey and Jersey. *Journal of Neurology, Neurosurgery, and Psychiatry*, **58**(1), pp. 22-26.

SHENG, J.G., MRAK, R.E. and GRIFFIN, W.S., (1994). S100 beta protein expression in Alzheimer disease potential role in the pathogenesis of neuritic plaques. *Journal of Neuroscience Research,* **39**, pp. 398-404.

SHIU, W. and SCHOR, S., (1987). Quantitative study of various factors influencing the migration of lymphocytes in vitro: glucocortico-steroid, PHA, cyclosporin A and hepain. *Cell Biology International Reports,* **11**(3), pp. 171-180.

SIEBERT, P.D. and CHENCHIK, A., (1993). Modified acid guanidinium thiocyanate- phenol - chloroform RNA extraction method which greatly reduces DNA contamination. *Nucleic Acids Research,* **21**(8), pp. 2019-2020.

SILANI, V. and COVA, L., (2008). Stem cell transplantation in Multiple Sclerosis: Safety and Ethics. *Journal of the Neurological Sciences,* **265**(1-2), pp. 116-121.

SIMARD, A.R. and RIVEST, S., (2004). Bone marrow stem cells have the ability to populate the entire central nervous system into fully differentiated parenchymal microglia. *FASEB Journal,* **18**(9), pp. 998-1000.

SIMPSON, J.E., NEWCOMBE, J., CUZNER, M.L. and WOODROOFE, M.N., (1998). Expression of monocyte chemoattractant protein-1 and other β-chemokines by resident glia and inflammatory cells in multiple sclerosis lesions. *Journal of Neuroimmunology,* **84**(2), pp. 238-249.

SIMPSON, J.E., REZAIE, P., NEWCOMBE, J., CUZNER, M.L., MALE, D. and WOODROOFE, M.N., (2000a). Expression of the β-chemokine receptors CCR2, CCR3 and CCR5 in multiple sclerosis central nervous system tissue. *Journal of Neuroimmunology,* **108**(1-2), pp. 192-200.

SIMPSON, J.E., NEWCOMBE, J., CUZNER, M.L. and WOODROOFE, M.N., (2000b). Expression of the interferon-gamma-inducible chemokines IP-10 and Mig and their receptor, CXCR3, in multiple sclerosis lesions. *Neuropathology and Applied Neurobiology,* **26**(2), pp. 133-142.

SINGH, A.K. and JIANG, Y., (2004). How does peripheral lipopolysaccharide induce gene expression in the brain of rats? *Toxicology,* **201**(1-3), pp. 197-207.

SMITH, I., (1983). Mitoxantrone (novantrone): a review of experimental and early clinical studies. *Cancer Treatment Reviews,* **10**(2), pp. 103-115.

SOBEL, R. and MITCHELL, M., (1989). Fibronectin in multiple sclerosis lesions. *American Journal of Pathology,* **135**(1), pp. 161-168.

SOILU-HANNINEN, M., AIRAS, L., MONONEN, I., HEIKKILA, A., VILJANEN, M. and HANNINEN, A., (2005). 25-Hydroxyvitamin D levels in serum at the onset of multiple sclerosis. *Multiple Sclerosis,* **11**(3), pp. 266-271.

SON, K., HWANG, J., KWON, B.S. and KIM, J., (2006). Human CC chemokine CCL23 enhances expression of matrix metalloproteinase-2 and invasion of vascular endothelial cells. *Biochemical and Biophysical Research Communications,* **340**(2), pp. 498-504.

SOOS, J., MORROW, J., ASHLEY, T., SZENTE, B., BIKOFF, E. and ZAMVIL, S., (1998). Astrocytes express elements of the class II endocytic pathway and process central nervous system autoantigen for presentation to encephalitogenic T cells. *Journal of Immunology,* **161**(11), pp. 5959-5966.

SØRENSEN, T.L., TANI, M., JENSEN, J., PIERCE, V., LUCCHINETTI, C., FOLCIK, V.A., QIN, S., ROTTMAN, J., SELLEBJERG, F., STRIETER, R.M., FREDERIKSEN, J.L. and RANSOHOFF, R.M., (1999). Expression of specific chemokines and chemokine receptors in the central nervous system of multiple sclerosis patients. *Journal of Clinical Investigation,* **103**, pp. 801–815.

SØRENSEN, B., HOJRUP, P., OSTERGARD, E., JORGENSEN, C., ENGHILD, J., RYDER, L. and HOUEN, G., (2002a). Silver staining of proteins on electroblotting membranes and intensification of silver staining of proteins separated by polyacrylamide gel electrophoresis. *Analytical Biochemistry,* **304**(1), pp. 33-41.

SØRENSEN, T.L., TREBST, C., KIVISÄKK, P., KLAEGE, K.L., MAJMUDAR, A., RAVID, R., LASSMANN, H., OLSEN, D.B., STRIETER, R.M., RANSOHOFF, R.M. and SELLEBJERG, F., (2002b). Multiple sclerosis: a study of CXCL10 and CXCR3 co-localization in the inflamed central nervous system. *Journal of Neuroimmunology,* **127**(1-2), pp. 59-68.

SØRENSEN, T.L., RANSOHOFF, R.M., STRIETER, R.M. and SELLEBJERG, F., (2004). Chemokine CCL2 and chemokine receptor CCR2 in early active multiple sclerosis. *European Journal of Neurology,* **11**(7), pp. 445-449.

SOTGIU, S., PUGLIATTI, M., FOIS, M.L., ARRU, G., SANNA, A., SOTGIU, M.A. and ROSATI, G., (2004). Genes, environment, and susceptibility to multiple sclerosis. *Neurobiology of Disease,* **17**(2), pp. 131-143.

SPERANDIO, M., PICKARD, J., UNNIKRISHNAN, S., ACTON, S. and LEY, K., (2006). Analysis of leukocyte rolling *in vivo* and *in vitro. Methods in Enzymology,* Ed. Minoru Fukuda, Academic Press, New York, pp. 346-371.

SPRENT, J. and SURH, C.D. (2001). Generation and maintenance of memory T cells. *Current Opinion in Immunology,* **13**(2), pp. 248-254.

STEINBRECHER, A., REINHOLD, D., QUIGLEY, L., GADO, A., TRESSER, N., IZIKSON, L., BORN, I., FAUST, J., NEUBERT, K., MARTIN, R., ANSORGE, S. and BROCKE, S., (2001). Targeting dipeptidyl peptidase IV (CD26) suppresses autoimmune encephalomyelitis and up-regulates TGF-β1 secretion *in vivo. Journal of Immunology,* **166**(3), pp. 2041-2048.

STEINER, J., BERNSTEIN, H., BIELAU, H., BERNDT, A., BRISCH, R., MAWRIN, C., KEILHOFF, G. and BOGERTS, B., (2007). Evidence for a wide extra-astrocytic distribution of S100B in human brain. *BMC Neuroscience,* **8**(1), pp. 2.

STEITZ, S., HASEGAWA, K., CHIANG, S., COBB, R., CASTRO, M., LOBL, T., YAMADA, M., LAZARIDES, E. and CARDARELLI, P., (1998). Mapping of MCP-1 functional domains by peptide analysis and site-directed mutagenesis. *FEBS Letters,* **430**(3), pp. 158-164.

STOCK, C., SCHILLING, T., SCHWAB, A. and EDER, C., (2006). Lysophosphatidylcholine stimulates IL-1beta release from microglia via a P2X7 receptor-independent mechanism. *Journal of Immunology,* **177**(12), pp. 8560-8568.

STRATTON, C. and WHELDON, D., (2006). Multiple sclerosis: an infectious syndrome involving *Chlamydophila pneumoniae. Trends in Microbiology,* **14**(11), pp. 474-479.

STREMENOVA, J., KREPELA, E., MARES, V., TRIM, J., DBALY, V., MAREK, J., VANICKOVA, Z., LISA, V., YEA, C. and SEDO, A., (2007). Expression and enzymatic activity of dipeptidyl peptidase-IV in human astrocytic tumours are associated with tumour grade. *International Journal of Oncology,* **31**(4), pp. 785-92.

STRONGIN, A.Y., COLLIER, I., BANNIKOV, G., MARMER, B.L., GRANT, G.A. and GOLDBERG, G.I., (1995). Mechanism of cell surface activation of 72-kDa type IV collagenase. Isolation of the activated form of the membrane metalloprotease. *Journal of Biological Chemistry,* **270**, pp. 5331–5338.

STRUYF, S., DE MEESTER, I., SCHARPÉ, S., LENAERTS, J-P., MENTEN, P., MING WANG, J., PROOST, P., and VAN DAMME, J., (1998). Natural truncation of RANTES abolishes signaling through the CC chemokine receptors CCR1 and CCR3, impairs its chemotactic potency and generates a CC chemokine inhibitor. *European Journal of Immunology,* **28**(4), pp. 1262-1271.

STRUYF, S., MENTEN, P., LENAERTS, J.P., PUT, W., D'HAESE, A., DE CLERCQ, E., SCHOLS, D., PROOST, P. and VAN DAMME, J., (2001). Diverging binding capacities of natural LD78β isoforms of macrophage inflammatory protein-1alpha to the CC chemokine receptors 1, 3 and 5 affect their anti-HIV-1 activity and chemotactic potencies for neutrophils and eosinophils. *European Journal of Immunology,* **31**(7), pp. 2170-2178.

STRUYF, S., PROOST, P. and VAN DAMME, J., (2003). Regulation of the immune response by the interaction of chemokines and proteases. *Advances in Immunology,* **81**, pp. 1-44.

STUART, D.A. and OORSCHOT, D.E., (1995). Embedding, sectioning, immunocytochemical and stereological methods that optimise research on the lesioned adult rat spinal cord. *Journal of Neuroscience Methods,* **61**(1-2), pp. 5-14.

STUVE, O., DOOLEY, N.P., UHM, J.H., ANTEL, J.P., FRANCIS, G.S., WILLIAMS, G. and YONG, V.W., (1996). Interferon β-1b decreases the migration of T lymphocytes in vitro: Effects on matrix metalloproteinase-9. *Annals of Neurology,* **40**(6), pp. 853-863.

SULIMAN, O., FOUILLET, A., ROMERO, I., KEYNES, M., SHARRACK, B. and WOODROOFE, M.N., (2006). Expression of CCL2, CXCL10 and their receptors CCR2 and CXCR3 by primary adult human astrocytes in vitro: Effect of pro-inflammatory cytokines. *Neurology,* **66**(5), Suppl. 2, pp. A371-A371.

SWAMINATHAN, G.J., HOLLOWAY, D.E., COLVIN, R.A., CAMPANELLA, G.K., PAPAGEORGIOU, A.C., LUSTER, A.D. and ACHARYA, K.R., (2003). Crystal structures of oligomeric forms of the IP-10/CXCL10 chemokine. *Structure,* **11**(5), pp. 521-532.

SZABO, K.A., ABLIN, R.J. and SINGH, G., (2004). Matrix metalloproteinases and the immune response. *Clinical and Applied Immunology Reviews,* **4**(5), pp. 295-319.

SZCZUCIŃSKI, J.L. and LOSY, J., (2007). Chemokines and chemokine receptors in multiple sclerosis. Potential targets for new therapies. *Acta Neurologica Scandinavica,* **115**(3), pp. 137-146.

TAKAHASHI, K., ROCHFORD, C.P. and NEUMANN, H., (2005). Clearance of apoptotic neurons without inflammation by microglial triggering receptor expressed on myeloid cells-2. *Journal of Experimental Medicine,* **201**(4), pp. 647-657.

TAKIZAWA, T., YANAGISAWA, M., OCHIAI, W., YASUKAWA, K., ISHIGURO, T., NAKASHIMA, K. and TAGA, T., (2001). Directly linked soluble IL-6 receptor–IL-6 fusion protein induces astrocyte differentiation from neuroepithelial cells via activation of STAT3. *Cytokine,* **13**(5), pp. 272-279.

TALLEY, C.L., (2005). The emergence of multiple sclerosis, 1870-1950: a puzzle of historical epidemiology. *Perspectives in Biology and Medicine,* **48**(3), pp. 383-395.

TANAKA, S., MURAKAMI, T., HORIKAWA, H., SUGIURA, M., KAWASHIMA, K. and SUGITA, T., (1997). Suppression of arthritis by the inhibitors of dipeptidyl peptidase IV. *International Journal of Immunopharmacology,* **19**(1), pp. 15-24.

TANAKA, T., CAMERINI, D., SEED, B., TORIMOTO, Y., DANG, N.H., KAMEOKA, J., DAHLBERG, H.N., SCHLOSSMAN, S.F. and MORIMOTO, C., (1992). Cloning and functional expression of the T cell activation antigen CD26. *Journal of Immunology,* **149**(2), pp. 481–486.

TANAKA, T., J KAMEOKA, J., YARON, A., SCHLOSSMAN, S.F. and MORIMOTO, C., (1993). The costimulatory activity of the CD26 antigen requires dipeptidyl peptidase IV enzymatic activity. *Proceedings of the National Academy of Sciences of the United States of America,* **90**(10), pp. 4586–4590.

TARRANT, J.M., (2005). The role of flow cytometry in companion animal diagnostic medicine. *Veterinary Journal,* **170**(3), pp. 278-288.

TELESHOVA, N., PASHENKOV, M., HUANG, Y., SODERSTROM, M., KIVISAKK, P., KOSTULAS, V., HAGLUND, M. and LINK, H., (2002). Multiple sclerosis and optic neuritis: CCR5 and CXCR3 expressing T cells are augmented in blood and cerebrospinal fluid. *Journal of Neurology,* **249**(6), pp. 723-729.

TENNAKOON, D., MEHTA, R., ORTEGA, S., RACKE, M. and KARANDIKAR, N., (2006). Sa.17. Glatiramer acetate (Copaxone) therapy restores regulatory, cytotoxic CD8+ T-cells in multiple sclerosis. *Clinical Immunology,* **119**(S1), pp. S110-S111.

THOMPSON, E.J. and KEIR, G., (1990). Laboratory investigation of cerebrospinal fluid proteins. *Annals of Clinical Biochemistry,* **27**(5), pp. 425-435.

THORPE, R., (2003). Chemokine/chemokine receptor nomenclature. *Cytokine,* **21**(1), pp. 48-49.

TIRUPPATHI, C., MIYAMOTO, Y., GANAPATHY, V. and LEIBACH, F.H., (1993). Genetic evidence for role of DPP IV in intestinal hydrolysis and assimilation of prolyl peptides. *American Journal of Physiology,* **265**, pp. G81–89.

TORIMOTO, Y., DANG, N.H., VIVIER, E., TANAKA, T., SCHLOSSMAN, S.F. and MORIMOTO, C., (1991). Coassociation of CD26 (dipeptidyl peptidase IV) with CD45 on the surface of human T lymphocytes. *Journal of Immunology,***147**(8), pp. 2514-2517.

TRAN, E.H., HOEKSTRA. K., VAN ROOIJEN, N., DIJKSTRA, C.D. and OWENS, T., (1998). Macrophages modulate immune invasion of the central nervous system. *Journal of Neuroimmunology*, **90**(1), pp. 22.

TRAPANI, J.A., DAVIS, J., SUTTON, V.R. and SMYTH, M.J., (2000). Proapoptotic functions of cytotoxic lymphocyte granule constituents *in vitro* and *in vivo. Current Opinion in Immunology,* **12**(3), pp. 323-329.

TREBST, C., STAUGAITIS, S.M., KIVISAKK, P., MAHAD, D., CATHCART, M.K., TUCKY, B., WEI, T., RANI, M.R.S., HORUK, R. and ALDAPE K.D., PARDO, C.A., LUCCHINETTI, C.F., LASSMANN, H. and RANSOHOFF, R.M., (2003). CC chemokine receptor 8 in the central nervous system is associated with phagocytic macrophages. *American Journal of Pathology,* **162**(2), pp. 427-438.

TSUJIMURA, K., TANAKA, J., ANDO, S., MATSUOKA, Y., KUSUBATA, M., SUGIURA, H., YAMAUCHI, T. and INAGAKI, M., (1994). Identification of phosphorylation sites on glial fibrillary acidic protein for cdc2 kinase and Ca2+-calmodulin-dependent protein kinase II. *Journal of Biochemistry,* **116**(2), pp. 426-434.

TURNER, L., WARD, S.G. and WESTWICK, J., (1995). RANTES-activated human T lymphocytes: a role for phosphoinositide 3-kinase. *Journal of Immunology*, **155**, pp. 2437–2444.

URRY, D. W. (2004). The change in Gibbs free energy for hydrophobic association - Derivation and evaluation by means of inverse temperature transitions. *Chemical Physics Letters,* **399**(1-3), pp.177-183

VAKNIN-DEMBINSKY, A. and WEINER, H., (2007). Relationship of immunologic abnormalities and disease stage in multiple sclerosis: Implications for therapy. *Journal of the Neurological Sciences,* **259**(1-2), pp. 90-94.

VAN BEEK, J., NICOLE, O., ALI, C., ISCHENKO, A., MACKENZIE, E.T., BUISSON, A. and FONTAINE, M., (2001). Complement anaphylatoxin C3a is selectively protective against NMDA-induced neuronal cell death. *Neuroreport,* **12**, pp. 289–293.

VAN COILLIE, E., PROOST, P., VAN AELST, I., STRUYF, S., POLFLIET, M., DE MEESTER, I., HARVEY, D.J., VAN DAMME, J. and OPDENAKKER, G., (1998). Functional comparison of two human monocyte chemotactic protein-2 isoforms, role of the amino-terminal pyroglutamic acid and processing by CD26/dipeptidyl peptidase IV. *Biochemistry,* **37**(36), pp. 12672-12680.

VAN DAMME, J., STRUYF, S. and OPDENAKKER, G., (2004). Chemokine-protease interactions in cancer. *Seminars in Cancer Biology,* **14**(3), pp. 201-208.

VAN DEN STEEN, P.E., PROOST, P., WUYTS, A., VAN DAMME, J. and OPDENAKKER, G., (2000). Neutrophil gelatinase B potentiates interleukin-8 tenfold by aminoterminal processing, whereas it degrades CTAP-III, PF-4, and GRO-alpha and leaves RANTES and MCP-2 intact. *Blood,* **96**(8), pp. 2673-2681.

VAN DEN STEEN, P.E., HUSSON, S., PROOST, P., VAN DAMME, J. and OPDENAKKER, G., (2003). Carboxyterminal cleavage of the chemokines MIG and IP-10 by gelatinase B and neutrophil collagenase. *Biochemical and Biophysical Research Communications,* **310**(3), pp. 889-896.

VAN DER VOORN, P., TEKSTRA, J., BEELEN, R.H., TENSEN, C.P., VAN DER VALK, P. and DE GROOT, C.J., (1999). Expression of MCP-1 by reactive astrocytes in demyelinating multiple sclerosis lesions. *American Journal of Pathology,* **154**(1), pp. 45-51.

VANGURI, P. and SHIN, M.L., (1986). Activation of complement by myelin: Identification of C1-binding proteins of human myelin from central nervous tissue. *Journal of Neurochemistry,* **46**(5), pp. 1535-1541.

VAN HOOF, G., GOOSSENS, F., DE MEESTER, I., HENDRIKS, D. and SCHARPE, S., (1995). Proline motifs in peptides and their biological processing. *FASEB Journal*, **9**(9), pp. 736-744.

VAN LINT, P. and LIBERT, C., (2007). Chemokine and cytokine processing by matrix metalloproteinases and its effect on leukocyte migration and inflammation. *Journal of Leukocyte Biology,* **82**(6), pp. 1375-1381.

VAN WEYENBERGH, J., LIPINSKI, P., ABADIE, A., CHABAS, D., BLANK, U., LIBLAU, R. and WIETZERBIN, J., (1998). Antagonistic action of IFN-β and IFN-γ on high affinity Fcγ receptor expression in healthy controls and multiple sclerosis patients. *Journal of Immunology,* **161**(3), pp. 1568-1574.

VEGA, F.D., LAZARUK, K., RHODES, M. and WENZ, M., (2005). Assessment of two flexible and compatible SNP genotyping platforms: TaqMan® SNP genotyping assays and the SNPlex™ genotyping system. *Mutation Research,* **573**(1-2), pp. 111-135.

VERMA, S., NAKAOKE, R., DOHGU, S. and BANKS, W.A., (2006). Release of cytokines by brain endothelial cells: A polarized response to lipopolysaccharide. *Brain, Behavior and Immunity* **20**(5), pp. 449-455.

VESTWEBER, D., (2000). Molecular mechanisms that control endothelial cell contacts. *Journal of Pathology,* **190**(3), pp. 281-291.

VESTWEBER, D., (2002). Regulation of endothelial cell contacts during leukocyte extravasation. *Current Opinion in Cell Biology,* **14**(5), pp. 587-593.

VICENTE-MANZANARES, M., WEBB, D.J. and HORWITZ, A.R., (2005). Cell migration at a glance. *Journal of Cell Science,* **118**(21), pp. 4917-4919.

VISSCHER, B.R., DETELS, R., COULSON, A.H., MALMGREN, R.M. and DUDLEY, J.P., (1977). Latitude, migration, and the prevalence of multiple sclerosis. *American Journal of Epidemiology,* **106**(6), pp. 470-475.

VON BERNHARDI, R. and RAMIREZ, G., (2001). Microglia astrocyte interaction in Alzheimer's disease: friends or foes for the nervous system? *Biological Research*, **34**(2), pp.123-128.

VON BREDOW, D.C., CRESS, A.E., HOWARD, E.W., BOWDEN, G.T. and NAGLE, R.B., (1998). Activation of gelatinase-tissue-inhibitors-of-metalloproteinase complexes by matrilysin. *Journal of Biochemistry,* **331**, pp. 965-972.

VON HUNDELSHAUSEN, P., PETERSEN, F. and BRANDT, E., (2007). Platelet-derived chemokines in vascular biology. *Thrombosis and Haemostasis,* **97**(5), pp. 704-713.

VOS, C.M.P., GEURTS, J.J.G., MONTAGNE, L., VAN HAASTERT, E.S., BO, L., VAN DER VALK, P., BARKHOF, F. and DE VRIES, H.E., (2005). Blood–brain barrier alterations in both focal and diffuse abnormalities on postmortem MRI in multiple sclerosis. *Neurobiology of Disease,* **20**(3), pp. 953-960.

WALDMANN, T.A. (1991). The interleukin-2 receptor. *Journal of Biological Chemistry,* **266**, pp. 2681-2684.

WALDMANN, T.A. (1993). The IL-2/IL-2 receptor system: A target for rational immune intervention. *Immunology Today,* **14**, pp. 264-269.

WALLENSTEIN, S., ZUCKER, C.L. and FLEISS, J.L., (1980). Some statistical methods useful in circulation research. *Circulation Research*, **47**, pp. 1-9.

WALZ, W., (2000). Controversy surrounding the existence of discrete functional classes of astrocytes in adult gray matter. *Glia,* **31**(2), pp. 95-103.

WATKINS, B.A., CROWLEY, R.W., DAVIS, A.E., LOUIE, A.T., REITZ, J., and MARVIN S., (1996). Expression of CD26 does not correlate with the replication of macrophage-tropic strains of HIV-1 in T-cell lines. *Virology,* **224**(1), pp. 276-280.

WEAVER, A.M., YOUNG, M.E., LEE, W. and COOPER, J.A., (2003). Integration of signals to the Arp2/3 complex. *Current Opinion in Cell Biology,* **15**(1), pp. 23-30.

WEBBER, D.J., COMPSTON, A. and CHANDRAN, S., (2007). Minimally manipulated oligodendrocyte precursor cells retain exclusive commitment to the oligodendrocyte lineage following transplantation into intact and injured hippocampus. *European Journal of Neuroscience,* **26**(7), pp. 1791-1800.

WEBER, K.S.C., VON HUNDELSHAUSEN, P., CLARK-LEWIS, I., WEBER, P.C., and WEBER, C. (1999). Differential immobilization and hierarchical involvement of chemokines in monocyte arrest and transmigration on inflamed endothelium in shear flow. *European Journal of Immunology,* **29**(2), pp. 700-712.

WELLS, W.A., (2003). Movement in Colorado: the keystone symposium on cell migration and invasion Breckenridge, CO January 18-23, 2003. *Journal of Cell Biology,* **160**(7), pp. 985-988.

WESTON, S. and PARISH, C., (1990). New fluorescent dyes for lymphocyte migration studies: analysis by flow cytometry and fluorescence microscopy. *Journal of Immunological Methods,* **133**(1), pp. 87-97.

WOLF, K., MAZO, I., LEUNG, H., ENGELKE, K., VON ANDRIAN, U.H., DERYUGINA, E.I., STRONGIN, A.Y., BROCKER, E. and FRIEDL, P., (2003). Compensation mechanism in tumor cell migration: mesenchymal-amoeboid transition after blocking of pericellular proteolysis. *Journal of Cell Biology,* **160**(2), pp. 267-277.

WOLF, M., ALBRECHT, S. and MÄRKI, C., (2008). Proteolytic processing of chemokines: Implications in physiological and pathological conditions. *International Journal of Biochemistry & Cell Biology,* **40**(6-7), pp. 1185-1198.

WONG, D. and DOROVINI-ZIS, K., (1996). Platelet/endothelial cell adhesion molecule-1 (PECAM-1) expression by human brain microvessel endothelial cells in primary culture. *Brain Research,* **731**(1-2), pp. 217-220.

WONG, D., DOROVINI-ZIS, K. and VINCENT, S., (2004). Cytokines, nitric oxide, and cGMP modulate the permeability of an in vitro model of the human blood–brain barrier. *Experimental Neurology,* **190**(2), pp. 446-455.

WONG, D., PRAMEYA, R. and DOROVINI-ZIS, K., (2007). Adhesion and migration of polymorphonuclear leukocytes across human brain microvessel endothelial cells are differentially regulated by endothelial cell adhesion molecules and modulate monolayer permeability. *Journal of Neuroimmunology,* **184**(1-2), pp. 136-148.

WOODROOFE, M.N., BELLAMY, A.S., FELDMANN, M., DAVISON, A.N. and CUZNER, M.L., (1986). Immunocytochemical characterisation of the immune reaction in the central nervous system in multiple sclerosis : possible role for microglia in lesion growth. *Journal of the Neurological Sciences,* **74**(2-3), pp. 135-152.

WYSOCZYNSKI, M., RECA, R., RATAJCZAK, J., KUCIA, M., SHIRVAIKAR, N., HONCZARENKO, M., MILLS, M., WANZECK, J., JANOWSKA-WIECZOREK, A. and RATAJCZAK, M.Z., (2005). Incorporation of CXCR4 into membrane lipid rafts primes homing-related responses of hematopoietic stem/progenitor cells to an SDF-1 gradient. *Blood,* **105**(1), pp. 40-48.

XIA, M.Q., BACSKAI, B.J., KNOWLES, R.B., QIN, S.X. and HYMAN, B.T., (2000). Expression of the chemokine receptor CXCR3 on neurons and the elevated expression of its ligand IP-10 in reactive astrocytes: *in vitro* ERK1/2 activation and role in Alzheimer's disease. *Journal of Neuroimmunology,* **108**(1-2), pp. 227-235.

XIAO, B. and LINK, H., (1998). Immune regulation within the central nervous system. *Journal of the Neurological Sciences,* **157**(1), pp. 1-12.

YAMADA, K.M., (2000). Fibronectin peptides in cell migration and wound repair. *Journal of Clinical Investigation,* **105**(11), pp. 1507-1509.

YAN, J. and MAMULA, M., (2002). Autoreactive T cells revealed in the normal repertoire: escape from negative selection and peripheral tolerance. *Journal of Immunology,* **168**(7), pp. 3188-3194.

YAN, Z., CALDWELL, G.W., JONES, W.J. & MASUCCI, J.A., (2000). A simple method to improve spectral quality in matrix-assisted laser desorption/ionization–time-of-flight–mass spectrometric analysis by using micro mate labeling tape as a sample support. *Analytical Biochemistry,* **277**(2), pp. 267-270.

YAO, P.J., O'HERRON, T.M. and COLEMAN, P.D., (2003). Immunohistochemical characterization of clathrin assembly protein AP180 and synaptophysin in human brain. *Neurobiology of Aging,* **24**(1), pp. 173-178.

YATES, J.R., SCHIELTZ, D., KOLLER, A. & VENABLE, J., (2006). Peptide sequencing by tandem mass spectrometry. *Cell Biology* (Third Edition), Ed. Julio E. Celis, Academic Press, Burlington, pp. 383-390.

YIN, K., CIRRITO, J.R., YAN, P., HU, X., XIAO, Q., PAN, X., BATEMAN, R., SONG, H., HSU, F., TURK, J., XU, J., HSU, C.Y., MILLS, J.C., HOLTZMAN, D.M. and LEE, J., (2006). Matrix metalloproteinases expressed by astrocytes mediate extracellular amyloid-beta peptide catabolism. *Journal of Neuroscience,* **26**(43), pp. 10939-10948.

YIP, S., TO, S., LEUNG, P.M., CHEUNG, T., CHENG, P.C. and LIM, W.L., (2005). Use of dual TaqMan® probes to increase the sensitivity of 1-step quantitative reverse transcription-PCR: application to the detection of SARS Coronavirus. *Clinical Chemistry,* **51**(10), pp. 1885-1888.

YONG, V.W., FORSYTH, P.A., BELL, R., KREKOSKI, C.A. and EDWARDS, D.R., (1998). Matrix metalloproteinases and diseases of the CNS. *Trends in Neurosciences,* **21**(2), pp. 75-80.

YONG, V.W., POWER, C., FORSYTH, P. and EDWARDS, D.R., (2001). Metalloproteinases in biology and pathology of the nervous system. *Nature Reviews. Neuroscience,* **2**(7), pp. 502-511.

YONG, V.W., AGRAWAL, S. and STIRLING, D., (2007a). Targeting MMPs in acute and chronic neurological conditions. *Neurotherapeutics,* **4**(4), pp. 580-589.

YONG, V.W., ZABAD, R.K., AGRAWAL, S., GONCALVES DASILVA, A. and METZ, L.M., (2007b). Elevation of matrix metalloproteinases (MMPs) in multiple sclerosis and impact of immunomodulators. *Journal of the Neurological Sciences,* **259**(1-2), pp. 79-84.

YOO, H.G., SHIN, B.A., PARK, J.S., LEE, K.H., CHAY, K.O., YANG, S.Y., AHN, B.W. and JUNG, Y.D., (2002). IL-1β induces MMP-9 via reactive oxygen species and NF-κB in murine macrophage RAW 264.7 cells. *Biochemical and Biophysical Research Communications,* **298**(2), pp. 251-256.

ZABAD, R.K., METZ, L.M., TODORUK, T.R., ZHANG, Y., MITCHELL, J.R., YEUNG, M., PATRY, D.G., BELL, R.B. and YONG, V.W., (2007).The clinical response to minocycline in multiple sclerosis is accompanied by beneficial immune changes: a pilot study. *Multiple Sclerosis,* **13**(4), pp. 517-526.

ZEINSTRA, E., WILCZAK, N. and DE KEYSER, J., (2003). Reactive astrocytes in chronic active lesions of multiple sclerosis express co-stimulatory molecules B7-1 and B7-2. *Journal of Neuroimmunology*, **135**(1-2), pp. 166-171.

ZHANG, H., UCHIMURA, K. and KADOMATSU, K., (2006). Brain keratan sulfate and glial scar formation. *Annals of the New York Academy of Sciences,* **1086**(1), pp. 81-90.

ZHANG, K., MCQUIBBAN, G.A., SILVA, C., BUTLER, G.S., JOHNSTON, J.B., HOLDEN, J., CLARK-LEWIS, I., OVERALL, C.M. and POWER, C., (2003). HIV-induced metalloproteinase processing of the chemokine stromal cell derived factor-1 causes neurodegeneration. *Nature Neuroscience,* **6**(10), pp. 1064-1071.